NEUROLOGIC CORRELATES OF MOTOR FUNCTION IN CEREBRAL PALSY: OPPORTUNITIES FOR TARGETED TREATMENT

EDITED BY: Jessica Rose, Christos Papadelis and Deborah Gaebler-Spira

PUBLISHED IN: Frontiers in Human Neuroscience and Frontiers in Neurology

frontiers Research Topics

frontiers

ISSN 1664-8714
ISBN 978-2-88966-354-5
DOI 10.3389/978-2-88966-354-5

About Frontiers

Frontiers is more than just an open-access publisher of scholarly articles: it is a pioneering approach to the world of academia, radically improving the way scholarly research is managed. The grand vision of Frontiers is a world where all people have an equal opportunity to seek, share and generate knowledge. Frontiers provides immediate and permanent online open access to all its publications, but this alone is not enough to realize our grand goals.

Frontiers Journal Series

The Frontiers Journal Series is a multi-tier and interdisciplinary set of open-access, online journals, promising a paradigm shift from the current review, selection and dissemination processes in academic publishing. All Frontiers journals are driven by researchers for researchers; therefore, they constitute a service to the scholarly community. At the same time, the Frontiers Journal Series operates on a revolutionary invention, the tiered publishing system, initially addressing specific communities of scholars, and gradually climbing up to broader public understanding, thus serving the interests of the lay society, too.

Dedication to Quality

Each Frontiers article is a landmark of the highest quality, thanks to genuinely collaborative interactions between authors and review editors, who include some of the world's best academicians. Research must be certified by peers before entering a stream of knowledge that may eventually reach the public - and shape society; therefore, Frontiers only applies the most rigorous and unbiased reviews.
Frontiers revolutionizes research publishing by freely delivering the most outstanding research, evaluated with no bias from both the academic and social point of view. By applying the most advanced information technologies, Frontiers is catapulting scholarly publishing into a new generation.

What are Frontiers Research Topics?

Frontiers Research Topics are very popular trademarks of the Frontiers Journals Series: they are collections of at least ten articles, all centered on a particular subject. With their unique mix of varied contributions from Original Research to Review Articles, Frontiers Research Topics unify the most influential researchers, the latest key findings and historical advances in a hot research area! Find out more on how to host your own Frontiers Research Topic or contribute to one as an author by contacting the Frontiers Editorial Office: researchtopics@frontiersin.org

NEUROLOGIC CORRELATES OF MOTOR FUNCTION IN CEREBRAL PALSY: OPPORTUNITIES FOR TARGETED TREATMENT

Topic Editors:
Jessica Rose, Stanford University, United States
Christos Papadelis, Cook Children's Medical Center, United States
Deborah Gaebler-Spira, Northwestern University, United States

Citation: Rose, J., Papadelis, C., Gaebler-Spira, D., eds. (2021). Neurologic Correlates of Motor Function in Cerebral Palsy: Opportunities for Targeted Treatment. Lausanne: Frontiers Media SA. doi: 10.3389/978-2-88966-354-5

Table of Contents

frontiers in Human Neuroscience

EDITORIAL
published: 19 November 2020
doi: 10.3389/fnhum.2020.615397

Editorial: Neurologic Correlates of Motor Function in Cerebral Palsy: Opportunities for Targeted Treatment

Jessica Rose[1]*, *Christos Papadelis*[2] and *Deborah Gaebler-Spira*[3]

[1] Division of Pediatric Orthopaedics, Stanford University School of Medicine, Stanford, CA, United States, [2] Jane and John Justin Neurosciences Center, Cook Children's Health Care System, Fort Worth, TX, United States, [3] Shirley Ryan AbilityLab, Chicago, IL, United States

Keywords: cerebral palsy, neurology, mobility, gait, upper limb function

Editorial on the Research Topic

Neurologic Correlates of Motor Function in Cerebral Palsy: Opportunities for Targeted Treatment

Cerebral palsy (CP) is the most common childhood motor disorder. It is a clinical syndrome with several etiologies and associated symptoms. These symptoms or impairments lead to varying degrees of gross and fine motor severity and impact functional activities such as gait, arm use, and speech. Current medical and surgical treatments for CP are only partially effective in improving these motor abnormalities and may cause significant muscle weakness and other complications. Thus, for persons with CP meaningful improvements remain elusive. We believe that a better understanding of the mechanisms underlying neuromuscular deficits of CP will lead to more effective treatments.

Abnormal tone interfering with the child's posture and development is a common feature of spastic, dyskinetic, and ataxic CP (Sanger et al., 2003, 2006, 2010), which arise from early injury to specific brain regions and result in characteristic neuromuscular deficits. Children with spastic CP, the most common form, have neuromuscular deficits associated with injury to the corticospinal motor track. Subsequent loss of descending neural activation and inhibition result in weak and short muscles that fail to grow sufficiently relative to skeletal growth, and affected muscles have increased sensitivity to stretch (Zhou et al., 2017). Additionally, voluntary movement is limited by impaired selective motor control (SMC), characterized by flexion and extension synergy patterns (Cahill-Rowley and Rose, 2014). Ironically, most research and medical interventions for spastic CP focus on tone, however, function is often most effected by muscle weakness and slow muscle growth relative to bone growth, in combination with impaired SMC. Muscle is frequently overlooked, and as the end organ, it is an area that needs focused attention and clinical research. Current treatments for joint contracture, such as surgical tendon lengthening and skeletal realignment address deformities that are years in the making and require hospitalization. Addressing the underlying impairments of muscle weakness and slow growth rate could prevent joint contracture and skeletal malalignment, and minimize the need for surgery. Muscle is highly responsive to input and substantially influences function, it is therefore a promising target for effective treatment. Understanding the neurological correlates of these neuromuscular impairments can inform more targeted and successful treatment.

Typically, CP is categorized by tone and topography. Many children with CP may have a mixed tone disorder that requires careful attention to identify. Dyskinetic CP is thought to arise primarily from injury to the basal ganglia, causing uncontrolled movements that impose on voluntary movements (Zhou et al., 2017). Ataxic CP is thought to arise primarily from injury to the cerebellum, causing impaired postural balance and targeting (Zhou et al., 2017).

OPEN ACCESS

Edited and reviewed by:
Lutz Jäncke,
University of Zurich, Switzerland

***Correspondence:**
Jessica Rose
jessica.rose@stanford.edu

Specialty section:
This article was submitted to Cognitive Neuroscience, a section of the journal Frontiers in Human Neuroscience

Received: *09 October 2020*
Accepted: *26 October 2020*
Published: *19 November 2020*

Citation:
Rose J, Papadelis C and Gaebler-Spira D (2020) Editorial: Neurologic Correlates of Motor Function in Cerebral Palsy: Opportunities for Targeted Treatment. Front. Hum. Neurosci. 14:615397. doi: 10.3389/fnhum.2020.615397

This research article collection, "*Neurologic correlates of motor function in cerebral palsy: opportunities for targeted treatment*" highlights current research from around the world that investigates important structure-function relationships underlying the neuromuscular deficits of CP. This exploratory research can inform and potentially translate into effective treatment.

Here we examine the links between regional brain injury, metabolic activity and motor impairments of the upper (Hung et al.; Papadelis et al.,) and lower limbs (Cahill-Rowley et al.; Fowler et al.; Papageorgiou et al.; Short et al.). In addition, the important role of sensorimotor (Zarkou et al.) and visuospatial (Maioli et al.) impairments in movement abnormalities are investigated. To guide effective treatment, it is vital to delineate motor control deficits from musculoskeletal limitations of gait abnormalities, this is explored using a physics-based simulation (Falisse et al.). An initial investigation of neuromuscular reflex characteristics to predict treatment outcome offers a step toward delivering more precise medicine for persons with CP (Bar-On et al.). Finally, the effects of treatment that targets underlying neuromuscular deficits of CP is examined (Beani et al.; Peeters et al.), including multichannel neuromuscular electrical stimulation that highlights need for lightweight wearable gait devices (Mooney and Rose). We envisioned that this research article collection would provide a context for developing an effective approach to addressing the etiology, diagnosis and treatment of CP. To this end, we appreciate your interest and hope that you will be inspired toward future research.

AUTHOR CONTRIBUTIONS

All authors listed have made a substantial, direct and intellectual contribution to the work, and approved it for publication.

ACKNOWLEDGMENTS

We wish to thank all of the research teams who have contributed to this article collection.

REFERENCES

Cahill-Rowley, K., and Rose, J. (2014). Etiology of impaired selective motor control: emerging evidence and its implications for research and treatment in cerebral palsy. *Dev. Med. Child Neurol.* 56, 522–528. doi: 10.1111/dmcn.12355

Sanger, T. D., Delgado, M. R., Gaebler-Spira, D., Hallet, M., and Mink, J. W. (2003). Classification and definition of disorders causing hypertonia in childhood. *Pediatrics* 111, e89–e97. doi: 10.1542/peds.111.1.e89

Sanger, T. D., Delgado, M. R., Gaebler-Spira, D., Hallet, M., and Mink, J. W. (2006). Definition and classification of negative motor symptoms in childhood. *Pediatrics* 118, 2159–2167. doi: 10.1542/peds.2005-3016

Sanger, T. D., Delgado, M. R., Gaebler-Spira, D., Hallet, M., and Mink, J. W. (2010). Definition and classification of hyperkinetic movements in childhood. *Mov. Disord.* 25, 1538–1549. doi: 10.1002/mds.23088

Zhou, J., Butler, E. E., and Rose, J. (2017). Neurologic correlates of gait abnormalities in cerebral palsy: implications for treatment. *Front. Hum. Neurosci.* 11:103. doi: 10.3389/fnhum.2017.00103

Conflict of Interest: The authors declare that the research was conducted in the absence of any commercial or financial relationships that could be construed as a potential conflict of interest.

frontiers in Human Neuroscience

ORIGINAL RESEARCH
published: 24 July 2019
doi: 10.3389/fnhum.2019.00254

Maturation of Corticospinal Tracts in Children With Hemiplegic Cerebral Palsy Assessed by Diffusion Tensor Imaging and Transcranial Magnetic Stimulation

Christos Papadelis[1,2†], Harper Kaye[3,4†], Benjamin Shore[5], Brian Snyder[5], Patricia Ellen Grant[2,6] and Alexander Rotenberg[3,4,7]*

[1]Laboratory of Children's Brain Dynamics, Division of Newborn Medicine, Boston Children's Hospital, Harvard Medical School, Boston, MA, United States, [2]Fetal-Neonatal Neuroimaging and Developmental Science Center, Division of Newborn Medicine, Boston Children's Hospital, Harvard Medical School, Boston, MA, United States, [3]Neuromodulation Program, Division of Epilepsy and Clinical Neurophysiology, Department of Neurology, Boston Children's Hospital, Boston, MA, United States, [4]F.M. Kirby Neurobiology Center, Boston Children's Hospital, Boston, MA, United States, [5]Department of Orthopedic Surgery, Boston Children's Hospital, Harvard Medical School, Boston, MA, United States, [6]Department of Radiology, Boston Children's Hospital, Harvard Medical School, Boston, MA, United States, [7]Department of Neurology, Berenson-Allen Center for Noninvasive Brain Stimulation, Division of Cognitive Neurology, Harvard Medical School and Beth Israel Deaconess Medical Center, Boston, MA, United States

OPEN ACCESS

Edited by:
Hubert Preissl,
Institute for Diabetes Research and Metabolic Diseases (IDM), Germany

Reviewed by:
Giovanni Pellegrino,
Montreal Neurological Institute and Hospital, McGill University, Canada
Martin Victor Sale,
University of Queensland, Australia

***Correspondence:**
Christos Papadelis
christos.papadelis@childrens.harvard.edu
orcid.org/0000-0001-6125-9217

†These authors share first authorship

Received: 27 February 2019
Accepted: 08 July 2019
Published: 24 July 2019

Citation:
Papadelis C, Kaye H, Shore B, Snyder B, Grant PE and Rotenberg A (2019) Maturation of Corticospinal Tracts in Children With Hemiplegic Cerebral Palsy Assessed by Diffusion Tensor Imaging and Transcranial Magnetic Stimulation. Front. Hum. Neurosci. 13:254. doi: 10.3389/fnhum.2019.00254

Aim: To assess changes in the developmental trajectory of corticospinal tracts (CST) maturation in children with hemiplegic cerebral palsy (HCP).

Methods: Neuroimaging data were obtained from 36 children with HCP for both the more affected (MA) and less affected (LA) hemispheres, and, for purposes of direct comparison, between groups, 15 typically developing (TD) children. With diffusion tensor imaging (DTI), we estimated the mean fractional anisotropy (FA), axial diffusivity (AD), mean diffusivity (MD), and radial diffusivity (RD) of the corticospinal tract, parameters indicative of factors including myelination and axon density. Transcranial magnetic stimulation (TMS) was performed as a neurophysiologic measure of corticospinal tract integrity and organization. Resting motor threshold (rMT) was obtained per hemisphere, per patient.

Results: We observed a significant AD and MD developmental trajectory, both of which were inversely related to age (decrease in AD and diffusivity corresponding to increased

Abbreviations: AD, Axial Diffusivity; ANOVA, Analysis of Variance; ANCOVA, Analysis of Covariance; APB, Abductor Pollicis Brevis; CC, Corpus Callosum; CE, Cystic Encephalomalacia; ChRIS, Children's Research Integration System; CST, Corticospinal Tracts; Dom, Dominant; DTI, Diffusion Tensor Imaging; EMG, Electromyogram; EP, Echo-Planar; FA, Fractional Anisotropy; FACT, Fiber Assignment by Continuous Tracking; FOV, Field of view; GMFCS, Gross Motor Function Classification System; HCP, Hemiplegic Cerebral Palsy; GRAPPA, Generalized Autocalibrating Partial Parallel Acquisition; LA, Less Affected; MA, More Affected; MACS, Manual Abilities Classification Scale; MD, Mean Diffusivity; MEP, Motor Evoked Potential; MO, Machine Output; MPRAGE, Magnetization-Prepared Rapid-Acquisition Gradient-Echo; MRI, Magnetic Resonance Imaging; NDom, Non-dominant; PrG, Pre-Central Gyrus; PV-WMI, Periventricular White Matter Injury; RD, Radial Diffusivity; rMT, Resting Motor Threshold; ROI, Region of Interest; SMU, Sensorimotor U-fibers; STh, Spinothalamic; TD, Typically Developing; TE, Echo Time; ThC, Thalamacortical; TMS, Transcranial Magnetic Stimulation; TR, Repetition Time.

age) in both hemispheres of TD children ($p < 0.001$). This maturation process was absent in both MA and LA hemispheres of children with HCP. Additionally, the TMS-derived previously established rMT developmental trajectory was preserved in the LA hemisphere of children with HCP ($n = 26$; $p < 0.0001$) but this trajectory was absent in the MA hemisphere.

Conclusions: Corticospinal tract maturation arrests in both hemispheres of children with HCP, possibly reflecting perinatal disruption of corticospinal tract myelination and axonal integrity.

Keywords: hemiplegic cerebral palsy, corticospinal tracts, development, maturation, transcranial magnetic stimulation

HIGHLIGHTS

- Linear age-dependent developmental trajectories of corticospinal tracts diffusion metrics
- Halted bilateral corticospinal tracts imaging metrics maturation in children with HCP
- Preserved resting motor threshold maturational trajectory in the less affected hemisphere of children with HCP
- Absent resting motor threshold maturational trajectory in the more affected hemisphere of children with HCP

INTRODUCTION

Hemiplegic cerebral palsy (HCP) is a common subtype of motor dysfunction, affecting one-third of patients with a clinical cerebral palsy diagnosis (Hagberg et al., 2001). Children with HCP reliably exhibit prominent impairment in skilled voluntary movements. The underlying etiology is a non-progressive lesion located most commonly in the periventricular white matter of the developing fetal or infant brain (Rosenbaum et al., 2007). This lesion impairs the structural integrity of the corticospinal tracts (CST), which are the most important tracts for fine motor skills, and among the first tracts to mature. Despite extensive literature showing microstructural damage in the CST of children with HCP (Scheck et al., 2012), little is known about how the underlying lesion affects the maturation process of these fibers.

CST maturation is a complex process affected by dynamic factors such as synaptic pruning and development (Eyre et al., 2001), myelination (Eyre et al., 1991), changes in axonal diameter and length (Eyre et al., 2002) and organization of pyramidal neuron firing patterns (Chiappa et al., 1991). Several studies have reported measurable CST developmental changes in healthy children using either transcranial magnetic stimulation (TMS) of the motor cortex (Koh and Eyre, 1988; Nezu et al., 1997; Paus et al., 2001) or diffusion tensor imaging (DTI; Lebel and Beaulieu, 2011; Yeo et al., 2014) of the CST. When measured by TMS, CST maturation in healthy children corresponds to a progressive increment of cortical excitability from infancy to adulthood that completes in mid-adolescence (Koh and Eyre, 1988; Nezu et al., 1997; Hameed et al., 2017; Kaye and Rotenberg, 2017). An analogous developmental trajectory is also seen when CST maturation is measured by DTI: a steep increase of the fiber volume and fractional anisotropy (FA) is observed in healthy children until early adolescence and a later gradual increase until adulthood (Lebel and Beaulieu, 2011; Yeo et al., 2014). The mechanistic relationship between these measures seems logical as larger myelinated fiber caliber should correspond to increased excitability. Yet, there are no TMS or DTI studies to examine whether and how normal CST maturation is affected by perinatal white matter injury, as occurs in HCP.

Here, we describe a cross-sectional study investigating the developmental trajectories of TMS and DTI CST metrics as a function of age in children with HCP to test whether perinatal injury arrests normal CST development, and whether such an arrest is confined to the more affected (MA) hemisphere of children with HCP. Specifically, by TMS, we measure the resting motor threshold (rMT), which reflects motor cortex excitability and the developmental stage of CST myelination, as well as the membrane characteristics and synaptic efficacy of the cortical and spinal motor neurons (Garvey et al., 2003). By DTI, we assess the structural integrity of the CST by measuring the FA, axial diffusivity (AD), mean diffusivity (MD), and radial diffusivity (RD), which are parameters indicative of myelination and axon density, among other factors (Grant et al., 2001).

MATERIALS AND METHODS

Participants

Neuroimaging data were obtained from 36 children and adolescents with HCP (age = 11.83 ± 3.79 years; range: 4.1–17.8 years; 17 females) and, for direct comparison, 15 age-matched typically developing (TD) children and adolescents (age = 12.05 ± 3.67 years; range: 7.13–18.02 years; 9 females). The inclusion criteria were: (i) mild to moderate spastic hemiplegia [Gross Motor Function Classification System (GMFCS) level I, II, or III; Manual Abilities Classification Scale (MACS) level I, II, or III]; (ii) sufficient cooperation to participate in a neuroimaging study; (iii) no contradiction for magnetic resonance imaging (MRI); i.e. presence of metallic implants, or pumps; and (iv) no severe intellectual developmental disability. The clinical characteristics of participants with HCP are shown in **Table 1**. The TD children were recruited from the local

TABLE 1 | Patient demographics and MRI findings.

ID	Age (Years)	Handedness	Epilepsy	GMFCS	MACS	MA hemisphere	Lesion type
CH 1	4	Left	Y	2	2	Left	Perinatal Stroke
CH 2	5	Right	Y	1	1	Right	Perinatal Stroke
CH 3	6	Left	Y	1	1	Left	Perinatal Stroke
CH 4	7	Right	N	2	1	Right	PV-WMI
CH 5	7	Right	Y	1	1	Left	CE
CH 6	7	Left	N	1	1	Left	Perinatal Stroke
CH 7	8	Right	Y	3	3	Right	Perinatal Stroke
CH 8	8	Left	Y	2	2	Left	Perinatal Stroke
CH 9	10	Right	Y	2	2	Left	PVNH
CH 10	10	Right	Y	2	2	Left	Perinatal Stroke
CH 11	10	AMBI	Y	1	1	Left	CE
CH 12	10	Left	Y	2	3	Left	Perinatal Stroke
CH 13	11	Right	Y	1	1	Left	CE
CH 14	11	Right	N	1	2	Right	Perinatal Stroke
CH 15	11	Right	N	1	1	Left	Parenchymal Atrophy
CH 16	11	Left	Y	1	1	Left	Perinatal Stroke
CH 17	11	Right	Y	2	2	Right	CE
CH 18	11	Left	Y	1	1	Left	CE
CH 19	11	Left	Y	2	3	Right	Perinatal Stroke
CH 20	12	AMBI	Y	1	1	Right	Perinatal Stroke
CH 21	12	Left	Y	1	1	Left	PV-WMI
CH 22	13	Left	Y	2	2	Left	CE
CH 23	13	Left	N	1	1	Left	PV-WMI
CH 24	14	Right	N	1	2	Right	Perinatal Stroke
CH 25	14	Right	N	1	2	Left	Parenchymal Defect
CH 26	15	Right	Y	2	2	Right	CE
CH 27	15	Right	Y	1	1	Right	Perinatal stroke
CH 28	16	Right	Y	1	1	Right	Perinatal stroke
CH 29	16	Right	Y	2	2	Right	CE
CH 30	16	Right	N	1	1	Right	PV Gliosis
CH 31	16	Left	Y	1	1	Left	Perinatal stroke
CH 32	17	Left	N	1	2	Left	CE
CH 33	17	AMBI	Y	1	1	Right	CE
CH 34	17	Right	Y	1	2	Left	CE
CH 35	18	Left	Y	1	2	Left	Perinatal stroke
CH 36	18	Left	N	1	2	Right	CE

Patient demographics include age in years; handedness; epileptic status; Gross Motor Function Classification System (GMFCS) level; Manual Abilities Classification Scale (MACS) level; the MA hemisphere; Lesion Type. AMBI, ambidextrous; PV-WMI, Periventricular White Matter Injury; PV Gliosis, Periventricular Gliosis; CE, Cystic Encephalomalacia; PVNH, Periventricular Nodular Heterotropia.

community. This study was carried out in accordance with the recommendations of Boston Children's Hospital (BCH) Internal Review Board (IRB). All subjects gave written informed consent in accordance with the Declaration of Helsinki. The protocol was approved by Boston Children's Hospital IRB (IRB-P00023570; PI: CP).

Image Acquisition

MRI scans were performed in a 3T Magnetom Tim Trio (Siemens Healthcare, Germany). The imaging protocol consisted of structural and diffusion-weighted sequences. The structural sequence was a T1-weighted magnetization-prepared rapid-acquisition gradient-echo acquisition (MPRAGE), which used volumetric echo-planar (EP) imaging navigators for real-time motion correction [voxel size (mm) = 1.0 × 1.0 × 1.0; field of view (FOV) = 19.2–22.0 cm; echo time (TE) = 1.74 ms; repetition time (TR) = 2,520 ms; flip angle = 7°]. The FOV was set to 256 mm and matrix size was 256 [TR = 3,200 ms, TE = 363 ms, Generalized Autocalibrating Partial Parallel Acquisition (GRAPPA) acceleration R = 2, echo-spacing of 3.63 ms for a total imaging time of 3:23 min]. The diffusion sequence (prescribed axially) used EP readouts [voxel size (mm) = 2.0 × 2.0 × 2.0; FOV = 11–12.8 cm; TE = 88 ms; TR = 8,320–10,934 ms; flip angle = 90°; 30 gradient diffusion directions at b = 1,000 s/mm^2; 10 acquisitions with b = 0 s/mm^2].

Identification of More and Less Affected Hemispheres

The MRI scans were reviewed by a pediatric radiologist (PEG). No structural abnormalities were observed in the MRIs of TD children. A unilateral structural abnormality was seen in 31 children with HCP. In five cases, bilateral abnormalities were observed. The MA hemisphere referred to the hemisphere where structural abnormalities were identified or were more prominent compared to the other hemisphere. For all children with HCP, the MA hemisphere was contralateral to the paretic hand. Each child in the TD group was assigned to have a randomly selected hemisphere (Hem1 and Hem2) to balance out possible inherent

differences in the functioning of the right and left hemispheres (Pihko et al., 2014).

DTI Analysis

From our cohort, DTI data were available for 17 children with HCP (mean: 12.93 ± 3.8 years; range: 6.59–17.80 years; nine females) and all TD children. Diffusion images were first processed to correct for distortions caused by minor eddy currents and simple head motions using FSL tools[1]. Diffusion tensor models were estimated with tractography plugin in the Children's Research Integration System (ChRIS) using the Fiber Assignment by Continuous Tracking (FACT) method and an angle threshold of 45° with no FA threshold (Mori et al., 1999). The algorithm also generated FA maps, vector maps, and a color-coded direction map. Colors were assigned by direction and orientation of the fibers (blue: superior-inferior, green: antero-posterior, red: left-right). Tracts within these directions were represented with a combination of these three colors. Volumetric segmentation and cortical surface reconstruction of T1-weighted images were performed with Freesurfer[2]. The T1 image was co-registered to the diffusion space using command-line tools from Freesurfer for visualization purposes of the tracts. The generated track file was uploaded into Trackvis[3] to analyze the diffusion data and create regions of interest (ROIs) for the targeted areas. To track the CST, the ROIs were placed over the pre-central gyrus (PrG) and cst at the brainstem level. The PrG and cst were manually defined using anatomical landmarks of the participant's MRI along with the color-coded direction maps and a diffusion atlas for reference. **Figure 1A** presents a 3D representation of the anatomically-defined ROIs and the corresponding CST for a TD and a child with HCP. Mean scalar measures of FA, AD, MD, and RD were derived for each fiber track. Data were analyzed separately for the two hemispheres identified as MA and less affected (LA) for the children with HCP and for both hemispheres of TD children. Only patients with identifiable CST in both hemispheres were considered for further analysis.

TMS

From our cohort, 26 children with HCP (age = 11.47 ± 3.79 years; range: 4.1–17.8 years; 12 females) underwent motor mapping with TMS. No TD children participated in the TMS motor mapping session. Each participant's T1-weighted MPRAGE was converted to a 3D head surface and brain reconstruction using Nexstim 4.3 software (Nexstim, Finland), and optimal cortical peel depth was chosen based upon individual cortical anatomy. TMS, coupled with surface electromyography (EMG), was delivered *via* a figure-of-eight coil with frameless stereotaxy and TMS neuronavigation software that allows for continuous visualization of the stimulation coil relative to the patient's individual brain MRI. Real-time stimulus-locked EMG was recorded from pre-determined target muscles, with one common-ground EMG amplifier (band-pass filter 10–500 Hz, sampling rate 3 KHz per channel). Surface EMG electrodes were placed on the right and the left abductor pollicis brevis (APB) muscles, and a ground electrode on the underside of the right forearm. With single-pulse TMS, stimuli were applied to scalp sites overlying the motor cortex, while muscle activity was monitored in real-time with stimulus-locked EMG. Motor evoked potentials (MEPs) were recorded bilaterally from the APB muscles and a hotspot, corresponding to location that produced peak APB MEP amplitudes were identified per hemisphere. Thereafter, rMT was determined as the minimum stimulation intensity (recorded as electric field strength, V/m) at the APB hotspot that was necessary to elicit a response from the APB, contralateral to the stimulated hemisphere, of 50 μV, on ≥50% of trials. The rMT was determined as percent machine output (MO) and in the corresponding units (V/m) of the induced electric field (e-field; Julkunen et al., 2012). Both rMT determination and motor mapping were performed separately in each hemisphere per child.

Statistical Analysis

Statistical analysis was performed using GraphPad Prism Software v.7 (GraphPad Prism Software, La Jolla, CA, USA). For the diffusion parameters, we compared the mean FA, AD, MD, and RD of the CST with a mixed 2 (group: HCP, TD) × 2 (hemisphere: LA, MA) analysis of variance (ANOVA), with group being a between-subject factor and hemisphere a within-subjects factor. To compensate for multiple comparisons and control the familywise Type I error rate at 5% in each family of four tests, we applied the Holm step-down criteria, setting the significance threshold for the strongest contrast at $p = 0.05/4$; for the second strongest at $p = 0.05/3$; and so forth (Bender and Lange, 2001). We calculated a Holm adjusted p-value as 4, 3, 2, or 1 times the observed value for the strongest, second strongest, and so forth. Normality assumption was tested with the Shapiro-Wilk test, sphericity assumption with the Mauchly test, and equality of variances with the Levene test. For the developmental trajectories of diffusion parameters, comparisons between hemispheres were performed by a linear mixed-effects model to account for within-subject correlations, with age, lesion and age × lesion interaction as fixed-effects. Comparisons between the two groups (HCP vs. TD) were also performed using a linear model. Linear regression analysis with a straight-line model was performed to test for a relationship between rMT and age. To test whether comparisons between slopes of the MA and LA hemispheres in children with HCP are significantly different, analysis of covariance (ANCOVA) was used. Since no TD children underwent motor mapping with TMS, only comparisons between the two hemispheres within the HCP group were performed for the rMT values. To avoid exclusion of patients with the highest rMTs, for those subjects ($n = 3$) whose APB rMT was >100% MO, the threshold for activation was estimated, per hemisphere, by sorting APB MEP peak-to-peak amplitudes, and obtaining the average e-field values (V/m) for the top 50th percentile. For all statistical analyses, the level of significance was set at $p < 0.05$.

[1]https://fsl.fmrib.ox.ac.uk/fsl/fslwiki/FDT
[2]http://surfer.nmr.mgh.harvard.edu/
[3]http://trackvis.org/

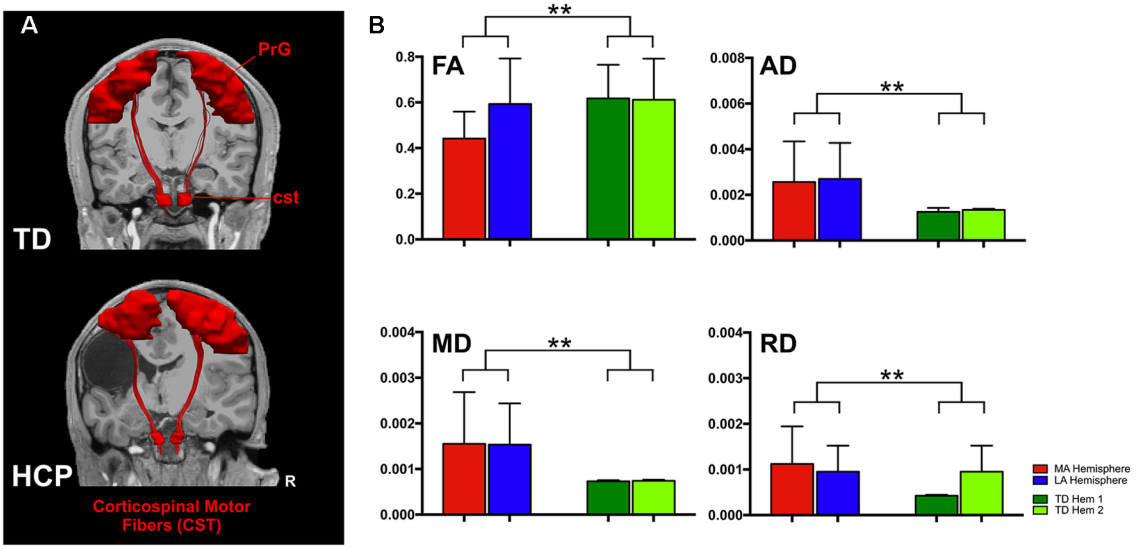

FIGURE 1 | Anatomically defined region of interest (ROI) and corticospinal tracts (CST). **(A)** The ROIs pre-central gyrus (PrG and cst) and their corresponding CST for a typically developing (TD) child (aged 18 years, upper panel) and a child with hemiplegic cerebral palsy (HCP) overlaid on their magnetic resonance imagings (MRIs). **(B)** Error bars (mean ± 95% confidence interval) of diffusion parameters [fractional anisotropy (FA), axial diffusivity (AD), mean diffusivity (MD), and radial diffusivity (RD)] for the CST for both hemispheres of TD children and the less affected (LA) and more affected (MA) hemispheres of children with HCP (**$p < 0.001$).

RESULTS

CST Diffusion Parameters for HCP and TD Children

ANOVA showed significant differences between the HCP and TD children for the FA ($F_{(1,64)} = 9.860$; $p = 0.003$), MD ($F_{(1,64)} = 6.492$; $p = 0.013$), AD ($F_{(1,64)} = 6.553$; $p = 0.013$), and RD ($F_{(1,64)} = 7.578$; $p = 0.008$; **Figure 1**). However, the main effect of hemisphere and the hemisphere × group interaction were not significant, indicating that the group difference was of similar magnitude in the MA and LA hemispheres.

Maturational Trajectory of Diffusion Parameters

In TD children, there is a progressive decline with age for both AD and MD that is essentially identical in both hemispheres (**Figure 2**). This developmental trajectory is significant for both hemispheres of TD children ($p < 0.05$). FA and RD measures for Hem1 and Hem2 show absence of inter-hemispheric difference (**Figure 1B**), and neither FA nor RD change with age ($p > 0.05$, n.s.).

In contrast to TD children, the AD and MD parameters in children with HCP have no significant interaction with age in the MA (MD, AD: $p > 0.05$, n.s.) or LA (MD, AD: $p > 0.05$, n.s.) hemispheres. Though in line with findings for the TD children, neither FA nor RD values change with age in the HCP cohort ($p > 0.05$, n.s.; **Table 2**). The difference in slopes for TD Hem1/Hem2 vs. CP MA/LA is significant for both MD and AD diffusion parameters ($p < 0.01$).

TMS Measure of CST Excitability and Maturation

The rMT was obtained per subject, per hemisphere for 26 subjects (**Figure 3**). Relevant to the present report, the rate of maturation differs between MA and LA hemispheres in patients with HCP. In the LA hemisphere, age is the major rMT determinant, which decreases by ∼10.42 V/m per year throughout childhood ($R^2 = 0.605$; $p < 0.0001$; **Figure 4A**). In contrast, rMT maturational trajectory is absent in the MA hemisphere ($R^2 = 0.012$; $p = 0.597$; **Figure 4B**), indicating absent CST maturation specific to the MA hemisphere.

DISCUSSION

Through a multimodal neuroimaging approach, this cross-sectional study shows for the first-time evidence of disrupted CST maturation in both hemispheres of children with HCP. With DTI, we identified a diffusivity decrement (reduced AD and MD) with increasing age in both hemispheres of TD children. In contrast, we identified a diffusivity increment (increased AD and MD) in the MA hemisphere of children with HCP, and a steady diffusivity across age in the LA hemisphere. In complement to the DTI findings, by TMS, we also found a halted electrophysiological maturation of the CST in the MA hemisphere of children with HCP, which contrasts to a normal maturation in the LA hemisphere of children with HCP (Hameed et al., 2017; Säisänen et al., 2018). Our findings support our main hypothesis that perinatal injury arrests normal CST development. This arrest occurs in both hemispheres of children with HCP but is more pronounced in the MA hemisphere.

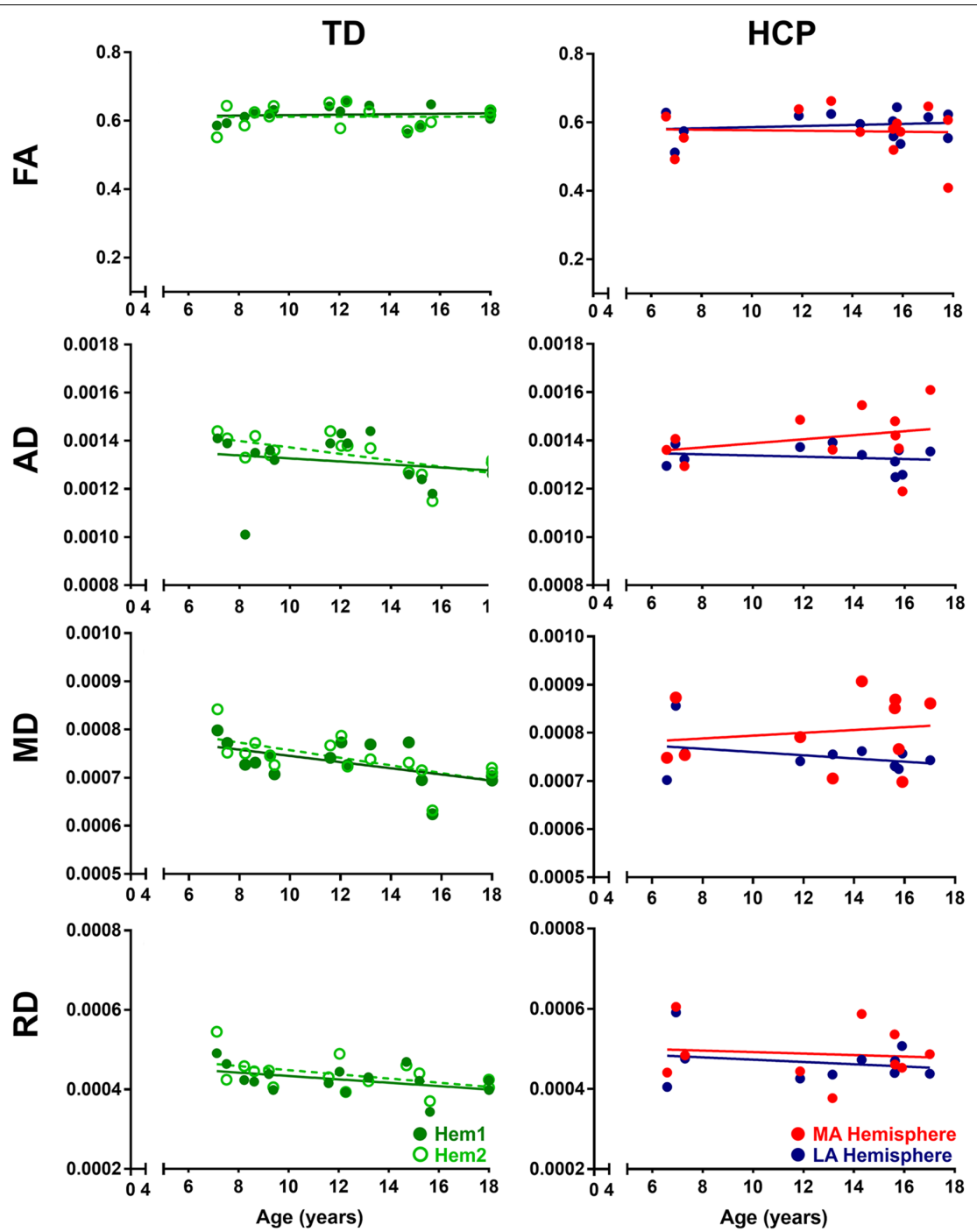

FIGURE 2 | Developmental trajectories of diffusion parameters. Mean FA, AD, MD, and RD for TD children (Hem1: dark green closed circles, Hem2: light green open circles), and children with HCP (MA: red closed circles, LA: blue closed circles) as a function of age. For FA TD (Hem1; $R^2 = 0.0080$, $p = 0.7506$), TD (Hem2; $R^2 = 0.0001$, $p = 0.9788$), HCP (LA; $R^2 = 0.0258$, $p = 0.5999$), HCP (MA; $R^2 = 0.0019$, $p = 0.8883$). For AD: TD (Hem1; $R^2 = 0.4101$, $p < 0.001$), TD (Hem2; $R^2 = 0.460$, $p < 0.001$), HCP (LA; $R^2 = 0.0395$; $p = 0.558$); HCP (MA; $R^2 = 0.081$, $p = 0.397$). For MD: TD (Hem1; $R^2 = 0.299$, $p < 0.001$), TD (Hem2; $R^2 = 0.419$, $p < 0.001$), HCP (LA; $R^2 = 0.116$, $p = 0.306$); HCP (MA; $R^2 = 0.025$, $p = 0.639$). For RD: TD (Hem1; $R^2 = 0.1931$, $p = 0.101$), TD (Hem2; $R^2 = 0.212$, $p = 0.085$), HCP (LA; $R^2 = 0.0479$, $p = 0.5437$); HCP (MA; $R^2 = 0.0117$, $p = 0.7665$).

Numerous cross-sectional studies have investigated age-related differences in DTI parameters in healthy children and adolescents. These studies consistently demonstrate an increasing FA, a parameter linked to axon packing and myelination (Beaulieu, 2002), and a decreasing MD, a parameter reflecting water content and density, throughout brain white

TABLE 2 | Maturational trajectory of diffusion parameters.

	AD	MD	FA	RD
TD (Hem1)	R^2 = 0.4101*, p = 0.014	R^2 = 0.2897*, p = 0.0385	R^2 = 0.008045, p = 0.7506	R^2 = 0.1932, p = 0.1012
TD (Hem2)	R^2 = 0.460*, p = 0.008	R^2 = 0.4099*, p = 0.0101	R^2 = 0.00005658, p = 0.9788	R^2 = 0.2118, p = 0.0843
HCP (MA)	R^2 = 0.08095, p = 0.3965	R^2 = 0.02547, p = 0.6393	R^2 = 0.001873, p = 0.8883	R^2 = 0.01167, p = 0.7665
HCP (LA)	R^2 = 0.0395, p = 0.558	R^2 = 0.1156, p = 0.3063	R^2 = 0.02583, p = 0.5999	R^2 = 0.04786, p = 0.5437

*$p < 0.05$.

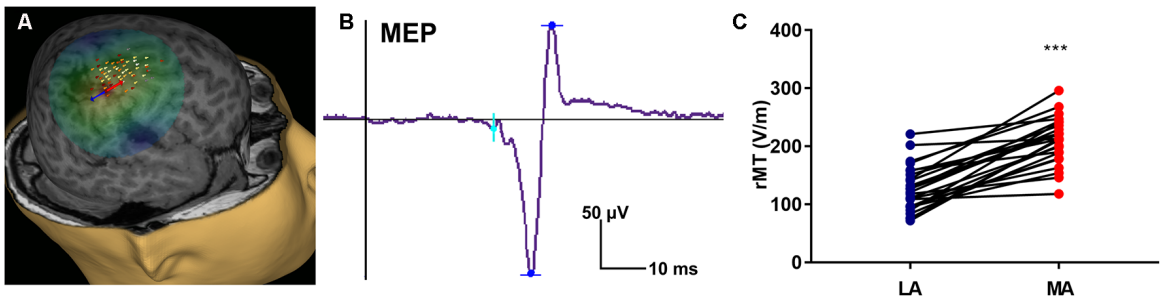

FIGURE 3 | Representative transcranial magnetic stimulation (TMS) motor map and resting motor threshold (rMT) measures. **(A)** An approximation of stimulating electric field induced by TMS is displayed on a 3D reconstruction of the cortical surface (for same subject as shown in **Figure 1A**), where field center is indicated by the junction between the red and blue arrows indicating the direction of induced current, and corresponding composite map of right hemispheric stimulation sites evoking motor evoked potentials (MEPs) of the left abductor pollicis brevis (APB) muscle. Intensity of response is color-coded from lowest (gray) to highest (white). **(B)** Representative left APB MEP sample where the vertical line (black) corresponds to stimulus time. **(C)** rMT of children with HCP for the LA and MA hemispheres (***$p < 0.0001$).

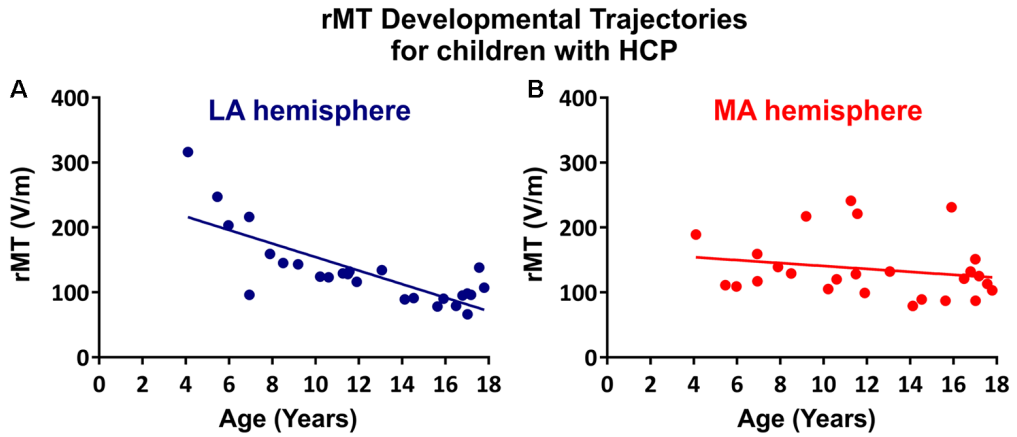

FIGURE 4 | rMT developmental trajectories. rMT as a function of age in the **(A)** LA hemisphere (R^2 = 0.6114, $p < 0.0001$) and **(B)** MA hemisphere (R^2 = 0.0313, p = 0.4991) for patients with HCP who underwent TMS (n = 26).

matter during childhood and adolescence (Schmithorst and Dardzinski, 2002; Eluvathingal et al., 2007; Mukherjee et al., 2008). Specifically, for the CST, Lebel and Beaulieu (2011) found a significant increase of the tract volume, decrease of FA, and increase of MD across ages 5–30 years. More recently, Yeo et al. (2014) observed a steep increase of FA until age 7 years and then a more gradual increase until adulthood, but did not examine other diffusion parameters, such as the AD, MD, or RD. As we have done, measuring all four diffusion parameters is important as each provides a distinct mechanistic insight into the HCP pathophysiology (Scheck et al., 2012), and each does not necessarily vary with age. For instance, while we identified a MD and AD reduction with increasing age we found no age-dependent FA change. Our findings are in line with previous DTI studies showing a maturation trajectory for the CST with decreasing diffusivity across age until the young adulthood. They are also consistent with the development of precise fine motor skills, which are dependent on CST maturation and continue to develop into young adulthood (Savion-Lemieux et al., 2009).

By DTI, we identified arrested maturation in both hemispheres of children with HCP as indicated by absent AD and MD change as a function of age (**Figure 2**). The arrest

in DTI maturation was more prominent in the MA compared to the LA hemisphere. AD is specific to axonal degeneration (Song et al., 2005). Increased AD is associated with axonal injury or damage, which leads to reduced axonal density or caliber, or axonal loss, increasing the extra-axonal space by allowing faster water molecule movement parallel to axons (Song et al., 2005; Sun et al., 2008). The MD is a measure of intra- and extra-cellular water diffusion (Neil et al., 1998) and provides valuable information about diffusivity and myelination (Grant et al., 2001). Increased MD suggests increased extracellular water content due to gliosis and microscopic cystic changes that are reliable pathologic features of cerebral palsy. An increasing or steady AD and MD with increasing age for both hemispheres of children with HCP indicates an arrested maturation of the CST possibly as a result of disrupted myelination due to perinatal oligodendrocyte or oligodendrocyte progenitor injury (Volpe, 2009).

Our TMS findings further support lateralized CST developmental compromise in HCP. Notably, whereas CST excitability, possibly reflecting improving myelination, increases with age, we found that the developmental rMT trajectory was absent in the MA hemisphere in our subjects. In principle, absent age-dependent decline in rMT (corresponding to increasing CST excitability) may be interpreted as either delayed or accelerated maturation. That is, the developmental trajectory may be halted because development does not occur, or because development completes prematurely. In our case, the relatively low rMT in the MA hemisphere likely indicates a premature acceleration of CST excitability, corresponding to an early increase in CST excitability, and perhaps an early closure of the critical period for motor development in the injured hemisphere—this electrophysiologic finding may correspond to absent CST myelination that is identified by DTI. Interestingly, while DTI metrics indicate bilateral abnormalities in patients with HCP, TMS found that the maturation trajectory of the rMT was absent only in the MA hemisphere, which may indicate that DTI is a more sensitive instrument for detecting CST developmental compromise. Alternatively, preserved maturation in the contralesional hemisphere that is identified by TMS indicates compensatory cortical or spinal changes that enable normal maturation despite modest abnormalities in myelination or other microstructural elements that are indicated by DTI.

LIMITATIONS

A limitation of this study is the lack of TMS data for TD children, and the fact that DTI and TMS data were not available for all participants with HCP given the risk (albeit small) of seizure or other adverse event associated with TMS, we could not justify administering this to healthy controls. Moreover, the participants with HCP had heterogeneities in the time, size, and location of the injury. Thus, the developmental changes observed in our cohort may not apply to all underlying pathologies of HCP. Finally, there are insufficient data to explain the differences in the changes of diffusion parameters. In particular, diffusion parameter differences may arise from a variety of factors, including differences in myelination, axonal fiber density and caliber, and fiber tract homogeneity, making it difficult to interpret the underlying pathology of the observed differences.

CONCLUSION

We present evidence of disrupted CST maturation in both hemispheres of children with HCP possibly as a result of the perinatal injury using a multimodal neuroimaging approach. Despite its limitations, this cross-sectional study provides detailed insights into the neurophysiological mechanisms of development that follow a perinatal brain injury and may help monitoring the efficiency of interventions during critical periods of life.

DATA AVAILABILITY

All datasets generated for this study are included in the manuscript.

ETHICS STATEMENT

This study was carried out in accordance with the recommendations of Boston Children's Hospital Internal Review Board (IRB). All subjects gave written informed consent in accordance with the Declaration of Helsinki. The protocol was approved by Boston Children's Hospital IRB (IRB-P00023570; PI: CP).

AUTHOR CONTRIBUTIONS

CP, HK and AR contributed to the conception and design of the study. CP and HK contributed to the acquisition and analysis of data. CP and HK contributed to the drafting of figures. All authors contributed to the drafting of a significant portion of the manuscript.

FUNDING

This work was supported by the Eunice Kennedy Shriver National Institute of Child Health and Human Development (NICHD) R21HD090549-01A1, NIMH R01 MH100186, Boston Children's Hospital Translational Research Program, Assimon Family (AR), and internal funding from BCH Division of Newborn Medicine.

REFERENCES

Beaulieu, C. (2002). The basis of anisotropic water diffusion in the nervous system—a technical review. *NMR Biomed.* 15, 435–455. doi: 10.1002/nbm.782

Bender, R., and Lange, S. (2001). Adjusting for multiple testing—when and how? *J. Clin. Epidemiol.* 54, 343–349.

Chiappa, K. H., Cros, D., Day, B., Fang, J. J., Macdonell, R., and Mavroudakis, N. (1991). Magnetic stimulation of the human motor cortex: ipsilateral and

contralateral facilitation effects. *Electroencephalogr. Clin. Neurophysiol.* 43, 186–201.

Eluvathingal, T. J., Hasan, K. M., Kramer, L., Fletcher, J. M., and Ewing-Cobbs, L. (2007). Quantitative diffusion tensor tractography of association and projection fibers in normally developing children and adolescents. *Cereb. Cortex* 17, 2760–2768. doi: 10.1093/cercor/bhm003

Eyre, J. A., Miller, S. I., and Clowry, G. J. (2002). "The development of the corticospinal tract in humans," in *Handbook of Transcranial Magnetic Stimulation*, eds A. Pascual-Leone, G. Davey, J. Rothwell and E. M. Wasserman (London: Arnold), 235–249.

Eyre, J. A., Miller, S., and Ramesh, V. (1991). Constancy of central conduction delays during development in man: investigation of motor and somatosensory pathways. *J. Physiol.* 434, 441–452. doi: 10.1113/jphysiol.1991.sp018479

Eyre, J. A., Taylor, J. P., Villagra, F., Smith, M., and Miller, S. (2001). Evidence of activity-dependent withdrawal of corticospinal projections during human development. *Neurology* 57, 1543–1554. doi: 10.1212/wnl.57.9.1543

Garvey, M. A., Ziemann, U., Bartko, J. J., Denckla, M. B., Barker, C. A., and Wassermann, E. M. (2003). Cortical correlates of neuromotor development in healthy children. *Clin. Neurophysiol.* 114, 1662–1670. doi: 10.1016/s1388-2457(03)00130-5

Grant, P. E., He, J., Halpern, E. F., Wu, O., Schaefer, P. W., Schwamm, L. H., et al. (2001). Frequency and clinical context of decreased apparent diffusion coefficient reversal in the human brain. *Radiology* 221, 43–50. doi: 10.1148/radiol.2211001523

Hagberg, B., Hagberg, G., Beckung, E., and Uvebrant, P. (2001). Changing panorama of cerebral palsy in Swede. VIII. Prevalence and origin in the birth year period 1991–94. *Acta Paediatr.* 90, 271–277. doi: 10.1080/08035250117296

Hameed, M. Q., Dhamne, S. C., Gersner, R., Kaye, H. L., Oberman, L. M., Pascual-Leone, A., et al. (2017). Transcranial magnetic and direct current stimulation in children. *Curr. Neurol. Neurosci. Rep.* 17:11. doi: 10.1007/s11910-017-0719-0

Julkunen, P., Säisänen, L., Hukkanen, T., Danner, N., and Könönen, M. (2012). Does second-scale intertrial interval affect motor evoked potentials induced by single-pulse transcranial magnetic stimulation? *Brain Stimul.* 5, 526–532. doi: 10.1016/j.brs.2011.07.006

Kaye, H. L., and Rotenberg, A. (2017). "nTMS in pediatrics: special issues and solutions," in *Navigated Transcranial Magnetic Stimulation in Neurosurgery*, ed. S. M. Krieg (New York, NY: Springer), 209–218.

Koh, T. H., and Eyre, J. A. (1988). Maturation of corticospinal tracts assessed by electromagnetic stimulation of the motor cortex. *Arch. Dis. Child.* 63, 1347–1352. doi: 10.1136/adc.63.11.1347

Lebel, C., and Beaulieu, C. (2011). Longitudinal development of human brain wiring continues from childhood into adulthood. *J. Neurosci.* 31, 10937–10947. doi: 10.1523/JNEUROSCI.5302-10.2011

Mori, S., Crain, B. J., Chacko, V. P., and van Zijl, P. C. (1999). Three-dimensional tracking of axonal projections in the brain by magnetic resonance imaging. *Ann. Neurol.* 45, 265–269. doi: 10.1002/1531-8249(199902)45:2<265::aid-ana21>3.0.co;2-3

Mukherjee, P., Berman, J. I., Chung, S. W., Hess, C. P., and Henry, R. G. (2008). Diffusion tensor MR imaging and fiber tractography: theoretic underpinnings. *AJNR Am. J. Neuroradiol.* 29, 632–641. doi: 10.3174/ajnr.a1051

Neil, J. J., Shiran, S. I., McKinstry, R. C., Schefft, G. L., Snyder, A. Z., Almli, C. R., et al. (1998). Normal brain in human newborns: apparent diffusion coefficient and diffusion anisotropy measured by using diffusion tensor MR imaging. *Radiology* 209, 57–66. doi: 10.1148/radiology.209.1.9769812

Nezu, A., Kimura, S., Uehara, S., Kobayashi, T., Tanaka, M., and Saito, K. (1997). Magnetic stimulation of motor cortex in children: maturity of corticospinal pathway and problem of clinical application. *Brain Dev.* 19, 176–180. doi: 10.1016/s0387-7604(96)00552-9

Paus, T., Collins, D. L., Evans, A. C., Leonard, G., Pike, B., and Zijdenbos, A. (2001). Maturation of white matter in the human brain: a review of magnetic resonance studies. *Brain Res. Bull.* 54, 255–266. doi: 10.1016/s0361-9230(00)00434-2

Pihko, E., Nevalainen, P., Vaalto, S., Laaksonen, K., Mäenpää, H., Valanne, L., et al. (2014). Reactivity of sensorimotor oscillations is altered in children with hemiplegic cerebral palsy: a magnetoencephalographic study. *Hum. Brain Mapp.* 35, 4105–4117. doi: 10.1002/hbm.22462

Rosenbaum, P., Paneth, N., Leviton, A., Goldstein, M., Bax, M., Damiano, D., et al. (2007). A report: the definition and classification of cerebral palsy April 2006. *Dev. Med. Child Neurol.* 49, 8–14. doi: 10.1111/j.1469-8749.2007.tb12610.x

Säisänen, L., Julkunen, P., Lakka, T., Lindi, V., Könönen, M., and Määttä, S. (2018). Development of corticospinal motor excitability and cortical silent period from mid-childhood to adulthood - a navigated TMS study. *Neurophysiol. Clin.* 48, 65–75. doi: 10.1016/j.neucli.2017.11.004

Savion-Lemieux, T., Bailey, J. A., and Penhune, V. B. (2009). Developmental contributions to motor sequence learning. *Exp. Brain Res.* 195, 293–306. doi: 10.1007/s00221-009-1786-5

Scheck, S. M., Boyd, R. N., and Rose, S. E. (2012). New insights into the pathology of white matter tracts in cerebral palsy from diffusion magnetic resonance imaging: a systematic review. *Dev. Med. Child Neurol.* 54, 684–696. doi: 10.1111/j.1469-8749.2012.04332.x

Schmithorst, V. J., and Dardzinski, B. J. (2002). Automatic gradient preemphasis adjustment: a 15-minute journey to improved diffusion-weighted echo-planar imaging. *Magn. Reson. Med.* 47, 208–212. doi: 10.1002/mrm.10022

Song, S. K., Yoshino, J., Le, T. Q., Lin, S. J., Sun, S. W., Cross, A. H., et al. (2005). Demyelination increases radial diffusivity in corpus callosum of mouse brain. *Neuroimage* 26, 132–140. doi: 10.1016/j.neuroimage.2005.01.028

Sun, S. W., Liang, H. F., Cross, A. H., and Song, S. K. (2008). Evolving Wallerian degeneration after transient retinal ischemia in mice characterized by diffusion tensor imaging. *Neuroimage* 40, 1–10. doi: 10.1016/j.neuroimage.2007.11.049

Volpe, J. J. (2009). Brain injury in premature infants: a complex amalgam of destructive and developmental disturbances. *Lancet Neurol.* 8, 110–124. doi: 10.1016/S1474-4422(08)70294-1

Yeo, S. S., Jang, S. H., and Son, S. M. (2014). The different maturation of the corticospinal tract and corticoreticular pathway in normal brain development: diffusion tensor imaging study. *Front. Hum. Neurosci.* 8:573. doi: 10.3389/fnhum.2014.00573

Conflict of Interest Statement: The authors declare that the research was conducted in the absence of any commercial or financial relationships that could be construed as a potential conflict of interest.

frontiers in Neurology

REVIEW
published: 21 August 2019
doi: 10.3389/fneur.2019.00887

A Scoping Review of Neuromuscular Electrical Stimulation to Improve Gait in Cerebral Palsy: The Arc of Progress and Future Strategies

Jake A. Mooney[1,2] *and Jessica Rose*[1,2]*

[1] Department of Orthopaedic Surgery, Stanford University, Stanford, CA, United States, [2] Motion & Gait Analysis Lab, Lucile Packard Children's Hospital, Stanford Children's Health, Stanford, CA, United States

Background: Neuromuscular deficits of children with spastic cerebral palsy (CP) limits mobility, due to muscle weakness, short muscle-tendon unit, spasticity, and impaired selective motor control. Surgical and pharmaceutical strategies have been partially effective but often cause further weakness. Neuromuscular electrical stimulation (NMES) is an evolving technology that can improve neuromuscular physiology, strength, and mobility. This review aims to identify gaps in knowledge to motivate future NMES research.

Methods: Research publications from 1990- July 20th 2019 that investigated gait-specific NMES in CP were reviewed using the PubMed and Google Scholar databases. Results were filtered by the National Institute of Neurological Disorder and Stroke common data elements guidelines for CP. The Oxford Centre for Evidence Based Medicine guidelines were used to determine levels of evidence for each outcome. Gait-specific NMES research protocols and trends are described, with implications for future research.

Results: Eighteen studies met inclusion criteria, reporting on 212 participants, 162 of whom received NMES while walking, average age of 9.8 years, GMFCS levels I–III. Studies included 4 randomized control trials, 9 cohort studies and 5 case studies. A historical trend emerged that began with experimental multi-channel NMES device development, followed by the commercial development of single-channel devices with inertial sensor-based gait event detection to facilitate ankle dorsiflexion in swing phase. This research reported strong evidence demonstrating improved ankle dorsiflexion kinematics in swing and at initial contact. Improved walking speed, step length, and muscle volume were also reported. However, improvements in global walking scores were not consistently found, motivating a recent return to investigating multi-channel gait-specific NMES applications.

Conclusions: Research on single-channel gait-specific NMES found that it improved ankle motion in swing but was insufficient to address more complex gait abnormalities common in CP, such as flexed-knee and stiff-knee gait. Early evidence indicates that multi-channel gait-specific NMES may improve gait patterns in CP, however significantly

OPEN ACCESS

Edited by:
Maurizio Ferrarin, Fondazione Don Carlo Gnocchi Onlus (IRCCS), Italy

Reviewed by:
Diane L. Damiano, National Institutes of Health (NIH), United States
Silmar Teixeira, Federal University of Piauí, Brazil

***Correspondence:**
Jessica Rose
jessica.rose@stanford.edu

Specialty section:
This article was submitted to Movement Disorders, a section of the journal Frontiers in Neurology

Received: *13 May 2019*
Accepted: *31 July 2019*
Published: *21 August 2019*

Citation:
Mooney JA and Rose J (2019) A Scoping Review of Neuromuscular Electrical Stimulation to Improve Gait in Cerebral Palsy: The Arc of Progress and Future Strategies. Front. Neurol. 10:887. doi: 10.3389/fneur.2019.00887

more research is needed. The conclusions of this review are highly limited by the low level of evidence of the studies available. This review provides a historical record of past work and a technical context, with implications for future research on gait-specific NMES to improve walking patterns and mobility in CP.

Keywords: NMES, FES, stimulation, cerebral palsy, gait, walking

HIGHLIGHTS

- Overview of gait-specific NMES for children with CP.
- Describes NMES-assisted gait technology and methods.
- Discusses history of gait-specific NMES in CP.
- Identifies gaps in knowledge and future research needs.

BACKGROUND

Cerebral palsy (CP) is the most common childhood motor disability and affects an estimated 1/323 children in the USA (1); reports of global prevalence range from 1.5 to more than 4 per 1,000 live births (2). While the initial brain injury is non-progressive, musculoskeletal impairments and functional limitations are progressive. Spastic CP affects 75% of children with CP, characterized by weak and short muscles, spasticity, and impaired selective motor control (SMC). Flexed-knee gait and stiff-knee gait are common and debilitating walking disorders in spastic CP. Many children with spastic CP lose independence in functional mobility as they age. Currently, surgical and pharmaceutical treatments for gait deficits are partially effective and often cause further muscle weakness.

Implanted or wearable electrical stimulation has been applied in a number of successful medical treatments in fields such as neurology, cardiology, and audiology. Deep brain stimulation has made groundbreaking progress in Parkinson's treatment. Electrical stimulation has been shown as an effective treatment for neurogenic bladder in patients with spinal cord injury (3) and pacemakers are now considered a standard of care in treating cardiac arrhythmias. Further, cochlear implants have returned hearing to hundreds of thousands of patients with hearing loss (4). Likewise, neuromuscular electrical stimulation (NMES) is an assistive technology in which electrical stimulation is applied either to the skin surface or via implanted electrodes to initiate or augment skeletal muscle contraction, through intact peripheral nerves (5). NMES has been used as a means to strengthen muscles in cases of stroke and CP (6), and there is promising evidence that it may do the same in cases of spinal cord injury (7).

When NMES is applied to achieve functional movements, the general term functional electrical stimulation (FES) is often used. In the context of gait, when electrical stimulation is applied during walking activities, the specific terminology used includes: gait-specific NMES or NMES-assisted gait. When stimulation is applied during functional activities related to gait such as cycling it can be termed gait-related NMES. Stimulation can also be applied as a purely muscle-strengthening application during physiotherapy, simply known as NMES. All references to electrical stimulation for the remainder of this review refer to NMES applied during walking activities, unless specified otherwise.

There is growing evidence that NMES may affect the four major neuromuscular deficits seen in spastic CP. NMES has been found to increase muscle fiber diameter and muscle size as well as strength in children with CP (8). In addition, increases in muscle fiber diameter may also increase overall muscle-tendon unit length due to the pennate angle of large lower limb muscles such as the rectus femoris and gastrocnemius. Further, there is early evidence that electrical stimulation may reduce spasticity in stroke by decreasing stretch reflex sensitivity (9, 10), indicating a need for further study of the impacts of NMES in CP. Finally, NMES may not directly improve SMC, however if applied during specific movement phases such as wrist extension when the elbow is flexed during a grasp, or knee extension when the hip is flexed at the end of swing phase of gait, it may compensate for impaired SMC, thereby improving movement patterns and functional ability.

The concept of electrical stimulation to induce muscle contractions can be traced at least as far back as 1776. The Italian physician and physicist, Luigi Galvani, famously elicited a muscular contraction from the leg of a frog using an electrical stimulus (11). Benjamin Franklin wrote about the possible role of electricity in human physiology and the digestive system in a letter to a South Carolina physician in 1757 (12). However, the successful use of NMES to achieve increased muscle strength and functional movement is a relatively new breakthrough with the majority of research conducted only in the past few decades, and on patients with spinal cord injury and stroke (6).

The miniaturization of electronics, such as inertial measurement units (IMU) and central processing units has allowed for the development of lightweight wearable NMES devices. Applied to improve gait, these devices are capable of sensing certain gait events and providing appropriate electrical stimulation in real-time (13). To date, the most common application has been single-channel stimulation to the tibialis anterior (TA) muscle during the swing phase of gait to improve foot clearance, in cases of foot drop. Control of a single muscle is termed single-channel NMES, whereas simultaneous control of multiple muscles is designated multi-channel NMES. The

Abbreviations: TA, tibialis anterior; QF, quadriceps femoris; G, gastrocnemius; S, soleus; Glu, gluteals; GMa, gluteus maximus; GMe, gluteus medius; BF, biceps femoris; VL, vastus lateralis; VM, vastus medialis; PAM, posterior adductor magnus; DF, dorsiflexion; PF, plantarflexion; IC, initial contact; TO, toe-off; SCALE, selective control assessment of the lower extremity; PCI, physiological cost index of walking; GMFM, gross motor function measure; COPM, Canadian occupational performance measure; 6MWT, 6-minute walk test; ROM, range of motion; OGS, observational gait score; GDI, gait deviation index.

purpose of this review is to examine the body of literature concerning gait-specific use of single and multi-channel NMES devices to improve gait in children with CP.

METHODOLOGY

A scoping review was chosen as the most appropriate form of review for this field at this time. The primary intention of this review was to provide a broad assessment of the historical trajectory and current state of this field of research. The secondary intention was to identify gaps in knowledge, and possible future directions. As such, a more broad-based review strategy was required. The Preferred Reporting Items for Systematic Reviews and Meta-Analyses extension for Scoping Reviews (PRISMA-ScR) Checklist was used to guide this review (14).

The literature search was conducted utilizing the PubMed database as well as Google Scholar. Additionally, relevant publications referenced through the primary search were also considered. The primary search was performed with a title and abstract keyword search using Boolean operators. Specifically, publications including "electrical stimulation" or "NMES" or "FES," and "cerebral palsy" or "CP" in their title or abstract and published from 1990 until July 20th 2019 were collected. Only articles available in English were reviewed.

Studies were extracted that investigated gait-specific application of NMES for children with CP, reported functional classification levels of participants, and reported standard outcome metrics for gait. Specifically, the criteria of reporting common data elements (CDE) was applied. The CDE for CP are now published by the National Institute of Neurological Disorder and Stroke (NINDS) working group on CP (15) and offer validated outcome measures that can be compared between and within participants with CP. Only publications that published the Gross Motor Functional Classification (GMFCS) of participants (16) and reported at least one CDE, were included in analysis. Of note, one study published the Gillette Gait Index (GGI), a precursor to the Gait Deviation Index (GDI). Although the GGI was not explicitly endorsed by the NINDS working group, this study was included since it pre-dates the development of the GDI. The results of these publications were then assessed and levels of evidence for various outcome metrics were assigned per the Oxford Centre for Evidence -Based Medicine 2011 Level of Evidence guidelines (17).

The grading of articles and outcome measures for level of evidence was done independently by two authors (JM and JR). Articles and outcome measures were downgraded at the authors discretion for small or poorly designed studies, as allowed by the guidelines. The randomized control trials included in this review were considered level II evidence, although they were small trials.

Finally, a Cochrane risk of bias assessment for seven elements across five domains was considered and adapted to the studies being assessed (18). Since a diversity of studies, ranging from RCT to case studies were included for review, a risk of bias tool may not be an entirely appropriate assessment at this stage. However, to provide a balanced perspective on the current state of research, a summary discussion of the findings can be found in Limitations (see section Limitations).

RESULTS

A flow chart schematic of the literature search and screening process can be seen in **Figure 1**. The search strategy outlined in the methodology resulted in 463 publications. These publications were screened at an abstract level to assess for possible relevance, specifically, if they met the broad inclusion criteria that they seemingly applied electrical stimulation in a population with CP. Studies were most commonly excluded for being done in the context of spinal cord injury or stroke, applying NMES in a non-gait-specific manner, or focusing on adult populations. This narrowed the results to 52 publications. These 52 publications were screened in their entirety to determine if they reported GMFCS levels of participants and at least one CDE outcome, in addition to confirming that they were completed studies in which NMES was used in a gait-specific manner in a pediatric population with CP. The only notable exception made was for one study (19) in which a single participant was 29 years old, and all others were under 18. The study was otherwise excellently executed with an entire year of gait-specific NMES therapy. Applying these exclusion filters eliminated 30 publications from consideration for reasons listed in the flow chart. The reasons for exclusion are listed in hierarchal order. This resulted in 22 publications reporting on 18 unique studies for inclusion in this review. Notably, the criteria of reporting at least one CDE did not solely exclude any paper.

Table 1 lists the results of the literature search, including the research study, level of evidence, as well as number, age, and functional level of participants. These 18 studies included 212 participants, 162 of whom actually received gait-specific NMES treatment, while the remainder served as controls. No study met the criteria for level 1 evidence. Four studies were small RCTs ranging from 14 to 34 total participants (level 2). Two studies were case-control cohort studies (level 3). Seven studies were cohort studies without control groups (level 3). The remaining five studies were case studies with three or fewer participants (level 4). Studies that included GMFCS I and II are most prevalent.

Table 2 specifies the details of the application of gait-specific NMES. The number of channels, trigger and electrode design, as well as the muscle groups targeted in each study are reported. An overall trend toward single-channel, surface stimulation to the tibialis-anterior, triggered by a tilt-sensor was observed.

Table 3 outlines the interventional protocol of each study, with the dosage and range of stimulator settings. If a known, commercially available NMES device was used, it is noted as well.

Table 4 shows the common data elements (CDE), per the NINDS guidelines, reported by each study. Improvements are compared to either baseline or a control group, as defined by each study. Carryover effects are noted. **Table 5** is a report of all CDE outcomes reported by studies included in this review, organized by outcome. Relevant studies are cited, and

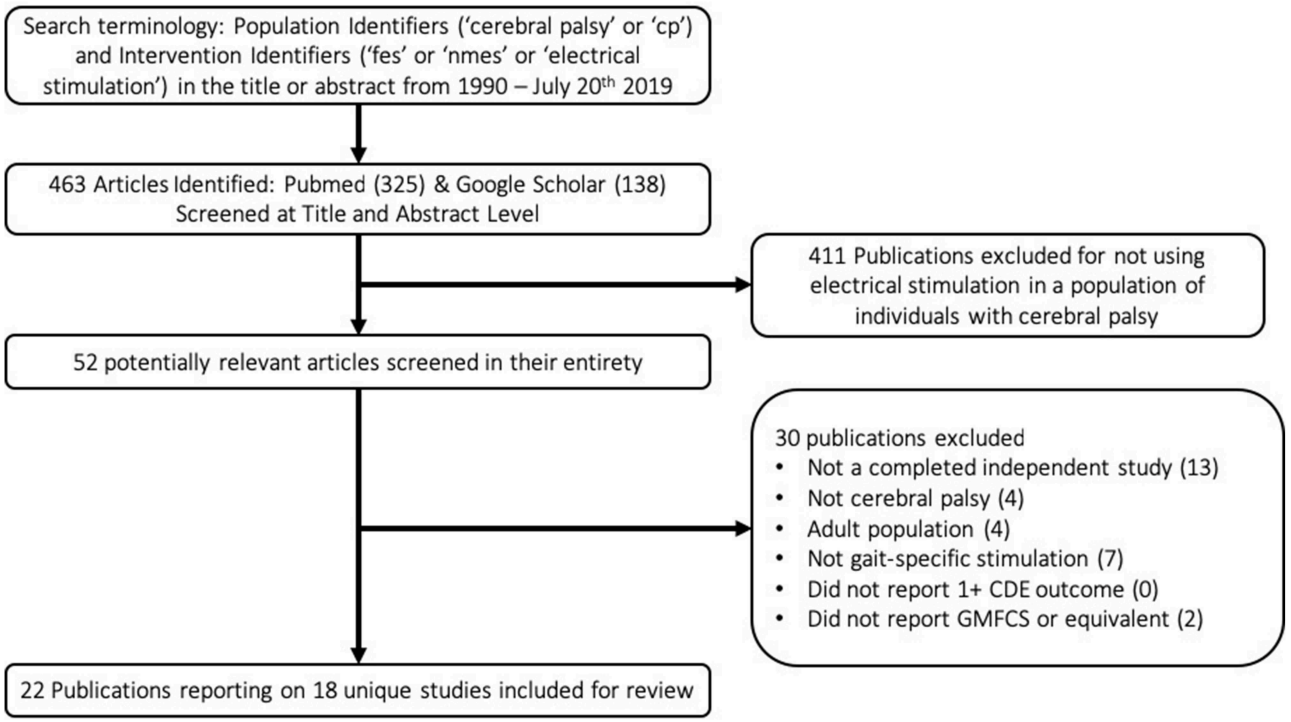

FIGURE 1 | Flow chart demonstrating the scoping review process.

a level of evidence for each outcome is assigned per the Oxford Center for Evidence-Based Medicine 2011 Levels of Evidence guidelines.

DISCUSSION

Overview

The use of electrical stimulation to improve gait in children with CP has undergone significant, and sometimes cyclic, changes over the past few decades. Early research demonstrated the approximate parameters to elicit reliable muscular contractions. This was followed by a period of exploratory NMES usage, in which a variety of NMES technologies and strategies were tested in small clinical trials. This early gait-specific usage of NMES was often ambitious, implementing complicated multi-channel systems in an attempt to normalize complex deficits. Then, driven by the development of commercial FES devices to address a single specific gait pathology in related neurological disorders, the field of NMES research in CP rapidly collapsed into the specific use of single-channel devices to augment ankle dorsiflexion in swing. This enabled a period of broader NMES usage, limited randomized controlled studies, and the first systematic reviews to be attempted. The results of this period seemed to strongly suggest that NMES can correct ankle dorsiflexion deficits in swing but is insufficient to improve more complex gait abnormalities common in CP. Now, the direction of progress is pointing back toward the use of multi-channel NMES devices.

The search criteria in this review considered publications as early as 1990, however no study met inclusion criteria until 2004. The 1990's were predominately a period of early NMES technology development in which systems capable of delivering reliable and precise electrical stimulation were developed, and the clinical applications were constrained to augmenting specific muscle strengthening exercises. It was this early body of work that allowed future investigators to make informed decisions regarding appropriate stimulation protocols. Ho et al. (36) most explicitly referenced prior work in justifying their rationalization of stimulation parameters, stating that prior work found the stimulation frequency threshold necessary to achieve fused muscle contraction (30 Hz) and the natural ramp-up time of gastrocnemius-soleus muscle contraction (0.2 s).

Standard methods and outcomes are only just emerging in this developing field. An effort was made to describe specific methods to promote standardization and repeatability. Too often, clinical expertise was cited as the rationale for customizing stimulation settings and timing. This does not promote repeatable results and limits interpretation and comparison with other studies. A concise report of stimulator settings is provided (**Table 3**) so that future researchers can have a better understanding of commonly used protocols. It is strongly advised to apply gait-specific NMES during normal muscle timing to promote normal sensorimotor input that can affect both neuroprosthetic and neurotherapeutic effects.

TABLE 1 | Research studies included in the review: study design and participant demographics with study number assigned.

Publication	Evidence level	Study design	Number of channels	Number of participants (# Control)	Age (*SD*)	GMFCS
1. Behbodi et al. (20)	4	Case	Multi	2 (0)	13 (0)	II–III
2. Rose et al. (21)	4	Case	Multi	3 (0)	11.3 (1.5)	I–II
3. Bailes et al. (22, 23)	3	Cohort	Single	11 (0)	9.9 (2.9)	I–II
4. Pool et al. (24–26)	2	RCT	Single	32 (16)	10.9 (3.8)	I–II
5. El-Shamy et al. (27)	2	RCT	Single	34 (17)	10.6 (0.8)	I–II
6. Khamis et al. (28)	4	Case	Single	1 (0)	18	II
7. Pool et al. (29)	3	Cohort	Single	12 (0)	9.2 (3.8)	I–II
8. Danino et al. (19)	3	Cohort	Single	4 (0)	18.5 (7.1)	I
9. Meilahn (30)	3	Cohort	Single	10 (0)	9.3 (1.7)	I
10. Prosser et al. (31); Damiano et al. (32)	3	Cohort	Single	19 (0)	12.9	I–II
11. Seifart et al. (33)	3	Cohort	Multi	5 (2)	5.1 (1.4)	I
12. Al-Abdulwahab and Al-Khatrawi (34)	2	RCT	Single	31 (10)	7.4 (2.0)	I–II[a]
13. van der Linden et al. (35)	2	RCT	Single	14 (7)[b]	8 (3.3)	I–II[c]
14. Ho et al. (36)	3	Cohort	Single	6 (0)	8.2 (2.6)	I
15. Orlin et al. (37)	3	Cohort	Multi	8 (0)	9.1 (1.3)	I–II
16. Pierce et al. (38)	4	Case	Single	1 (0)	11	I
17. Johnston et al. (39)	3	Cohort	Multi	17 (9)	7.7 (1.8)	I–III
18. Pierce et al. (40)	4	Case	Multi	2 (0)	8, 10	I

[a] *Estimated GMFCS determined via inclusion criteria and qualitative description of participants.*
[b] *All participants received some form of NMES treatment, see* ***Table 3*** *for details.*
[c] *Gillette Functional Assessment Questionnaire was reported, estimated GMFCS is reported (41).*

Initial Studies: 2004–2010

NMES in CP began to be applied in a gait-specific manner and was first reported in 2004. For the first time electrical stimulation was applied synchronized with the individual's walking cycle. These early experiments were exploratory in nature, less focused on answering specific research or clinical questions, and more concerned with identifying future directions. These initial gait-specific studies and the ones that followed soon after, explored a greater diversity of potential NMES applications than has been seen since. Over this time period, 84 children participated in studies involving gait-specific NMES, 63 of whom received NMES treatment. The average age of recipients of NMES treatment during this period was 7.7 years old. All stimulation parameters were within the range of 20–50 Hz, pulse width of 3–350 μs and 10–70 mA. All studies, except one (34), applied stimulation according to normal gait timing. Percutaneous electrodes were implanted in 4 studies, and surface electrodes were used in 5, with one study directly comparing the efficacy of electrode types.

Perhaps the most defining feature of this time period in NMES usage, was the implementation of a force sensitive resistor (FSR) footswitch as the trigger for gait cycle timing and stimulation, which was ubiquitous across all studies. As a timing mechanism, this provided a reliable, albeit simplistic control scheme. Footswitches are capable of detecting initial contact and toe-off with high reliability, however, provide little to no information about the gait phase between these events. As such, this control architecture is dependent on manually preprogramming time delays into the stimulation patterns based on these two specific gait events. This approach limits real-time adaptability of the system as it is reliant on pre-determined timing, as well as its generalizability as it depends on clinician determined settings to optimize affect.

Single-Channel NMES-Assisted Gait

Between 2004 and 2010, four studies reported on single-channel NMES. Single-channel devices targeted the tibialis anterior (35, 38, 40), quadriceps femoris (35), gastrocnemius-soleus (36), or gluteus medius (34).

The single-channel NMES studies demonstrated that isolated stimulation of the quadriceps femoris or gastrocnemius did not significantly improve knee or ankle kinematics, respectively. Comparatively, isolated stimulation or stimulation as part of a multi-channel system of the tibialis anterior did consistently improve ankle kinematics in swing phase and at IC. One study assessing both single-channel stimulation of the tibialis anterior, and quadriceps femoris, reported significantly improved kinematics in the ankle during swing and not the knee in swing, however neither had a clinically significant impact on the GGI (35). The two studies that showed improved ankle kinematics via single-channel stimulation of the tibialis anterior also reported significantly decreased walking speeds (35, 40). The only single-channel study to demonstrate significantly improved walking speeds, stride length or step length, stimulated only the

TABLE 2 | Research studies included in the review: NMES treatment and device design.

Publication	Number of channels	Stimulation trigger	Percutaneous or surface	Muscle groups stimulated
Behbodi et al. (20)	Multi (3–4)	Tilt-sensor	Surface	Glu, QF, TA, G-S[a]
Rose et al. (21)	Multi (3)	Manual	Surface	QF, Gluteus, G–S
Bailes et al. (22, 23)	Single	Footswitch	Surface	TA
Pool et al. (24–26)	Single	Tilt-sensor	Surface	TA
El-Shamy et al. (27)	Single	Tilt-sensor	Surface	TA
Khamis et al. (28)	Single	Tilt-sensor	Surface	QF
Pool et al. (29)	Single	Tilt-sensor	Surface	TA
Danino et al. (19)	Single	Footswitch	Surface	TA
Meilahn et al. (30)	Single	Tilt-sensor	Surface	TA
Prosser et al. (31); Damiano et al. (32)	Single	Tilt-sensor	Surface	TA
Seifart et al. (33)	Multi (2)	Footswitch	Surface	TA, G
Al-Abdulwahab and Al-Khatrawi (34)	Single	Continuous	Surface	GMe
van der Linden et al. (35)	Single	Footswitch	Surface	TA, QF
Ho et al. (36)	Single	Footswitch	Surface	G-S
Orlin et al. (37)	Multi (2)	Footswitch	Percutaneous	TA, G
Pierce et al. (38)	Single	Footswitch	Both	TA
Johnston et al. (39)	Multi	Footswitch	Percutaneous	TA (8), S (10), BF (2), VM (14), VL(14), PAM (2), GMe (16), GMa(16)[b]
Pierce et al. (40)	Multi (2)	Footswitch	Percutaneous	TA, G

[a] *Targeted muscle groups described as "ankle dorsiflexors" were assumed to be TA, and those described as "ankle plantarflexors" were assumed to be G-S.*
[b] *Individual participant data was not reported. Instead the cumulative number of electrodes implanted across all 8 participants was reported.*

gluteus medius (34). The researchers reasoned that hip adductor spasticity was a primary cause of the stereotypical "scissor gait" seen in many patients with spastic CP, a debilitating gait. As a novel treatment strategy, they provided continual, low level stimulation to the hip abductors (gluteus medius) to promote less hip adduction. Despite the positive results of the study, continual single-channel stimulation of the gluteus medius has not been attempted since.

In all, the most persistent finding from single-channel research in this time period was that stimulation of the tibialis anterior improved ankle dorsiflexion in swing and foot clearance. Temporal-spatial parameters were significantly improved only in the study that assessed continual single-channel stimulation of the gluteus medius (34). Single-channel stimulation of either the gastrocnemius-soleus or quadriceps femoris appeared to have little effect on gait.

Multi-channel NMES-Assisted Gait

Between 2004 and 2010, four studies reported on multi-channel NMES. Three studies utilized two-channel devices, targeting both the gastrocnemius and tibialis anterior (33, 37, 40). One study applied NMES in a truly multi-channel manner, stimulating muscle groups actuating the hip, knee, and ankle joints (39).

All three studies that investigated ankle dorsiflexion in swing or at IC reported improvements (37, 39, 40). The results of these studies were otherwise highly variable, likely due to relatively few participants (21 children in total received NMES treatment), and inconsistent methodologies across studies. Temporal-spatial parameters were either improved or unchanged across these studies. One study assessed the effects of gait-specific NMES to the gastrocnemius and tibialis anterior after the individuals received Botox injections to the gastrocnemius and reported improved plantar flexion strength in the NMES treatment group (33).

Recent Studies: 2010—Present

The time period since 2010 has seen significant progress in NMES technology use in the CP population. In large part, this is due to the advent of commercially available foot drop stimulators. These devices, developed initially for the stroke population, are single-channel stimulators that target the common fibular nerve to stimulate ankle dorsiflexion via the tibialis anterior in swing, thus attempting to correct foot drop, improve foot clearance, and reduce incidences of tripping. Although these devices were approved by the FDA as early as 2005, their use in pediatric populations was not approved until years later.

From 2010 to April of 2019, 128 children participated in studies involving gait-specific NMES, 99 of whom received gait-specific NMES treatment. The average age at time of treatment during this period was 10.9 years old. This is a notable increase in both number and age of participants since before 2010. The Walkaide commercial stimulator was used in 5 studies, the Bioness stimulator in 3 studies, the RT50-Z in 1 study, the Odstock 2 channel stimulator in 1 study, and the Hasomed RehaStim in 1 study. This is a drastic shift away from the research grade stimulators used in the past, to a complete uniformity in using commercial devices. Reported stimulation parameters were within the range of frequency of 16.7–45 Hz,

TABLE 3 | The NMES protocol reported in each study, with dosage and stimulator settings listed to the extent reported.

Publication	Intervention	Reported stimulator settings
Behbodi et al. (20)	Device: Hasomed RehaStim GmbH (Maqdeburg, Germany) and custom motion sensors. Protocol: Five six-minute walking periods. NMES alternated on/off every minute within each 6-min walking bout. Achieved 60–80% maximum heart rate. Timing: Typical muscle timing and clinical recommendations. Duration: 12 weeks, 3 days/week, 30 min/day. Dosage: 1,080 min.	Frequency: 40 Hz. PW: 275–440 μs. Current: 35–60 mA.
Rose et al. (21)	Device: RT50-Z (Restorative Therapies, Baltimore, MD, USA). Protocol: Manually triggered stimulation train at IC. 30 m walk for accommodation before data collection. Timing: Typical muscle timing. Duration: Single session, 10 trials walking through the viewing volume. Dosage: <20 min.	Frequency: 40 Hz. PW: 50 μs. Current: 30 mA.
Bailes et al. (22, 23)	Device: Ness L300. Protocol: Community ambulation. Timing: Typical muscle timing. Duration: 7 days, 15 min/day (accommodation) then 12 weeks, 7 days/week, 6 h/day (intervention). Dosage: 30,345 min.	Frequency: 30–45 Hz. PW: 200–300 μs. Current: Not reported.
Pool et al. (24–26)	Device: Walkaide. Protocol: Community ambulation. Timing: Typical muscle timing. Duration: 8 weeks, 6 days/week, avg 6.2 h/day. Dosage: 17,856 min avg.	Frequency: 33 Hz. PW: 25–100 μs. Current: Variable.
El-Shamy et al. (27)	Device: Walkaide. Protocol: Community Ambulation. Timing: Typical muscle timing Duration: 7 days, 15 min/day (accommodation) then 12 weeks, at least 3 days/week, 2 h/day (intervention). Dosage: 4,425 min.	Frequency: 33 Hz. PW: 300 μs. Current: Variable.
Khamis et al. (28)	Device: Ness L300 Plus. Protocol: (1) Walking only. (2) Walking and non-gait related stimulation. (3) Walking and stair climbing 2 floors. Timing: QF stimulation from heel strike through pre-swing. Duration: (1) 20 min of accommodation. (2) 8 weeks, 7 days/week, 25 min/day of walking, 20 min of non-gait stimulation. (3) 16 weeks, 7 days/week, 30 min/day of walking and stair climbing. Dosage: 4,780 min (gait) + 1,120 min (non-gait).	Frequency: 40 Hz. PW: 300 μs. Current: 40 mA.
Pool et al. (29)	Device: Walkaide. Protocol: Community Ambulation. Timing: Typical muscle timing. Duration: 8 weeks, 6 days/week, 1 h/day. Dosage: 2,880 min.	Frequency: 25–33 Hz. PW: 25–300 μs. Current: Variable.
Danino et al. (19)	Device: Ness L300. Protocol: Community Ambulation. Timing: Typical muscle timing. Duration: 1 year, continuous daily. Dosage: Unknown.	Individually calibrated—not reported.
Meilahn (30)	Device: Walkaide. Protocol: Community Ambulation. Timing: Typical muscle timing. Duration: 12 weeks, 7 days/week, 0.9–19.5 hrs/day. Dosage: 25,724 min avg (range 6,384–55,974 min).	Frequency: Not reported. Pulse width 50 μs. Current: Not reported. Min time 0.3 sec, max time 0.6 s.
Prosser et al. (31); Damiano et al. (32)	Device: Walkaide. Protocol: Community Ambulation with (1) accommodation and (2) intervention phases. Timing: Typical muscle timing. Duration: (1) 4 weeks, 7 days/week, 30 min to 6 hrs/day. (2) 12 weeks, 7 days/week, avg 5.6 h/day (1.5–9.4 h/day). Dosage: (1) >840 min. (2) 28,224 min avg (7,560–47,376 min range).	Frequency: 16.7–33 Hz. PW: 25–300 μs. Current: Variable
Seifart et al. (33)	Device: Odstock 2 channel stimulator (O2CHSPI version 3.0, United Kingdom). Protocol: Subjects first received a botulin-toxin injection to the gastrocnemius, then home-based NMES program. Timing: Typical muscle timing. Duration: 4 weeks, 5 days/week, 30 min/day. Dosage: 600 min.	No parameters reported.

(Continued)

TABLE 3 | Continued

Publication	Intervention	Reported stimulator settings
Al-Abdulwahab and Al-Khatrawi (34)	Device: Dual-channel TENS programmable stimulator model 120Z. Protocol: Laboratory based walking with (1) accommodation and (2) intervention phases. Timing: Continuous stimulation. Duration: (1) 2 minutes. (2) 7 days, 3 × 15 min/day. Dosage: 315 min.	Frequency: 20 Hz. PW: 20 μs. Current: <20 mA.
van der Linden et al. (35)	Device: Odstock. Protocol: (1) Non-gait stimulation applied at rest to either ankle DF or knee extensors in the treatment group only, followed by (2) Community ambulation. Timing: Typical muscle timing. Duration: (1) 14 days, 1 h/day. (2) 8 weeks, 4–7 days/week, continuous. Dosage: 11,520 min[a].	Frequency: 40 Hz. PW: 3–350 μs. Current: 20–70 mA.
Ho et al. (36)	Device: Respond II Select (Medtronic Inc, Minneapolis, MN). Protocol: Laboratory-based walking. Timing: Stimulation applied from IC to toe-off. Duration: Single session, 30 trials walking through the viewing volume. Dosage: 20–30 min.	Frequency: 32 Hz. PW: 300 μs. Current: 10–40 mA.
Orlin et al. (37)	Device: Custom research device. Protocol: Laboratory-based walking, participants assigned to either TA only, gastrocnemius only, or TA and gastrocnemius. Timing: Typical muscle timing. Duration: 7 days, 2 × 45 min/day. Dosage: 630 min.	Frequency: 20–50 Hz. PW: 12–200 μs. Current: 20 mA.
Pierce et al. (38)	Device: Surface FES (S-FES) EMPI 300PV stimulator (Empi, St. Paul, MN). Percutaneous FES (P-FES) Custom research device. Protocol: Laboratory-based walking, (1) first with S-FES, (2) then P-FES. Timing: Typical muscle timing. Duration: (1) 3 months, 30 min/week. (2) 8 months, 30 min/week. Dosage: (1) 360 min S-FES. (2) 960 min P-FES.	S-FES: Frequency: 30 Hz. PW: 300 μs. Current: 20 mA. P-FES: Frequency: 20 Hz. PW: 17 μs. Current: 20 mA.
Johnston et al. (39)	Device: Custom research grade 24-channel stimulator Protocol: All study subjects underwent surgical ablative operations; the experimental group received a more limited surgery and NMES. Individualized muscle groups targeted (not reported). NMES program consisted of (1) Non-gait exercise based NMES program, then (2) gait-specific NMES. Timing: Typical muscle timing. Duration: (1) 4 weeks, 5 days/week, 1 h/day. (2) 1 year, continuous daily use. Dosage: (1) 1,200 min. (2) Unknown.	Frequency: 20 Hz. PW: up to 200 μs. Current: 20 mA.
Pierce et al. (40)	Device: Custom research device Protocol: Laboratory-based walking, each participant underwent all 3 conditions: TA only, then TA and gastrocnemius, then gastrocnemius only. Timing: Typical muscle timing. Duration: 7 days, 2 × 45 min/day. Dosage: 630 min.	Frequency: 20–50 Hz (TA) 50 Hz (gastroc.). PW: up to 200 μs. Current: 20 mA.

PW, pulse width.

[a]*From van der Linden et al. (35), "All children except one used the stimulator for 4–6 days or more a week and for 6 or more hours a day".*

pulse width of 25–440 μs and current of 30–60 mA. These parameters are not drastically different from the earlier studies, however notably, the use of commercial devices seemingly encouraged less precise reporting of specific parameters used. Specifically, the Walkaide and Bioness devices provide a user-controlled intensity setting, which presumably alters the current, since no study that implemented these devices in a community setting reported current settings. All studies, except one (20), applied stimulation according to normal physiological timing. All studies utilized surface electrodes. An outlier in stimulation protocols was the most recent study which utilized a multi-channel device in two individuals (20). They used a substantially higher pulse width, up to 440 μs, and current up to 60 mA. No other study reported a pulse width above 300 μs or current above 45 mA. The authors stated these pulse width and current values were determined by considering both the results of a thresholding procedure and the desired muscle activation. Further discussion explaining the deviation from prior stimulation settings was not provided. Additionally, they did not necessarily provide stimulation at normal muscle timing. As the authors explained, normal muscle timing was used as a basis, however final stimulation timing was determined by the observations and recommendations of three independent physical therapists.

Gait event detection technologies were more varied in recent studies. Two studies achieved gait event detection by a footswitch

TABLE 4 | Common data elements (CDE) outcomes reported by each study.

Publication	Common data elements (CDE) reported		
	Improved	**No change**	**Declined**
Behbodi et al. (20)	Step width*, stride length*, walking distance*, knee and ankle kinematics*	VO_2, walking speed	
Rose et al. (21)	GDI	Walking speed	
Bailes et al. (22, 23)	COPM, DF at IC, 6MWT, walking speed		
Pool et al. (24–26)	Muscle volume (MRI of TA and Gastrocnemius*), Isometric DF strength, DF at IC, maximum ankle DF in swing, time in stance, step length, modified Tardieu*, COPM	SCALE, walking speed,	
El-Shamy et al. (27)	Stride length, walking speed, cadence, percent stance, VO_2		
Khamis et al. (28)	Kinematics (maximal knee extension at midstance and at the stance phase)		
Pool et al. (29)	Ankle ROM*, modified Tardieu*, isometric DF strength*, concentric PF strength*	OGS	
Danino et al. (19)	Kinematics (ankle DF, foot progression angle), GDI		
Meilahn et al. (30)	Walking Speed	ROM (Ankle DF)	
Prosser et al. (31); Damiano et al. (32)	Kinematics (ankle DF in swing and at IC, ankle PF at TO), Muscle volume (ultrasound of TA)*	Walking speed, cadence, step length,	
Seifart et al. (33)	Isometric PF strength	Isometric DF strength, walking speed	
Al-Abdulwahab and Al-Khatrawi (34)	Walking speed, step length, stride length, hip adductor tone		
van der Linden et al. (35)	Ankle DF in swing and at IC, GGI		Walking speed
Ho et al. (36)		Stride length, cadence	
Orlin et al. (37)	Ankle DF in swing and at IC (TA and TA+GA only)	Walking speed, stride length	
Pierce et al. (38)	Ankle DF in swing and at IC	Stride length	Cadence, walking speed
Johnston et al. (39)	Passive ROM (hip extension/abduction, popliteal angle, knee extension, ankle DF). Temporal-spatial (step length, cadence, walking speed). GMFM (standing)	VO_2, GMFM (crawling, walking, running, climbing)	
Pierce et al. (40)	Ankle DF in swing and at IC (TA and TA+GA only)		

For cohort and randomized control trials, outcomes are reported as improved or declined only if reported as significant differences. For case studies, outcomes are reported as improved or declined only if ubiquitous across all subjects, otherwise reported under no change.
**Denotes observation of a carryover, neurotherapeutic, effect.*

trigger, using the older model Bioness device (19, 22, 23). The newer Bioness model (28) and Walkaide studies use an inertial measurement unit (IMU) based tilt sensor. Similarly, one study (20) utilized an IMU to detect seven phases of gait by shank angular velocity. IMU based technology removes the need to install additional footswitch hardware in the sole of the user's shoe. Additionally, a tilt sensor is capable of continuous gait cycle monitoring, rather than detecting only toe-off and initial contact. This has the potential to provide a higher resolution of stimulation control, as was demonstrated in one recent study which cited the ability to detect seven phases of gait with bilateral IMUs (20). A case study of 3 children with CP, using the RT50 stimulator, had a trained observer manually trigger a stimulation chain at observation of initial contact (21).

Single-Channel NMES-Assisted Gait

Since 2010, most publications have applied only single-channel stimulation to the tibialis anterior, except for three case studies (**Table 2**). Although the focus of studies has been narrowed to largely only single-channel stimulation of the tibialis anterior, a number of significant improvements have been identified. Improvement were demonstrated in kinematics, temporal-spatial parameters, and physiological metrics such as muscle volume, muscle strength, Modified Tardieu test of spasticity, and energy expenditure. These reported improvements are likely due to a combination of delivering better NMES timing, stimulation application, and higher-powered studies. Additionally, outcome evaluations such as muscle strength and volume, were not assessed until more recently. Lasting neurotherapeutic effects have also been demonstrated. Specifically, the Modified Tardieu (26, 29) and the muscle volume of the tibialis anterior (31) and gastrocnemius (26) were reported to have significant carry-over effect, suggesting that the neuromuscular deficits of weakness and spasticity can be improved with gait-specific NMES in persons with CP.

This shift in NMES research toward a focused attention on single-channel stimulation of the tibialis anterior to augment dorsiflexion brought both benefits and potential missed

TABLE 5 | Common data element (CDE) outcomes across all studies, grouped by outcome metric, with study number noted.

Outcomes	Improved	No change	Declined	Effect, level of evidence
TEMPORAL-SPATIAL PARAMETERS				
Walking Speed	3, **5**, 9, **12**	2, **4**, 10, 11, 15	**13**, 16	Mixed
Step Length	**4**, **12**, 17	10		Improvement, II
Stride Length	1, **5**, **12**	14, 15, 16		Improvement, II
Step Width	1			Improvement IV
Cadence	**5**, 17	10, 14	16	Improvement, III
Time in Stance	**4**, **5**			Improvement, II
KINEMATICS				
Ankle				
DF in swing	1, **4**, 8, 10, **13**, 15, 16, 18			Improvement, I
DF at IC	1, 2, **4**, 10, **13**, 15, 16, 18			Improvement, I
PF at TO	10			Improvement, III
Foot Progression Angle	8			Improvement, IV
Knee				
Maximal Knee Extension	6			Improvement, IV
PHYSIOLOGICAL OUTCOMES				
Muscle Volume				
TA	**4**, 10			Improvement, II
Gastrocnemius	**4**			Improvement, II
Muscle Strength				
Isometric DF	**4**, 7	11		Improvement, II
Isometric PF	11			Improvement, IV
Concentric PF	7			Improvement, III
Modified Tardieu				
Ankle	**4**, 7			Improvement, II
Energy Expenditure				
VO_2	**5**	1, 17		Improvement, II
Hip Adductor Tone (Mod. Ashworth)	**12**			Improvement, III
SCALE		**4**		No Change, II
ROM	7, 17	9		Improvement, III
FUNCTIONAL ASSESSMENTS				
GMFM	17	17		Improvement, III
GDI	2, 8			Improvement, IV
GGI	13			Improvement, III
COPM	3, **4**			Improvement, II
6MWT	3			Improvement, III
OGS		7		No Change, III

Associated Oxford Centre for Evidence Based Medicine Level of Evidence is provided along with a cumulative assessment of the effect seen for a given CDE outcome metric. Randomized control trials have been bolded.

opportunities. Such ubiquitous attention has allowed for the first credible systematic review to be attempted in the field (8). With a review question limited to the effect of functional electrical stimulation during walking on ankle dorsiflexors in children with CP, the reviewers concluded that improvements in active ankle dorsiflexion range of motion, strength, selective motor control, balance and gait kinematics could be achieved. However, they could not draw a conclusion on whether or not functional metrics such as self-reported frequency of toe-drag and falls were improved.

Apart from tibialis anterior single-channel NMES, one study examined single-channel stimulation to the quadriceps femoris and reported significant improvements in knee kinematics (28). This finding is at odds with a prior publication (35) and could be due to improvements in stimulation technology and timing. However, there is insufficient evidence either way, as the older publication included only four children receiving stimulation to the quadriceps, and the newer study was a case study of one participant.

Multi-channel NMES-Assisted Gait

Since 2010, only two case studies have reported on multi-channel NMES use in persons with CP (**Table 2**). Rose et al. (21) applied stimulation to the gluteals, quadriceps femoris, and gastric-soleus

muscles bilaterally, in a three subject single-session case study, and Behboodi et al. (20) applied stimulation to 3–4 muscle groups bilaterally in a two subject case study.

Rose et al. (21) recruited children specifically with flexed-knee gait, defined as 20–40°C of knee flexion in stance. Stimulation was then applied to the quadriceps and gluteus muscles from initial contact through 50% of the gait cycle, and gastrocnemius-soleus complex from 15 to 60% of the gait cycle. They demonstrated improved velocity and GDI in 2 out of 3 participants with improved hip, knee and ankle joint kinematics during a single-session of NMES-assisted gait. The multi-channel NMES study published by Behboodi et al. (20) demonstrated a number of promising findings in their small case study. Their 12-week program of gait-specific NMES training did appear to be beneficial to the two individuals in the study. In all, the study demonstrated a normalization of temporal-spatial parameters with improved fitness in the participant with GMFCS III, and improved efficiency in the participant with GMFCS II, as determined by peak VO_2 and O_2 cost of walking, respectively.

The Arc of Progress of Multi-channel NMES

The largest study to assess the effect of multi-channel NMES in children with CP included 17 children, 8 of whom received NMES, and was conducted in 2004 (39). This publication, and the three others studying multi-channel NMES prior to 2010 (33, 37, 40), were in the early stages of NMES research, utilizing percutaneous electrodes and custom stimulator systems. Furthermore, they were either limited in dosage (37), underpowered (40), or highly confounded by extraneous factors, such as major surgeries (39) or Botox injections (33). They were appropriate for their time, as exploratory studies, however an assessment of the efficacy of multi-channel stimulation by modern technological standards has not been attempted beyond case studies. The targeted augmentation of ankle DF in swing is an appropriate intervention for patients whose primary gait abnormality is the lack of ankle DF during swing due to DF weakness. However, it is likely to be insufficient in the majority of children with CP. It would not be expected that normalization of the kinematics of a single joint during the non-weight bearing phase would have substantive effects on proximal muscle weakness and control during stance phase. The success of achieving improvements in ankle DF by single-channel NMES is encouraging but in large part due to the muscular demand being relatively small; ankle DF in swing is non-weight bearing and acts on a small load (the foot). Similarly, forces of hip flexors in early swing and knee extensors in terminal swing are low relative to the forces necessary to achieve upright gait during stance phase. This was leveraged and partially demonstrated in the case study by Behboodi et al. in stimulating the quadriceps in terminal swing, achieving greater knee extension and a resulting increased stride length (20).

Moving forward, the results of this review suggest a possible return to the study of multi-channel stimulation in children with CP. Stimulation of the tibialis anterior and augmentation of ankle DF is likely to be a critical component of such future systems; however, it appears unlikely that it alone will resolve gait deficits seen in this population. Interestingly, gait-specific NMES applied to the tibialis anterior was shown to only improve ankle kinematics (8), while the singular recent case study on gait-specific NMES applied to the quadriceps femoris showed only improvements in knee joint kinematics (28). This taken in conjunction with the findings of earlier studies that multi-channel stimulation can have additive beneficial effects, would suggest that normalization of more involved gait deficits, would require a multi-channel gait-specific NMES acting across multiple joints. This early hypothesis is supported by the case studies published in Rose et al. (21) and Behboodi et al. (20). Additionally, a single subject case study published in 2015, assessing the effects of gait-specific multi-channel stimulation to the tibialis anterior and hamstrings in an adult with CP, demonstrated improvements in the Dynamic Gait Index, Performance Oriented Mobility Assessment, Observational Gait Scale, and Activities-specific Balance Confidence Scale scores (42). However, these are all case study examples, and the benefits of a multi-channel NMES system must be born out in a larger study.

Multi-channel gait-specific NMES development is a task not only for clinicians to carry out, but also the medical device industry and research groups. Currently, two double-channel NMES devices were found capable of initiating gait-specific stimulation in a self-regulated manner, the Bioness L300 Plus and Odstock 2 Channel Stimulator. The L300 Plus system employs a tilt-sensor to control a common fibular nerve stimulator, and a thigh mounted stimulator, for either quadricep or hamstring stimulation. Comparatively, the Odstock device uses a foot switch sensor to trigger stimulation of the gastrocnemius and tibialis anterior at mid-stance and during swing, respectively. Early stages of multi-channel device development can leverage lessons learned from wearable robotic development such as the idea that that bi-directional control of a joint is vastly more difficult than unidirectional control (43). As such, early implementations of multi-channel NMES may benefit from limiting the amount of bi-directional joint actuation.

In general, a multi-channel device is likely best utilized by applying stimulation within the normal timing of the muscle, and providing unidirectional control of the hip, knee, and ankle joints. For example, a device that provided quadriceps stimulation from terminal swing through loading response, gluteal stimulation from initial contact through loading, gastrocnemius-soleus stimulation from loading through mid-stance, and tibialis anterior stimulation in swing phase. Applying gait-specific NMES across the three major lower limb joints within periods of physiologically normal timing could provide vital sensorimotor input and biomechanical support, and lead to greater normalization of gait as compared to stimulation at a single joint.

Limitations

The findings of this review must be taken in the context of the quality and size of the studies it is comprised of. Only eighteen

relevant studies have been conducted, four of which are RCTs, all with 34 or fewer participants. Amongst the RCTs, the two larger and best conducted studies asses only TA stimulation in swing. The remaining two studies are smaller, and asses single-channel stimulation of other muscle groups, one of which being the gluteus medius which has not been repeated since. Many of the findings of this review are based on small cohort and case studies. Ultimately, at this stage in this field, this review can largely only highlight what has and what has not been observed. The authors recognize the absence of evidence in this field and have attempted to present the findings scaled with that expectation.

The recruitment and retention of study subjects from a pediatric population with cerebral palsy is difficult. Electrical stimulation, while comfortable for most, can be an uncomfortable sensation for some users. The challenges are even greater using un-refined research grade devices for many of the more ambitious multi-channel studies. The physical appearance of these devices is an additional barrier to acceptance for parents and children, and their technical requirements often constrain them to laboratory use only. It is remarkable that some of these studies maintained intervention programs and follow up out to 1 year. But it is also why many of these studies ultimately become either case studies, or single sessions. This fundamental limitation will remain until commercially available multi-channel devices are available for home and community use.

The Cochrane guidelines for risk of bias assessment for both randomized and non-randomized studies were consulted to guide an assessment of risk across all studies considered. The risk of bias across nearly all seven elements is considered high for a few key factors, mostly stemming from this being such preliminary research. The study population is a self-selected subset of patients and families both willing to try and interested in NMES technology, as well as being capable of tolerating the electrical stimulation. Although adequate random sequence generation was performed in some, recruitment is fundamentally non-random. One cohort study even defined its control group, as those who could not tolerate the electrical stimulation (33). The effects of this non-random recruitment make the smaller studies at an even higher risk for bias due to ideal patient selection. The intervention itself, is practically impossible to blind participants from, and no study blinded the personnel from. Finally, since so many studies were small cohort or case studies, there is an even higher risk of bias due to inherent selective reporting bias stemming from the results not being statistically significant in such small studies. Additionally, the reporting of small case studies could also be influenced by selective reporting of best responders. Even objective outcome data could be potentially biased by effort, since the participants are aware of the intervention. Considering the high risk of bias, the outcomes in this review are at a high risk of over-estimating the potential benefits of NMES technology.

Conducting a more focused review to address a specific clinical question was considered, however due to the under-developed nature of this field, it was determined that insufficient evidence exists to adequately answer any specific question and a broader review would be more beneficial. A systematic review at this early point, would have unduly limited the diversity of studies. It would have placed an over-emphasis on a limited few randomized control trials which have all assessed the same technology—a tibialis anterior stimulator for ankle dorsiflexion in swing. As a consequence, the results of this review do not provide the strength of evidence that a systematic review would provide.

CONCLUSION

CP is a common neurological disorder presenting early in childhood with progressive musculoskeletal and functional impairments. Current pharmaceutical and surgical treatments are inadequate, with only partial benefits. Neuromuscular electrical stimulation is a well-established technology that has demonstrated recent progress due to advances in wearable electromechanical technology that can improve functional electrical stimulation treatment. The study of NMES during gait in persons with CP is still limited, however these early studies are promising in showing that NMES may offer unique benefits for gait rehabilitation. Improvements seen with NMES, such as joint kinematics and muscle volumes, still must translate to other functionally meaningful metrics such as degree of community ambulation. Further advancement of NMES technology, particularly in the arena of multi-channel devices and the targeting of major muscle groups, may yield even greater improvement in the gait of individuals with CP. Electrical stimulation is a particularly appealing technological solution as it may play a restorative or compensatory role in the four major defining musculoskeletal deficits of spastic CP, while remaining non-invasive and highly individually tunable. Overall, NMES is a well-accepted and tolerated intervention, with high reported rates of patient satisfaction and retention.

AUTHOR CONTRIBUTIONS

JM and JR conducted the literature search, contributed to writing and editing the manuscript, conceptualized the framework within which to conduct the review, and have reviewed and approved the final manuscript.

FUNDING

This work was supported in part by the Stanford University Medical Scholars Fellowship.

REFERENCES

1. Christensen D, Van Naarden Braun K, Doernberg NS, Maenner MJ, Arneson CL, Durkin MS, et al. Prevalence of cerebral palsy, co-occurring autism spectrum disorders, and motor functioning–Autism and Developmental Disabilities Monitoring Network USA 2008. *Dev Med Child Neurol.* (2014) 56:59–65. doi: 10.1111/dmcn.12268
2. Stavsky M, Mor O, Mastrolia SA, Greenbaum S, Than NG, Erez O. Cerebral palsy—trends in epidemiology and recent development in prenatal mechanisms of disease, treatment, and prevention. *Front Pediatr.* (2017) 5:21. doi: 10.3389/fped.2017.00021
3. Radziszewski K. Outcomes of electrical stimulation of the neurogenic bladder: results of a two-year follow-up study. *NeuroRehabilitation.* (2013) 32:867–73. doi: 10.3233/NRE-130911
4. Foundation The Ear. *Cochlear Implant Information Sheet.* (2016). Available online at: https://www.earfoundation.org.uk/hearing-technologies/cochlear-implants/cochlear-implant-information-sheet (accessed January 17, 2019).
5. Sheffler LR, Chae J. Neuromuscular electrical stimulation in neurorehabilitation. *Muscle Nerve.* (2007) 35:562–90. doi: 10.1002/mus.20758
6. Takeda K, Tanino G, Miyasaka H. Review of devices used in neuromuscular electrical stimulation for stroke rehabilitation. *Med Devices.* (2017) 10:207–13. doi: 10.2147/MDER.S123464
7. de Freitas GR, Szpoganicz C, Ilha J. Does neuromuscular electrical stimulation therapy increase voluntary muscle strength after spinal cord injury? *A systematic review. Top Spinal Cord Inj Rehabil.* (2018) 24:6–17. doi: 10.1310/sci16-00048
8. Moll I, Vles JSH, Soudant DLHM, Witlox AMA, Staal HM, Speth LAWM, et al. Functional electrical stimulation of the ankle dorsiflexors during walking in spastic cerebral palsy: a systematic review. *Dev Med Child Neurol.* (2017) 59:1230–6. doi: 10.1111/dmcn.13501
9. Stein C, Fritsch CG, Robinson C, Sbruzzi G, Plentz RD. Effects of electrical stimulation in spastic muscles after stroke systematic review and meta-analysis of randomized controlled trials. *Stroke.* (2015) 46:2197–205. doi: 10.1161/STROKEAHA.115.009633
10. Sahin N, Ugurlu H, Albayrak I. The efficacy of electrical stimulation in reducing the post-stroke spasticity: a randomized controlled study. *Disabil Rehabil.* (2012) 34:151–6. doi: 10.3109/09638288.2011.593679
11. Dibner B. *Luigi Galvani.* (2018). Available online at: https://www.britannica.com/biography/Luigi-Galvani (accessed January 17, 2019).
12. Shashkevich A. *Benjamin Franklin as the Social Network Genius of His Time? Yes, Says One Stanford Scholar.* Stanford University (2018). Available online at: https://news.stanford.edu/2018/11/12/benjamin-franklin-social-genius-18th-century/ (accessed January 17, 2019).
13. Zahradka N, Lee S. *When and What to Stimulate? An Evaluation of a Custom Functional Electrical Stimulation System and Its Neuroprosthetic Effect on Gait in Children With Cerebral Palsy.* Newark, DE: University of Delaware Library, Museums and Press (2016). Available online at: http://udspace.udel.edu/handle/19716/23624 (accessed March 01, 2019).
14. Tricco AC, Lillie E, Zarin W, O'Brien CH, Levac D, Moher D, et al. PRISMA extension for scoping reviews (PRISMA-ScR): checklist and explanation. *Ann Int Med.* (2018) 169:467–73. doi: 10.7326/M18-0850
15. Grinnon ST, Miller K, Marler JR, Lu Y, Stout A, Odenkirchen J, et al. National Institute of Neurological Disorders and Stroke Common Data Element Project - approach and methods. *Clin Trials.* (2012) 9:322–9. doi: 10.1177/1740774512438980
16. Palisano R, Rosenbaum P, Walter S, Russell D, Wood E, Galuppi B. Development and reliability of a system to classify gross motor function in children with cerebral palsy. *Dev Med Child Neurol.* (1997) 39:214–23. doi: 10.1111/j.1469-8749.1997.tb07414.x
17. Howick J, Chalmers I, Glasziou P, Greenhalgh T, Heneghan C, Liberati A, et al. *The Oxford 2011 Levels of Evidence.* Oxford, UK: Oxford Centre for Evidence-Based Medicine (2011).
18. Higgins JPT, Altman DG, Sterne JAC. Chapter 8: assessing risk of bias in included studies. In: Higgins JPT, Green S, Editors. *Cochrane Handbook for Systematic Reviews of Interventions Version 5.1.0.* The Cochrane Collaboration (2011).
19. Danino B, Khamis S, Hemo Y, Batt R, Snir E, Wientroub S, et al. The efficacy of neuroprosthesis in young hemiplegic patients, measured by three different gait indices: early results. *J Child Orthop.* (2013) 7:537–42. doi: 10.1007/s11832-013-0540-5
20. Behboodi A, Zahradka N, Wright H, Alesi J, Lee SCK. Use of a Novel Functional Electrical Stimulation Gait Training System in 2 Adolescents With Cerebral Palsy: A Case Series Exploring Neurotherapeutic Changes. *Phys. Ther.* (2019) 99:739–47. doi: 10.1093/ptj/pzz040
21. Rose J, Cahill-Rowley K, Butler EE. Artificial walking technologies to improve gait in cerebral palsy: multichannel neuromuscular stimulation. *Artif Organs.* (2017) 41:233–9. doi: 10.1111/aor.13058
22. Bailes AF, Caldwell C, Clay M, Tremper M, Dunning K, Long J. An exploratory study of gait and functional outcomes after neuroprosthesis use in children with hemiplegic cerebral palsy. *Disabil Rehabil.* (2017) 39:2277–85. doi: 10.1080/09638288.2016.1225827
23. Bailes AF, Caldwell C, Clay M, Tremper M, Dunning K, Long J. Participation and community-based walking activity after neuroprosthesis use in children with hemiplegic cerebral palsy: a pilot study. *J Pediatr Rehabil Med.* (2017) 10:71–9. doi: 10.3233/PRM-170434
24. Pool D, Valentine J, Blackmore AM, Colegate J, Bear N, Stannage K, et al. Daily functional electrical stimulation during everyday walking activities improves performance and satisfaction in children with unilateral spastic cerebral palsy: a randomized controlled trial. *Arch Physiother.* (2015) 5:5. doi: 10.1186/s40945-015-0005-x
25. Pool D, Valentine J, Bear N, Donnelly CJ, Elliott C, Stannage K. The orthotic and therapeutic effects following daily community applied functional electrical stimulation in children with unilateral spastic cerebral palsy: a randomised controlled trial. *BMC Pediatr.* (2015) 15:154. doi: 10.1186/s12887-015-0472-y
26. Pool D, Elliott C, Bear N, Donnelly CJ, Davis C, Stannage K, et al. Neuromuscular electrical stimulation-assisted gait increases muscle strength and volume in children with unilateral spastic cerebral palsy. *Dev Med Child Neurol.* (2016) 58:492–501. doi: 10.1111/dmcn.12955
27. El-Shamy SM, Abdelaal AA. Walkaide efficacy on gait and energy expenditure in children with hemiplegic cerebral palsy: a randomized controlled trial. *Am J Phys Med Rehabil.* (2016) 95:629–38. doi: 10.1097/PHM.0000000000000514
28. Khamis S, Martikaro R, Wientroub S, Hemo Y, Hayek S. A functional electrical stimulation system improves knee control in crouch gait. *J Child Orthop.* (2015) 9:137–43. doi: 10.1007/s11832-015-0651-2
29. Pool D, Blackmore AM, Bear N, Valentine J. Effects of short-term daily community walk aide use on children with unilateral spastic cerebral palsy. *Pediatr Phys Ther.* (2014) 26:308–17. doi: 10.1097/PEP.0000000000000057
30. Meilahn JR. Tolerability and effectiveness of a neuroprosthesis for the treatment of footdrop in pediatric patients with hemiparetic cerebral palsy. *PMR.* (2013) 5:503–9. doi: 10.1016/j.pmrj.2012.11.005
31. Prosser LA, Curatalo AKE, Damiano DL. Acceptability and potential effectiveness of a foot drop stimulator in children and adolescents with cerebral palsy. *Dev Med Child Neurol.* (2012) 54:1044–9. doi: 10.1111/j.1469-8749.2012.04401.x
32. Damiano DL, Prosser LA, Curatalo LA, Alter KE. Muscle plasticity and ankle control after repetitive use of a functional electrical stimulation device for foot drop in cerebral palsy. *Neurorehabil Neural Repair.* (2013) 27:200–7. doi: 10.1177/1545968312461716
33. Seifart A, Unger M, Burger M. Functional electrical stimulation to lower limb muscles after botox in children with cerebral palsy. *Pediatr Phys Ther.* (2010) 22:199–206. doi: 10.1097/PEP.0b013e3181dbd806
34. Al-Abdulwahab SS, Al-Khatrawi WM. Neuromuscular electrical stimulation of the gluteus medius improves the gait of children with cerebral palsy. *NeuroRehabilitation.* (2009) 24:209–17. doi: 10.3233/NRE-2009-0470
35. van der Linden ML, Hazlewood ME, Hillman SJ, Robb JE. Functional electrical stimulation to the dorsiflexors and quadriceps in children with cerebral palsy. *Pediatr Phys Ther.* (2008) 20:23–9. doi: 10.1097/PEP.0b013e31815f39c9
36. Ho C, Holt KG, Saltzman E, Wagenaar RC. Functional electrical stimulation changes dynamic resources in children with spastic cerebral palsy. *Phys. Ther.* (2006) 86:987–1000. doi: 10.1093/ptj/86.7.987

37. Orlin MN, Pierce SR, Stackhouse CL, Smith BT, Johnston T, Shewokis PA, et al. Immediate effect of percutaneous intramuscular stimulation during gait in children with cerebral palsy: a feasibility study. *Dev Med Child Neurol.* (2005) 47:684–90. doi: 10.1017/S0012162205001398
38. Pierce SR, Orlin MN, Lauer RT, Johnston TE, Smith BT, McCarthy JJ. Comparison of percutaneous and surface functional electrical stimulation during gait in a child with hemiplegic cerebral palsy. *Am J Phys Med Rehabil.* (2004) 83:798–805. doi: 10.1097/01.PHM.0000137318.92035.8C
39. Johnston TE, Finson RL, McCarthy JJ, Smith BT, Betz RR, Mulcahey MJ. Use of functional electrical stimulation to augment traditional orthopaedic surgery in children with cerebral palsy. *J Pediatr Orthop.* (2004) 24:283–91. doi: 10.1097/01241398-200405000-00009
40. Pierce SR, Laughton CA, Smith BT, Orlin MN, Johnston TE, McCarthy JJ. Direct effect of percutaneous electric stimulation during gait in children with hemiplegic cerebral palsy: a report of 2 cases. *Arch Phys Med Rehabil.* (2004) 85:339–43. doi: 10.1016/S0003-9993(03)00473-8
41. Gunel MK, Tarsuslu T, Mutlu A, Livanelioglu A. Investigation of interobserver reliability of the gillette functional assessment questionnaire in children with spastic diparetic cerebral palsy. *Acta Orthop Traumatol Turc.* (2010) 44:63–9. doi: 10.3944/AOTT.2010.2218
42. Robinson BS, Williamson EM, Cook JL, Harrison KS, Lord EM. Examination of the use of a dual-channel functional electrical stimulation system on gait, balance and balance confidence of an adult with spastic diplegic cerebral palsy. *Physiother Pract.* (2015) 31:214–20. doi: 10.3109/09593985.2014.982774
43. Mooney LM, Rouse EJ, Herr HM. Autonomous exoskeleton reduces metabolic cost of human walking during load carriage. *J NeuroEng Rehabil.* (2014) 11:80. doi: 10.1186/1743-0003-11-80

Conflict of Interest Statement: The authors declare that the research was conducted in the absence of any commercial or financial relationships that could be construed as a potential conflict of interest.

frontiers in Human Neuroscience

ORIGINAL RESEARCH
published: 18 September 2019
doi: 10.3389/fnhum.2019.00305

Prediction of Gait Impairment in Toddlers Born Preterm From Near-Term Brain Microstructure Assessed With DTI, Using Exhaustive Feature Selection and Cross-Validation

*Katelyn Cahill-Rowley[1,2], Kornél Schadl[1,3], Rachel Vassar[1,3], Kristen W. Yeom[4], David K. Stevenson[5] and Jessica Rose[1,2,3]**

[1] Division of Pediatric Orthopaedics, Stanford University School of Medicine, Stanford, CA, United States, [2] Motion & Gait Analysis Laboratory, Lucile Packard Children's Hospital, Stanford, CA, United States, [3] Neonatal Neuroimaging Research Lab, Stanford University School of Medicine, Stanford, CA, United States, [4] Department of Radiology, Lucile Packard Children's Hospital, Stanford University School of Medicine, Stanford, CA, United States, [5] Division of Neonatal and Developmental Medicine, Stanford University School of Medicine, Stanford CA, United States

OPEN ACCESS

Edited by:
Muthuraman Muthuraman, University Medical Center of the Johannes Gutenberg University Mainz, Germany

Reviewed by:
Xiaobo Li, New Jersey Institute of Technology, United States
Rathinaswamy Bhavanandhan Govindan, Children's National Health System, United States

***Correspondence:**
Jessica Rose
jessica.rose@stanford.edu

Specialty section:
This article was submitted to Motor Neuroscience, a section of the journal Frontiers in Human Neuroscience

Received: 18 March 2019
Accepted: 19 August 2019
Published: 18 September 2019

Citation:
Cahill-Rowley K, Schadl K, Vassar R, Yeom KW, Stevenson DK and Rose J (2019) Prediction of Gait Impairment in Toddlers Born Preterm From Near-Term Brain Microstructure Assessed With DTI, Using Exhaustive Feature Selection and Cross-Validation. Front. Hum. Neurosci. 13:305. doi: 10.3389/fnhum.2019.00305

Aim: To predict gait impairment in toddlers born preterm with very-low-birth-weight (VLBW), from near-term white-matter microstructure assessed with diffusion tensor imaging (DTI), using exhaustive feature selection, and cross-validation.

Methods: Near-term MRI and DTI of 48 bilateral and corpus callosum regions were assessed in 66 VLBW preterm infants; at 18–22 months adjusted-age, 52/66 participants completed follow-up gait assessment of velocity, step length, step width, single-limb support and the Toddle Temporal-spatial Deviation Index (TDI). Multiple linear models with exhaustive feature selection and leave-one-out cross-validation were employed in this prospective cohort study: linear and logistic regression identified three brain regions most correlated with gait outcome.

Results: Logistic regression of near-term DTI correctly classified infants high-risk for impaired gait velocity (93% sensitivity, 79% specificity), right and left step length (91% and 93% sensitivity, 85% and 76% specificity), single-limb support (100% and 100% sensitivity, 100% and 100% specificity), step width (85% sensitivity, 80% specificity), and Toddle TDI (85% sensitivity, 75% specificity). Linear regression of near-term brain DTI and toddler gait explained 32%–49% variance in gait temporal-spatial parameters. Traditional MRI methods did not predict gait in toddlers.

Interpretation: Near-term brain microstructure assessed with DTI and statistical learning methods predicted gait impairment, explaining substantial variance in toddler gait. Results indicate that at near term age, analysis of a set of brain regions using statistical learning methods may offer more accurate prediction of outcome at toddler age. Infants high risk for single-limb support impairment were most accurately predicted.

As a fundamental element of biped gait, single-limb support may be a sensitive marker of gait impairment, influenced by early neural correlates that are evolutionarily and developmentally conserved. For infants born preterm, early prediction of gait impairment can help guide early, more effective intervention to improve quality of life.

What This Paper Adds:

- Accurate prediction of toddler gait from near-term brain microstructure on DTI.
- Use of machine learning analysis of neonatal neuroimaging to predict gait.
- Early prediction of gait impairment to guide early treatment for children born preterm.

Keywords: MRI, DTI, diffusion tensor imaging, very-low-birth-weight preterm infant, toddler gait, gait impairment, motor development, machine learning

INTRODUCTION

At near-term age, the infant brain is rapidly developing (Brody et al., 1987; Dubois et al., 2006; Huang et al., 2006; Oishi et al., 2011; Nossin-Manor et al., 2013; Rose et al., 2014). Brain microstructure abnormalities assessed at this age have been found to correlate to neurodevelopment in preterm children, suggesting potential as early biomarkers for neurodevelopmental impairment (Mukherjee et al., 2002; Arzoumanian et al., 2003; Rose et al., 2007, 2009, 2015; Alvarez et al., 2011; Van Kooij et al., 2011; Woodward et al., 2012; Aeby et al., 2013). Although advances in neonatal medicine have improved outcomes among children born preterm, 40% of very preterm infants develop motor impairments such as cerebral palsy (CP) and developmental coordination disorder, rates that are substantially higher than the general population (Williams et al., 2010; Spittle et al., 2011). Neonatal identification of at-risk children could enable high-impact early intervention during optimal developmental periods of rapid growth and neuronal plasticity.

Diffusion tensor imaging (DTI) is a promising neuroimaging technique that reflects white matter (WM) microstructural injury and can be used to assess early brain development. DTI reveals the amount and direction of water diffusion. In the brain, water diffusion is restricted by neural development, in particular, the presence and isotropy of cellular membranes and myelination. Thus, brain DTI can be used as a metric of brain neurodevelopment and organization (Hüppi et al., 1998; Counsell et al., 2002; Basser and Pierpaoli, 2011). DTI quantifies fractional anisotropy (FA), mean diffusivity (MD), radial diffusivity (RD), and axial diffusivity (AD). FA represents the anisotropy of diffusion, i.e., the extent to which water diffuses in one particular direction (Basser and Pierpaoli, 2011); in WM it is altered by fiber coherence, diameter, density, and myelination. MD is the average amount of water diffusion; AD is the amount of diffusion occurring in the dominant direction or primary axis; and RD is the amount of diffusion occurring perpendicular to the dominant direction. Generally, higher FA and AD indicate more developed microstructure, whereas higher MD and RD indicate less developed microstructure. Brain development alters the dynamics of diffusion, e.g., decreased water content, contraction of extracellular space, myelination, and increased coherence of axonal structures (Kinney et al., 1994; Dubois et al., 2008; Nossin-Manor et al., 2013). The DTI metrics of FA, MD, AD, and RD are affected by these changes and therefore reflect brain development and maturation.

For preterm infants, prognosis based structural brain MRI findings have demonstrated partial success (Miller and Ferriero, 2009; Spittle et al., 2011; Hintz et al., 2015; Anderson et al., 2017). Children at high risk, such as VLBW preterm infants, generally undergo neuroimaging as standard-of-care prior to discharge from the neonatal intensive care unit (NICU). Although currently, DTI is not routinely obtained in NICU clinical brain imaging assessment, it is a promising extension of neuroimaging techniques that may better identify WM microstructural injuries affecting early development (Arzoumanian et al., 2003; Rose et al., 2007, 2009, 2015).

We previously reported on neonatal correlates of toddler gait, analyzing near-term DTI in six subcortical WM regions. We analyzed four bilateral regions and two regions of the corpus callosum (CC) which were selected based on previously reported relevance, using standard statistical techniques in the same cohort of VLBW preterm children (Rose et al., 2015). The current study aims to improve the predictive value of DTI assessment at this early age of brain development. Here we include a broader set of brain regions that may more precisely predict gait impairments and ultimately, may inform neuroprotective treatment to improve outcomes for preterm children.

The current study applies exhaustive feature selection and leave-one-out cross-validation of WM in 99 brain regions, including 48 bilateral regions and three regions of the CC, in order to investigate the use of linear statistical models on DTI metrics for early prognosis of toddler gait impairment. A prior study of this cohort employed similar statistical learning methods to investigate prediction of cognitive and motor neurodevelopment, as measured by the Bayley Scales of Infant Development-Third Edition (Schadl et al., 2018). In this study, we employed a supervised statistical learning approach to determine the predictive value of near-term WM microstructure in VLBW preterm neonates in relation to temporal-spatial gait metrics at 18–22 months adjusted age. We hypothesized that applying a

more comprehensive approach using DTI metrics of FA, MD, AD, and RD in a subset of three near-term brain regions, identified using statistical learning approach of exhaustive feature selection and cross-validation, would demonstrate higher predictive value for gait impairment at 18–22 months adjusted age, compared to using standard techniques.

MATERIALS AND METHODS

Participants born with VLBW (birth weight ≤1500 g), gestational age at birth ≤32 weeks, and no evidence of genetic disorder or congenital brain abnormalities were recruited. 102 infants treated at Lucile Packard Children's Hospital (LPCH) NICU from 1/1/10-12/31/11 participated, representing 76% of eligible infants admitted over the 2-year period. All parents of eligible infants were approached prior to scheduled routine MRI and written informed consent was obtained for this IRB-approved prospective cohort study. 66 of 102 neonates had successful DTI scans at near-term age, collected at end of routine MRI scan, prior to discharge from the NICU.

Of the 66 neonates who had both near-term MRI and DTI, 52 completed follow-up gait assessment at 18–22 months of age, adjusted for prematurity (**Table 1**). Gait was assessed for 2–3 walking trials on an instrumented mat, as described previously (Cahill-Rowley and Rose, 2016a). Walking trials included at least four consecutive footfalls with at least one foot always touching the ground. Temporal-spatial gait metrics included walking velocity, step length, step width, and single-limb support as a percent of the gait cycle (SLS). These temporal-spatial parameters are accurately assessed at toddler age, reflect different aspects of gait function such as symmetry, single limb balance, dynamic postural balance, and overall gait function, and are sensitive to differences in gait pattern and impairment (Cahill-Rowley and Rose, 2016a,b). The Toddle Temporal-spatial Deviation Index (Toddle TDI), an assessment which quantifies deviation of temporal-spatial gait parameters from normal and is sensitive to gross motor function in toddlers (Cahill-Rowley and Rose, 2016b), was calculated. Gait impairment was defined as having a gait outcome score worse than one standard deviation from the mean value of a typically-developing cohort (n = 42) at 18–22 months adjusted age, previously published (Cahill-Rowley and Rose, 2016a,b).

TABLE 1 | Demographic and neonatal characteristics of all neonates and neonates with both DTI and gait assessment.

	All neonates (n = 102)	Neonates with DTI and gait assessment (n = 52)
Males, n (%)	42 (41)	20 (38)
Females, n (%)	60 (59)	32 (62)
GA (weeks) mean (SD)	28.7 (2.4)	29.0 (2.4)
BW (g) mean (SD)	1087.3 (278.8)	1081.5 (270.0)
Maternal age (years) mean (SD) (n = 99; 51)	31.6 (6.0)	32.1 (6.0)
PMA at scan (weeks) mean (SD) (n = 102)	36.6 (1.8)	36.5 (1.2)
Multiple gestation mean (SD)	1.7 (1.0)	1.9 (0.9)
Apgar at 5-minute mean (SD) (n = 100; 51)	7.4 (1.9)	7.5 (1.8)
Days on ventilation mean (SD) (n = 99; 51)	11.1 (18.4)	8.5 (14.7)
BPD[a], n (%)	30 (29)	15 (29)
NEC, n (%)	14 (14)	5 (10)
ROP[b], n (%)	29 (28)	15 (29)
Sepsis[c], n (%)	12 (12)	5 (10)
Mean CRP[d], mg/dl, mean (SD) (n = 97; 49)	0.45 (0.58)	0.31 (0.35)
Peak CRP[d], mg/dl, mean (SD) (n = 97; 49)	1.00 (1.49)	0.63 (0.84)

BPD, bronchopulmonary dysplasia; BW, birth weight; GA, gestational age; NEC, necrotizing enterocolitis; PMA, postmenstrual age; ROP, retinopathy of prematurity. [a]BPD: history of respiratory distress syndrome, treated with oxygen >21% at 36 wk PMA. [b]Presence of ROP stage 2 or 3. [c]Sepsis, confirmed by positive blood culture. [d]Measured over first two postnatal weeks.

MRI Data Acquisition

Brain MRI scans were performed on a 3T MRI (GE Discovery MR750, 8-Channel HD head coil, Little Chalfont, United Kingdom) at LPCH. A 3-plane localizer was used and an asset calibration was prescribed to utilize parallel imaging. Sagittal T1 FLAIR image parameters were: TE = 9l ms, TR = 2200 ms, FOV = 20 cm, matrix size = 320 × 224, slice thickness 3.0 × 0.5 mm spacing, NEX = 1. T2, DWI, and DTI axial scans were prescribed using a single acquisition full-phase field of view (FOV). The axial fast spin echo T2 imaging parameters were: TE = 85 ms, TR = 2500 ms, FOV = 20 cm, matrix = 384 × 224; slice = 4.0 × 0.0 mm spacing. Axial T2 FLAIR parameters were: TE = 140 ms, TR = 9500 ms, FOV = 20 cm, slice = 4.0 × 0.0 mm, inversion time 2300 ms, fluid-attenuated inversion recovery matrix = 384 × 224. Axial DWI parameters were: TE = 88.8 ms, TR = 10000 ms, FOV = 20 cm, slice = 4.0 × 0.0 mm spacing, matrix = 128 × 128. Coronal T1 SPGR parameters were: TE = 8 ms, TR = 3 s, slice = 1.0 × 0.0 mm spacing, FOV = 24 cm, matrix = 256 × 256.

Radiological Assessment

Structural MRI was assessed for degree of White Matter Abnormality (WMA) and significant cerebellar abnormality. Radiological evaluation was performed by an experienced pediatric neuroradiologist (XS) and confirmed by a second (KY), both were masked to all other participant data. A form validated for near-term neuroradiological assessment (Hintz et al., 2015) was used to score WMA (1–4) according to a widely used classification system (Woodward et al., 2006 Horsch et al., 2010; Hintz et al., 2015): (i) extent of WM signal abnormality, (ii) periventricular WM volume loss, (iii) cystic abnormalities, (iv) ventricular dilation, and (v) thinning of the CC. High inter-rater agreement (96–98%) for moderate-severe WMA using this classification was reported (Woodward et al., 2006 Hintz et al., 2015). Significant cerebellar abnormalities included significant cerebellar lesions defined by Hintz et al. and/or significant cerebellar asymmetry of ≥3 mm in the anterior-posterior or medial-lateral direction (Hintz et al., 2015). The structural MRI findings in this cohort were previously reported (Rose et al., 2015).

Diffusion tensor imaging was calculated based on diffusion-weighted images (DWI) obtained along 25 orientations with slice thickness of 3 mm, matrix size of 128 × 128, and 90-degree flip

angle on a 3T MRI (GE Discovery MR750, 8-Channel HD head coil) at LPCH at the end of routine MRI acquisition. A repetition of DTI sequence was successfully collected in 64 of 66 cases. Thus, in 64 subjects, a full scan was motion free. For 2 out of 66 cases, a composite image was generated by selecting the best slices out of two repetitions manually and combining them to a composite image. Infants were swaddled and fed and typically remained asleep during the scan. Sedation typically was not utilized for routine near-term MRI and was not utilized as part of the research protocol.

DTI Processing

A trained inspector selected the best DTI repetition to eliminate MRI scans with artifacts or evidence of motion. As noted above, for 2 out of the 66 cases, due to the lack of usable full repetition, a composite repetition was generated from the best image slices. Eddy current distortions were corrected by applying affine transformation. Skull stripping was performed based on B0 and trace (vectorial sum of diffusivity) maps using a ROI editor, and manually rotated to align with the JHU neonatal template, which is a template based on a neonatal brain atlas integrating DTI data with co-registered anatomical MRI (Oishi et al., 2011). Scans were analyzed in a semi-automated, atlas-based manner, using DTI-studio with settings detailed in Oishi et al. (2011).

Diffusion tensor imaging images were processed using DiffeoMap using FA and trace map to perform a large deformation diffeomorphic metric mapping transformation. Amplitude of trace > 0.006 mm^2/s and FA < 0.15 were considered cerebrospinal fluid (CSF) and gray matter, respectively, and were used to obtain the mask of WM regions. WM regions were then segmented into 126 regions based on the JHU parcellation atlas, and the average FA, MD, AD, and RD values were calculated for each region. The number of regions was then narrowed to apical regions ensuring quality of registration, resulting in 48 regions of both sides in addition to the splenium and genu of the CC, and the overall CC (**Table 2**). Further examination was performed on the FA, MD, AD, and RD values of a total of 99 regions adjusted for postmenstrual age (PMA) at scan.

TABLE 2 | Brain regions, based on JHU parcellation atlas and segmented using DiffeoMap; DTI metrics (FA, MD, AD, RD) were used as features to find sets of three metrics best predicting outcome.

Corpus Callosum	Body of corpus callosum	
	Genu of the corpus callosum	
	Splenium of the corpus callosum	
Bilateral regions:	Amygdala	Middle occipital gyrus
	Angular gyrus	Middle temporal gyrus
	Anterior corona radiata	Parahippocampal gyrus
	Anterior limb of the internal capsule	Postcentral gyrus
	Caudate nucleus	Posterior corona radiata
	Cingular part of cingulum	Posterior limb of the internal capsule
	Cingulum gyrus	Posterior thalamic radiation
	Cuneus	Precentral gyrus
	External capsule	Precuneus
	Fornix	Putamen
	Frontal medial orbital gyrus	Retrolenticular capsule
	Fusiform gyrus	Sagittal stratum
	Globus pallidus	Stria terminalis
	Gyrus rectus	Superior corona radiata
	Hippocampal part of the cingulum	Superior frontal gyrus
	Hippocampus	Superior longitudinal fasciculus
	Inferior frontal gyrus	Superior occipital gyrus
	Inferior fronto-occipital fasciculus	Superior occipitofrontal fasciculus
	Inferior occipital gyrus	Superior parietal gyrus
	Inferior temporal gyrus	Superior temporal gyrus
	Insular cortex	Supramarginal gyrus
	Lateral orbitofrontal gyrus	Tapetum
	Lingual gyrus	Thalamus
	Middle frontal gyrus	Uncinate fasciculus

Statistical Analysis

For each temporal-spatial gait metrics, including velocity, step length, step width, SLS, and Toddle TDI, distinct linear models were generated to examine their correlations with DTI measures. Using an exhaustive search in the feature space, multiple linear regression models were evaluated with leave-one-out cross-validation, L2 regularization, and regularization strength 1.0 to find a set of 3 regions (features) most correlated with gait metrics. Logistic regression models were evaluated with leave-one-out cross-validation, L2 regularization and regularization strength 1.0 on DTI to find a set of 3 regions that best classified high-risk infants scoring worse than one standard deviation from typically developing mean values previously reported (Cahill-Rowley and Rose, 2016a). Best models were selected based on leave-one-out cross-validated, adjusted coefficient of determination (R^2) for linear regression, and leave-one-out cross-validated area under the curve (AUC) of the receiver operator characteristic (ROC) for the binary classification with logistic regression. Logistic regression models were also evaluated on the structural MRI for presence of WMA, cerebellar signal abnormality, cerebellar asymmetry, and intraventricular hemorrhage (IVH, grade 3 or 4) on structural MRI.

Diffusion tensor imaging scalars were adjusted for PMA at scan and normalized to have zero mean and unit variance. To ensure model generalization and robustness, and avoid overfitting, performance measures, i.e., adjusted R^2 and AUC, were evaluated with leave-one-out cross-validation (LOOCV), such that for both regression and classification tasks, N distinct models (N = number of subjects) using the same set of features were evaluated leaving out the n-th subject during the determination of the model parameters. Ultimately, each model was evaluated on the left-out subject, and the N distinct results in pair with their ground truth values were used to calculate the cross-validated performance metrics. For the classification tasks (high-risk vs. low-risk), balanced sensitivity and specificity were

determined by maximizing the sum of the squares of sensitivity and specificity (sensitivity^2 + specificity^2). Coefficients of logistic regression reported in **Table 3** determine the magnitude and direction with which a feature contributed to the probability of considering a subject as high risk. A positive coefficient implies, that a higher feature value increases the risk, whereas a negative coefficient indicates that a higher feature value lowers the risk, and shifts the evaluation of the logistic function toward the normally developing range. Results were obtained using Scikit-learn (Pedregosa et al., 2011) and Statsmodels (Seabold and Perktold, 2010).

RESULTS

Near-term MRI and DTI were collected at 36.6 ± 1.8 weeks postmenstrual age in 66 children born preterm (28.9 ± 2.3 weeks postmenstrual age) with very-low-birth-weight (1090 ± 266 g). Follow-up gait temporal-spatial parameters were collected in 52 children at 20.2 ± 1.0 months adjusted age; all participants had complete neuroimaging and gait data sets. **Table 3** reports the prediction of gait impairment classification based on DTI and MRI using logistic regression with exhaustive feature selection and cross-validation.

Gait impairment was correctly classified for: velocity with 93% sensitivity and 79% specificity (**Figures 1A,B**); right step length with 91% sensitivity and 85% specificity (**Figures 2A,B**); left step length with 93% sensitivity and 76% specificity (**Figures 3A,B**); step width with 85% sensitivity and 80% specificity (**Figures 4A,B**); right SLS with 100% sensitivity and 100% specificity (**Figures 5A,B**); left SLS with 100% sensitivity and 100% specificity (**Figures 6A,B**); and Toddle TDI with 85% sensitivity and 75% specificity (**Table 3**).

Clinical findings on structural MRI were also evaluated for their predictive value (**Table 4**) using logistic regression with LOOCV. Presence of WMA, cerebellar signal abnormality, cerebellar asymmetry, and IVH (grade 3 or 4) identified on MRI did not correctly classify children with impaired gait compared to children with typical gait based on TDI; no clinical findings on structural MRI correctly identified more than one child with a particular gait metric abnormality. Logistic regression of near-term structural MRI results did not correctly classify infants as high-risk for impaired velocity, step width, SLS, or step length. Cross-validation revealed that models built on structural MRI assessments, which only included six metrics, were not sufficiently robust to maintain findings with cross-validation. Thus, impairments in gait were not predicted from traditional MRI findings.

Gait temporal-spatial values were predicted using cross-validated linear regression on near-term DTI with exhaustive feature selection of three brain regions (**Table 5**). The three most predictive brain regions for gait explained 22% of variance in velocity; 34% in step width; 16 and 15% in right and left step length, respectively; 19 and 16% in right and left SLS, respectively; and 16% of variance in Toddle TDI.

TABLE 3 | Classification of gait impairment determined by logistic regression of near-term white matter DTI with exhaustive feature selection and leave-one-out cross-validation.

			Without cross-validation			With cross-validation		
Variable	**Brain region (DTI measure)**	**Coefficients**	**AUC**	**Sensitivity**	**Specificity**	**AUC**	**Sensitivity**	**Specificity**
Velocity	R inferior frontal gyrus (FA)	−3.13	0.93	0.93	0.87	0.90	0.93	0.79
	L hippocampus (AD)	1.98						
	Genu (MD)	2.81						
Step width	L lingual gyrus (FA)	−3.13	0.93	0.85	0.85	0.90	0.85	0.80
	L hippocampus (FA)	1.98						
	R putamen (RD)	2.81						
Step length (R)	Genu (MD)	2.22	0.93	0.91	0.88	0.89	0.91	0.85
	L hippocampus (AD)	−3.60						
	R inferior frontal gyrus (FA)	1.64						
Step length (L)	L supramarginal gyrus (MD)	−1.36	0.85	0.93	0.79	0.80	0.93	0.76
	R superior parietal gyrus (AD)	1.32						
	R hippocampus (MD)	−1.29						
Single-limb support (R)	R fusiform gyrus (FA)	−30.68	1	1	1	1	1	1
	Splenium (AD)	61.98						
	Genu (FA)	−43.26						
Single-limb support (L)	R middle frontal gyrus (RD)	−18.83	1	1	1	1	1	1
	R superior occipital gyrus (RD)	47.97						
	L lateral fronto-orbital gyrus (FA)	33.94						
Toddle TDI	R parahippocampal gyrus (RD)	−0.88	0.88	0.90	0.84	0.83	0.85	0.75
	R posterior corona radiata (MD)	−2.21						
	L sagittal striatum (AD)	1.71						

The three most predictive brain regions for each gait metric are listed. Right (R), Left (L). Significance of all AUC values, $p < 0.0001$.

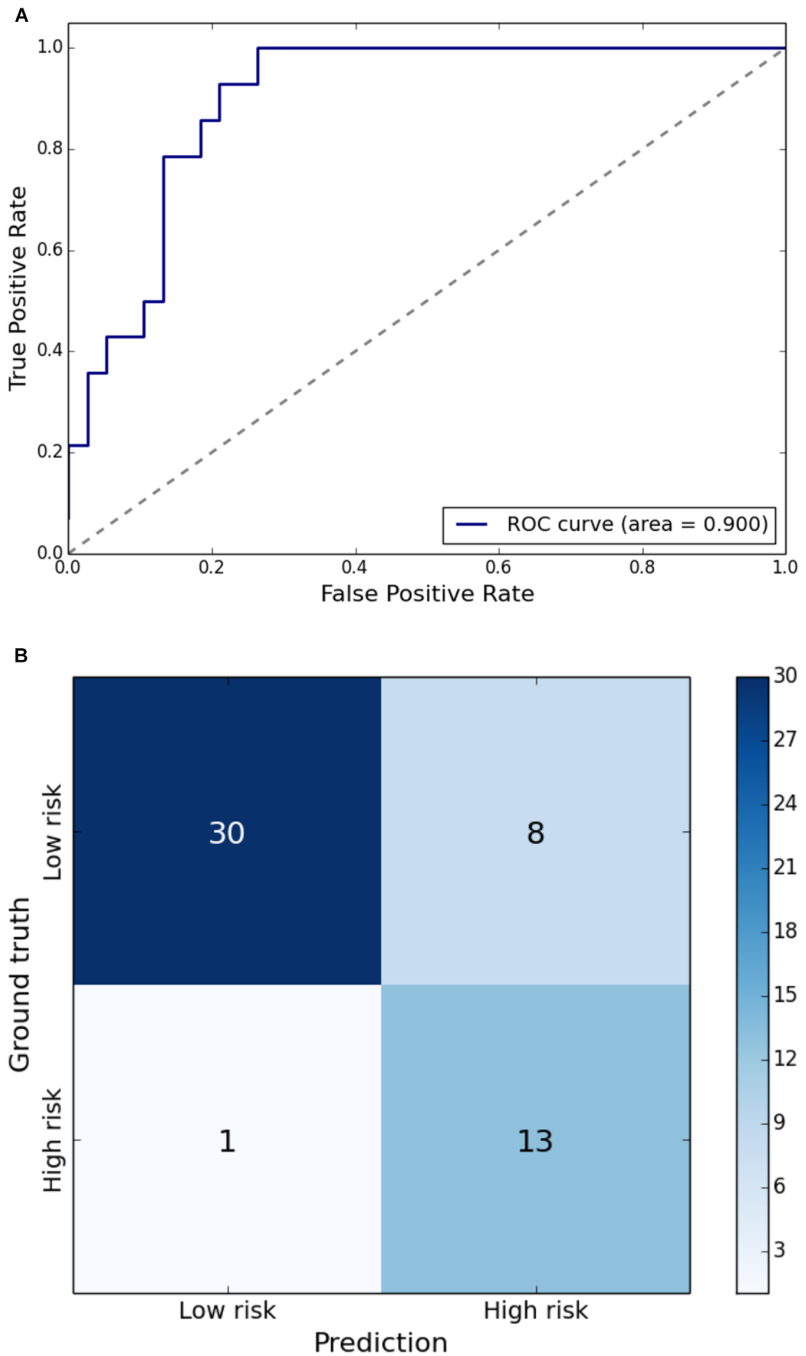

FIGURE 1 | (A) Receiver Operating Characteristic curve of leave-one-out cross-validated classification of toddlers having gait velocity below one standard deviation of the mean. **(B)** Balanced confusion matrix of leave-one-out cross-validated classification of toddlers having gait velocity below one standard deviation of the mean.

DISCUSSION

Statistical learning is an area in statistics, referring to a set of tools for modeling complex datasets. It blends parallel developments in computer science, in particular to machine learning, and has been successfully applied to numerous fields. It is also a promising method to improve prognostic accuracy and guide early treatment of preterm infants. We built supervised statistical models using exhaustive feature search applied on near-term brain microstructure assessed on DTI to predict temporal-spatial gait in preterm toddlers at 18–22 months adjusted age. Due to the multiple comparisons inherent to exhaustive search, leave-one-out cross-validation was applied to reduce over-fitting and optimize robustness of generalization. Application of exhaustive

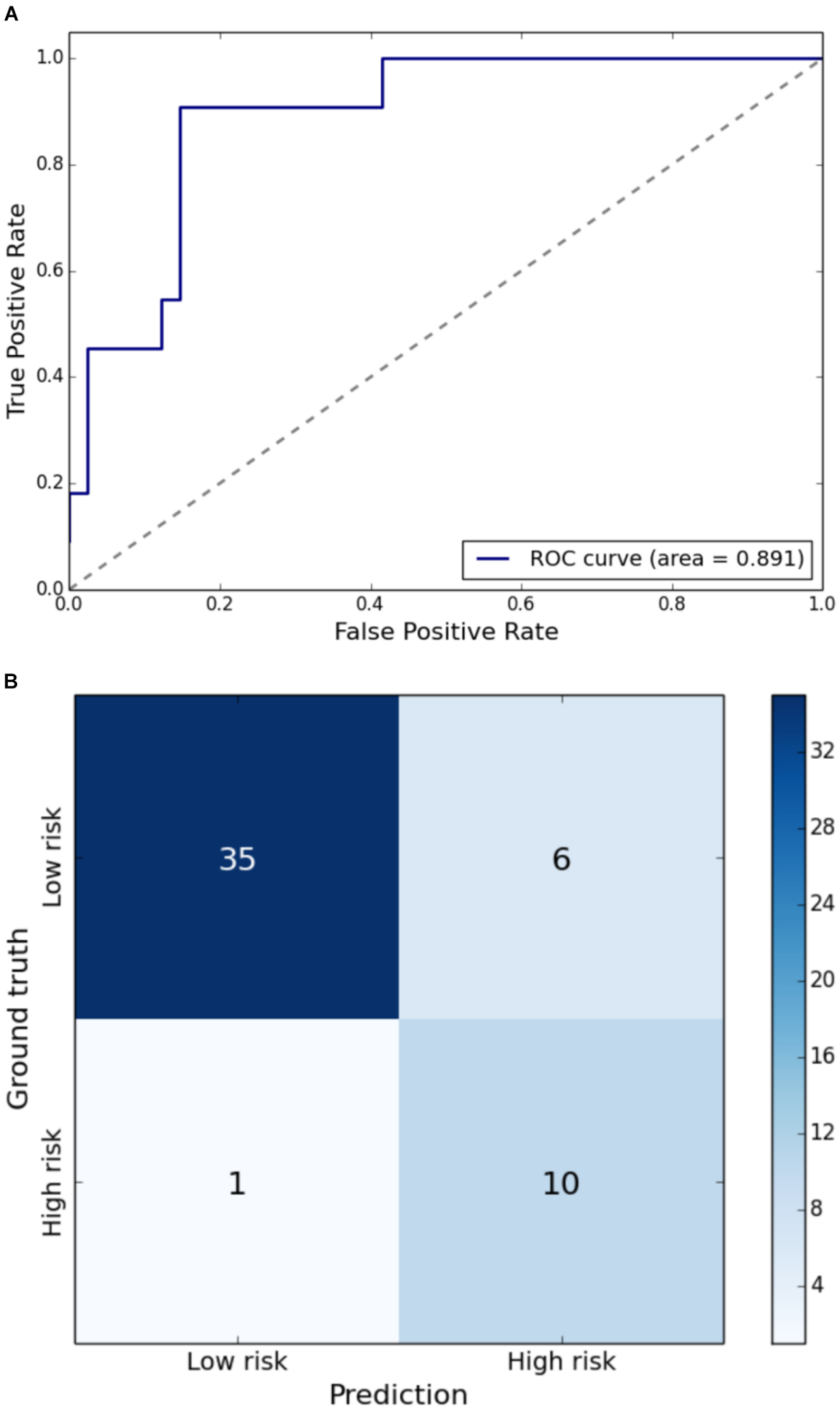

FIGURE 2 | (A) Receiver Operating Characteristic curve of leave-one-out cross-validated classification of toddlers having right step length below one standard deviation of the mean. **(B)** Balanced confusion matrix of leave-one-out cross-validated classification of toddlers having right step length below one standard deviation of the mean.

feature search with cross-validation on DTI generated relatively high predictive values, compared to standard techniques using structural MRI at near-term age.

Infants were classified with high sensitivity and specificity as high-risk for gait impairment based on near-term WM microstructure (**Table 3**). Most commonly, the genu of the CC

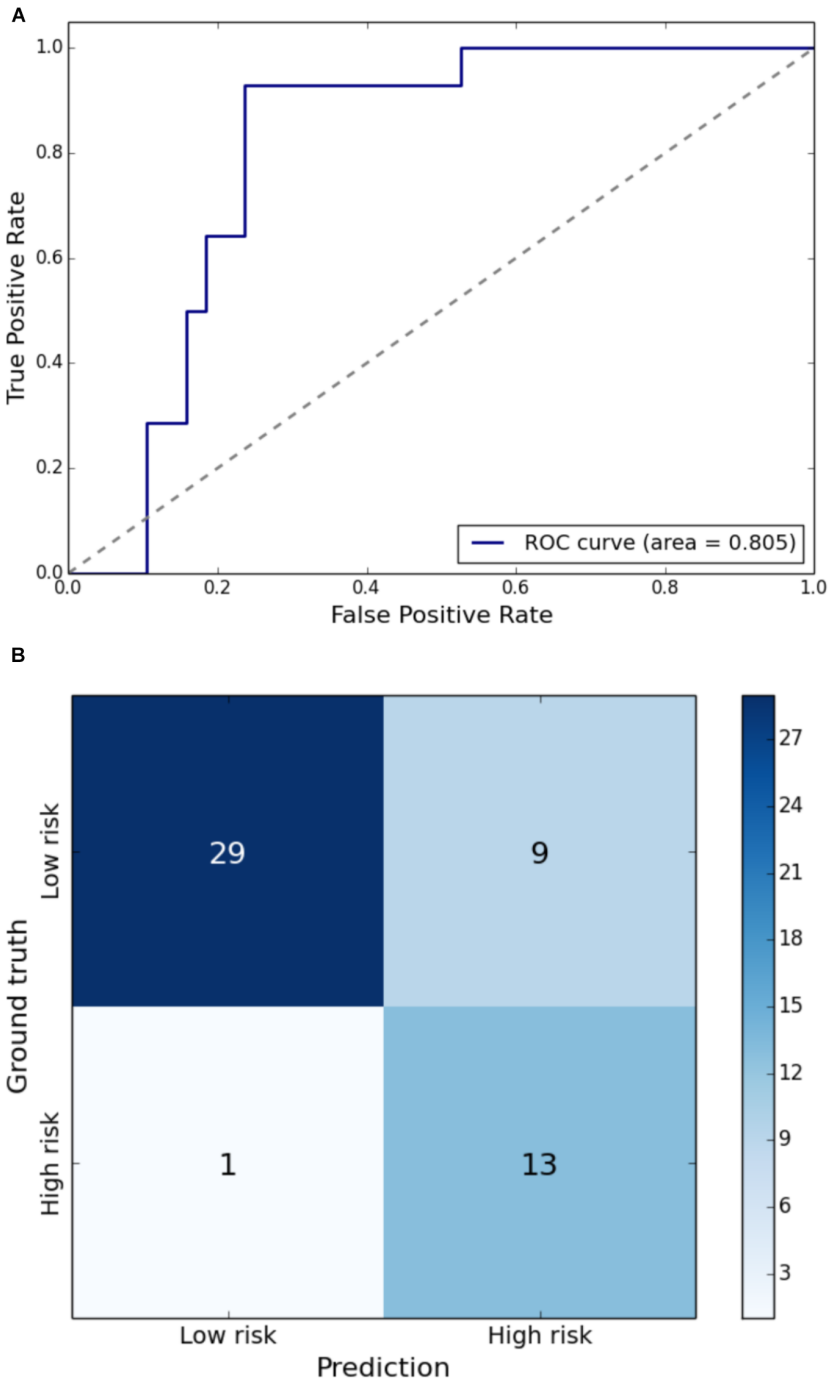

FIGURE 3 | (A) Receiver Operating Characteristic curve of leave-one-out cross-validated classification of toddlers having left step length below one standard deviation of the mean. **(B)** Balanced confusion matrix of leave-one-out cross-validated classification of toddlers having left step length below one standard deviation of the mean.

contributed to best performing logistic and linear models (for 3/6 gait parameters and 4/6 gait parameters, respectively) as one of the three selected features, suggesting its strong predictive value for gait metrics. The CC has been previously found to be associated with neurodevelopmental outcome. Anderson et al. (2006) examined 61 VLBW infants and found that poor growth of the CC length was associated with severe motor delay and cerebral palsy by age 2. Mathew et al. (2013) found associations between WM microstructure of the CC as assessed on DTI and motor function in eight very preterm infants. Rose et al. (2008) examined 23 preterm infants and found reduced FA mainly within the posterior regions of the CC. Malavolti et al. (2017)

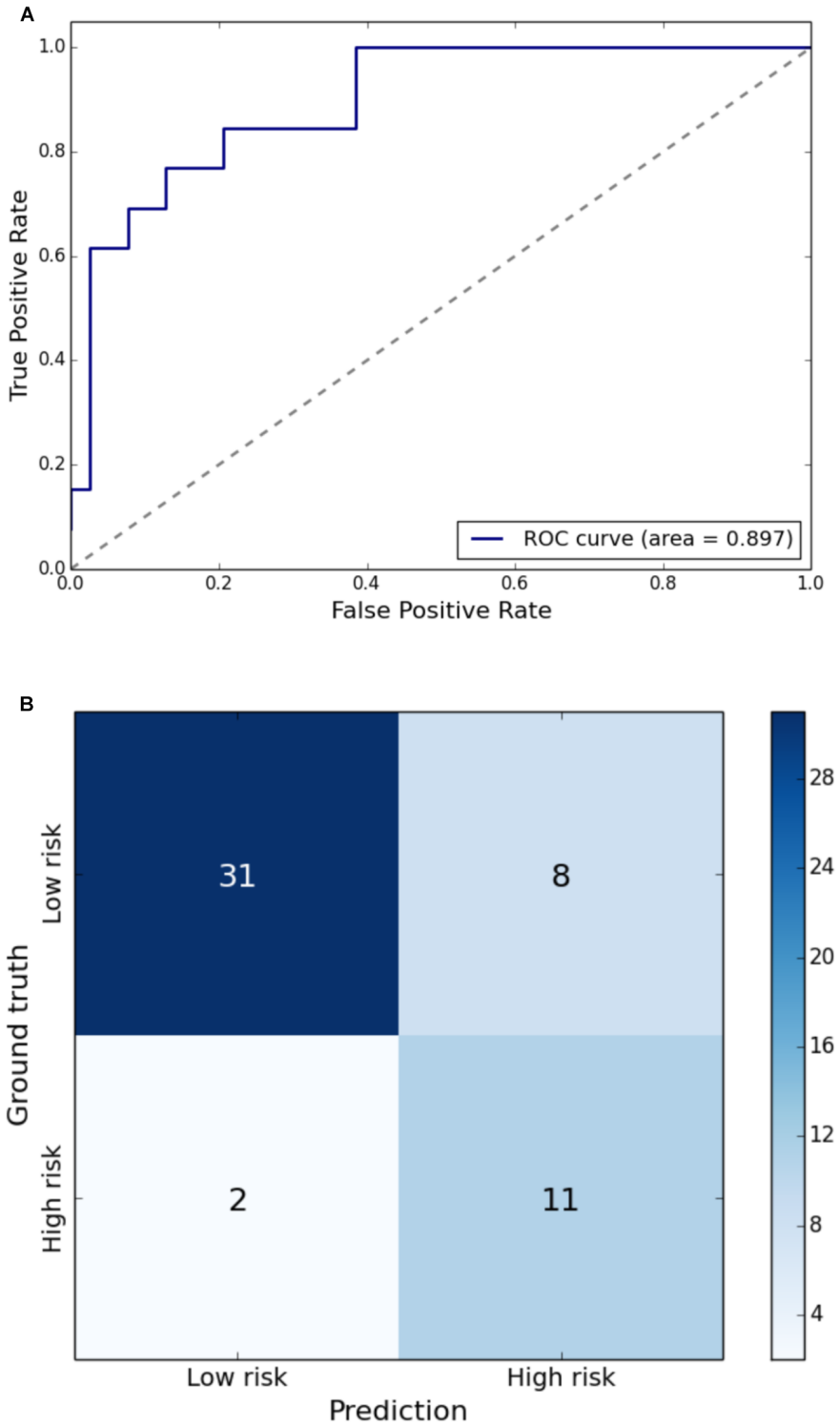

FIGURE 4 | (A) Receiver Operating Characteristic curve of leave-one-out cross-validated classification of toddlers having step width above one standard deviation of the mean. **(B)** Balanced confusion matrix of leave-one-out cross-validated classification of toddlers having step width above one standard deviation of the mean.

found that adverse motor outcome at 18 months corrected age was associated with smaller neonatal CC size in the posterior subdivision ($p = 0.003$).

Both the hippocampus and the inferior frontal gyrus contributed to several best performing logistic and linear models. The hippocampus contributed to logistic regression of 4/6 gait

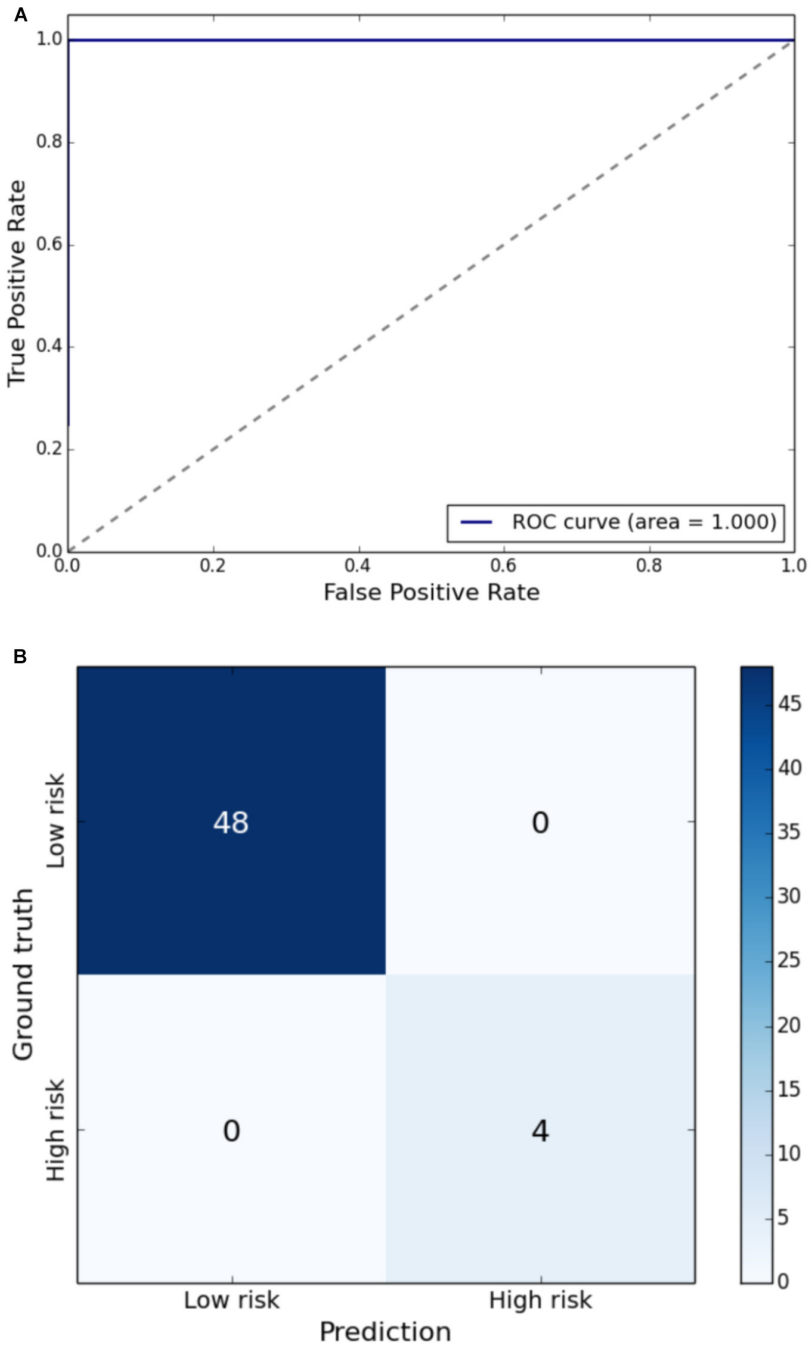

FIGURE 5 | (A) Receiver Operating Characteristic curve of leave-one-out cross-validated classification of toddlers having right SLS below one standard deviation of the mean. **(B)** Balanced confusion matrix of leave-one-out cross-validated classification of toddlers having right SLS below one standard deviation of the mean.

parameters (**Table 3**) and is involved in working memory. The inferior frontal gyrus contributed to logistic regression of 3/6 gait parameters (**Table 3**) and to linear regression of 3/6 gait parameters (**Table 5**), and has previously been shown to control motor responses (Swick et al., 2008).

Toddler's with the gait impairment of SLS time were most accurately predicted from near-term brain microstructure. This may be explained because as a toddler learns to walk, achieving sufficient SLS requires single limb strength and balance as well as bilateral stability and symmetry. As a fundamental element of human biped gait, SLS may be a sensitive marker of toddler gait impairment influenced by early neural correlates that are evolutionarily and developmentally conserved. Classification with the logistic function fitted on the

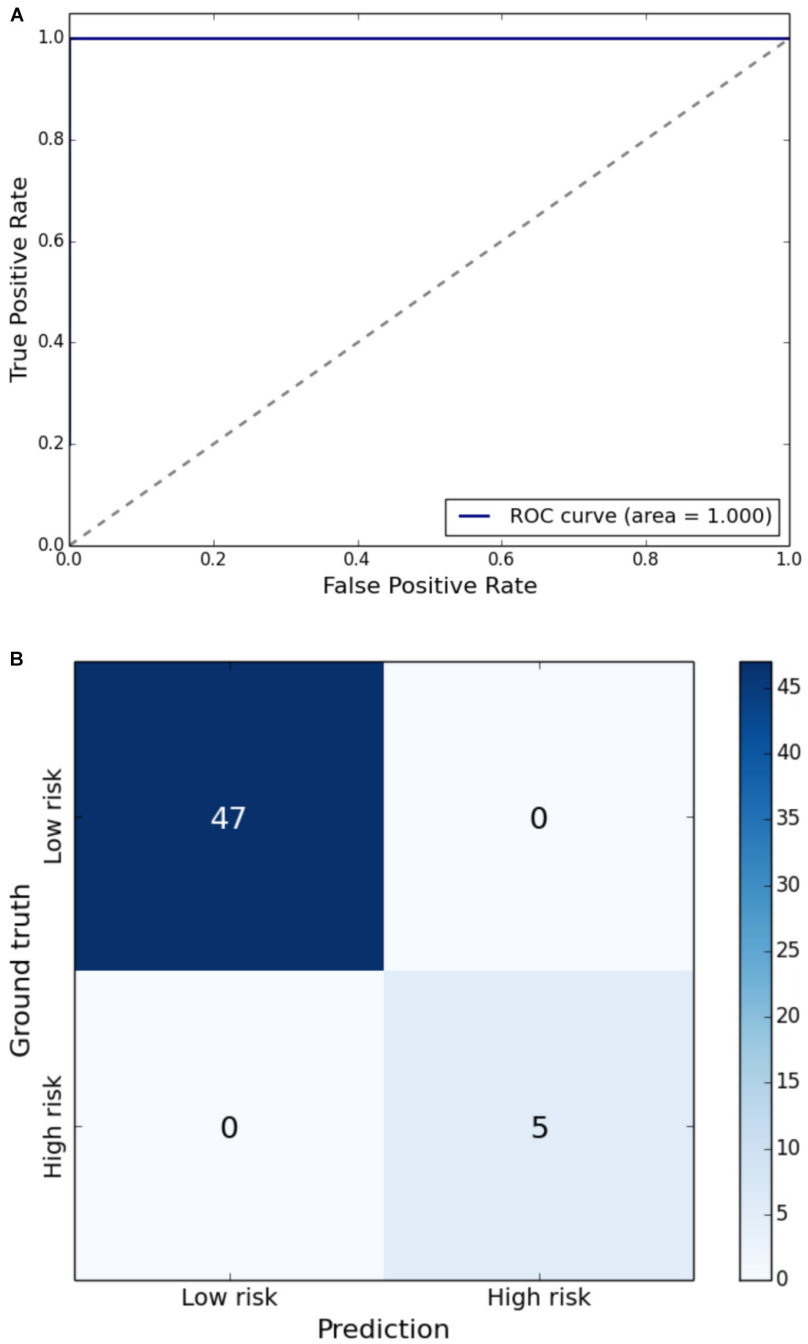

FIGURE 6 | (A) Receiver Operating Characteristic curve of leave-one-out cross-validated classification of toddlers having left SLS below one standard deviation of the mean. **(B)** Balanced confusion matrix of leave-one-out cross-validated classification of toddlers having left SLS below one standard deviation of the mean.

right fusiform gyrus FA, splenium AD, and genu FA predicted right SLS with 100% sensitivity and 100% specificity; logistic function fitted on the right middle frontal gyrus RD, right superior occipital RD, and left lateral fronto-orbital gyrus FA predicted left SLS with 100% sensitivity and 100% specificity (**Table 3**). In addition, linear regression of left anterior limb of the internal capsule MD, genu RD, and right inferior frontal gyrus RD was most predictive of right SLS; and right retrolenticular part of the internal capsule RD, genu RD, and right superior occipital gyrus FA were most predictive of left SLS (**Table 5**).

Step width was also well predicted in the present study, the linear regression with exhaustive feature search and cross-validation found that the left and right globus pallidus, along with the right tapetum, were predictive of step width, a gait metric that typically reflects development of postural balance.

TABLE 4 | Prediction from near-term brain DTI and MRI of gait impairment at 18–22 months.

	Velocity		Step width		Step length				Single-limb support				Toddle TDI	
					Right		Left		Right		Left			
Methods	**True +**	**False +**	**True +**	**False +**	**True +**	**False +**	**True +**	**False +**	**True +**	**False +**	**True +**	**False +**	**True +**	**False +**
DTI logistic regression	13/14	5/38	11/13	6/39	10/11	5/41	13/14	8/38	4/4	0/48	5/5	0/47	18/20	5/32
DTI logistic regression with cross-validation	13/14	8/38	11/13	8/39	10/11	6/41	13/14	9/38	4/4	0/48	5/5	0/47	17/20	8/32
White matter abnormality	0/14	3/38	1/13	2/39	0/11	3/41	0/14	3/38	0/4	3/48	0/5	3/47	0/20	3/32
Cerebellar signal abnormality	0/14	6/38	1/13	5/39	0/11	6/41	1/14	5/38	0/4	6/48	0/5	6/47	0/20	6/32
Cerebellar asymmetry	1/14	4/38	1/13	4/39	0/11	5/41	0/14	5/38	0/4	5/48	0/5	5/47	1/20	4/32
Intraventricular hemorrhage, grade 3 or 4	0/14	2/38	0/13	2/39	0/11	2/41	0/14	2/38	0/4	2/48	0/5	2/47	0/20	2/32

Logistic regression with exhaustive feature selection was able to predict gait impairment, while standard MRI findings were not. Single-limb support (SLS) was perfectly predicted by logistic regression, bilaterally.

Coefficients of logistic regression models (**Table 3**) reinforce prior findings, that in white matter regions with negligible crossing fibers, as compared to gray matter regions, fiber coherence is well measured and reflects neurodevelopment. The direction of the DTI metrics of FA, MD, and AD values of the CC were as expected in affecting the probability of being high risk. Gray matter features provide less ease of interpretation due to higher cortical connectivity, relatively later development, and associated variability in direction of DTI metrics.

TABLE 5 | Multiple linear regression models using exhaustive feature selection found the set of three brain regions most correlated with gait metrics.

		Without cross-validation	With cross-validation
Variable	**Brain regions**	**Adj. R^2**	**Adj. R^2**
Velocity	L parahippocampal cingulum (RD)	0.32	0.22
	Genu (RD)		
	R inferior frontal gyrus (FA)		
Step width	R tapetum (FA)	0.45	0.34
	L globus pallidus (AD)		
	R globus pallidus (RD)		
Step length (R)	L cingulum cingular part (AD)	0.28	0.16
	L cuneus (FA)		
	L superior occipital gyrus (FA)		
Step length (L)	L supramarginal gyrus (MD)	0.28	0.15
	L inferior temporal gyrus (FA)		
	Genu (RD)		
Single-limb support (R)	L anterior limb of the internal capsule (MD)	0.32	0.19
	Genu (RD)		
	R inferior frontal gyrus (RD)		
Single-limb support (L)	R retrolenticular part of internal capsule (RD)	0.30	0.16
	Genu (RD)		
	R superior occipital gyrus (FA)		
Toddle TDI	L insular cortex (RD)	0.27	0.16
	L inferior temporal gyrus (FA)		
	L anterior limb of the internal capsule (RD)		

Right (R), Left (L).

We found that prediction by the models using DTI outperformed models using structural MRI (**Table 4**), consistent with prior studies that found DTI provided higher predictive value for neurodevelopmental outcome compared to structural MRI for Arzoumanian et al. (2003), Rose et al. (2007, 2009), De Bruïne et al. (2013). In our comparison, however, we used metrics that were derived by manual inspection from structural MRI. In further studies, we encourage comparing and examining structural MRI that is segmented and assessed on a regional basis similar to our approach with DTI. Analysis with DTI using the statistical learning approach of exhaustive feature selection and cross-validation has potential to improve prognostic accuracy of neonatal neuroimaging. The clinical feasibility of using DTI is increased by advances in automated data processing that improve its ease of use, repeatability, and thus prognostic value. In this study we used a linear model logistic regression and therefore both its implementation and interpretation are relatively straightforward. These methods could be implemented clinically to improve prognostic accuracy, if replicated in a larger population. Individual patient DTI metrics of most predictive brain regions could be input into a simple spreadsheet to identify infants at high risk for cognitive and motor impairment.

We previously reported data from the same cohort, and evaluated velocity and SLS with respect to WM and cerebellar abnormality as assessed on structural MRI, and in 6 different subcortical WM regions assessed on DTI, using standard partial correlation analyses (Rose et al., 2015). The MRI findings did not correlate with velocity or SLS; genu DTI did correlate with both velocity and SLS. DTI metrics of the other five regions (splenium, anterior limb of the internal capsule, posterior limb of the internal capsule, thalamus, and globus pallidus) did not.

In the current study, the genu and splenium of CC, as well as fusiform gyrus, superior-occipital gyrus, lateral fronto-orbital gyrus, and right middle frontal gyrus contributed to 100%

accurate prediction of SLS impairment. Further, the anterior limb of the internal capsule and retrolenticular part of the internal capsule and inferior frontal gyrus also contributed to explaining approximately 15% of the variation of toddler SLS, a sensitive gait metric that reflects gait stability, weight bearing, and symmetry. These findings suggest that a set of brain regions taken together may be more sensitive to outcome than a single region in isolation.

To ensure ease of interpretability we used linear models, which limit accuracy due to the highly non-linear nature of the solution space. Study limitations also include that we analyzed a relatively small cohort which requires the use of statistical tools that are less robust compared to state-of-the-art machine learning approaches (i.e., deep learning), and that classification on imbalanced dataset can be biased, even when using ROC-AUC or precision and recall as performance metrics. Furthermore, evaluation of cortical WM can be confounded by imaging resolution and signal-to-noise ratio. Methods outlined in this study need to be validated on larger preterm populations.

Applying machine learning algorithms on near-term regional WM microstructure may help identify risk of neurodevelopmental delay, guide early intervention and ultimately, may inform neuroprotective treatment to improve quality of life for preterm children. In this study, we employed an exhaustive feature selection algorithm to identify a set of 3 brain regions that best predicted outcomes. Results indicate a relatively high prognostic value for temporal-spatial gait parameters, in particular SLS, and warrant further investigation in larger preterm populations.

DATA AVAILABILITY

The datasets generated for this study are available on request to the corresponding author.

ETHICS STATEMENT

This study was approved by the Stanford University Institutional Review Board and consent was obtained from parents or guardians.

AUTHOR CONTRIBUTIONS

KC-R, RV, JR, and KS contributed to the concept, data collection, data analysis and interpretation, and writing the manuscript. KS, KY, and DS contributed to the concept, data analysis and interpretation, and writing the manuscript.

FUNDING

This research was supported by the Chiesi Foundation, Parma Italy; NIH Clinical and Translational Science Award UL!RR025744 for the Stanford Center for Clinical and Translational Education and Research (Spectrum) and for Stanford Center for Clinical Informatics, Stanford Translational Research Integrated Database Environment (STRIDE); Lucile Packard Foundation for Children's Health; NSF Graduate Research Fellowship grant no. DGE-1147470, and by the Mary Baracchi Research Fund, Lucile Packard Children's Hospital at Stanford. The authors have stated that they have no interests that might be perceived as posing a conflict or bias and there was no involvement of funders in the study design, data collection, analysis, article preparation or publication decisions.

ACKNOWLEDGMENTS

We wish to thank Dr. John Tamaresis, Dr. Ron Cohen, Elizabeth Loi, and Dr. Megan Thompson for valuable discussions and assistance.

REFERENCES

Aeby, A., De Tiège, X., Creuzil, M., David, P., Balériaux, D., Van Overmeire, B., et al. (2013). Language development at 2 years is correlated to brain microstructure in the left superior temporal gyrus at term equivalent age: a diffusion tensor imaging study. *NeuroImage* 78, 145–151. doi: 10.1016/j.neuroimage.2013.03.076

Alvarez, R. P., Chen, G., Bodurka, J., Kaplan, R., and Grillon, C. (2011). Phasic and sustained fear in humans elicits distinct patterns of brain activity. *Neuroimage* 55, 389–400. doi: 10.1016/j.neuroimage.2010.11.057

Anderson, N. G., Laurent, I., Woodward, L. J., and Inder, T. E. (2006). Detection of impaired growth of the corpus callosum in premature infants. *Pediatrics* 118, 951–960. doi: 10.1542/peds.2006-0553

Anderson, P. J., Treyvaud, K., Neil, J. J., Cheong, J. L., Hunt, R. W., Thompson, D. K., et al. (2017). Associations of newborn brain magnetic resonance imaging with long-term neurodevelopmental impairments in very preterm children. *J. Pediatr.* 187, 58–65. doi: 10.1016/j.jpeds.2017.04.059

Arzoumanian, Y., Mirmiran, M., Barnes, P. D., Woolley, K., Ariagno, R. L., Moseley, M. E., et al. (2003). Diffusion tensor brain imaging findings at term-equivalent age may predict neurologic abnormalities in low birth weight preterm infants. *Am. J. Neuroradiol.* 24, 1646–1653.

Basser, P. J., and Pierpaoli, C. (2011). Microstructural and physiological features of tissues elucidated by quantitative-diffusion-tensor MRI. *J. Magn. Reson.* 213, 560–570. doi: 10.1016/j.jmr.2011.09.022

Brody, B. A., Kinney, H. C., Kloman, A. S., and Gilles, F. H. (1987). Sequence of central nervous system myelination in human infancy. I. An autopsy study of myelination. *J. Neuropathol. Exp. Neurol.* 46, 283–301. doi: 10.1097/00005072-198705000-00005

Cahill-Rowley, K., and Rose, J. (2016a). Temporal-spatial gait parameters and neurodevelopment in very-low-birth-weight preterm toddlers at 18–22 months. *Gait Posture* 45, 83–89. doi: 10.1016/j.gaitpost.2016.01.002

Cahill-Rowley, K., and Rose, J. (2016b). Toddle temporal-spatial deviation index: assessment of pediatric gait. *Gait Posture* 49, 226–231. doi: 10.1016/j.gaitpost.2016.06.040

Counsell, S. J., Maalouf, E. F., Fletcher, A. M., Duggan, P., Battin, M., Lewis, H. J., et al. (2002). MR imaging assessment of myelination in the very preterm brain. *Am. J. Neuroradiol.* 23, 872–881.

De Bruïne, F. T., Van Wezel-Meijler, G., Leijser, L. M., Steggerda, S. J., Van Den Berg-Huysmans, A. A., Rijken, M., et al. (2013). Tractography of white-matter tracts in very preterm infants: a 2-year follow-up study. *Dev. Med. Child Neurol.* 55, 427–433. doi: 10.1111/dmcn.12099

Dubois, J., Dehaene-Lambertz, G., Perrin, M., Mangin, J. F., Cointepas, Y., Duchesnay, E., et al. (2008). Asynchrony of the early maturation of white matter

bundles in healthy infants: quantitative landmarks revealed noninvasively by diffusion tensor imaging. *Hum. Brain Mapp.* 29, 14–27. doi: 10.1002/hbm.20363

Dubois, J., Hertz-Pannier, L., Dehaene-Lambertz, G., Cointepas, Y., and Le Bihan, D. (2006). Assessment of the early organization and maturation of infants' cerebral white matter fiber bundles: a feasibility study using quantitative diffusion tensor imaging and tractography. *Neuroimage* 30, 1121–1132. doi: 10.1016/j.neuroimage.2005.11.022

Hintz, S. R., Barnes, P. D., Bulas, D., Slovis, T. L., Finer, N. N., Wrage, L. A., et al. (2015). Neuroimaging and neurodevelopmental outcome in extremely preterm infants. *Pediatrics* 135, e32–e42. doi: 10.1542/peds.2014-0898

Horsch, S., Skiöld, B., Hallberg, B., Nordell, B., Nordell, A., Mosskin, M., et al. (2010). Cranial ultrasound and MRI at term age in extremely preterm infants. *Arch. Dis. Child. Fetal Neonatal Ed.* 95, F310–F314. doi: 10.1136/adc.2009.161547

Huang, H., Zhang, J., Wakana, S., Zhang, W., Ren, T., Richards, L. J., et al. (2006). White and gray matter development in human fetal, newborn and pediatric brains. *Neuroimage* 33, 27–38. doi: 10.1016/j.neuroimage.2006.06.009

Hüppi, P. S., Maier, S. E., Peled, S., Zientara, G. P., Barnes, P. D., Jolesz, F. A., et al. (1998). Microstructural development of human newborn cerebral white matter assessed in vivo by diffusion tensor magnetic resonance imaging. *Pediatr. Res.* 44, 584–590. doi: 10.1203/00006450-199810000-00019

Kinney, H. C., Karthigasan, J., Borenshteyn, N. I., Flax, J. D., and Kirschner, D. A. (1994). Myelination in the developing human brain: biochemical correlates. *Neurochem. Res.* 19, 983–996. doi: 10.1007/bf00968708

Malavolti, A. M., Chau, V., Brown-Lum, M., Poskitt, K. J., Brant, R., Synnes, A., et al. (2017). Association between corpus callosum development on magnetic resonance imaging and diffusion tensor imaging, and neurodevelopmental outcome in neonates born very preterm. *Dev. Med. Child Neurol.* 59, 433–440. doi: 10.1111/dmcn.13364

Mathew, P., Pannek, K., Snow, P., D'Acunto, M. G., Guzzetta, A., Rose, S. E., et al. (2013). Maturation of corpus callosum anterior midbody is associated with neonatal motor function in eight preterm-born infants. *Neural Plast.* 2013:359532. doi: 10.1155/2013/359532

Miller, S. P., and Ferriero, D. M. (2009). From selective vulnerability to connectivity: insights from newborn brain imaging. *Trends Neurosci.* 32, 496–505. doi: 10.1016/j.tins.2009.05.010

Mukherjee, P., Miller, J. H., Shimony, J. S., Philip, J. V., Nehra, D., Snyder, A. Z., et al. (2002). Diffusion-tensor MR imaging of gray and white matter development during normal human brain maturation. *Am. J. Neuroradiol.* 23, 1445–1456.

Nossin-Manor, R., Card, D., Morris, D., Noormohamed, S., Shroff, M. M., Whyte, H. E., et al. (2013). Quantitative MRI in the very preterm brain: assessing tissue organization and myelination using magnetization transfer, diffusion tensor and T1 imaging. *Neuroimage* 64, 505–516. doi: 10.1016/j.neuroimage.2012.08.086

Oishi, K., Mori, S., Donohue, P. K., Ernst, T., Anderson, L., Buchthal, S., et al. (2011). Multi-contrast human neonatal brain atlas: application to normal neonate development analysis. *Neuroimage* 56, 8–20. doi: 10.1016/j.neuroimage.2011.01.051

Pedregosa, F., Varoquaux, G., Gramfort, A., Michel, V., Thirion, B., Grisel, O., et al. (2011). Scikit-learn: machine learning in Python. *J. Mach. Learn. Res.* 12, 2825–2830.

Rose, J., Butler, E. E., Lamont, L. E., Barnes, P. D., Atlas, S. W., and Stevenson, D. K. (2009). Neonatal brain structure on MRI and diffusion tensor imaging, sex, and neurodevelopment in very-low-birthweight preterm children. *Dev. Med. Child Neurol.* 51, 526–535. doi: 10.1111/j.1469-8749.2008.03231.x

Rose, J., Cahill-Rowley, K., Vassar, R., Yeom, K. W., Stecher, X., Stevenson, D. K., et al. (2015). Neonatal brain microstructure correlates of neurodevelopment and gait in preterm children 18–22 mo of age: an MRI and DTI study. *Pediatr. Res.* 78, 700–708. doi: 10.1038/pr.2015.157

Rose, J., Mirmiran, M., Butler, E. E., Lin, C. Y., Barnes, P. D., Kermoian, R., et al. (2007). Neonatal microstructural development of the internal capsule on diffusion tensor imaging correlates with severity of gait and motor deficits. *Dev. Med. Child Neurol.* 49, 745–750. doi: 10.1111/j.1469-8749.2007.00745.x

Rose, J., Vassar, R., Cahill-Rowley, K., Guzman, X. S., Stevenson, D. K., and Barnea-Goraly, N. (2014). Brain microstructural development at near-term age in very-low-birth-weight preterm infants: an atlas-based diffusion imaging study. *Neuroimage* 86, 244–256. doi: 10.1016/j.neuroimage.2013.09.053

Rose, S. E., Hatzigeorgiou, X., Strudwick, M. W., Durbridge, G., Davies, P. S., and Colditz, P. B. (2008). Altered white matter diffusion anisotropy in normal and preterm infants at term-equivalent age. *Magn. Reson. Med.* 60, 761–767. doi: 10.1002/mrm.21689

Schadl, K., Vassar, R., Cahill-Rowley, K., Yeom, K. W., Stevenson, D. K., and Rose, J. (2018). Prediction of cognitive and motor development in preterm children using exhaustive feature selection and cross-validation of near-term white matter microstructure. *Neuroimage Clin.* 17, 667–679. doi: 10.1016/j.nicl.2017.11.023

Seabold, S., and Perktold, J. (2010). "Statsmodels: econometric and statistical modeling with python," in *Proceedings of the 9th Python in Science Conference* (Austin: Scipy society), 61.

Spittle, A. J., Cheong, J., Doyle, L. W., Roberts, G., Lee, K. J., Lim, J., et al. (2011). Neonatal white matter abnormality predicts childhood motor impairment in very preterm children. *Dev. Med. Child Neurol.* 53, 1000–1006. doi: 10.1111/j.1469-8749.2011.04095.x

Swick, D., Ashley, V., and Turken, U. (2008). Left inferior frontal gyrus is critical for response inhibition. *BMC Neurosci.* 9:102. doi: 10.1186/1471-2202-9-102

Van Kooij, B. J., van Pul, C., Benders, M. J., van Haastert, I. C., de Vries, L. S., and Groenendaal, F. (2011). Fiber tracking at term displays gender differences regarding cognitive and motor outcome at 2 years of age in preterm infants. *Pediatr. Res.* 70, 626–632. doi: 10.1203/PDR.0b013e318232a963

Williams, J., Lee, K. J., and Anderson, P. J. (2010). Prevalence of motor-skill impairment in preterm children who do not develop cerebral palsy: a systematic review. *Dev. Med. Child Neurol.* 52, 232–237. doi: 10.1111/j.1469-8749.2009.03544.x

Woodward, L. J., Anderson, P. J., Austin, N. C., Howard, K., and Inder, T. E. (2006). Neonatal MRI to predict neurodevelopmental outcomes in preterm infants. *N Engl. J. Med.* 355, 685–694. doi: 10.1056/nejmoa053792

Woodward, L. J., Clark, C. A., Bora, S., and Inder, T. E. (2012). Neonatal white matter abnormalities an important predictor of neurocognitive outcome for very preterm children. *PLoS One* 7:e51879. doi: 10.1371/journal.pone.0051879

Conflict of Interest Statement: The authors declare that the research was conducted in the absence of any commercial or financial relationships that could be construed as a potential conflict of interest.

frontiers in Human Neuroscience

BRIEF RESEARCH REPORT
published: 24 September 2019
doi: 10.3389/fnhum.2019.00334

Relationship Between Integrity of the Corpus Callosum and Bimanual Coordination in Children With Unilateral Spastic Cerebral Palsy

Ya-Ching Hung[1], Maxime T. Robert[2,3], Kathleen M. Friel[3] and Andrew M. Gordon[2]*

[1] Department of Family, Nutrition, and Exercise Sciences, Queens College, The City University of New York, New York, NY, United States, [2] Department of Biobehavioral Sciences, Teachers College, Columbia University, New York, NY, United States, [3] Burke Neurological Institute, Weill Cornell Medicine, White Plains, NY, United States

Children with unilateral spastic cerebral palsy (USCP) have shown impaired bimanual coordination. The corpus callosum (CC) connects the two hemispheres and is critical for tasks that require inter-hemisphere communication. The relationship between the functional bimanual coordination impairments and structural integrity of the CC is unclear. We hypothesized that better integrity of the CC would relate to better bimanual coordination performance during a kinematic bimanual drawer-opening task. Thirty-nine children with USCP (Age: 6–17 years old; MACS levels: I-III) participated in the study. Measurement of the CC integrity was performed using diffusion tensor imaging. The CC was measured as a whole and was also divided into three regions: genu, midbody, and splenium. Fractional anisotropy, axial diffusivity (AD), radial diffusivity, mean diffusivity, number of voxels, and number of streamlines were evaluated in whole and within each region of the CC. 3-D kinematic analyses of bimanual coordination were also assessed while children performed the bimanual task. There were negative correlations between bimanual coordination measures of total movement time and AD of whole CC (p = 0.037), number of streamlines and voxels of splenium (p = 0.038, 0.032, respectively); goal synchronization and AD of whole CC (p = 0.04), and number of streamlines and voxels of splenium (p = 0.001, 0.01, respectively). The current results highlight the possible connection between the integrity of the CC, especially between the splenium region and temporal bimanual coordination performance for children with USCP.

Keywords: corpus callosum, pediatric, diffusion MRI, kinematics, upper extremity, cerebral palsy

OPEN ACCESS

Edited by:
Jessica Rose,
Stanford University, United States

Reviewed by:
Kenichi Oishi,
Johns Hopkins University, United States
Rachel Vassar,
University of California, San Francisco, United States

****Correspondence:***
Ya-Ching Hung
yaching.hung@qc.cuny.edu

Specialty section:
This article was submitted to Motor Neuroscience, a section of the journal Frontiers in Human Neuroscience

Received: *20 June 2019*
Accepted: *10 September 2019*
Published: *24 September 2019*

Citation:
Hung Y-C, Robert MT, Friel KM and Gordon AM (2019) Relationship Between Integrity of the Corpus Callosum and Bimanual Coordination in Children With Unilateral Spastic Cerebral Palsy. Front. Hum. Neurosci. 13:334. doi: 10.3389/fnhum.2019.00334

INTRODUCTION

Children with unilateral spastic cerebral palsy (USCP) have early brain damage that leads to various motor and sensory impairments particularly on their more-affected side, such as slower movement and impaired hand grasping control (e.g., Eliasson et al., 1995; Forssberg et al., 1999; Gordon et al., 2003; Steenbergen et al., 2008). Severity of impairments on the more-affected hand has been showed to be associated with poorer bimanual coordination (Hung et al., 2004). Studies of children with USCP also indicated impaired bimanual hand function performance using clinical

tests [e.g., assisting hand assessment (AHA)] and kinematic tasks (e.g., Utley and Sugden, 1998; Hung et al., 2004, 2010; Utley et al., 2004; Gaillard et al., 2018). Kinematic analysis showed that bimanual coordination impairments are associated with reduced temporal coordination between the two hands during symmetric and asymmetric bimanual tasks in children with USCP (e.g., Utley and Sugden, 1998; Hung et al., 2004, 2010; Utley et al., 2004). All of these movement impairments affect their ability to perform daily functional activities and their independence (e.g., Lee, 2017).

It is essential to better understand the connection between brain white matter integrity and movement performances for children with USCP to better predict their prognosis and to develop specific effective treatments. Reid et al. (2015) indicated that severe white matter loss of both hemispheres and the corpus callosum (CC) measured by magnetic resonance imaging (MRI) is associated with poor gross motor function [gross motor function classification (GMFCS)]. They further suggested that MRI may not be sensitive enough to detect microstructural impairments such as connectivity within the white matter. More advanced neuroimaging techniques such as diffusion tensor imaging (DTI) provides a more sensitive measure of white matter microstructure allowing the reconstruction of neuronal pathways (Mori et al., 1999). Diffusion parameters such as number of streamlines, number of voxels, and fractional anisotropy (FA, directional preference of white matter water molecular diffusion measure; higher value reflecting better axonal integrity) are often reported in studies on individuals with USCP (e.g., Thomas et al., 2005). Children with USCP were found to have decreased fiber count on the corticobulbar tract, increased mean diffusivity (MD, degree of restriction to diffusion of white matter water molecules irrespective to direction; lower value reflecting better axonal integrity) and decreased FA on the primary white matter lesion site (e.g., Thomas et al., 2005). Cortico-spinal tract diffusion properties (lower FA and higher MD) were also shown to be correlated with the severity of movement impairments (Kuczynski et al., 2018).

Using diffusion tensor imaging, Weinstein et al. (2014) showed that poorer integrity of the CC is associated with more-severe unimanual and bimanual hand function evaluated by clinical measures of AHA and children's hand experience questionnaire. CC is the main pathway between the hemispheres. A larger CC size has been shown to be related to better motor performance in children with periventricular leukomalacia and children born prematurely (Davatzikos et al., 2003; Rademaker et al., 2004; Pannek et al., 2014). The communication role between the hemispheres of the CC is especially important for motor control involving bimanual coordination (see review, Bloom and Hynd, 2005). The less-affected hand was suggested to compensate for the more affected hand during some bimanual tasks for children with USCP (e.g., Utley and Sugden, 1998; Hung et al., 2004, 2010; Utley et al., 2004). Such compensatory strategies between the two hands would depend on interhemispheric communication and should correlate to microstructure impairments of the CC.

In our previous studies, children with USCP showed impaired temporal bimanual coordination during a functional bimanual drawer task using kinematic analysis (Hung et al., 2004, 2010). The test was sensitive in order to identify differences in improvements after intensive unimanual and bimanual interventions (Hung et al., 2011, 2017a). Thus, this drawer task can be an ideal test to evaluate the connection between the integrity of the CC and kinematic bimanual performance in children with USCP.

Our objective is to explore the relationship between the integrity of the CC and the kinematics of bimanual performance during a functional bimanual drawer task in children with USCP. We hypothesized that DTI parameters of the CC will be correlated with temporal bimanual coordination measures.

MATERIALS AND METHODS

Participants

A subset of thirty-nine children with USCP (20 males, 19 females, age 6–17 years, MACS I-III, **Table 1**) from a prior randomized control trial (RCT, NCT02918890) were recruited over 4 years (2014–2017) to participate in this study. The RCT recruited participants from the website[1], clinics in the NYC area, and online support groups. All potential participants were screened by an on-site physical examination or a videotaped examination by their physical/occupational therapist first. The inclusion criteria were selected based on our prior USCP studies: (1) attending a mainstream school, (2) the ability to follow instructions during screening, (3) the ability to lift the more affected arm 15 cm above a table and grasp light objects, and (4) the ability to complete all testing. The exclusion criteria were: (1) botulinum toxin in the upper extremity within the last 6 months, (2) other health problems unassociated with CP, (3) current/unstable seizures, (4) visual problems interfering with testing, and (5) surgery on the more affected hand within 1 year. Informed consents were

[1]http://www.tc.edu/centers/cit/

TABLE 1 | Participant characteristics.

Affected Side	Right (*n* = 15)	Left (*n* = 24)
Mean Age (*SD*) y,m	9,9 (3,2)	9,3 (3,3)
Age range y	6–17	6–17
Gender		
Male	6	14
Female	9	10
MACS		
I	4	8
II	8	12
III	3	4
AHA (*SD*) AHA units	55.60 (7.43)	56.33 (10.11)

SD, standard deviation; MACS, manual ability classification system for individuals with cerebral palsy; AHA, assisting hand assessment.

obtained from all the participants and guardians. The current study was approved by the University Institutional Review Board.

Procedures

All participants were part of a RCT to have intensive upper extremity training. Neuroimaging, bimanual coordination using a 3D motion capture system, and AHA score were assessed before their training to elucidate the mechanisms between the integrity of the CC and bimanual coordination.

MRI Data Acquisition

Diffusion MRI was acquired on all 39 children. DTI was used to reconstruct the interhemispheric connections of the CC. The MRI protocol was performed on a 3T Scanner (Siemens Magnetom Trio, Citigroup Biomedical Imaging Center, Weill Cornell Medical College). A total of 75 slices were acquired (matrix 112 × 112, FOV = 224 mm, 65 directions, b-value = 800 s/mm^2, TR = 9000 ms, and TE = 83 ms). The participants were positioned in a supine position with padding around the head to minimize the movement and reduce noise. The participants were not physically constrained nor received any sedation.

MRI Data Analysis

Diffusion tensor imaging analysis was performed using DTI Studio (John Hopkins University, Baltimore, MD, United States), which included FA, vector maps, and color-coded maps. An image was first created to mask the background noise at the threshold of 30 dB, using standard linear regression for tensor calculation. Images containing movement artifacts were excluded by visually inspecting the original images using the apparent diffusion constant function (Jiang et al., 2006). Reconstruction of the interhemispheric connections was done using the Continuous Tracking method (Mori et al., 1999). Fiber tracking started <0.15 and was terminated if the tract turning angle was >70.

Regions of interest were determined using anatomical location through orientation-based color-coding maps by hand. The CC was segmented into the following three segments based on the Witelson parcelation scheme: genu, midbody, and splenium (Witelson, 1989).

The FA, axial diffusivity (AD, reflecting axonal growth and injury), radial diffusivity (RD, indicating myelination and demyelination processes), and MD, number of streamlines and voxels were calculated. Data was analyzed by a trained researcher (second author) blinded to the kinematic results of participants. To ensure good reliability of the DTI findings, we evaluated both inter-rater and intra-rater variability. Good to excellent reliability was found: coefficient ranging of inter-rater from 0.816 (CI 0.079–0.963) to 0.979 (CI 0.896–0.996) and intra-rater from 0.746 (CI −0.267–0.949) to 0.988 (CI 0.940–0.998).

Kinematic Bimanual Coordination Testing

Participants were instructed to open a spring-loaded drawer (load 0.3 kg) with the less affected (drawer hand) and to insert their more affected hand (task hand) in the drawer to activate a light switch (14 cm × 10 cm) while seated. Participants were seated in front of the table (15 cm from the trunk) with both elbows flexed at right angles, and hands placed 30 cm apart at the edge of the table initially. The drawer (15 cm × 15 cm) equipped with a loop handle (9 cm in length and 3 cm in depth) and was placed at midline 30 cm from the edge of the table from the subject.

The drawer task was performed at a self-selected speed while 3-D kinematic data were collected with eight infrared cameras using Workstation 4.6 (VICON, Denver, CO, United States). Each trial ended after the subject activated the light switch inside the drawer. Total of five trials were collected after two practice trials. Seven reflective markers were placed on bilateral shoulder (acromion process), elbow (lateral epicondyle), wrist (ulnar styloid process), and spinous process of the seventh cervical vertebra (C7) of the participants. Calibration was performed on the space with a set external x (medial-lateral axis), y (anterior-posterior axis), and z (vertical axis) coordinates. The digitizing rate was 120 Hz. All digitized signals were processed using a low pass digital filter with a cutoff frequency of 6 Hz.

The velocity onset/offset threshold was set at a criterion of 5% peak velocity of the wrist tangential velocity. The onset of hand movement was defined when the wrist tangential velocity exceeded the criterion and constantly moved forward thereafter. The end of drawer opening (offset of drawer hand) was defined as the velocity falling below the criterion. The offset of the more affected hand was defined as the time when the wrist tangential velocity fell below the velocity criterion or when the light switch inside the drawer was activated.

The overall task completion time was defined by the time between the onset of the drawer hand and the offset of the task hand movements. The goal synchronization of the two hands was measured by the time difference between the offset of the two hands (the drawer hand fully opening the drawer and the task hand reaching inside the drawer). The normalized movement overlap time was calculated by the overlapping movement time of the two hands, as a percentage of the total task completion time. These three temporal measures were used to evaluate bimanual coordination performance. 3-D displacement of C7 marker was also calculated to indicate the trunk motion during task performance.

Quality of Bimanual Hand Use

The assisting hand assessment (AHA, version 5.0) quantifies the effectiveness to which children with unilateral impairments utilize their more affected hand to assist various bimanual play activities and has excellent validity/reliability (Holmefur et al., 2007; Krumlinde-Sundholm et al., 2007). All participants were videotaped during testing and were scored offsite by an experienced blinded evaluator. Data were reported in logit-based units.

Statistical Analysis

Statistical analysis was performed using SPSS (version 23, Statistical Production and Service Solutions, Chicago, IL, United States). To better understand the relationship between the DTI parameters and the kinematic measures of bimanual coordination, partial Spearman's correlations controlling for

age was used. To explore the connection between the current temporal bimanual coordination measures and trunk control with clinical measure of AHA, a separate partial Spearman's correlations controlling for age was carried out. In order to examine the possible effects of the side of hemiplegia on all the kinematic measures and AHA, a simple *t*-test with either side of hemiplegia (left or right) was performed. All of the data were approximately normally distributed (Shapiro-Wilk test). Significance was set at $p < 0.05$.

RESULTS

Temporal Bimanual Coordination and DTI Parameters

Correlations controlling for age between temporal bimanual coordination and DTI parameters are shown in **Table 2**. The total movement time was negatively correlated with AD of the whole CC (**Figure 1A**, $r = -0.33$, $p = 0.037$), number of streamlines of splenium (**Figure 1B**, $r = -0.34$, $p = 0.038$), and number of voxels of the splenium (**Figure 1C**, $r = -0.35$, $p = 0.032$). Goal synchronization differences were negatively correlated with AD of the whole CC (**Figure 1D**, $r = -0.33$, $p = 0.04$), number of streamlines of the splenium (**Figure 1E**, $r = -0.40$, $p = 0.01$), and number of splenium voxels (**Figure 1F**, $r = -0.42$, $p = 0.01$). No correlation was observed for the genu and midbody for any measure.

Clinical AHA Test and Kinematic Bimanual Coordination Variables

Table 3 shows the correlation summary of AHA scores with temporal bimanual coordination and trunk involvement. There were significant negative correlations between AHA scores and most kinematic valuables; i.e., better bimanual coordination was associated with higher AHA scores (see **Table 3**, except normalized overlap movement). The three temporal bimanual coordination variables were significantly correlated to one another (total time and goal synchronization: $r = 0.92$ $p = 0.001$; total time and normalized overlap $r = -0.42$, $p = 0.009$; goal synchronization and normalized overlap: $r = -0.55$, $p = 0.001$), but not with trunk control. Trunk control was negatively correlated with AHA score ($r = -0.43$, $p = 0.008$).

Effects of Hemiplegia Side

No significant findings of hemiplegic side effects on temporal bimanual coordination measures, trunk control, or AHA score were found.

DISCUSSION

This study investigated the relationship between the CC diffusion properties and bimanual coordination performance during a functional bimanual drawer task in children with USCP. As we hypothesized, the integrity of the CC was correlated with temporal bimanual coordination performance for children with USCP. AD of the whole CC and the splenium region were correlated with bimanual coordination performance. Genu and midbody diffusion properties were not related to any measure. There were also significant correlations between clinical bimanual AHA scores and bimanual coordination and trunk control measures.

TABLE 2 | Correlation analyses between temporal coordination measures and DTI variables.

Region	DTI variables	Total movement time		Goal synchronization		Normalized movement overlap	
		R	*p* value	*R*	*p* value	*R*	*p* value
Whole CC	FA	−0.003	0.98	−0.07	0.69	−0.15	0.39
	Streamlines	−0.12	0.47	−0.23	0.17	−0.09	0.61
	Voxels	−0.14	0.39	−0.26	0.12	−0.07	0.70
	AD	−0.33	0.037*	−0.33	0.04*	0.09	0.61
	RD	0.18	0.28	0.22	0.18	−0.02	0.93
	MD	−0.24	0.14	−0.23	0.17	−0.05	0.77
Genu CC	FA	−0.033	0.84	−0.03	0.87	−0.08	0.62
	Streamlines	−0.20	0.23	−0.27	0.11	0.06	0.72
	Voxels	−0.19	0.26	−0.28	0.09	0.10	0.56
	AD	−0.29	0.075	−0.28	0.09	−0.15	0.38
	RD	−0.14	0.40	−0.14	0.42	−0.06	0.72
	MD	−0.23	0.16	−0.22	0.18	−0.11	0.51
Midbody CC	FA	−0.02	0.92	−0.03	0.87	−0.03	0.85
	Streamlines	−0.10	0.55	−0.21	0.20	0.09	0.56
	Voxels	−0.11	0.52	−0.22	0.19	0.11	0.51
	AD	−0.30	0.064	−0.27	0.11	−0.18	0.29
	RD	−0.08	0.65	−0.05	0.76	−0.06	0.70
	MD	−0.21	0.22	−0.17	0.30	−0.13	0.44
Splenium CC	FA	−0.08	0.63	−0.14	0.40	−0.02	0.93
	Streamlines	−0.34	0.038*	−0.40	0.01*	0.07	0.68
	Voxels	−0.35	0.032*	−0.42	0.01*	0.01	0.95
	AD	−0.17	0.40	−0.19	0.25	−0.03	0.87
	RD	0.004	0.98	0.04	0.82	0.01	0.93
	MD	0.08	0.62	−0.07	0.67	−0.01	0.98

*CC, corpus callosum; DTI, diffusion tensor imaging; FA, fractional anisotropy; AD, axial diffusivity; RD, radial diffusivity; MD, mean diffusivity; Streamlines, number of streamlines; Voxels, number of voxels; *, significant correlation.*

Correlation Between Bimanual Coordination and Integrity of the Splenium

There were significant negative correlations between total movement time and goal synchronization measures and AD of the whole CC, number of streamlines of the splenium, and the number of voxels of the splenium. Shorter total movement time and goal synchronization time differences both indicated better temporal bimanual coordination during the current task. Children with USCP showed impaired temporal bimanual coordination during a drawer task similar to the current one when compared with typically developed children (Hung et al., 2004, 2010). They had longer total movement time, reduced goal synchronization (longer goal

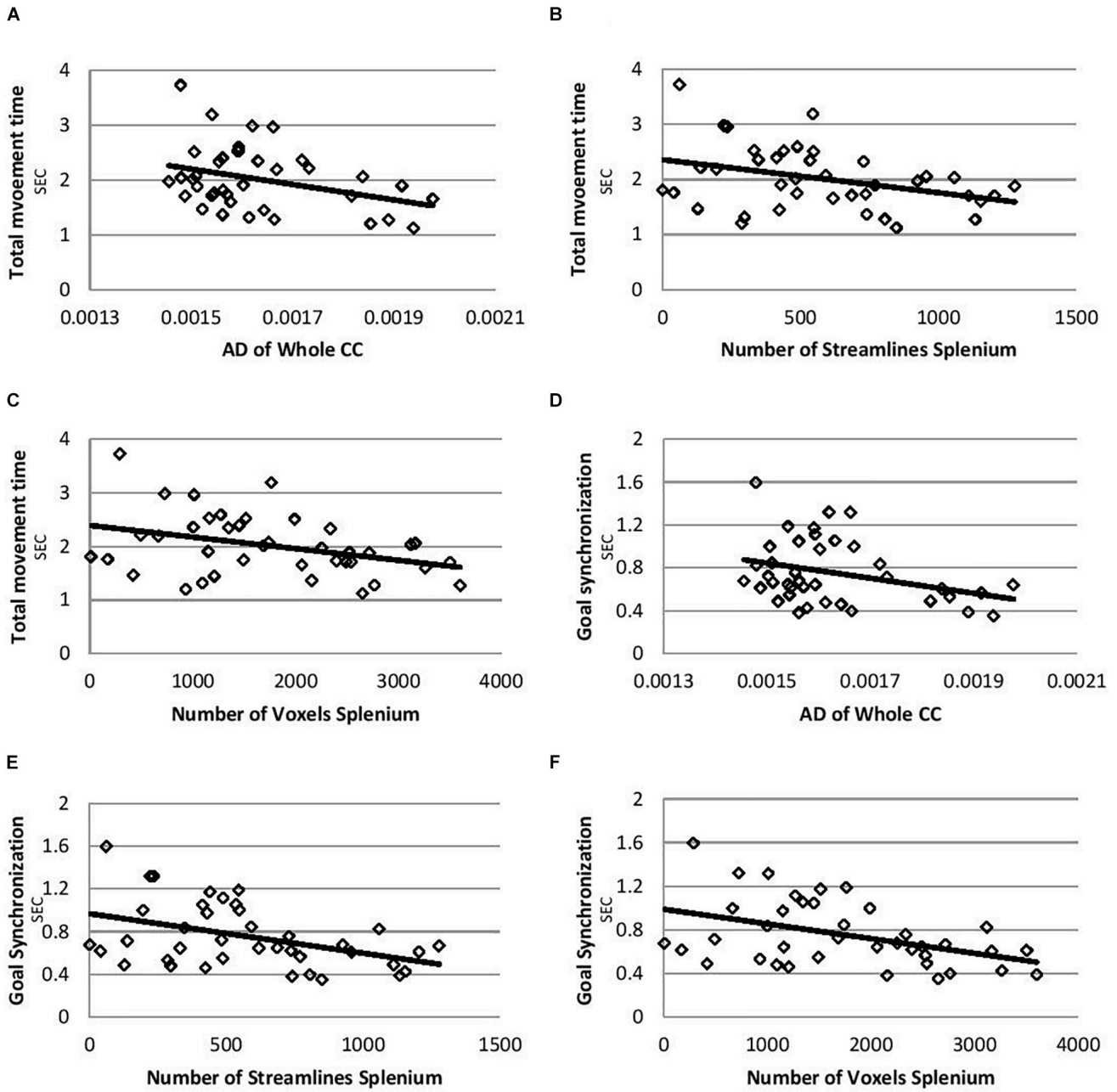

FIGURE 1 | Correlation plots for total movement time and goal synchronization. **(A)** Correlation between total movement time and AD of whole CC. **(B)** Correlation between total movement time and number of streamlines of splenium. **(C)** Correlation between total movement time and number of voxels of splenium. **(D)** Correlation between goal synchronization and AD of whole CC. **(E)** Correlation between goal synchronization and number of streamlines of splenium. **(F)** Correlation between goal synchronization and number of voxels of splenium. AD, axial diffusivity; CC, corpus callosum.

accomplished time differences between the two hands), and reduced normalized movement overlap (Hung et al., 2004, 2010). Thus the current negative correlations indicated better bimanual control correlated with integrity of microstructure of the CC, especially the splenium. The number of streamlines of the splenium was also correlated with AHA scores (clinical bimanual measure) for children with USCP in a previous study (Davatzikos et al., 2003).

Weinstein et al. (2014) showed only correlations between the splenium region integrity (FA, MD, and RD measures) and clinical hand function measures (questionnaire of more affected hand use during daily bimanual tasks) in children with USCP. Weinstein et al. (2014) further suggested the possible reason of their findings was the important role of the splenium region for visual-spatial control and spatial awareness of the more affected hand. Thus the number of streamlines of the splenium region that

TABLE 3 | Correlation analyses between AHA scores and kinematic measures.

	AHA		Total movement time		Goal synchronization		Normalized movement overlap	
	R	*p* value	*R*	*p* value	*R*	*p* value	*R*	*p* value
Total movement time	−0.33	0.041*						
Goal synchronization	−0.35	0.03*	0.92	0.001*				
Normalized movement overlap	−0.016	0.33	−0.42	0.009*	−0.55	0.001*		
Trunk control	−0.33	0.042*	0.74	0.055	0.63	0.08	0.20	0.21

*AHA, assisting hand assessment; *, significant correlation.*

influenced bimanual coordination performance (such as current kinematic measures and AHA scores of previous study), and the quality of fibers (integrity) seemed to be connected with spatial temporal movement control of the more affected hand. Since we did not assess unimanual spatial temporal control of the more affected hand, we cannot evaluate the suggestion from Weinstein et al. (2014).

The possible reason for failing to find correlation between splenium integrity (FA, MD, and RD measures) and kinematic bimanual coordination in the current study could be the influence of developmental factors. The number of streamlines may not be affected as greatly as integrity changes of the splenium during development. Muetzel et al. (2008) evaluated the relationship between development of the CC and bimanual performances for healthy adolescents. They found that splenium FA measures correlated greatly with bimanual finger tapping performance. They did not measure number of streamlines or voxels. However, they suggested increase splenium FA in DTI studies to be related to splenium white matter volume. Muetzel et al. (2008) suggested that white matter integrity (measured by FA) in the splenium continued to develop until 18 years old for healthy adolescents. The developmental process and influence factors of such white matter integrity (such as measure of FA) for children with USCP is unclear and most likely prolonged with a different developing rate. The current study had a wide age range (6–17 years old) and was more likely to be influenced by developing factors even though the correlation findings were controlled for age statistically. The age effect of CC integrity changes between 6 and 7 years old is not likely to be the same as between 15 and 16 years old. A future study with more participants to evaluate the developmental effects of the number of streamlines and voxels, and integrity measures (control for severity) could help answer this question. The other possible reason could be that other neural pathways (e.g., Cortico-spinal tract, cerebellum) provide additional compensatory mechanisms.

In the current study, AD of the whole CC was also negatively correlated with total movement time and goal synchronization performance for children with USCP. AD was suggested to evaluate axonal integrity (Harsan et al., 2006; Sun et al., 2006). However, most microstructure studies of the CC failed to indicate significant AD findings (e.g., Weinstein et al., 2014). In a previous study that evaluated changes of white matter microstructure of the CC after after-school additional physical activity program (9 month program) for children indicated changes in FA and RD measures of the CC, but not AD values (Chaddock-Heyman et al., 2018). AD measure of the CC may be less likely to change over training or it has less sensibility to detect small changes. The previous studies only evaluated the connection between AD of the CC and clinical measures which may be less sensitive to movement coordination than kinematic analysis (Hung et al., 2011, 2017a,b; Weinstein et al., 2014; Serrien, 2017).

AHA and Bimanual Kinematic Measures

It is interesting to see the connection between the AHA score (clinical bimanual measure) and kinematic bimanual coordination measures of total movement time, goal synchronization, and trunk control during the current drawer task. Most of the previous studies failed to find any significant correlation between the AHA and kinematic bimanual coordination measures (Hung et al., 2011, 2017a). A larger group of participants and wider age range of participants with the developmental effects may lead to significant correlation findings.

Trunk control was significantly correlated to AHA scores, but not other temporal bimanual coordination measures. Proximal trunk compensation (excessive trunk forward movement) for the reduced distal joint motion of the more affected upper extremity was shown in previous studies for children with USCP (e.g., Coluccini et al., 2007; Hung et al., 2012). Therefore, trunk control during the current task might be more related to impairments of the more affected hand than the temporal quality of bimanual movement coordination. The AHA also emphasizes how the more affected hand performs hand assists for the less affected hand during bimanual tasks. The AHA does not measure the coordination between the two hands (e.g., how less affected hand slows down to compensate for the more affected hand).

Limitations

The current project has a wide age range of participants. This may increase the possibility of developmental influences even if we statistically tried to control for the age effect. No control group was included in the study, which could provide better age-specific comparison. We only focused on the integrity of the CC; however, there are many other regions of the brain or descending tracts that might be correlated to bimanual coordination performance as well. Multiple correlations are evaluated in our study, and may increase type I error. To avoid false significant findings

due to multiple correlations, we confirmed same findings with linear regressions.

CONCLUSION

The current study investigated the connection between the CC diffusion properties (assessed by DTI) and bimanual coordination performance during a functional bimanual drawer opening task for children with USCP. The integrity of the CC, specifically the splenium, was found to play a role in bimanual coordination performance. This means that the splenium might be important for temporal coordination for movement control. Future studies are required to further understand the underlying mechanisms between the microstructure of the central nervous system (e.g., connections between the different neuronal pathways and other structures) and the various movement performance. Therefore, we can potentially predict the movement impairments. It would also be important to determine the interaction of the integrity of the CC and changes in bimanual coordination following intensive therapies.

DATA AVAILABILITY STATEMENT

The datasets generated for this study are available on request to the corresponding author.

ETHICS STATEMENT

The studies involving human participants were reviewed and approved by the Teachers College, Columbia University Burke Neurological Institute, Weill Cornell Medicine Queens College, and City University of New York. Written informed consent to participate in this study was provided by the participants' legal guardian/next of kin.

AUTHOR CONTRIBUTIONS

Y-CH and MR designed and conducted the experiments. Y-CH analyzed the data and wrote the manuscript. AG and KF helped to discuss the data and edited the manuscript.

FUNDING

KF and AG were funded by the NIH R01 HD07436-A01 and R01 HD095663. MR was supported by a postdoctoral training award from the Fonds de Recherche en Santé du Québec (Québec, Canada).

ACKNOWLEDGMENTS

We thank the children and their families for participating in this study.

REFERENCES

Bloom, J. S., and Hynd, G. W. (2005). The role of the corpus callosum in interhemispheric transfer of information: excitation or inhibitation? *Neuropsychol. Rev.* 15, 59–71. doi: 10.1007/s11065-005-6252-y

Chaddock-Heyman, L., Erichson, K. I., Kienzler, C., Drollette, E. E. S., Raine, L. B., Kao, S. C., et al. (2018). Physical activity increase white matter microstructure in children. *Front. Neurosci.* 12:950. doi: 10.3389/fnins.2018.00950

Coluccini, M., Maini, E. S., Martelloni, C., Sgandurra, G., and Cioni, G. (2007). Kinematic characterization of functional reach to grasp in normal and in motor disables children. *Gait Posture* 25, 493–501. doi: 10.1016/j.gaitpost.2006.12.015

Davatzikos, C., Barzi, A., Lawrie, T., Hoon, A. H. Jr., and Melhem, E. R. (2003). Correlation of corpus callosal morphometry with cognitive and motor function in periventricular leukomalacia. *Neuropediatrics* 34, 247–252. doi: 10.1055/s-2003-43259

Eliasson, A. C., Gordon, A. M., and Forssberg, H. (1995). Tactile control of isometric fingertip forces during grasping in children with cerebral palsy. *Dev. Med. Child. Neurol.* 37, 72–84. doi: 10.1111/j.1469-8749.1995.tb11933.x

Forssberg, H., Eliasson, A. C., Redon-Zonitenn, C., Mercuri, E., and Dubowitz, L. (1999). Impaired grip-lift synergy in children with unilateral brain lesions. *Brain* 122, 1157–1168. doi: 10.1093/brain/122.6.1157

Gaillard, F., Cretual, A., Cordillet, S., Le Cornec, C., Gonthier, C., Bouvier, B., et al. (2018). Kinematic motion abnormalities and bimanual performance in children with unilateral cerebral palsy. *Dev. Med. Child. Neurol.* 60, 839–845. doi: 10.1111/dmcn.13774

Gordon, A. M., Lewis, S. R., Eliasson, A. C., and Duff, S. V. (2003). Object release under varying task constraints in children with hemiplegic cerebral palsy. *Dev. Med. Child Neurol.* 45, 240–248. doi: 10.1111/j.1469-8749.2003.tb00338.x

Harsan, L. A., Poulet, P., Guignard, B., Steibel, J., Parizel, N., de Sousa, P. L., et al. (2006). Brain dysmyelination and recovery assessment by noninvasive in vivo diffusion tensor magnetic resonance imaging. *J. Neurosci. Res.* 83, 392–402. doi: 10.1002/jnr.20742

Holmefur, M., Krumlinde-Sundholm, L., and Eliasson, A. C. (2007). Interrater and intrarater reliability of the assistinf hand assessment. *Am. J. Occup. Ther.* 61, 79–84. doi: 10.5014/ajot.61.1.79

Hung, Y. C., Brandao, J. M., and Gordon, A. M. (2017a). Structured skill practice during intensive bimanual training leads to better trunk and arm control than unstructured practice in children with unilateral spastic cerebral palsy. *Res. Dev. Disabil.* 60, 65–76. doi: 10.1016/j.ridd.2016.11.012

Hung, Y. C., Friel, K. M., and Gordon, A. M. (2017b). Response: commentary: skilled bimanual training drives motor cortex plasticity in children with unilateral cerebral palsy. *Front. Hum. Neurosci.* 11:619. doi: 10.3389/fnhum.2017.00619

Hung, Y. C., Casertano, L., Hillman, A., and Gordon, A. M. (2011). The effect of training specificity on bimanual coordination in children with hemiplegia. *Res. Dev. Disabil.* 32, 2724–2731. doi: 10.1016/j.ridd.2011.05.038

Hung, Y. C., Charles, J., and Gordon, A. M. (2004). Bimanual coordination during a goal-directed task in children with hemiplegic cerebral palsy. *Dev. Med. Child Neurol.* 46, 746–753. doi: 10.1111/j.1469-8749.2004.tb00994.x

Hung, Y. C., Charles, J., and Gordon, A. M. (2010). The influence of task constraints in bimanual coordination for children with hemiplegic cerebral palsy. *Exp. Brain Res.* 201, 421–428. doi: 10.1007/s00221-009-2049-1

Hung, Y. C., Enderson, E., Akbashev, F., Valte, L., Ke, W. S., and Gordon, A. M. (2012). Joint Coordination during a reach-grasp-eat Task in children with hemiplegia. *Res. Dev. Disabil.* 33, 1649–1657. doi: 10.1016/j.ridd.2012.04.003

Jiang, H., van Zijl, P. C., Kim, J., Pearlson, G. D., and Mori, S. (2006). DtiStudio: resource program for diffusion tensor computation and fiber bundle tracking. *Comput. Methods Programs Biomed.* 81, 106–116. doi: 10.1016/j.cmpb.2005.08.004

Krumlinde-Sundholm, L., Holmefur, M., Kottorp, A., and Eliasson, A. C. (2007). The assisting hand assessment: current evidence of validity, reliability, and responsiveness to change. *Dev. Med. Child Neurol.* 49, 259–264. doi: 10.1111/j.1469-8749.2007.00259.x

Kuczynski, A. M., Dukelow, S. P., Hodge, J. A., Carison, H. L., Lebel, C., Semrau, J. A., et al. (2018). Corticospinal tract diffusion properties and robotic visually

guided reaching in children with hemiplegic cerebral palsy. *Hum. Brain Mapp.* 39, 1130–1144. doi: 10.1002/hbm.23904

Lee, B. H. (2017). Relationship between gross motor function and the function, activity and participation components of the international classification of functioning in children with spastic cerebral palsy. *J. Phys. Ther. Sci.* 29, 1732–1736. doi: 10.1589/jpts.29.1732

Mori, S., Crain, B., Chacko, V. P., and van Zijl, P. C. (1999). Three-dimensional tracking of axonal projections in the brain by magnetic resonance imaging. *Ann. Neurol.* 45, 265–269. doi: 10.1002/1531-8249(199902)45:2<265::aid-ana21>3.0.co;2-3

Muetzel, R. L., Collins, P. F., Mueller, B. A., Schissel, A. M., Lim, K. O., and Luciana, M. (2008). The development of corpus callosum microstructure and associations with bimanual task performance in healthy adolescents. *Neuroimage* 39, 1918–1925. doi: 10.1016/j.neuroimage.2007.10.018

Pannek, K., Boyd, R. N., Fiori, S., Guzzetta, A., and Rose, S. E. (2014). Assessment of the structural brain network reveals altered connectivity in children with unilateral cerebral palsy due to periventricular white matter lesions. *Neuroimage Clin.* 5, 84–92. doi: 10.1016/j.nicl.2014.05.018

Rademaker, K. J., Lam, J. N., Van Haastert, I. C., Uiterwaal, C. S., Lieftink, A. F., Groenendaal, F., et al. (2004). Large corpus callosum size with better motor performance in prematurely born children. *Semin. Perinatol* 28, 279–287. doi: 10.1053/j.semperi.2004.08.005

Reid, S. M., Ditchfield, M. R., Bracken, J., and Reddihough, D. S. (2015). Relationship between characteristics on magnetic resonance imaging and motor outcomes in children with cerebral palsy and white matter injury. *Res. Dev. Disabil.* 4, 178–187. doi: 10.1016/j.ridd.2015.07.030

Serrien, D. J. (2017). Commentary: skilled bimanual training drives motor cortex plasticity in children with unilateral cerebral palsy. *Front. Hum. Neurosci.* 11:297. doi: 10.3389/fnhum.2017.00297

Steenbergen, B., Charles, J., and Gordon, A. M. (2008). Fingertip force control during bimanual object lifting in hemiplegic cerebral palsy. *Exp. Brain Res.* 186, 191–201. doi: 10.1007/s00221-007-1223-6

Sun, S. W., Liang, H. F., Trinkaus, K., Cross, A. H., Armstrong, R. C., and Song, S. K. (2006). Noninvasive detection of cuprizone induced axonal damage and demyelination in the mouse corpus callosum. *Magn. Reson. Med.* 55, 302–308. doi: 10.1002/mrm.20774

Thomas, B., Eyssen, M., Peeters, R., MOlenaers, G., Van Hecke, P., De Cock, P., et al. (2005). Qualitative diffusion tensor imaging in cerebral palsy due to periventricular white matter injury. *Brain* 128, 2562–2577. doi: 10.1093/brain/awh600

Utley, A., Steenbergen, B., and Sugden, D. A. (2004). The influence of object size on discrete bimanual co-ordination in children with hemiplegic cerebral palsy. *Disabil. Rehabil.* 26, 603–613. doi: 10.1080/09638280410001696674

Utley, A., and Sugden, D. (1998). Interlimb coupling in children with hemiplegic cerebral palsy during reaching and grasping at speed. *Dev. Med. Child Neurol.* 40, 396–404. doi: 10.1111/j.1469-8749.1998.tb08215.x

Weinstein, M., Green, D., Geva, R., Schertz, M., Fattal-Valevski, A., Artzi, M., et al. (2014). Interhemispheric and intrahemispheric connectivity and manual skills in children with unilateral cerebral palsy. *Brain Struct. Funct.* 219, 1025–1040. doi: 10.1007/s00429-013-0551-5

Witelson, S. F. (1989). Hand and sex differences in the isthmus and genu of the human corpus callosum. A postmortem morphological study. *Brain* 112, 799–835. doi: 10.1093/brain/112.3.799

Conflict of Interest: The authors declare that the research was conducted in the absence of any commercial or financial relationships that could be construed as a potential conflict of interest.

frontiers in Human Neuroscience

ORIGINAL RESEARCH
published: 08 November 2019
doi: 10.3389/fnhum.2019.00392

Visuospatial Attention and Saccadic Inhibitory Control in Children With Cerebral Palsy

Claudio Maioli[1], Luca Falciati[1], Jessica Galli[1,2], Serena Micheletti[2], Luisa Turetti[1], Michela Balconi[3] and Elisa M. Fazzi[1,2]*

[1]Department of Clinical and Experimental Sciences, University of Brescia, Brescia, Italy, [2]Unit of Child Neurology and Psychiatry, ASST Spedali Civili of Brescia, Brescia, Italy, [3]Research Unit in Affective and Social Neuroscience, Department of Psychology, Catholic University of Milan, Milan, Italy

Cerebral palsy (CP) is a non-progressive syndrome due to a pre-, peri- or post-natal brain injury, which frequently involves an impairment of non-motor abilities. The aim of this article was to examine visuospatial attention and inhibitory control of prepotent motor responses in children with CP showing a normal IQ or mild cognitive impairment, measuring their performance in oculomotor tasks. Ten children (9–16-year-old) with spastic CP and 13 age-matched, typically developing children (TDC) participated in the study. Subjects performed a simple visually-guided saccade task and a *cue-target* task, in which they performed a saccade towards a peripheral target, after a non-informative visual cue was flashed 150 ms before the imperative target, either at the same (*valid*) or at a different (*invalid*) spatial position. Children with CP showed severe executive deficits in maintaining sustained attention and complying with task instructions. Furthermore, saccadic inhibitory control appeared to be significantly impaired in the presence of both stimulus-driven and goal-directed captures of attention. In fact, patients showed great difficulties in suppressing saccades not only to the cue stimuli but also to the always-present target placeholders, which represented powerful attentional attractors that had to be covertly attended throughout the task execution. Moreover, impairment did not affect in equal manner the whole visual field but showed a marked spatial selectivity in each individual subject. Saccade latencies in the *cue-target* task were faster in the *valid* than in the *invalid* condition in both child groups, indicating the preservation of low-level visuospatial attentive capabilities. Finally, this study provides evidence that these impairments of executive skills and in inhibitory control, following early brain injuries, manifest in childhood but recover to virtually normal level during adolescence.

Keywords: cerebral palsy, eye movements, inhibitory control, executive skills, visuospatial attention, saccades, oculomotor control, cueing paradigm

OPEN ACCESS

Edited by:
Christos Papadelis, Cook Children's Medical Center, United States

Reviewed by:
Corinna M. Bauer, Harvard Medical School, United States
Donatas Jonikaitis, Ludwig Maximilian University of Munich, Germany

****Correspondence:***
Claudio Maioli
claudio.maioli@unibs.it

Specialty section:
This article was submitted to Motor Neuroscience, a section of the journal Frontiers in Human Neuroscience

Received: *18 July 2019*
Accepted: *21 October 2019*
Published: *08 November 2019*

Citation:
Maioli C, Falciati L, Galli J, Micheletti S, Turetti L, Balconi M and Fazzi EM (2019) Visuospatial Attention and Saccadic Inhibitory Control in Children With Cerebral Palsy. Front. Hum. Neurosci. 13:392. doi: 10.3389/fnhum.2019.00392

INTRODUCTION

Cerebral palsy (CP) designates a group of non-progressive neurological disorders, because of a pre-, peri- or post-natal brain injury, affecting the development of movement and postural abilities (Bax et al., 2005; Rosenbaum et al., 2007). However, cerebral damage in this neurodevelopmental condition is in general not restricted to the motor system. Children with CP (CPC) frequently

manifest a varying degree of neurovisual, cognitive and learning deficits (Rosenbaum et al., 2007; Fazzi et al., 2009, 2012; MacLennan et al., 2015). In fact, lesions of the periventricular white matter and of the cortical deep gray matter are very common in CP, leading to the involvement not only of motor abilities, but also of non-motor developing abilities, such as visuospatial, attentive and executive functions (Krägeloh-Mann and Horber, 2007; Galli et al., 2018).

Severity of non-motor symptoms varies substantially in CP. However, even children with cognitive functions within or above the normal range manifest a higher prevalence of learning disorders (Frampton et al., 1998) and dysfunctions in sustained and divided attention (Kolk and Talvik, 2000; Pirila et al., 2004; Bottcher et al., 2010). These dysfunctions are associated with increased distractibility and inattention and may explain why CPC have often a lower academic performance and problems in emotional and social relationships (Nadeau and Tessier, 2006; Parkes et al., 2009; Whittingham et al., 2010). Visuospatial attention plays a pivotal role as a filter mechanism for selecting which parts of the visual scene are relevant in a given behavioral context. In a limited-capacity system, such as that of the brain in processing an enormous amount of information, the ability of selecting relevant stimuli from background is not only essential for sensorimotor integration but is also critical for the development of executive and academic skills (Anderson, 2002). Furthermore, a causal link has been proposed between visuospatial attention and reading acquisition (Hari and Renvall, 2001; Vidyasagar and Pammer, 2010; Franceschini et al., 2012; Collis et al., 2013). In view of the high incidence of reading difficulties in CPC (Frampton et al., 1998; Schenker et al., 2005; Gillies et al., 2018), deficits in selective attention may be responsible also for learning disorders in CP (Bottcher, 2010).

Attention and executive dysfunctions have been mostly ascertained in CP by means of neuropsychological tests and questionnaires (e.g., White and Christ, 2005; Bottcher et al., 2010; Bodimeade et al., 2013; Whittingham et al., 2014). Only few articles investigated visual attention in children with spastic diplegic CP by using an orienting task (Craft et al., 1994; Schatz et al., 2001). These studies employed a reaction-time paradigm, developed by Posner and colleagues, in which a manual response follows a covert orientation of attention to a peripheral visual target (i.e., maintaining gaze at a central fixation point), after presenting a visual cue at the same or at a different spatial location (Posner, 1980; Posner et al., 1985). Both reports described a pattern of impairments in basic attentional mechanisms, which was associated with a prevalent damage of anterior brain regions, suggesting that frontal cortical areas play a critical role in the development of visual attention. Since frontal lobes are well known to play an important role also in the developing of executive abilities (Stuss et al., 1997; Casey, 2001), one could expect that attentive and executive impairments coexist in CPC.

The evaluation of oculomotor functions represents in many aspects an ideal tool to investigate at once both selective attention and the competence of executive abilities. Specifically, in this article we adopted a saccadic task, similar to the Posner cuing protocol, in which however the participant must perform an eye movement towards the peripheral target after a non-informative visual cue is flashed either at the same or at a different spatial position. By monitoring only the eye movements, the limitations in posture and limb movements that characterize CP become irrelevant in determining the accuracy and the timing of the motor response. In fact, in the absence of strabismus, nystagmus or ocular motor apraxia (Lanzi et al., 1998; Jacobson and Dutton, 2000), the saccadic system of most CPC does not differ, or shows only very modest abnormalities, with respect to typically developing children (TDC; Katayama and Tamas, 1987; Christ et al., 2003; Saavedra et al., 2009).

The correct execution of the oculomotor task adopted in this article requires a proper operation of a number of cognitive abilities. First, the task requires the capacity of actively keeping a steady fixation, maintaining sustained attention for a long time at a specific point of the visual scene. Second, selective attention must identify the sensory event that is relevant to the immediate goal, discarding a distracting cue that is irrelevant to the task. Third, inhibitory mechanisms must suppress unwanted motor responses. The abrupt onset of the cue in the perceptual space elicits an automatic, bottom-up selection process for action, even if it is in contrast with the prescriptions of the task. The suppression of this motor response requires the activation of inhibitory mechanisms by the prefrontal executive system, possibly with the involvement of frontostriatal circuits (Casey, 2001). Finally, if a visual cue attracts attention at the same spatial location of the target, shortly before its onset, a facilitation effect determines an increase of the response speed. In TDC, as in normal adults, a cuing paradigm of this kind induces faster reaction times for both manual and saccadic responses (Posner et al., 1984; Maylor, 1985; Briand et al., 2000).

The aim of this article is to examine visuospatial attention and executive abilities of CPC, measuring their performance in an oculomotor task. We employed a cue-target paradigm for a quantitative evaluation of the ability to discard distracting, task-irrelevant stimuli, of engaging attentive resources for a long-lasting time span and of the capacity of inhibiting an unwanted, prepotent motor response, which is in contrast with the behavioral goal. It can be surmised that accessing the integrity of these basic skills in CP, even in children with a mild degree of disability, could be essential in view of their relevance for the development of a large number of cognitive functions. This knowledge may also address more properly therapeutic and rehabilitation approaches in order to early detect or treat learning disabilities and social difficulties, which frequently affect children with CP and adolescents (Frampton et al., 1998; Bottcher et al., 2010; Whittingham et al., 2014).

MATERIALS AND METHODS

Ethical Approval

This study was conducted in accordance with the ethical guidelines set forth by the Declaration of Helsinki and had the approval from the Ethics Committee of "ASST Spedali Civili" of Brescia, Italy (protocol. N. 1324, 08/04/2013). Informed

consent was obtained both in verbal form from the participants, as well as in written form from their parents, prior to the experimental sessions.

Subjects

Ten children with CP (five males and five females) and 13 age-matched children (six males and seven females) with typical development (TD) participated in the study. All participants were naïve to the purpose of the experiment. CPC were enrolled in the Unit of Child Neurology and Psychiatry, at the "ASST Spedali Civili" of Brescia (Italy) and were aged from 8 years and 11 months to 16 years and 1 month (mean age: 11 years and 4 months ± 2 years and 10 months). TDC were aged from 9 years and 6 months to 15 years and 7 months (mean age: 13 years and 1 month ± 2 years and 6 months) and had no history of head trauma, neurological or psychiatric diseases, cognitive disabilities or oculomotor/neurovisual impairments.

The inclusion criteria for CPC were as follows: (1) diagnosis of spastic CP documented by neurological examination and neuroimaging according to the International Classification of CP (Bax et al., 2005; Rosenbaum et al., 2007); (2) normal IQ or mild cognitive impairment (full-scale intelligence quotient, FIQ, >50 standard scores and verbal intelligence quotient, VIQ, >70 standard scores), according to WISC-III scores (Wechsler, 2006), performed within last 12 months (see **Table 1**); (3) normal or near-normal visual acuity (not less than 6/10 in binocular vision); and (4) ability to understand the verbal instructions for executing the experimental task. Exclusion criteria were a history of uncontrolled epilepsy seizures and the presence of oculomotor disturbances such as nystagmus, strabismus or oculomotor apraxia (Fazzi et al., 2012).

Table 1 reports the demographic characteristics of the recruited CPC. Three CPC (CP3, CP8, CP10) were excluded from the study because of problems arising during the experimental session. Two children were unable to keep a sufficiently stable head posture on the head-support device. Consequently, it has been impossible to obtain a workable calibration for the remote eye-tracker. The third child manifested a latent strabismus during the recording session. Therefore, the average measure of the binocular gaze point showed a quite erratic behavior along the horizontal axis, yielding only very few trials with an apparently normal eye convergence. Therefore, the CPC group was composed by seven participants.

A visual field test was performed for both eyes in all CPC. The examination yielded a normal visual field in five subjects (CP2, CP4, CP6, CP7, CP9). By contrast, a visual defect was found in the lower right quadrant in CP5 and in the right hemifield in CP1. However, in these children only the peripheral vision was affected, sparing the central part of the visual field for at least 10° around the fovea. Since stimuli were presented at an eccentricity of 7°, the detected visual defects were not such to interfere with the execution of the oculomotor tasks of this study. In any case, we carefully checked, before running the experimental sessions, that all children could clearly see without effort the stimuli while looking at a fixation cross placed in the center of the visual field.

Apparatus and Stimuli

Participants sat in a dimly illuminated and quiet room. A combination of chin rest and head-support device was used to restrain head movements. Visual stimuli were displayed on a full HD 21.5" LED monitor (ASUS VH226H, Taiwan), located 80 cm in front of the subject. A light gray central fixation cross and four light gray square frames were displayed on the screen throughout the experimental session, against a black background. The cross subtended a visual angle of 0.36°. By contrast, the frames subtended an angle of 1.64° and served as placeholders for the visual targets. Each placeholder was located at one vertex of an imaginary square surrounding the central cross, at an eccentricity of 7° (**Figure 1A**).

Visual stimuli acting as saccade targets consisted of a 0.43° green solid square appearing at the center of one placeholder. Eye-movements were recorded by the remote eye-tracker Tobii X120 (Tobii AB, Stockholm, Sweden), at a sampling rate of 120 Hz and with an accuracy of 0.5°. Tobii's image-processing algorithm, based on the reflection pattern of near-infrared light on the eyes, provided the X-Y coordinates of the gaze point on the screen in pixels, by averaging the values computed from the left and the right eyes.

The experiment was performed using Presentation® software (Version 16.3, Neurobehavioral Systems, Inc., Berkeley, CA, USA[1]) and the TobiiEyetrackerExtension v1.1 for interfacing the eye tracker with the Presentation software[2].

Experimental Procedures

In an experimental session, participants had to perform two tasks in a sequence. The first task, hereinafter called *saccadic task* (**Figure 1B**), consisted in performing simple visually-guided saccades. The trial began with the central fixation cross and the four placeholders displayed on the screen. After a fixed delay of 1,150 ms from a warning tone, a green square target turned on inside one of the placeholders for 2,000 ms. The target onset was the go-signal for shifting the gaze to it, as quickly as possible. After the target disappearance, only the fixation cross and the empty placeholders remained on the visual scene for the other 1,300 ms. Afterward, a new warning tone marked the beginning of the next trial. Participants were instructed to quickly return with their gaze to the central fixation cross only after the offset of the green saccadic target. The experimental block comprised 40 trials, allowing 10 repetitions at random of each possible target location.

The second task consisted in a cuing paradigm, hereinafter called *cue-target task* (**Figure 1C**). This paradigm was identical to that of the *saccadic task*, except for the appearance of a visual cue 150 ms before the onset of the saccade target. The cue was represented by the doubling the luminance of one placeholder for 50 ms. The cue could occur either at the same (*valid*) or at a different (*invalid*) spatial location with respect to the saccade target. The participant had to disregard the visual cue and make, as fast as possible, an eye movement only to the green target. The cue was very little informative about the position

[1] www.neurobs.com
[2] idk.fh-joanneum.at/2018/04/22/visionspace

TABLE 1 | Demographic characteristics of Children with cerebral palsy (CPC).

Participant code	Handedness	GA (weeks)	CP type (Hagberg)	Motor abnormalities: nature and typology	Motor abnormalities: functional motor abilities	Associted impairments: epilepsy	Visual acuity right eye	Visual acuity left eye	FIQ	VIQ	Brain images	Brain injury causation and timing
CP1	Left	39	Right hemiplegia	Unilateral spastic hypertonia	GMFCS: 1 MACS: 2	focal epilepsy	10/10	10/10	83	93	Multicystic encephalopathy (left parietal-occipital-temporal areas; MRI)	Chronic circulatory insufficiency
CP2	Left	n.a.	Right hemiplegia	Unilateral spastic hypertonia	GMFCS: 1 MACS: 1	no	10/10	10/10	99	112	Bilateral Periventricular leukomalacia (MRI)	n.a.
CP3	Right	40	Left hemiplegia	Unilateral spastic hypertonia	GMFCS: 1 MACS: 3	focal epilepsy	8/10	8/10	70	63	Right porencephaly (MRI)	Prenatal
CP4	Left	40	Right hemiplegia	Unilateral spastic hypertonia	GMFCS: 2 MACS: 3	focal epilepsy	10/10	10/10	55	77	Left periventricular leukomalacia (MRI)	Hypoxic-ischemeic damage; perinatal
CP5	Left	41	Right hemiplegia	Unilateral spastic hypertonia	GMFCS: 2 MACS:2	no	10/10	10/10	67	86	Left cortical-subcortical frontal-temporal-parietal encephalomalacia (MRI)	Stroke; perinatal
CP6	Right	29	Diplegia (left > right)	Bilateral spastic hypertonia	GMFCS: 2 MACS: 1	focal epilepsy	10/10	10/10	82	89	Bilateral Periventricular leukomalacia (MRI)	Hypoxic-ischemeic damage; perinatal
CP7	Left	37	Right hemiplegia	Unilateral spastic hypertonia	GMFCS: 1 MACS: 2	no	6.3/10	6.3/10	99	92	Left periventricular leukomalacia (MRI)	Hypoxic-ischemeic damage; perinatal
CP8	Right	31	Diplegia (left > right)	Bilateral spastic hypertonia	GMFCS: 2 MACS: 1	no	9/10	9/10	87	99	Bilateral Periventricular leukomalacia (MRI)	Hypoxic-ischemeic damage; perinatal
CP9	Left	40	Right hemiplegia	Unilateral spastic hypertonia	GMFCS: 2 MACS: 2	no	10/10	10/10	99	101	Bilateral basal ganglia (putamen, thalamus) hyperintensity (MRI)	Hypoxic-ischemeic damage; perinatal
CP10	Right	29	Diplegia (left > right)	Bilateral spastic hypertonia	GMFCS: 1 MACS: 2	no	10/10	10/10	100	104	Right periventricular leukomalacia (CUS)	Hypoxic-ischemeic damage; perinatal

CUS, cranial ultrasound; FIQ, Full-scale intelligence quotient; GA (weeks), Gestational Age (weeks); GMFCS, Gross Motor Function Classification System; MACS, Manual Ability Classification System; MRI, Magnetic Resonance Imaging; n.a., not available; VIQ, verbal intelligence quotient.

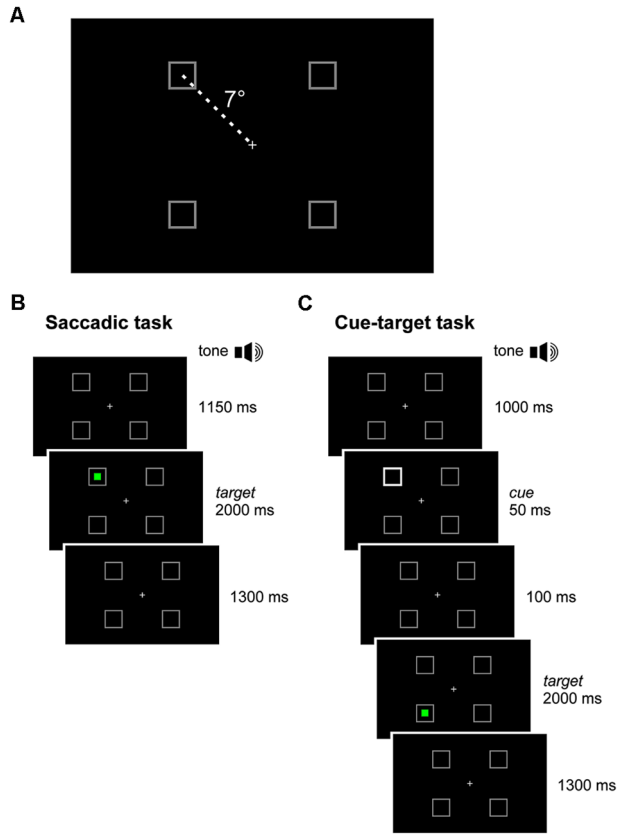

FIGURE 1 | Experimental paradigm. **(A)** In each quadrant of the visual field, a square-shaped gray placeholder was displayed at 7° of eccentricity from a central cross throughout the recording session. **(B)** *Saccadic task*: the subject executed a visually-guided saccade towards a green target, randomly occurring inside one of the placeholders. **(C)** *Cue-target task*: the subject executed a saccade to the green target, disregarding a non-informative cue (50 ms luminance increase of a placeholder), which occurred 150 ms before target onset, either at the same (valid-cue condition) or at a different (invalid-cue condition) spatial location.

of the forthcoming saccadic target, as it occurred at the same placeholder where the target was presented in only 40% of the trials. It is fair to assume that the small preponderance of valid cues, with respect to a completely random distribution among the placeholders, did not represent a reliable predictor of the direction of the saccadic response. In the remaining 60% of invalid-cue trials, the cue occurred randomly at one of the three placeholders with a different spatial location from the saccade target. The aim of this experimental design was to reduce the difference in sample size between valid- and invalid-cue trials. Within each experimental session, we presented 80 valid-cue trials (equally distributed among the four placeholders) and 120 invalid-cue trials (with all possible cue-target combinations occurring with equal probability), yielding a total number of 200 trials. To reduce the level of fatigue and to maintain high level of attention, we divided the *cue-target task* into five blocks of 40 trials (each one lasting about 3 min), leaving a rest period of 5 min between blocks.

All subjects received practice trials of both tasks before performing the experimental session. The calibration of the eye tracker was repeated before each block, by using a five-point routine. A correct comprehension of task instructions was carefully ascertained verbally from each child. Unfortunately, some children were unable to complete all five blocks of trials in the *cue-target task*, by manifesting restlessness in the last part of the recording session. Thus, one CP child (CP5) was able to conclude just four blocks of trials, while only three blocks were recorded in two TDC (TD2 and TD7) and in two CPC (CP2 and CP7).

Data Processing

In order for a trial to be included in the quantitative analysis of the oculomotor response, participant gaze had to be directed within a circle of 1° radius around the central fixation cross (in the absence of eye blinking) at the time of the target appearance in the *saccadic task* or at the appearance of the cue in the *cue-target task*.

Oculomotor responses were analyzed off-line by a custom-written Visual Basic application, developed in a Microsoft Visual Studio 2015 environment. Statistical analyses were performed in the R environment (R Core Team, 2016).

RESULTS

Saccadic Task

The *saccadic task* was meant to ascertain whether CPC were able to perform visually-guided saccades with similar characteristics with respect to TDC. To this end, reaction time and spatial error (distance between target position and eye position at the end of the first saccadic movement following the target onset) were measured for simple visually-guided saccades in both groups of children.

The scatter plot of **Figure 2** shows the mean latencies and the mean errors of saccadic movements for every CP and TD subject. The mean saccade latency across all TDC was 234.7 ms (SD ±39.14 ms), while the mean saccadic error was 1.83° (SD ±0.46°). The average values for CPC were 241.1 ms (SD ±91.14 ms) for the latency and 1.59° (SD ±0.39°) for the saccadic error. The mean values of both parameters were not statistically different for the two children groups (Wilcoxon Test, $p > 0.39$). However, the standard deviation of mean saccadic latencies was significantly larger for CPC than for TDC ($F_{(6,12)} = 5.422$; two-tailed $p = 0.013$).

This larger variability was due to the very fast and very low response speed of subjects CP9 and CP5, respectively. The mean saccadic latency of CP9 (9 years) was 127.8 ms (SD ±34.4 ms). In fact, 76% of the responses of this child were express saccades, i.e., with a latency shorter than 140 ms (Fischer and Ramsperger, 1984; Fischer and Weber, 1993). By contrast, responses of CP5 ($15\frac{1}{2}$ years) had an average latency of 385.0 ms (SD ±151.1 ms), with no express saccades. Both mean latencies fell outside the 95% confidence interval of TDC distribution ($t_{(12)} = 2.842$, $p = 0.015$ and $t_{(12)} = 4.220$, $p = 0.001$, respectively).

Moreover, latency in TDC was shorter for upward than for downward saccades, the mean intra-subject difference being

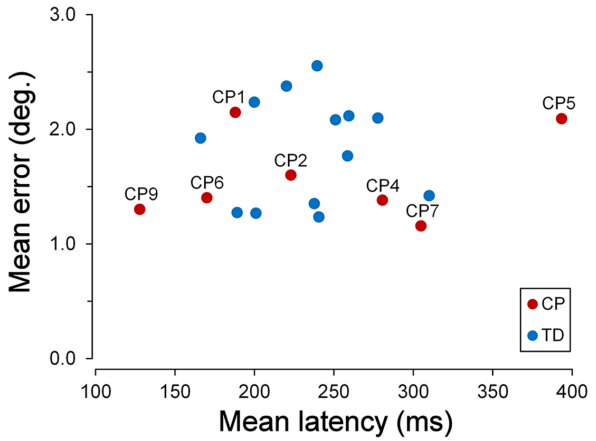

FIGURE 2 | Latency and accuracy of ocular responses in the *saccadic task*. Scatter plot of the mean latencies vs. the mean errors of saccadic movements for every cerebral palsy (CP) and typically developing (TD) participant, tested in the *saccadic task*. For Children with CP (CPC), subject identifiers are shown.

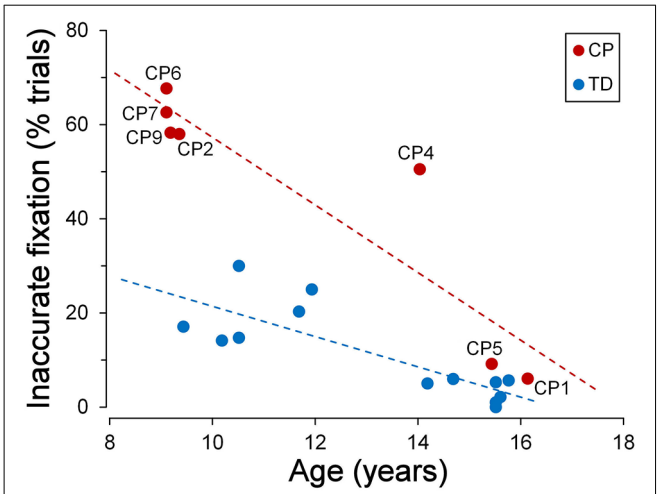

FIGURE 3 | Fixation stability during the *cue-target task*. Scatter plot showing the relationship between the percentage of trials with inaccurate fixation and participant's age. Subject identifiers are reported near CPC data points. Statistically significant regression lines (dashed) are depicted for typically developing children (TDC; blue) and CPC (red), separately.

31.4 ms (SD ±35.9 ms). A paired *t*-test demonstrated that this difference was statistically significant ($t_{(12)} = 3.153$, $p = 0.008$). By contrast, the difference between upward and downward saccade mean latencies in CPC was found to be statistically non-significant ($t_{(6)} = 2.043$, $p = 0.087$).

Cue-Target Task

Fixation Stability During Task Execution

Besides inhibiting a prepotent saccadic response towards the task-irrelevant visual cue, a correct execution of the *cue-target task* required the capacity of actively keeping a steady fixation, maintaining sustained attention for a long time at a specific point of the visual scene.

Fixation during trials was considered to be accurate when no eye movements larger than few degrees were made away from the central cross during the initial part of the task, or from the peripheral target once the latter was reached after the presentation of the cue-target sequence. Therefore, in our analysis, fixation accuracy measured the overall child's ability to execute the task, independently of whether or not he/she succeeded in suppressing an eye movement towards the visual cue.

TDC were generally quite good in keeping a steady fixation. However, we found a significant correlation between fixation accuracy and child age. The graph of **Figure 3** depicts the relationship between the percentage of the trials with inaccurate fixation and the participant age, for both TDC and CPC. It can be clearly seen that older TDC (14–16 years) were very good in performing the task, as eye movements breaking the fixation periods occurred, on average, in only 3.6% of the trials, while in younger TDC (9–12 years) the mean percentage increased to 20.2%. A linear regression analysis to test the dependence of the percentage of trials with inaccurate fixation on age yielded statistically highly significant results ($\beta = -0.031$; $t = -4.606$; $p < 0.001$).

Figure 3 also neatly shows that younger CPC were much less accurate in task execution with respect to TDC, suggesting an impairment of executive functions. The most frequent observed incorrect behaviors were: looking towards empty areas of the visual field during task performance (sometimes even outside the computer screen), directing gaze towards "inactive" placeholders, returning to the fixation cross shortly after the eye response to the target (often with to-and-fro movements between central cross and target), "forgetting" to return to the fixation cross after the target turned off (sometimes remaining on the empty placeholder for the all duration of the next trial), or a combinations of these actions. Indeed, 62% of the trials, in the CPC below the age of 10, suffered on average of some type of error in task execution. Furthermore, these fixation inaccuracies were unlikely to depend on visual fatigue, since their frequency did not increase during a block of trials, neither towards the end of the experimental session.

Interestingly, fixation accuracy was much more accurate in the two older CPC (>15 years), at a level comparable to that of age-matched TDC. The percentage of trials with inappropriate saccadic movements was 6.1% for CP1 and 9.2% for CP5. A *t*-test to compare these values with those measured in the 7 TDC with age >14 years, yielded a statistically non-significant difference for CP1 ($t_{(6)} = 1.081$; $p = 0.321$) and a marginally significant difference in CP5 ($t_{(6)} = 2.447$; $p = 0.050$). The linear regression coefficient between percentage of trials with inaccurate fixation and age in CPC was highly significant ($\beta = -0.072$; $t = -4.927$; $p = 0.004$) and was twice as steep of that of TDC. Therefore, the difference between TDC and CPC in trial execution errors is large at a younger age but is virtually absent at an age of about 15.

Saccadic Intrusions Towards Placeholders

Saccadic intrusions towards "inactive" placeholders (i.e., when they did not exhibit any change in their luminance intensity)

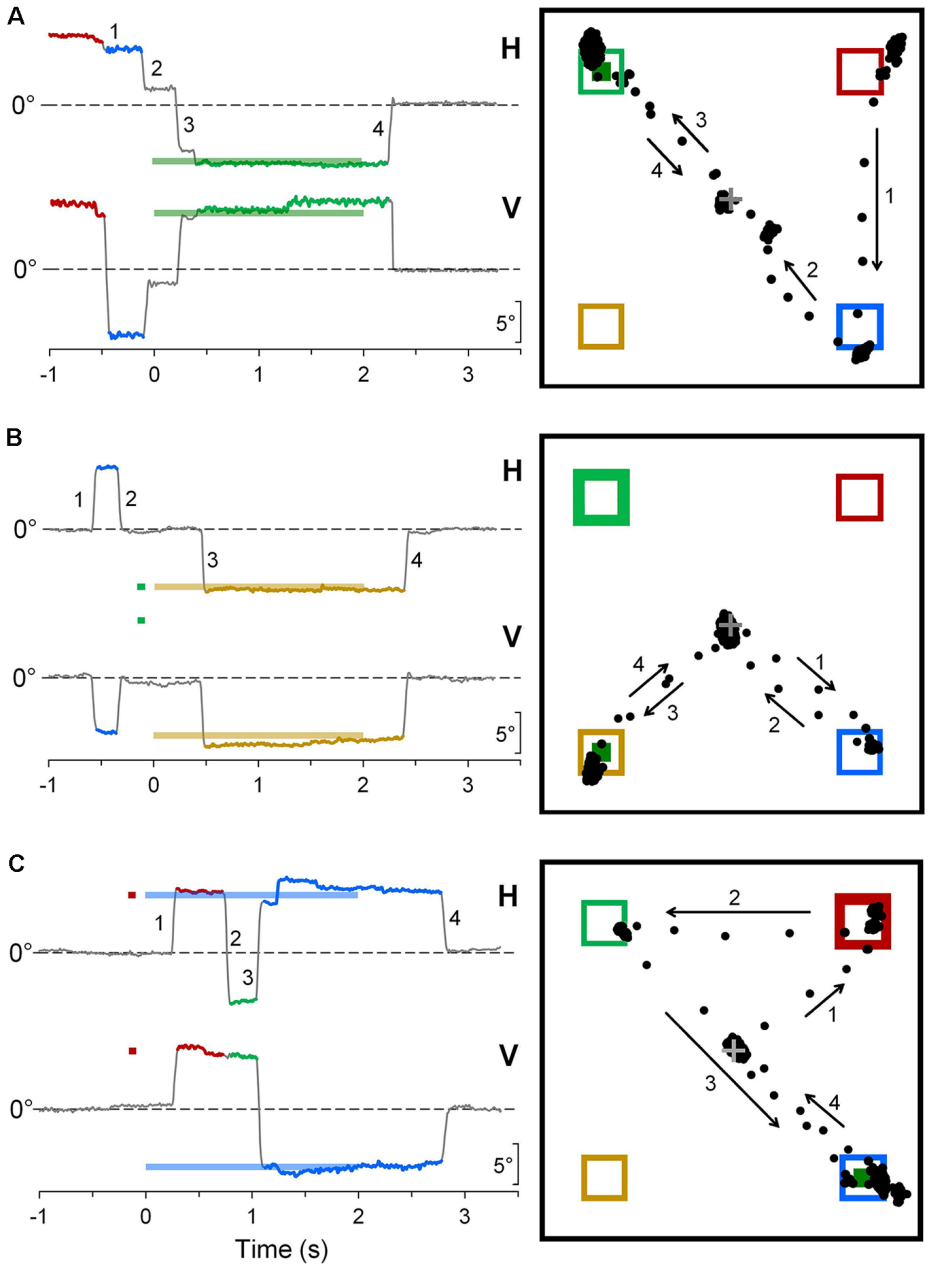

FIGURE 4 | Representative recordings of saccadic intrusions towards placeholders in CPC. **(A)** A *saccadic task* trial; **(B,C)** trials during the *cue-target task*. Color codes are used to identify more easily the placeholders on which visual stimuli are presented and eye movements are directed to. On the column at the left-hand side, traces represent the time courses of horizontal (H) and vertical (V) eye movement recordings (up: rightwards and upwards direction), with respect to central fixation cross (dashed line). Bold horizontal lines, with the color corresponding to the placeholder of appearance, indicate timing and position of saccadic target and cue. Eye movement traces are also drawn with the color code corresponding to the placeholder to which gaze was directed. Insets on the right-hand column depict the projections of the line of gaze on the computer screen during the trial. Numbers and arrows mark sequence and direction of saccades, respectively, to ease the comparison between the two ways of representing the eye movements. Bold frames indicate the placeholder of cue appearance; little green squares indicate the place of occurrence of the saccadic target.

constituted the most common reason for fixation breakdown in both TDC and CPC.

Some representative examples of saccadic intrusions in CPC are shown in **Figure 4**. Panel A depicts an eye movement recording during a *saccadic task* trial in subject CP6. Although instructions were to keep a steady fixation of the central cross until target onset, the subject gaze was jumping from one placeholder to another, landing in the proximity of the central cross only 110 ms before the appearance of the peripheral visual stimulus. Nevertheless, the occurrence of a subsequent

correct saccadic response to the target, with a very fast reaction time of 156 ms, denotes a normal performance of visually-guided saccades. **Figures 4B,C** show a correct and an erroneous response, respectively, in *cue-target task* trials, in another CP subject (CP4). In **Figure 4B**, an eye movement to the cue was correctly inhibited, but a saccade to an "inactive" placeholder was performed during the fixation period before stimulus presentation. In **Figure 4C**, instead, the first saccadic response was erroneously made towards the cue with a latency of 351 ms. Gaze eventually reached the target location about 1 s after its onset, but only after the intrusion of a task-inappropriate saccade to an "inactive" placeholder.

Figure 5A depicts the frequency of occurrence of saccadic intrusions towards placeholders during the entire experimental session (measured as mean intrusions per trial) as a function of age, for both TDC and CPC. In TDC, they occurred on average about once every 12 trials (0.084 intrusions/trial, SD ±0.077). Moreover, as for fixation accuracy, also the frequency of saccadic intrusions to placeholders had an inverse linear relationship with age, reaching an almost perfect inhibition of these incorrect gaze shifts at the age of about 15 years. The regression analysis on TDC data yielded a statistically significant regression coefficient ($\beta = -0.020$; $t = -2.742$; $p = 0.019$).

By contrast, younger CPC made much more frequent gaze movements towards "inactive" placeholders than TDC, often performing several saccadic intrusions within the same trial. The number of intrusions per trial ranged from 0.391 (CP2) to 0.884 (CP6), falling largely outside the two-tailed 95% confidence interval of the distribution found in the TDC population. Interestingly, saccadic intrusions were scanty in the two older CPC (CP1 and CP5), with a frequency of occurrence very similar to that of age-matched TDC (15–16 years). Not surprisingly, these two subjects were also very good in maintaining a steady fixation during the execution of the task (see **Figure 3**).

The execution of saccadic intrusions towards placeholders was of particular interest in CPC since most subjects showed a quadrant preponderance in their occurrence. **Figure 5B** represents the distribution of saccadic intrusions among visual quadrants, in each of the five CPC with a high rate of intrusion occurrence. For each participant, the total area of the four circles is proportional to the overall frequency of occurrence per trial. Moreover, the area of each circle reflects the proportion of intrusions (whose percent value is reported nearby) directed to the placeholder located in the corresponding visual quadrant. In all subjects shown in **Figure 5B**, a χ^2 test indicates that the observed frequencies differed significantly ($p \leq 0.001$) from those expected if the distribution of saccadic intrusions were the same among the four quadrants. Subjects CP2 and CP4 showed a neat left-right asymmetry, with a marked preponderance of saccadic intrusions to the right visual hemifield. By contrast, in subject CP9 the visual field preponderance was towards the upper quadrants. Finally, in CP6 and CP7 the distribution of saccadic intrusions was clearly non-uniform, with an obvious lower frequency of occurrence towards the lower-left and upper-left quadrants, respectively.

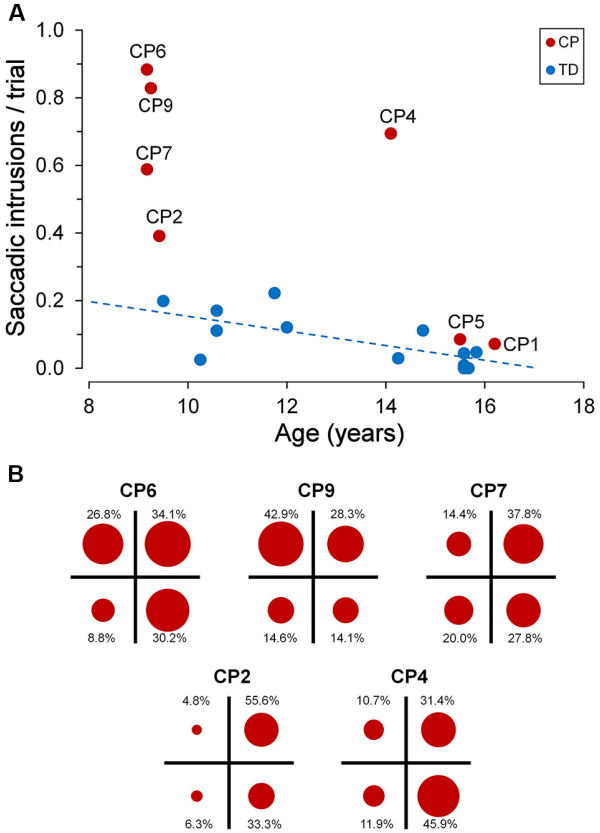

FIGURE 5 | Saccadic intrusions towards "inactive" placeholders. **(A)** Scatter plot illustrating mean saccadic intrusions per trial as a function of participant age, for TDC and CPC. Subject identifiers are reported near CPC data points. The blue dashed line indicates the presence of a statistically significant linear regression for TDC data. **(B)** Distribution of saccadic intrusions among visual quadrants, made by CPC with a high rate of intrusion occurrence. In each plot, the circle areas are proportional to the relative frequency of intrusions in the corresponding quadrant (see text for details).

Responses to Cue

A goal of the cue-target paradigm was to ascertain the operation of the inhibitory control in CPC in presence of a stimulus-driven capture of attention: the task-irrelevant cue is a prepotent attentional stimulus, eliciting a foveating saccade that must be suppressed. For the purpose of this analysis, we considered a saccadic response as erroneously elicited by the cue appearance: (1) an *invalid* trial in which the first saccade following the presentation of the cue-target pair of stimuli was directed towards the cue; and (2) a *valid* trial in which the eye movement was directed towards the target with a latency shorter than 90 ms. In fact, below this very short latency, it is safe to assume that the response was driven by the luminance change of the placeholder (cue), rather than by the presentation of the target.

Interestingly, the ability to suppress an automatic response towards the cue was markedly affected by the subject's "response readiness" in performing visually-guided saccades, as measured by the rate of the express saccades recorded during the *saccadic task*. Express saccades are saccades that are characterized by an extremely short latency (Fischer and Ramsperger, 1984;

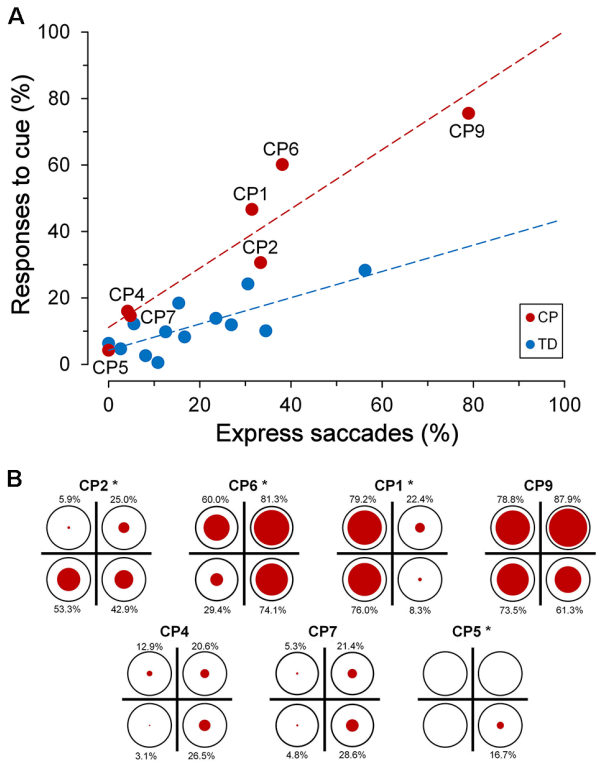

FIGURE 6 | Inhibitory control of reflexive saccades in the *cue-target task*. **(A)** Scatter plot depicting the percentage of eye responses towards the cue as a function of the percentage of express saccades made by each subject. Subject identifiers are reported near CPC data points. The red dashed line indicates the presence of a statistically significant linear regression for CPC data. **(B)** Distribution of responses towards the cue among visual quadrants for each CP subject. In each plot, the size of the red circles reflects the percentage of responses (whose value is reported nearby), with respect to the number of trials in which the cue fell in the corresponding quadrant (indicated as reference by a black circumference). Asterisks near the subject identifiers indicate a non-random distribution of cue-directed saccades.

Fischer and Weber, 1993). It has been reported that a relatively high number of express saccades determines a reduced ability to suppress reflexive saccades (Fischer et al., 1997), suggesting the presence of a poorly developed fixation system. In this article, a saccade has been defined as "express" when its latency falls within the range of 90–140 ms. In agreement with literature data, we found, in both TDC and CPC, a statistically significant linear correlation between the percentage of eye responses elicited by the cue and the number of express saccades made by each subject (**Figure 6A**).

A linear regression analysis was conducted to compare the relationship of the percentage of responses to cue to the rate of express saccades, for each group of children. The analysis yielded a highly significant correlation between the percentage of responses to the cue and the express saccade frequency, for both TDC ($\beta = 0.396$, $R^2 = 0.577$, $p = 0.003$) and CPC ($\beta = 0.892$, $R^2 = 0.886$, $p = 0.002$). A significant interaction in the relationship was found for the two groups of children ($F_{(1,16)} = 8.73$, $p = 0.009$), indicating a statistically significant difference between the regression coefficients. Finally, the two groups of children did not show a significant difference in the rate of occurrence of expressed saccades (Wilcoxon test, $p = 0.663$), suggesting that CP does not determine *per se* a variation in the tendency to make saccades with a very short latency. Notwithstanding the lack of a statistical difference between the population means, it is worth noting that subject CP9 made an unusually high number of express saccades (78.9%), yielding an extremely short overall saccadic mean latency (127.8 ms).

To summarize, in both TD and CP children, the ability to suppress an eye movement towards a prepotent attentional stimulus strongly depends, in an inverse manner, on the individual leaning to make saccadic responses with very short latencies. Thus, CPC that idiosyncratically make most saccades with a regular latency are as successful as TDC to inhibit gaze shifts towards task-irrelevant captures of attention. An impairment of the inhibitory control of reflexive saccades with respect to TDC manifests only in CPC who have the tendency to make visually-guided saccades with very short reaction times: the highest the rate of express saccades, the worst is an effective suppression of a response to the cue stimulus.

Alike to the observed spatial preponderance for the saccadic intrusions towards placeholder, also the ability of most CPC to suppress a saccade towards the cue was not equally compromised in the various quadrants of the visual field. **Figure 6B** depicts, for every CP subject, the distribution among quadrants of the responses to cue. The size of the red circles reflects the percentage of responses (whose value is reported nearby), with respect to the number of trials in which the cue fell in the corresponding quadrant (indicated as reference by a black circumference). Asterisks near the subject identifiers indicate that the observed percentages of responses to cue differed significantly from those expected if they were equally distributed in all quadrants (χ^2 test at $p < 0.05$ level). Specifically, differences in distribution among quadrants were found to be statistically highly significant ($p < 0.001$) in CP1, CP5 and CP6, while in CP2 the χ^2 test yielded $p = 0.021$.

By taking into account the four CPC who manifested the biggest impairment in suppressing the responses to the cue, one can notice that inhibitory control was indeed normal or near-to-normal in some quadrants, but was highly defective in others. Thus, in CP1 inhibitory control was almost completely lost in the left visual hemifield, but was very similar to that of the TDC population on the right hemifield. In CP2, the impairment affected only the lower hemifield, while CP6 failed in suppressing cue-directed saccades in the whole visual field, except the lower-left quadrant. Finally, inhibitory control was almost completely lost in the whole visual field in CP9, with no statistically significant differences among quadrants ($\chi^2 = 6.394$; $p = 0.094$).

Interestingly, the quadrants in which a subject made more frequently saccadic intrusions to placeholders did not correspond, in general, to those in which responses to cue were prevailing. For instance, saccadic intrusions were almost absent in CP1, but saccades to the cue occurred in the large majority of trials in the left hemifield. Subject CP2 made saccadic intrusions mostly in the right hemifield but showed a preponderance of responses to the cue in the lower quadrants. Conversely, a good

spatial correspondence of saccadic intrusions and responses to the cue was present in subject CP6.

Effect of Cue Validity on Saccade Latency

In the *cue-target task*, the participant had to perform a saccade to the peripheral target, after a visual cue was flashed a short time interval (150 ms) before the target onset, either at the same (valid cue) or at a different (invalid cue) spatial position. Under these conditions, saccadic responses were expected to be faster when the target occurred at cued, relative to uncued, locations.

Our cueing paradigm proved to be very effective in inducing faster responses in TDC when the cue occurred at the same location as the saccade target. We performed a two-way repeated-measure ANOVA, with "*validity*" and "*target quadrant*" as grouping factors, on the within-subject mean response latencies, computed from all correctly performed trials. Analysis yielded highly significant principal effects for both factors, with a non-significant interaction. Cue validity accounted for an average increase of 49.3 ms in saccade latency of invalid with respect to valid trials ($F_{(1,84)} = 66.293$, $p < 0.0001$). Mean latency across subjects was 211.0 ms and 260.3 ms for valid and invalid trials, respectively. Also the "*target quadrant*" principal effect was highly significant ($F_{(3,84)} = 9.391$, $p < 0.0001$). This effect was largely accounted for by the fact that response latencies towards the upper visual hemifield (221.7 ms, SD ±88.3 ms) were faster than those towards the lower hemifield (249.6 ms, SD ±94.2 ms). Accordingly, a two-way repeated-measure ANOVA yielded very significant "*up-down*" ($F_{(1,36)} = 15.141$, $p = 0.0004$) and "*validity*" ($F_{(1,36)} = 47.298$, $p < 0.0001$) principal effects, with a non-significant interaction.

The effect of cue validity on saccade latency was more difficult to ascertain in CPC as a population, because of a non-homogeneous behavior in the *cue-target task* relative to the visual quadrants and the scantiness of usable responses in some subjects. In fact, as described above, many trials had to be discarded for this type of analysis, either for the preponderance of cue-directed responses or for the presence of saccadic intrusions or other fixation inaccuracies. Nevertheless, a two-way repeated-measure ANOVA on the within-subject mean response latencies revealed a significant effect of the factor "*validity*" ($F_{(1,45)} = 4.427$, $p = 0.041$) and a non-significant effect of the factor "*target quadrant*" ($F_{(3,45)} = 1.167$, $p = 0.333$). The reason for the low level of significance of the "*validity*" effect is possibly to be ascribed to the large statistical variability of the data, due to the reduced number of available trials per quadrant in some subjects. In any case, the mean intra-subject increase in response latency for the invalid trials with respect to the valid ones was 57.7 ms, that is, quite similar to that found in the TDC population.

DISCUSSION

This article investigated attentional and inhibitory control in CPC, with normal IQ or mild cognitive impairment, by using oculomotor tasks. This approach was meant to overcome the difficulties arising from postural and limb movement disabilities when tests are based on manual responses. Furthermore, the intimate relationship between eye movements and spatial attention constitutes a vantage point to discern deviant attention engagements, increased distractibility or deficits in discarding irrelevant sensory stimuli to the ongoing task.

The present study extends recent research demonstrating that CPC might show significant impairments in inhibitory control (Christ et al., 2003) and of attentional and executive skills (Bottcher et al., 2010; Bodimeade et al., 2013). Indeed, our results indicate that CPC show severe deficits in maintaining sustained attention and complying with instructions of the oculomotor task. Furthermore, inhibitory control appears to be significantly impaired. Patients show great difficulties in suppressing saccades not only to the cue stimuli but also to "inactive" placeholders, which represent powerful attentional attractors that must be covertly attended during task execution. Altogether, results provide evidence that CPC often manifests significant executive impairments, even in the presence of normal or mildly impaired intelligence.

These findings have relevant implications from a clinical and rehabilitative viewpoint. It is widely accepted that the maturation of attentional control and of the ability to suppress responses to stimuli, that are irrelevant or conflicting with the ongoing task, is essential for the development of cognitive abilities through childhood and adolescence (Dempster, 1993; Anderson et al., 2002). Accordingly, a number of studies have shown that CPC often manifests specific learning disabilities, lower academic performance and problems in emotional and social relationships (Frampton et al., 1998; Nadeau and Tessier, 2006; Parkes et al., 2009; Whittingham et al., 2010).

Saccadic Inhibitory Control After Stimulus-Driven Captures of Attention

There is a large body of evidence that spatial attention and saccade programming are driven by overlapping neural mechanisms (Rizzolatti et al., 1987; Awh et al., 2006). Because of the drop in visual acuity with increasing retinal eccentricity, a saccade is the normal motor response to bring into the fovea a salient visual object for a better perceptual processing. However, the system has evolved to make covert shifts of attention (i.e., without the overt deployment of an eye movement), whenever the motor response is inadequate to the behavioral goal. Because of the tight link between selective attention and saccade planning, a covert shift of attention relays on a successful inhibition of the programmed eye movement. Our data show that a deficit in the saccadic inhibitory control following an attentive engagement is a common outcome of CP.

Capture of attention can be driven by two distinct mechanisms, controlled by two partially segregated neural systems (Corbetta and Shulman, 2002). Stimulus-driven (*bottom-up*) capture of attention takes place at the occurrence of an unexpected or salient stimulus. By doing so, these events gain high priority over brain activity, in order to advantage the perceptual processing of the novel stimulus. By contrast, goal-directed (*top-down*) shifts of selective attention are controlled by cognitive factors, such as expectancies, task-related instructions and behavioral goals. In the *cue-target task* of this study, both stimulus-driven and goal-directed captures of attention are present.

Cue stimuli in the *cue-target task*, although uninformative, represent novel events that increase the saliency of a specific spatial location and generate a stimulus-driven capture of attention. The attentive engagement by the cue event is demonstrated by a well-known spatial priming effect, which determines faster responses and an enhanced stimulus detection when a target stimulus occurs at the same location within a time interval shorter than 200 ms (Posner et al., 1984; Fecteau et al., 2005; as opposed to the phenomenon called "inhibition of return" occurring at longer time intervals; Posner and Cohen, 1984; Fecteau et al., 2005). At the cue-target onset asynchrony employed in this study of 150 ms, therefore, valid cues are expected to have a facilitatory effect on the latency of the eye movement towards the target. Accordingly, a significant decrease of the saccadic reaction time in the valid-cue trials, with respect to the invalid ones, is observed in both the TDC and CPC populations. This finding demonstrates that cue stimuli in our experimental protocol are effective in inducing a *bottom-up* engagement of spatial attention and that the basic mechanisms of stimulus-driven capture of attention are preserved in our sample of CPC. However, data show that many CPC have much greater difficulties, with respect to TDC, in suppressing a saccadic response towards the task-irrelevant visual cues. By comparison, TDC on average fail to inhibit an eye movement to the cue only in about 12% of the trials. Instead, there are quadrants of the visual field in which 4 out of 7 CPC make a saccade to the cue in more than 50% of the responses, reaching in some subjects percentages higher than 75–80%. The correct suppression in some quadrants of the responses to the cue in all CPC (except CP9), to a level comparable to TDC performance, demonstrates that, in spite of the presence of a mild cognitive impairment in some participants, the deficit in saccadic inhibitory control cannot be ascribed to a poor understanding of the instructions of the *cue-target task*. In fact, if performance errors were due to a lack of comprehension of the task, we would expect a uniform spatial distribution of the responses to the cue in the visual field. In addition, the number of execution errors does not seem to be related to the VIQ or FIQ scores of the participant (see **Table 1**).

Interestingly, in both TDC and CPC, the ability to inhibit stimulus-driven saccades towards the cue is inversely proportional to the frequency of express saccades made by the subject during a visually-guided saccade task. Express saccades are generally produced in low numbers, especially with an overlap paradigm as in the *saccadic task* of this study, i.e., when the fixation point remains visible during the presentation of the saccade target. According to Fischer et al. (1997), the rate of express saccades in the overlap condition is <20% in young subjects (less than 20 years old). Munoz et al. (1998), instead, reports a percentage range of 0–35% (mean 9.3%) in children with ages between 5 and 8.

In the present study, the rate of occurrence of express saccades does not show a statistical difference between TD and CP children. The percentage is <40% for the majority of participants, independently of age. It should be noted, however, that two children make an extraordinarily high number of express saccades: 56.3% (TD child) and 78.9% (CP9). The higher rate of express saccades in this study, with respect to that reported in the literature, may find a plausible explanation in the difference in the experimental protocol. In our paradigm, placeholders are always present, possibly exerting a priming effect on the locations where the saccade target will appear. In addition, a warning acoustic tone occurs at a fixed interval from the target onset, enhancing the subject readiness to respond to the visual stimulus. Finally, a note on the two children who perform a very high number of express saccades. One could hypothesize that, independently of being affected by CP, these subjects belong to the minority of individuals, known as "express saccade makers," who produce unusually high numbers of express saccades in the overlap paradigm (Biscaldi et al., 1996; Cavegn and Biscaldi, 1996). This condition has been proposed to result from a poor development of the fixation system and is associated with a marked difficulty to suppress reflexive saccades and with a reduced voluntary control over saccade generation. Therefore, based on our data, it is not possible to conclude that the observed tendency in some CPC to make a high number of express saccades is a consequence of the early brain lesion.

The relationship between the percentage of responses to the cue and express saccade rate is also in full agreement with literature data. In fact, it has been reported that the capability of suppressing reflexive saccades in an antisaccade task (subject has to inhibit a saccade towards a visual stimulus and move his gaze to its mirror location; Hallett, 1978) or in a memory-guided saccade paradigm (execution of a delayed eye movement towards the spatial location of a briefly presented visual stimulus) is reduced as a function of the rate of express saccades that each subject makes in a visually-guided saccade task (Fischer et al., 1997; Munoz et al., 1998).

In this context, however, the most relevant result is that, at equal percentages of express saccade execution, CPC make more saccadic responses to the cue than TDC. This represents a clear demonstration of an impairment of the saccadic inhibitory control in the presence of a stimulus-driven capture of attention. Interestingly, this difficulty in suppressing task-irrelevant, reflexive saccades becomes manifest only in CPC who tend to make visually-guided saccadic responses with very low latencies. Patients normally performing saccades with regular/long reaction times are able to inhibit responses to the cue stimuli as efficiently as TDC.

Cognitive Control of Oculomotor Behavior

Placeholders in our experimental setup constitute powerful goal-directed attentional attractors, inasmuch as they are locations in which behaviorally relevant sensory stimuli are expected to occur. They are always present throughout the recording session, representing areas of interest that are covertly attended while the subject is looking to the detection of the target onset. The occurrence of a *top-down* attentive engagement (together with an associated oculomotor program) is indicated by the occasional presence, even in TDC, of escape saccades during the periods of visual fixation, bringing temporarily the subject's gaze on an "inactive" placeholder. This interpretation is also supported by the notion that expectancy can induce a sustained neuronal activity in the fronto-parietal network

subserving selective attention, even in the absence of a novel visual stimulus (Kastner et al., 1999). It is noteworthy that, in our group of TDC, the inhibitory control of inappropriate saccades towards goal-directed attentional attractors improves with age, attaining a very high level of performance at 15–16 years (**Figure 5A**).

As for stimulus-driven shifts of attention, our data show that saccadic inhibitory control in CPC is impaired also with goal-directed attentive engagements. This is especially evident in younger children, who make many more saccadic intrusions to placeholders than TDC. Also in this case, performance appears to improve with age. Although the low number of subjects does not allow drawing definitive conclusions, 15–16-year-old CPC exhibit an almost perfect ability to suppress saccades towards placeholders, to a degree that is virtually identical to that shown by age-matched TDC.

To summarize, the present study supports that an outcome of early brain lesions is a deficit in the saccadic inhibitory control in the presence of both stimulus-driven and goal-directed captures of attention. This impairment does not affect in equal manner the whole visual field but shows a marked spatial selectivity in each individual subject. Furthermore, the quadrant spatial preponderance of this deficit is often different for *bottom-up* and *top-down* attentive engagements. This result can find an explanation in the ordered spatial topography of the multiple neural representations of the attentive map (e.g., Fecteau and Munoz, 2006) and the fact that partially segregated brain networks control the two types of attention mechanisms (Corbetta and Shulman, 2002).

Maturation Timing of a Stable Fixation

Several studies in the literature investigated in TDC the maturation of the ability to suppress context-inappropriate saccades and to maintain a stable fixation for a prolonged time-span. There is a wide consensus that these abilities, like many other executive skills (e.g., Anderson, 2002), attain an adult level of performance by the age of 15–20 years (Fischer et al., 1997; Munoz et al., 1998). For instance, the rate of directional errors of saccadic responses in the antisaccade task decreases from about 50% to 10% between age 8–9 and 15–17 years, according to Munoz et al. (1998), and from 60% to 22% between age of 9 and 15 years, according to Fischer et al. (1997). The ability to maintain a stable central fixation, in the presence of distracting peripheral visual stimuli, also markedly improves between 9 and 10 years of age (Paus et al., 1990). However, 10-year-old children are still unable to suppress verbally forbidden saccades in about 40% of the trials, a rate well above adult level. Saavedra et al. (2009) reported similar results regarding the ability to maintain central fixation at the appearance of a peripheral target. In that study, the rate of fixation breakdowns in CPC decreases from 80% at the age of 6–9 to about 40% at the age of 11–16, against an about 20% of errors in age-matched TDC.

Our data in TDC are in good agreement with the literature. Task instructions were to keep a steady fixation either on the central fixation cross or on the target, depending on the phase of the task paradigm. Between the age of 9 and 12, the average percentage of trials with fixation inaccuracies is about 20%. More importantly, an inverse correlation is present between rate of fixation breakdowns and age, with the achievement of a high level of fixation accuracy at 15–16 years. Therefore, there is a clear evidence that, within the age-span of this study, the executive abilities required to perform the oculomotor tasks of this study are still undergoing a process of maturation.

The ability to maintain a stable fixation is far worse in younger CPC. If we take into account children below the age of 10, one or more fixation breakdowns occur in the large majority of trials, as described in more detail in the section "Fixation Stability During Task Execution" of the "Results" section. It should be noted that visual field is normal in younger CPC. Therefore, the more frequent execution of saccades cannot be ascribed to a compensatory strategy in the presence of a visual field constriction. It should be stressed, however, that both saccadic intrusions towards placeholders and fixation inaccuracies decrease with age more steeply in CPC than in TDC. This trend leads to a reduction over time of the gap in performance, until a similar executive high level is attained by the age of about 15 years. This time course of performance improvement is very similar to that described by White and Christ (2005), although in a different context of executive abilities.

Concluding Remarks

Our results provide compelling evidence that early brain injuries determine in childhood deficits of some executive skills in the oculomotor behavior, which recover to virtually normal level during adolescence. A development delay of executive abilities is not an adequate explanation for this observation, since: (1) also TDC exhibit, in the age-span of this study, an improvement of the saccadic inhibitory control and of fixation accuracy, although showing a considerably higher level of performance with respect to CPC; and (2) both TD and CP children attain the same high level of performance at about 15–16 years. Therefore, it looks more a matter of a greater incompetence of immature executive skills in CPC, rather than a delay in the attainment of abilities that are normally achieved at an earlier age.

We can make some speculations about the neural substrate underlying these observations. It is widely accepted that the development of the cognitive control is bound to the maturation of the frontal lobes and of basal ganglia thalamo-cortical circuits (Krasnegor et al., 1997; Casey et al., 2001), which typically occurs during the second decade of life. While the dependency of executive processes from the prefrontal cortex (PFC) in the adult brain is undisputed, recent studies have shown that the integrity of the entire brain is essential in childhood for typical executive performance (Jacobs et al., 2011; Long et al., 2011). During the maturation process, executive functions are not yet localized in the PFC but have a more diffuse neural representation. Accordingly, functional MRI studies have shown that children recruit different brain regions from adults in executive tasks involving response inhibition or interference suppression (Luna et al., 2001; Bunge et al., 2002) and early focal lesions induce similar patterns of executive deficits, regardless of their localization (Jacobs et al., 2011). Furthermore, contrary to adults and to 14–17-year-old adolescents (Luna et al., 2001),

activation of PFC does not occur in younger children, in whom executive abilities are bound to an activation of more posterior cortical areas. One could then surmise that the deficits occurring at a younger age, following an early brain injury, could result from a greater difficulty of extra-frontal regions in providing for executive functions, which afterward will become a main prerogative of the frontal lobes.

Along this way of reasoning, it is possible to hypothesize that the maturation process of PFC circuits, and consequently the unfolding of the related cognitive abilities, do not have a very dissimilar time course in TD and CP children, leading to an alike executive competence at about the age of 15–16 years. By contrast, the lower level of performance we observed during the earlier development period (in abilities such as suppressing saccades towards attentive stimuli, focusing attention for extended periods and exerting a cognitive control of oculomotor responses) mainly occurs in the time epoch in which executive skills seem to depend on the involvement of extra-frontal regions, conceivably through alternative executive strategies. A possible explanation of the larger executive deficits in younger CPC is that early brain lesions make this functional substitution process more difficult, determining a worse capacity to control behavior from cognitive factors.

Obviously, this condition should not be considered as a temporary situation that produces only transitory effects. The first decades of life constitute a critical period for the cognitive development and the achievement of behavioral competence. An insufficient ability to discard task-irrelevant sensory stimuli, to engage sustained attention or to inhibit a prepotent motor response, may represent a relevant factor facilitating the emergence of learning disorders and social difficulties, frequently affecting CP children and adolescents (Frampton et al., 1998; Bottcher et al., 2010; Whittingham et al., 2014).

DATA AVAILABILITY STATEMENT

The datasets generated for this study are available on request to the corresponding author.

ETHICS STATEMENT

The studies involving human participants were reviewed and approved by Ethics Committee of "ASST Spedali Civili" of Brescia, Italy (protocol. N. 1324, 08/04/2013). Written informed consent to participate in this study was provided by the participants' legal guardian/next of kin.

AUTHOR CONTRIBUTIONS

CM, LF, EF and MB contributed to the conception and design of the study. EF, JG, SM and LT performed participant recruitment. LF, JG, SM and LT performed data collection and eye movement recordings. CM and LF performed the data analysis. CM wrote the first draft of the manuscript. All authors contributed to manuscript revision, read and approved the submitted version.

ACKNOWLEDGMENTS

We are grateful to Laura Laghetto for helping in data analysis. We also thank Anna Alessandrini and Nicole D'Adda (occupational therapists), Nadia Pasini and Alessandra Franzoni (ophthalmologists) and Alice Bertoletti (orthoptist) for their valuable professional assistance in evaluating the children in this study.

REFERENCES

Anderson, P. (2002). Assessment and development of executive function (EF) during childhood. *Child Neuropsychol.* 8, 71–82. doi: 10.1076/chin.8.2.71.8724

Anderson, V. A., Anderson, P., Northam, E., Jacobs, R., and Mikiewicz, O. (2002). Relationships between cognitive and behavioral measures of executive function in children with brain disease. *Child Neuropsychol.* 8, 231–240. doi: 10.1076/chin.8.4.231.13509

Awh, E., Armstrong, K. M., and Moore, T. (2006). Visual and oculomotor selection: links, causes and implications for spatial attention. *Trends Cogn. Sci.* 10, 124–130. doi: 10.1016/j.tics.2006.01.001

Bax, M., Goldstein, M., Rosenbaum, P., Leviton, A., Paneth, N., Dan, B., et al. (2005). Proposed definition and classification of cerebral palsy, April 2005. *Dev. Med. Child Neurol.* 47, 571–576. doi: 10.1111/j.1469-8749.2005.tb01195.x

Biscaldi, M., Fischer, B., and Stuhr, V. (1996). Human express saccade makers are impaired at suppressing visually evoked saccades. *J. Neurophysiol.* 76, 199–214. doi: 10.1152/jn.1996.76.1.199

Bodimeade, H. L., Whittingham, K., Lloyd, O., and Boyd, R. N. (2013). Executive function in children and adolescents with unilateral cerebral palsy. *Dev. Med. Child Neurol.* 55, 926–933. doi: 10.1111/dmcn.12195

Bottcher, L. (2010). Children with spastic cerebral palsy, their cognitive functioning, and social participation: a review. *Child Neuropsychol.* 16, 209–228. doi: 10.1080/09297040903559630

Bottcher, L., Flachs, E. M., and Uldall, P. (2010). Attentional and executive impairments in children with spastic cerebral palsy. *Dev. Med. Child Neurol.* 52, e42–e47. doi: 10.1111/j.1469-8749.2009.03533.x

Briand, K. A., Larrison, A. L., and Sereno, A. B. (2000). Inhibition of return in manual and saccadic response systems. *Percept. Psychophys.* 62, 1512–1524. doi: 10.3758/bf03212152

Bunge, S. A., Dudukovic, N. M., Thomason, M. E., Vaidya, C. J., and Gabrieli, J. D. (2002). Immature frontal lobe contributions to cognitive control in children: evidence from fMRI. *Neuron* 33, 301–311. doi: 10.1016/s0896-6273(01)00583-9

Casey, B. J. (2001). "Disruption of inhibitory control in developmental disorders: a mechanistic model of implicated fronto-striatal circuitry," in *Mechanisms of Cognitive Development: Behavioral and Neural Perspectives*, eds J. L. McClelland and R. S. Siegler (Mahwah, NJ: Erlbaum), 662–665.

Casey, B. J., Durston, S., and Fossella, J. A. (2001). Evidence for a mechanistic model of cognitive control. *Clin. Neurosci. Res.* 1, 267–282. doi: 10.1016/s1566-2772(01)00013-5

Cavegn, D., and Biscaldi, M. (1996). Fixation and saccade control in an express-saccade maker. *Exp. Brain Res.* 109, 101–116. doi: 10.1007/bf00228631

Christ, S., White, D., Brunstrom, J., and Abrams, R. (2003). Inhibitory control following perinatal brain injury. *Neuropsychology* 17, 171–178. doi: 10.1037/0894-4105.17.1.171

Collis, N. L., Kohnen, S., and Kinoshita, S. (2013). The role of visual spatial attention in adult developmental dyslexia. *Q. J. Exp. Psychol.* 66, 245–260. doi: 10.1080/17470218.2012.705305

Corbetta, M., and Shulman, G. L. (2002). Control of goal-directed and stimulus-driven attention in the brain. *Nat. Rev. Neurosci.* 3, 201–215. doi: 10.1038/nrn755

Craft, S., White, D. A., Park, T. S., and Figiel, G. (1994). Visual attention in children with perinatal brain injury: asymmetric effects of bilateral lesions. *J. Cogn. Neurosci.* 6, 165–173. doi: 10.1162/jocn.1994.6.2.165

Dempster, F. N. (1993). "Resistance to interference: developmental changes in a basic processing mechanism," in *Emerging Themes in Cognitive Development, Volume I: Foundations*, eds M. L. Howe and R. Pasnak (New York, NY: Springer-Verlag), 3–27.

Fazzi, E., Bova, S., Giovenzana, A., Signorini, S., Uggetti, C., and Bianchi, P. (2009). Cognitive visual dysfunctions in preterm children with periventricular leukomalacia. *Dev. Med. Child Neurol.* 51, 974–981. doi: 10.1111/j.1469-8749.2009.03272.x

Fazzi, E., Signorini, S. G., La Piana, R., Bertone, C., Misefari, W., Galli, J., et al. (2012). Neuro-ophthalmological disorders in cerebral palsy: ophthalmological, oculomotor, and visual aspects. *Dev. Med. Child Neurol.* 54, 730–736. doi: 10.1111/j.1469-8749.2012.04324.x

Fecteau, J. H., and Munoz, D. P. (2006). Salience, relevance, and firing: a priority map for target selection. *Trends Cogn. Sci.* 10, 382–390. doi: 10.1016/j.tics.2006.06.011

Fecteau, J. H., Bell, A. H., Dorris, M. C., and Munoz, D. P. (2005). "Neurophysiological correlates of the reflexive orienting of spatial attention," in *Encyclopedia on the Neurobiology of Attention*, eds L. Itti, G. Rees and J. Tsotsos (San Diego, CA: Elsevier), 389–394.

Fischer, B., Biscaldi, M., and Gezeck, S. (1997). On the development of voluntary and reflexive components in human saccade generation. *Brain Res.* 754, 285–297. doi: 10.1016/s0006-8993(97)00094-2

Fischer, B., and Ramsperger, E. (1984). Human express saccades: extremely short reaction times of goal directed eye movements. *Exp. Brain Res.* 57, 191–195. doi: 10.1007/bf00231145

Fischer, B., and Weber, H. (1993). Express saccades and visual attention. *Behav. Brain. Sci.* 16, 553–567. doi: 10.1017/s0140525x00031575

Frampton, I., Yude, C., and Goodman, R. (1998). The prevalence and correlates of specific learning difficulties in a representative sample of children with hemiplegia. *Br. J. Educ. Psychol.* 68, 39–51. doi: 10.1111/j.2044-8279.1998.tb01273.x

Franceschini, S., Gori, S., Ruffino, M., Pedrolli, K., and Facoetti, A. (2012). A causal link between visual spatial attention and reading acquisition. *Curr. Biol.* 22, 814–819. doi: 10.1016/j.cub.2012.03.013

Galli, J., Ambrosi, C., Micheletti, S., Merabet, L. B., Pinardi, C., Gasparotti, R., et al. (2018). White matter changes associated with cognitive visual dysfunctions in children with cerebral palsy: a diffusion tensor imaging study. *J. Neurosci. Res.* 96, 1766–1774. doi: 10.1002/jnr.24307

Gillies, M. B., Bowen, J. R., Patterson, J. A., Roberts, C. L., and Torvaldsen, S. (2018). Educational outcomes for children with cerebral palsy: a linked data cohort study. *Dev. Med. Child Neurol.* 60, 397–401. doi: 10.1111/dmcn.13651

Hallett, P. E. (1978). Primary and secondary saccades to goals defined by instructions. *Vision Res.* 18, 1279–1296. doi: 10.1016/0042-6989(78)90218-3

Hari, R., and Renvall, H. (2001). Impaired processing of rapid stimulus sequences in dyslexia. *Trends Cogn. Sci.* 5, 525–532. doi: 10.1016/s1364-6613(00)01801-5

Jacobs, R., Harvey, A. S., and Anderson, V. (2011). Are executive skills primarily mediated by the prefrontal cortex in childhood? Examination of focal brain lesions in childhood. *Cortex* 47, 808–824. doi: 10.1016/j.cortex.2010.06.002

Jacobson, L. K., and Dutton, G. N. (2000). Periventricular leukomalacia: an important cause of visual and ocular motility dysfunction in children. *Surv. Ophthalmol.* 45, 1–13. doi: 10.1016/S0039-6257(00)00134-X

Kastner, S., Pinsk, M. A., De Weerd, P., Desimone, R., and Ungerleider, L. G. (1999). Increased activity in human visual cortex during directed attention in the absence of visual stimulation. *Neuron* 22, 751–761. doi: 10.1016/s0896-6273(00)80734-5

Katayama, M., and Tamas, L. B. (1987). Saccadic eye-movements of children with cerebral palsy. *Dev. Med. Child Neurol.* 29, 36–39. doi: 10.1111/j.1469-8749.1987.tb02105.x

Kolk, A., and Talvik, T. (2000). Cognitive outcome of children with early-onset hemiparesis. *J. Child Neurol.* 15, 581–587. doi: 10.1177/088307380001500903

Krägeloh-Mann, I., and Horber, V. (2007). The role of magnetic resonance imaging in elucidating the pathogenesis of cerebral palsy: a systematic review. *Dev. Med. Child Neurol.* 49, 144–151. doi: 10.1111/j.1469-8749.2007.00144.x

Krasnegor, N. A., Lyon, G. R., and Goldman-Rakic, P. S. (1997). *Development of the Prefrontal Cortex: Evolution, Neurobiology, and Behavior*. Baltimore: Paul H Brookes Publishing.

Lanzi, G., Fazzi, E., Uggetti, C., Cavallini, A., Danova, S., Egitto, M. G., et al. (1998). Cerebral visual impairment in periventricular leukomalacia. *Neuropediatrics* 29, 145–150. doi: 10.1055/s-2007-973551

Long, B., Spencer-Smith, M. M., Jacobs, R., Mackay, M., Leventer, R., Barnes, C., et al. (2011). Executive function following child stroke: the impact of lesion location. *J. Child Neurol.* 26, 279–287. doi: 10.1177/0883073810380049

Luna, B., Thulborn, K. R., Munoz, D. P., Merriam, E. P., Garver, K. E., Minshew, N. J., et al. (2001). Maturation of widely distributed brain function subserves cognitive development. *Neuroimage* 13, 786–793. doi: 10.1006/nimg.2000.0743

MacLennan, A. H., Thompson, S. C., and Gecz, J. (2015). Cerebral palsy: causes, pathways, and the role of genetic variants. *Am. J. Obstet. Gynecol.* 213, 779–788. doi: 10.1016/j.ajog.2015.05.034

Maylor, E. A. (1985). "Facilitatory and inhibitory components of orienting in visual space," in *Attention and Performance 11*, eds M. I. Posner and O. Marin (Hillsdale, NJ: Erlbaum), 189–207.

Munoz, D. P., Broughton, J. R., Goldring, J. E., and Armstrong, I. T. (1998). Age-related performance of human subjects on saccadic eye movement tasks. *Exp. Brain Res.* 121, 391–400. doi: 10.1007/s002210050473

Nadeau, L., and Tessier, R. (2006). Social adjustment of children with cerebral palsy in mainstream classes: peer perception. *Dev. Med. Child Neurol.* 48, 331–336. doi: 10.1017/s0012162206000739

Parkes, J., White-Koning, M., McCullough, N., and Colver, A. (2009). Psychological problems in children with hemiplegia: a European multicentre survey. *Arch. Dis. Child.* 94, 429–433. doi: 10.1136/adc.2008.151688

Paus, T., Babenko, V., and Radil, T. (1990). Development of an ability to maintain verbally instructed central gaze fixation studied in 8- to 10-year-old children. *Int. J. Psychophysiol.* 10, 53–61. doi: 10.1016/0167-8760(90)90045-f

Pirila, S., van der Meere, J., Korhonen, P., Ruusu-Niemi, P., Kyntaja, M., Nieminen, P., et al. (2004). A retrospective neurocognitive study in children with spastic diplegia. *Dev. Neuropsychol.* 26, 679–690. doi: 10.1207/s15326942dn2603_2

Posner, M. I., and Cohen, Y. (1984). "Components of visual orienting," in *Attention and Performance X: Control of Language Processes*, eds H. Bouma and D. G. Bouwhuis (Hillsdale, NJ: Erlbaum), 531–556.

Posner, M. I., Rafal, R. D., Choate, L., and Vaughan, J. (1985). Inhibition of return: neural basis and function. *Cogn. Neuropsychol.* 2, 211–228. doi: 10.1080/02643298508252866

Posner, M. I., Walker, J. A., Friedrich, F. J., and Rafal, R. D. (1984). Effects of parietal lobe injury on covert orienting of visual attention. *J. Neurosci.* 4, 1863–1874. doi: 10.1523/JNEUROSCI.04-07-01863.1984

Posner, M. I. (1980). Orienting of attention. *Q. J. Exp. Psychol.* 32, 3–25. doi: 10.1080/00335558008248231

R Core Team. (2016). *R: A Language and Environment for Statistical Computing*. Vienna: R Foundation for Statistical Computing. Avlaible online at: https://www.R-project.org/.

Rizzolatti, G., Riggio, L., Dascola, I., and Umiltá, C. (1987). Reorienting attention across the horizontal and vertical meridians: evidence in favor of a premotor theory of attention. *Neuropsychologia* 25, 31–40. doi: 10.1016/0028-3932(87)90041-8

Rosenbaum, P., Paneth, N., Leviton, A., Goldstein, M., Bax, M., Damiano, D., et al. (2007). Report: the definition and classification of cerebral palsy April 2006. *Dev. Med. Child Neurol. Suppl.* 109, 8–14. doi: 10.1111/j.1469-8749.2007.tb12610.x

Saavedra, S., Joshi, A., Woollacott, M., and van Donkelaar, P. (2009). Eye hand coordination in children with cerebral palsy. *Exp. Brain Res.* 192, 155–165. doi: 10.1007/s00221-008-1549-8

Schatz, J., Craft, S., White, D., Park, T. S., and Figiel, G. S. (2001). Inhibition of return in children with perinatal brain injury. *J. Int. Neuropsychol. Soc.* 7, 275–284. doi: 10.1017/s1355617701733012

Schenker, R., Coster, W. J., and Parush, S. (2005). Neuroimpairments, activity performance, and participation in children with cerebral palsy mainstreamed in elementary schools. *Dev. Med. Child Neurol.* 47, 808–814. doi: 10.1017/s0012162205001714

Stuss, D. T., Alexander, M. P., and Benson, D. F. (1997). "Frontal lobe functions," in *Contemporary Behavioral Neurology*, eds M. R. Trimble and J. L. Cummings (Boston, MA: Butterworth-Heinemann), 169–187.

Vidyasagar, T. R., and Pammer, K. (2010). Dyslexia: a deficit in visuo-spatial attention, not in phonological processing. *Trends Cogn. Sci.* 14, 57–63. doi: 10.1016/j.tics.2009.12.003

Wechsler, D. (2006). *WISC-III Wechsler Intelligence Scale for Children.* 3rd Edn. Italy: Giunti, OS Editore.

White, D. A., and Christ, S. E. (2005). Executive control of learning and memory in children with bilateral spastic cerebral palsy. *J. Int. Neuropsychol. Soc.* 11, 920–924. doi: 10.1017/s1355617705051064

Whittingham, K., Bodimeade, H. L., Lloyd, O., and Boyd, R. N. (2014). Everyday psychological functioning in children with unilateral cerebral palsy: does executive functioning play a role? *Dev. Med. Child Neurol.* 56, 572–579. doi: 10.1111/dmcn.12374

Whittingham, K., Fahey, M., Rawicki, B., and Boyd, R. (2010). The relationship between motor abilities and early social development in a preschool cohort of children with cerebral palsy. *Res. Dev. Disabil.* 31, 1346–1351. doi: 10.1016/j.ridd.2010.07.006

Conflict of Interest: The authors declare that the research was conducted in the absence of any commercial or financial relationships that could be construed as a potential conflict of interest.

frontiers in Human Neuroscience

ORIGINAL RESEARCH
published: 14 February 2020
doi: 10.3389/fnhum.2020.00036

Children With Unilateral Cerebral Palsy Utilize More Cortical Resources for Similar Motor Output During Treadmill Gait

*Matthew R. Short[1], Diane L. Damiano[1], Yushin Kim[1,2] and Thomas C. Bulea[1]**

[1] *Functional and Applied Biomechanics Section, Rehabilitation Medicine Department, National Institutes of Health, Bethesda, MD, United States,* [2] *Sports Health Rehabilitation, Cheongju University, Cheongju, South Korea*

Children with unilateral cerebral palsy (CP) walk independently although with an asymmetrical, more poorly coordinated pattern compared to their peers. While gait biomechanics in unilateral CP and their alteration from those without CP have been well documented, cortical mechanisms underlying gait remain inadequately understood. To the best of our knowledge, this is the first study utilizing electroencephalography (EEG) during treadmill gait in older children with and without CP. Lower limb surface electromyographic (EMG) data were collected and muscle synergy analyses performed to quantify motor output. Our primary goal was to evaluate the relationships between cortical and muscle activation within and across groups and hemispheres to provide novel insights into neural control of gait and how it may be disrupted by an early unilateral brain injury. Participants included 9 children with unilateral CP, mean age 16.0 ± 2.7 years, and 12 with typical development (TD), mean age 14.8 ± 3.0 years. EEG data were collected during a standing baseline and treadmill walking at self-selected speed. EMG of 16 lower limb muscles were also collected bilaterally and synchronized with EEG. No significant group differences were found in synergy number or structure across groups. Six cortical clusters were identified as having gait-related activation and all contained participants from both CP and TD groups; however, the percent of individuals per group appearing in different clusters varied. Notably, the cluster least represented in CP was the non-dominant motor region. Both groups showed mu-band ERD in the motor clusters during gait although sustained beta-band ERD was not evident in TD. The CP group showed greater cortical activation than TD during walking as measured by mu- and beta-ERD in the dominant and non-dominant motor and parietal regions and elevated low gamma-activity in the frontal and parietal areas, a unique finding in CP. CP showed greater bilateral motor EEG-EMG coherence in the gamma-band with the hallucis longus compared to TD. In summary, individuals with CP display increased cortical activation during gait possibly relating to differences in distal motor control of the more affected side. Strategies that iteratively reduce cortical activation while improving selective motor control are needed in CP.

Keywords: electroencephalography, hemiplegia, muscle synergies, coherence, walking, pediatric, electromyography

OPEN ACCESS

Edited by:
Jessica Rose,
Stanford University, United States

Reviewed by:
Yi-Ning Wu,
University of Massachusetts Lowell, United States
Kornél Schadl,
Stanford University, United States

***Correspondence:**
Thomas C. Bulea
thomas.bulea@nih.gov

Specialty section:
This article was submitted to Motor Neuroscience, a section of the journal Frontiers in Human Neuroscience

Received: *01 October 2019*
Accepted: *27 January 2020*
Published: *14 February 2020*

Citation:
Short MR, Damiano DL, Kim Y and Bulea TC (2020) Children With Unilateral Cerebral Palsy Utilize More Cortical Resources for Similar Motor Output During Treadmill Gait. Front. Hum. Neurosci. 14:36. doi: 10.3389/fnhum.2020.00036

INTRODUCTION

Cerebral palsy (CP) describes a group of functional motor disabilities that are the consequences of brain injuries early in development. Movement difficulties may be predominantly unilateral (one side of the body) or bilateral (both sides), and the range of disability can vary from mild coordination problems to being totally dependent for mobility and care, as categorized by the Gross Motor Functional Classification System (GMFCS) (Palisano et al., 1997). Nearly all children with unilateral CP learn to walk independently. However, their motor patterns and coordination differ from their peers without CP with distal limb involvement most prominent (Winters et al., 1987). While gait analysis has been used extensively to describe temporal, spatial and kinematic characteristics of walking in unilateral CP, the cortical mechanisms that influence gait function in CP are not well understood and are likely to vary across and within CP subtypes, and perhaps are best characterized at the individual level (Weinstein et al., 2018).

The advancement of mobile neuroimaging technologies [e.g., functional near infrared spectroscopy (fNIRS) and electroencephalography (EEG)] and associated signal processing techniques have provided novel insights on the role of cortical activity in walking. fNIRS measures the concentration of oxygenated and de-oxygenated hemoglobin in cortical tissue, corresponding to changes in neural activity. Gait-related increases in hemodynamic activity have been reported in multiple brain regions using fNIRS, including prefrontal, premotor, primary motor and supplementary motor areas (Miyai et al., 2001; Suzuki et al., 2004). Walking tasks of greater complexity (Koenraadt et al., 2014) or requiring increased precision (Kurz et al., 2012) have been shown to further elevate hemodynamic activity.

Electroencephalography has a higher temporal resolution than hemodynamic methods such as fNIRS and therefore is commonly used to quantify movement planning and execution. Despite its low spatial resolution, high density EEG provides scalp coverage that, when combined with sophisticated processing, can resolve movement-related activations to focal scalp and/or source regions. Notably, recent EEG studies have shown that modulation of cortical activity in multiple frequency bands and originating from distinct brain regions is coupled with gait cycle phases during walking in healthy adults (Gwin et al., 2011; Severens et al., 2012; Seeber et al., 2014; Bradford et al., 2015; Bulea et al., 2015). This cortical activity is typically evaluated using relative changes in the power spectra over time, termed event-related spectral perturbations (ERSPs) (Makeig, 1993). When computed for analysis of activity within a stride, ERSPs represent differences in spectral power between a given time point in the gait cycle relative to the mean. Cortical involvement in gait can also be characterized by increases or decreases in spectral power relative to a quiet baseline (e.g., standing), termed event-related synchronization (ERS) or event-related desynchronization (ERD), respectively. Mu- (8–13 Hz) and beta- (14–30 Hz) band ERD in the motor areas of the brain are well established correlates of movement preparation and execution while beta-ERS has been associated with movement suppression or inhibition (Pfurtscheller and Da Silva, 1999; Solis-Escalante et al., 2012). During walking in adults, mu- and beta-ERD have been reported in the sensorimotor and posterior parietal regions relative to quiet standing (Severens et al., 2012; Seeber et al., 2014; Bulea et al., 2015). Mu- and beta-ERD magnitude also appear to be proportional to task difficulty as studies have found enhanced ERD in more challenging walking conditions such as those requiring active speed control (Bulea et al., 2015; Nordin et al., 2019), walking with robotic assistance (Wagner et al., 2012) and during adaptation of step length in response to perturbations (Wagner et al., 2016). Cortical modulations in other frequency bands, in particular low gamma (25–50 Hz), have also been identified during gait in prefrontal, sensorimotor and parietal areas with preliminary evidence suggesting that these rhythms may also be task-related given their modulation across different walking tasks (Wagner et al., 2012, 2014; Bulea et al., 2015; Seeber et al., 2015).

Because of the relatively low signal-to-noise ratio, EEG signals recorded from scalp electrodes during walking contain broadband contamination from movement-related artifacts (Castermans et al., 2014; Kline et al., 2015). However, studies have also shown that decomposition of EEG channels using principal component analysis applied over sliding windows (Mullen et al., 2013; Bulea et al., 2014) and independent component analysis (ICA) (Snyder et al., 2015) can parse movement artifacts from cortical activity based on their power spectra, scalp maps, dipolarity, time-frequency decompositions and lack of correlation with neighboring channels (i.e., volume conduction). The same techniques can also be used to separate electrocortical activity from physiological sources of artifact such as scalp and neck EMG, EOG, and EKG and non-physiological noise such as parasitic voltage drops from sudden skin-electrode impedance changes and electrical line noise (Makeig et al., 1996; Delorme et al., 2012). Thus, careful application of advanced signal processing techniques is necessary to ensure that the ERSPs and ERD/ERS computed from EEG collected during walking represent signal changes originating from the cortex.

While data are beginning to accumulate in healthy adults, studies that utilize mobile neuroimaging techniques to evaluate gait in typically developing children or in individuals with brain injuries are very limited, especially in children with CP. One small pilot study found that children with bilateral CP exhibited increased sensorimotor and parietal activity during walking compared to children without CP, as measured with fNIRS (Kurz et al., 2014). Perhaps relevant to gait performance, another study showed that children with bilateral CP demonstrated stronger beta-band ERD in the premotor cortex and mu-band (or alpha-band) ERD, measured via magnetoencephalography, in the anterior cingulate cortex during the motor execution phase of a knee extension task (Kurz et al., 2017). *To our knowledge, this is the first EEG study of walking in CP as well as in a healthy pediatric cohort*. In upper limb tasks, EEG-based studies have found that, compared to children with typical development, individuals with child-onset brain injury (before age 13) have reduced ERD in the affected hemisphere during wrist extension (Kukke et al., 2015), hand grasping (Weinstein et al., 2018), and reach to grasp (Inuggi et al., 2018).

Muscle activation patterns as assessed by electromyography (EMG) have long been regarded as a major source of indirect evidence of central nervous system (CNS) control. Human gait involves extensive integration of CNS commands (e.g., supraspinal and spinal circuitry) and peripheral feedback, resulting in the coordinated recruitment of multiple muscles. Recent studies in the field of motor control have posed numerous theories regarding the characterization and quantification of modular control strategies describing this recruitment (Latash et al., 2007; d'Avella et al., 2015). One widely recognized interpretation of modularity suggests that groups of muscles are recruited via *synergies* representing motor outputs organized by the CNS (Tresch et al., 2002; Ivanenko et al., 2004; d'Avella and Bizzi, 2005). Sets of muscle synergies constitute task-specific and low-dimensional decompositions of complex movements. In this way, functional behaviors that require high-level coordination and balance, such as gait, are spatiotemporally simplified, thus minimizing the issues of redundancy in muscle recruitment and kinematic degrees-of-freedom. For example, previous studies have shown that six or fewer synergies, identified through non-negative matrix factorization (NNMF) of lower-limb EMG signals, account for over 90% variance of the EMG activity associated with asymptomatic walking patterns (Ivanenko et al., 2004; Chvatal and Ting, 2012; Kim et al., 2016). Furthermore, these synergies appear to activate concurrently with one or more phases of locomotion such as forward propulsion and leg deceleration during swing.

In individuals with brain injuries, the number of synergies identified during walking (based on the aforementioned 90% variance criteria) is reduced (Clark et al., 2009; Kim et al., 2018); and a lower synergy number has been shown to correlate with greater clinical severity in individuals post-stroke (Bowden et al., 2010) and with CP (Hashiguchi et al., 2018). Additionally, synergy structures exhibited by children with CP across a bout of walking show higher variability than by those with typical development (Kim et al., 2018) while maintaining repeatable weighting and activation matrices at the individual level (Steele et al., 2019) during overground walking.

In this study, we evaluated and compared cortical and muscle activation patterns in age-matched children with unilateral CP and typical development (TD) during treadmill walking. EEG source localization was used to examine and compare group and hemispheric differences in cortical activation in multiple brain regions. Cluster analysis of identified muscle synergies, as described previously (Kim et al., 2016, 2018), was utilized for the comparison of muscle activation patterns across groups. Finally, corticomuscular coherence was performed to relate cortical and EMG data. We did not expect to find a different number of cortical sources involved in gait between groups but hypothesized that there would be differences in the magnitude, extent and location of cortical activation, particularly in the sensorimotor areas of the predominantly affected hemisphere of those with unilateral CP. We also expected group differences in the power spectra modulation within the gait cycle. Consistent with previous gait studies, we hypothesized that the CP group would exhibit fewer synergies per stride on average as well as a broader range of synergy structures compared to the TD group. Finally, we hypothesized that children with TD and CP would display mu- and beta-band desynchronization during the gait cycle overlapping with significant synergy activations and that these relationships may differ in CP. The overall goal of this project was to link cortical and peripheral mechanisms and/or output to identify potential novel targets for neurorehabilitation aimed at improving mobility in those with unilateral CP.

MATERIALS AND METHODS

Participants

In this study, participants included 9 children with unilateral CP (7 females, 2 males; age: 16.0 ± 2.7 years) and 12 with TD (8 females, 4 males; age: 14.8 ± 3.0 years) (**Table 1**). In recruiting for this experiment, participants with TD were selected as age-matched controls. There were no significant differences in mean age ($p = 0.345$, independent t-test), height ($p = 0.922$) or weight ($p = 0.556$) between groups. Of the nine children with CP, six were GMFCS Level I and three were Level II (**Table 1**). This protocol was approved by the Institutional Review Board (#13-CC-0110). All participants and legal guardians provided informed assent and consent before participating, respectively.

Procedure and Data Collection

The data analyzed in this study were part of a larger protocol investigating cortical and muscle activation differences across different treadmill walking conditions in children with CP and TD. Prior to data collection, each participant's preferred treadmill walking speed was determined based on average pelvic velocity during overground walking, adjusted according to their level of comfort while walking on the treadmill. Participants walked for 5 min at this self-selected speed during data collection. Prior to the walking trials, participants were instructed to stand still for 2 min to obtain a non-walking (resting) baseline.

A 64-channel, wireless, active electrode EEG system (Brain Products, Morrisville, NC, United States) was positioned on each participant's head using the 5% 10–20 international system (Easy Cap, Germany) for electrode placement and FCz as reference. Electrode impedance was maintained below 20 kΩ throughout the experiment. EEG data were collected at 1000 Hz. EMG was recorded wirelessly (Trigno Wireless, Delsys, Boston, MA, United States) at 1000 Hz from bipolar surface electrodes positioned bilaterally on the tibialis anterior (TA), medial gastrocnemius (MG), soleus (SOL), peroneus longus (PL), rectus femoris (RF), vastus lateralis (VL), medial hamstrings (MH) and hallucis longus (HL). Kinematic data were collected using ten motion capture cameras (Vicon, Denver, CO, United States) at 100 Hz. Reflective markers were placed over anatomic locations on the pelvis and lower extremities and kinematic data collection was synchronized with both EMG and EEG recordings via manual trigger. After the experiment, motion capture data were processed offline using Visual 3D (C-Motion, Germantown, MD, United States). All other data analyses were performed using custom scripts in Matlab (Mathworks, Natick, MA, United States) in conjunction with functions from the EEGLAB v13 software (Delorme and Makeig, 2004).

TABLE 1 | Participant Demographics.

	Age (yrs)	Height (cm)	Weight (kg)	Handedness	Gender	GMFCS
CP1	14	162	43.7	Right	Female	I
CP2	21	166	54.0	Left	Female	II
CP3	12	149	41.2	Right	Female	I
CP4	16	180	89.2	Left	Male	I
CP5	17	161	75.7	Right	Female	I
CP6	17	178	63.3	Right	Male	I
CP7	13	156	51.1	Left	Female	II
CP8	17	156	57.2	Left	Female	I
CP9	17	174	82.9	Left	Female	II
TD1	14	171	56.5	Right	Male	–
TD2	14	167	81.6	Right	Female	–
TD3	16	165	56.4	Right	Female	–
TD4	18	166	62.8	Right	Female	–
TD5	16	171	92.4	Right	Female	–
TD6	14	154	50.5	Right	Male	–
TD7	17	160	73.9	Right	Female	–
TD8	18	177	100.4	Right	Male	–
TD9	16	164	65.9	Right	Female	–
TD10	13	168	63.9	Right	Female	–
TD11	7	123	20.8	Right	Female	–
TD12	15	183	81.1	Right	Male	–

Gross motor functional classification system (GMFCS).

Motion Capture Analysis

Kinematic data from foot markers and force plate data were used to segment walking trials into gait cycles comprised of a dominant heel-strike (DHS) followed by a non-dominant toe-off (nDTO), a non-dominant heel-strike (nDHS), a dominant toe-off (DTO) and ending just before the next DHS. The synchronized EEG and EMG data were similarly segmented into gait cycles. After gait cycle segmentation, gait speed, cadence, stance time and step length (distance between feet at DHS and nDHS) were extracted from the kinematics and compared across groups using independent *t*-tests (alpha = 0.05, two-tailed).

EEG Data Analysis

EEG channel data were high-pass filtered at 1 Hz (5th order Butterworth). The filtered datasets of walking and quiet standing conditions were then concatenated to create a single, merged set for each subject. Channels were removed from the merged set based on the following criteria: prolonged, flat-line periods longer than 5 s, significant noise contamination indicated by a kurtosis greater than 4 standard deviations from the mean and channels insufficiently correlated with neighboring channel activity ($r < 0.7$) (Gwin et al., 2011). Channels removed from the merged data set were also removed from each individual condition (walking and standing). An average of 61 acceptable channels were retained per subject (range: 53–64). One participant in the TD group was excluded from EEG analysis because of an excessive number of noisy channels ($n = 36$). Next, an artifact subspace reconstruction (ASR) algorithm was utilized to remove movement related artifact and improve the accuracy of subsequent independent component analysis and source localization (Mullen et al., 2013). In brief, ASR identifies time periods which contain high amplitude artifacts in EEG data by comparison with a calibration EEG dataset recorded from the same subject. Channels identified to contain artifacts within each time window are removed and reconstructed from neighboring channels using a covariance matrix computed from the calibration data. For our analysis, a variance threshold of 4 standard deviations and a sliding window of 400 ms were used to identify channels containing corrupted data. The calibration dataset was derived from the merged (standing rest and walking) set, excluding time points where the fraction of removed channels using the above criteria was greater than 0.075. After ASR, EEG data were re-referenced to a common average. Channels that were removed were interpolated prior to common average referencing, but were not included in any subsequent analysis.

An extended independent component analysis algorithm (RUNICA) was applied to the merged, ASR-cleaned datasets (Makeig et al., 1996). RUNICA is a blind source separation technique that transforms EEG channel data containing cortical and non-cortical sources into static, spatially distinct and temporally independent components (ICs). Because ASR can potentially attenuate and/or remove cortical signals of physiological relevance, only the sphering and weighting matrices produced by the RUNICA decomposition of the ASR-cleaned data were kept for further analysis (Bulea et al., 2015). The IC sphering and weighting matrices were then applied to the preprocessed, unmerged datasets associated with each subject's treadmill walking and standing conditions. These individual datasets were subject to the same process for noisy channel removal and common average referencing as the merged dataset, but were not subject to ASR. The best fitting dipole for each

IC was computed using the DIPFIT toolbox in EEGLAB with a template 3-shell boundary element head model (Oostenveld and Oostendorp, 2002). EEG channel locations for each individual were warped to match the MNI brain template (Montreal Neurological Institute, Quebec, Canada) before dipole fitting. ICs with equivalent dipole fits containing greater than 20% residual variance (RV) were rejected (Bulea et al., 2015).

For the retained ICs of each subject, walking epochs (3 s in duration) were extracted starting 1 s before DHS to ensure a complete stride in each. Non-overlapping baseline epochs (3 s in duration) were generated from the quiet standing condition. Walking and standing epochs were rejected if the IC magnitude exceeded a manually determined noise threshold of 20 μV for more than one IC at any time point. To maintain consistency between measures, the same set of epochs were retained for the EEG and raw EMG data.

Power spectral density (PSD) was computed with a Fast Fourier Transform (FFT) for each walking epoch (0–500 Hz). We then computed the time-frequency decomposition [2–50 Hz, 400 points, time-warped to the median gait event latencies across groups (Bulea et al., 2015)] with FFT for the IC walking epochs to obtain gait cycle spectrograms. ERSPs were computed by subtracting the mean spectral power (averaged across time points and strides) from the epoched walking spectrograms (Gwin et al., 2011). Gait-related ICs were identified as those which had significant power modulations within the ERSP; significance thresholds were computed for ERSPs using the *bootstat* function in EEGLAB (1000 points of surrogate data shuffled across time points and strides, alpha = 0.05, two-tailed). Scalp topographies, PSDs and time-frequency decompositions were visually inspected to confirm and remove of any remaining artifactual components from each dataset (e.g., EMG components which have high power modulations above 20 Hz and topographies located at the periphery of the head model). An average of 5 dipoles were retained (range: 3–9) for each subject. One participant in the CP group was excluded from further IC analyses as no dipoles were retained (all but 2 ICs for this subject had greater than 20% residual variance; the remaining 2 were removed based on the above criteria). To assess cortical activity relative to rest, time-frequency decompositions (2–50 Hz, 400 points) were computed for the standing epochs; standing spectrograms (averaged across time points and epochs) were subsequently subtracted from the epoched walking spectrograms to produce gait-related ERD/ERS plots (Bulea et al., 2015).

Finally, ICs from both groups (CP and TD) were pooled and clustered globally by *k*-means using parameters from ERSPs (ERSP magnitudes from 8 to 30 Hz), PSD (2–50 Hz), scalp topographies (absolute value) and dipole coordinates (Talairach space). The first ten dimensions identified by principal component analysis (PCA) were retained for each clustering measure except for the dipole coordinates (3 dimensions) (Gwin et al., 2010; Bulea et al., 2015). The resulting feature vector was further reduced to 17 principal dimensions with PCA. Previous studies have used feature vectors incorporating some combination of dipole locations, scalp projections and PSD for clustering brain ICs with *k*-means (Gwin et al., 2010; Bulea et al., 2015; Luu et al., 2017). Because dipole locations and scalp projections were expected to be more variable across subjects in the CP group, we chose to include ERSPs in the feature space to more stringently classify the cortical function of each IC. The *k*-value was set to the total number of components divided by the total number of subjects across groups, rounded up to the nearest whole number. An IC was reallocated to an outlier cluster if it was 3 or more standard deviations from its assigned cluster centroid. For *post hoc* comparisons, global clusters were split into two subclusters: one containing the ICs from CP participants and one with ICs from TD participants. Owing to the unilateral involvement of our CP cohort, IC clusters that were lateralized and symmetric about the midline were reorganized from left and right to dominant (less affected) and non-dominant (more affected) clusters based on clinical assessment by the study physician in CP and the Edinburgh Handedness Inventory (Oldfield, 1971) in TD. In this data-driven approach to clustering, it is expected that not all individuals will appear in a given cluster. Overall, this method allowed for a more functionally relevant and direct comparison of ICs across groups.

Grand mean cluster ERSPs were computed by subtracting the mean spectral power (averaged globally across all time points and strides); significance thresholds for these ERSPs were recomputed using the *bootstat* function in EEGLAB (1000 points of surrogate data shuffled across time points and strides, alpha = 0.05, two-tailed). ERD/ERS plots were averaged across strides for each IC cluster. To compare the ERSPs and ERD/ERS between groups, a non-parametric bootstrapping function, *condstat*, was implemented in EEGLAB (1000 points of surrogate data shuffled across strides, alpha = 0.05, two-tailed). Time points exhibiting significant reduction in power (suppression) in the ranges of 8 to 13 Hz (mu-band) and 14 to 30 Hz (beta-band), respectively, were also marked for each IC. Previous studies have shown that frequency bands of motor related ERD can vary by age in children (Cuevas et al., 2014), however, no differences in group level ERD results were found when individual specific mu- and beta-bands were used in our cohort.

EMG Data Analysis

Electromyographic channel data were detrended, high-pass filtered (3rd order Butterworth, 35 Hz), full-wave rectified and low-pass filtered (3rd order Butterworth, 5 Hz) to create linear envelopes. Each EMG envelope was segmented by gait cycle (DHS to DHS), normalized by the maximum activation value per channel in each gait cycle and time-interpolated (cubic spline) to 150 points. EMG signals were linearly time-warped using the built-in EEGLAB function, *timewarp* (Delorme and Makeig, 2004) to match the EEG data and ensure gait events occurred at the same median latency across outcome measures. The resulting EMG signals were averaged across strides for each individual subject.

For each participant, muscle synergies were extracted from the pre-processed, averaged EMG data using non-negative matrix factorization (NNMF) (Lee and Seung, 1999). NNMF

decomposes a set of EMG into weighting and activation matrices as described by the following equation:

$$EMG_o = \sum_{i=1}^{n} W_i C_i + e;\ EMG_r = \sum_{i=1}^{n} W_i C_i$$

where, EMG_o is the original, mean EMG matrix (muscles x time), n is the number of muscle synergies ranging from one to sixteen, W is a synergy matrix (muscles $\times$ n) representing weighting coefficients of individual synergies, C is a synergy matrix (n $\times$ time) representing temporal profiles of synergy activations and e is the residual error. Matrix multiplication of W and C results in the reconstructed EMG matrix, EMG_r (muscles $\times$ time). Here, a 16-synergy reconstruction is equivalent to the original set of processed EMG signals. To prevent a local minima, the NNMF procedure was performed with 100 replicates for each synergy number.

Synergy number was determined by the total variance accounted for (VAF), computed as follows:

$$VAF = 1 - \frac{||EMG_o - EMG_r||^2}{||EMG_o - mEMG_o||^2}$$

where $mEMG_o$ is the channel-wise average of EMG_o. We set a VAF threshold of 90% as in previous studies (Kim et al., 2016, 2018) and selected the lowest synergy number that satisfied this requirement. The weighting coefficients and activation profiles were normalized by the maximum channel weightings and activation values, respectively, confining the magnitude of each synergy to a range of 0 to 1.

To match similar synergies within each group, k-means clustering with 100 replicates was utilized with squared-Euclidean distance as the evaluative distance metric. Although previous gait studies have clustered synergies using only weighting coefficients (Steele et al., 2015; Kim et al., 2016, 2018; Shuman et al., 2016) here we added the latency of peak synergy activation during the normalized gait cycle (16 weights + 1 peak time index = 17-dimensional feature space) for clustering. The peak time index was divided by the length of the normalized time vector to ensure equal parameter weighting. Incorporating this temporal index is advantageous for correctly classifying and separating synergies which have similar weight coefficients, but differ in the time domain. Calinski-Harabasz (CH) index was used to evaluate the separation between synergies of different clusters and compactness of synergies within each cluster (squared-Euclidean distance) (Maulik and Bandyopadhyay, 2002; Cappellini et al., 2016). Clustering was repeated 100 times with k-values of two to the total number of synergies in each group; the k-value that produced the local maximum in the corresponding CH indices was identified as the optimal number. The most frequently occurring optimal cluster number and the greatest CH index across the 100 iterations was selected for further analysis. Finally, synergy cluster compactness within groups and clusters was computed using the mean intraclass correlation coefficient (ICC).

Synergy-IC Overlap

As a preliminary comparison of brain and muscle activity, we explored the relationship between IC and synergy activity at the group level for each IC cluster. Synergy activations extracted from individuals contained in each cluster were averaged and the overlap between significant periods of cluster mean ERSP modulation and temporal synergy activation was quantified. Percentage overlap (rather than correlation coefficient) was chosen due to the different frequency content between ERSP and synergy activation signal to provide a descriptive examination of the correlation between the brain and peripheral activity. Significant ERSP modulations were defined as above. Significant periods of synergy activation were marked as regions that exceeded half of the maximum temporal profile after offset subtraction and overlap were visually compared between significant ERSP modulations and synergy activations at the group level. The proposed analysis makes no assumptions regarding the type of relationship between cortical signals and synergy activations as in previously described, regression-based studies (Pirondini et al., 2017; Pei et al., 2019) and is used only as a preliminary investigation.

EMG-IC Coherence

Coherence between EMG channels and IC activations for the motor clusters (DM, NDM) was evaluated by computing the coherence between high-pass filtered (5th order Butterworth, 1 Hz) and rectified EMG signals and IC activations, both linearly time-warped by median gait cycle latencies. EMG-IC cross-coherence was computed using zero-padded FFT across fixed-windows (400 time points, 2–50 Hz, *newcross* in EEGLAB) and was masked for significance using *bootstat* (1000 points of surrogate data shuffled across time points and strides, alpha = 0.05). Coherence values are complex numbers and therefore can be decomposed into phase and magnitude components. Phase, in this computation, represents the time lag between input signals and can be used to determine which signal is leading/lagging relative to the gait cycle. For visualization of efferent activity, we additionally masked coherence magnitude plots to only display time points where IC activations were leading EMG signals.

RESULTS

Spatiotemporal Metrics

Non-dominant limb stance time relative to the gait cycle was significantly lower in the CP group (TD: 67.2 $\pm$ 0.90%, CP: 64.2 $\pm$ 2.30%; $p < 0.001$) with no significant difference in dominant limb stance time between groups (**Table 2**). There were no significant differences in mean treadmill speed, normalized step length and cadence between groups (**Table 2**), however, mean walking speed (TD: 0.99 $\pm$ 0.11 m/s, CP: 0.89 $\pm$ 0.10 m/s; $p = 0.053$), non-dominant step length (TD: 0.30 $\pm$ 0.02, CP: 0.29 $\pm$ 0.02; $p = 0.052$), and non-dominant limb cadence (TD: 104 $\pm$ 5.74 step/min, CP: 96.1 $\pm$ 10.9 steps/min; $p = 0.055$) were all greater in TD, but failed to reach statistical threshold. Comparing across limbs in the CP group, stance time ($p < 0.001$)

TABLE 2 | Spatiotemporal metrics during treadmill walking.

	Preferred treadmill speed (m/s)	Normalized step length[a]		Stance time (%)		Cadence (steps/min)		
		Non-dominant	Dominant	Non-dominant	Dominant	Non-dominant	Dominant	Average
TD	0.99 ± 0.11	0.30 ± 0.02	0.31 ± 0.01	67.2 ± 0.90	67.4 ± 0.82	104 ± 5.74	104 ± 4.92	104 ± 5.17
CP	0.89 ± 0.10	0.29 ± 0.02	0.30 ± 0.03	64.2 ± 2.30	68.4 ± 1.61	96.1 ± 10.9	108 ± 10.8	102 ± 10.1
p	0.053	0.052	0.539	**<0.001**	0.072	0.055	0.287	0.598

Mean ± standard deviation; Bold values indicate significant differences between groups ($p < 0.05$, independent t-test) [a]Step length was normalized by participant height in meters.

and cadence ($p = 0.002$) were significantly lower in the non-dominant compared to dominant limb with no difference in normalized step length.

EEG Component Clusters

At the group level, global *k*-means clustering resulted in six IC clusters for preferred speed walking (2 outlier components). Clustered scalp topographies and grand mean ERSPs (**Figure 1**) were spatially determined to represent activity from the frontal (FR), dominant parietal (DP), dominant motor (DM), non-dominant motor (NDM), non-dominant parietal (NDP) and prefrontal (PF) regions based on the cluster centroid dipole locations in the MNI template. Brodmann areas were identified in a ±2 mm range of all individual dipoles within a given cluster (**Table 3**; Lancaster et al., 2000). Each of these clusters contained subsets of individuals that were considered to be representative of each group. With regard to group representation, the percentages of total subjects (respective of each group) contained in each IC cluster were most different between groups in the NDM cluster (91% of subjects with TD; 38% of subjects with CP) with differences also observed in the DP cluster (82% of subjects with TD; 56% of subjects with CP), the DM cluster (55% of subjects with TD; 75% of subjects with CP), and the PF cluster (36% of subjects with TD; 75% of subjects with CP).

At the group level, instances of mu- and beta-suppression most often occurred during single limb stance and/or swing, evidenced by the grand mean ERSPs (**Figure 1**). In the TD group, the DM and NDM clusters exhibited a consistent decrease in power for the duration of single stance and swing, respectively, across both the mu- and beta-bands. Low gamma-band power (25–50 Hz), in phase with mu- and beta-band modulations, also decreased in the TD motor clusters. In the CP group, the DM and NDM clusters showed periods of decreased power in the same phases of the gait cycle (single stance and swing); however, these instances were spectrally discontinuous across the mu- and beta-bands after significance masking. Additionally, gamma-band power in the DM cluster was in phase with beta-band power during early swing but appeared offset from mu- and beta-band modulations in the NDM cluster, exhibiting significant activity instead from initial contact through mid-stance.

Statistical comparison of ERSPs between groups showed significant differences in mu- and beta-band power in the DP, NDM, and FR clusters (**Figure 1**). In the DP cluster, the CP group had significantly more mu-band power centered around initial contact. In the NDM cluster, the CP group briefly displayed increased power in the mu-band at the beginning of single stance and decreased power in the same frequency range during loading response and terminal swing. While, descriptively, the CP group exhibited more mu-band power before and after toe-off in the FR cluster, differences in the mu- and beta-bands were not largely apparent. Significant changes in gamma-band power were observed between groups for all clusters except the DM cluster. In the DP, NDP, and PF clusters, the CP group consistently showed more gamma-band power during mid-stance. Similarly, the CP group had increased gamma-band power during double stance in the FR and NDM clusters.

The percentage of the gait cycle with mu-suppression relative to the mean was significantly greater in the TD group for the DM cluster ($p < 0.001$) (**Table 4**). For the NDM cluster, the percentage of mu-suppression was also greater in the TD group, however, this trend was not significant ($p = 0.075$). Conversely, the percentage of mu-suppression for the NDP cluster was greater, but not significantly, in the CP group ($p = 0.055$). No other significant differences were found when comparing mu- and beta-suppression between groups in the remaining IC clusters.

Spectrograms computed relative to quiet standing (i.e., ERD/ERS) revealed continuous desynchronization in the mu- and beta-bands across groups and clusters (**Figure 2**). In both groups, the strongest instances of mu-band desynchronization were present from mid-stance to initial contact in the NDM clusters and from swing to late stance in the DM clusters. In the TD group, increased gamma-band power was observed throughout the gait cycle in the DM, NDM, NDP, and PF clusters. The same clusters exhibited increased gamma-band activity in the CP group, with the addition of the FR cluster.

When comparing ERD/ERS plots between groups (**Figure 2**), upper mu-ERD was significantly greater for the CP group in all motor and parietal clusters with significant differences persisting throughout the gait cycle. These differences were also present in various segments of the beta-band for the DP, DM, and NDM clusters. Despite predominant instances of greater ERD in the motor clusters of the CP group, we also found phasic periods of less ERD in the CP group. These phenomena occurred in the lower mu-band during single stance and swing for the DM cluster and during terminal swing and loading response for the DP cluster as well in the lower beta-band during single and double stance for the NDM cluster. Similarly, lower beta-ERD was significantly decreased before and after toe-off in the CP group for the FR cluster. In the PF cluster, upper mu- and beta-ERD were both lower for the CP group during single and double stance.

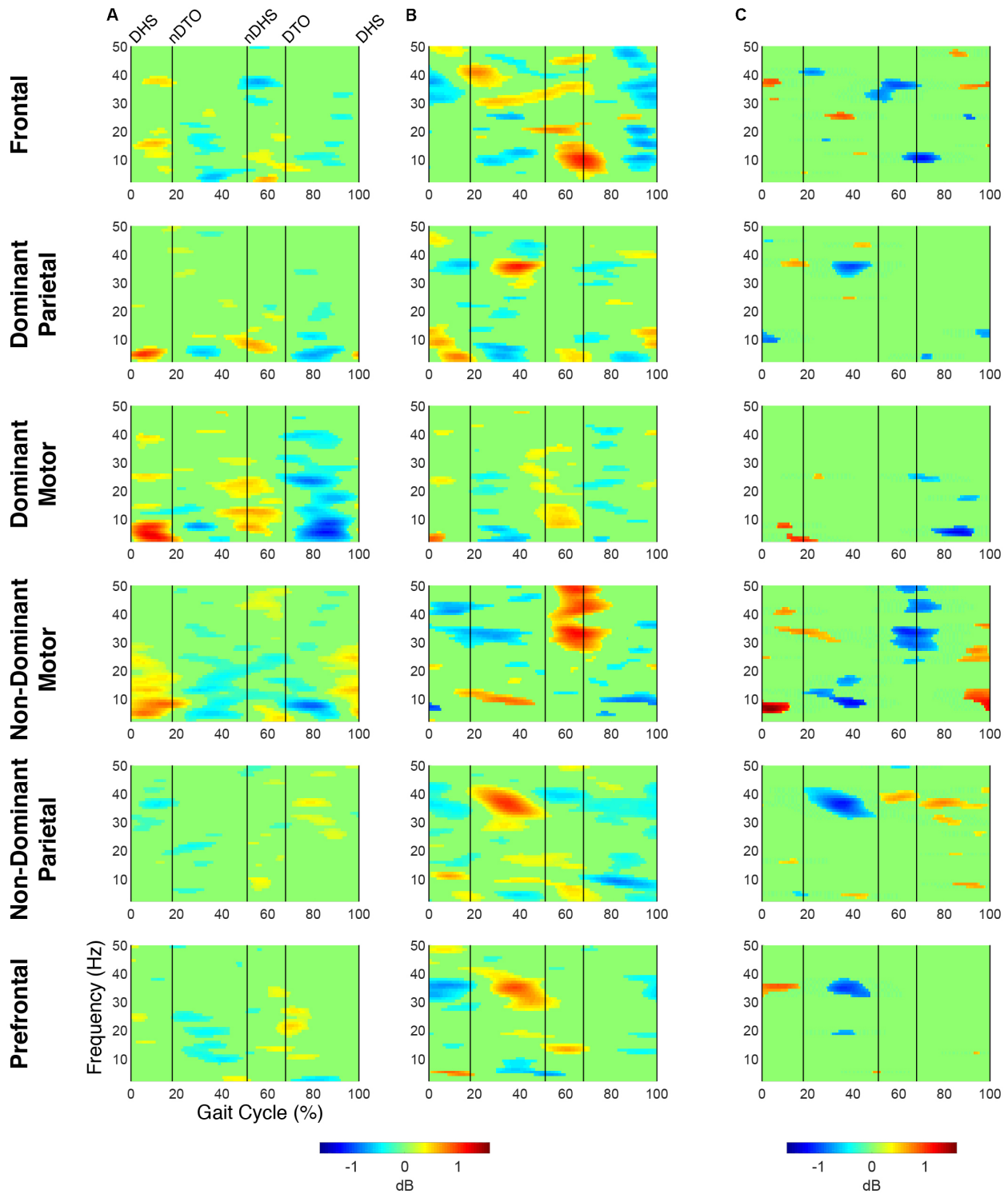

FIGURE 1 | Time-frequency modulations relative to mean gait cycle activity during treadmill walking. Grand mean gait event related spectral perturbations (ERSPs) computed for each cortical cluster in **(A)** TD and **(B)** CP, displayed in dB. **(C)** Between group differences of spectrograms calculated by subtracting grand mean ERSPs in CP from TD, displayed in dB. ERSPs and difference spectrograms were masked for significance (alpha <0.05); non-significant values were set to 0 dB (green).

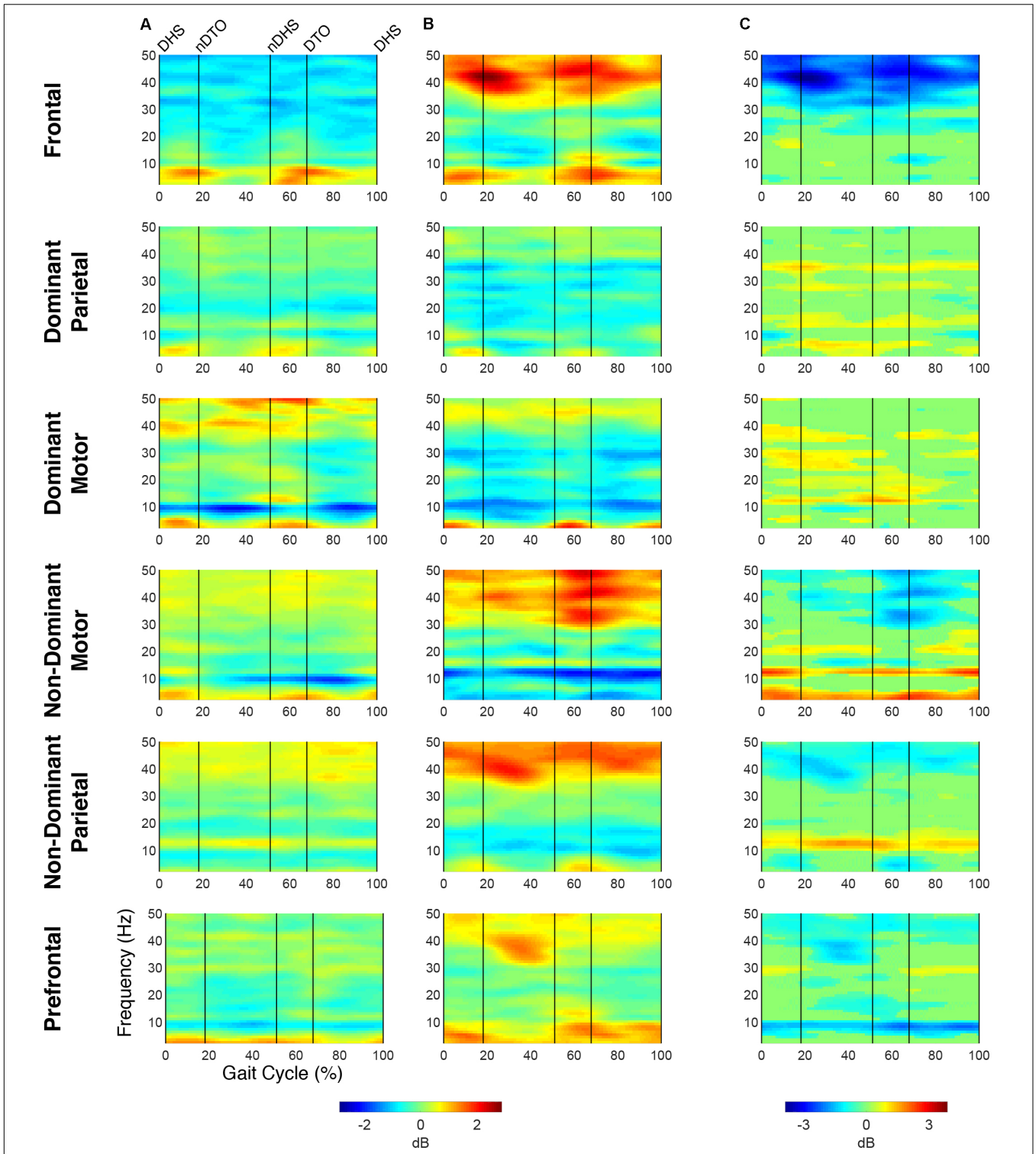

FIGURE 2 | Time-frequency activity relative to quiet standing during treadmill walking. Grand mean event-related desynchronization (ERD)/event-related synchronization (ERS) plots for each cortical cluster in **(A)** TD and **(B)** CP, displayed in dB. **(C)** Between group differences of spectrograms calculated by subtracting grand mean ERD/ERS plots in CP from TD, displayed in dB. Difference spectrograms were masked for significance (alpha <0.05); non-significant values were set to 0 dB (green).

TABLE 3 | IC Cluster characteristics.

IC Cluster location	Brodmann areas[a]	Scalp topographies[b]		# of Subjects (ICs)		% of total subjects	
		TD	CP	TD	CP	TD	CP
Frontal	6, 8, 32	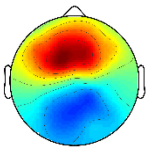		5 (6)	3 (5)	45%	38%
Dominant parietal	5, 7, 18, 19, 31, 39, 40	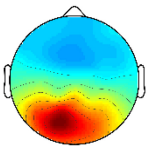		9 (10)	5 (7)	82%	56%
Dominant motor	3, 4, 6, 8, 9, 22	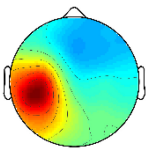		6 (9)	6 (7)	55%	75%
Non-dominant motor	3, 4, 6, 8, 22, 24	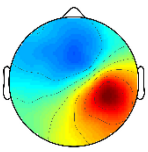		10 (12)	3 (3)	91%	38%
Non-dominant parietal	5, 7, 13, 18, 19, 22, 31, 39, 40	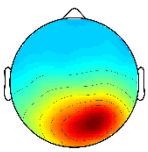		7 (13)	6 (12)	64%	75%
Prefrontal	6, 8, 9, 10, 24, 32	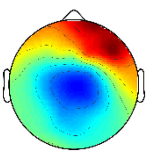		4 (6)	6 (8)	36%	75%

[a]Brodmann Areas were found within a ±2 mm area of all individual dipoles in each cluster [b]Individual scalp topographies were inverted to best match the cluster polarity; individual topographies of the motor and parietal clusters were mirrored about the y-axis according to hemisphere dominance.

TABLE 4 | Mu- and Beta-suppression percentage relative to gait cycle.

IC cluster location	Mu-suppression (%)			Beta-suppression (%)		
	TD	CP	*p*	TD	CP	*p*
Frontal	25.3 ± 11.5	32.9 ± 6.78	0.228	43.4 ± 10.8	46.3 ± 13.4	0.707
Dominant parietal	22.9 ± 8.20	25.9 ± 14.5	0.597	32.1 ± 12.6	39.0 ± 6.17	0.209
Dominant motor	**42.8 ± 12.7**	**17.0 ± 8.42**	**<0.001**	48.1 ± 10.8	44.7 ± 16.2	0.621
Non-dominant motor	38.6 ± 16.2	18.9 ± 13.2	0.075	44.3 ± 15.5	45.8 ± 16.1	0.884
Non-dominant parietal	17.5 ± 13.9	27.8 ± 11.3	0.055	38.3 ± 13.3	44.8 ± 9.68	0.175
Prefrontal	19.8 ± 13.9	30.3 ± 8.99	0.109	39.8 ± 14.8	35.3 ± 16.8	0.616

Mean ± standard deviation; Bold values indicate significant differences between groups ($p < 0.05$, independent t-test).

The CP group exhibited significantly greater gamma-band power throughout the gait cycle in all IC clusters excluding those from the dominant hemisphere (DP and DM). Interestingly, the TD group showed greater gamma-band power, particularly during single stance, in the DP and DM clusters. Delta- (2–4 Hz) and theta- (4–7 Hz) band differences varied between clusters.

While power was significantly decreased throughout the gait cycle in the CP group for the DP and NDM clusters, power increased during all phases of the gait cycle except single stance in the CP group for the NDP cluster at these frequencies.

EMG Synergy Clusters

For all subjects and conditions, 4 to 6 synergies were extracted from the averaged strides using the 90% VAF criteria. The mean extracted synergy numbers for unrestricted walking in TD and CP were 5.0 ± 0.4 (12 subjects; VAF = 0.92 ± 0.02) and 5.0 ± 0.5 (9 subjects; VAF = 0.93 ± 0.02), respectively, with no significant differences discerned between groups (synergy number: $p = 1.0$; VAF: $p = 0.74$).

The optimal synergy cluster number from *k*-means was five for both the TD and CP group (**Figures 3**, **4**). These five clusters were ordered by the peak timing of their activation profiles and determined to be similar across groups in terms of mean activation profiles (**Figures 3A,B**) and weight coefficients (**Figures 4A,B**) (Activation Profiles: $r = 0.95 \pm 0.02$; Weight Coefficients: $r = 0.77 \pm 0.16$). Descriptions of the synergy clusters (referred to as Synergy Cluster A, B, C, D and E for each group) are provided below and in **Table 5**. With regard to cluster compactness, the TD group generally had higher average ICC values computed across weight coefficients, but lower ICC values across activation profiles compared to the CP group.

Cluster A, active primarily during terminal swing and loading response, promoted knee extension and foot stabilization. In the TD group, this cluster was associated with dominant TA, RF, VL, MH, and HL activity as well as non-dominant SOL, PL, and RF activity. In the CP group, this cluster exhibited similar muscle activity, with the addition of increased non-dominant MG activity. Notably, in the CP group, this cluster exhibited the lowest average ICC calculated across weight coefficients (ICC = 0.30).

Cluster B was active from loading response through mid-stance and was primarily responsible for hip extension and knee stabilization for forward progression. In the TD group, this cluster involved dominant RF, VL and MH activity as well as non-dominant TA, RF and HL activity. In the CP group, dominant RF and VL (two primary knee extensors) activity were diminished while non-dominant TA and MG activity increased.

Cluster C, active primarily during terminal stance, accounted for hip and knee extension throughout the stance phase and ankle plantarflexion in preparation of toe-off. In the TD group, this cluster was associated with dominant MG, SOL, and PL activity as well as non-dominant TA, MH, and HL activity. In the CP group, muscle activity was similar with the exception of increased non-dominant MG, PL, RF, and VL activity.

Cluster D acts as a reciprocal to cluster B, promoting support and stabilization during terminal swing and initial contact of the contralateral leg. Muscle activity was similar between groups with the exception of increased non-dominant MG, SOL, and PL activity in the CP cluster.

Cluster E acts reciprocally to cluster C, maintaining extension and initiating leg lift during mid- to terminal stance of the contralateral leg. Muscle activity was again similar between groups with the exception of increased non-dominant MG, activity in the TD group and increased non-dominant MH activity in the CP group.

Synergy-IC Overlap

Plotting of significant synergy and IC activations across the gait cycle revealed no clear pattern of correlation between the two signals (**Figure 5**). The activation profiles of synergy clusters A-E were averaged relative to the subset of subjects contained in each IC cluster. Despite this reorganization, mean activation profiles were relatively consistent with grand mean results from **Figures 3**, **4**. Synergy activation was distributed across strides, with each of the five synergy clusters locked to a particular phase of the gait cycle. Mu- and beta-suppression, as previously described, were typically coupled and occurred during multiple phases of the gait cycle, primarily during single stance and swing. Therefore IC activity overlapped with many synergies, but showed no preference in terms of timing to one particular synergy, regardless of IC cluster location or group. Most often, mu- and beta-suppression overlapped with synergy clusters B, C, and E, with the onset of suppression leading the onset of muscle activation in many cases.

EMG-IC Coherence

For both groups, significant periods of coherence were found across many frequencies between EMG channels and IC activations (**Figures 6**, **7**). In the DM cluster of the TD group (**Figure 6**), delta-band coherence was observed in the non-dominant MG and SOL during initial double stance. Similarly, in the DM cluster of the CP group, delta-band coherence appeared in the dominant MG and non-dominant VL during terminal double stance. The CP group additionally showed gamma-band coherence bilaterally in the HL during single stance. Mu- and beta-coherence were present in the DM cluster of both groups, though these instances were scattered and not consistent across muscles.

In the NDM cluster (**Figure 7**), the TD group displayed less coherence compared to the DM cluster, however, mu-coherence was observed briefly during terminal double stance in the dominant RF and VL. In the NDM cluster of the CP group, delta-coherence was present during initial double stance in the dominant MG, SOL, RF, and VL. The strongest gamma-coherence in this cluster occurred during single stance, appearing bilaterally in the HL and, to a lesser extent, unilaterally in the dominant PL. These instances of gamma-coherence were similar to those found in the DM cluster in terms of timing and frequency.

DISCUSSION

This study represents the first evaluation of cortical activity using EEG during walking in two pediatric cohorts, one with TD and one with CP. The evaluation was performed on a treadmill rather than overground for logistical reasons, mainly to minimize motion artifact and maximize the number of strides for EEG analyses. It is important to note that the participants in the CP group were at the highest levels of functional mobility in CP

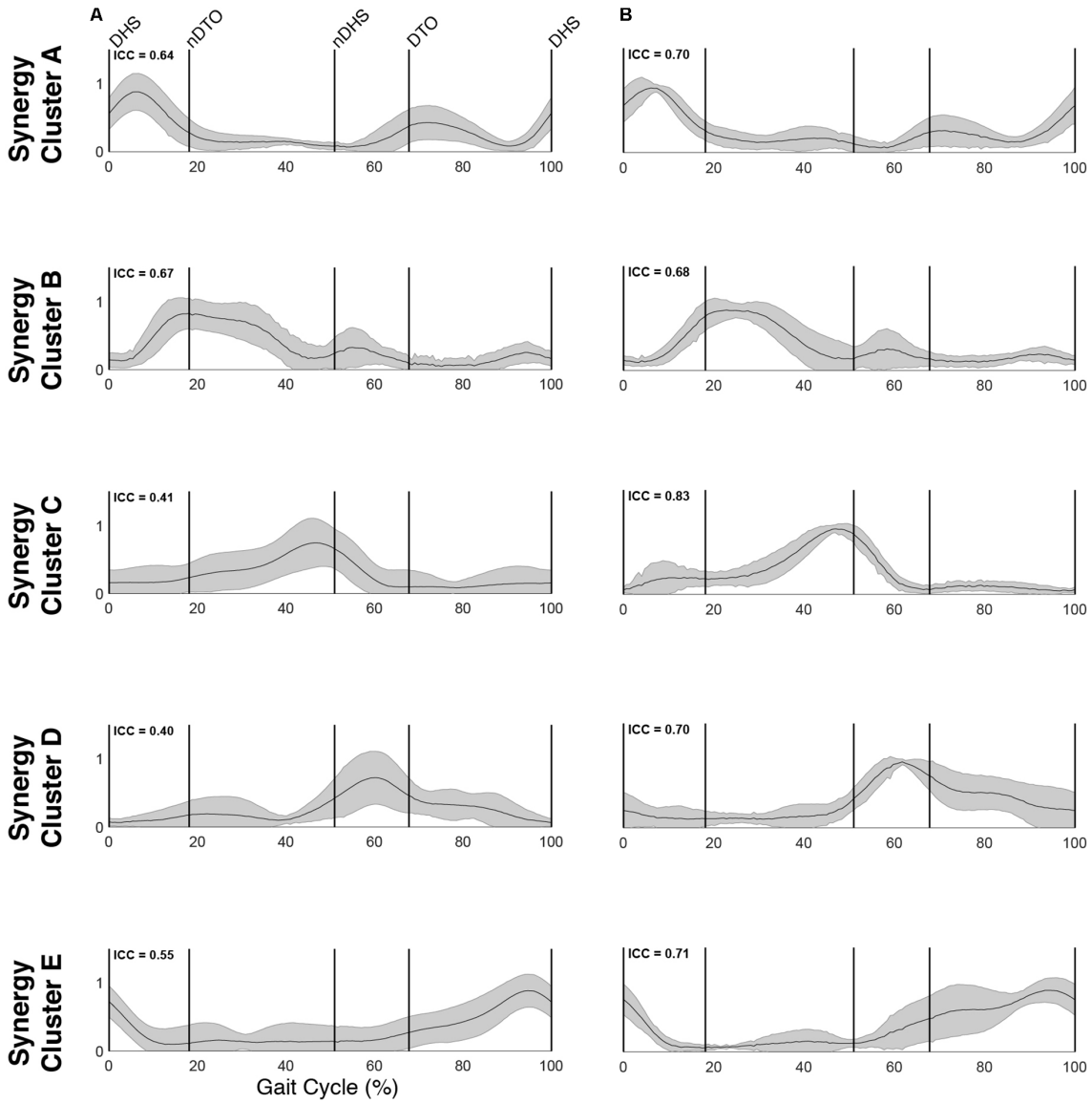

FIGURE 3 | Muscle synergy activations. Mean (standard deviation) activation profiles for each synergy cluster in **(A)** TD and **(B)** CP. Mean intraclass correlation coefficients (ICC) are reported in the upper left corner of each plot.

and were minimally, but not significantly, slower in comfortable gait speed and in cadence on the more involved side than those with TD. Consequently, the groups showed many similarities, particularly in the synergy analyses, however, some potentially important differences were also identified. In addition, both groups, while under 21 years of age, were comprised mainly of adolescents whose gait patterns are likely to be highly similar to those of adults.

With respect to the EMG data, consistent with previous studies, between 4 to 6 synergies extracted via NNMF were able to sufficiently recreate individual channel EMG during normal walking (Ivanenko et al., 2004; Chvatal and Ting, 2012; Kim et al., 2016). However, in contrast with other findings (Steele et al., 2015; Kim et al., 2018), no significant differences were found in mean synergy numbers and VAF between individuals with CP and TD across conditions with an average of 5 synergies identified for each group. This inconsistency could be attributed in part to the high level of functioning in the CP cohort as well the number of muscles used in the synergy extraction (Kim et al., 2016) and the procedure of averaging the EMG data across strides. Comparing synergy clusters between CP and TD, activation and weight matrices were highly correlated for paired clusters. Overall, though correlated between groups, the synergy weight coefficients of the CP clusters exemplified much more non-dominant (affected) limb activity, evidenced especially in Synergy Cluster C (**Figure 4**). The observed differences in weight coefficients can be attributed to abnormalities in selective motor control seen in children with CP (Leonard et al., 1991;

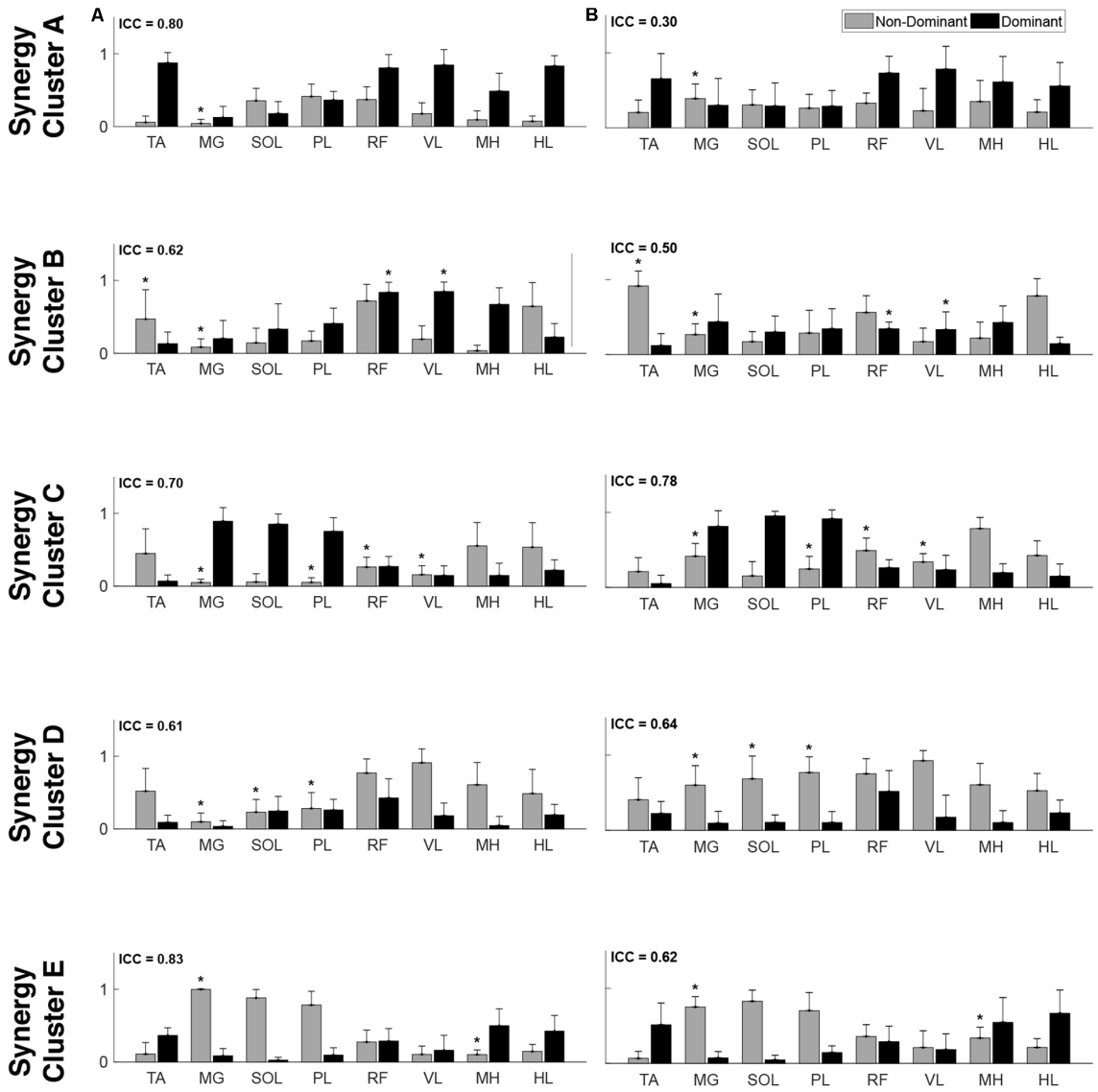

FIGURE 4 | Muscle synergy weightings. Mean (standard deviation) weight coefficients for each synergy cluster in **(A)** TD and **(B)** CP. Asterisks (*) indicate significant differences between groups for individual muscle weightings, relative to each synergy cluster ($p < 0.01$, independent t-test). Mean intraclass correlation coefficients (ICC) are reported in the upper left corner of each plot.

Crenna, 1998), supported by previous synergy studies in this population (Kim et al., 2018).

A previous cohort study demonstrated that children with unilateral and bilateral CP exhibited a combination of similar and disparate synergies relative to those of children with TD on a stride-to-stride basis (Kim et al., 2018). Our observation of similar synergy numbers between groups after averaging can be interpreted to represent the most frequently occurring synergies of each group. While averaging and concatenating strides has been shown to exclude relevant stride-to-stride variability of muscle activity (Oliveira et al., 2014), this was deemed a necessary step in our methodology. EEG time-frequency analysis requires a relatively large number of trials to make meaningful conclusions. Consequently, in order to directly compare synergy results with cortical activity, this stride averaging procedure was utilized consistently for both the EMG and EEG datasets.

Similar to the finding of the same number of muscle synergies in each group, the IC clustering results showed six distinct clusters that all contained cortical sources from both CP and TD participants. At the group level, we observed roughly the same peripheral output (no extraneous, voluntary movements in CP and no significant difference in gait speed) but consistent differences in cortical activation between groups within each cluster. These differences may reflect altered cognitive and/or motor requirements for execution of the same task. These results are also similar to the results found in healthy adults using nearly

TABLE 5 | Synergy structure characteristics.

Synergy cluster	# of Subjects (Synergies)		Activation profiles			Weight coefficients		
			ICC		*r*	ICC		*r*
	TD	CP	TD	CP	Between groups	TD	CP	Between groups
A	11 (11)	9 (10)	0.64	0.70	0.94	0.80	0.30	0.86
B	8 (8)	9 (10)	0.67	0.68	0.94	0.62	0.50	0.52
C	12 (15)	9 (9)	0.41	0.83	0.98	0.70	0.78	0.86
D	12 (14)	8 (8)	0.40	0.70	0.92	0.61	0.64	0.70
E	12 (12)	8 (8)	0.55	0.71	0.94	0.83	0.62	0.92

r indicates Pearson correlation coefficient computed between mean structures for each cluster.

identical methods (Bulea et al., 2015). However, the distribution of individuals across clusters revealed some important group and hemispheric differences. Fewer subjects with CP were found to have ICs in the non-dominant motor cluster; this cluster was represented by the lowest percentage of CP across all clusters. The highest percentages of individuals with CP were in the DM and PF clusters, both of which had appreciably lower percentages in TD. These results suggest an under-reliance on the NDM region and an over-reliance on the PF and DM regions in CP, which is not surprising based on upper limb studies that demonstrate a reorganization that favors use of the dominant hemisphere over the non-dominant one in both unilateral non-dominant side and bilateral tasks (Kukke et al., 2015; Inuggi et al., 2018; Weinstein et al., 2018). These results may also be attributed to the elevated functional role of the dominant limb during walking in our cohort, as evidenced by increased dominant limb stance time and cadence compared to the non-dominant side. While the representation of individuals within each cluster varied in both groups, the results for TD were more consistent than for CP, as shown by the high percentage (91%) of those with TD represented in the NDM cluster as one example. This result is similar to earlier findings from Weinstein et al. (2018), demonstrating that each child with CP likely has their own neural signature on how their brain develops in response to early injury. Neurorehabilitation strategies that demonstrate effectiveness in shifting the reliance more toward the NDM or in lowering the PF activation during tasks that involve the more affected side warrant further exploration and development.

In line with previous work from healthy adults (Gwin et al., 2011; Severens et al., 2012; Seeber et al., 2014; Bulea et al., 2015), we observed, *for the first time* in a younger cohort, cortical activity modulated relative to the gait cycle in mu-, beta- and low gamma-bands. The motor (dominant and non-dominant) regions in the TD group had stronger within stride modulations of mu- and beta-band activity and slightly different timing patterns but were generally quite similar to CP. In the low gamma-band, the CP group had significantly greater modulations in all regions except for the dominant motor cluster. This suggests more cortical activation during gait in brain regions beyond the affected sensory and motor areas in CP. Compared to standing, the CP group displayed a greater increase in low gamma-band activity than the TD group in the frontal areas, also suggesting increased cortical resources attending to the walking task. These findings are similar to results showing elevated frontal activity in more demanding walking tasks in adults (Bulea et al., 2015; Seeber et al., 2015; Wagner et al., 2016). The frontal cortex has been implicated in elevated top-down or executive control of motor tasks (Miller and Cohen, 2001; Danielmeier et al., 2011) and thus our results suggest that children with unilateral CP dedicate more executive control to the treadmill walking task than TD. Interestingly, low gamma-modulation is also elevated in the non-dominant (more affected) motor and parietal areas of CP compared to TD. Given previous studies indicating that greater sensorimotor gamma activity is linked to tasks requiring greater dynamic control (Mehrkanoon et al., 2014), this suggests that walking is also more challenging for children with CP.

When evaluating mu-band ERD, we found that both groups showed significant desynchronization, or elevated cortical activity, in walking compared to standing as had been shown previously in healthy adults. The TD group here, however, differed from earlier results in adults (Bulea et al., 2015; Seeber et al., 2015) in that, compared to standing, strong beta-ERD in the motor and parietal areas was not present. In general, the CP group showed greater cortical activations than TD during walking as measured by mu- and beta-ERD in the NDM, DM, NDP, and DP areas. These results are interesting because they are in disagreement with some upper extremity EEG studies that show *less* task-related ERD in the motor areas. However, fNIRS results from our group (Sukal-Moulton et al., 2018) also show that children with bilateral CP display more widespread motor cortex activation than those with TD for bilateral lower extremity tasks. Greater cortical activation was associated with greater muscle activation in our earlier study, suggesting that brain effort reflects peripheral effort. We found here that, whereas the overall synergy number did not differ between groups during walking, there was increased non-dominant limb activity across multiple synergy clusters in the CP cohort (**Figure 4**). Enhanced mu- and beta-ERD, particularly in motor areas, is indicative of elevated sensorimotor activation during walking (Pfurtscheller and Da Silva, 1999; Severens et al., 2012; Seeber et al., 2014; Bulea et al., 2015). Interestingly, recent results also show mu- and beta-ERD in parietal areas when comparing across walking tasks of varying difficulty [e.g., active vs. passive walking (Wagner et al., 2012; Bulea et al., 2015), fast vs. slow walking (Bulea et al., 2015;

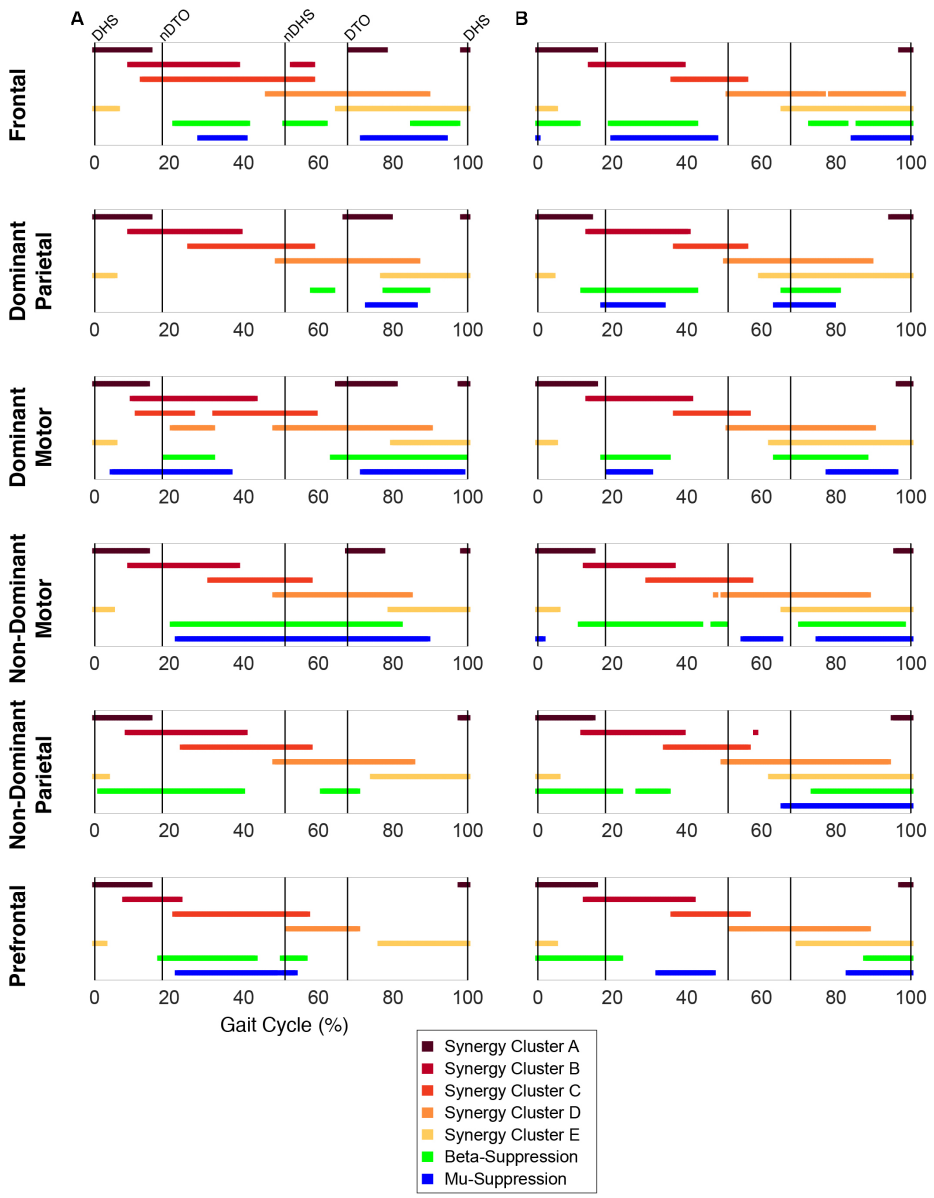

FIGURE 5 | Overlap between synergy and cortical component activity. Significant periods of synergy activation plotted with mu- and beta-suppression throughout the gait cycle for each cortical cluster in **(A)** TD and **(B)** CP.

Nordin et al., 2019), and step shortening adaptations (Wagner et al., 2016)]. Collectively, these results suggest that children with CP require enhanced cortical output to achieve a similar motor output as those with TD.

The primary goal of this study was to relate cortical and muscle activity during a complex bilateral task. Characterization of this relationship can be explored through simultaneous evaluation of cortical activity and synergy output. This concept has been demonstrated in a previous study using multivariate regression to model the influence of EEG frequency-band power on kinematic synergies during hand grasping (Pei et al., 2019). Another study found significant similarities between EEG microstates and muscle synergies via canonical correlation during hand reaching and grasping (Pirondini et al., 2017). To our knowledge, comparative analyses incorporating EEG and muscle synergies have not been applied to ambulation. However, at this level of analysis, we failed to find significant correlations between synergies and activation in cortical sources. The cortical motor sources presented here were active throughout the gait cycle with some relative fluctuations at specific phases, differing slightly across groups. Given that ICs represent coherent activity of large groups (i.e., thousands or more) of neurons, it is perhaps not surprising that we did not find significant associations between ICs and synergy activations.

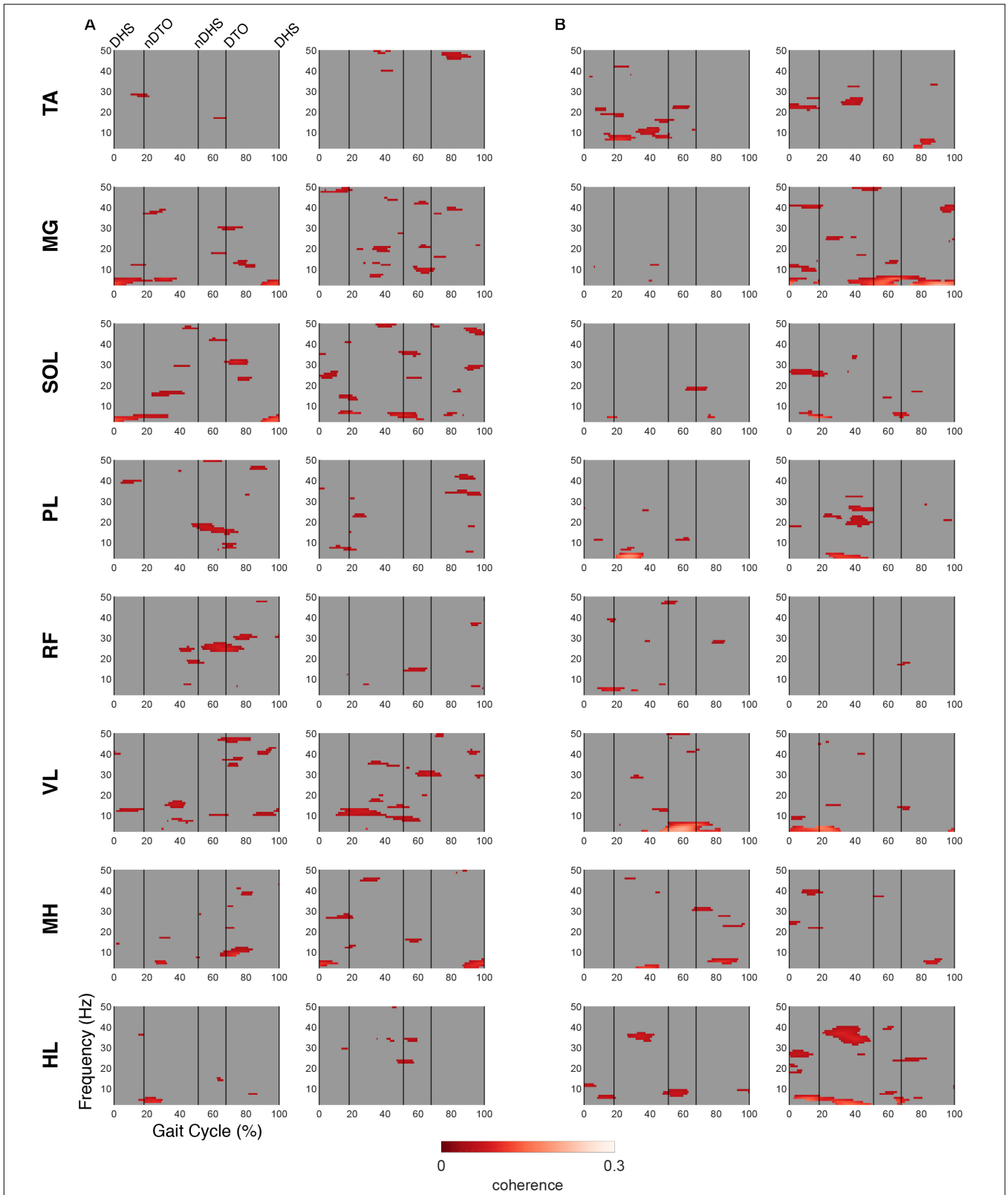

FIGURE 6 | EMG-IC coherence relative to dominant motor clusters. Linear coherence magnitudes between non-dominant (left)/dominant (right) EMG signals and dominant motor IC activations in **(A)** TD and **(B)** CP. Coherence plots were masked for significance (alpha <0.05); non-significant values and time points where EMG signals led IC activations (phase >0 radians) were set to 0 (gray).

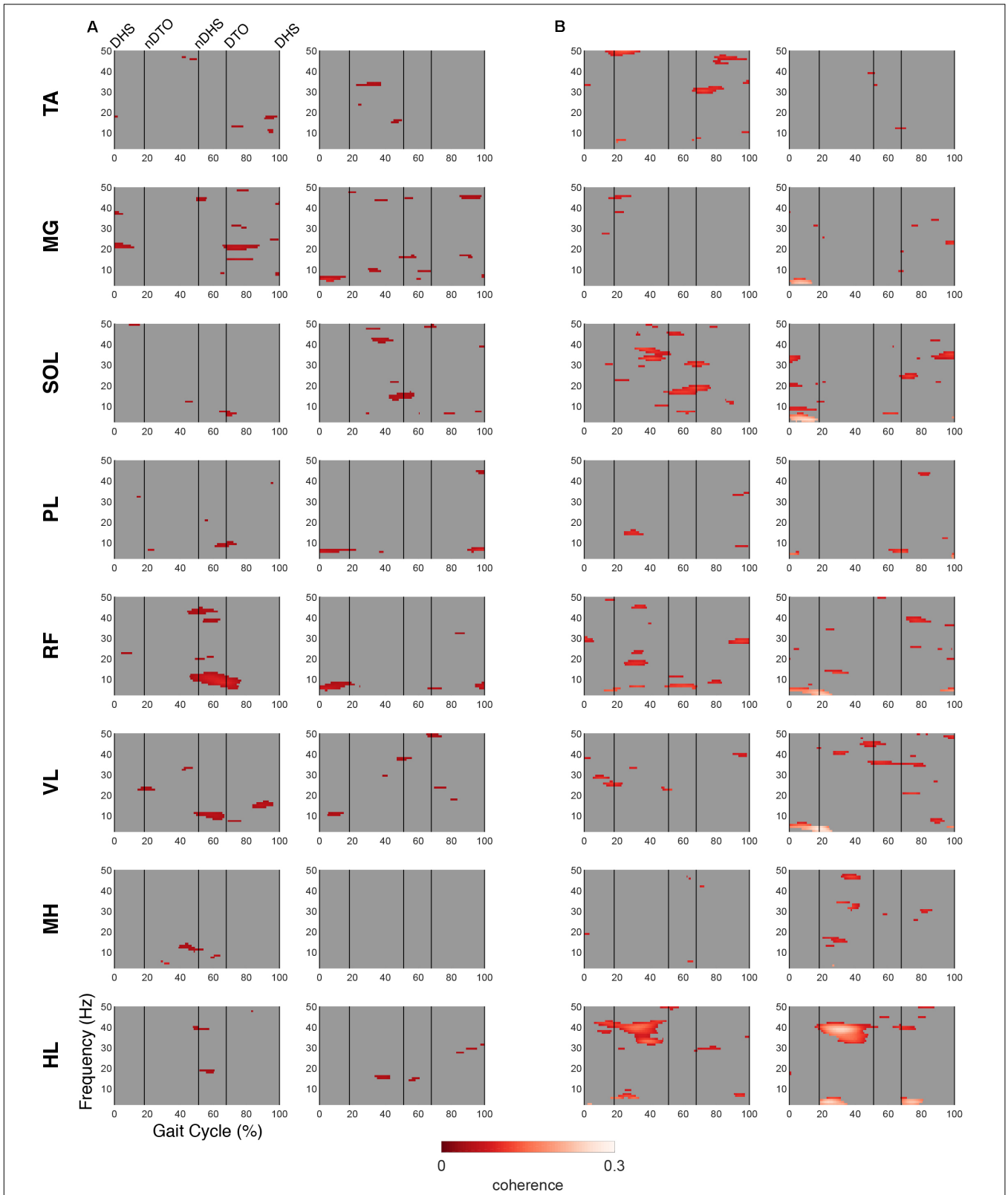

FIGURE 7 | EMG-IC coherence relative to non-dominant motor clusters. Linear coherence magnitudes between non-dominant (left)/dominant (right) EMG signals and non-dominant motor IC activations in **(A)** TD and **(B)** CP. Coherence plots were masked for significance (alpha <0.05); non-significant values and time points where EMG signals led IC activations (phase >0 radians) were set to 0 (gray).

It is expected that for a task such as gait, which coordinates subcortical and spinal pathways to move the entire body while ensuring dynamic stability and forward progression, mapping cortical to peripheral output would be far more difficult, if not impossible. However, EMG–EEG coherence studies have identified significant relationships that tend to be stronger and more consistent in static tasks isolated to a few joints, requiring higher force or effort levels (Mima and Hallett, 1999). As a next step, we performed coherence analyses relating the motor sources to EMG activation of individual muscles, focusing on the efferent control where the cortical activity would presumably lead the muscle activity. Similar patterns of delta-band coherence were found across groups for the DM region. Coherence in this frequency range persisted for the NDM region in the CP group but was not apparent in TD. In both motor regions, the CP group uniquely showed gamma-band coherence for the HL, primarily on the dominant limb, a distal muscle predominantly affected in unilateral CP, with some evidence that the dominant side may try to overcompensate to maintain optimal mobility (Wiley and Damiano, 1998).

One limitation of this study is the loss of stride-to-stride variability via gait cycle averaging as well as intra-subject variability due to group-level analysis. Averaging spectrograms at the group-level has the potential to obscure subject-specific evidence of cortical contributions to muscle recruitment. This issue is more consequential in the CP group due to the distinctive nature of each individual's brain injury and the subsequent reorganization of cortical processes. Of particular note is the inclusion of only three children with CP in the NDM cluster. To this effect, we clustered brain ICs with an equivalent focus on spatial and functional organization using dipole locations and time-frequency parameters. However, the chance of inaccurately grouping these ICs still persists. Therefore applying the same clustering analysis at the individual level may prove more effective in characterizing relationships between the CNS and periphery, which is particularly important for clinical applications where the rehabilitation program should be tailored to the individual. Regarding EMG processing, differences in specific parameters for time-interpolation, normalization and filtering can affect the results of synergy extraction by NNMF (Shuman et al., 2017) and should be considered when comparing synergy results across studies. Finally, the group results here are based on a relatively small number of subjects, especially when comparing ICs within clusters and therefore, we did not control for multiple comparisons when looking at ERSP and ERD/ERS difference plots. Also, the cohort with CP was mildly affected with unilateral involvement and thus, these results warrant further investigation in larger samples and in different CP subtypes.

CONCLUSION

Electrocortical measurements and muscle synergy analysis are independently, potentially powerful tools for neurorehabilitation to better understand and address motor control abnormalities that impact daily functional activities. However, a quantitative understanding of how motor control strategies are encoded by the CNS and communicated to the periphery is generally lacking. In this study, we compared a subtype of CP with the highest mobility levels to a group with typical development. Therefore, finding that muscle synergy weights and activations were not significantly different at the group level is not unreasonable. Still, we were able to detect unique differences in distribution of individuals across brain regions active during gait as well as significant differences that reflect the unilateral injury that primarily disrupts distal control and its cortical representation in the sensorimotor brain regions in CP. Based on our results, we advocate for the development and implementation of strategies for CP that are more personalized and which iteratively reduce cortical activation while improving selective motor control using brain-computer interface (BCI) methodologies similar to studies in stroke.

DATA AVAILABILITY STATEMENT

The datasets generated for this study are available on request to the corresponding author.

ETHICS STATEMENT

The studies involving human participants were reviewed and approved by the Combined Neuroscience Institutional Review Board, National Institutes of Health. Written informed consent to participate in this study was provided by the participants' legal guardian.

AUTHOR CONTRIBUTIONS

TB, YK, and DD conceived and designed the study. MS performed the data analysis, interpreted the data, wrote the manuscript, and created the figures. DD supervised the clinical aspects of the study, interpreted the data, and wrote the manuscript. YK collected and analyzed the data and reviewed the manuscript. TB collected the data, supervised the data analysis, interpreted the data, wrote the manuscript, and created the figures.

FUNDING

This work was funded by the Intramural Research Program of the National Institutes of Health Clinical Center.

ACKNOWLEDGMENTS

The authors thank Cris Zampieri-Gallagher for assistance with data collection, Chris Stanley for assistance with motion capture and EMG data analysis and Jason Chou for assistance with EEG data analysis.

REFERENCES

Bowden, M. G., Clark, D. J., and Kautz, S. A. (2010). Evaluation of abnormal synergy patterns poststroke: relationship of the fugl-meyer assessment to hemiparetic locomotion. *Neurorehabil. Neural Repair* 24, 328–337. doi: 10.1177/1545968309343215

Bradford, J. C., Lukos, J. R., and Ferris, D. P. (2015). Electrocortical activity distinguishes between uphill and level walking in humans. *J. Neurophysiol.* 115, 958–966. doi: 10.1152/jn.00089.2015

Bulea, T. C., Kim, J., Damiano, D. L., Stanley, C. J., and Park, H.-S. (2015). Prefrontal, posterior parietal and sensorimotor network activity underlying speed control during walking. *Front. Hum. Neurosci.* 9:247. doi: 10.3389/fnhum.2015.00247

Bulea, T. C., Prasad, S., Kilicarslan, A., and Contreras-Vidal, J. L. (2014). Sitting and standing intention can be decoded from scalp EEG recorded prior to movement execution. *Front. Neurosci.* 8:376. doi: 10.3389/fnins.2014.00376

Cappellini, G., Ivanenko, Y. P., Martino, G., MacLellan, M. J., Sacco, A., Morelli, D., et al. (2016). Immature spinal locomotor output in children with cerebral palsy. *Front. Physiol.* 7:478. doi: 10.3389/fphys.2016.00478

Castermans, T., Duvinage, M., Cheron, G., and Dutoit, T. (2014). About the cortical origin of the low-delta and high-gamma rhythms observed in EEG signals during treadmill walking. *Neurosci. Lett.* 561, 166–170. doi: 10.1016/j.neulet.2013.12.059

Chvatal, S. A., and Ting, L. H. (2012). Voluntary and reactive recruitment of locomotor muscle synergies during perturbed walking. *J. Neurosci.* 32, 12237–12250. doi: 10.1523/JNEUROSCI.6344-11.2012

Clark, D. J., Ting, L. H., Zajac, F. E., Neptune, R. R., and Kautz, S. A. (2009). Merging of healthy motor modules predicts reduced locomotor performance and muscle coordination complexity post-stroke. *J. Neurophysiol.* 103, 844–857. doi: 10.1152/jn.00825.2009

Crenna, P. (1998). Spasticity andspastic'gait in children with cerebral palsy. *Neurosci. Biobehav. Rev.* 22, 571–578. doi: 10.1016/s0149-7634(97)00046-8

Cuevas, K., Cannon, E. N., Yoo, K., and Fox, N. A. (2014). The infant EEG mu rhythm: methodological considerations and best practices. *Dev. Rev.* 34, 26–43. doi: 10.1016/j.dr.2013.12.001

Danielmeier, C., Eichele, T., Forstmann, B. U., Tittgemeyer, M., and Ullsperger, M. (2011). Posterior medial frontal cortex activity predicts post-error adaptations in task-related visual and motor areas. *J. Neurosci.* 31, 1780–1789. doi: 10.1523/JNEUROSCI.4299-10.2011

d'Avella, A., and Bizzi, E. (2005). Shared and specific muscle synergies in natural motor behaviors. *Proc. Natl. Acad. Sci. U.S.A.* 102, 3076–3081. doi: 10.1073/pnas.0500199102

d'Avella, A., Giese, M., Ivanenko, Y. P., Schack, T., and Flash, T. (2015). Modularity in motor control: from muscle synergies to cognitive action representation. *Front. Comput. Neurosci.* 9:126. doi: 10.3389/fncom.2015.00126

Delorme, A., and Makeig, S. (2004). EEGLAB: an open source toolbox for analysis of single-trial EEG dynamics including independent component analysis. *J. Neurosci. Methods* 134, 9–21. doi: 10.1016/j.jneumeth.2003.10.009

Delorme, A., Palmer, J., Onton, J., Oostenveld, R., and Makeig, S. (2012). Independent EEG sources are dipolar. *PLoS one* 7:e30135. doi: 10.1371/journal.pone.0030135

Gwin, J. T., Gramann, K., Makeig, S., and Ferris, D. P. (2010). Removal of movement artifact from high-density EEG recorded during walking and running. *J. Neurophysiol.* 103, 3526–3534. doi: 10.1152/jn.00105.2010

Gwin, J. T., Gramann, K., Makeig, S., and Ferris, D. P. (2011). Electrocortical activity is coupled to gait cycle phase during treadmill walking. *Neuroimage* 54, 1289–1296. doi: 10.1016/j.neuroimage.2010.08.066

Hashiguchi, Y., Ohata, K., Osako, S., Kitatani, R., Aga, Y., Masaki, M., et al. (2018). Number of synergies is dependent on spasticity and gait kinetics in children with cerebral palsy. *Pediatr. Phys. Therapy* 30, 34–38. doi: 10.1097/pep.0000000000000460

Inuggi, A., Bassolino, M., Tacchino, C., Pippo, V., Bergamaschi, V., Campus, C., et al. (2018). Ipsilesional functional recruitment within lower mu band in children with unilateral cerebral palsy, an event-related desynchronization study. *Exp. Brain Res.* 236, 517–527. doi: 10.1007/s00221-017-5149-3

Ivanenko, Y. P., Poppele, R. E., and Lacquaniti, F. (2004). Five basic muscle activation patterns account for muscle activity during human locomotion. *J. Physiol.* 556, 267–282. doi: 10.1113/jphysiol.2003.057174

Kim, Y., Bulea, T. C., and Damiano, D. L. (2016). Novel methods to enhance precision and reliability in muscle synergy identification during walking. *Front. Hum. Neurosci.* 10:455. doi: 10.3389/fnhum.2016.00455

Kim, Y., Bulea, T. C., and Damiano, D. L. (2018). Children with cerebral palsy have greater stride-to-stride variability of muscle synergies during gait than typically developing children: implications for motor control complexity. *Neurorehabil. Neural Repair* 32, 834–844. doi: 10.1177/1545968318796333

Kline, J. E., Huang, H. J., Snyder, K. L., and Ferris, D. P. (2015). Isolating gait-related movement artifacts in electroencephalography during human walking. *J. Neural Eng.* 12:046022. doi: 10.1088/1741-2560/12/4/046022

Koenraadt, K. L., Roelofsen, E. G., Duysens, J., and Keijsers, N. L. (2014). Cortical control of normal gait and precision stepping: an fNIRS study. *Neuroimage* 85, 415–422. doi: 10.1016/j.neuroimage.2013.04.070

Kukke, S. N., de Campos, A. C., Damiano, D., Alter, K. E., Patronas, N., and Hallett, M. (2015). Cortical activation and inter-hemispheric sensorimotor coherence in individuals with arm dystonia due to childhood stroke. *Clin. Neurophysiol.* 126, 1589–1598. doi: 10.1016/j.clinph.2014.11.002

Kurz, M. J., Proskovec, A. L., Gehringer, J. E., Heinrichs-Graham, E., and Wilson, T. W. (2017). Children with cerebral palsy have altered oscillatory activity in the motor and visual cortices during a knee motor task. *Neuroimage* 15, 298–305. doi: 10.1016/j.nicl.2017.05.008

Kurz, M. J., Wilson, T. W., and Arpin, D. J. (2012). Stride-time variability and sensorimotor cortical activation during walking. *Neuroimage* 59, 1602–1607. doi: 10.1016/j.neuroimage.2011.08.084

Kurz, M. J., Wilson, T. W., and Arpin, D. J. (2014). An fNIRS exploratory investigation of the cortical activity during gait in children with spastic diplegic cerebral palsy. *Brain Dev.* 36, 870–877. doi: 10.1016/j.braindev.2014.01.003

Lancaster, J. L., Woldorff, M. G., Parsons, L. M., Liotti, M., Freitas, C. S., Rainey, L., et al. (2000). Automated Talairach atlas labels for functional brain mapping. *Hum. Brain Mapp.* 10, 120–131. doi: 10.1002/1097-0193(200007)10:3<120::aid-hbm30>3.0.co;2-8

Latash, M. L., Scholz, J. P., and Schöner, G. (2007). Toward a new theory of motor synergies. *Mot. Control* 11, 276–308. doi: 10.1123/mcj.11.3.276

Lee, D. D., and Seung, H. S. (1999). Learning the parts of objects by non-negative matrix factorization. *Nature* 401:788. doi: 10.1038/44565

Leonard, C. T., Hirschfeld, H., and Forssberg, H. (1991). The development of independent walking in children with cerebral palsy. *Dev. Med. Child Neurol.* 33, 567–577. doi: 10.1016/j.braindev.2019.03.005

Luu, T. P., Brantley, J. A., Zhu, F., and Contreras-Vidal, J. L. (2017). "Electrocortical amplitude modulations of human level-ground, slope, and stair walking," in *Proceedings of the 2017 39th Annual International Conference of the IEEE Engineering in Medicine and Biology Society EMBC*, Piscataway, NJ, 1913–1916.

Makeig, S. (1993). Auditory event-related dynamics of the EEG spectrum and effects of exposure to tones. *Electroencephalogr. Clin. Neurophysiol.* 86, 283–293. doi: 10.1016/0013-4694(93)90110-h

Makeig, S., Bell, A. J., Jung, T.-P., and Sejnowski, T. J. (1996). Independent component analysis of electroencephalographic data. *Adv. Neural Inform. Process. Syst.* 8, 145–151.

Maulik, U., and Bandyopadhyay, S. (2002). Performance evaluation of some clustering algorithms and validity indices. *IEEE Trans. Pat. Anal. Mach. Intell.* 24, 1650–1654. doi: 10.1109/tpami.2002.1114856

Mehrkanoon, S., Breakspear, M., and Boonstra, T. W. (2014). The reorganization of corticomuscular coherence during a transition between sensorimotor states. *Neuroimage* 100, 692–702. doi: 10.1016/j.neuroimage.2014.06.050

Miller, E. K., and Cohen, J. D. (2001). An integrative theory of prefrontal cortex function. *Ann. Rev. Neurosci.* 24, 167–202. doi: 10.1146/annurev.neuro.24.1.167

Mima, T., and Hallett, M. (1999). Corticomuscular coherence: a review. *J. Clin. Neurophysiol.* 16, 501–511. doi: 10.1097/00004691-199911000-00002

Miyai, I., Tanabe, H. C., Sase, I., Eda, H., Oda, I., Konishi, I., et al. (2001). Cortical mapping of gait in humans: a near-infrared spectroscopic topography study. *Neuroimage* 14, 1186–1192. doi: 10.1006/nimg.2001.0905

Mullen, T., Kothe, C., Chi, Y. M., Ojeda, A., Kerth, T., Makeig, S., et al. (2013). "Real-time modeling and 3D visualization of source dynamics and connectivity using wearable EEG," in *Proceedings of the 2013 35th Annual International Conference of the IEEE Engineering in Medicine And Biology Society*, Piscataway, NJ, 2184–2187.

Nordin, A. D., Hairston, W. D., and Ferris, D. P. (2019). Faster gait speeds reduce alpha and beta EEG spectral power from human sensorimotor cortex. *IEEE Trans. Biomed. Eng.* (in press).

Oldfield, R. C. (1971). The assessment and analysis of handedness: the Edinburgh inventory. *Neuropsychologia* 9, 97–113. doi: 10.1016/0028-3932(71)90067-4

Oliveira, A. S., Gizzi, L., Farina, D., and Kersting, U. G. (2014). Motor modules of human locomotion: influence of EMG averaging, concatenation, and number of step cycles. *Front. Hum. Neurosci.* 8:335. doi: 10.3389/fnhum.2014.00335

Oostenveld, R., and Oostendorp, T. F. (2002). Validating the boundary element method for forward and inverse EEG computations in the presence of a hole in the skull. *Hum. Brain Mapp.* 17, 179–192. doi: 10.1002/hbm.10061

Palisano, R., Rosenbaum, P., Walter, S., Russell, D., Wood, E., and Galuppi, B. (1997). Development and reliability of a system to classify gross motor function in children with cerebral palsy. *Dev. Med. Child Neurol.* 39, 214–223. doi: 10.1111/j.1469-8749.1997.tb07414.x

Pei, D., Patel, V., Burns, M., Chandramouli, R., and Vinjamuri, R. (2019). Neural decoding of synergy-based hand movements using electroencephalography. *IEEE Access.* 7, 18155–18163. doi: 10.1109/access.2019.2895566

Pfurtscheller, G., and Da Silva, F. L. (1999). Event-related EEG/MEG synchronization and desynchronization: basic principles. *Clin. Neurophysiol.* 110, 1842–1857. doi: 10.1016/s1388-2457(99)00141-8

Pirondini, E., Coscia, M., Minguillon, J., Millán, J. D. R., Van De Ville, D., and Micera, S. (2017). EEG topographies provide subject-specific correlates of motor control. *Sci. Rep.* 7:13229. doi: 10.1038/s41598-017-13482-1

Seeber, M., Scherer, R., Wagner, J., Solis-Escalante, T., and Müller-Putz, G. R. (2014). EEG beta suppression and low gamma modulation are different elements of human upright walking. *Front. Hum. Neurosci.* 8:485. doi: 10.3389/fnhum.2014.00485

Seeber, M., Scherer, R., Wagner, J., Solis-Escalante, T., and Müller-Putz, G. R. (2015). High and low gamma EEG oscillations in central sensorimotor areas are conversely modulated during the human gait cycle. *Neuroimage* 112, 318–326. doi: 10.1016/j.neuroimage.2015.03.045

Severens, M., Nienhuis, B., Desain, P., and Duysens, J. (2012). "Feasibility of measuring event related desynchronization with electroencephalography during walking," in *Proceedings of the 2012 Annual International Conference of the IEEE Engineering in Medicine and Biology Society*, Piscataway, NJ, 2764–2767.

Shuman, B., Goudriaan, M., Bar-On, L., Schwartz, M. H., Desloovere, K., and Steele, K. M. (2016). Repeatability of muscle synergies within and between days for typically developing children and children with cerebral palsy. *Gait Posture* 45, 127–132. doi: 10.1016/j.gaitpost.2016.01.011

Shuman, B. R., Schwartz, M. H., and Steele, K. M. (2017). Electromyography data processing impacts muscle synergies during gait for unimpaired children and children with cerebral palsy. *Front. Comput. Neurosci.* 11:50. doi: 10.3389/fncom.2017.00050

Snyder, K. L., Kline, J. E., Huang, H. J., and Ferris, D. P. (2015). Independent component analysis of gait-related movement artifact recorded using EEG electrodes during treadmill walking. *Front. Hum. Neurosci.* 9:639. doi: 10.3389/fnhum.2015.00639

Solis-Escalante, T., Müller-Putz, G. R., Pfurtscheller, G., and Neuper, C. (2012). Cue-induced beta rebound during withholding of overt and covert foot movement. *Clin. Neurophysiol.* 123, 1182–1190. doi: 10.1016/j.clinph.2012.01.013

Steele, K. M., Munger, M. E., Peters, K. M., Shuman, B. R., and Schwartz, M. H. (2019). Repeatability of electromyography recordings and muscle synergies during gait among children with cerebral palsy. *Gait Posture* 67, 290–295. doi: 10.1016/j.gaitpost.2018.10.009

Steele, K. M., Rozumalski, A., and Schwartz, M. H. (2015). Muscle synergies and complexity of neuromuscular control during gait in cerebral palsy. *Dev. Med. Child Neurol.* 57, 1176–1182. doi: 10.1111/dmcn.12826

Sukal-Moulton, T., de Campos, A. C., Alter, K. E., Huppert, T. J., and Damiano, D. L. (2018). Relationship between sensorimotor cortical activation as assessed by functional near infrared spectroscopy and lower extremity motor coordination in bilateral cerebral palsy. *Neuroimage Clin.* 20, 275–285. doi: 10.1016/j.nicl.2018.07.023

Suzuki, M., Miyai, I., Ono, T., Oda, I., Konishi, I., Kochiyama, T., et al. (2004). Prefrontal and premotor cortices are involved in adapting walking and running speed on the treadmill: an optical imaging study. *Neuroimage* 23, 1020–1026. doi: 10.1016/j.neuroimage.2004.07.002

Tresch, M. C., Saltiel, P., d'Avella, A., and Bizzi, E. (2002). Coordination and localization in spinal motor systems. *Brain Res. Rev.* 40, 66–79. doi: 10.1016/s0165-0173(02)00189-3

Wagner, J., Makeig, S., Gola, M., Neuper, C., and Müller-Putz, G. (2016). Distinct β band oscillatory networks subserving motor and cognitive control during gait adaptation. *J. Neurosci.* 36, 2212–2226. doi: 10.1523/jneurosci.3543-15.2016

Wagner, J., Solis-Escalante, T., Grieshofer, P., Neuper, C., Müller-Putz, G., and Scherer, R. (2012). Level of participation in robotic-assisted treadmill walking modulates midline sensorimotor EEG rhythms in able-bodied subjects. *Neuroimage* 63, 1203–1211. doi: 10.1016/j.neuroimage.2012.08.019

Wagner, J., Solis-Escalante, T., Scherer, R., Neuper, C., and Müller-Putz, G. (2014). It's how you get there: walking down a virtual alley activates premotor and parietal areas. *Front. Hum. Neurosci.* 8:93. doi: 10.3389/fnhum.2014.00093

Weinstein, M., Green, D., Rudisch, J., Zielinski, I. M., Benthem-Muñiz, M., Jongsma, M. L., et al. (2018). Understanding the relationship between brain and upper limb function in children with unilateral motor impairments: a multimodal approach. *Eur. J. Paediatr. Neurol.* 22, 143–154. doi: 10.1016/j.ejpn.2017.09.012

Wiley, M. E., and Damiano, D. L. (1998). Lower-extremity strength profiles in spastic cerebral palsy. *Dev. Med. Child Neurol.* 40, 100–107. doi: 10.1111/j.1469-8749.1998.tb15369.x

Winters, T., Gage, J., and Hicks, R. (1987). Gait patterns in spastic hemiplegia in children and young adults. *J. Bone Joint Surg. Am.* 69, 437–441. doi: 10.2106/00004623-198769030-00016

Conflict of Interest: The authors declare that the research was conducted in the absence of any commercial or financial relationships that could be construed as a potential conflict of interest.

frontiers in Human Neuroscience

ORIGINAL RESEARCH
published: 18 February 2020
doi: 10.3389/fnhum.2020.00040

Physics-Based Simulations to Predict the Differential Effects of Motor Control and Musculoskeletal Deficits on Gait Dysfunction in Cerebral Palsy: A Retrospective Case Study

Antoine Falisse[1], Lorenzo Pitto[1], Hans Kainz[1], Hoa Hoang[1], Mariska Wesseling[1], Sam Van Rossom[1], Eirini Papageorgiou[2], Lynn Bar-On[2,3], Ann Hallemans[4], Kaat Desloovere[2], Guy Molenaers[5,6], Anja Van Campenhout[5,6], Friedl De Groote[1] and Ilse Jonkers[1]*

[1] Department of Movement Sciences, KU Leuven, Leuven, Belgium, [2] Department of Rehabilitation Sciences, KU Leuven, Leuven, Belgium, [3] Department of Rehabilitation Medicine, Amsterdam Movement Sciences, Amsterdam UMC, VU University Medical Center, Amsterdam, Netherlands, [4] Department of Rehabilitation Sciences and Physiotherapy, University of Antwerp, Antwerp, Belgium, [5] Department of Orthopaedic Surgery, UZ Leuven, Leuven, Belgium, [6] Department of Development and Regeneration, KU Leuven, Leuven, Belgium

OPEN ACCESS

Edited by:
Jessica Rose,
Stanford University, United States

Reviewed by:
Pavel Lindberg,
INSERM U1266 Institut de Psychiatrie et Neurosciences de Paris, France
Kornél Schadl,
Stanford University, United States

***Correspondence:**
Antoine Falisse
antoine.falisse@kuleuven.be

Specialty section:
This article was submitted to Motor Neuroscience, a section of the journal Frontiers in Human Neuroscience

Received: *30 September 2019*
Accepted: *27 January 2020*
Published: *18 February 2020*

Citation:
Falisse A, Pitto L, Kainz H, Hoang H, Wesseling M, Van Rossom S, Papageorgiou E, Bar-On L, Hallemans A, Desloovere K, Molenaers G, Van Campenhout A, De Groote F and Jonkers I (2020) Physics-Based Simulations to Predict the Differential Effects of Motor Control and Musculoskeletal Deficits on Gait Dysfunction in Cerebral Palsy: A Retrospective Case Study. Front. Hum. Neurosci. 14:40. doi: 10.3389/fnhum.2020.00040

Physics-based simulations of walking have the theoretical potential to support clinical decision-making by predicting the functional outcome of treatments in terms of walking performance. Yet before using such simulations in clinical practice, their ability to identify the main treatment targets in specific patients needs to be demonstrated. In this study, we generated predictive simulations of walking with a medical imaging based neuro-musculoskeletal model of a child with cerebral palsy presenting crouch gait. We explored the influence of altered muscle-tendon properties, reduced neuromuscular control complexity, and spasticity on gait dysfunction in terms of joint kinematics, kinetics, muscle activity, and metabolic cost of transport. We modeled altered muscle-tendon properties by personalizing Hill-type muscle-tendon parameters based on data collected during functional movements, simpler neuromuscular control by reducing the number of independent muscle synergies, and spasticity through delayed muscle activity feedback from muscle force and force rate. Our simulations revealed that, in the presence of aberrant musculoskeletal geometries, altered muscle-tendon properties rather than reduced neuromuscular control complexity and spasticity were the primary cause of the crouch gait pattern observed for this child, which is in agreement with the clinical examination. These results suggest that muscle-tendon properties should be the primary target of interventions aiming to restore an upright gait pattern for this child. This suggestion is in line with the gait analysis following muscle-tendon property and bone deformity corrections. Future work should extend this single case analysis to more patients in order to validate the ability of our physics-based simulations to capture the gait patterns of individual patients pre- and post-treatment. Such validation would open the door for identifying targeted treatment strategies with the aim of designing optimized interventions for neuro-musculoskeletal disorders.

Keywords: computational biomechanics, Hill-type muscle-tendon model, human locomotion, magnetic resonance imaging, muscle-tendon unit, optimal control, spasticity, synergy

1. INTRODUCTION

Cerebral palsy (CP) is the most common cause of motor disability amongst children, affecting 2 to 3 per 1000 live births in Europe (Surveillance of Cerebral Palsy in Europe, 2002). CP is caused by a non-progressive lesion in the immature brain that may induce inabilities to selectively control muscles, spasticity, and weakness. These deficits undermine walking performance and, over time, lead to secondary impairments, such as bone deformities and muscle contracture, that may further deteriorate walking abilities (Gage et al., 2009). Numerous treatments target these impairments with the aim of improving walking performance, such as single-event multi-level orthopedic surgeries (SEMLS) to correct multiple bone and muscle impairments in a single intervention (McGinley et al., 2012). Yet walking involves complex interactions between the musculoskeletal and motor control systems, which are both impaired in CP. Hence, the treatment outcome does not only depend on the success of the intervention in terms of musculoskeletal remediation but also on the remaining motor control (Schwartz et al., 2016). As a result, over the last decades, only modest, unpredictable, and stagnant treatment outcomes have been documented for children with CP (Schwartz, 2018). For example, SEMLS have been reported to improve walking performance in only 25 to 43% of the patients (Chang et al., 2006; Filho et al., 2008) and to lead to clinically meaningful improvements over natural progression in only 37% of the cases (Rajagopal et al., 2018). Physics-based computer models that can predict the functional outcome of treatments on walking performance have the potential to improve this success rate by allowing clinicians to optimize the clinical decision-making (e.g., by discriminating the effects of musculoskeletal restoration due to surgical interventions to those from tone reduction and physical therapy targeting motor control impairments). However, predictive simulations are not yet applied in clinical practice, in part due to computational and modeling challenges.

Physics-based predictive simulations generate novel movements based on a mathematical model of the neuro-musculoskeletal system without relying on measured movement data. Typically, these simulations consist in identifying muscle excitations that follow a certain control strategy and drive the musculoskeletal model to achieve a movement-related goal (e.g., moving forward at a given speed). The relationship between input muscle excitations and output joint kinematics is thus fully determined by physics-based models, which allows qualifying our simulations as predictive as typically referred to in the literature (e.g., Miller, 2014; Lin et al., 2018). For such simulations to be valuable in predicting the functional outcome of treatments on walking performance, they should be based on models that are complex enough to describe the musculoskeletal structures and motor control processes underlying walking that may be impaired and thus affected by treatment. Yet these complex models are computationally expensive in predictive simulations (Anderson and Pandy, 2001; Miller, 2014; Song and Geyer, 2015; Lin et al., 2018; Ong et al., 2019) and, therefore, their ability to predict the variety of gaits encountered under different conditions (e.g., healthy and pathological gaits) has been only scarcely explored in the literature. We recently developed a simulation framework to generate rapid (i.e., about 30 min of computational time) predictive simulations of gait with complex models (Falisse et al., 2019b). Further, we demonstrated the ability of our framework to predict the mechanics and energetics of a broad range of gaits, suggesting that our models and simulations were sufficiently generalizable for use in clinical applications. Nevertheless, the ability of our simulations to identify the main treatment targets in specific patients remains untested. Specifically, for children with CP, simulations should allow distinguishing the effects of musculoskeletal vs. motor control impairments on walking performance to be able to help clinicians optimize treatments.

Predicting the effects of impairments on walking performance in children with CP requires the neuro-musculoskeletal model to take these impairments into account. In this work, we focus on two types of impairments: motor control impairments that include spasticity and non-selective muscle control, and musculoskeletal impairments that include bone deformities and altered muscle-tendon properties.

The neural component of spasticity has been described as a velocity-dependent increase in tonic stretch reflex responses resulting from hyper-excitability of the stretch reflex (Lance, 1980). Following such description, models based on feedback from muscle velocity have been developed to describe spastic muscle activity [i.e., electromyography (EMG)] measured in response to passive stretches (van der Krogt et al., 2016). However, we previously showed that a model based on feedback from muscle force and force rate better explains the muscle activity response of spastic hamstrings and gastrocnemii to passive stretches than length- and velocity-based models (Falisse et al., 2018). Further, we found that a force-based model could predict muscle activity in agreement with pathological EMG during gait. Our simulations were nevertheless based on measured movement data, which prevents investigating the influence of spasticity on gait kinematics; an influence that remains subject to debate (Dietz and Sinkjaer, 2007). Predictive simulations have the potential to provide insights into the role of spasticity during gait. In more detail, incorporating the aforementioned spasticity models into the neuro-musculoskeletal model theoretically allows evaluating the impact of spasticity on gait performance by predicting the spastic contribution to the generated muscle activations as well as the resulting effects on the predicted joint kinematics and gait energetics. Modeling spasticity is also a prerequisite to simulating the effects of treatments aiming to reduce spasticity, such as botulinum toxin-A (BTX) injections.

The inability to selectively control muscles has been described through muscle synergies (Ivanenko et al., 2004), which are independent groups of muscles activated in a fixed ratio by a single input signal. Children with CP have been shown to use fewer synergies (i.e., a simpler neuromuscular control strategy) than typically developing (TD) individuals during walking (Steele et al., 2015) as well as to use synergies exhibiting a greater stride-to-stride variability (Kim et al., 2018). However, assessing the relationship between simpler neuromuscular control and impaired gait is difficult. For example, Shuman et al. (2019)

showed that treatments such as BTX injections, selective dorsal rhizotomy, and SEMLS minimally affected synergies despite changing the walking patterns. Predictive simulations have the potential to relate synergy complexity to impaired walking abilities, which might help designing specific treatments (e.g., physical therapy protocols) targeting impaired selective motor control.

Bone deformities and resultant altered muscle path trajectories make the use of generic musculoskeletal models linearly-scaled to the subjects' anthropometry inappropriate for clinical analyses in children with CP. A well established approach to capture these aberrant geometries is the use of personalized models created from Magnetic Resonance Imaging (MRI) (Arnold et al., 2001; Scheys et al., 2009, 2011a), where personalized indicates that certain model parameters (e.g., muscle insertion points and joint axes) are fitted to the subject. Such personalization has been shown to improve, for example, the accuracy of moment arm estimation in children with CP (Scheys et al., 2011b). Besides geometries, the muscle-tendon properties are also altered in these children (e.g., smaller muscle volumes and shorter fiber lengths as compared to TD individuals) (Barrett and Lichtwark, 2010; Barber et al., 2011a,b, 2012; Smith et al., 2011). This makes the use of Hill-type muscle-tendon models with generic (i.e., anthropometry-based) parameters unsuited for clinical studies. Indeed, such parameters may not reflect altered muscle force generating capacities and, therefore, result in unrepresentative simulations. To capture the impact of altered muscle-tendon properties on walking performance, the muscle-tendon parameters should be personalized. Different approaches have been proposed for such purpose, including methods based on angle-torque relationships from functional movements (Lloyd and Besier, 2003; Falisse et al., 2017).

Predictive simulations have the potential to shed light upon the influence of altered musculoskeletal properties, impaired selective motor control, and spasticity on walking performance by evaluating the isolated effects of these impairments. Yet only few predictive analyses have used simulations for such purpose. Recent modeling work showed that a musculoskeletal model could reproduce an unimpaired walking pattern with five synergies but not with two synergies similar to those seen after neurological injury, suggesting that impaired control affects walking performance (Meharbi et al., 2019). Another predictive analysis explored the effects of aging on walking performance by adjusting skeletal and neuromuscular parameters and reported a predominant contribution of loss in muscle strength and mass to reduced energy efficiency (Song and Geyer, 2018). Both studies, however, relied on simple two-dimensional (2D) models, neglecting motor control mechanisms in the frontal plane. To the authors' knowledge, no study has yet attempted to relate patients' clinical examination reports to the outcome of predictive simulations evaluating the effects of musculoskeletal and motor control impairments on walking performance based on three-dimensional (3D) personalized models.

The purpose of this study was to evaluate the ability of our predictive simulation platform to differentiate the effects of musculoskeletal and motor control impairments on the impaired walking pattern (i.e., crouch gait) of a specific child with CP. To this aim, we evaluated the effect of these impairments on gait patterns predicted by performance optimization (**Figure 1A**). We first investigated the influence of using personalized rather than generic muscle-tendon parameters, thereby assessing the contribution of the child's altered muscle-tendon properties to the crouch gait pattern. We then evaluated the impact of imposing a number of synergies lower than typically reported for unimpaired individuals, thereby testing how reducing neuromuscular control complexity affects walking performance. We finally investigated the effect of spasticity modeled based on muscle force and force rate feedback. In all cases, we used a MRI-based musculoskeletal model of the child to take the aberrant geometries into account. We found that altered muscle-tendon properties rather than motor control impairments alone caused a crouch gait pattern. As an additional analysis, we investigated whether the child's impairments impede a walking pattern similar to TD walking or rather make such a walking pattern less optimal. To this aim, we extended the performance criterion of the predictive simulations with a tracking term that penalized deviations from a TD walking pattern. We found that the musculoskeletal impairments did not prevent an upright walking pattern resembling TD walking but that upright walking was less optimal than walking in crouch. Further work is necessary to extend this single case analysis to more patients in order to validate the ability of our physics-based simulations to capture the gait patterns of individual patients pre- and post-treatment.

2. MATERIALS AND METHODS

The overall process to evaluate the effects of impairments on walking performance through predictive simulations is outlined in **Figure 1B**. The following sections provide details of this process.

2.1. Experimental Data

We collected data from one child with diplegic CP (age: 10–15 years; height: 125–150 cm; mass: 30–40 kg). The data collection was approved by the Ethics Committee at UZ Leuven (Belgium) and written informed consent was obtained from the child's parents. The child was instrumented with retro-reflective skin mounted markers whose 3D trajectories were recorded (100 Hz) using a motion capture system (Vicon, Oxford, UK) during overground walking at self-selected speed. Ground reaction forces were recorded (1,000 Hz) using force plates (AMTI, Watertown, USA). EMG was recorded (2,000 Hz) using a telemetric Zerowire system (Cometa, Milan, Italy) from eight muscles of each leg (rectus femoris, biceps femoris short head, semitendinosus, tibialis anterior, gastrocnemius lateralis, vastus lateralis, soleus, and gluteus medius). EMG from the rectus femoris and vastus lateralis was of poor quality and excluded from the analysis.

On the same day as the gait analysis, spasticity of the right medial hamstrings and gastrocnemii was assessed using an instrumented passive spasticity assessment [IPSA; described in detail by Bar-On et al. (2013)]. Hamstrings and gastrocnemii were passively stretched by moving knee and ankle, respectively, one at a time from a predefined position throughout the full

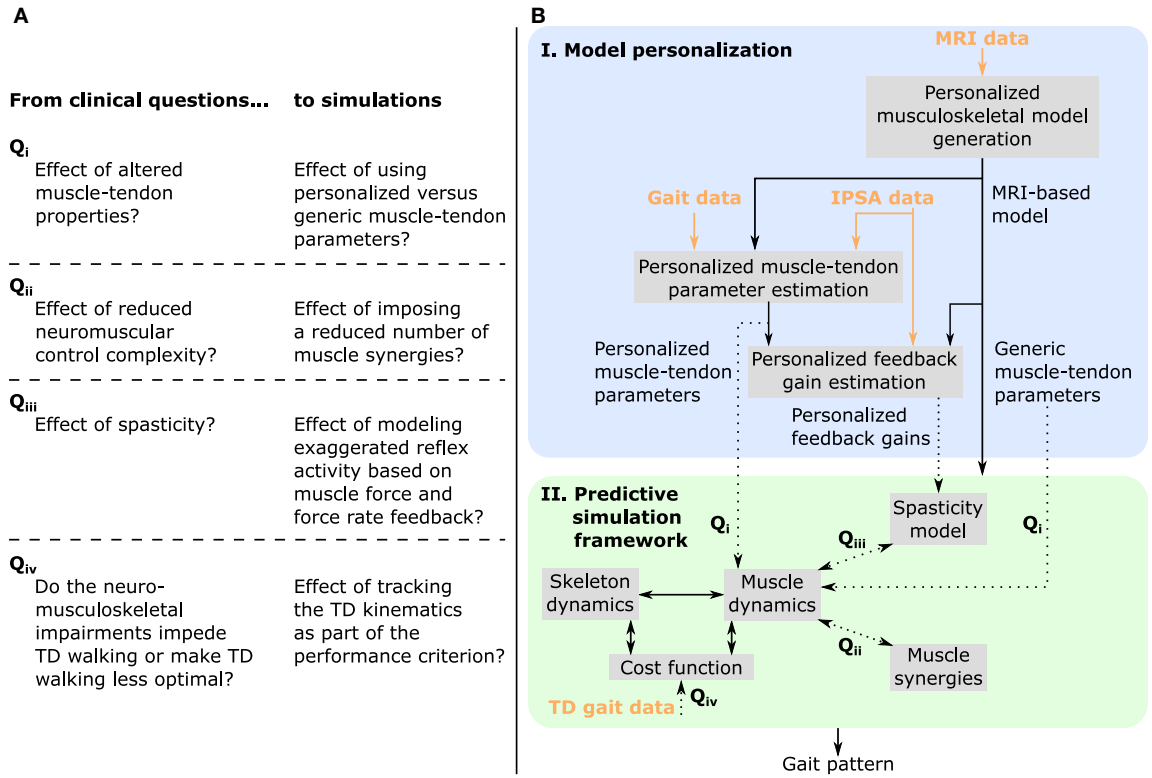

FIGURE 1 | Overview of **(A)** clinical questions and corresponding simulations, and **(B)** methodology. MRI images are used to generate a musculoskeletal model of the child with personalized geometries. This MRI-based model as well as experimental data collected during walking and instrumented passive spasticity assessments (IPSA) are inputs to optimization procedures providing personalized estimates of Hill-type muscle-tendon parameters characterizing altered muscle-tendon properties and personalized feedback gains characterizing spasticity. The framework for predictive simulations generates gait patterns by optimizing a cost function, describing a walking-related performance criterion, subject to the muscle and skeleton dynamics of the MRI-based musculoskeletal model. We investigated the effects of impairments on predicted gait patterns (dotted arrows): in Q_i we evaluated the effect of altered vs. unaltered muscle-tendon properties by using personalized vs. generic muscle-tendon parameters in the muscle dynamics; in Q_{ii} we assessed the influence of reducing the neuromuscular control complexity by imposing a reduced number of muscle synergies; in Q_{iii} we explored the impact of spasticity on walking performance. Details on how we modeled these impairments are described in the methods. As an additional analysis, Q_{iv}, we evaluated how well the model was able to reproduce the gait pattern of a typically developing (TD) child by adding a term in the cost function penalizing deviations between predicted gait pattern and measured gait data of a TD child. All these analyses can be combined as well as performed in isolation. Details are provided in section "model-based analyses".

range of motion (ROM). The stretches were performed at slow and fast velocities. EMG was collected from four muscles (semitendinosus, gastrocnemius lateralis, rectus femoris, and tibialis anterior) using the same system and electrode placement as used for gait analysis. The motion of the distal and proximal segments were tracked using two inertial measurement units (Analog Devices, ADIS16354). The forces applied to the segment were measured using a hand-held six degrees of freedom load-cell (ATI Industrial Motion, mini45). The position of the load-cell relative to the joint axis was manually measured by the examiner.

Muscle strength, selectivity, and ROM were evaluated (**Table 1**) with a standardized clinical examination protocol (Desloovere et al., 2006). The child had close to normal ROM at the hip and ankle but bilateral knee extension deficits, bilateral spasticity in most muscles, good strength in most muscles although slight deficits in hip extensors, knee extensors, and hip abductors, and good to perfect selectivity in most muscles. MRI images were collected for the hip region [i.e., pelvis and femur according to the protocol described by Bosmans et al. (2014)]. The child was classified at a level II in the Gross Motor Function Classification System (GMFCS).

We processed the experimental gait and IPSA data, used as input for the estimation of muscle-tendon parameters and feedback gains (**Figure 1**; details below), with OpenSim 3.3 (Delp et al., 2007) using the MRI-based model described below.

2.2. Personalized Musculoskeletal Model Generation

A 3D musculoskeletal model with personalized geometries was created from MRI images (Scheys et al., 2009, 2011a; Bosmans et al., 2014). Bones of the lower limbs and pelvis were segmented using Mimics (Materialize, Leuven, Belgium). Anatomical reference frames, joint axes, and muscle origin and insertion points were defined using a previously developed workflow (Scheys et al., 2008). The model consisted of 21 degrees of freedom (six between the pelvis and the ground; three at each hip joint; one at each knee, ankle, and subtalar joint; and

TABLE 1 | Clinical examination.

	ROM			Spasticity	
	Left	**Right**		**Left**	**Right**
Hip flexion	145°	140°	Hip flexion MAS	**2**	**2**
Hip extension	**–10°**	**–10°**	Hip adduction (Knee 0°) MAS	**1.5**	**1.5**
Hip abduction (Knee 0°)	25°	25°	Hip adduction (Knee 90°) MAS	0	0
Hip abduction (Knee 90°)	45°	45°	Hamstrings MAS	**1.5**	**1**
Hip adduction	0°	0°	Hamstrings Tardieu	**–70°**	/
Hip internal rotation (prone)	60°	70°	Duncan-Ely MAS	**1.5**	**1.5**
Hip external rotation (prone)	25°	25°	Soleus MAS	0	0
Hip internal rotation (supine)	25°	30°	Soleus Tardieu	/	/
Hip external rotation (supine)	55°	50°	Gastrocnemius MAS	**1.5**	**1.5**
Knee flexion	120°	120°	Gastrocnemius Tardieu	0°	**5°**
Knee extension	**–20°**	**–15°**	Tibialis posterior MAS	0	0
Knee spontaneous position	**–30°**	**–25°**	Clonus	0	0
Popliteal angle Unilateral	**–70°**	**–65°**			
Popliteal angle Bilateral	**–65°**	**–60°**			
Ankle dorsiflexion (Knee 90°)	20°	25°		**Alignment**	
Ankle dorsiflexion (Knee 0°)	15°	15°		**Left**	**Right**
Ankle plantarflexion	35°	35°	Femoral anteversion	35°	35°
Ankle inversion	40°	45°	Tibia-femoral angle	25°	25°
Ankle eversion	10°	10°	Bimalleor angle	40°	40°

	Selectivity			Strength	
	Left	**Right**		**Left**	**Right**
Hip flexion	2	2	Hip flexion	4	4
Hip extension	1.5	1.5	Hip extension	**3**	**3**
Hip abduction	1.5	1.5	Hip abduction	**3+**	**3+**
Hip adduction	2	2	Hip adduction	4	4
Knee flexion	1.5	1.5	Knee flexion	4	**3+**
Knee extension	**1**	1.5	Knee extension	**3+**	**3+**
Ankle dorsiflexion (Knee 90°)	1.5	1.5	Ankle dorsiflexion (Knee 90°)	4	4
Ankle dorsiflexion (Knee 0°)	1.5	1.5	Ankle dorsiflexion (Knee 0°)	4	4
Ankle plantarflexion	1.5	1.5	Ankle plantarflexion	4	**3+**
Ankle inversion	1.5	1.5	Ankle inversion	4	4
Ankle eversion	2	1.5	Ankle eversion	4	4

ROM is range of motion. Spasticity, MAS is for Modified Ashworth Scale: 1 is low, 1+ is medium, and 2 is high spastic involvement. Selectivity: 1 is medium, 1.5 is good, and 2 is perfect selective control. Strength: 3 is medium and 4 is good strength; strength from 3 indicates ability to move against gravity. Clinically meaningful deviations from unimpaired individuals are in bold.

three at the lumbar joint), 86 muscles actuating the lower limbs (43 per leg), three ideal torque actuators at the lumbar joint, and four contact spheres per foot (Delp et al., 1990, 2007). We added passive torques to the joints of the lower limbs and the trunk to model the role of the ligaments and other passive structures (Anderson and Pandy, 2001). These passive torques varied exponentially with joint positions and linearly with joint velocities.

We used Raasch's model (Raasch et al., 1997; De Groote et al., 2009) to describe muscle excitation-activation coupling (muscle activation dynamics) and a Hill-type muscle-tendon model (Zajac, 1989; De Groote et al., 2016) to describe muscle-tendon interaction and the dependence of muscle force on fiber length and velocity (muscle contraction dynamics). We modeled skeletal motion with Newtonian rigid body dynamics and smooth approximations of compliant Hunt-Crossley foot-ground contacts (Delp et al., 2007; Sherman et al., 2011; Seth et al., 2018; Falisse et al., 2019b). We calibrated the Hunt-Crossley contact parameters (transverse plane locations and contact sphere radii) through muscle-driven tracking simulations of the child's experimental walking data as described in previous work (Falisse et al., 2019b). To increase computational speed, we defined muscle-tendon lengths, velocities, and moment arms as a polynomial function of joint positions and velocities (van den Bogert et al., 2013; Falisse et al., 2019b).

2.3. Personalized Muscle-Tendon Parameter Estimation

The force-length-velocity relationships describing the force generating capacity of the Hill-type muscle-tendon model are dimensionless and can be scaled to a specific muscle through five muscle-tendon parameters: the maximal isometric force $F_m^{\max}$, the optimal fiber length l_m^{opt}, the tendon slack length l_t^s, the optimal pennation angle α_m^{opt}, and the maximal fiber contraction velocity $v_m^{\max}$ (assigned to ten times l_m^{opt}). In this study, we used generic and personalized parameters when generating predictive simulations of walking (**Figure 1**).

The generic parameters were derived by linearly scaling the parameters of a generic musculoskeletal model (Delp et al., 1990) to the child's anthropometry. The linear scaling was only performed for the optimal fiber lengths and tendon slack lengths. The maximal isometric muscle forces were scaled based on body mass M (van der Krogt et al., 2016):

$$F_{m,\text{subject}}^{\max} = F_{m,\text{gait2392}}^{\max} \left(\frac{M_{\text{subject}}}{M_{\text{gait2392}}} \right)^{(2/3)}, \quad (1)$$

where gait2392 refers to the OpenSim gait2392 model (Delp et al., 1990, 2007).

The personalized parameters reflect the muscle force generating capacity of the subject. Only optimal fiber lengths and tendon slack lengths were personalized as gait simulations have been shown to be the most sensitive to these two parameters (De Groote et al., 2010). The personalization process was based on an extension of an optimal control approach to solve the muscle redundancy problem while accounting for muscle dynamics (De Groote et al., 2016; Falisse et al., 2017). Solving the muscle redundancy problem identifies muscle excitations that reproduce joint torques underlying a given movement while minimizing a performance criterion (e.g., muscle effort). We augmented this formulation in different ways. First, we added optimal fiber lengths and tendon slack lengths as optimization variables. Second, we introduced a term in the cost function minimizing the difference between muscle activations and scaled EMG signals where scale factors were included as optimization variables. Third, we assumed that muscles operate around their optimal fiber lengths, and that maximal and minimal fiber

lengths across movements should hence be larger and smaller, respectively, than their optimal fiber lengths. Fourth, we assumed that resistance encountered when evaluating the ROM during the clinical examination may be, at least in part, attributed to passive muscle forces. Hence, we included a term in the cost function minimizing the difference between fiber lengths at these extreme positions of the ROM and reference fiber lengths generating large passive forces (Pitto et al., 2019). Finally, we minimized optimal fiber lengths, assuming that children with CP have short fibers (Barrett and Lichtwark, 2010). The problem thus consisted in identifying muscle excitations and parameters that minimized a multi-objective cost function:

$$J_{\text{estimation}} = \int_{t_0}^{t_f} \left(\underbrace{w_1 \|a\|_2^2}_{\substack{\text{Muscle} \\ \text{effort}}} + \underbrace{w_2 \|a - EMG\|_2^2}_{\substack{\text{EMG} \\ \text{deviation}}} + \underbrace{w_3 \left\| l_m^{\max} - l_{\text{ref}}^{\max} \right\|_2^2}_{\substack{\text{Passive forces in} \\ \text{extreme positions}}} + \underbrace{w_4 \left\| l_m^{\text{opt}} \right\|_1}_{\substack{\text{Short} \\ \text{fibers}}} + \underbrace{w_5 \|a_r\|_2^2}_{\substack{\text{Reserve} \\ \text{actuators}}} \right) dt, \tag{2}$$

where t_0 and t_f are initial and final times, a are muscle activations, $l_m^{\max}$ and $l_{\text{ref}}^{\max} = 1.5$ are simulated and reference fiber lengths, respectively, at the extreme positions of the ROM, a_r are reserve actuators, w_{1-5} are weight factors, and t is time. This cost function was subject to constraints enforcing muscle dynamics, that resultant muscle forces should reproduce joint torques calculated from inverse dynamics, that fiber lengths should cross their optimal fiber lengths during the movement, and that the difference between activations and EMG should not be larger than 0.1. Reserve actuators are non-physiological ideal actuators added to muscle-generated torques to ensure that joint torques from inverse dynamics can be reproduced. The weights were manually adjusted to the following: $w_1 = 10 \times 10^{-4}$, $w_2 = 30 \times 10^{-4}$, $w_3 = 3550 \times 10^{-4}$, $w_4 = 1010 \times 10^{-4}$, and $w_5 = 5400 \times 10^{-4}$. These weights primarily penalized the use of reserve actuators and encouraged the generation of passive forces in the extreme positions of the ROM. We solved this problem while simultaneously considering data from four gait trials of each leg and six passive stretches (IPSA measurements) of the right hamstrings, rectus femoris, and gastrocnemii at slow and fast velocities (one stretch per muscle per speed). Data from 14 trials (gait and passive trials combined) was thus included. Data from passive stretches of left leg muscles was not available. Hence, we imposed that corresponding parameters of both legs could not differ by more than 5%. The parameters were allowed to vary between 50 and 200% of the generic values.

2.4. Spasticity Model–Personalized Feedback Gain Estimation

We modeled spasticity through delayed feedback from muscle-tendon force and its first time derivative (i.e., force rate) (Falisse et al., 2018). The model relates sensory information s (i.e., muscle force and force rate) to feedback muscle activations a_s through a first order differential equation:

$$\tau_s \frac{da_s}{dt} = \begin{cases} -a_s, & s \leq T_s \\ -a_s + g_s(s - T_s), & s > T_s \end{cases} \tag{3}$$

where T_s is a feedback threshold, g_s is a feedback gain, and $\tau_s = 30$ ms is a time delay.

We calibrated this model, separately for the hamstrings and gastrocnemii, to reproduce the spastic muscle activity measured in response to fast passive stretches during IPSA measurements. The resulting personalized models describe the neural component of spasticity measured through exaggerated muscle activity. In more detail, we first determined the threshold for force feedback as the value 20 ms before the EMG onset (Staude and Wolf, 1999) and used a zero threshold for force rate feedback. We then identified the personalized feedback gains that minimized the difference between muscle activations from muscle force and force rate feedback and EMG measured during fast passive stretches (IPSA measurements). We performed such optimization for the right medial hamstrings (i.e., biceps femoris long head, semitendinosus, and semimembranosus) and for the right gastrocnemii (i.e., gastrocnemius lateralis and medialis). We used semitendinosus EMG to drive the three hamstrings and gastrocnemius lateralis EMG to drive both gastrocnemii. We normalized EMG using scale factors identified when estimating the personalized muscle-tendon parameters. We described the optimization process in detail in previous work (Falisse et al., 2018). Finally, we incorporated the spasticity models with personalized feedback gains in our framework for predictive simulations to evaluate the spastic contribution to generated muscle activations and the resulting effects on predicted joint kinematics and gait energetics (**Figure 1**). Since we only had IPSA measurement for the right leg, we used feedback gains and thresholds identified with right leg data for left leg muscles. Gait EMG data and spasticity, as clinically assessed (**Table 1**), were comparable for both legs.

2.5. Muscle Synergies

We modeled the reduced neuromuscular control complexity through muscle synergies. These synergies consisted of two matrices: a $N_{\text{syn}} \times N_f$ matrix H, where N_{syn} is the number of synergies and N_f is the number of frames, containing synergy activations and a $N_m \times N_{\text{syn}}$ matrix W, where N_m is the number of muscles, containing weights that determine the contribution of each muscle in each synergy. Individual muscle activations were composed from synergies as follows:

$$a = W \times H, \tag{4}$$

where a has dimensions $N_m \times N_f$. Importantly, we did not impose personalized synergies when generating predictive simulations (**Figure 1**). Instead, we modeled the effect of reducing the neuromuscular control complexity by limiting the number of

synergies per leg to four or three, thereby limiting the selection of independent muscle activations. This represents a reduction of the neuromuscular control complexity under the assumption that five synergies describe healthy human locomotion (Ivanenko et al., 2004).

2.6. Problem Formulation

We predicted gait patterns by optimizing a gait-related cost function, independent of measured movement data, based on the MRI-based musculoskeletal model described above. In addition to optimizing performance, we imposed average gait speed and periodicity of the gait pattern. We optimized for a full gait cycle to account for asymmetry of CP gait. We solved the resultant optimal control problem via direct collocation. The problem formulation and computational choices are detailed in previous work (Falisse et al., 2019b).

The cost function represents the goal of the motor task. Based on previous work (Falisse et al., 2019b), we modeled this task-level goal as a weighted sum of gait-related performance criteria including metabolic energy rate, muscle fatigue, joint accelerations, passive joint torques, and trunk actuator excitations:

$$J_{\text{prediction}} = \int_0^{t_f} \frac{1}{d} \left(\underbrace{w_1 \left\| \dot{E} \right\|_2^2}_{\substack{\text{Metabolic} \\ \text{energy rate}}} + \underbrace{w_2 \| a \|_{10}^{10}}_{\substack{\text{Muscle} \\ \text{fatigue}}} + \underbrace{w_3 \left\| \ddot{q} \right\|_2^2}_{\substack{\text{Joint} \\ \text{accelerations}}} + \underbrace{w_4 \left\| T_p \right\|_2^2}_{\substack{\text{Passive} \\ \text{torques}}} + \underbrace{w_5 \| e_t \|_2^2}_{\substack{\text{Trunk} \\ \text{excitations}}} \right) dt, \quad (5)$$

where t_f is unknown gait cycle duration, d is distance traveled by the pelvis in the forward direction, $\dot{E}$ are metabolic energy rates, a are muscle activations, $\ddot{q}$ are joint accelerations, T_p are passive joint torques, e_t are excitations of the trunk torque actuators, w_{1-5} are weight factors, and t is time. We modeled metabolic energy rate using a smooth approximation of the phenomenological model described by Bhargava et al. (2004). This metabolic model requires parameters for fiber type composition and muscle specific tension, which we obtained from the literature (Uchida et al., 2016). We manually adjusted the weight factors until we found a set of weights that predicted human-like walking: $w_1 = \left(25/86/\text{body mass}\right) \times 10^{-2}$, $w_2 = 25/86 \times 10^2$, $w_3 = 50/21$, $w_4 = 10/15 \times 10^2$, and $w_5 = 1/3 \times 10^{-1}$. The weight factors were kept constant across simulations. We added several path constraints enforcing a prescribed average gait speed corresponding to the child's average gait speed ($d/t_f = 1$ m s^{-1}), imposing periodic states over the complete gait cycle (except for the pelvis forward position), and preventing inter-penetration of body segments. It is worth mentioning that the values of the weight factors strongly depend on the scaling of the cost function terms (Falisse et al., 2019b), which explains the different orders of magnitude. Proper scaling of the cost function terms might allow using the same weight factors across subjects. Yet it is also possible that such common cost function does not exist and that weight factors should be personalized to capture inter-subject differences in performance criteria. This is an area for future research.

2.7. Model-Based Analyses

We investigated the differential effects of altered muscle-tendon properties, reduced neuromuscular control complexity, and spasticity on gait patterns predicted with the MRI-based musculoskeletal model (**Figure 1**). In particular, we compared predicted joint kinematics and kinetics, muscle activity, and stride lengths to their experimental counterparts. We also evaluated how impairments affected the metabolic cost of transport (COT), defined as metabolic energy consumed per unit distance traveled.

First, we tested the influence of altered vs. unaltered muscle-tendon properties by using personalized vs. generic muscle-tendon parameters in the muscle dynamics (Q_i in **Figure 1**). In this initial analysis, we did not include spasticity, nor imposed synergies.

Second, we assessed the impact of reducing the neuromuscular control complexity by imposing fixed numbers of synergies (Q_{ii} in **Figure 1**). To assess the effect of reducing the number of synergies, we compared the synergy activations resulting from simulations with three and four synergies using the coefficient of determination R^2 and the synergy weights using Pearson's coefficient of correlation r. We generated simulations with both sets of muscle-tendon parameters to explore the effect of synergies in isolation as well as in combination with altered muscle-tendon properties.

Finally, we evaluated the effect of spasticity in the three medial hamstrings and two gastrocnemii of both legs (Q_{iii} in **Figure 1**). We modeled muscle activations as the sum of feedforward muscle activations and feedback muscle activations determined based on the personalized (i.e., calibrated based on IPSA measurements) spasticity models:

$$a_{\text{sum}} = a_{f_f} + a_{F_t} + a_{dF_t}, \quad (6)$$

where a_{f_f} are feedforward muscle activations, and a_{F_t} and a_{dF_t} are muscle activations from muscle force and force rate feedback, respectively, computed based on Equation (3). Feedback and feedforward activations can be interpreted as spastic and non-spastic muscle activations, respectively. We only tested the effect of spasticity based on the model with personalized muscle-tendon parameters, since these parameters were used to estimate the feedback gains. We tested the effect of spasticity in combination with fine selective control (i.e., no synergy constraints) as well as with a reduced number of muscle synergies.

As an additional analysis, we investigated whether the child adopted an impaired crouch gait pattern because of neuro-mechanical constraints or because it was more optimal (Q_{iv} in

Figure 1). To this aim, we added a term in the cost function that penalized deviations from measured kinematics of a TD child:

$$J_{\text{tracking}} = \int_0^{t_f} \left(\underbrace{w_6 \left\| q - \hat{q} \right\|_2^2}_{\substack{\text{TD kinematics} \\ \text{deviation}}} \right) dt, \tag{7}$$

where q are joint positions, $\hat{q}$ are measured joint positions of a TD child, and $w_6 = 100/20$ is a weight factor. We generated these simulations with personalized parameters as well as with and without synergies. We did not include spasticity in this analysis since it had little influence on the walking pattern in the simulations described above.

We formulated our problems in MATLAB using CasADi (Andersson et al., 2019), applied direct collocation using a third order Radau quadrature collocation scheme with 150 mesh intervals per gait cycle, and solved the resulting nonlinear programming problems with the solver IPOPT (Wächter and Biegler, 2006). We applied algorithmic differentiation to compute derivatives (Falisse et al., 2019a). We started each optimization from multiple initial guesses and selected the result with the lowest optimal cost. Initial guesses for joint variables were based on experimental data. Specifically, for all simulations, we used two initial guesses derived from experimental kinematics of the CP and TD child, respectively. For simulations accounting for synergies, we added initial guesses derived from simulated kinematics with the lowest optimal costs produced without synergies and with more synergies (e.g., with three synergies,

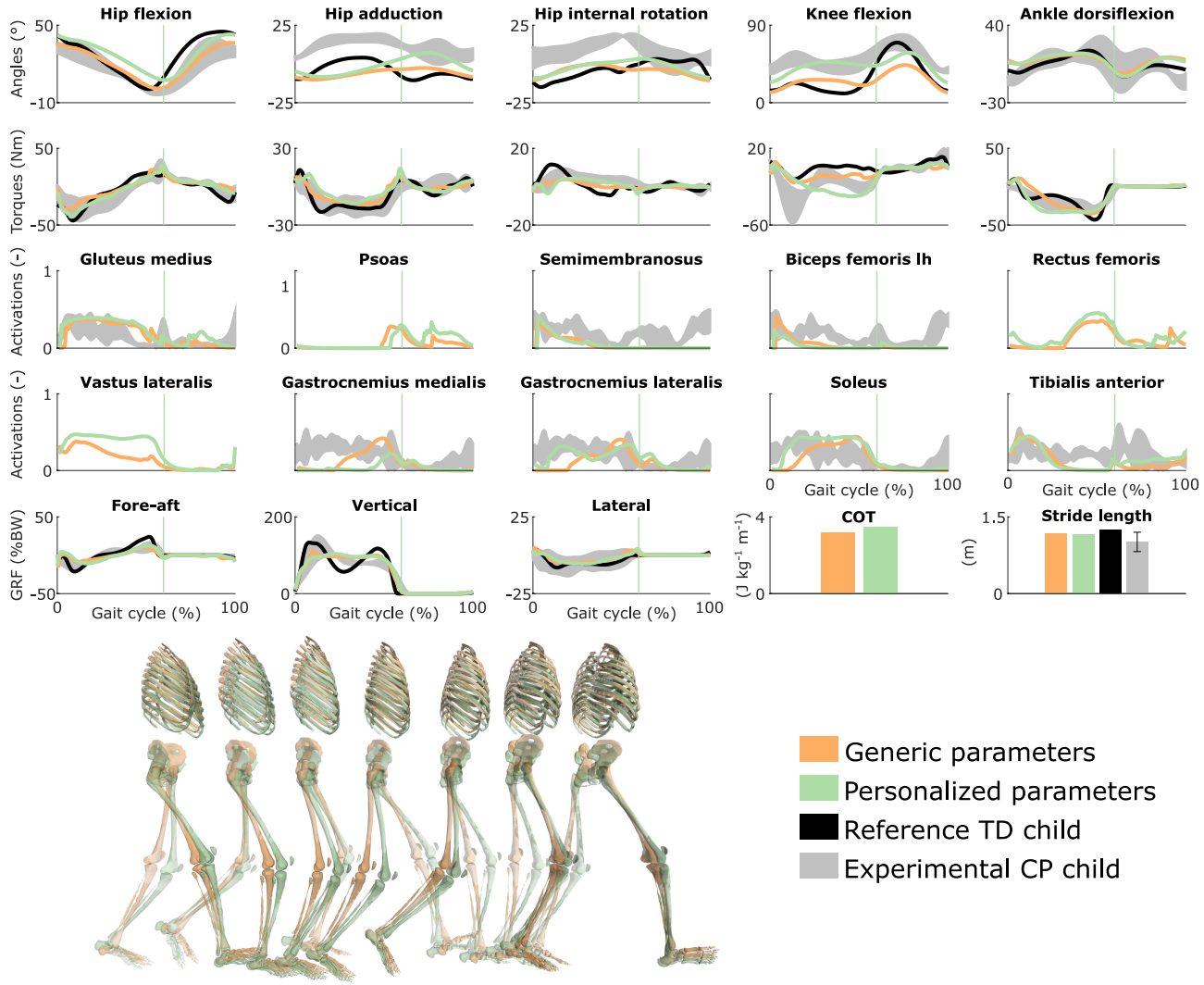

FIGURE 2 | Influence of the muscle-tendon parameters on the predicted walking gaits. Variables from the right leg are shown over a complete gait cycle; left leg variables are shown in **Figure S1**. Vertical lines indicate the transition from stance to swing. Experimental data is shown as mean ± two standard deviations. Experimental EMG data was normalized to peak activations. GRF is for ground reaction forces; BW is for body weight; COT is for metabolic cost of transport; lh is for long head. Gait snapshots cover a gait cycle starting at right heel strike; left leg segments are more transparent.

initial guesses were derived from the best kinematic solutions with four synergies and without synergies). For simulations accounting for spasticity, we added initial guesses derived from simulated kinematics with the lowest optimal costs produced without spasticity. In all cases, initial guesses for muscle, trunk, and synergy variables were constant across time and not informed by experimental data. Initial guesses for synergy weights were constant across muscles and independent of experimental data.

3. RESULTS

3.1. Gait Analysis

The child walked with a pronounced crouch gait pattern characterized by bilateral knee extension deficits with reduced knee ROM during swing, a lack of right ankle dorsiflexion at the end of swing, excessive left ankle dorsiflexion, excessive and deficient right and left hip adduction, respectively, and excessive bilateral hip internal rotation (**Figure 2** and **Figure S1**; **Movies 1, 2**).

3.2. Influence of the Muscle-Tendon Parameters

Using personalized vs. generic muscle-tendon parameters resulted in a crouch (i.e., excessive knee flexion) vs. a more upright gait pattern (**Figure 2** and **Figure S1**; **Movies 3, 4**). Personalized optimal fiber lengths and tendon slack lengths were generally smaller and larger, respectively, than their generic counterparts (**Tables S1, S2**). The use of personalized parameters resulted in decreased deviations [smaller root mean square error (RMSE)] between measured and predicted knee angles (RMSE of 17° and 11° for the left and right leg, respectively) as compared to the use of generic parameters (RMSE of 43° and 25°). The gastrocnemius lateralis and soleus (ankle plantarflexors) were activated earlier in stance with the crouch gait, as observed in the child's EMG. The vasti (knee extensors) activity was also increased during stance when the model walked in crouch. The COT was higher with the personalized parameters (crouch gait; 3.45 J $kg^{-1}m^{-1}$) than with the generic parameters (more upright gait; 3.18 J $kg^{-1}m^{-1}$). Predicted stride lengths were larger than the average stride length of the child but were within two standard deviations.

3.3. Influence of the Synergies With Generic Muscle-Tendon Parameters

Reducing the number of synergies in combination with generic muscle-tendon parameters did not induce the amount of crouch that was experimentally measured in the child, although it altered muscle coordination and increased COT (**Figure 3** and **Figure S2**, **Movie 5**). The right knee flexion angles increased during stance with the reduction of the neuromuscular control complexity but were still smaller than experimentally measured. This was accompanied with increased rectus femoris (knee extensor) activity. The synergies had a limited effect on the left leg that had a straight knee pattern during stance. The COT increased with the reduction of the neuromuscular control complexity (3.58 and 3.90 J $kg^{-1}m^{-1}$ with four and three synergies, respectively). The synergies had little effect on the predicted stride lengths that were larger than the child's average stride length but were within two standard deviations. The synergies of the three-synergy case were similar to the first three synergies of the four-synergy case (average R^2 and r over three common synergy activations and weight vectors, respectively, of both legs: 0.84 ± 0.19 and 0.83 ± 0.10). The additional synergy in the four-synergy case was activated in early stance and at the transition between stance and swing, and mainly consisted of hip adductors.

3.4. Influence of the Synergies With Personalized Muscle-Tendon Parameters

Reducing the number of synergies in combination with personalized muscle-tendon parameters had a minor effect on gait kinematics but altered muscle coordination and increased COT (**Figure 4** and **Figure S3**, **Movie 6**). Specifically, synergies only had a slight effect on the kinematics during the swing phase of the right leg but affected the activation pattern of certain muscles (e.g., gastrocnemius medialis and lateralis). The COT increased with the reduction of the neuromuscular control complexity (3.94 and 4.09 J $kg^{-1}m^{-1}$ with four and three synergies, respectively). Stride lengths slightly decreased with synergies but remained larger than the child's average stride length. The synergies of the three-synergy case were similar to the first three synergies of the four-synergy case (average R^2 and r: 0.85 ± 0.05 and 0.87 ± 0.09, respectively). The additional synergy in the four-synergy case was activated in early stance and at the transition between stance and swing, and mainly consisted of the gemellus, piriformis, tibialis posterior, and several ankle plantarflexors.

3.5. Influence of Spasticity

Spasticity had a limited effect on muscle coordination and almost no influence on gait kinematics (**Figure 5** and **Figure S4**, **Movie 7**). Specifically, spastic activity was predicted in the medial hamstrings in early stance but this had, overall, a minor effect on the total (i.e., combined spastic and non-spastic contributions) medial hamstrings activity when compared to simulations without spasticity. Bursts of spastic activity were also observed in early swing. Medial hamstrings activity contributes to knee flexion but since similar (timing and magnitude) activity profiles were predicted with and without spasticity, there was no difference in predicted knee flexion angles. A constant low spastic contribution was predicted for the gastrocnemius lateralis during stance, whereas a minor contribution was predicted for the gastrocnemius medialis during stance and at the transition between stance and swing. Spasticity hence does not explain the lack of right ankle dorsiflexion (i.e., increased plantarflexion) observed at the end of swing in experimental data. Similar observations hold with and without synergies. The COT increased when incorporating spasticity (3.75 and 4.18 J $kg^{-1}m^{-1}$ with zero and four synergies, respectively).

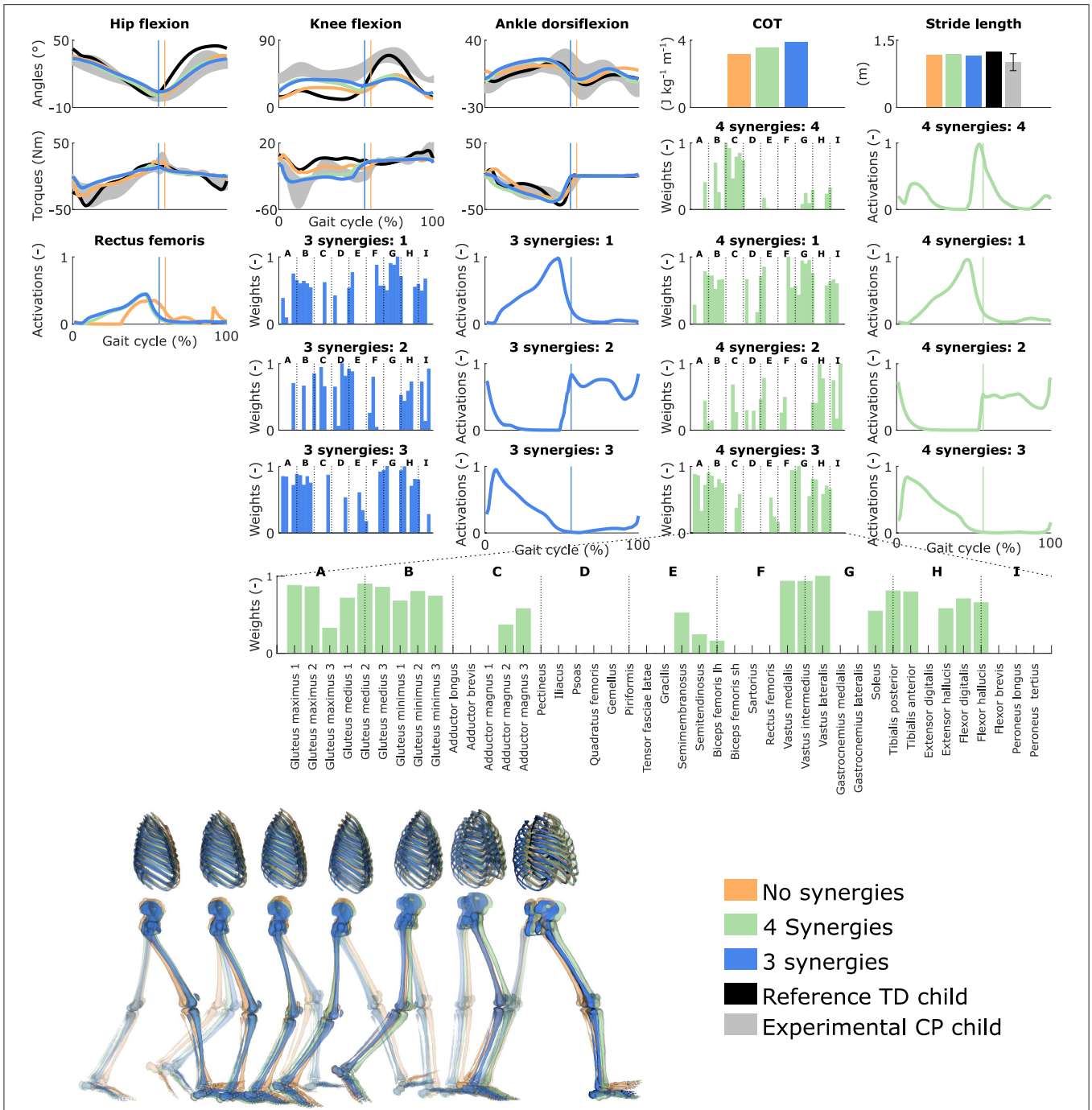

FIGURE 3 | Influence of the synergies on walking gaits predicted with the generic muscle-tendon parameters. Variables from the right leg are shown over a complete gait cycle; left leg variables are shown in **Figure S2**. Vertical lines (solid) indicate the transition from stance to swing. Panels of synergy weights are divided into sections (A-I) to relate bars to muscle names provided in the bottom bar plot, which is an expanded version of the plot of weights with title 4 synergies: 3. Lh and sh are for long and short head, respectively. Weights were normalized to one. Experimental data is shown as mean ± two standard deviations. Gait snapshots cover a gait cycle starting at right heel strike; left leg segments are more transparent.

3.6. Influence of Tracking the Kinematics of a TD Child

Tracking the TD kinematics while using personalized muscle-tendon parameters produced an upright gait pattern when not incorporating synergies, but decreased the overall gait performance (**Figure 6** and **Figure S5**, **Movie 8**). Specifically, the simulated gait had a similar COT (3.46 J $kg^{-1}m^{-1}$) as the crouch gait pattern predicted without such tracking term but

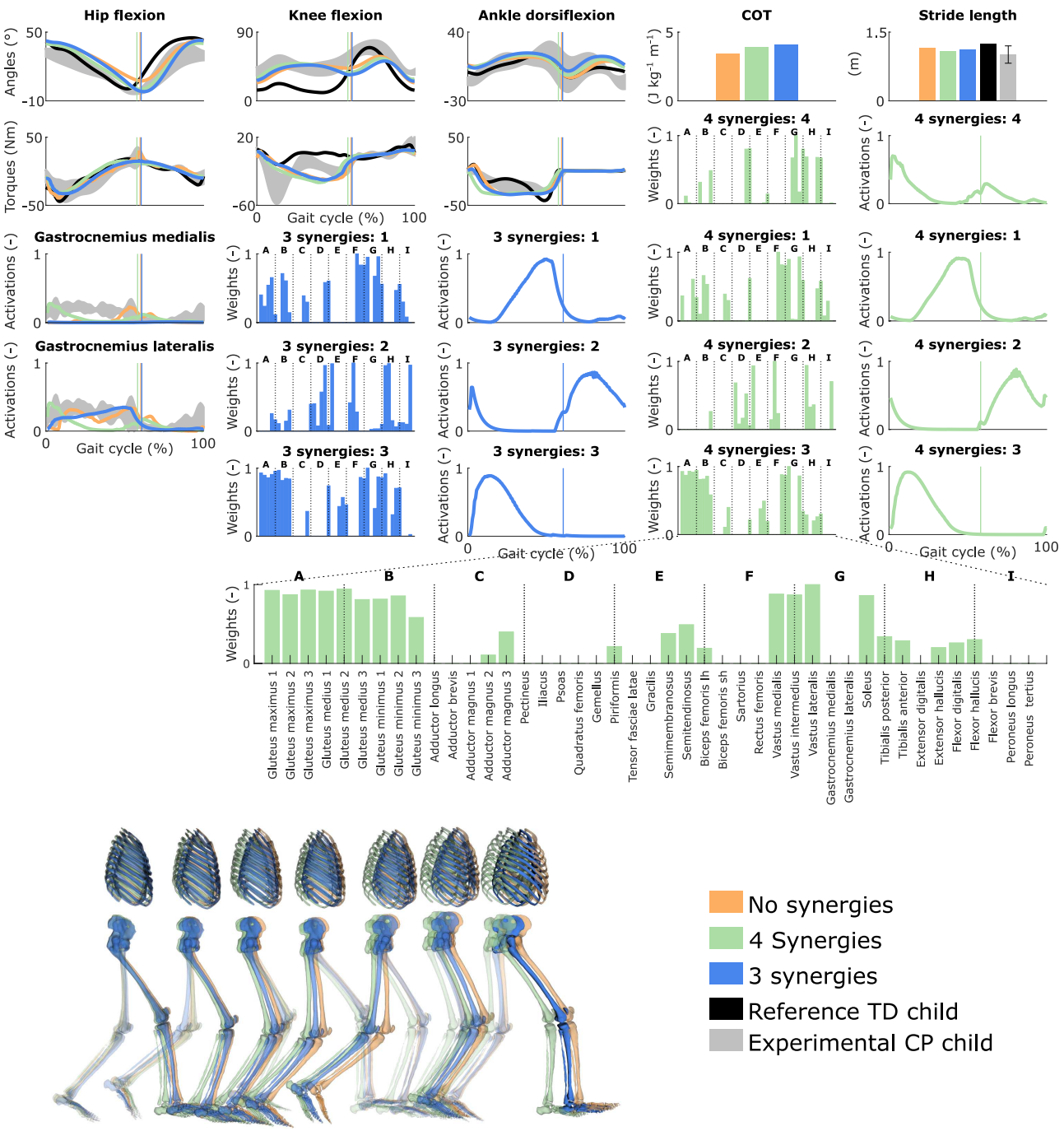

FIGURE 4 | Influence of the synergies on walking gaits predicted with the personalized muscle-tendon parameters. Variables from the right leg are shown over a complete gait cycle; left leg variables are shown in **Figure S3**. Vertical lines (solid) indicate the transition from stance to swing. Panels of synergy weights are divided into sections (A-I) to relate bars to muscle names provided in the bottom bar plot, which is an expanded version of the plot of weights with title 4 synergies: 3. Lh and sh are for long and short head, respectively. Weights were normalized to one. Experimental data is shown as mean ± two standard deviations. Experimental EMG data was normalized to peak activations. Gait snapshots cover a gait cycle starting at right heel strike; left leg segments are more transparent.

the contribution of most terms in the cost function increased, suggesting that walking upright is not prevented by mechanical constraints (i.e., aberrant musculoskeletal geometries and altered muscle-tendon properties) but is less optimal, due to these mechanical constraints, than walking in crouch for this child. The contribution of the muscle fatigue term increased by 29%, in part driven by higher activations of the glutei. The contribution of the joint acceleration, metabolic energy rate, and passive joint

torque terms increased by 15, 15, and 36%, respectively, when walking upright. Similarly, passive muscle forces increased when walking upright for the iliacus and psoas (hip flexors), and biceps femoris short head (knee flexor). Knee flexion increased when adding synergies but did not reach the angle that was experimentally measured in the child (**Figure S6**). Nevertheless, this suggests that reduced neuromuscular control complexity may contribute to crouch gait. The gastrocnemius lateralis and soleus (ankle plantarflexors) were also activated earlier during stance with synergies. Imposing synergies increased the COT (4.12 and 4.05 J $kg^{-1}m^{-1}$ with four and three synergies, respectively).

4. DISCUSSION

We demonstrated the ability of predictive simulations to explore the differential effects of musculoskeletal and motor control impairments on the gait pattern of a child with CP. In this specific case study, aberrant musculoskeletal geometries combined with altered muscle-tendon properties explained the key gait deviation of the child, namely the crouch gait pattern. Accounting for aberrant geometries alone (i.e., MRI-based model with generic muscle-tendon parameters) did not result in a crouch gait pattern. Despite altered muscle-tendon properties and aberrant geometries, the model could still adopt a more upright gait pattern (TD kinematics tracking). Yet such pattern was less optimal as it induced higher muscle fatigue compared to the crouch gait pattern. These simulations thus suggest that adopting an upright gait pattern for this child might produce an early onset of fatigue, which might explain in part why the child walks in crouch. Importantly, not only fatigue, but also joint accelerations, passive joint torques, and metabolic energy rates increased with an upright gait pattern, potentially contributing to the child's selection of a crouch gait pattern. It is worth underlining that we performed a single case study to demonstrate the ability of physics-based simulations to explore causal relations between musculoskeletal mechanics and motor control impairments on the one hand and gait mechanics and energetics on the other hand. This case study therefore does not validate the ability of our framework to predict subject-specific gait patterns. Future work will focus on validating the framework for predicting post-treatment gait patterns based on a larger population.

Decreasing the neuromuscular control complexity through a reduced number of synergies had, for this child, a lower effect on the simulated gait patterns than muscular deficits as evaluated when comparing simulated gait patterns obtained with personalized and generic muscle-tendon parameters. Nevertheless, the synergies resulted in increased knee flexion in several simulations, indicating that impaired selective motor control may contribute to gait deficits as suggested in prior simulation studies (Meharbi et al., 2019). In this study, we imposed the number of synergies but not the synergy structure (synergy weights and activations were optimization variables and not informed by experimental data). We thus explored the effect of reducing the neuromuscular control complexity but not the impact of imposing the child's experimental synergies. We expect this impact to be limited for this child since he had a good selectivity.

Our predictive simulations generated both movement patterns and the underlying synergies. Only imposing the number of synergies resulted in synergies that presented common features with those reported in the literature, such as one synergy activated during early stance and composed by the glutei and vasti, and one synergy activated during late stance consisting of the glutei, ankle plantarflexors, and iliacus (De Groote et al., 2014). This suggests that synergy structures might emerge from mechanical constraints and performance optimization during walking. Future research should explore this hypothesis based on a larger population.

Decreasing the number of synergies resulted in a larger COT for this child, as may be expected with a higher level of co-activations. This finding has been hypothesized in previous studies (Steele et al., 2017; Meharbi et al., 2019) but not tested explicitly. It is indeed difficult to dissociate the influence of the neuromuscular control complexity on the COT through experiments or based on measured data, since many other factors [e.g., spasticity (Hemingway et al., 2001) and weakness (van der Krogt et al., 2012)] might also play a role. Overall, our predictive simulations allow exploring the effects of isolated impairments on gait energetics, which was not possible through analyses based on measured data.

Spasticity had a minor influence on the predicted gait kinematics, suggesting a low impact of spasticity on gait performance for this child. This hypothesis is in agreement with several studies reporting a lack of correlation between spasticity as diagnosed during passive movements and determinants of gait (Ada et al., 1998; Marsden et al., 2012; Willerslev-Olsen et al., 2014). However, it would be premature to draw such conclusion based on this single case study. First, spasticity was only taken into account for the medial hamstrings and gastrocnemii, whereas the rectus femoris and several hip flexors and adductors were also reported to be spastic (**Table 1**). Including these other muscles may have an influence on walking performance. Second, experimental data from the spasticity assessment was only collected for the right leg, whereas bilateral spasticity was reported (**Table 1**). We optimized the feedback parameters using that data but used the resulting parameters for both legs, which might affect our predictions. Third, we used feedback parameters optimized from passive stretches to predict spasticity (i.e., reflex activity) during gait, assuming no reflex modulation. This assumption is in line with the decreased reflex modulation reported for patients with spasticity (Sinkjaer et al., 1996; Faist et al., 1999; Dietz, 2002; Dietz and Sinkjaer, 2007). Yet further research is needed to ensure that the same model is valid in passive and active conditions. Note that the current model does not distinguish between concentric and eccentric contractions, whereas spasticity is presumably only manifest upon muscle stretch. Finally, the optimized feedback gains depend on EMG that was normalized using scale factors optimized during the muscle-tendon parameter estimation. However, these factors may not truly reflect the magnitude of the spastic responses, which may result in an under- or over-estimation of the predicted

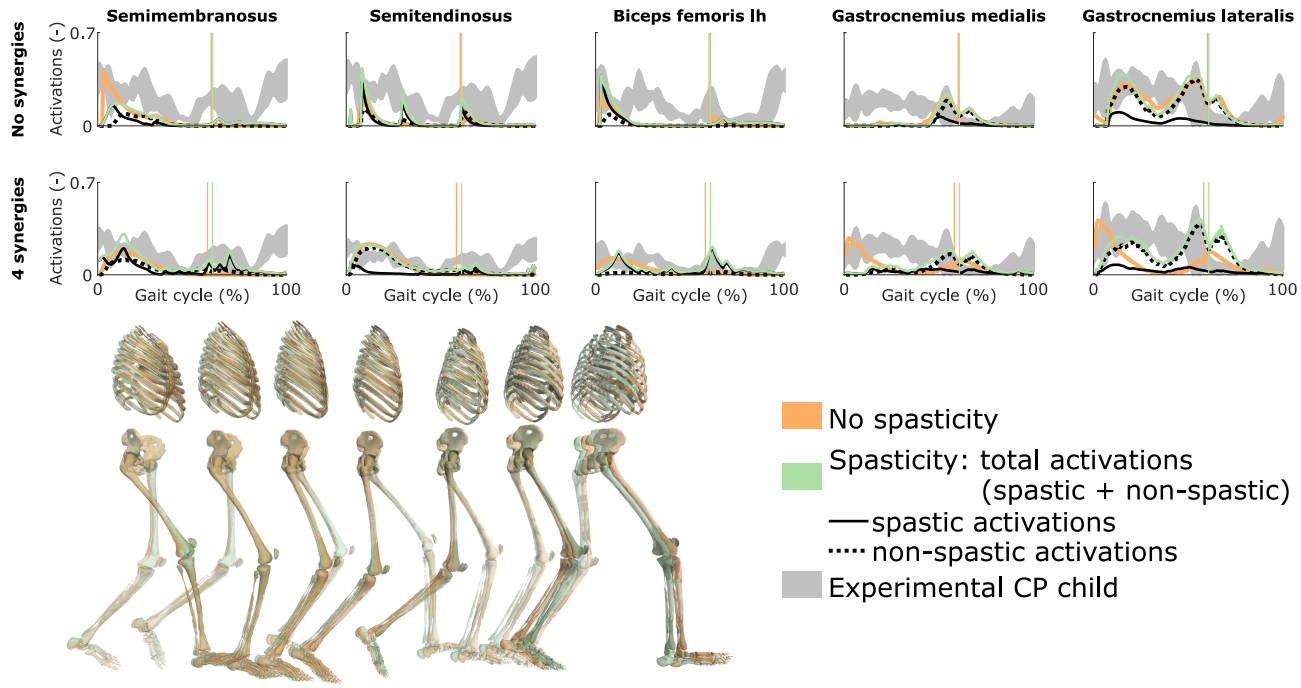

FIGURE 5 | Influence of spasticity on the predicted muscle activity. Activations from right leg muscles only are shown over a complete gait cycle; left leg activations are shown in **Figure S4**. When accounting for spasticity, total activations (green) combine spastic (solid black) and non-spastic (dotted black) activations. Vertical lines indicate the transition from stance to swing. Experimental data is shown as mean ± two standard deviations. Experimental EMG data was normalized to peak activations. Lh is for long head. Gait snapshots cover a gait cycle starting at right heel strike; left leg segments are more transparent; the snapshots are for the case with no synergies.

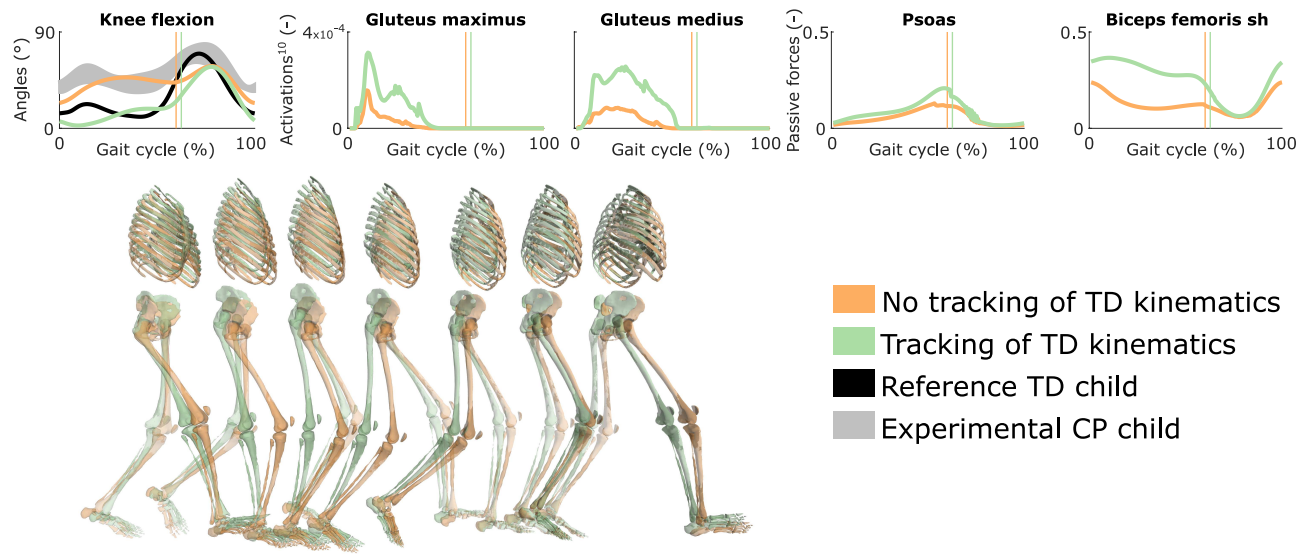

FIGURE 6 | Influence of tracking the TD kinematics on predicted walking gaits. Variables from the right leg are shown over a complete gait cycle; left leg variables are shown in **Figure S5**. Vertical lines indicate the transition from stance to swing. Experimental data is shown as mean ± two standard deviations. Muscle fatigue is modeled by activations at the tenth power. Passive muscle forces are normalized by maximal isometric muscle forces. Sh is for short head. Gait snapshots cover a gait cycle starting at right heel strike; left leg segments are more transparent. The influence of synergies on predicted walking gaits is depicted in **Figure S6**.

spastic activity during gait. In previous work (Falisse et al., 2018), we showed that predicted spastic responses of the gastrocnemii were in agreement with large EMG signals observed in early stance in subjects landing on their toes. In this study, the child had a flat foot landing and we did not observe such EMG rise, therefore suggesting that the effect of spasticity of the gastrocnemii during gait might be limited for this child. Interestingly, our model captured this phenomenon as it did not predict large spastic activity in early stance.

Our analysis suggests that muscle-tendon properties rather than selective motor control and spasticity should be the target of interventions aiming to restore an upright posture for this child. This suggestion is in line with the surgical report and one-year post-operative gait analysis. Specifically, the child underwent SEMLS consisting of bilateral rectus femoris transfer, distal femur extension and derotation osteotomy, tibia derotation, and patella distalization that successfully addressed the knee extension deficits and restored the upright gait pattern. The intervention also included bilateral BTX injections in the psoas (hip flexor) and gracilis (hip flexor, adductor, and knee flexor) to reduce spasticity. However, BTX injections are unlikely to have had an effect one year post-treatment (Molenaers et al., 2010), suggesting a limited contribution of reduced psoas and gracilis spasticity on restored knee extension. Note that our study did not investigate the sensitivity of the predicted walking patterns to bone misalignment as we considered the same aberrant geometries for all analyses. Studying the effect of bone deformities on the gait pattern should be considered in future work.

Our simulations with personalized muscle-tendon parameters captured salient features of the child's walking pattern. Nevertheless, they deviated from measured data in different ways. In particular, our model did not adopt the observed flat foot landing. Such pattern might have different underlying roots. On the one hand, it might be an ankle strategy to add functional limb length and compensate for the knee extension deficits. Our simulations did not predict such compensation strategy but also lacked knee flexion in early stance as compared to measured data (**Figure 2**). Increased knee flexion might strengthen the need for ankle compensation, causing the model to adopt a flat foot landing. On the other hand, it might be due to contracture of the plantarflexors (Wren et al., 2005; Mathewson et al., 2015) although this hypothesis is less likely for this child who had a normal ROM in terms of plantarflexion.

Other factors might have contributed to the deviations between predicted and measured movements. First, the musculoskeletal model had generic rather than personalized (i.e., MRI-based) geometries for feet and tibias. Since the child later underwent a surgery that included bilateral tibia derotation, these generic geometries might have contributed to the gait deviations. Second, the clinical examination indicated that the child's trunk was leaning forward. This is likely a compensation strategy, since no fixed lordosis was reported. However, our model had a very simple trunk representation (i.e., one joint with three degrees of freedom), limiting the emergence of compensation strategies. How to model the trunk to capture such compensations remains an open question. Third, our control strategy likely did not capture all complex control mechanisms that might be at play during gait. For instance, we did not consider in our cost function criteria such as head stability (Menz et al., 2003) and pain that might contribute to gait control. Further, we designed our cost function based on previous work with a healthy adult but the same performance criterion might not hold for children with CP. Nevertheless, our cost function predicted, as expected, a crouch gait pattern with personalized parameters and a more upright gait pattern with generic parameters, suggesting that it captured at least part of the child's control strategy. Finally, the personalized muscle-tendon parameters might not accurately capture the effect of the child's altered muscle-tendon properties. In previous work (Falisse et al., 2017), we underlined the importance of incorporating experimental data from multiple functional movements when calibrating muscle-tendon parameters in order to obtain valid parameter estimates (i.e., representative of the subject). In this study, the available experimental data was limited to walking trials and passive stretches from one leg. Hence, it is likely that some parameters were calibrated to fit the experimental data but did not truly reflect the force-generating capacities of the child. When used in conditions different from the experiments, these parameters may hence result in non-representative force predictions. A challenge for upcoming research will be the design of experimental protocols to collect experimental data that contains sufficient information for providing valid muscle-tendon parameter estimates while accounting for physiological limitations of impaired individuals and practical limitations of clinical contexts. It is also worth noting that our parameter estimation procedure only adjusted optimal fiber lengths and tendon slack lengths, whereas other parameters may need to be personalized, such as maximal isometric muscle forces, tendon compliance, or maximal muscle contraction velocities. The muscle force-length-velocity relationships might also be altered in children with CP due to their longer sarcomere lengths. Overall, further tuning of the neuro-musculoskeletal model and validation of the simulation framework outcome with a large population are necessary for augmenting the representativeness of the simulations.

5. CONCLUSION

This study used predictive simulations to identify the main treatment targets for a child with CP. The results showed that, in the presence of aberrant musculoskeletal geometries, altered muscle-tendon properties rather than reduced neuromuscular control complexity and spasticity were the primary driver of the impaired crouch gait pattern observed for the child. Based on this observation, we would recommend altered muscle-tendon properties to be the primary target of clinical interventions aiming to restore a more upright posture, which is in line with the surgical report and one-year post-operative gait analysis. Validation of our simulation workflow through analysis of more cases is, however, necessary to build confidence in the simulation outcomes. Such validation would open the door for predicting the functional outcome of treatments on

walking performance by allowing *in silico* assessment of the effect of changes in the neuro-musculoskeletal system on the gait pattern.

DATA AVAILABILITY STATEMENT

All data and code used for this study can be found in the SimTK repository: https://simtk.org/projects/predictcpgait.

ETHICS STATEMENT

The studies involving human participants were reviewed and approved by the Ethics Committee at UZ Leuven (Belgium). Written informed consent to participate in this study was provided by the participants' legal guardian/next of kin.

AUTHOR CONTRIBUTIONS

AF, FD, and IJ conceptualized the methods, conducted the investigation, and validated the research outputs. AF, LP, HK, HH, MW, SV, EP, and LB-O processed the data. AF performed the formal analysis, developed the software, prepared the data visualization, and drafted the manuscript. AF, HK, LB-O, AH, KD, GM, AV, FD, and IJ acquired funding. AF and FD developed the methodology. AH, KD, GM, AV, FD, and IJ administrated the project. EP, LB-O, AH, KD, GM, and AV provided resources. FD and IJ supervised the project. All authors edited the manuscript.

FUNDING

This work was supported by the IWT-TBM grant SimCP (140184). AF also received a Ph.D. grant (1S35416N) from the Research Foundation Flanders (FWO). HK received a H2020-MSCA individual fellowship (796120). LB-O received a postdoctoral grant (12R4215N) from the Research Foundation Flanders (FWO) and a grant (016.186.144) from the Netherlands Organization for Scientific Research (NWO).

SUPPLEMENTARY MATERIAL

The Supplementary Material for this article can be found online at: https://www.frontiersin.org/articles/10.3389/fnhum.2020.00040/full#supplementary-material

REFERENCES

Ada, L., Vattanasilp, W., O'Dwyer, N. J., and Crosbie, J. (1998). Does spasticity contribute to walking dysfunction after stroke? *J Neurol. Neurosurg. Psychiatry* 64, 628–635.

Anderson, F. C., and Pandy, M. G. (2001). Dynamic optimization of human walking. *J. Biomechan. Eng.* 123, 381–390. doi: 10.1115/1.1392310

Andersson, J. A. E., Gillis, J., Horn, G., Rawlings, J. B., and Diehl, M. (2019). CasADi : a software framework for nonlinear optimization and optimal control. *Math. Programm. Comput.* 11, 1–36. doi: 10.1007/s12532-018-0139-4

Arnold, A. S., Blemker, S. S., and Delp, S. L. (2001). Evaluation of a deformable musculoskeletal model for estimating muscle-tendon lengths during crouch gait. *Ann. Biomed. Eng.* 29, 263–274. doi: 10.1114/1.1355277

Barber, L., Barrett, R., and Lichtwark, G. (2011a). Passive muscle mechanical properties of the medial gastrocnemius in young adults with spastic cerebral palsy. *J. Biomechan.* 44, 2496–2500. doi: 10.1016/j.jbiomech.2011.06.008

Barber, L., Barrett, R., and Lichtwark, G. (2012). Medial gastrocnemius muscle fascicle active torque-length and Achilles tendon properties in young adults with spastic cerebral palsy. *J. Biomechan.* 45, 2526–2530. doi: 10.1016/j.jbiomech.2012.07.018

Barber, L., Hastings-Ison, T., Baker, R., Barrett, R., and Lichtwark, G. (2011b). Medial gastrocnemius muscle volume and fascicle length in children aged 2 to 5years with cerebral palsy. *Dev. Med. Child Neurol.* 53, 543–548. doi: 10.1111/j.1469-8749.2011.03913.x

Bar-On, L., Aertbeliën, E., Wambacq, H., Severijns, D., Lambrecht, K., Dan, B., et al. (2013). A clinical measurement to quantify spasticity in children with cerebral palsy by integration of multidimensional signals. *Gait Post.* 38, 141–147. doi: 10.1016/j.gaitpost.2012.11.003

Barrett, R. S., and Lichtwark, G. A. (2010). Gross muscle morphology and structure in spastic cerebral palsy: a systematic review. *Dev. Med. Child Neurol.* 52, 794–804. doi: 10.1111/j.1469-8749.2010.03686.x

Bhargava, L. J., Pandy, M. G., and Anderson, F. C. (2004). A phenomenological model for estimating metabolic energy consumption in muscle contraction. *J. Biomechan.* 37, 81–88. doi: 10.1016/S0021-9290(03)00239-2

Bosmans, L., Wesseling, M., Desloovere, K., Molenaers, G., Scheys, L., and Jonkers, I. (2014). Hip contact force in presence of aberrant bone geometry during normal and pathological gait. *J. Orthopaedic Res.* 32, 1406–1415. doi: 10.1002/jor.22698

Chang, F. M., Seidl, A. J., Muthusamy, K., Meininger, A. K., and Carollo, J. J. (2006). Effectiveness of instrumented gait analysis in children with cerebral palsy - Comparison of outcomes. *J. Pediat. Orthopaed.* 26, 612–616. doi: 10.1097/01.bpo.0000229970.55694.5c

De Groote, F., Jonkers, I., and Duysens, J. (2014). Task constraints and minimization of muscle effort result in a small number of muscle synergies during gait. *Front. Comput. Neurosci.* 8, 1–11. doi: 10.3389/fncom.2014.00115

De Groote, F., Kinney, A. L., Rao, A. V., and Fregly, B. J. (2016). Evaluation of direct collocation optimal control problem formulations for solving the muscle redundancy problem. *Ann. Biomed. Eng.* 44, 2922–2936. doi: 10.1007/s10439-016-1591-9

De Groote, F., Pipeleers, G., Jonkers, I., Demeulenaere, B., Patten, C., Swevers, J., et al. (2009). A physiology based inverse dynamic analysis of human gait: potential and perspectives. *Comput. Methods Biomechan. Biomed. Eng.* 12, 563–574. doi: 10.1080/10255840902788587

De Groote, F., Van Campen, A., Jonkers, I., and De Schutter, J. (2010). Sensitivity of dynamic simulations of gait and dynamometer experiments to hill muscle model parameters of knee flexors and extensors. *J. Biomechan.* 43, 1876–1883. doi: 10.1016/j.jbiomech.2010.03.022

Delp, S. L., Anderson, F. C., Arnold, A. S., Loan, P., Habib, A., John, C. T., et al. (2007). OpenSim: open-source software to create and analyze dynamic simulations of movement. *IEEE Trans. Biomed. Eng.* 54, 1940–1950. doi: 10.1109/TBME.2007.901024

Delp, S. L., Loan, J. P., Hoy, M. G., Zajac, F. E., Topp, E. L., and Rosen, J. M. (1990). An interactive graphics-based model of the lower extremity to study orthopaedic surgical procedures. *IEEE Trans. Biomed. Eng.* 37, 757–767. doi: 10.1109/10.102791

Desloovere, K., Molenaers, G., Feys, H., Huenaerts, C., Callewaert, B., and Van de Walle, P. (2006). Do dynamic and static clinical measurements correlate with gait analysis parameters in children with cerebral palsy? *Gait Post.* 24, 302–313. doi: 10.1016/j.gaitpost.2005.10.008

Dietz, V. (2002). Proprioception and locomotor disorders. *Nat. Rev. Neurosci.* 3, 781–790. doi: 10.1038/nrn939

Dietz, V., and Sinkjaer, T. (2007). Spastic movement disorder: impaired reflex function and altered muscle mechanics. *Lancet Neurol.* 6, 725–733. doi: 10.1016/S1474-4422(07)70193-X

Faist, M., Ertel, M., Berger, W., and Dietz, V. (1999). Impaired modulation of quadriceps tendon jerk reflex during spastic gait: differences between spinal and cerebral lesions. *Brain* 122, 567–579. doi: 10.1093/brain/122.3.567

Falisse, A., Bar-On, L., Desloovere, K., Jonkers, I., and De Groote, F. (2018). A spasticity model based on feedback from muscle force explains muscle activity during passive stretches and gait in children with cerebral palsy. *PLoS ONE* 13:e0208811. doi: 10.1371/journal.pone.0208811

Falisse, A., Serrancolí, G., Dembia, C. L., Gillis, J., and De Groote, F. (2019a). Algorithmic differentiation improves the computational efficiency of OpenSim-based trajectory optimization of human movement. *PLoS ONE* 14:e0217730. doi: 10.1371/journal.pone.0217730

Falisse, A., Serrancolí, G., Dembia, C. L., Gillis, J., Jonkers, I., and De Groote, F. (2019b). Rapid predictive simulations with complex musculoskeletal models suggest that diverse healthy and pathological human gaits can emerge from similar control strategies. *J. R. Soc. Interf.* 16:20190402. doi: 10.1098/rsif.2019.0402

Falisse, A., Van Rossom, S., Jonkers, I., and De Groote, F. (2017). EMG-driven optimal estimation of subject-specific Hill model muscle-tendon parameters of the knee joint actuators. *IEEE Trans. Biomed. Eng.* 64, 2253–2262. doi: 10.1109/TBME.2016.2630009

Filho, M. C. d. M., Yoshida, R., Carvalho, W. d. S., Stein, H. E., and Novo, N. F. (2008). Are the recommendations from three-dimensional gait analysis associated with better postoperative outcomes in patients with cerebral palsy? *Gait Post.* 28, 316–322. doi: 10.1016/j.gaitpost.2008.01.013

Gage, J. R., Schwartz, M. H., Koop, S. E., and Novacheck, T. F. (eds.). (2009). *The Identification and Treatment of Gait Problems in Cerebral Palsy, 2nd Edn*. London: Mac Keith Press.

Hemingway, C., McGrogan, J., and Freeman, J. M. (2001). Energy requirements of spasticity. *Dev. Med. Child Neurol.* 43:277. doi: 10.1017/S0012162201000524

Ivanenko, Y. P., Poppele, R. E., and Lacquaniti, F. (2004). Five basic muscle activation patterns account for muscle activity during human locomotion. *J. Physiol.* 556, 267–282. doi: 10.1113/jphysiol.2003.057174

Kim, Y., Bulea, T. C., and Damiano, D. L. (2018). Children with cerebral palsy have greater stride-to-stride variability of muscle synergies during gait than typically developing children: implications for motor control complexity. *Neurorehabilit. Neural Repair* 32, 834–844. doi: 10.1177/1545968318796333

Lance, J. (1980). "Pathophysiology of spasticity and clinical experience with baclofen," in *Spasticity: Disordered Motor Control,* eds J. Lance, R. Feldman, R. Young, and W. Koella (Chicago, IL: Year Book Medical), 185–204.

Lin, Y.-C., Walter, J. P., and Pandy, M. G. (2018). Predictive simulations of neuromuscular coordination and joint-contact loading in human gait. *Ann. Biomed. Eng.* 46, 1216–1227. doi: 10.1007/s10439-018-2026-6

Lloyd, D. G., and Besier, T. F. (2003). An EMG-driven musculoskeletal model to estimate muscle forces and knee joint moments *in vivo*. *J. Biomechan.* 36, 765–776. doi: 10.1016/S0021-9290(03)00010-1

Marsden, J., Ramdharry, G., Stevenson, V., and Thompson, A. (2012). Muscle paresis and passive stiffness: key determinants in limiting function in hereditary and sporadic spastic paraparesis. *Gait Post.* 35, 266–271. doi: 10.1016/j.gaitpost.2011.09.018

Mathewson, M. A., Ward, S. R., Chambers, H. G., and Lieber, R. L. (2015). High resolution muscle measurements provide insights into equinus contractures in patients with cerebral palsy. *J. Orthopaed. Res.* 33, 33–39. doi: 10.1002/jor.22728

McGinley, J. L., Dobson, F., Ganeshalingam, R., Shore, B. J., Rutz, E., and Graham, H. K. (2012). Single-event multilevel surgery for children with cerebral palsy: a systematic review. *Dev. Med. Child Neurol.* 54, 117–128. doi: 10.1111/j.1469-8749.2011.04143.x

Meharbi, N., Schwartz, M. H., and Steele, K. M. (2019). Can altered muscle synergies control unimpaired gait? *J. Biomechan.* 90, 84–91. doi: 10.1016/j.jbiomech.2019.04.038

Menz, H. B., Lord, S. R., and Fitzpatrick, R. C. (2003). Acceleration patterns of the head and pelvis when walking on level and irregular surfaces. *Gait Post.* 18, 35–46. doi: 10.1016/S0966-6362(02)00159-5

Miller, R. H. (2014). A comparison of muscle energy models for simulating human walking in three dimensions. *J. Biomechan.* 47, 1373–1381. doi: 10.1016/j.jbiomech.2014.01.049

Molenaers, G., van Campenhout, A., Fagard, K., De Cat, J., and Desloovere, K. (2010). The use of botulinum toxin A in children with cerebral palsy, with a focus on the lower limb. *J. Children's Orthopaed.* 4, 183–195. doi: 10.1007/s11832-010-0246-x

Ong, C. F., Geijtenbeek, T., Hicks, J. L., and Delp, S. L. (2019). Predicting gait adaptations due to ankle plantarflexor muscle weakness and contracture using physics-based musculoskeletal simulations. *PLoS Computat. Biol.* 15:e1006993. doi: 10.1371/journal.pcbi.1006993

Pitto, L., Kainz, H., Falisse, A., Wesseling, M., Van Rossom, S., Hoang, H., et al. (2019). SimCP: A simulation platform to predict gait performance following orthopedic intervention in children with cerebral palsy. *Front. Neurorobot.* 13:19. doi: 10.3389/fnbot.2019.00054

Raasch, C. C., Zajac, F. E., Ma, B., and Levine, W. S. (1997). Muscle coordination of maximum-speed pedaling. *J. Biomechan.* 30, 595–602. doi: 10.1016/S0021-9290(96)00188-1

Rajagopal, A., Kidziński, Ł., McGlaughlin, A. S., Hicks, J. L., Delp, S. L., and Schwartz, M. H. (2018). Estimating the effect size of surgery to improve walking in children with cerebral palsy from retrospective observational clinical data. *Sci. Rep.* 8, 1–11. doi: 10.1038/s41598-018-33962-2

Scheys, L., Desloovere, K., Spaepen, A., Suetens, P., and Jonkers, I. (2011a). Calculating gait kinematics using MR-based kinematic models. *Gait Post.* 33, 158–164. doi: 10.1016/j.gaitpost.2010.11.003

Scheys, L., Desloovere, K., Suetens, P., and Jonkers, I. (2011b). Level of subject-specific detail in musculoskeletal models affects hip moment arm length calculation during gait in pediatric subjects with increased femoral anteversion. *J. Biomechan.* 44, 1346–1353. doi: 10.1016/j.jbiomech.2011.01.001

Scheys, L., Loeckx, D., Spaepen, A., Suetens, P., and Jonkers, I. (2009). Atlas-based non-rigid image registration to automatically define line-of-action muscle models: a validation study. *J. Biomechan.* 42, 565–572. doi: 10.1016/j.jbiomech.2008.12.014

Scheys, L., Van Campenhout, A., Spaepen, A., Suetens, P., and Jonkers, I. (2008). Personalized MR-based musculoskeletal models compared to rescaled generic models in the presence of increased femoral anteversion: effect on hip moment arm lengths. *Gait Post.* 28, 358–365. doi: 10.1016/j.gaitpost.2008.05.002

Schwartz, M. H. (2018). O 046 - A flexible omnibus matching algorithm (FOMA) to support treatment decisions for children with cerebral palsy. *Gait Post.* 65, 93–94. doi: 10.1016/j.gaitpost.2018.06.064

Schwartz, M. H., Rozumalski, A., and Steele, K. M. (2016). Dynamic motor control is associated with treatment outcomes for children with cerebral palsy. *Dev. Med. Child Neurol.* 58, 1139–1145. doi: 10.1111/dmcn.13126

Seth, A., Hicks, J. L., Uchida, T. K., Habib, A., Dembia, C. L., Dunne, J. J., et al. (2018). OpenSim: simulating musculoskeletal dynamics and neuromuscular control to study human and animal movement. *PLOS Computat. Biol.* 14:e1006223. doi: 10.1371/journal.pcbi.1006223

Sherman, M. A., Seth, A., and Delp, S. L. (2011). Simbody: multibody dynamics for biomedical research. *Procedia IUTAM* 2, 241–261. doi: 10.1016/j.piutam.2011.04.023

Shuman, B. R., Goudriaan, M., Desloovere, K., Schwartz, M. H., and Steele, K. M. (2019). Muscle synergies demonstrate only minimal changes after treatment in cerebral palsy. *J. NeuroEng. Rehabil.* 16, 1–10. doi: 10.1186/s12984-019-0502-3

Sinkjaer, T., Andersen, J. B., and Nielsen, J. F. (1996). Impaired stretch reflex and joint torque modulation during spastic gait in multiple sclerosis patients. *J. Neurol.* 243, 566–574.

Smith, L. R., Lee, K. S., Ward, S. R., Chambers, H. G., and Lieber, R. L. (2011). Hamstring contractures in children with spastic cerebral palsy result from a stiffer extracellular matrix and increased *in vivo* sarcomere length. *J. Physiol.* 589, 2625–2639. doi: 10.1113/jphysiol.2010.203364

Song, S., and Geyer, H. (2015). A neural circuitry that emphasizes spinal feedback generates diverse behaviours of human locomotion. *J. Physiol.* 593, 3493–3511. doi: 10.1113/JP270228

Song, S., and Geyer, H. (2018). Predictive neuromechanical simulations indicate why walking performance declines with ageing. *J. Physiol.* 596, 1199–1210. doi: 10.1113/JP275166

Staude, G., and Wolf, W. (1999). Objective motor response onset detection in surface myoelectric signals. *Med. Eng. Phys.* 21, 449–467.

Steele, K. M., Rozumalski, A., and Schwartz, M. H. (2015). Muscle synergies and complexity of neuromuscular control during gait in cerebral palsy. *Dev. Med. Child Neurol.* 57, 1176–1182. doi: 10.1111/dmcn.12826

Steele, K. M., Shuman, B. R., and Schwartz, M. H. (2017). Crouch severity is a poor predictor of elevated oxygen consumption in cerebral palsy. *J. Biomechan.* 60, 170–174. doi: 10.1016/j.jbiomech.2017.06.036

Surveillance of Cerebral Palsy in Europe (2002). Prevalence and characteristics of children with cerebral palsy in Europe. *Dev. Med. Child Neurol.* 44, 633–640. doi: 10.1111/j.1469-8749.2002.tb00848.x

Uchida, T. K., Hicks, J. L., Dembia, C. L., and Delp, S. L. (2016). Stretching your energetic budget: how tendon compliance affects the metabolic cost of running. *PLoS ONE* 11:e0150378. doi: 10.1371/journal.pone.0150378

van den Bogert, A. J., Geijtenbeek, T., Even-Zohar, O., Steenbrink, F., and Hardin, E. C. (2013). A real-time system for biomechanical analysis of human movement and muscle function. *Med. Biol. Eng. Comput.* 51, 1069–1077. doi: 10.1007/s11517-013-1076-z

van der Krogt, M. M., Bar-On, L., Kindt, T., Desloovere, K., and Harlaar, J. (2016). Neuro-musculoskeletal simulation of instrumented contracture and spasticity assessment in children with cerebral palsy. *J. NeuroEng. Rehabil.* 13:64. doi: 10.1186/s12984-016-0170-5

van der Krogt, M. M., Delp, S. L., and Schwartz, M. H. (2012). How robust is human gait to muscle weakness? *Gait Post.* 36, 113–119. doi: 10.1016/j.gaitpost.2012.01.017

Wächter, A., and Biegler, L. T. (2006). On the implementation of an interior-point filter line-search algorithm for large-scale nonlinear programming. *Math. Programm.* 106, 25–57. doi: 10.1007/s10107-004-0559-y

Willerslev-Olsen, M., Andersen, J. B., Sinkjaer, T., and Nielsen, J. B. (2014). Sensory feedback to ankle plantar flexors is not exaggerated during gait in spastic hemiplegic children with cerebral palsy. *J. Neurophysiol.* 111, 746–754. doi: 10.1152/jn.00372.2013

Wren, T. A., Rethlefsen, S., and Kay, R. M. (2005). Prevalence of specific gait abnormalities in children with cerebral palsy. *J. Pediat. Orthopaed.* 25, 79–83. doi: 10.1097/00004694-200501000-00018

Zajac, F. (1989). Muscle and tendon: properties, models, scaling, and application to biomechanics and motor control. *Crit. Rev. Biomed. Eng.* 17, 359–411.

Conflict of Interest: The authors declare that the research was conducted in the absence of any commercial or financial relationships that could be construed as a potential conflict of interest.

frontiers in Human Neuroscience

ORIGINAL RESEARCH
published: 26 February 2020
doi: 10.3389/fnhum.2020.00045

Foot and Ankle Somatosensory Deficits Affect Balance and Motor Function in Children With Cerebral Palsy

Anastasia Zarkou[1]*, *Samuel C. K. Lee*[2,3], *Laura A. Prosser*[4] and *John J. Jeka*[5]

[1]Spinal Cord Injury Research Laboratory, Crawford Research Institute, Shepherd Center, Atlanta, GA, United States, [2]Department of Physical Therapy and Interdisciplinary Graduate Program in Biomechanics and Movement Science, University of Delaware, Newark, DE, United States, [3]Research Department, Shriners Hospital for Children, Philadelphia, PA, United States, [4]Department of Pediatrics, University of Pennsylvania & The Children's Hospital of Philadelphia, Philadelphia, PA, United States, [5]Department of Kinesiology and Applied Physiology, University of Delaware, Newark, DE, United States

Sensory dysfunction is prevalent in cerebral palsy (CP). Evidence suggests that sensory deficits can contribute to manual ability impairments in children with CP, yet it is still unclear how they contribute to balance and motor performance. Therefore, the objective of this study was to investigate the relationship between lower extremity (LE) somatosensation and functional performance in children with CP. Ten participants with spastic diplegia (Gross Motor Function Classification Scale: I-III) and who were able to stand independently completed the study. Threshold of light touch pressure, two-point discriminatory ability of the plantar side of the foot, duration of cutaneous vibration sensation, and error in the joint position sense of the ankle were assessed to quantify somatosensory function. The balance was tested by the Balance Evaluation System Test (BESTest) and postural sway measures during a standing task. Motor performance was evaluated by using a battery of clinical assessments: (1) Gross Motor Function Measure (GMFM-66-IS) to test gross motor ability; (2) spatiotemporal gait characteristics (velocity, step length) to evaluate walking ability; (3) Timed Up and Go (TUG) and 6 Min Walk (6MWT) tests to assess functional mobility; and (4) an isokinetic dynamometer was used to test the Maximum Volitional Isometric Contraction (MVIC) of the plantar flexor muscles. The results showed that the light touch pressure measure was strongly associated only with the 6MWT. Vibration and two-point discrimination were strongly related to balance performance. Further, the vibration sensation of the first metatarsal head demonstrated a significantly strong relationship with motor performance as measured by GMFM-66-IS, spatiotemporal gait parameters, TUG, and ankle plantar flexors strength test. The joint position sense of the ankle was only related to one subdomain of the BESTest (Postural Responses). This study provides preliminary evidence that LE sensory deficits can possibly contribute to the pronounced balance and motor impairments in CP. The findings emphasize the importance of developing a thorough LE sensory test battery that can guide traditional treatment protocols toward a more holistic therapeutic approach by combining both motor and sensory rehabilitative strategies to improve motor function in CP.

Keywords: cerebral palsy, somatosensation, sensory function, balance, postural control, motor function

OPEN ACCESS

Edited by:
Christos Papadelis, Cook Children's Medical Center, United States

Reviewed by:
Rahul Goel, Stanford University, United States
Hossein Ehsani, University of Maryland, College Park, United States

***Correspondence:**
Anastasia Zarkou
anastasia.zarkou@shepherd.org

Specialty section:
This article was submitted to Motor Neuroscience, a section of the journal Frontiers in Human Neuroscience

Received: *01 October 2019*
Accepted: *31 January 2020*
Published: *26 February 2020*

Citation:
Zarkou A, Lee SCK, Prosser LA and Jeka JJ (2020) Foot and Ankle Somatosensory Deficits Affect Balance and Motor Function in Children With Cerebral Palsy. Front. Hum. Neurosci. 14:45. doi: 10.3389/fnhum.2020.00045

INTRODUCTION

Sensory inputs are crucial for the developing nervous system because they allow for the proper synaptic organization of the brain. In particular, somatosensory information is important for motor learning in the early stages of development and provides the foundation for acquiring more complex behavioral skills (Cascio, 2010; Maitre et al., 2012). Abnormal somatosensory processing has been associated with communication, motor, and social skill deficits in a range of neurodevelopmental disorders like cerebral palsy (CP; Cascio, 2010). Even though CP has been traditionally characterized as a developmental disorder of movement and posture, the reclassification of CP acknowledges coexistent sensory information and sensory processing deficits associated with this pathology (Rosenbaum et al., 2007).

Sensory deficits in CP have been primarily attributed to the injury of the immature brain and, secondarily, stem as a result of limited learning experience (Clayton et al., 2003; Rosenbaum et al., 2007) because motor impairments may not allow environmental exploration; a crucial element in development. Numerous imaging studies showed thalamocortical pathway disruption and aberrant somatosensory cortical activation in children with spastic CP (Burton et al., 2009; Kurz et al., 2014a,b, 2015; Papadelis et al., 2014, 2018), suggesting sensory processing dysfunction. Further, evidence demonstrated that the desynchronization of neuronal discharges in the somatosensory cortex has been related to the amount of error in ankle force performance (Kurz et al., 2014b), indicating that impaired feedback mechanisms can affect the skeletal musculature's ability of persons with CP to adapt in a changing environment. Abnormal sensorimotor oscillatory activity during a knee extension task has shown that children with CP may have anticipatory feedforward control deficits, as their limited environmental exploration early in life does not allow them to develop appropriate internal models for a successful motor response (Kurz et al., 2014a). Altogether, the aforementioned findings suggest that sensory processing deficits associated with this pathology may lead to impaired motor planning and diminished postural control.

Clinical studies have reported somatosensory impairments in upper extremities (Cooper et al., 1995; Wingert et al., 2008, 2010; Auld et al., 2012a,b) affecting up to 90% of children with hemiplegia (Bleyenheuft and Gordon, 2013). Most of these studies showed tactile deficits that have been associated with poor unimanual and bimanual motor performance and inability to characterize an object by its properties (i.e., weight, texture, shape, etc.; Auld et al., 2012b). Additionally, impaired somatosensory integration has negatively influenced feedforward motor control mechanisms during precision grip tasks even in cases where only one hand was primarily affected as in unilateral CP (Bleyenheuft and Gordon, 2013). By using a fingertip force paradigm, Gordon et al. (1999) showed that children with hemiplegia presented anticipatory control deficits in the affected hand due to disrupted sensory information (Gordon and Duff, 1999). In a systematic review of the precision grip and sensory impairments in CP, it was concluded that the relationship between sensory dysfunction and prehension deficits needs to be delineated to improve the design of more focused and effective neurorehabilitation approaches for manual function (Bleyenheuft and Gordon, 2013).

Studies have also found that children with CP exhibit lower extremity (LE) somatosensation deficits (McLaughlin et al., 2005; Wingert et al., 2009). Specifically, impairments in pain (McLaughlin et al., 2005), position sense of the knee (McLaughlin et al., 2005) and hip (Wingert et al., 2009), and direction of scratch (McLaughlin et al., 2005) have been reported in spastic CP. Kurz et al. (2015) provided evidence on the relationship between somatosensory cortical activation and mobility as they showed that an abnormal cortical response to plantar tactile stimulation may have a negative impact on walking ability and plantar flexors' strength in this population. Also, hip proprioception deficits in children with unilateral and bilateral CP have been linked to increased postural sway and decreased gait velocity, even when visual information was upregulated (Damiano et al., 2013). Overall, deficits in sensory information and processing contribute to motor impairments; however, for children with CP, the relationship between foot and ankle somatosensory function and balance performance is not clear.

The aim of the current study was to delineate the contribution of decreased plantar cutaneous feedback and inaccurate ankle proprioceptive input on balance control and motor performance in children with CP. We hypothesized that plantar cutaneous and ankle proprioception deficits would be related to impaired balance and motor function in this population. The findings shed light on how to design more effective sensory-oriented rehabilitative protocols in CP.

MATERIALS AND METHODS

Participants

Ten ambulatory children with spastic diplegia, who were able to stand without any assistive device, were recruited from the outpatient CP clinic at Shriners Hospital for Children in Philadelphia, PA, USA. All participants were able to follow multiple-step commands to complete the somatosensory assessments and clinical measures. Children with a history of the selective dorsal rhizotomy, a score of 4 on the modified Ashworth scale, severe scoliosis (primary curve $>40°$), LE joint instability, and marked visual, hearing, and vestibular deficits were excluded from the study. Additional exclusion criteria were: LE orthopedic surgery or fracture in the year prior participation, botulinum toxin injections within the past 6 months, and pregnancy if the participant was female. The protocol was approved by the Western Institution Review Board (IRB) and the IRB of Temple University and the University of Delaware. Informed parental consent and child assent or consent forms in accordance with the Declaration of Helsinki were obtained prior to participation.

Experimental Procedures

Somatosensory Function

All the children completed a comprehensive clinical evaluation to document their foot and ankle somatosensory function. *Light touch pressure* sensation was assessed by using the 6-item

Monofilaments kit (Baseline®, White Plains, New York, NY, USA) at the first and fifth metatarsal heads and heel of the plantar side of each foot (Meyer et al., 2004; Citaker et al., 2011; Cruz-Almeida et al., 2014). The light touch pressure threshold was defined as the thinner monofilament value the participant correctly identified twice out of three trials for each application site. *Two-point discrimination* was assessed by using an aesthesiometer (Baseline®, White Plains, New York, NY, USA) on the forefoot and heel of the plantar side of each foot (Meyer et al., 2004; Citaker et al., 2011), and scored as the minimum distance in mm between two stimulus points (Meyer et al., 2004; Citaker et al., 2011; Auld et al., 2012a), which were correctly identified as distinct points twice out of three trials for each site. *Cutaneous vibration sensation* was evaluated by using a 128 Hz tuning fork (Rydel–Seiffer graduated tuning fork, Martin Tuttlingen, Germany) at the first metatarsal head and medial malleolus bilaterally (McLaughlin et al., 2005; Citaker et al., 2011). This is a reliable and valid clinical tool that is used to evaluate vibration perception impairments (Alanazy et al., 2018; Marcuzzi et al., 2019). The duration of the perceived vibration stimulus (average of three trials) for each site was recorded. For the ankle *joint position sense* assessment, the participant was instructed to actively reproduce, as accurately as possible, a target joint angle position for each leg. The magnitude of error between the performance and target joint angle was recorded to the nearest degree (average of three trials) for each ankle (Wingert et al., 2009; Damiano et al., 2013).

All the aforementioned testing procedures were performed in random order, without visual feedback, and the total testing duration was approximately 1 h. To determine an individual's threshold for each somatosensory test (overall score) and each site of sensory stimulus application (site-specific score), the average of the combined left and right side scores were computed. In addition, the overall score for each somatosensory test was calculated by averaging the values of all the application sites for every somatosensory modality. Both overall and site-specific scores were used in the analyses.

Balance Performance

Postural Control

The Balance Evaluation Systems Test (BESTest) is a 36-item physical performance scale and was employed to assess balance in the following postural control domains: (1) Biomechanical Constraints; (2) Stability Limits/Verticality; (3) Anticipatory Postural Adjustments; (4) Postural Responses; (5) Sensory Orientation; and (6) Stability in Gait (Horak et al., 2009). Each item was assessed on a four-point scale and percentage scores were calculated for each domain with higher scores suggesting better balance performance. An overall BESTest score was also computed. The BESTest can discriminate postural control abilities in children with typical development with high reproducibility (Dewar et al., 2017) and has been also used previously in children with CP to evaluate balance after the completion of a treadmill training protocol (Kurz et al., 2011).

Standing Balance

Standing balance was assessed by postural sway measures (COP-based measures; Zarkou et al., 2018). Children stood barefoot on two force plates with their feet in a neutral position—the distance between heels was approximately 11% of each subject's height and at a 14° degrees angle between each foot and the midline (Hwang et al., 2014). Tape traces of the feet on the force plates were used to ensure consistent positioning between trials. The children were instructed to stay as motionless and upright as possible and were asked to keep their gaze straight ahead at the eye level. The duration of each trial was 25 s for a total of two trials and the resting interval between trials depended on each participant's comfort and fatigue level. Finally, an overhead harness system was used to prevent falls during each trial.

For kinetic assessment of balance, two AMTI force plates (OR6-7-1000, Advanced Mechanical Technology Inc., Watertown, MA, USA) were used. The force plate data were collected by using Vicon Nexus software (v1.8.5) at 100 Hz sampling rate and filtered with a fourth-order, zero-phase response, low-pass Butterworth filter with a cutoff frequency of 5 Hz (Prieto et al., 1996; Ross et al., 2013). Then, the resultant COP velocity (COPV) and 95% COP Confidence ellipse area (COPA) were computed (Zarkou et al., 2018) and used to investigate their relationship with LE light touch pressure, two-point discrimination, cutaneous vibration, and ankle joint position sense.

Motor Performance

Gross Motor Ability

The Gross Motor Function Measure Item Set (GMFM-66-IS), the abbreviated version of Gross Motor Function Measure 66 (GMFM-66), is a standardized instrument designed to measure the change in gross motor function in children with CP (Russell et al., 2010). For GMFM-66-IS, an algorithm of three decision items from GMFM-66 (items 23, 67, and 85) was used to define which of the four available item sets can be administered (Russell et al., 2010) to more accurately represent each child's function level. It has been reported that there is no systematic difference between different item sets (Russell et al., 2010) with high levels of validity and reliability (ICC $>$ 0.98; Brunton and Bartlett, 2011). For the purposes of this study, the item sets 3 (n = 39 items) and 4 (n = 22 items) were used since our participants had only mild mobility impairments (GMFCS I- III; they were able to stand without the assistive device). Each item was graded on a four-point scale ranging from 0 (does not initiate the required task) to 3 (completes the required task) and was scored by a physical therapist using GMAE software.

Walking Ability

Spatiotemporal characteristics of gait were evaluated while children walked on an instrumented walkway (GAITRite®, CIR Systems Inc., Franklin, NJ, USA). The GAITRite mat was positioned on the floor and children started walking 1.2 m before the beginning of the mat (acceleration walkway) and continued walking 1.2 m after reaching the end of the mat (deceleration walkway). The acceleration and deceleration walkways ensured that the children walked on a steady speed over the instrumented walkway. Subjects were tested in bare feet walking at their fast speed and without using any assistive device. Two to six trials were collected depending on children's number of steps per trial (i.e., at least 16 steps). To qualify as a valid walking

pass, trials had to include at least four consecutive footfalls on the instrumented walkway. The first four gait cycles for each side (right and left) were used for further analyses; thus, collecting a total of eight strides allowed for reliable estimation of gait parameters in children with CP (GMFCS I-III; Redekop et al., 2008). The following spatiotemporal parameters were collected: gait speed and step length normalized to height (Non-Dimensional approach; Stansfield et al., 2003). All values from the selected gait cycles were averaged for each variable of interest.

Functional Mobility

The Timed Up and Go (TUG) test quantifies functional mobility. Children rose from a seated position, walked 3 m, turned around, and walked back to the chair and sat down as quickly and safely as possible (Williams et al., 2005). The test was repeated three times and the average time was recorded. Participants performed the test barefoot without using an assistive device. The 6-Minute Walk Test (6MWT) assessed children's walking aerobic capacity (Maher et al., 2008; Fitzgerald et al., 2016). Each subject was asked to ambulate around a fixed course as safely and quickly as possible. The distance that the individual was able to traverse in the allotted time was recorded. Only one child with CP needed to use a walker to complete the test.

Strength

The Maximum Volitional Isometric Contraction (MVIC) of triceps surae, bilaterally, was assessed by a computerized controlled dynamometer (KinCom II, Chattecx Corporation, Chattanooga, TN). Children were positioned in the dynamometer for triceps surae testing as previously described in the literature (Stackhouse et al., 2005). A total of three trials for each side were collected with a 3-min resting period between trials. During each trial, visual feedback and enthusiastic verbal encouragement were provided to children. The peak MVIC value was normalized with each subject's body weight and then the left and right MVIC were averaged and used for subsequent analyses.

Statistical Analyses

Due to the small sample size of this pilot study, median and interquartile ranges (IQR) were computed for the demographic characteristics and the sensory and motor function clinical assessments. Further, Spearman rank correlation coefficients were calculated to determine the relationships between somatosensory function and the respective clinical measures that assess balance and motor performance. According to Cohen's standards, rho coefficients greater than 0.5 indicate strong relationships, 0.3–0.5 moderate relationships, and 0.1–0.3 weak relationships (Cohen, 1988). Statistical significance was set at $p < 0.05$. The SPSS (version 23; SPSS Inc., Chicago, IL, USA) statistical software was used for the analyses.

RESULTS

A total of 10 children with CP participated in this study. The median and IQR for age, height, and weight were 15.62 years (13.37–18.15), 165.8 cm (150.5–170), and 58.25 kg (38.25–74.23) respectively. The demographic characteristics of each individual are presented in **Table 1**.

TABLE 1 | Participants' demographic information. All children were diagnosed with spastic diplegic cerebral palsy (CP).

	Age	Sex	GMFCS	Height	Weight
1	9 years 1 month	M	I	142 cm	33 kg
2	17 years 8 months	M	II	182.5 cm	127 kg
3	18 years 0 months	M	I	158.5 cm	58.3 kg
4	15 years 7 months	M	III	164.6 cm	49.1 kg
5	13 years 1 month	M	I	146 cm	30.2 kg
6	18 years 6 months	M	II	170 cm	66 kg
7	18 years 6 months	M	I	170 cm	58.2 kg
8	15 years 2 months	M	III	169 cm	98.9 kg
9	15 years 6 months	M	III	167 cm	59.3 kg
10	13 years 5 months	F	II	152 cm	40 kg

Abbreviations: GMFCS, Gross Motor Function Classification Scale.

For the rest of the foot and ankle somatosensory tests and motor function clinical measures, the median and IQR values are presented in **Table 2**.

Relationships Between Somatosensation and Balance

Spearman rho correlation coefficients, presented in **Table 3**, were computed to assess the relationship between somatosensory function (overall scores) and balance performance.

Two-point discrimination was strongly related with the BESTest score in all subdomains (rho = −0.57 to −0.83, $p < 0.05$)—except for the *Anticipatory Postural Adjustments* subdomain—and the COPA (rho = 0.86, $p = 0.001$). A strong relationship was also revealed between vibration sensation and the *Stability Limits/Verticality* subdomain of BESTest (rho = −0.56, $p = 0.048$) and COP measures (COPV: rho = 0.69, $p = 0.014$; COPA: rho = 0.73, $p = 0.008$). Scatterplots partially summarize these results (**Figure 1**).

Ankle joint position sense was significantly associated with the *Postural Responses* subdomain of BESTest (**Figure 2**: rho = −0.70, $p = 0.019$). For all the above relationships, the rho coefficients' negative value indicated that the higher the somatosensory assessment thresholds indicating greater impairment, the lower children's score in the BESTest; whereas, the positive value suggested that the higher the somatosensory thresholds the larger the postural sway measures during the standing balance test.

Spearman rho correlation coefficients were also computed to characterize the relationships between the site-specific scores of the somatosensory tests and the balance clinical measures (**Table 4**). In particular, there was a negative correlation between the two-point discrimination in the forefoot area with two of the subdomains of the BESTest (Stability Limits/Verticality: rho = −0.68, $p = 0.015$; Stability in Gait: rho = −0.58, $p = 0.04$). Similarly, two-point discrimination in the heel area was strongly related to three of the subdomains of BESTest (rho = −0.62 to −0.65, $p < 0.05$). Vibration sensation in the first metatarsal site demonstrated a strong negative relationship with the overall BESTest score (rho = −0.60, $p = 0.033$) and the score in Stability Limits/Verticality, Postural Responses, and Stability in Gait

TABLE 2 | Median and Interquartile Range (IQR) values for somatosensory and motor function assessments in children with CP.

Sensory assessments	Median (IQR)	Motor ability assessments	Median (IQR)
Light touch pressure (level)		Postural control (%)	
1st Metatarsal	4.31 (4.14–4.61)	BESTest *Overall*	62.96 (40.28–83.10)
5th Metatarsal	4.31 (4.14–4.9)	BESTest 1 *Biomechanical Constraints*	56.67 (33.33–81.67)
Heel	4.38 (4.22–5.18)	BESTest 2 *Stability Limits/Verticality*	78.57 (63.10–85.71)
Overall	4.33 (4.14–4.79)	BESTest 3 *Anticipatory Postural Adjustments*	52.78 (48.61–91.67)
Two-point discrimination (mm)		BESTest 4 *Postural Responses*	30.55 (19.44–55.55)
Forefoot	17.5 (13.75–21.25)	BESTest 5 *Sensory Orientation*	76.67 (48.33–100.00)
Heel	17.5 (16.88–25.63)	BESTest 6 *Stability in Gait*	64.29 (28.57–95.24)
Overall	17.5 (16.56–21.56)	Balance Performance	
Vibration (s)		COPA (cm^2)	81.10 (15.49–109.39)
1st Metatarsal	15.5 (14.46–20.58)	COPV (cm/s)	5.55 (4.16–7.25)
Medial Malleolus	16.17 (11.09–19.25)	Gross Motor Ability (%)	
Overall	16.79 (12.83–19.19)	GMFM-66-IS	75.00 (68.78–89.03)
Joint Position Sense (degrees)		Walking Ability (ND)	
Ankle	4.5 (3.10–5.17)	Velocity	0.33 (0.26–0.36)
		Step Length	0.35 (0.31–0.37)
		Functional Ability	
		TUG (s)	7.84 (5.93–12.10)
		6MWT (min)	467.72 (381.10–534.31)
		Strength	
		MVIC (N/Kg)	4.69 (2.04–6.83)

Abbreviation: BESTest, Balance Evaluation Systems Test; COPV, center of pressure resultant velocity; COPA, 95% eclipse area of center of pressure; GMFM-66-IS, Gross Motor Function Measure Item Set; ND, Non-Dimensional; TUG, Timed Up and Go; 6MWT, 6-Minute Walk Test; MVIC, Maximum Volitional Isometric Contraction.

TABLE 3 | Spearman's rank correlations between the somatosensation thresholds and balance control scores in children with CP.

	Somatosensory ability measures			
	Light touch pressure	Two-point discrimination	Vibration	JPS
Postural control				
BESTest *overall*	0.00	−0.64*	−0.31	−0.28
BESTest 1 *Biomechanical Constraints*	0.01	−0.62*	−0.12	−0.19
BESTest 2 *Stability Limits/Verticality*	0.24	−0.83**	−0.56*	−0.34
BESTest 3 *Anticipatory Postural Adjustments*	−0.25	−0.48	−0.39	0.00
BESTest 4 *Postural Responses*	0.35	−0.57*	−0.26	−0.70*
BESTest 5 *Sensory Orientation*	0.06	−0.58*	−0.14	−0.52
BESTest 6 *Stability in Gait*	−0.14	−0.69*	−0.52	−0.11
Balance Performance				
COPA	−0.31	0.86**	0.73**	0.23
COPV	0.01	0.45	0.69*	−0.09

Asterisks indicate significant relationships ($p < 0.05$; **$p < 0.01$). Abbreviations: JPS, Joint Position Sense; BESTest, Balance Evaluation Systems Test; COPV, the center of pressure resultant velocity; COPA, 95% eclipse area of the center of pressure.*

subdomains of BESTest (rho = −0.62 to −0.70, $p < 0.05$). These correlations suggested that the higher the two-point discrimination thresholds and the longer the vibration stimulus was perceived the poorer that participants performed in the BESTest, showing impaired postural control in these children (**Table 4**).

Two-point discrimination in the forefoot and heel sites and cutaneous vibration sensation in the first metatarsal site showed a strong positive relationship with the COPA (rho = 0.72–0.77, $p < 0.01$). Additionally, increased two-point discrimination thresholds and longer vibration perception in the forefoot and medial malleolus areas, respectively, were significantly associated with the increased velocity of COP sway (rho = 0.65, $p = 0.02$ and rho = 0.77, $p = 0.004$). Finally, none to weak relationships were found between site-specific scores for light touch pressure and the balance performance measures.

Relationships Between Somatosensation and Motor Function

Children with higher light touch pressure thresholds in their plantar side of the foot (overall score) were more likely to cover a shorter distance during the 6MWT, as indicated by the negative rho coefficient of −0.55 ($p = 0.048$; **Figure 3**).

Furthermore, only the cutaneous vibration sensation of the first metatarsal head demonstrated a significantly strong relationship with motor performance as measured by GMFM-66-IS, spatiotemporal gait parameters, TUG, and plantar flexor strength (**Figure 4**). More specifically, the longer the children were able to perceive the vibration stimulus in the first metatarsal area the more likely they were to have limitations in gross motor function (rho = −0.63, $p = 0.025$), and walking ability (gait velocity: rho = −0.78, $p = 0.004$; step length: rho = −0.59, $p = 0.036$), functionality (TUG: rho = 0.66, $p = 0.02$), and plantar flexors' strength (rho = −0.61, $p = 0.029$). The rest of

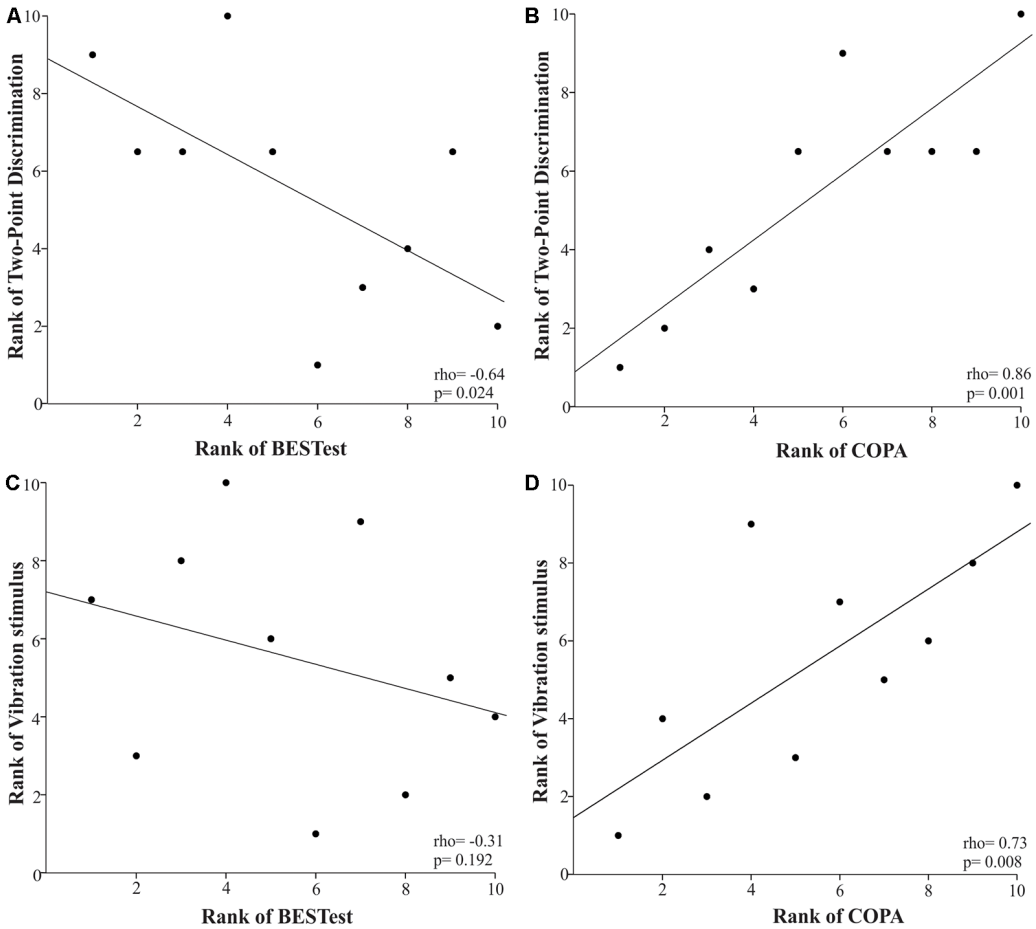

FIGURE 1 | Scatter plots of the relationships between two-point discrimination **(A,B)** and vibration **(C,D)** senses and balance ability using Spearman's rank correlations in the children with cerebral palsy (CP). Each data point reflects a participant.

the somatosensory site-specific scores were weakly to moderately associated with motor function tests, and these relationships were not statistically significant.

DISCUSSION

This study investigated the relationship between foot and ankle somatosensory and motor function in children with spastic diplegic CP. Our results demonstrated that foot and ankle somatosensation is strongly related to standing balance and motor performance; thus, supporting the notion that plantar cutaneous and ankle proprioceptive deficits may contribute to the postural control and mobility impairments in this population. These clinical findings emphasized the importance of developing a thorough LE sensory test battery that can identify subject-specific sensory deficits and, therefore, guide traditional treatment protocols toward a more comprehensive therapeutic approach by combining motor and sensory rehabilitative strategies to improve motor function in CP. Also, our findings are particularly noteworthy in light of existing evidence indicating that enhancing sensory inputs through stochastic resonance stimulation applications can improve balance in children with CP (Zarkou et al., 2018).

Relationship Between Somatosensation and Balance

Flexible postural control and motor planning require organizing and integrating visual, vestibular, and somatosensory inputs to efficiently coordinate motor actions (Shumway-Cook and Woollacott, 2012). Research indicates that individuals with CP may depend primarily on feedback from their visual and vestibular systems in environments that challenge balance compared to individuals without CP (Yu et al., 2019). Impairments in at least one of the aforementioned sensory systems could be a contributing factor in the poor balance control exhibited by children with CP. Postural control deficits in this population have been attributed to biomechanical changes in postural alignment as well as to central nervous system (CNS) sensory processing impairments (Papadelis et al., 2014; Kurz et al., 2015; Pavão et al., 2015). Our results showed that LE somatosensory function is strongly related to balance performance in CP and, therefore, impairments in the plantar

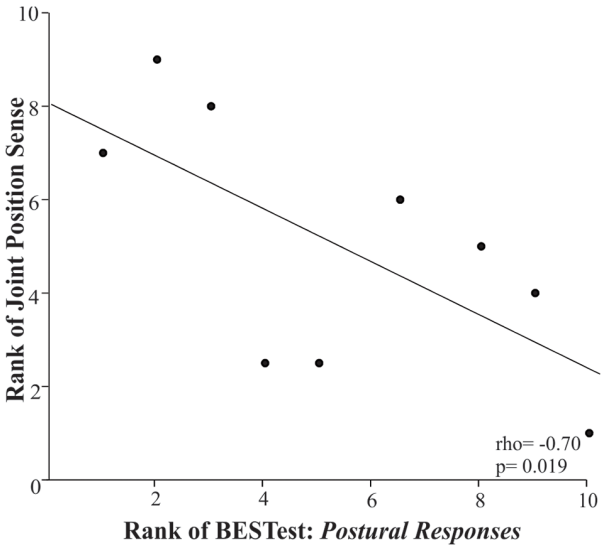

FIGURE 2 | Scatter plot of the rank of the Balance Evaluation System Test (BESTest) score in the 4th Subdomain (postural responses) and the rank of the ankle joint position sense in the children with CP. Each data point reflects a participant.

cutaneous and ankle proprioceptive function may partially contribute to balance deficits.

Among the tested somatosensory modalities, two-point discrimination in the plantar side of the foot was significantly associated with all but one of the subdomains of BESTest and the area of COP sway during quiet stance. Specifically, the larger the distance between the two applied stimuli that children perceived as distinct, the poorer they performed in five different underlying systems that contributed to postural control, hence suggesting generalized balance problems in CP. When investigating the site-specific scores for two-point discrimination, we found that both the forefoot and heel areas contributed to the observed poor balance performance. These findings indicated that limited spatial and temporal tactile information from the anterior and posterior supporting zones of the foot (i.e., forefoot and heel areas; Kavounoudias et al., 1998) may result in inability to trigger the appropriate compensatory responses to maintain a stable upright stance in CP.

Vibration sensation in the first metatarsal area showed significant relationships with three subcategories of BESTest and the area of COP sway. These findings suggested that when children were able to perceive vibration sensation for a longer period of time, they showed decreased functional stability limits, impaired compensatory postural responses, and dynamic and static stability deficits. Previous research in vibration sensation reported that children with CP were not able to properly identify a vibration stimulus in their LE (McLaughlin et al., 2005). Further, we showed that children with CP, although they did not perform significantly different compared to controls, they perceived the vibration stimulus for a longer period (Zarkou, 2017). Conversely, for individuals with multiple sclerosis (Citaker et al., 2011) the duration of the perceived vibration is shorter compared to healthy adults and this has been attributed to spinal dorsal column abnormalities associated with this pathology (Zackowski et al., 2009). Temlett (2009) showed that the duration of the vibration sensation also declines with age due to nerve fibers degeneration and deterioration of Pacinian corpuscles, which are the primary mechanoreceptors of cutaneous vibration sensation. Evidence suggests that vibrotactile stimulation at the foot activates Pacinian corpuscles, but can also modulate ankle joint proprioception, thus indicating an interplay between tactile and proprioceptive inputs (Mildren and Bent, 2016) that both contribute to postural control (Kavounoudias et al., 2001). In this study, the recorded longer period of vibration sensation in CP may have indicated aberrant and prolonged processing and integration of the afferent vibratory input by the CNS that resulted in impaired balance control. This corroborates brain imaging findings proposing that sensory processing deficits contribute to the motor planning and execution impairments in spastic diplegia (Burton et al., 2009; Kurz et al., 2014a,b; Kurz et al., 2015).

Ankle joint position sense errors were significantly related to the *Postural Responses* subdomain of BESTest. In particular, for this category's balance tasks, children were required to regain their equilibrium with and without taking a step following

TABLE 4 | Spearman's rank correlations between two-point discrimination and vibration senses, at different application sites, and balance ability measures in children with CP.

	Two-point discrimination		Vibration	
	Forefoot	Heel	1st Metatarsal	Medial Malleolus
Postural control				
BESTest *Overall*	−0.45	−0.54	−0.60*	−0.05
BESTest 1 *Biomechanical Constraints*	−0.29	−0.62*	−0.54	0.13
BESTest 2 *Stability Limits/Verticality*	−0.68*	−0.65*	−0.69*	−0.15
BESTest 3 *Anticipatory Postural Adjustments*	−0.35	−0.29	−0.54	−0.22
BESTest 4 *Postural Responses*	−0.33	−0.64*	−0.70*	0.07
BESTest 5 *Sensory Orientation*	−0.31	−0.53	−0.51	0.21
BESTest 6 *Stability in Gait*	−0.58*	−0.47	−0.62*	−0.24
Balance Performance				
COPA	0.72**	0.74**	0.77**	0.46
COPV	0.65*	0.36	0.33	0.77**

*Asterisks indicate significant relationships (*p < 0.05; **p < 0.01). Abbreviations: BESTest, Balance Evaluation Systems Test; COPV, the center of pressure resultant velocity; COPA, 95% eclipse area of the center of pressure.*

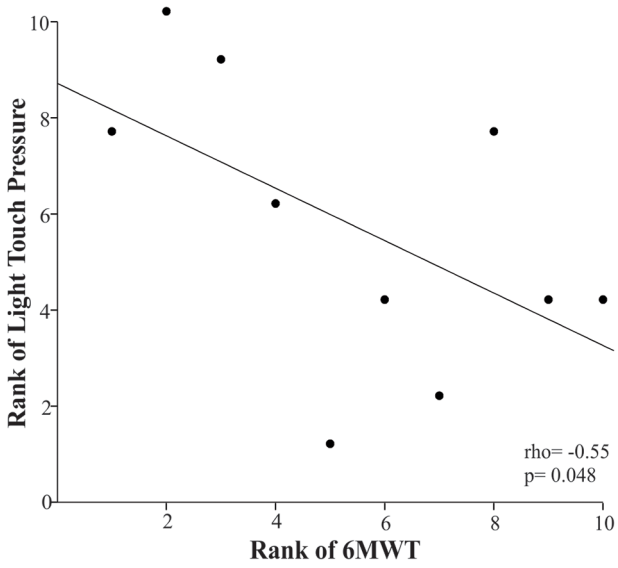

FIGURE 3 | Scatter plot of the rank of the 6-Minute Walk Test (6MWT) and the rank of the light touch pressure in the children with CP. Each data point reflects a participant.

perturbations in different directions (i.e., forward, backward, or lateral) induced by the examiner's hands (Horak et al., 2009). Children with CP were unable to elicit an appropriate postural response to unexpected perturbations, receiving a median group score of 30.55 out of the maximum 100. The lower they scored in this subdomain, they presented larger errors in reproducing the target ankle position during the joint position sense test. These findings potentially demonstrate that ankle proprioceptive deficits did not allow for proper sensory feedback during the execution of the motor response and, therefore, children with CP were unable to regain equilibrium during a challenging balance task. Similarly, Damiano et al. (2013) reported that increased hip proprioception errors were significantly related to increased postural sway during quiet stance and decreased gait velocity in CP. Altogether, the findings suggested that evaluation of proprioception should be incorporated into LE sensory battery tests, especially in light of evidence that proprioceptive deficits can be exacerbated by the loss of plantar cutaneous inputs affecting balance stability (Meyer et al., 2004).

Relationship Between Somatosensation and Motor function

In our previous work, we showed that light touch pressure thresholds significantly increased in children with CP compared to their age-matched typically developing peers (Zarkou, 2017). Although higher light touch pressure thresholds have been associated with poor balance performance in older adults (Cruz-Almeida et al., 2014), individuals with multiple sclerosis (Citaker et al., 2011), and peripheral neuropathy (Perkins et al., 2001; Kars et al., 2009), this study demonstrated that the only significant relationship in children with CP was between light touch pressure and the 6MWT, yet it was not associated with balance measures. Specifically, higher light touch pressure thresholds were significantly related to shorter distances covered over a 6 min period. A possible explanation is that during dynamic activities like gait, in which the loading response may be equivalent to several times the bodyweight of the individual, the plantar mechanoreceptors' thresholds are more likely to be reached compared to simpler balance tasks that involve lower levels of plantar pressure like the ones that occur during postural shifts to maintain standing balance (Cruz-Almeida et al., 2014). Therefore, the impact of the plantar light touch pressure deficits on postural stability in CP may be more evident during a prolonged walking task, like the 6MWT.

Interestingly, the cutaneous vibration sensation at the first metatarsal head was the only sensory modality that was significantly related to the majority of the clinical motor assessments. In particular, longer duration of the vibration perception was significantly related to impaired gross motor and walking function, functional mobility, and plantar flexors' strength. These findings implied that vibratory inputs from the first metatarsal head, as provided by the stimulation of Pacinian corpuscles that are located at both the subcutaneous tissue, bony periosteum, and joint ligaments (Temlett, 2009), are crucial for static and dynamic postural control. Moreover, our findings corroborate previous work reporting that decreased sensory inputs from the first metatarsal head area have been associated with decreased score in the Berg Balance Scale and walking speed in older adults (Cruz-Almeida et al., 2014). Hence, future studies should focus on delineating the reweighting of LE somatosensory cues—especially from the first metatarsal head area- and how it affects motor function not only during static but also dynamic and prolonged activities.

This work highlighted the strong relationship between somatosensory function and variables of balance and motor performance in CP even with small sample size. These observations may imply that somatosensory dysfunction is highly pervasive in children with CP, however, we urge caution in interpreting these results because of the small sample size. Furthermore, we acknowledge the fact that musculoskeletal deficits, along with poor somatosensory ability, can contribute to the noted motor impairments witnessed in children with CP as this pathology is multifactorial. Finally, over the course of the past decade, neuroimaging evidence has supported the existence of somatosensory processing deficits and abnormal sensorimotor connectivity in this population (Burton et al., 2009; Kurz et al., 2014a,b, 2015; Papadelis et al., 2014, 2018), however, there is limited research on the clinically detectable LE somatosensory impairments. Combining brain-imaging techniques with our clinical assessment methods may have further strengthened the results of this study.

CONCLUSION

Somatosensory system is essential to motor control by providing information for the formulation of the appropriate feedforward anticipatory strategy and for the regulation of the feedback

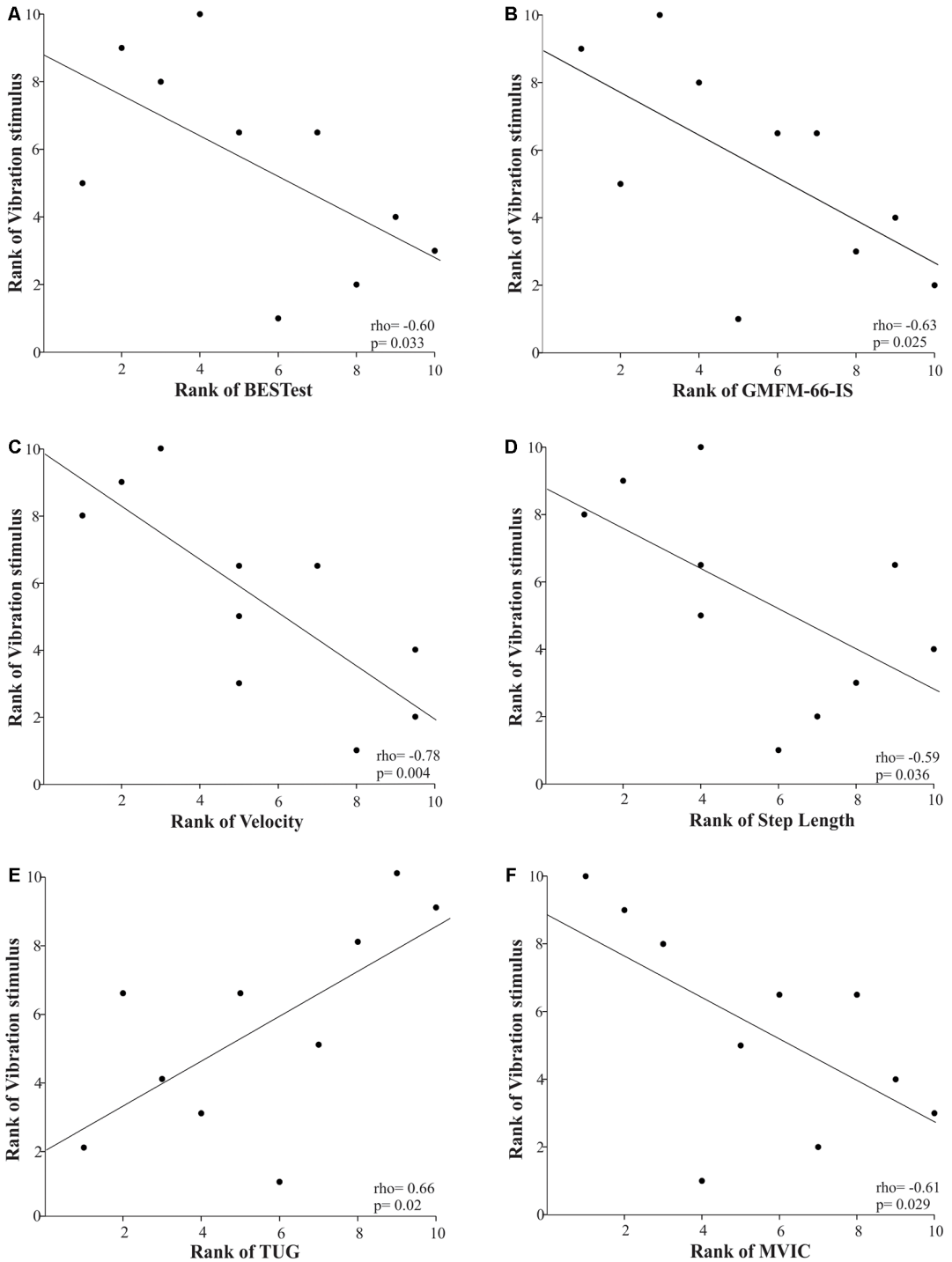

FIGURE 4 | Scatter plots of the Spearman's rank correlations between the rank of the vibration stimulus when applied in the first metatarsal area and the rank of motor performance variables [i.e., postural control **(A)**, gross motor function **(B)**, gait velocity **(C)**, step length **(D)**, functional mobility **(E)**, and plantar flexors' strength **(F)**] in children with CP. Each data point reflects a participant.

mechanism, which allows the correction of performance errors during the execution of a motor plan (Ghez, 1991; Schmidt and Lee, 2011); therefore, impairments in this system may impact motor behavior. In support of prior imaging work (Burton et al., 2009; Kurz et al., 2014a,b, 2015; Papadelis et al., 2014, 2018), our clinical findings suggested that sensory processing dysfunction is partially contributed to the motor planning and execution impairments that affect postural control and motor function

in CP. Specifically, we provided evidence that somatosensory deficits in the LEs, especially two-point discrimination and cutaneous vibration sensation, appear to strongly influence balance and motor performance in children with spastic diplegia. Therefore, addressing the reported somatosensory impairments may contribute to postural stability and functional mobility improvements in this population.

Our research proposed that using a simple battery of clinical tests to assess somatosensation allows for the identification of tactile and proprioceptive deficits, and thus provides important information for clinical care in CP. Further research is required to investigate the minimum necessary number of somatosensory assessments that should be included in the clinical practice. A short screening tool that includes modality and site-specific tests besides being administered in a timely manner can potentially identify motor function declines in CP. In addition, it can guide traditional treatment protocols toward a more holistic therapeutic approach by combining motor and sensory rehabilitative strategies to improve overall functionality and quality of life in CP.

DATA AVAILABILITY STATEMENT

The raw data supporting the conclusions of this article will be made available by the authors, without undue reservation, to any qualified researcher.

ETHICS STATEMENT

The studies involving human participants were reviewed and approved by Western Institution Review Board (IRB), Temple University IRB, and University of Delaware IRB. Written informed consent to participate in this study was provided by the participants' legal guardian/next of kin. Child assents were also obtained prior participation.

AUTHOR CONTRIBUTIONS

All authors contributed to the design of the study. AZ and LP ran the experiments. AZ analyzed the data, interpreted the results, drafted the manuscript and submitted the manuscript. SL, LP, and JJ provided thorough feedback and revised the manuscript. All authors approved the final manuscript.

FUNDING

This research was supported by Shriners Hospital for Children (grant 22173) to JJ and partial support by the Onassis Foundation to AZ.

ACKNOWLEDGMENTS

This research project was conducted in partial fulfillment of the requirements for the Ph.D. dissertation of AZ (Biomechanics and Movement Science Program, University of Delaware, Newark, DE, USA). Part of this work has been presented at the 70th Annual Meeting of AACPDM, Hollywood, FL, USA (Zarkou et al., 2016). We thank our participants and their families for taking part in this study. We also thank Peter Agada and Dr. Sungjae Hwang for their assistance during the instrumented static balance assessments.

REFERENCES

Alanazy, M. H., Alfurayh, N. A., Almweisheer, S. N., Aljafen, B. N., and Muayqil, T. (2018). The conventional tuning fork as a quantitative tool for vibration threshold. *Muscle Nerve* 57, 49–53. doi: 10.1002/mus.25680

Auld, M. L., Boyd, R. N., Moseley, G. L., Ware, R. S., and Johnston, L. M. (2012a). Impact of tactile dysfunction on upper-limb motor performance in children with unilateral cerebral palsy. *Arch. Phys. Med. Rehabil.* 93, 696–702. doi: 10.1016/j.apmr.2011.10.025

Auld, M. L., Boyd, R. N., Moseley, G. L., Ware, R. S., and Johnston, L. M. (2012b). Tactile function in children with unilateral cerebral palsy compared to typically developing children. *Disabil. Rehabil.* 34, 1488–1494. doi: 10.3109/09638288.2011.650314

Bleyenheuft, Y., and Gordon, A. M. (2013). Precision grip control, sensory impairments and their interactions in children with hemiplegic cerebral palsy: a systematic review. *Res. Dev. Disabil.* 34, 3014–3028. doi: 10.1016/j.ridd.2013.05.047

Brunton, L. K., and Bartlett, D. J. (2011). Validity and reliability of two abbreviated versions of the gross motor function measure. *Phys. Ther.* 91, 577–588. doi: 10.2522/ptj.20100279

Burton, H., Dixit, S., Litkowski, P., and Wingert, J. R. (2009). Functional connectivity for somatosensory and motor cortex in spastic diplegia. *Somatosens. Mot. Res.* 26, 90–104. doi: 10.3109/08990220903335742

Cascio, C. J. (2010). Somatosensory processing in neurodevelopmental disorders. *J. Neurodev. Disord.* 2, 62–69. doi: 10.1007/s11689-010-9046-3

Citaker, S., Gunduz, A. G., Guclu, M. B., Nazliel, B., Irkec, C., and Kaya, D. (2011). Relationship between foot sensation and standing balance in patients with multiple sclerosis. *Gait Posture* 34, 275–278. doi: 10.1016/j.gaitpost.2011.05.015

Clayton, K., Fleming, J. M., and Copley, J. (2003). Behavioral responses to tactile stimuli in children with cerebral palsy. *Phys. Occup. Ther. Pediatr.* 23, 43–62. doi: 10.1080/j006v23n01_04

Cohen, J. (1988). *Statistical Power Analysis for the Behavioral Sciences.* 2nd Edn. Hillsdale, NJ: Lawrence Erlbaum Associates.

Cooper, J., Majnemer, A., Rosenblatt, B., and Birnbaum, R. (1995). The determination of sensory deficits in children with hemiplegic cerebral palsy. *J. Child Neurol.* 10, 300–309. doi: 10.1177/088307389501000412

Cruz-Almeida, Y., Black, M. L., Christou, E. A., and Clark, D. J. (2014). Site-specific differences in the association between plantar tactile perception and mobility function in older adults. *Front. Aging Neurosci.* 6:68. doi: 10.3389/fnagi.2014.00068

Damiano, D. L., Wingert, J. R., Stanley, C. J., and Curatalo, L. (2013). Contribution of hip joint proprioception to static and dynamic balance in cerebral palsy: a case control study. *J. Neuroeng. Rehabil.* 10:57. doi: 10.1186/1743-0003-10-57

Dewar, R., Claus, A. P., Tucker, K., Ware, R., and Johnston, L. M. (2017). Reproducibility of the balance evaluation systems test (BESTest) and the mini-BESTest in school-aged children. *Gait Posture* 55, 68–74. doi: 10.1016/j.gaitpost.2017.04.010

Fitzgerald, D., Hickey, C., Delahunt, E., Walsh, M., and O'Brien, T. (2016). Six-minute walk test in children with spastic cerebral palsy and children developing typically. *Pediatr. Phys. Ther.* 28, 192–199. doi: 10.1097/pep.0000000000000224

Ghez, C. (1991). "The control of movement," in *Principles of Neural Science*, 3rd Edn. eds E. Kandel, J. Schwartz and T. Jessell (New York, NY: Elsevier Science Publishing Co. Inc.), 534–547.

Gordon, A. M., Charles, J., and Duff, S. V. (1999). Fingertip forces during object manipulation in children with hemiplegic cerebral palsy. II: bilateral coordination. *Dev. Med. Child Neurol.* 41, 176–185. doi: 10.1017/s0012162299000365

Gordon, A. M., and Duff, S. V. (1999). Relation between clinical measures and fine manipulative control in children with hemiplegic cerebral palsy. *Dev. Med. Child Neurol.* 41, 586–591. doi: 10.1017/s0012162299001231

Horak, F. B., Wrisley, D. M., and Frank, J. (2009). The balance evaluation systems test (BESTest) to differentiate balance deficits. *Phys. Ther.* 89, 484–498. doi: 10.2522/ptj.20080071

Hwang, S., Agada, P., Kiemel, T., and Jeka, J. J. (2014). Dynamic reweighting of three modalities for sensor fusion. *PLoS One* 9:e88132. doi: 10.1371/journal.pone.0088132

Kars, H. J. J. C., Hijmans, J. M., Geertzen, J. H. B., and Zijlstra, W. (2009). The effect of reduced somatosensation on standing balance: a systematic review. *J. Diabetes Sci. Technol.* 3, 931–943. doi: 10.1177/193229680900300441

Kavounoudias, A., Roll, R., and Roll, J.-P. (1998). The plantar sole is a 'dynamometric map' for human balance control. *Neuroreport* 9, 3247–3252. doi: 10.1097/00001756-199810050-00021

Kavounoudias, A., Roll, R., and Roll, J. P. (2001). Foot sole and ankle muscle inputs contribute jointly to human erect posture regulation. *J. Physiol.* 532, 869–878. doi: 10.1111/j.1469-7793.2001.0869e.x

Kurz, M. J., Becker, K. M., Heinrichs-Graham, E., and Wilson, T. W. (2014a). Neurophysiological abnormalities in the sensorimotor cortices during the motor planning and movement execution stages of children with cerebral palsy. *Dev. Med. Child Neurol.* 56, 1072–1077. doi: 10.1111/dmcn.12513

Kurz, M. J., Heinrichs-Graham, E., Arpin, D. J., Becker, K. M., and Wilson, T. W. (2014b). Aberrant synchrony in the somatosensory cortices predicts motor performance errors in children with cerebral palsy. *J. Neurophysiol.* 111, 573–579. doi: 10.1152/jn.00553.2013

Kurz, M. J., Corr, B., Stuberg, W., Volkman, K. G., and Smith, N. (2011). Evaluation of lower body positive pressure supported treadmill training for children with cerebral palsy. *Pediatr. Phys. Ther.* 23, 232–239. doi: 10.1097/PEP.0b013e318227b737

Kurz, M. J., Heinrichs-Graham, E., Becker, K. M., and Wilson, T. W. (2015). The magnitude of the somatosensory cortical activity is related to the mobility and strength impairments seen in children with cerebral palsy. *J. Neurophysiol.* 113, 3143–3150. doi: 10.1152/jn.00602.2014

Maher, C. A., Williams, M. T., and Olds, T. S. (2008). The six-minute walk test for children with cerebral palsy. *Int. J. Rehabil. Res.* 31, 185–188. doi: 10.1097/MRR.0b013e32830150f9

Maitre, N. L., Barnett, Z. P., and Key, A. P. F. (2012). Novel assessment of cortical response to somatosensory stimuli in children with hemiparetic cerebral palsy. *J. Child Neurol.* 27, 1276–1283. doi: 10.1177/0883073811435682

Marcuzzi, A., Wainwright, A., Costa, D., and Wrigley, P. (2019). Vibration testing: optimizing methods to improve reliability. *Muscle Nerve* 59, 229–235. doi: 10.1002/mus.26373

McLaughlin, J. F., Felix, S. D., Nowbar, S., Ferrel, A., Bjornson, K., and Hays, R. M. (2005). Lower extremity sensory function in children with cerebral palsy. *Pediatr. Rehabil.* 8, 45–52. doi: 10.1080/13638490400011181

Meyer, P. F., Oddsson, L. I. E., and De Luca, C. J. (2004). The role of plantar cutaneous sensation in unperturbed stance. *Exp. Brain Res.* 156, 505–512. doi: 10.1007/s00221-003-1804-y

Mildren, R. L., and Bent, L. R. (2016). Vibrotactile stimulation of fast adapting cutaneous afferents from the foot modulates proprioception at the ankle joint. *J. Appl. Physiol.* 120, 855–864. doi: 10.1152/japplphysiol.00810.2015

Papadelis, C., Ahtam, B., Nazarova, M., Nimec, D., Snyder, B., Grant, P. E., et al. (2014). Cortical somatosensory reorganization in children with spastic cerebral palsy: a multimodal neuroimaging study. *Front. Hum. Neurosci.* 8:725. doi: 10.3389/fnhum.2014.00725

Papadelis, C., Butler, E. E., Rubenstein, M., Sun, L., Zollei, L., Nimec, D., et al. (2018). Reorganization of the somatosensory cortex in hemiplegic cerebral palsy associated with impaired sensory tracts. *NeuroImage Clin.* 17, 198–212. doi: 10.1016/j.nicl.2017.10.021

Pavão, S. L., dos Silva, F. P. S., Savelsbergh, G. J. P., and Rocha, N. A. C. F. (2015). Use of sensory information during postural control in children with cerebral palsy: systematic review. *J. Mot. Behav.* 47, 291–301. doi: 10.1080/00222895.2014.981498

Perkins, B. A., Olaleye, D., Zinman, B., and Bril, V. (2001). Simple screening tests for peripheral neuropathy in the diabetes clinic. *Diabetes Care* 24, 250–256. doi: 10.2337/diacare.24.2.250

Prieto, T. E., Myklebust, J. B., Hoffmann, R. G., Lovett, E. G., and Myklebust, B. M. (1996). Measures of postural steadiness: differences between healthy young and elderly adults. *IEEE Trans. Biomed. Eng.* 43, 956–966. doi: 10.1109/10.532130

Redekop, S., Andrysek, J., and Wright, V. (2008). Single-session reliability of discrete gait parameters in ambulatory children with cerebral palsy based on GMFCS level. *Gait Posture* 28, 627–633. doi: 10.1016/j.gaitpost.2008.04.008

Rosenbaum, P., Paneth, N., Leviton, A., Goldstein, M., Bax, M., Damiano, D., et al. (2007). A report: the definition and classification of cerebral palsy April 2006. *Dev. Med. Child Neurol.* 49, 8–14. doi: 10.1111/j.1469-8749.2007.tb12610.x

Ross, S. E., Linens, S. W., Wright, C. J., and Arnold, B. L. (2013). Customized noise-stimulation intensity for bipedal stability and unipedal balance deficits associated with functional ankle instability. *J. Athl. Train.* 48, 463–470. doi: 10.4085/1062-6050-48.3.12

Russell, D. J., Avery, L. M., Walter, S. D., Hanna, S. E., Bartlett, D. J., Rosenbaum, P. L., et al. (2010). Development and validation of item sets to improve efficiency of administration of the 66-item gross motor function measure in children with cerebral palsy. *Dev. Med. Child Neurol.* 52, e48–e54. doi: 10.1111/j.1469-8749.2009.03481.x

Schmidt, R. A., and Lee, T. D. (2011). *Motor Control and Learning: Sensory Contribution in Motor Control.* Champaign, IL: Human Kinetics.

Shumway-Cook, A., and Woollacott, M. H. (2012). *Motor Control: Translating Research into Clinical Practice (Vol. 4th).* Philadelphia, PA: Wolters Kluwer Health/Lippincott Williams and Wilkins.

Stackhouse, S. K., Binder-Macleod, S. A., and Lee, S. C. K. (2005). Voluntary muscle activation, contractile properties, and fatigability in children with and without cerebral palsy. *Muscle Nerve* 31, 594–601. doi: 10.1002/mus.20302

Stansfield, B. W., Hillman, S. J., Hazlewood, M. E., Lawson, A. M., Mann, A. M., Loudon, I. R., et al. (2003). Normalisation of gait data in children. *Gait Posture* 17, 81–87. doi: 10.1016/s0966-6362(02)00062-0

Temlett, J. A. (2009). An assessment of vibration threshold using a biothesiometer compared to a C128-Hz tuning fork. *J. Clin. Neurosci.* 16, 1435–1438. doi: 10.1016/j.jocn.2009.03.010

Williams, E. N., Carroll, S. G., Reddihough, D. S., Phillips, B. A., and Galea, M. P. (2005). Investigation of the timed "Up and Go" test in children. *Dev. Med. Child Neurol.* 47, 518–524. doi: 10.1017/s0012162205001027

Wingert, J. R., Burton, H., Sinclair, R. J., Brunstrom, J. E., and Damiano, D. L. (2008). Tactile sensory abilities in cerebral palsy: deficits in roughness and object discrimination. *Dev. Med. Child Neurol.* 50, 832–838. doi: 10.1111/j.1469-8749.2008.03105.x

Wingert, J. R., Burton, H., Sinclair, R. J., Brunstrom, J. E., and Damiano, D. L. (2009). Joint-position sense and kinesthesia in cerebral palsy. *Arch. Phys. Med. Rehabil.* 90, 447–453. doi: 10.1016/j.apmr.2008.08.217

Wingert, J. R., Sinclair, R. J., Dixit, S., Damiano, D. L., and Burton, H. (2010). Somatosensory-evoked cortical activity in spastic diplegic cerebral palsy. *Hum. Brain Mapp.* 31, 1772–1785. doi: 10.1002/hbm.20977

Yu, Y., Tucker, C. A., Lauer, R. T., and Keshner, E. A. (2019). Influence of visual dependence on inter-segmental coordination during upright stance in cerebral palsy. *J. Mot. Behav.* doi: 10.1080/00222895.2019.1610860 [Epub ahead of print].

Zackowski, K. M., Smith, S. A., Reich, D. S., Gordon-Lipkin, E., Chodkowski, B. A., Sambandan, D. R., et al. (2009). Sensorimotor dysfunction in multiple sclerosis and column-specific magnetization transfer-imaging abnormalities in the spinal cord. *Brain* 132, 1200–1209. doi: 10.1093/brain/awp032

Zarkou, A. (2017). *Somatosensory Deficits Affect Balance and Motor Function in Children with Cerebral Palsy: Stochastic Resonance Stimulation can Modulate Somatosensation to Enhance Balance*. Newark, DE: University of Delaware. [Dissertation thesis].

Zarkou, A., Lee, S., Prosser, L., Hwang, S., and Jeka, J. (2016). The role of lower extremities' somatosensory ability on motor function in children with cerebral palsy. *Dev. Med. Child Neurol.* 58, 73–74. doi: 10.1111/dmcn.107_13224

Zarkou, A., Lee, S. C. K., Prosser, L. A., Hwang, S., and Jeka, J. (2018). Stochastic resonance stimulation improves balance in children with cerebral palsy: a case control study. *J. Neuroeng. Rehabil.* 15:115. doi: 10.1186/s12984-018-0467-7

Conflict of Interest: The authors declare that the research was conducted in the absence of any commercial or financial relationships that could be construed as a potential conflict of interest.

frontiers in Neurology

ORIGINAL RESEARCH
published: 28 February 2020
doi: 10.3389/fneur.2020.00016

Feasibility of a Home-Based Action Observation Training for Children With Unilateral Cerebral Palsy: An Explorative Study

Elena Beani[1], *Valentina Menici*[1], *Adriano Ferrari*[2,3], *Giovanni Cioni*[1,4] *and Giuseppina Sgandurra*[1,4]*

[1] Department of Developmental Neuroscience, IRCCS Fondazione Stella Maris, Pisa, Italy, [2] Children Rehabilitation Unit, Azienda USL - IRCCS Reggio Emilia, Reggio Emilia, Italy, [3] Department of Neuroscience, University of Modena and Reggio Emilia, Modena, Italy, [4] Department of Clinical and Experimental Medicine, University of Pisa, Pisa, Italy

Unilateral Cerebral Palsy (UCP), the most frequent form of Cerebral Palsy, usually affects more the upper limb (UL) than the lower limb. Rehabilitation programs are addressed to improve manual abilities and UL use. In recent years, Information and Communication Technology (ICT) has been introduced in rehabilitation to increase treatment opportunities for patients, and also in home-based intervention. Moreover, the discovery of the Mirror Neuron System allowed to insert a new paradigm of treatment that is the Action Observation Training (AOT). The aim of the present study was to investigate the feasibility of a new rehabilitative home-based approach, called Tele-UPCAT (Tele-monitored UPper Limb Children Action Observation Training), based on the principles of AOT, in a group of Italian children and adolescents with UCP. This investigation was to provide information about the possibility of introducing ICT in telerehabilitation field. Twenty-nine children aged 11.73 ± 3.65 years (range 6.00–18.75) with a diagnosis of UCP participated in the study. They carried out 15 days of training based on the AOT paradigm with Tele-UPCAT system while wearing Actigraphs on both wrists. The feasibility of both training and study design and procedures was assessed through nine criteria taken from existent literature and from a questionnaire designed and realized *ad hoc* for the purpose, based on standard items of usability and acceptability. All feasibility criteria were met: 80% of training sessions were completed in the planned time and no significant technical issues were found. From the questionnaire, total scores were all above 82.15%, while the four sections obtained the following scores: (i) customization of exercises 80.00%; (ii) acceptability at home, 77.50%; (iii) required effort 80.00%; and (iv) suitability of manual and software 95.00%. No differences were found for age and sex. Tele-UPCAT demonstrated to be feasible as a home-based AOT for children and adolescents with UCP. Trial registration NCT03094455.

Keywords: feasibility, home-based training, action-observation training, upper limb, unilateral cerebral palsy, children

OPEN ACCESS

Edited by:
Deborah Gaebler-Spira, Northwestern University, United States

Reviewed by:
Sandeep K. Subramanian, The University of Texas Health Science Center at San Antonio, United States
Pedro Ribeiro, Federal University of Rio de Janeiro, Brazil

***Correspondence:**
Giuseppina Sgandurra
g.sgandurra@fsm.unipi.it

Specialty section:
This article was submitted to Movement Disorders, a section of the journal Frontiers in Neurology

Received: *04 November 2019*
Accepted: *08 January 2020*
Published: *28 February 2020*

Citation:
Beani E, Menici V, Ferrari A, Cioni G and Sgandurra G (2020) Feasibility of a Home-Based Action Observation Training for Children With Unilateral Cerebral Palsy: An Explorative Study. Front. Neurol. 11:16. doi: 10.3389/fneur.2020.00016

INTRODUCTION

Unilateral Cerebral Palsy (UCP) is the most frequent form of Cerebral Palsy, representing 30–40% of all affected children (1, 2). Due to the fact that in the majority of cases the upper limb (UL) is more affected than the lower limb (LL), rehabilitation programs are mainly addressed to improve manual abilities and UL use and integration. Together with the traditional methods of rehabilitative intervention, the discovery of the Mirror Neuron System allowed to insert a new paradigm of treatment, that is, the Action Observation Training (AOT) (3). The AOT is based on neurophysiological knowledge that the observation of a goal-directed action activates the same neural substrate, the Mirror Neuron System, as the physical execution of the same action (4, 5). AOT evidence is rising in literature, mainly in adult population, but in some works, it has been used also in pediatric samples (6–10).

Beside face-to-face trials, the recent introduction of Information and Communication Technologies (ICTs) has increased treatment opportunities for patients directly at home. Home-based therapies, defined as "therapeutic activities that the child performs with parental assistance in the home environment with the goal of achieving desired health outcomes" (11), represent a way to facilitate children and adolescent access to rehabilitation and to enhance motivation.

Innovative rehabilitation trainings based on ICT devices have been introduced to increase opportunities and to add objective data in rehabilitation. The use of ICT for rehabilitation purposes at home is referred to as telerehabilitation (12, 13). Telerehabilitation allows care continuity and limits time and economic demands for families and institutes. Moreover, it enables precise monitoring of patients' performance through online tracking (14, 15).

From the union between the innovative paradigm of treatment that is the AOT and the innovative approach represented by the home-based therapy, the Tele-UPCAT (Tele-monitored UPper Limb Children Action Observation Training), built by the BioRobotics Institute of Scuola Superiore Sant'Anna in collaboration with IRCCS Fondazione Stella Maris, has been recently introduced in the panorama of rehabilitative proposals for children with UCP (16).

Tele-UPCAT is a platform to practice AOT at home, designed to be user-friendly both for children and adolescents, at home in a playful setting with integrated smart features. In fact, two age-related interfaces have been developed, following the interest and motivational factors of the two age ranges; moreover, the management of the entire system is very simple for families, as the software has an automatic process of execution and continuation of the program just needs to push a button; finally, the integrated camera has a reminder for being turned on and off.

Given the economic and energy advantages that home therapy brings, the issues of usability and acceptability of a technology-based therapy into the home environment need to be investigated. It is crucial to investigate the end-user opinions during the use at home of a new tool. A new home rehabilitation system could be effective, but its use could be not feasible from the user's point of view; this highlights the importance of evaluating the feasibility aspects before evaluating the effectiveness.

Based on these aspects, the aim of the present study is to investigate the feasibility, acceptability, and usability of the Tele-UPCAT in a group of Italian children and adolescents with UCP. This investigation will provide information about the possibility of introducing ICT in the telerehabilitation field.

MATERIALS AND METHODS

This study was a part of a wider study, aimed to investigate if a new Information and Communication Technology platform, called Tele-UPCAT, could be able to deliver the AOT in a home setting and test its feasibility and efficacy in children and adolescents with UCP.

The study has been approved by Tuscany Pediatric Ethics Committee (169/2016), and it was registered (NCT03094455) on Clinical Trials.gov.

According to CONSORT guidelines (17), the sample size estimate has been based on projected treatment effect on the primary outcome measure, the Assisting Hand Assessment (AHA). Taking into account the study design and the stratification, a minimum sample size of 10 per group was required in order to detect a 1.40 effect size [the value based on our preliminary data; (8, 18)] at a significant level of 0.05% and 80% power. Considering 20% of possible dropouts, a minimum of 12 participants per group were recruited, with a total sample of 24 participants.

Protocol and system description, together with the psychometric properties of the selected outcome measures, have been already extensively reported elsewhere (16). Briefly, the study has been designed as a randomized, allocation concealed (waitlist control) and evaluator-blinded clinical trial with two investigative arms, which were AOT vs. standard care (SC). Both groups are assessed with clinical tools (Assisting Hand Assessment, Melbourne Assessment 2, Box and Block Test, ABILHAND-Kids, Participation and Environment Measure—Children and Youth and Cerebral Palsy Quality of Life Questionnaire) and technological outcome measures (a purpose-designed sensorized toy and Actigraphs). The experimental group, after the first assessment (T0), proceeded with a home-based 3-week AOT with the Tele-UPCAT system, then the assessment is repeated immediately after this period (T1) and after 8 (T2) and 24 (T3) weeks after the end of the training. The control group starts with a 3-week period of SC, then follows the same pathway as the experimental group, which meant the AOT and the follow-up assessments. Parents of the enrolled participants were asked to provide written informed consent in order to allow data collection and analysis for study purposes. All parents provided informed consent. For subjects of ages above 12 years, an additional consensus has been asked to the child, with a dedicated form.

Participants

Participants were recruited among children and adolescents with congenital UCP referring to IRCCS Fondazione Stella Maris

(Pisa) and Unit of Children Rehabilitation of S. Maria Nuova Hospital (Reggio Emilia).

The main inclusion criteria were as follows: age between 5 and 20 years, confirmed diagnosis of spastic motor type of UCP, minimum ability of manual function defined as the ability to passively hold an object placed in the hand or hold and stabilize an object with a hand while the other manipulates it (i.e., House Functional Classification System, HFCS $\geq$ 2), a normal cognitive level (i.e., IQ $\geq$ 70), and no disabling behavioral disorders. The main exclusion criteria were as follows: previous orthopedic surgery or botulinum toxin A (BoNT-A) injection in the UL within 6 months prior to the enrolment of this study.

Patients' recruitment was conducted by a research team member who assisted, when necessary and requested, families during the AOT and proposed to fill in a questionnaire specifically designed for the purpose (described below) of assessing the feasibility at the end of the training. In case of assent, parents and/or children were requested to complete the questionnaire in the printed or electronic version.

Recruitment for this preliminary study on feasibility started after the approval of the research project by the Ethics Committee.

Study Design and Procedure

This study represents a part of the Tele-UPCAT trial, an exploratory randomized, allocation concealed (waitlist controlled) and evaluator-blinded clinical trial with two investigative arms using an AOT intensive rehabilitation program of home-based AOT compared with SC in children and adolescents with UCP, whose recruitment started on March 2017 and was completed on November 2018. The total minimum sample size was planned for 24 children.

As shown in the study design (16), participants were assessed at baseline and randomly allocated to the immediate AOT group or waitlist SC.

The primary outcome measure was the AHA. The Melbourne Assessment 2, Box and Block Test, ABILHAND-Kids, Participation and Environment Measure—Children and Youth, and Cerebral Palsy Quality of Life Questionnaire were included as secondary measures. In addition, quantitative measures from the available ICT were added, i.e., the assessment with a sensorized object and two wearable sensors on both wrists (Actigraphs GXT3+), used both during the assessments and in the intervention period (AOT and SC). The assessment points were the week before (T0) and after (T1) the period of AOT/SC. Further assessments were then carried out in the week after the AOT period for the waitlist group (T1 plus) and at 8 weeks (T2) and 24 weeks (T3) after the AOT.

Concerning the intervention, the experimental group performed the AOT at home for 3 weeks using a customized Tele-UPCAT system. Participants were asked to complete 15 sessions of the AOT at home for 45 to 60 min per working day for 3 weeks (5 days per week). Through the Tele-UPCAT system, they watched 3-min first-person video sequences of unimanual or bimanual goal-directed actions, and then they had to execute the same action for 3 min. Three different actions were proposed twice each day. The type and the order of the games were identical for all participants in terms of actions (unilateral or bilateral and increasing complexity) but variable in terms of objects (the same goal but different shape of toys) in order to be suitable for different hand abilities.

The Tele-UPCAT platform has been delivered to the participant's home by the engineers in charge of system installation together with a research team member, who assisted families for the beginning of the training. Weekly telephone-based contact with the participants and their parents was then conducted by the research team member, with the aim of assisting them for the training, sustaining training compliance and motivation, and recording the reasons of any eventual issue.

The control group received usual care for 3 weeks, which might include UL training, and then they were asked to receive the AOT at home by means of the Tele-UPCAT system after 3 weeks. In each case, participants were asked to wear an Actigraph at both wrists to measure the UL mean activity and to fill in a daily diary with notes related to the time of main activities of the day and the time with and without Actigraphs. In this way, some quantitative data were added not only during the assessments but also during the 3 week period of training and SC.

Data on training performance were collected on a remote database available at IRCCS Fondazione Stella Maris. The number of days for completing the program (15 days of training) and effective time with/without wearing Actigraphs were recorded for each patient. An *ad hoc* questionnaire has been created and administered to all participants at the post-training assessment (T1 for the AOT group and T1 plus for the control group) by an operator who structured it as an interview to the child/adolescents with the presence of parents.

Intervention

Tele-UPCAT system (**Figure 1**) is composed of two different modules: *the observation module (OM)*, which is mainly dedicated to the presentation of videos for the "observational task," and the *motor performance module (MPM)*, for the "exercise execution," which consists of objects and toys for executing the action observed in videos and two Actigraphs (wGT3X-BT) for recording UL activities.

All the actions were chosen based on some daily activities, goal-directed to meaningful actions of children and adolescents that evocate hand and arm movements to be stimulated because of their impairment due to the UCP. In the first half of the sessions, movements require the use of the affected side and, in the second half, the bimanual cooperation. The selected objects are mainly toys (e.g., some glitter glue with some marbles to be attached to a plastic frame) or tools that remind one of some daily objects (such as a bottle and a glass). Details of actions of the training are presented in the study protocol description (16).

Each daily session is composed of three goal-directed actions with increasing difficulty within days of the training. As described above, the training is planned in 15 sessions to be performed once a day in 3 weeks, 5 days a week.

Each activity is presented with an age-appropriate software package for motivating participants and explaining the training rules: the cartoon with the adventures of an explorer called Ubi and its missions in the galaxy for children aged <12 years and a

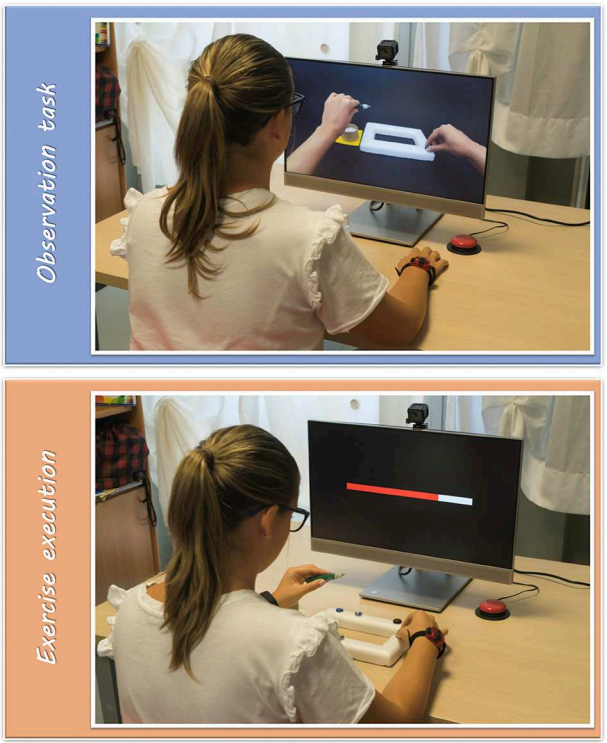

FIGURE 1 | The Tele-UPCAT system.

PowerPoint presentation with simple slides and voice guide for adolescents (>12 years).

Outcome Measures

The feasibility of the AOT with Tele-UPCAT was investigated by three measures: the acceptability and usability from the questionnaire, the criteria for the feasibility taken from the literature, and the acceptability in terms of wearing time of Actigraphs.

First, the study of the acceptability and usability was assessed through the *ad hoc* purpose-designed questionnaire (widely described below). According to the study design (16), the questionnaire was administrated during the post-training assessment (T1 or T1 plus for the immediate AOT and the waitlist group, respectively).

Moreover, feasibility outcome measures were taken from the literature (19–21), and they are criteria based on relevant recommendations for conducting research on feasibility. In details, there are nine feasibility measures: four relative to training intervention (accessibility, training motivation, technical smoothness, and training compliance) and five for the procedures and study design (participation willingness, participation rates, loss to follow-up, assessment timescale, and assessment procedures).

These criteria have been adapted for the Tele-UPCAT study and in details measures have been fixed as follows:

Feasibility of Intervention:

- *Acceptability*: intelligibility of rules of the activity in terms of preparation and execution;
- *Training compliance*: duration of the training (at least 3 weeks, that is, the fixed interval of the training);
- *Technical smoothness*: good functioning of the system, defined as the quantity of issues and malfunctioning experienced with the system;
- *Training motivation*: motivation and perceived effort in carrying out the training.

Feasibility of Study Design and Procedures:

- *Participation willingness*: Acceptance of the participation in the study;
- *Participation rates*: Completion of the training (no dropout);
- *Loss to follow-up*: Possibility to collect all data from all outcome measures;
- *Assessment time scale*: Required time for collecting all outcome measures (at least 1 week);
- *Assessment procedures*: Loss to follow-up rates.

The Questionnaire:

To assess the usability and acceptability of the whole therapy, a 32-query questionnaire was created. The questionnaire was tailored for the Tele-UPCAT program, but it is conformed to the standard definitions of usability (22–24) and acceptability (25, 26), respecting items generally evaluated in this kind of assessments.

The questions are divided into four sections composed of eight queries that analyze crucial items of the therapy, from exercises' features to the acceptability of the Actigraphs and enjoyment of the whole therapy. The groups are as follows:

- "Customization of the exercises": how the participants perceived the exercises as personalized following their abilities and needs, how difficult they were perceived, their preference about the kind of exercise.
- "Acceptability of the Tele-UPCAT system at home in daily life": how participants coped with a technology system directly installed in their home and the commitment to the therapy in everyday life.
- "Required effort": whether the participants perceived the whole treatment as tiring and strenuous and the use of Actigraphs every day as bothersome.
- "Suitability of the manual/software": whether the manual was complete and clear in delivering the instruction to use the system and if the software (including the program) was enjoyable and easy to use, without technical issues.

The questions were structured to be easy to understand for even the youngest participant. When necessary, the parent's perception was taken into account. The questions are followed by a five-point Likert scale, ranging from 1 to 5, where 1 identifies the most negative response and 5 the most positive one. Younger children were helped with a smiley meter to facilitate them in expressing their feelings: they had five illustrated faces with

five different expressions, from the saddest to the happiest, and they were asked to indicate the one that better described their thoughts.

Every section of the questionnaire can range from a minimum of 8 (strongly negative) to a maximum of 40 (strongly positive), for a total of 160 for the whole questionnaire, indicating the greatest level of acceptability and usability.

Participants were asked to supply personal thought on every item of the questionnaire to have a wider view on the patient's feedback.

Finally, the wearing time of Actigraphs extracted both from the data and the diary has been considered to have an additional index of acceptability.

Data Collection

The questionnaire was delivered immediately after the end of the AOT therapy period (T1 or T1 plus) in a face-to-face interview with the patient, with or without the help of the parents. The face-to-face interview allowed the interviewer to explain the queries when necessary and the participant to give their perception more easily.

Daily diaries were also collected to have the data about the wearing time of Actigraphs and parameters about the training time for the analysis of the nine criteria of feasibility.

Statistical Analysis

Clinical and quantitative data were analyzed by means of the Statistical Package for Social Sciences (SPSS, version 20.0). Median and 95% confidence intervals were calculated. For the questionnaire, raw total score and total for each questionnaire groups and relative percentages were calculated. As a first step, a descriptive analysis of the whole enrolled sample was carried out. Normality of data distribution was verified by Shapiro–Wilk's test, and in relation to the non-normal distribution, we treated the data with nonparametric analyses. In order to assess potential differences between the experiences in the two different age-appropriated software packages (Ubi vs. slides), the Mann–Whitney U independent sample test was performed for the raw scores.

RESULTS

From the developers' point of view (clinicians and engineers), the Tele-UPCAT platform was designed, realized, and used for its features, judged as optimal at the end of the study: (i) it is possible to present videos and activities based on the developmental needs of each subject; (ii) it can provide a cycle of 15 sessions of daily training, more intensive than the traditional rehabilitative training (which occupies no more than once a week) with low daily duration (no more than 1 h a day), without requiring excessive efforts to be added to the everyday demands of school and other activities; and iii) it is easily transportable and adaptable for in-home use.

Participants

Participants of this feasibility study were those who were accepted to participate in the wider research project and answered to the *ad hoc* questionnaire, created and developed for the purpose: 29 children and adolescents carried out the Tele-UPCAT training, and all of them filled in the questionnaires on which the present feasibility study is based.

TABLE 1 | Sample characteristics.

Age (year)	Mean	11.73
	SD	3.65
Sex	F	14
	M	15
Affected side	Right	19
	Left	10
HFCS	2–3	5
	4–5	13
	6–8	11

HFCS, House Function Classification System; SD, Standard Deviation.

Demographic characteristics of the 29 participants are shown in **Table 1**. The mean age was 11.73 ± 3.65 years, with a similar number of males and females, 15 and 14, respectively. The affected limb was on the left side in 10 cases and on the right side in 19 cases. According to House Function Classification System (HFCF), five children were in the range between 2 and 3 (meaning a possible hold of the object passively with the affected hand); 13 in the range between 4 and 5 (which means that it is possible to actively stabilize the object with the affected hand); and 11 between 6 and 8 (that is a good or active use of the affected hand).

Training Outcome

All participants completed the training. In details, the mean value of days for achieving the 15 sessions was 20.48 days, ranging from 17 to a maximum of 24, and this was due to the fact that seven patients required more than 21 days (the 3 weeks originally planned) to finish the training.

The wearing time of Actigraph was high in majority of the cases, with a mean of 74.56% and a range from 26.81 to 99.83%.

Feasibility Outcome

Feasibility of Intervention

All four criteria regarding the feasibility of the training intervention were met:

1) All participants figured out instructions both from the printed manual and the software without requiring further explanations and correctly understood goals and ways to proceed each training activity.
2) Overall, all participants reached the criterion of completing at least 80% of the training in 3 weeks; only seven participants completed the whole training in a period ranging from 22 to 24 days.
3) Only two participants experienced a technical issue in the software. These issues were fixed with a phone call with the technical support. One participant had an issue with the camera and it was substituted with a new one.

TABLE 2 | Results of Tele-UPCAT questionnaire.

	All Sample ($n = 29$)		Ubi ($n = 14$)		Slides ($n = 15$)		Ubi vs. Slides
	Median [95% CI]		Median [95% CI]		Median [95% CI]		z score* (p)§
	Raw scores	%	Raw scores	%	Raw scores	%	
Customization of exercises	32.00 [29.23–33.38]	80.00 [71.23–82.03]	33.00 [31.18–35.15]	80.00 [73.04–86.55]	32.00 [25.31–33.01]	80.00 [63.83–82.54]	−1.642 (0.104)
Acceptability at home	31.00 [29.43–33.00]	77.50 [73.07–81.71]	32.00 [29.72–34.78]	77.50 [73.27–85.47]	31.00 [27.30–32.88]	77.50 [68.24–82.21]	−0.957 (0.347)
Required effort	32.00 [30.96–33.99]	80.00 [76.73–83.49]	33.00 [31.21–35.79]	80.00 [76.77–86.57]	30.00 [29.23–33.49]	75.00 [73.08–83.73]	−1.360 (0.190)
Suitability of manual/software	38.00 [36.78–38.35]	95.00 [91.37–95.58]	38.50 [37.39–31.11]	96.25 [91.88–97.70]	36.00 [35.48–38.16]	90.00 [88.70–95.39]	−1.761 (0.091)
TOTAL	132.00 [127.70–137.43]	82.15 [79.81–85.90]	135.50 [130.56–143.77]	84.69 [81.60–89.86]	130.00 [120.61–134.48]	81.25 [75.38–84.05]	−1.666 (0.104)

*Mann–Whitney sample test.
§2-sides significant level at 0.05.
CI: 95% confidence interval.

Nevertheless, all participants managed to continue with the training.

4) Regarding the training compliance, all participants showed a positive score (only in one case, just a bit more than neutral) in the "required effort" section of the questionnaire.

Feasibility of Study Design and Procedures

All criteria regarding the feasibility of the study design and procedures were met:

5) All eligible participants (100%) agreed to join the project. In three cases, families asked to organize the training in periods in which the required time by the school was reduced (i.e., winter or summer holidays).
6) The totality of enrolled participants agreed to perform the training intervention (i.e., the AOT at home). In one case, a participant started with the SC period (see study design for further details) but did not give the consensus for carrying out the home AOT.
7) All outcome measures (both feasibility and efficacy measures) were collected during assessments and there were no missing data.
8) Follow-up data were collected within a week after the training period, as planned.
9) There was no follow-up loss for any participant who finished the training program; 100% of the participants completed all assessments.

The Questionnaire

All the 29 children and adolescents gladly accepted the interview or the online questionnaire, adding also some personal comments.

In general, all participants showed a good level of acceptability and usability, with total scores all above 103 points (64.38%). Regarding the four sections: "customization of the exercises" is the one with the lowest range of raw scores (range 18–38); then "acceptability of the Tele-UPCAT system at home in daily life" with a range of 22–38; "required effort" presented a range from 26 to 40; and "suitability of the manual/software" presented a range of 34–40.

There were no differences in the total scores of answers related to the sex of the subjects ($p > 0.05$) and the HFCS level ($p > 0.05$) or the different versions of the software used (Ubi or slides) ($p > 0.05$).

The general opinion of the interviewed sample was globally positive, and there were no significant differences within groups.

Median and 95% confidence interval of scores in the questionnaire (both total and section scores) are shown in **Table 2.**

Even if the median values between the two age groups were similar, the younger subjects (Ubi) showed larger and higher ranges (**Figure 2**).

Customization of the Exercises

This section showed the lowest scores. The median values between the two groups were similar, but the distribution of the answers was toward higher values in younger subjects and lower in older ones (**Figure 3**).

Acceptability of the Tele-UPCAT System at Home in Daily Life

In this section, the younger children showed more variability in their answers than adolescents, who gave more similar answers (**Figure 4**).

Required Effort

This section presented similar median values between the two groups, but the distribution is different: in fact, for children aged <12 years (Ubi group), the required effort is perceived as feasible and the tendency of the scores is toward higher values, while for adolescents, the distribution is equal around the median value and globally lower than children's scores (**Figure 5**).

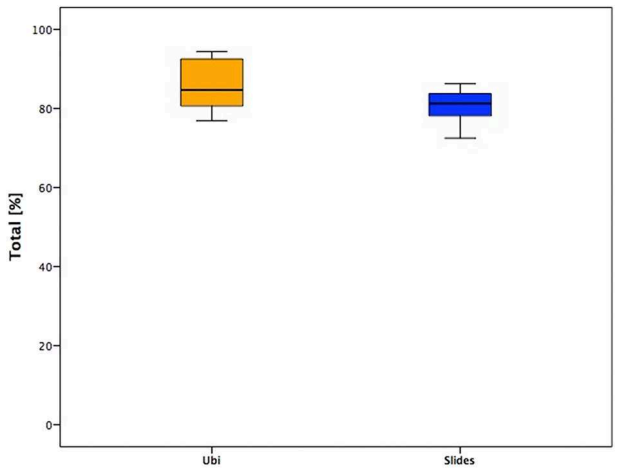

FIGURE 2 | Total answers of the two groups.

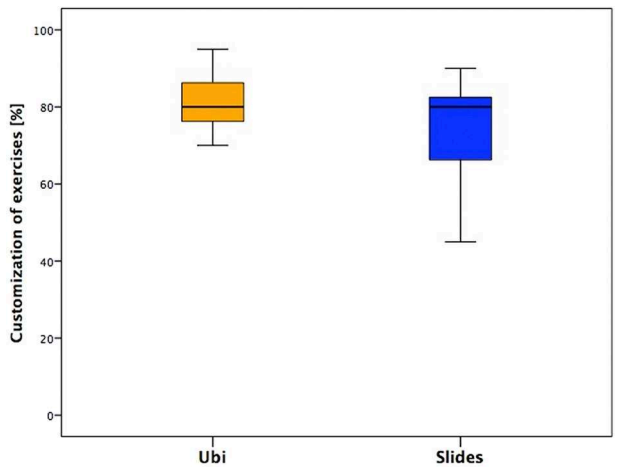

FIGURE 3 | Answers of the section "Customization of the exercises" of the two groups.

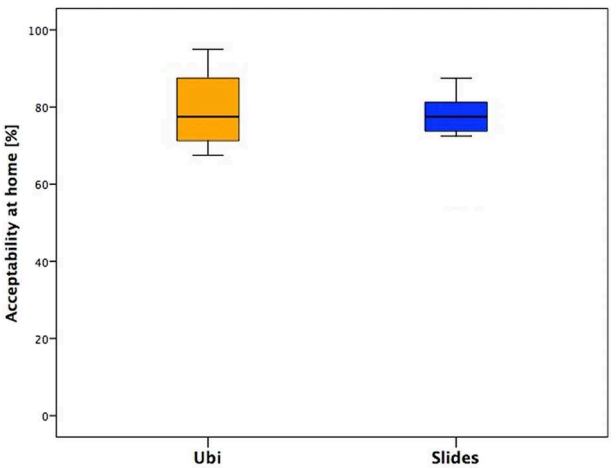

FIGURE 4 | Answers of the section "Acceptability of the Tele-UPCAT system at home in daily life" of the two groups.

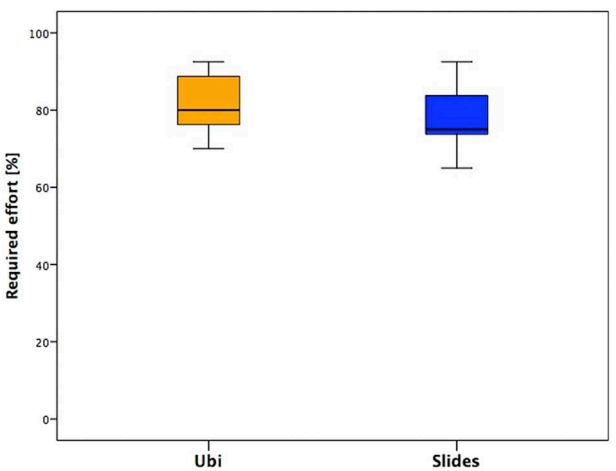

FIGURE 5 | Answers of the section "Required effort" of the two groups.

Suitability of the Manual/Software

In the last section, one positive aspect is that almost no one needed technical assistance or encountered technical issues during the training, and this supports the stability of the system and its consequent appropriateness for home trainings (**Figure 6**).

DISCUSSION

It is widely known that the success of a trial also depends on end users' opinions and satisfaction, which motivate patients to carry out the training and the research staff to improve and optimize the intervention; as a consequence, these two aspects can be positively influenced.

In the present work, we tested the feasibility of a rehabilitative intervention based on the AOT delivered at home, in a sample of children and adolescents with UCP, by the use of an ICT platform. Moreover, we tested also the feasibility of the study design and procedures. To test both these feasibility aspects, in addition to the *ad hoc* questionnaire and data about the wearing time of Actigraphs, a series of previously set and validated measures (21) based on relevant literature (19, 20) have been used.

Based on the data of the number of days to complete the training, the absence of dropouts, and the results of the questionnaires, the Tele-UPCAT platform was demonstrated to be acceptable and usable for home-based training. In addition to this, the platform has shown its stability; in fact, no errors of hardware or software issues have been experienced. In the *ad hoc* questionnaire on training acceptability, most participants indicated a positive commitment to the training program and, together with their parents, they reported high levels of perceived usefulness of the program. For this reason, also the training program can be considered sustainable and relevant, although if

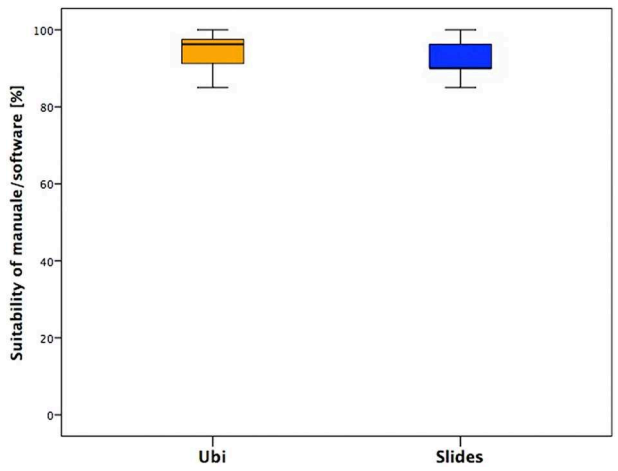

FIGURE 6 | Answers of the section "Suitability of the Manual/Software" of the two groups.

we can hypothesize that, weekly contacts with the staff could have a role in sustaining motivation and adherence to the training. This hypothesis has been already reported in the literature (27, 28); in fact, it has been demonstrated how the presence of a tutor could be motivating for participants of a trial. Another explanation could be that in telerehabilitation programs, subjects perceive the planning of competent drivers (i.e., the rehabilitation staff) who remotely guide the training to be behind the training activities. programs, while performed without the technologies, could leave the subjects alone. They can perceive the stress of executing the exercises, while the use of technology can give them the perception that they are executed as in the real rehabilitation setting.

As we included a sample of patients with a wide range of age, the current data can be considered quite representative of the population of children and adolescents with UCP; this suggests that the AOT exercises may be successfully proposed for a telemonitored intervention directly at families' houses. The use of telerehabilitation might increase the accessibility of rehabilitation to a large number of UCP children (e.g., children that live far from the clinical center). It could become cheaper than traditional treatment because telemonitored rehabilitation games could allow the possibility of reducing the "number of children per therapist," guaranteeing an individualized and intensive training for each patient.

Concerning the feasibility of study design and procedures, we registered a high involvement of participants and families, since all the eligible families accepted to participate. This suggests that families of UCP children and adolescents are highly motivated to introduce ICT platforms for UL rehabilitation at their home.

The participation rate was extremely high, as none of the participants dropped out of the study neither during the AOT home training period nor at follow-up assessments, and also the adherence to the training was very good: only some participants required more than 3 weeks (21 days) to finish the 15 sessions. From their comments, it emerged that this was due to the period of the training execution, i.e., during the school, because during the week, they had many scheduled appointments (therapies, homework, sport, etc.), and they sometimes had a lack of free time to dedicate to the AOT. On the other hand, many participants asked to carry out the training during holidays (Christmas, Easter, and summer) in order to facilitate the organization.

According to the results of the questionnaires, the general opinion of the interviewed sample was globally positive, and there were no significant differences between children (<12 years, Ubi sample) and adolescents (>12 years, Slides sample). This is the first interesting data, because it means that the effort of creating a customized training, which takes care of sex and age preferences, was well-rewarded: all the opinions were coherent and showed appreciation and positive feedback.

When observing the total score of answers, the median values were similar in the two groups, but the score distribution showed higher values in younger subjects. This could be explained because children lived the training in a playful way and performed the exercises with a more motivational software package (Ubi had to achieve missions). This result could also be due to the presence of their parents during the treatment. On the other hand, some adolescents demonstrated to like less the training, and a deeper analysis of the answers of the four sessions gave a clearer view on this aspect.

Customization of the Exercises

This section showed that the lowest scores with similar values between groups, slightly higher in younger subjects and lower in adolescents.

This could be explained by the fact that the objects selected for the exercises were more suitable for younger children in terms of sizes and features. In fact, the pool of objects and toys has been originally selected to be suitable for a wide range of ages, thinking about making them more compliant for younger children. However, this could mean that sometimes the toys resulted to be not suitable or excessively small for adolescents; moreover, children aged <12 years probably preferred to play with toys, while adolescents could have appreciated something more appropriate for their age and interests. This could clarify the different opinions between the two groups.

In addition, the exercises maybe resulted poorly engaging and boring for adolescents because of their repetitiveness. Despite this, some interesting opinions came from the adolescents. Although they seem to have less appreciated the training, they were more conscious about its relevance, as reported by an example of their personal comments as follows: "I have used some movements of the training in daily life," "I have used the hand to do certain movements I didn't know I was able to do," "Now I think about the right movement I've seen during the training and I can do it better," and "I'm more aware of my hand now."

Acceptability of the Tele-UPCAT System at Home in Daily Life

Focusing on the specific answers, more variable in younger children than in adolescents, we noticed that an intensive training at home, which means dedicated time and space for subjects and

their family, is feasible but requires organization of home spaces and daily activities. In the children's group, answers' variability is probably related to the weekly routine: there were subjects who had many therapies and other family activities during the days and consequently attending the daily training for them was more demanding; on the other hand, some others were less busy, and the steady commitment of the training represented an appreciated routine.

Required Effort

This section presented similar median values between the two groups, with a little difference between younger children and adolescents, in fact the second group presented values slightly lower and less variable.

The questions of this section were more focused on the use of Actigraphs and the level of difficulty of exercises. From the free comments in the questionnaire, it emerged that the wristbands were not quite comfortable; some adolescents reported itchiness or being bothered and, in some cases, also embarrassment while wearing Actigraphs in social contexts (school, parties, free time).

Furthermore, the difficulty in performing some actions emerged more in adolescents. It has been explained because they were more aware of exercise movement features, and they reported pain or complaint due to the frequency of the requested movements (done with two intervals of 3 min each).

Several subjects found the duration of the videos excessive, and thus the evaluation of the exercises as boring. They understood the meaning of the two observational intervals, and they demonstrated good levels of attention to the videos, but all of them judged the situation as boring and the videos a little bit too long.

Suitability of the Manual/Software

In the last section, emerged the stability of the system and its consequent appropriateness for home trainings.

The manual and software were overall considered as clear and complete. Especially the children found the game of their specific software amusing and fun. The slight difference in the answers is basically related to the already reported different software features of the two groups.

CONCLUSIONS

Action Observation Therapy is a new innovative tool that, according to the literature, seems to bring a significant improvement in activity and body function in ICF domains in children and adults. Since the first AOT treatment was carried out by Ertelt et al. (29), the number of studies on adults and children increased and, in this framework, also a new type of innovative therapy, such as the AOT with an ICT platform, has recently been proposed directly at patients' home (30).

We can gladly conclude that, thanks to the presented findings, the home-based AOT is feasible for children and adolescents with UCP. Of course, the next perspective will be to analyze the results of the RCT study in order to understand if this kind of training could have some effects in promoting UL use and performance, immediately after the training and both at the medium and long terms. These parameters will be extracted both from clinical scales and technological measures (Actigraphs).

More and more emphasis should be placed on home-based care and therapies for a number of reasons. Besides cutting costs, this would not only increase efficiency and alleviate the workload of the hospital staff, but also it would offer a wider population the opportunity to avail this treatment. If the ICT solution used in the Tele- UPCAT study was made available, cost-efficient rehabilitation programs could be developed. At the moment, children and young people in non-urban areas are usually at a disadvantage, as often they cannot access treatment easily due to the downsizing or closure of hospitals in their area. The use of technology for rehabilitation also allows an intervention provided remotely and in a non-medical setting, but in a more acceptable and comfortable environment, which is the child's home (14, 31).

Moreover, this type of approach would more than likely reduce family stress, as already demonstrated in another study where a rehabilitative training has been carried out at home with parents (32).

In addition to this, thanks to the remote role of the clinical staff, it is possible, on one hand, to follow in parallel many patients and, on the other hand, to have quantitative results that enrich the clinical data.

In order to investigate also therapists' point of view, it could be useful to develop also a questionnaire addressed to the clinical staff, and this tool is in fact under construction. The analysis of the different end user's perspectives is crucial for ensuring the optimal designing of study protocols and medical devices. There is a growing literature on the development of methods for assessing usability and acceptability of technologies for home-based rehabilitation (33).

From our data, what emerged is that the only disadvantage of an intensive home-based training could be represented by the daily and weekly family routine, as some participants reported to prefer holiday periods to carry out the training. A future perspective could be to organize the 15 sessions in free-time periods (e.g., summer time), perhaps structuring the training without weekend interruption in order to make it last only 2 weeks. On the contrary, another solution could be to shorten the daily training or to provide multiple shorter sections per day in order to guarantee the continuity of the treatment during longer periods. The use of technology gives an advantage of offering multiple and customized solutions in relation to the different rehabilitation needs.

In conclusion, this study demonstrated the feasibility of a home-based AOT with the Tele-UPCAT system in children and adolescents with UCP. The home environment represents an accessible opportunity for rehabilitation among population. Thanks to end users' opinion, the Tele-UPCAT platform can be improved and optimized to further increase its acceptability and usability and, as a consequence, motivation and adherence to the training.

This can, on one hand stimulate, the creation of new platforms for home rehabilitation and, on the other hand, sensitize to follow this methodology for the assessment of the feasibility of the systems to be used for rehabilitation.

The availability of ICT solutions and the rapid progresses of the technology could help to integrate in the Tele-UPCAT system also new hardware and software for better recording of the kinematic aspects of the movement.

Finally, near-future perspective also offers this kind of treatment to other participants, in particular those with bilateral forms of CP, as well as for LL rehabilitation.

DATA AVAILABILITY STATEMENT

The datasets generated for this study are available on request to the corresponding author.

ETHICS STATEMENT

The studies involving human participants were reviewed and approved by Tuscany Pediatric Ethics Committee (169/2016). Written informed consent to participate in this study was provided by the participants' legal guardian/next of kin. Written informed consent was obtained from the individual(s) for the publication of any potentially identifiable images or data included in this article.

AUTHOR CONTRIBUTIONS

GS conceived the idea for this original research, and all other authors contributed to the conception and the design of the study. All authors participated in the design of the study. GS, GC, and AF carried out the enrollment of all children for the study. EB, VM, and GS designed and realized the questionnaire. EB performed all the assessments. VM assisted the families and children within the training. GS performed the statistical analysis. EB prepared the manuscript. GS, VM, GC, and AF read, critically revised, and approved the final manuscript.

FUNDING

This project has been partially supported by the Italian Ministry of Health Grant GR-2011-02350053, Grant RC2019, and 5 X 1000 health Research 2015.

ACKNOWLEDGMENTS

We gratefully thank all the families involved in the project for their trust in the Tele-UPCAT approach.

REFERENCES

1. Cioni G, Sgandurra G, Muzzini S, Paolicelli PB, Ferrari A. Forms of hemiplegia. In: Cioni G, Ferrari A, editors. *The Spastic Forms of Cerebral Palsy: A Guide to the Assessment of Adaptive Functions.* Milano: Springer-Verlag. (2010). p. 331–56. doi: 10.1007/978-88-470-1478-7_16
2. Novak I, Morgan C, Adde L, Blackman J, Boyd RN, Brunstrom-Hernandez J, et al. Early, accurate diagnosis and early intervention in cerebral palsy: advances in diagnosis and treatment. *JAMA Pediatr*. (2017) 171:897–907. doi: 10.1001/jamapediatrics.2017.1689
3. Sakzewski L, Ziviani J, Boyd RN. Efficacy of upper limb therapies for unilateral cerebral palsy: a meta-analysis. *Pediatrics*. (2014) 133:e175–204. doi: 10.1542/peds.2013-0675
4. Buccino G, Binkofski F, Fink GR, Fadiga L, Fogassi L, Gallese V, et al. Action observation activates premotor and parietal areas in a somatotopic manner: an fMRI study. *Eur J Neurosci*. (2001) 13:400–4. doi: 10.1046/j.1460-9568.2001.01385.x
5. Zhu MH, Wang J, Gu XD, Shi MF, Zeng M, Wang CY, et al. Effect of action observation therapy on daily activities and motor recovery in stroke patients. *Int J Nurs Sci*. (2015) 2:279–82. doi: 10.1016/j.ijnss.2015.08.006
6. Buccino G, Arisi D, Gough P, Aprile D, Ferri C, Serotti L, et al. Improving upper limb motor functions through action observation treatment: a pilot study in children with cerebral palsy. *Dev Med Child Neurol*. (2012) 54:822–8. doi: 10.1111/j.1469-8749.2012.04334.x
7. Buccino G, Molinaro A, Ambrosi C, Arisi D, Mascaro L, Pinardi C, et al. Action observation treatment improves upper limb motor functions in children with cerebral palsy: a combined clinical and brain imaging study. *Neural Plast*. (2018) 11:2018. doi: 10.1155/2018/4843985
8. Sgandurra G, Ferrari A, Cossu G, Guzzetta A, Fogassi L, Cioni G. Randomized trial of observation and execution of upper extremity actions versus action alone in children with unilateral cerebral palsy. *Neurorehabil Neural Rep*. (2013) 27:808–15. doi: 10.1177/1545968313497101
9. Kirkpatrick E, Pearse J, James P, Basu A. Effect of parent-delivered action observation therapy on upper limb function in unilateral cerebral palsy: a randomized controlled trial. *Dev Med Child Neurol*. (2016) 58:1049–56. doi: 10.1111/dmcn.13109
10. Buchignani B, Beani E, Iacono O, Sicola E, Perazza S, Bieber E, et al. Action observation training for rehabilitation in brain injuries: a systematic review and meta-analysis. *BMC Neurol*. (2019) 19:344. doi: 10.1186/s12883-019-1533-x.
11. Novak I, Cusick A, owe K. A pilot study on the impact of occupational therapy home programming for young children with cerebral palsy. *Am J Occup Ther*. (2007) 61:463–8. doi: 10.5014/ajot.61.4.463
12. Brennan DM, Mawson S, Brownsell S. Telerehabilitation: enabling the remote delivery of healthcare, rehabilitation, and self management. *Stud Health Technol Inform*. (2009) 145:231–248. doi: 10.3233/978-1-60750-018-6-231
13. Peretti A, Amenta F, Tayebati SK, Nittari G, Mahdi SS. Telerehabilitation: review of the state-of-the-art and areas of application. *JMIR Rehabil Assist Technol*. (2017) 4:e7. doi: 10.2196/rehab.7511
14. Zampolini M, Todeschini E, Bernabeu Guitart M, Hermens H, Ilsbroukx S, Macellari V, et al. Tele-rehabilitation: present and future. *Ann Ist Super Sanita*. (2008) 44:125–34.
15. Galea MD. Telemedicine in rehabilitation. *Phys Med Rehabil Clin N Am*. (2019) 30:473–83. doi: 10.1016/j.pmr.2018.12.002
16. Sgandurra G, Cecchi F, Beani E, Mannari I, Maselli M, Falotico FP, et al. Tele-UPCAT: study protocol of a randomised controlled trial of a home-based tele-monitored UPper limb children action observation training for participants with unilateral cerebral palsy. *BMJ Open*. (2018) 8:e017819. doi: 10.1136/bmjopen-2017-017819.
17. Cobos-Carbó A, Augustovski F. 2011. CONSORT. Declaration: updated guideline for reporting parallel group randomised trials. *Med Clin*. (2010) 137:213–5. doi: 10.1016/j.medcli.2010.09.034
18. Sgandurra G, Ferrari A, Cossu G, Guzzetta A, Biagi L, Tosetti M, et al. (2011). Upper limb children action observation training (UP-CAT): a randomised controlled trial in hemiplegic cerebral palsy. *BMC Neurol*. 11:80. doi: 10.1186/1471-2377-11-80
19. Leon AC, Davis, LL., Kraemer HC. The role and interpretation of pilot studies in clinical research. *J Psychiatr Res*. (2011) 45:626–9. doi: 10.1016/j.jpsychires.2010.10.008
20. Thabane L, Ma J, Chu R, Cheng J, Ismaila A, Rios LP, et al. A tutorial on pilot studies: the what, why and how. *BMC Med Res Methodol*. (2010) 10:1. doi: 10.1186/1471-2288-10-1
21. Verhelst H, Vander Linden C, Vingerhoets G, Caeyenberghs K. How to train an Injured Brain? A pilot feasibility study of a home-based

computerized cognitive training. *Games Health J.* (2017) 6:28–38. doi: 10.1089/g4h.2016.0043
22. Wixon D, Wilson C. The usability engineering framework for product design and evaluation. In: Helander MG, Landauer TK, Prabhu PV, editors. *Handbook of Human-Computer Interaction 2nd edn*. New York, NY: North Holland (1997). p.653–88. doi: 10.1016/B978-044481862-1.50093-5
23. Abran A, Khelifi A, Suryn W, Seffah A. Usability meanings and interpretations in ISO standards. *Softw Qual J*. (2003) 11:325. doi: 10.1023/A:1025869312943
24. Jokela T, Iivari N, Matero J, Karukka M. The standard of user-centered design and the standard definition of usability: analyzing ISO 13407 against ISO 9241-11. *CLIHC*. (2003) 53–60. doi: 10.1145/944519.944525
25. Davis FD. *A Technology Acceptance Model for Empirically Testing New End-User Information Systems: Theory and Results*. Massachusetts Institute of Technology (1986). Avaialable online at: http://hdl.handle.net/1721.1/15192 (accessed September 11, 2019).
26. Dillon, AP, Morris MG. User acceptance of new information technology: theories and models. Ann Rev Inform Sci Technol. (1996) 31:3–32.
27. Gard G. Work motivating factors in rehabilitation: a brief review. *Phys Ther Rev*. (2001) 6:85–9. doi: 10.1179/ptr.2001.6.2.85
28. Sadeghi M, Barlow-Krelina E, Gibbons C, Shaikh KT, Fung WLA, Meschino WS, et al. Feasibility of a computerized working memory training in individuals with Huntington disease. *PLoS ONE*. (2017) 12:e0176429. doi: 10.1371/journal.pone.0176429
29. Ertelt D, Small S, Solodkin A, Dettmers C, McNamara A, Binkofski F, et al. Action observation has a positive impact on rehabilitation of motor deficits after stroke. *Neuroimage*. (2007) 36:T164–73. doi: 10.1016/j.neuroimage.2007.03.043
30. Nuara A, Avanzini P, Rizzolatti G, Fabbri-Destro M. Efficacy of a home-based platform for child-to-child interaction on hand motor function in unilateral cerebral palsy. *Dev Med Child Neurol.* (2019) 61:1314–22. doi: 10.1111/dmcn.14262
31. Schmeler MR, Schein RM, McCue M, Betz K. Telerehabilitation clinical and vocational applications for assistive technology: research, opportunities, and challenges. *Int J Telerehabil*. (2009) 4:59–72. doi: 10.5195/IJT.2009.6014
32. Sgandurra G, Beani E, Inguaggiato E, Lorentzen J, Nielsen JB, Cioni G. Effects on parental stress of early home-based caretoy intervention in low-risk preterm infants. *Neural Plast.* (2019) 22:7517351. doi: 10.1155/2019/7517351
33. Sgherri G, Avola G, Beani E, Chisari C, Cioni G, Sgandurra G. Methods to assess Usability and Acceptability of technologies for home-based rehabilitation: a systematic review. *Int J Emerg Technol.* (2020) 10:434–43.

Conflict of Interest: The authors declare that the research was conducted in the absence of any commercial or financial relationships that could be construed as a potential conflict of interest.

frontiers in Neurology

ORIGINAL RESEARCH
published: 21 April 2020
doi: 10.3389/fneur.2020.00210

Joint and Muscle Assessments of the Separate Effects of Botulinum NeuroToxin-A and Lower-Leg Casting in Children With Cerebral Palsy

Nicky Peeters[1,2]*, *Anja Van Campenhout*[3], *Britta Hanssen*[1,2], *Francesco Cenni*[2], *Simon-Henri Schless*[4], *Christine Van den Broeck*[2], *Kaat Desloovere*[1,5†] and *Lynn Bar-On*[1,6†]

[1] Department of Rehabilitation Sciences, KU Leuven, Leuven, Belgium, [2] Department of Rehabilitation Sciences, University of Ghent, Ghent, Belgium, [3] Department of Development and Regeneration, KU Leuven, Leuven, Belgium, [4] Motion Analysis and Biofeedback Laboratory, Alyn Hospital, Jerusalem, Israel, [5] Clinical Motion Analysis Laboratory, UZ Leuven, Pellenberg, Belgium, [6] Department of Rehabilitation Medicine, Amsterdam UMC, Amsterdam Movement Sciences, Amsterdam, Netherlands

OPEN ACCESS

Edited by:
Pedro J. Garcia-Ruiz, University Hospital Fundación Jiménez Díaz, Spain

Reviewed by:
Samuel Ignacio PAscual Pascual, Autonomous University of Madrid, Spain
Jane Patricia Valentine, Child and Adolescent Health Service, Australia

***Correspondence:**
Nicky Peeters
nicky.peeters@kuleuven.be

† These authors have contributed equally to this work and share senior authorship

Specialty section:
This article was submitted to Movement Disorders, a section of the journal Frontiers in Neurology

Received: 02 December 2019
Accepted: 09 March 2020
Published: 21 April 2020

Citation:
Peeters N, Van Campenhout A, Hanssen B, Cenni F, Schless S-H, Van den Broeck C, Desloovere K and Bar-On L (2020) Joint and Muscle Assessments of the Separate Effects of Botulinum NeuroToxin-A and Lower-Leg Casting in Children With Cerebral Palsy. Front. Neurol. 11:210. doi: 10.3389/fneur.2020.00210

Botulinum NeuroToxin-A (BoNT-A) injections to the medial gastrocnemius (MG) and lower-leg casts are commonly combined to treat ankle equinus in children with spastic cerebral palsy (CP). However, the decomposed treatment effects on muscle or tendon structure, stretch reflexes, and joint are unknown. In this study, BoNT-A injections to the MG and casting of the lower legs were applied separately to gain insight into the working mechanisms of the isolated treatments on joint, muscle, and tendon levels. Thirty-one children with spastic CP (GMFCS I-III, age 7.4 ± 2.6 years) received either two weeks of lower-leg casts or MG BoNT-A injections. During full range of motion slow and fast passive ankle rotations, joint resistance and MG stretch reflexes were measured. MG muscle and tendon lengths were assessed at resting and at maximum dorsiflexion ankle angles using 3D-freehand ultrasound. Treatment effects were compared using non-parametric statistics. Associations between the effects on joint and muscle or tendon levels were performed using Spearman correlation coefficients ($p < 0.05$). Increased joint resistance, measured during slow ankle rotations, was not significantly reduced after either treatment. Additional joint resistance assessed during fast rotations only reduced in the BoNT-A group (−37.6%, $p = 0.013$, effect size = 0.47), accompanied by a reduction in MG stretch reflexes (−70.7%, $p = 0.003$, effect size = 0.56). BoNT-A increased the muscle length measured at the resting ankle angle (6.9%, $p = 0.013$, effect size = 0.53). Joint angles shifted toward greater dorsiflexion after casting (32.4%, $p = 0.004$, effect size = 0.56), accompanied by increases in tendon length (5.7%, $p = 0.039$, effect size = 0.57; $r = 0.40$). No associations between the changes in muscle or tendon lengths and the changes in the stretch reflexes were found. We conclude that intramuscular BoNT-A injections reduced stretch reflexes in the MG

accompanied by an increase in resting muscle belly length, whereas casting resulted in increased dorsiflexion without any changes to the muscle length. This supports the need for further investigation on the effect of the combined treatments and the development of treatments that more effectively lengthen the muscle.

Keywords: cerebral palsy, tendon length, muscle length, spasticity, hyper-resistance, casting, Botulinum NeuroToxin, muscle stretch reflex

INTRODUCTION

Cerebral palsy (CP), the most common childhood disability, is caused by an injury to the developing brain that occurs prior to, or shortly after, birth. In case of spastic CP, disturbed muscle innervation and biomechanical loading is combined with progressively worsening muscle contractures and joint hyper-resistance to movement. In the ankle joint, this hyper-resistance impairs the joint's passive range of motion (ROM), resulting in gait impairments such as equinus or excessive knee flexion (1).

Numerous studies have tried to establish the mechanisms that contribute to the development of ankle joint hyper-resistance in spastic CP. Recent literature indicates that hyperactive stretch reflexes, commonly labeled as spasticity, are considered to have less impact (2, 3). Instead, alterations such as reduced muscle volume and atrophy, cellular and genetic factors have been related to the increased joint resistance (4–6). Despite the likelihood of multifactorial contributions, the most common non-surgical treatment for joint hyper-resistance is intramuscular injection of Botulinum NeuroToxin-A (BoNT-A) which, mainly targets hyperactive stretch reflexes by causing temporary muscle paralysis. There is no known effect of BoNT-A in treating the non-neural components of joint hyper-resistance. The effectiveness of BoNT-A in correcting gait deviations, and passive joint ROM on the short-term, has been shown to improve when BoNT-A is combined with casting (7–9). The rational of this treatment combination is that paralysis, followed by passive immobilization in a neutral position, results in tissue elongation through physiological adaptation to prolonged stretch. However, few clinical studies reported the effects of BoNT-A treatment at the muscle level (10–18). Synthesis of existing clinical studies that include post-treatment assessment of muscle morphology is hindered by methodological differences between studies and lack of normalization to account for natural muscle growth. Therefore, results are inconclusive and whether the improved joint ROM occurs due to muscle remodeling or at the expense of other soft tissues, is not well-understood (19).

Given the frequent use of BoNT-A and casting in clinical practice, and the current uncertainties about their effect on muscle, more research is required. Knowledge of the working mechanism of the treatments will help understand how to combine them more efficiently. This will support the development of individually tailored treatments, where BoNT-A and casting are prescribed according to individually assessed causes of joint hyper-resistance. As a first step toward such patient-tailored medicine, careful assessment of the individual effects of BoNT-A and casting on different levels, ranging from joint to muscle and tendon, is required. The aim of the current study is to contribute to the understanding of the individual mechanisms by comprehensively evaluating the separate short-term effects of BoNT-A and lower-leg casting on ankle joint hyper-resistance, plantar flexor stretch reflexes, and muscle-tendon complex lengths. Additionally, the effects between the two treatments will be compared and the relations between treatment effects at the different levels are explored within each treatment group. It is hypothesized that BoNT-A will reduce hyperactive stretch reflexes, whereas casting will reduce the joint hyper-resistance by lengthening the muscle and tendon. Furthermore, any changes that occur at the joint level will be more related to alterations in the muscle and tendon lengths than to a reduction in stretch reflexes.

METHODS

Participants

Children with spastic CP, aged between 4 and 17 years, were recruited from the Clinical Motion Laboratory of the University Hospital Pellenberg (Belgium), and included when the multidisciplinary clinical team concluded that there was an indication for BoNT-A treatment of the medial gastrocnemius (MG) and casting of their ankle joint. This decision was based on the results of routine clinical assessments of spasticity by means of Modified Ashworth scale (20) and Tardieu R1 angle (21), ROM (by means of goniometry), strength and selectivity (by means of manual muscle testing and clinical selectivity scores), and a 3D gait analysis. Furthermore, included children had a minimum of 20° ankle ROM in the most involved limb, no behavioral problems that would impede the ability to understand and perform the test procedure, and no dyskinesia, dystonic or ataxic features. Children who received BoNT-A injections in the calf muscles within 6 months prior to the first assessment, a Selective Dorsal Rhizotomy (SDR), or orthopedic surgery on the lower-leg, were excluded. Children with a Modified Ashworth Scale score of 2 or higher in the hamstrings and psoas muscles, indicating greater proximal compared to distal muscle involvement (and therefore not suited to receive ankle stretching casts without multilevel BoNT-A injections), were also excluded. The local University Hospitals' Ethics Committee (study number s57384) approved this study. All participants were informed on the content of the study and written informed consent for participation was obtained from all parents/legal guardians and children above the age of 12 years.

Interventions

This investigation describes the first part of a larger study including a crossover design whereby BoNT-A (Botox®; Allergan Ltd, Buckinghamshire, UK) and lower-leg casting were applied in two treatment sessions, rather than during the same session. The treatment sessions were separated by a two-week period. This approach allowed investigation of the individual effects of BoNT-A and casting at a group level, but also ensured that all patients eventually received both of their prescribed clinical treatments. Patients were randomly allocated by an independent researcher to one of two groups by minimization such that each allocation minimized imbalance between the groups across multiple factors including Gross Motor Functional Classification Scale (GMFCS) level, topographic classification (unilateral or bilateral involvement), age, and gender. Children allocated to the first group received BoNT-A in the MG as part of their multi-level treatment. BoNT-A dosage and muscle selection was based on patient weight, medical history, findings of a clinical examination, 3D gait analysis, and the clinician's experience. Injection was given under short masked anesthesia, and was ultrasound guided for visual identification of muscles and needle depth.

Children allocated to the second group received two weeks of lower-leg casting. Polyester casts were applied conform clinical guidelines by a specialized nurse, supervised by the treating orthopedic surgeon.

In the two weeks following treatment, children in both groups continued with their usual post-treatment physical therapy. Children allocated to the BoNT-A group continued their usual use of their ankle-foot orthoses.

Assessments

Assessments were carried out on the most affected leg, defined by the most recent clinical examination. In the case of equal involvement, the left leg was assessed. Clinical examination of the plantar flexors including the Modified Ashworth Scale (20) and Tardieu R1 angle (21) as well as measurements of body weight and height were carried out before the treatment. Assessments of muscle and tendon lengths, ankle joint resistance and stretch reflexes were carried out before, and two weeks after, the individual treatments by the same experienced assessor.

Muscle and Tendon Lengths

Muscle and tendon lengths were assessed using 3D freehand ultrasound (3DfUS); combining conventional B-mode 2D ultrasound (Telemed EchoBlaster128, Vilnius, Lithuania) with 3D motion analysis (Optitrack NaturalPoint, USA), as previously described (22). The US acquisition parameters were kept constant between the different acquisitions (frequency, 10 MHz; depth, 5 cm; focus, 1.8–2.8 cm; gain, 46%; dynamic range, 44 dB and unaltered time-gain compensation) (23). This method has proven to be valid with a strong inter acquirer reliability in both healthy and pathological muscles (23, 24).

Subjects lay prone with the lower-leg supported by a small triangular cushion allowing ∼20° of knee flexion and the ankle to rest comfortably over the edge of the cushion, to reduce bi-articular stretch on the plantar flexor muscles. This position is referred to as the resting ankle position. First, the MG was imaged at this resting ankle position. Secondly, imaging was carried out with the ankle at maximum dorsiflexion. Maximum dorsiflexion was achieved by a second examiner who manually fixated the ankle in this position while ensuring that maximal motion occurred at the subtalar joint, avoiding foot add-/abduction or pro-/supination. The US images were recorded by an experienced examiner starting from the medial femoral condyle until the most distal edge of the calcaneus. Two 3DfUS sweeps over the MG were carried out at each ankle position. The knee and ankle joint angles were measured with a goniometer at both positions.

Instrumented Assessment of Ankle Joint Resistance and Stretch Reflexes

A previously described assessment was used to distinguish between neural and non-neural components of ankle joint resistance during slow and fast passive joint rotations that stretched the plantar flexors (25). Participants were assessed supine with the lower-limb supported. Three inertial measurement units (IMU's) were used to track the movement of the upper-leg with respect to the lower-leg and the lower-leg with respect to foot. Calibration trials were carried out to define a known angular position and the direction of rotation. A six degrees-of-freedom torque load-cell (ATI mini45: Industrial Automation), attached to a foot orthosis, was used to move the ankle and measure the forces and moments applied to the ankle (25). Surface electromyography (EMG) data (Zerowire, Cometa, Milan, IT) were collected from the MG, lateral gastrocnemius, soleus and tibialis anterior. With the subject fully relaxed, three passive ankle rotations over the full ROM were performed, first at slow velocity (5 s to complete full ROM) and then as fast as possible. Between repeated rotations, there was at least a 7 s rest interval, to avoid post-activation depression (26).

Data Processing

Muscle and Tendon Lengths

An open-source software library, developed in Python, was used to create a 3-dimensional view of the MG by integrating 2D US data and motion tracking (22). The 3D reconstruction of the muscle-tendon complex was visualized in a custom-made workflow in Mevislab (www.mevislab.de) (22). Visualization in three planes allowed for accurate identification of the following anatomical landmarks: the most superficial part of the femoral condyle used to define the MG muscle origin; the muscle-tendon junction (MTJ), as the muscle insertion and tendon origin; and the most proximal point on the calcaneus as the tendon insertion. The lengths of the MG and corresponding tendon in the two ankle positions were extracted by calculating the Euclidean distances between these landmarks (**Figure 1**). Muscle-tendon complex length was calculated as the summation of muscle (ML) and tendon length (TL). The same assessor, who was blinded for group allocation and assessment session, extracted all lengths twice. Average lengths were calculated and used for the final statistical analysis. In addition, the standard error of measurement (SEM) associated with extracting the lengths was calculated from the square root of the mean square error from one-way ANOVA (27). The change in joint angle,

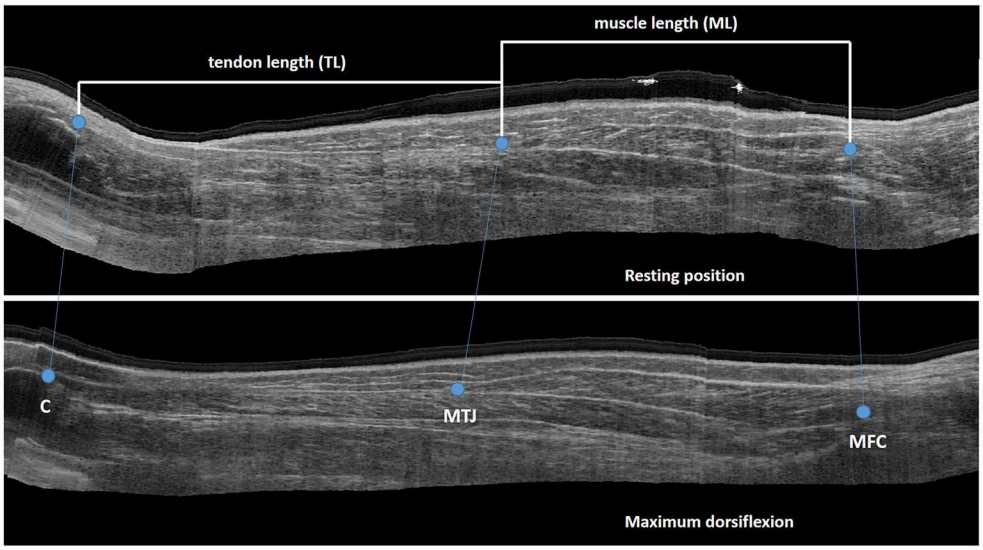

FIGURE 1 | Sagittal US image with landmarks for extraction of muscle and tendon length *C, calcaneus; MTJ, muscle tendon junction; MFC, medial femoral condyle*.

ML and TL between the two joint positions was calculated and indicated the degree of the joint (Δ ankle angle) and muscle/tendon "extensibility."

Instrumented Assessment of Ankle Joint Resistance and Stretch Reflexes

Data collected during the ankle joint resistance assessment were processed offline using a custom-made Matlab program (Mathworks, R2015a) as previously described (25). Raw EMG signals were filtered with a 6th order zero-phase Butterworth bandpass filter from 20 to 500Hz. The root mean square (rms) envelope of the EMG signal was defined by taking the square root after applying a low-pass 30 Hz 6th order zero-phase Butterworth filter on the squared raw signal. Joint angle and angular velocity were calculated from the IMU data by applying a Kalman filter (28). The net ankle joint moment was calculated from the forces and moments applied on the load-cell, the external moment arms, and the predicted torque caused by gravity on the orthotic (25).

ROM and maximum angular velocity were extracted from slow and fast passive ankle rotations. Average rms-EMG was calculated during an interval 200 ms before maximum velocity to 90% of the ROM, thereby emphasizing the velocity dependency of the hyperactive stretch reflex and excluding the effects of end ROM. To quantify the hyperactive stretch reflexes, average rms-EMG during slow velocity rotations was subtracted from average rms-EMG during fast rotations.

To quantify joint resistance, work during slow and fast passive rotations was defined as the average area underneath the torque-angle graph from maximum velocity to 90% ROM (25). Work during the slow passive rotation represented the non-neural component of joint resistance. The work during slow rotation was subtracted from that during fast rotation to calculate the neural component of joint resistance (25).

Statistical Analysis

An overview of the used statistical analyses is included in **Figure 2**.

Statistical analyses were performed using SPSS statistics (version 25 IBM). Normality of data distribution was evaluated using the Kolmogorov-Smirnov test. Outlier analysis was performed visually. Within-group treatment effects were evaluated with Wilcoxon signed ranks tests. Between groups, the treatment-induced changes were compared using Mann-Whitney U-tests. In addition to being statistically significant, treatment-induced changes were only considered meaningful when larger than the SEM.

Associations between treatment-induced changes in ankle angles, muscle/tendon lengths, extensibility, ankle joint hyper-resistance and stretch reflex parameters were assessed by Spearman rank correlation coefficients for both treatment groups separately. Correlation values of 0.6 or higher were considered as strong (29).

Effect sizes were calculated according the formula: $r = Z/\sqrt{N}$ (30). The Z-score was extracted from the SPSS output of the Wilcoxon signed rank test. N represents the total number of observations. *R*-values of 0.5 or higher were considered as large effect sizes, whereas *r*-values above 0.3 were considered moderate.

RESULTS

Thirty-one children with spastic CP (GMFCS I-III, age 7.4 ± 2.6 years) were included in this investigation. During the course of this study, some data were lost due to dropout and/or

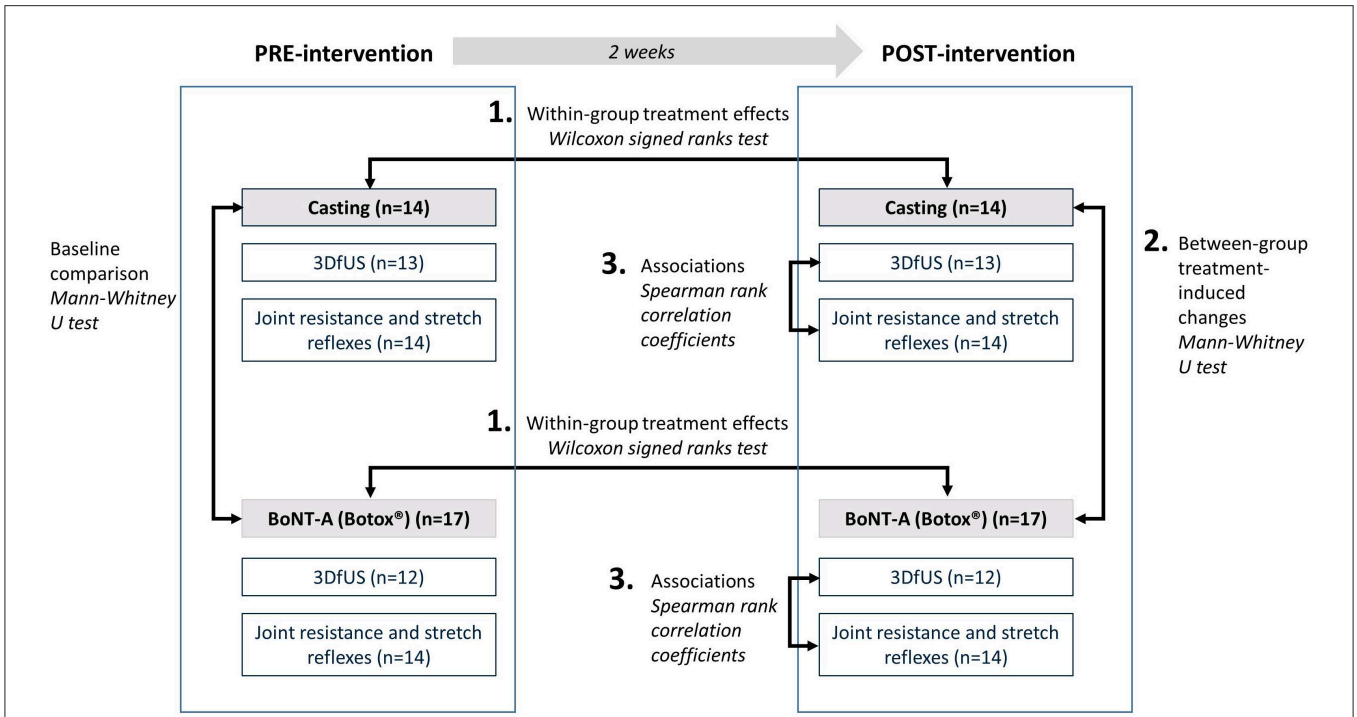

FIGURE 2 | Overview of statistical analyses. *3DfUS, 3D freehand ultrasound; BoNT-A, Botulinum NeuroToxin-A.*

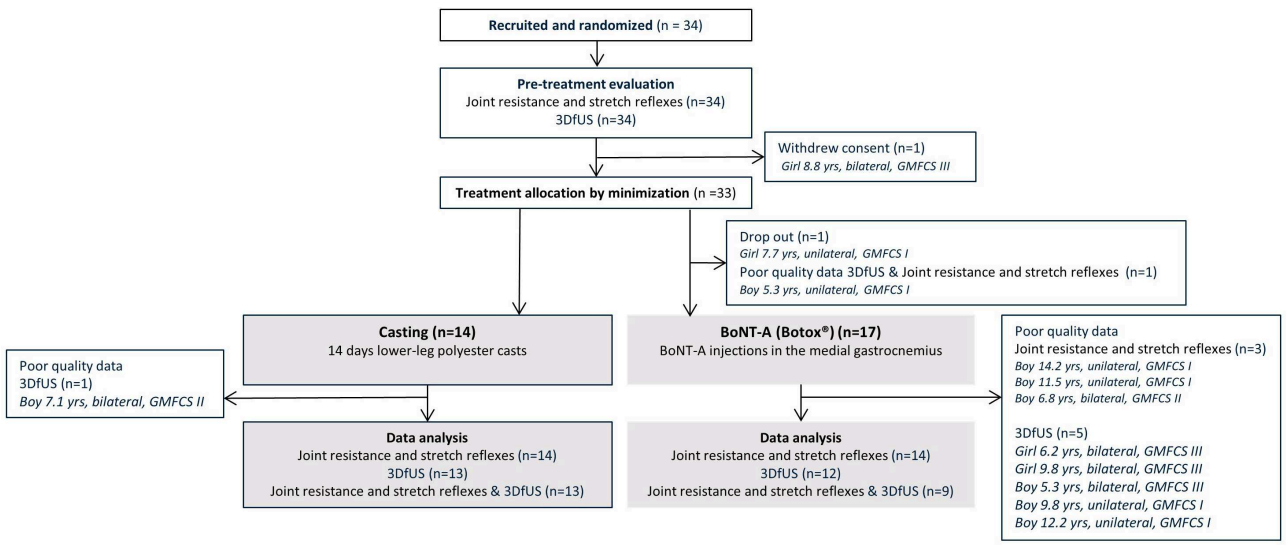

FIGURE 3 | Flowchart of the inclusion of participants with an overview of the available and missing data. *3DfUS, 3D freehand ultrasound; GMFCS, gross motor functional classification scale; BoNT-A, Botulinum NeuroToxin-A.*

technical issues with measurement equipment. The flowchart of the patient enrolment and all available data that were included in the final data analyses, and subdivided per outcome, are presented in **Figure 3**. At baseline (**Table 1**), the two intervention groups did not differ in age, body weight, height, maximum dorsiflexion ankle angle, Modified Ashworth Scale, Tardieu R1 angle, the difference in ankle angle between resting and maximum dorsiflexion position (Δ ankle angle), extensibility of the muscle or tendon, muscle/tendon lengths, ROM, angular velocity, hyperactive stretch reflexes, and work. The number of included patients and their characteristics per sub-analysis are included in **Supplementary Table 1**.

TABLE 1 | Participant characteristics.

	Casting ($n = 14$)	**BoNT-A ($n = 17$)**
Age (years)	7 (5–8.3)	7 (5.5–10.5)
Body weight (kg)	23.6 (18.4–28.7)	25 (19–27.6)
GMFCS level	I = 6, II = 6, III = 2	I = 11, II = 4, III = 2
Involvement	Unilateral = 7, Bilateral = 7	Unilateral = 12, Bilateral = 5
Gender	Male = 8, Female = 6	Male = 12, Female = 5
MAS*, knee extended	2 (1.5–3)	2 (1–3)
MTS R1*, knee extended (degrees)	−12.5 (−35 to −5)	−12.5 (−25 to 0)
Treatment details	2 weeks of lower-leg casting: $n = 14$ 2 weeks of removable upper- leg casts worn during the night: $n = 3$	BoNT-A (Botox®) plantar flexors: 4 Units/kg (2.33–6.12) BoNT-A (Botox®) MG: 2.47 Units/kg (1.93–3.66) BoNT-A (Botox®) LG: 0.37 Units/kg (0.00–0.71) BoNT-A (Botox®) SOL: 1.49 Units/kg (0.00–2.04)
Use of day orthoses, prior to treatment	Frequently used (≥50% of the day) $n = 11$ Not frequently used (<50% of the day) $n = 1$ Not used $n = 2$	Frequently used (≥50% of the day) $n = 14$ Not frequently used (<50% of the day) $n = 1$ Not used $n = 2$
Use of night orthoses, prior to treatment	Frequently used (≥50% of the night) $n = 2$ Not frequently used (<50% of the night) $n = 7$ Not used $n = 5$	Frequently used (≥50% of the night) $n = 2$ Not frequently used (<50% of the night) $n = 4$ Not used $n = 11$

*Values are presented as medians with corresponding quartiles (p25–p75), or numbers (n). *median, minimum-maximum values. BoNT-A, Botulinum NeuroToxin-A; GMFCS, Gross Motor Functional Classification Scale; MAS, modified ashworth scale; MTS, modified tardieu scale; MG, medial gastrocnemius muscle; LG, lateral gastrocnemius muscle; SOL, soleus muscle.*

Muscle and Tendon Lengths

There was a positive significant treatment effect of casting on the resting ($p = 0.004$, pre median: −31.5°, inter quartile range (IQR): 20.0°; post median: −25.0°, IQR: 10.0°, effect size = 0.56) and maximum dorsiflexion ($p = 0.026$, pre median: 0.0°, IQR: 3.8°; post median: 10.0°, IQR: 10.0°, effect size = 0.44) angles (**Figure 4**). Knee angles remained constant between the assessments of muscle/tendon lengths before and after treatment. The SEM values for determining the muscle and tendon lengths were 2.25 and 2.54 mm, respectively. SEM values were found to be comparable to those previously reported (23). The absolute muscle and tendon lengths pre- and post-treatment are presented in **Figure 4** and the treatment-induced change values are presented in **Supplementary Table 2**. Two weeks of casting caused a significant increase in the TL and muscle-tendon complex length at maximum dorsiflexion (5.6%, $p = 0.039$, effect size = 0.40, and 4.1%, $p = 0.005$, effect size = 0.63, respectively). These treatment-induced changes were also significantly larger than those found in the BoNT-A group ($p = 0.002$ and $p = 0.001$, respectively).

A significant increase in MG ML at the resting ankle position was found after BoNT-A injections (6.9%, $p = 0.013$, effect size = 0.53). Additionally, a significant increase in the TL at maximum dorsiflexion occurred, however this increase was within the range of the SEM. At the resting ankle position, ML after BoNT-A injections and the treatment-induced change in ML were significantly larger compared to those assessed following casting ($p = 0.023$ and $p = 0.036$, respectively).

Post-treatment, the extensibility of the ML and of the muscle-tendon complex length were significantly reduced after BoNT-A injections (−34.1%, $p = 0.010$, effect size = 0.55 and −36.3%, $p = 0.013$, effect size = 0.56, respectively), but unaltered by casting.

Instrumented Assessment of Ankle Joint Resistance and Stretch Reflexes

The ankle joint ROM and angular velocities applied during passive joint rotation remained unchanged after either treatment. Effects of the treatments on plantar flexor stretch reflexes and joint work are displayed in **Figure 4**. Two weeks of casting caused a significant reduction in the stretch reflexes of the lateral gastrocnemius (−29.5%, $p = 0.047$, effect size = 0.44), and soleus (−17.5%, $p = 0.034$, effect size = 0.43). Post-casting, the average work assessed during slow, and fast minus slow stretch remained unchanged.

BoNT-A injections resulted in a significant reduction in the stretch reflexes of the MG (−72.4%, $p = 0.003$, effect size = 0.56) together with a reduction in work during fast minus slow stretch (−22.4%, $p = 0.013$, effect size = 0.47). There was a trend that this reduction in work was larger in the group receiving BoNT-A compared to casting ($p = 0.050$).

Associations

Few correlations were found between the changes in joint angles, muscle/tendon lengths and ankle joint resistance. An overview of all correlation values and significance can be found in **Supplementary Tables 4, 5**.

In the casting group, there was a moderate positive correlation ($r = 0.56$, $p = 0.049$) between the change in TL at maximum dorsiflexion and the change in ankle angle (Δ ankle angle). Additionally, the increase in TL at maximum dorsiflexion was negatively related ($r = −0.67$, $p = 0.050$) to the reduction in stretch reflexes in the lateral gastrocnemius and the amount of work at high velocity ($r = −0.60$, $p = 0.03$). Furthermore, the increase in muscle-tendon complex length at rest was associated ($r = −0.821$,

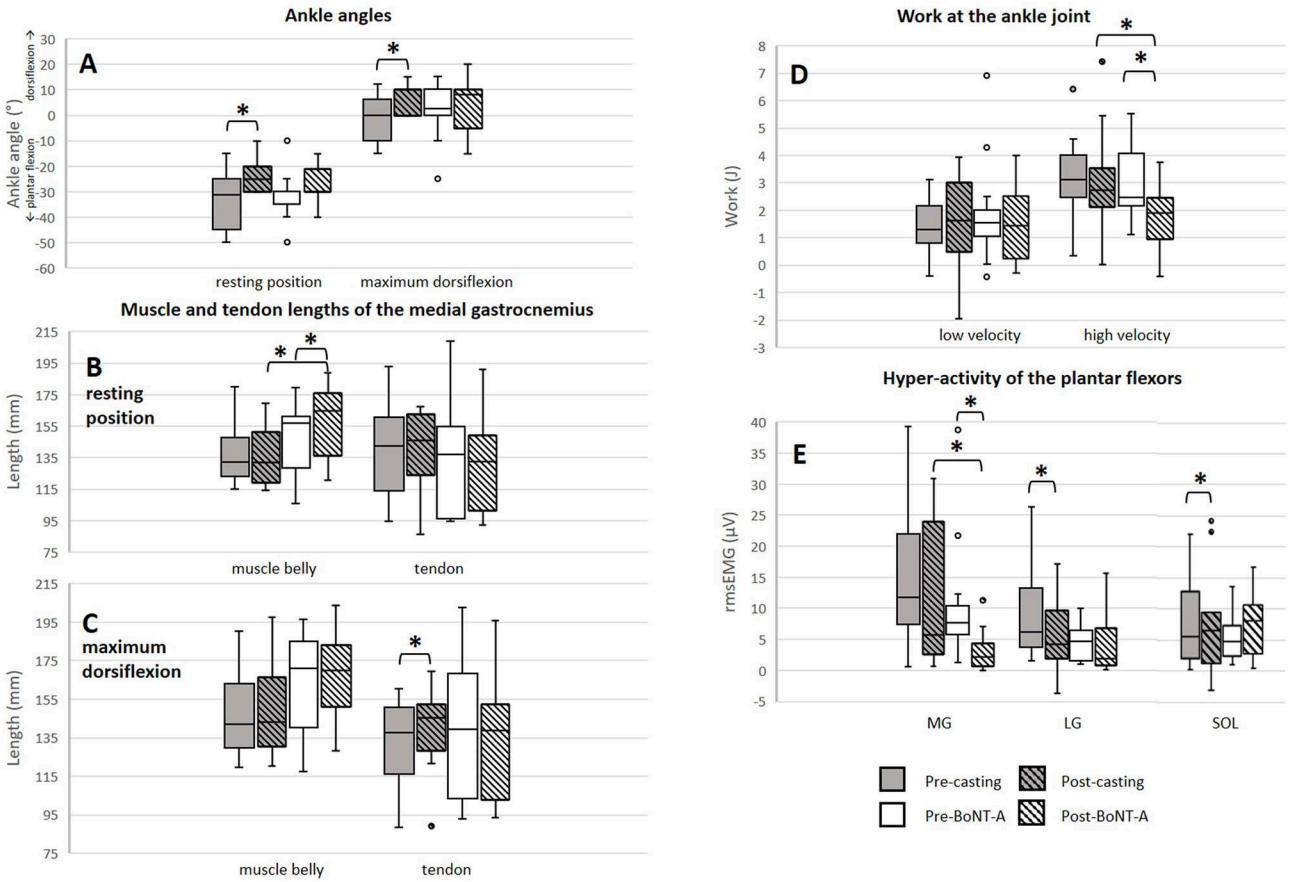

FIGURE 4 | Results of muscle/tendon lengths, ankle joint resistance and stretch reflex assessments. **(A)** Change in ankle angles. **(B)** Muscle and tendon lengths at resting position. **(C)** Muscle and tendon lengths at maximum dorsiflexion. **(D)** Work at the ankle joint during slow and fast joint rotations. **(E)** Stretch reflexes of the plantar flexors during fast rotations. *****significant results ($p < 0.05$, difference > SEM). mm, millimeter; J, Joule; rms EMG, root mean square of the electromyographic signal; μV, microvolt; MG, medial gastrocnemius muscle; LG, lateral gastrocnemius muscle; SOL, soleus muscle; BoNT-A, Botulinum NeuroToxin-A.*

$p = 0.02$) with the reduction in stretch reflexes in the lateral gastrocnemius.

In the BoNT-A group, the reduction in hyperactive stretch reflexes of the soleus muscle was strongly correlated ($r = 0.79$, $p = 0.036$) to the increase in ML of the MG at rest. In addition, the reduction in work at fast minus slow velocity was strongly correlated ($r = -0.77$, $p = 0.016$) with the change in ML at the maximum dorsiflexion angle.

DISCUSSION

Summary of Findings

The aim of this study was to gain more insight into the working mechanisms of BoNT-A and casting at the joint and muscle levels in children with spastic CP. Our hypotheses that BoNT-A targets the muscles' stretch reflexes, whereas casting targets the muscle belly and tendon length, were partly confirmed. Two weeks of casting increased the dorsiflexion angle, lowered the stretch reflexes in the lateral gastrocnemius and soleus muscles and increased the tendon length measured at maximum dorsiflexion position. BoNT-A reduced the stretch reflexes in the MG, reduced the joint resistance measured during fast passive ankle joint rotation, and increased the muscle length measured at the resting ankle position. Only a few associations between the treatment-induced alterations in joint angles, muscle or tendon lengths and measures of ankle joint resistance, and stretch reflexes were found. In summary, this study found rather minor changes at the muscle level after either intervention, with limited relationships between the effects at the joint, muscle or tendon lengths and stretch reflexes.

Casting

We confirmed previous findings that maximum dorsiflexion increases after lower-leg casting (31, 32). However, since the joint angle at rest also moved toward greater dorsiflexion, the total joint ROM and change in ankle angle (Δ ankle angle) remained unchanged after treatment. While this result may make it easier to fit a foot into an ankle-foot orthosis configured toward dorsiflexion, it remains unclear to what

extent this new biomechanical configuration is functionally useful. In the two subjects whose ROM did increase, this was mainly explained by an increase in their maximum dorsiflexion angle with an accompanied increased tendon length (**Supplementary Figure 1**). Interestingly, the three children who additionally received removable upper leg casts during the night showed an increase in muscle belly length at maximum dorsiflexion.

Since the plantar flexor muscles of children with spastic CP have been described as stiff and short (33), lengthening of these muscles through treatment is desirable. In clinical practice, it is thereby commonly hypothesized that an increase in dorsiflexion angle following casting is a result of lengthening the muscle. However, our results showed that the increase in maximum dorsiflexion angle post-casting was related to the increase in tendon length rather than alterations in muscle belly length. Hösl et al. (2015) reported increased tendon length following a period of ankle foot orthotic use (34) and Theis et al. (2013) reported similar results after a manual stretching intervention (35). As far as we are aware, our study is the first to report this effect following two weeks of casts.

Previous studies suggested that children with CP have a more compliant Achilles tendon (36, 37). In ambulant children with CP, this adaptation may be beneficial for achieving sufficient dorsiflexion during the stance phase of gait, but may compromise push-off power as the tendon may offer less resilience. Therefore, given that TL is already increased in CP, our findings highlight that caution has to be paid when applying passive stretches due to potentially enhancing the negative effects on the tendon. This is especially important when considering the coherence of the muscle-tendon unit as a complex and the efficiency of the muscle and tendon to interact during function. A recent study by Kalkman et al. (2019) concluded that increased tendon compliance in CP may result in reduced stretch stimulus to the muscle during ankle rotation, thus explaining the minimal effects of stretching interventions on muscle remodeling (38). In a follow-up study, they then confirmed that initially increasing tendon stiffness, by means of strength training, resulted in more efficient muscle stretch (38). Similarly, the group of Zhao et al. (2010) accomplished a reduction in Achilles tendon length and increased stiffness by combining passive stretching with active movement therapy (39). These findings suggest that stretching should be combined with strengthening exercises in order to optimally target the muscle belly.

The reduction in hyperactive stretch reflexes of the lateral gastrocnemius and soleus following casting was unexpected, but might be explained by the alteration in starting ankle angle, as the ankle was spontaneously more dorsiflexed after casting. Meinders et al. (1996) suggested that specifically at the ankle, stretch reflexes are reduced at a longer starting muscle-tendon complex lengths (40). Confirming this, we found that the reduction in hyperactive stretch reflex in the lateral gastrocnemius following casts was associated with an increase in tendon length.

BoNT-A

BoNT-A targets the neural component of ankle joint resistance by reducing the hyperactive stretch reflexes. Reduction of hyperactive stretch reflexes is thought to create the opportunity for the muscle to act over a larger ROM and thereby improve its function (41). Our results confirmed the reduction of MG stretch reflexes, shown by a reduction in rms-EMG of the MG and in the reduced work needed to move the ankle joint during a high-velocity stretch of the plantar flexors. The question remains whether these changes additionally translate to morphological changes at the muscle level. Post BoNT-A, we observed an increase in the resting length of the MG muscle belly. Since spastic muscles have been described with a higher resting muscle tone (42), the increased MG muscle belly length may be a direct result of muscle tone reduction and the ability of the muscle to relax in this position. On the other hand, there were no changes to the muscle length measured at maximum dorsiflexion. Therefore, we found little evidence that the reduction in hyperactive stretch reflex of the MG post BoNT-A induced muscle remodeling. It is known that the muscle needs more time than the current short-term (two weeks) follow-up to adapt and no conclusions can be drawn about the medium- and long-term effect of BoNT-A on muscle length (43). Furthermore, muscle remodeling might take place after combining with casting.

Combined Treatment

Answers regarding the combination of the treatments are currently being analyzed as the second part of this research project, which includes a crossover design with all the participants receiving the other treatment. In addition, this second part includes 3D gait analysis before and after receiving the two interventions allowing us to understand effects of the interventions on the functional level. Desloovere et al. (2007) showed that BoNT-A combined with casting was more effective in improving gait, compared to casting alone (44). However, it is unclear how these effects were achieved and additional insight, which we expect to gain with the second stage of this project, will likely facilitate the understanding of these findings. Following BoNT-A injections only, there were no changes in the ankle angles or joint ROM. Given the effects of casting on these parameters, there is reason to believe that the best results may be achieved when the two treatments are combined. Ideally, the changes seen on the muscle level following BoNT-A, in combination with static stretch as applied from casting, will result in the desired effect of increasing the joints ROM by promoting muscle length. Such an effect should result in greater ankle mobility that would be transferrable to the child's gait. However, given the finding that casting only increased the tendon length, very careful monitoring of how ankle mobility is achieved post-casting is essential, as it may be subject-specific. This highlights that an individualized and fine-tuned combination of the treatments is required. Furthermore, we can question whether a primarily passive stretch applied by casts is beneficial, as evidence shows that muscle activity is required to efficiently stretch the muscle and maintain an optimal configuration of the muscle-tendon complex (39).

Importantly, since neither treatment in isolation affected the increased joint resistance assessed during slow passive stretch, it is unlikely that the combination of the two treatments will affect resistance during slow stretch. If confirmed, this suggests that

we need more effective treatments that address hyper-resistance over the full ROM, and not only increases the maximum dorsiflexion. If combined results are still not satisfactory, new treatment modalities should be developed to more efficiently target the muscle.

Our data showed a lack of strong responses on the group level. This reflects the large heterogeneity of the children with CP included in this study and therefore the need for larger samples. Given that the sample was taken from the clinical population seeking treatment for ankle joint hyper-resistance, this finding emphasizes the need to generate muscle-specific profiles and establish patient-tailored treatment. Furthermore, we highlight the importance of evaluating the underlying muscle and tendon structures rather than providing treatment based only on conclusions drawn from evaluations at the joint level.

Limitations

The study has limitations that need to be acknowledged. This study investigated only the very short-term effects of the treatments. This allowed us to evaluate the separate effects without having to compromise on the children's clinical intervention plan. A study design in which the same study sample received both treatments including a wash-out period would have been methodically stronger. However, implementing such an investigation would differ too much from normal clinical treatment and would not be considered ethical (nor would including control groups from whom treatment was denied). In addition, considering the long time span of such a study, other parameters would influence the response.

This clinical study included a small dataset with missing data. As a result, not all participants were included in all analyses. When only including subjects who underwent both assessments ($n = 23$, BoNT-A $n = 9$, casting $n = 13$), most of our conclusions were still valid (**Supplementary Table 3**). Nevertheless, more studies need to be conducted to confirm the initial results of this study. Randomization by minimization was applied in order to minimize differences between groups in terms of pathology, age, body weight and height. Even though the groups did not perfectly match, there were no differences reported at baseline. Heterogeneity in treatment history and current treatment adherence are limitations when performing randomized controlled trials in children with CP. It is well-described that muscle morphology of children with CP is different from typically developing peers, although it remains unclear to what extent treatment history contributes to these alterations. This should be focus for further investigation. In addition, given the wide age range, and the effect of age on the ability of the muscle fiber to adapt, it is possible that the muscle fiber stage influenced our results.

The full data set of this investigation is published (DOI: https://doi.org/10.6084/m9.figshare.12009375.v1). When more data becomes available, sub analyses according to baseline characteristics may be carried out that will contribute to clinical implementation.

This study only investigated the muscle and tendon lengths of the MG as this is the muscle that is most frequently treated with BoNT-A in daily clinical practice. Future investigations with larger samples investigating more muscles are needed to confirm these initial findings. Given recent validation of the clinical applicability of the methods used in this study (23, 45), such investigations should be feasible in the near future.

We studied the alterations in the length of the entire muscle belly. Yet, this does not provide information on the fascicle behavior, especially since the MG is pennated. More-over, local fascicle remodeling in specific regions of the muscle may have occurred. Furthermore, since neither muscle length nor fascicle length necessarily represent sarcomere number or length, it is important to continue investigations that combine macro- and micro-structure responses to the applied treatments.

CONCLUSION

This study presents initial findings on treatment response in a heterogeneous group of children with spastic CP. Intramuscular BoNT-A injections reduced the stretch reflex in the MG accompanied by an increase in resting muscle belly length, whereas casting resulted in increased dorsiflexion without any changes to the muscle length. These results indicate limited treatment-induced MG muscle remodeling. This supports the need for further investigation once the treatments are combined and for the development of treatments that more effectively lengthen the muscle belly. Additionally, future implementation of objective assessments will contribute to a better understanding of treatment effects, which could support clinical decision-making and help to identify responders.

DATA AVAILABILITY STATEMENT

The datasets generated for this study can be found in the Figshare repository DOI: https://doi.org/10.6084/m9.figshare.12009375.v1.

ETHICS STATEMENT

The studies involving human participants were reviewed and approved by Ethical-Committee of the University Hospitals of Leuven/KU Leuven. Written informed consent to participate in this study was provided by the participants' parents/legal guardians.

AUTHOR CONTRIBUTIONS

This study was designed by LB, KD, and AV. NP, BH, and S-HS were responsible for data collection. FC and LB wrote the software for data analysis. AV evaluated eligibility of subjects. NP and LB conducted all presented analyses. All authors have had complete access to the study data throughout the study. NP, AV, BH, FC, S-HS, CV, KD, and LB contributed to the interpretation of the results and were involved in the critical revision and editing of the manuscript that was written by NP and LB. All authors approve the final version of the

manuscript and agree to be accountable for the content of the work.

FUNDING

LB received postdoctoral grants (12R4215N) from the Research Foundation Flanders (FWO) and (016.186.144) from the Netherlands Organization for Scientific Research (NWO). The work was also supported by the TBM grant (TAMTA-T005416N) from the Research Foundation Flanders (FWO), Belgium and from La Fondation Motrice, contract 2016/8.

ACKNOWLEDGMENTS

The research team is very grateful to all the children and parents who participated in this study.

SUPPLEMENTARY MATERIAL

The Supplementary Material for this article can be found online at: https://www.frontiersin.org/articles/10.3389/fneur.2020.00210/full#supplementary-material

REFERENCES

1. Gage JR, Schwartz MH, Koop SE, Novacheck TF. *The Identification And Treatment Of Gait Problems In Cerebral Palsy*. 2nd Edn. London: Mac Keith Press; John Wiley & Sons (2009).
2. Gough M, Shortland AP. Could muscle deformity in children with spastic cerebral palsy be related to an impairment of muscle growth and altered adaptation? *Dev Med Child Neurol.* (2012) 54:495–9. doi: 10.1111/j.1469-8749.2012.04229.x
3. Willerslev-Olsen M, Choe Lund M, Lorentzen J, Barber L, Kofoed-Hansen M, Nielsen JB. Impaired muscle growth precedes development of increased stiffness of the triceps surae musculotendinous unit in children with cerebral palsy. *Dev Med Child Neurol.* (2018) 60:672–9. doi: 10.1111/dmcn.13729
4. Domenighetti XAA, Mathewson MA, Pichika R, Sibley LA, Zhao L, Chambers HG, et al. Loss of myogenic potential and fusion capacity of muscle stem cells isolated from contractured muscle in children with cerebral palsy. *Am J Physiol Cell Physiol.* (2019) 315:C247–57. doi: 10.1152/ajpcell.00351.2017
5. Von Walden F, Gantelius S, Liu C, Borgström H, Björk L, Gremark O, et al. Muscle contractures in patients with cerebral palsy and acquired brain injury are associated with extracellular matrix expansion, pro-inflammatory gene expression, and reduced rRNA synthesis. *Muscle Nerve.* (2018) 58:277–85. doi: 10.1002/mus.26130
6. Dayanidhi S, Dykstra PB, Lyubasyuk V, McKay BR, Chambers HG, Lieber RL. Reduced satellite cell number in situ in muscular contractures from children with cerebral palsy. *J Orthop Res.* (2015) 33:1039–45. doi: 10.1002/jor.22860
7. Molenaers G, Schörkhuber V, Fagard K, Van Campenhout A, De Cat J, Pauwels P, et al. Long-term use of botulinum toxin type A in children with cerebral palsy: treatment consistency. *Eur J Paediatr Neurol.* (2009) 13:421–9. doi: 10.1016/j.ejpn.2008.07.008
8. Molenaers G, Fagard K. Botulinum toxin A treatment of the lower extremities in children with cerebral palsy. *J Child Orthop*. (2013) 7:383–7. doi: 10.1007/s11832-013-0511-x
9. Martín Lorenzo T, Rocon E, Martínez Caballero I, Ramírez Barragán A, Lerma Lara S. Prolonged stretching of the ankle plantarflexors elicits muscle-tendon adaptations relevant to ankle gait kinetics in children with spastic cerebral palsy. *Med Hypotheses.* (2017) 109:65–9. doi: 10.1016/j.mehy.2017.09.025
10. Alexander C, Elliott C, Valentine J, Stannage K, Bear N, Donnelly CJ, et al. Muscle volume alterations after first botulinum neurotoxin A treatment in children with cerebral palsy : a 6-month prospective cohort study. *Dev Med Child Neurol*. (2018) 60:1165–72. doi: 10.1111/dmcn.13988
11. Boyaci A, Tutoglu A, Boyaci N, Koca I, Calik M, Sakalar A, et al. Changes in spastic muscle stiffness after botulinum toxin A injections as part of rehabilitation therapy in patients with spastic cerebral palsy. *NeuroRehabilitation.* (2014) 35:123–9. doi: 10.3233/NRE-141107
12. Barber L, Hastings-Ison T, Baker R, Kerr Graham H, Barrett R, Lichtwark G. The effects of botulinum toxin injection frequency on calf muscle growth in young children with spastic cerebral palsy: A 12-month prospective study. *J Child Orthop.* (2013) 7:425–33. doi: 10.1007/s11832-013-0503-x
13. Reid S, Elliott C, Shipman P, Valentine J. Muscle volume alterations in spastic muscles immediately following botulinum toxin type-A treatment in children with cerebral palsy. *Dev Med Child Neurol.* (2013) 55:813–20. doi: 10.1111/dmcn.12200
14. Williams SA, Elliott C, Valentine J, Gubbay A, Shipman P, Reid S. Combining strength training and botulinum neurotoxin intervention in children with cerebral palsy: the impact on muscle morphology and strength. *Disabil Rehabil.* (2013) 35:596–605. doi: 10.3109/09638288.2012.711898
15. Kawano A, Yanagizono T, Kadouchi I, Umezaki T, Chosa E. Ultrasonographic evaluation of changes in the muscle architecture of the gastrocnemius with botulinum toxin treatment for lower extremity spasticity in children with cerebral palsy. *J Orthop Sci.* (2017) 23:389–93. doi: 10.1016/j.jos.2017.10.012
16. Schless S-H, Cenni F, Bar-On L, Hanssen B, Kalkman BM, O'Brien TD, et al. Medial gastrocnemius volume and echo-intensity after botulinum neurotoxin A interventions in children with spastic cerebral palsy. *Dev Med Child Neurol.* (2019) 61:783–90. doi: 10.1111/dmcn.14056.
17. Park ES, Sim E, Rha D-W, Jung S. Architectural changes of the gastrocnemius muscle after botulinum toxin type A injection in children with cerebral palsy. *Yonsei Med J.* (2014) 55:1406. doi: 10.3349/ymj.2014.55.5.1406
18. Van Campenhout A, Verhaegen A, Pans S, Molenaers G. Botulinum toxin type A injections in the psoas muscle of children with cerebral palsy: muscle atrophy after motor end plate-targeted injections. *Res Dev Disabil.* (2013) 34:1052–8. doi: 10.1016/j.ridd.2012.11.016
19. Huijing PA, Bénard MR, Harlaar J, Jaspers RT, Becher JG. Movement within foot and ankle joint in children with spastic cerebral palsy : a 3-dimensional ultrasound analysis of medial gastrocnemius length with correction for effects of foot deformation. *BMC Musculoskelet Disord*. (2013) 14:365. doi: 10.1186/1471-2474-14-365
20. Bohannon RW, Smith MB. Interrater reliability of a modified ashworth scale of muscle spasticity. *Phys Ther.* (1987) 67:206–7. doi: 10.1093/ptj/67.2.206
21. Boyd RN, Graham HK. Objective measurement of clinical findings in the use of botulinum toxin type A for the management of children with cerebral palsy. *Eur J neurol.* (1999). 6(suppl. 4):23–35. doi: 10.1111/j.1468-1331.1999.tb00031.x
22. Cenni F, Monari D, Desloovere K, Aertbeliën E, Schless S-H, Bruyninckx H. The reliability and validity of a clinical 3D freehand ultrasound system. *Comput Methods Programs Biomed.* (2016) 136:179–87. doi: 10.1016/j.cmpb.2016.09.001
23. Cenni F, Schless SH, Bar-On L, Aertbeliën E, Bruyninckx H, Hanssen B, et al. Reliability of a clinical 3D freehand ultrasound technique: analyses on healthy and pathological muscles. *Comput Methods Programs Biomed.* (2018) 156:97–103. doi: 10.1016/j.cmpb.2017.12.023
24. Cenni F, Schless S-H, Bar-On L, Molenaers G, Van Campenhout A, Aertbeliën E, et al. Can *in vivo* medial gastrocnemius muscle–tendon unit lengths be reliably estimated by two ultrasonography methods? A within-session analysis. *Ultrasound Med Biol.* (2018) 44:110–8. doi: 10.1016/j.ultrasmedbio.2017.09.018
25. Bar-On L, Aertbelien E, Wambacq H, Severijns D, Lambrecht K, Dan B, et al. A clinical measurement to quantify spasticity in children with cerebral palsy by integration of multidimensional signals. *Gait Posture.* (2013) 38:141–7. doi: 10.1016/j.gaitpost.2012.11.003
26. Aymard C, Katz R, Lafitte C, Lo E, Penicaud A, Pradat-Diehl P, et al. Presynaptic inhibition and homosynaptic depression: a comparison between

lower and upper limbs in normal human subjects and patients with hemiplegia. *Brain.* (2000) 123:1688–702. doi: 10.1093/brain/123.8.1688
27. Weir JP. Quantifying test-retest reliability using the intraclass correlation coefficient and the SEM. *J strength Cond Res.* (2005) 19:231–40. doi: 10.1519/00124278-200502000-00038
28. Rauch HE, Tung F, Striebel C. Maximum likelihood estimates of linear dynamic systems. *Am Inst Aeronaut Astronaut J.* (1965) 3:1445–50. doi: 10.2514/3.3166
29. Altman D. *Practical Statistics for Medical Research*. Boca Raton, FL: Chapman and Hall/CRC (1991).
30. Rosenthal R. Meta-analytic procedures for social research. In: Starika MR, editor *Meta-analytic Procedures for Social Research.* Newbury Park, CA: Sage Publications (1991). p. 14–20.
31. Harvey LA, Katalinic OM, Herbert RD, Moseley AM, Lannin NA, Schurr K. Stretch for the treatment and prevention of contracture: an abridged republication of a Cochrane Systematic Review. *J Physiother*. (2017) 63:67–75. doi: 10.1016/j.jphys.2017.02.014.
32. Guissard N, Duchateau J. Neural aspects of muscle stretching. *Exerc Sport Sci Rev*. (2006) 34:154–8. doi: 10.1249/01.jes.0000240023.30373.eb
33. Graham HK, Rosenbaum P, Paneth N, Dan B, Lin J-P, Damiano DL, et al. Cerebral palsy. *Nat Rev Dis Prim.* (2016) 2:15082. doi: 10.1038/nrdp.2016.5
34. Hösl M, Böhm H, Arampatzis A, Döderlein L. Effects of ankle–foot braces on medial gastrocnemius morphometrics and gait in children with cerebral palsy. *J Child Orthop.* (2015) 9:209–19. doi: 10.1007/s11832-015-0664-x
35. Theis N, Korff T, Kairon H, Mohagheghi AA. Does acute passive stretching increase muscle length in children with cerebral palsy? *Clin Biomech.* (2013) 28:1061–7. doi: 10.1016/j.clinbiomech.2013.10.001
36. Zhao H, Wu Y, Liu J, Ren Y, Gaebler-spira DJ, Zhang L. Changes of calf muscle-tendon properties due to stretching and active movement of children with cerebral palsy a pilot study. *Annu Int Conf IEEE Eng Med Biol Soc.* (2009) 2009:5287–90. doi: 10.1109/IEMBS.2009.5333518
37. Theis N, Mohagheghi AA, Korff T. Mechanical and material properties of the plantarflexor muscles and achilles tendon in children with spastic cerebral palsy and typically developing children. *J Biomech.* (2016) 49:3004–8. doi: 10.1016/j.jbiomech.2016.07.020
38. Kalkman BM, Holmes G, Bar-on L, Maganaris CN, Barton GJ, Bass A, et al. Resistance training combined with stretching increases tendon stiffness and is more effective than stretching alone in children with cerebral palsy : a randomized controlled trial. *Front Pediatr*. (2019). 7:333. doi: 10.3389/fped.2019.00333
39. Zhao H, Wu Y, Hwang M, Ren Y, Gaebler-Spira DJ, Zhang L. Changes of calf muscle-tendon biomechanical properties induced by passive stretching and active movement training in children with cerebral palsy. *Dev Med Child Neurol.* (2010) 52:40–2. doi: 10.1152/japplphysiol.01361.2010.
40. Meinders M, Price R, Lehmann JF, Questad KA. The stretch reflex response in the normal and spastic ankle effect of ankle position. *Arch Phys Med Rehabil.* (1996) 77:487–92. doi: 10.1016/S0003-9993(96)90038-6
41. El-Etribi MA, Salem ME, El-Shakankiry HM, El-Kahky AM, El-Mahboub SM. The effect of botulinum toxin type-A injection on spasticity, range of motion and gait patterns in children with spastic diplegic cerebral palsy: an Egyptian study. *Int J Rehabil Res Int Zeitschrift fur Rehabil Rev Int Rech Readapt.* (2004) 27:275–81. doi: 10.1097/00004356-200412000-00004
42. Sloot LH, van der Krogt MM, de Gooijer-van de Groep KL, van Eesbeek S, de Groot J, Buizer AI, et al. The validity and reliability of modelled neural and tissue properties of the ankle muscles in children with cerebral palsy. *Gait Posture.* (2015) 42:7–15. doi: 10.1016/j.gaitpost.2015.04.006
43. Multani I, Manji J, Ison TH, Khot A, Graham K. Botulinum toxin in the management of children with cerebral palsy. *Pediatr Drugs.* (2019) 21:261–81. doi: 10.1007/s40272-019-00344-8
44. Desloovere K. Motor function following multilevel botulinum toxin type A treatment in children with cerebral palsy. *Dev Med Child Neuro*. (2007) 49:56–61. doi: 10.1017/S001216220700014X.x
45. Bar-On L, Aertbeliën E, Molenaers G, Van Campenhout A, Vandendoorent B, Nieuwenhuys A, et al. Instrumented assessment of the effect of botulinum toxin-A in the medial hamstrings in children with cerebral palsy. *Gait Posture.* (2014) 39:17–22. doi: 10.1016/j.gaitpost.2013.05.018

Conflict of Interest: The authors declare that the research was conducted in the absence of any commercial or financial relationships that could be construed as a potential conflict of interest.

frontiers in Human Neuroscience

BRIEF RESEARCH REPORT
published: 25 May 2020
doi: 10.3389/fnhum.2020.00159

Brain Metabolism During A Lower Extremity Voluntary Movement Task in Children With Spastic Cerebral Palsy

Eileen G. Fowler[1,2], William L. Oppenheim[1], Marcia B. Greenberg[1], Loretta A. Staudt[1], Shantanu H. Joshi[3,4] and Daniel H. S. Silverman[5,6]*

[1]Center for Cerebral Palsy, Department of Orthopaedic Surgery, University of California, Los Angeles, Los Angeles, CA, United States, [2]Tarjan Center at UCLA, Los Angeles, CA, United States, [3]Department of Neurology, University of California, Los Angeles, Los Angeles, CA, United States, [4]Department of Bioengineering, University of California, Los Angeles, Los Angeles, CA, United States, [5]Department of Molecular and Medical Pharmacology, University of California, Los Angeles, Los Angeles, CA, United States, [6]Ahmanson Translational Imaging Division, UCLA Health System, Los Angeles, CA, United States

OPEN ACCESS

Edited by:
Christos Papadelis,
Cook Children's Medical Center,
United States

Reviewed by:
Claudio Luis Ferre,
Burke Neurological Institute (BNI),
United States
Yanlong Song,
University of Texas at Arlington,
United States
Hsing-Ching Cherie Kuo,
UC Davis Medical Center,
United States

***Correspondence:**
Eileen G. Fowler
efowler@mednet.ucla.edu

Specialty section:
This article was submitted to Motor Neuroscience, a section of the journal Frontiers in Human Neuroscience

Received: 08 February 2020
Accepted: 14 April 2020
Published: 25 May 2020

Citation:
Fowler EG, Oppenheim WL, Greenberg MB, Staudt LA, Joshi SH and Silverman DHS (2020) Brain Metabolism During a Lower Extremity Voluntary Movement Task in Children with Spastic Cerebral Palsy. Front. Hum. Neurosci. 14:159. doi: 10.3389/fnhum.2020.00159

Reduced selective voluntary motor control (SVMC) is a primary impairment due to corticospinal tract (CST) injury in spastic cerebral palsy (CP). There are few studies of brain metabolism in CP and none have examined brain metabolism during a motor task. Nine children with bilateral spastic CP [Age: 6-11 years, Gross Motor Function Classification System (GMFCS) Levels II–V] completed this study. SVMC was evaluated using Selective Control Assessment of the Lower Extremity (SCALE) ranging from 0 (absent) to 10 (normal). Brain metabolism was measured using positron emission tomography (PET) scanning in association with a selective ankle motor task. Whole brain activation maps as well as ROI averaged metabolic activity were correlated with SCALE scores. The contralateral sensorimotor and superior parietal cortex were positively correlated with SCALE scores ($p < 0.0005$). In contrast, a negative correlation of metabolic activity with SCALE was found in the cerebellum ($p < 0.0005$). Subsequent ROI analysis showed that both ipsilateral and contralateral cerebellar metabolism correlated with SCALE but the relationship for the ipsilateral cerebellum was stronger ($R^2 = 0.80$, $p < 0.001$ vs. $R^2 = 0.46$, $p = 0.045$). Decreased cortical and increased cerebellar activation in children with less SVMC may be related to task difficulty, activation of new motor learning paradigms in the cerebellum and potential engagement of alternative motor systems when CSTs are focally damaged. These results support SCALE as a clinical correlate of neurological impairment.

Keywords: spastic cerebral palsy, PET—positron emission tomography, brain metabolism, selective voluntary motor control, ankle motor task

INTRODUCTION

Children with spastic cerebral palsy (CP) have developmental brain injuries primarily affecting the motor systems. Impairments of motor control are observed early in development (Fetters et al., 2004; Sargent et al., 2017) often preceding the detection of spasticity in children with CP. Deficits in gross motor function including mobility, strength, and balance are additional impairments. Spastic CP results from damage to the periventricular white matter containing descending motor tracts including the corticospinal tracts (CSTs) responsible for voluntary motor control (Bax et al., 2006;

Volpe, 2009). White matter damage including the CSTs has been described and quantified in CP and correlated with motor and sensory function measures using magnetic resonance imaging (MRI) with diffusion tensor imaging (DTI) techniques (Hoon et al., 2009; Lee et al., 2011). While damage to the developing CSTs is a primary etiology in spastic CP, resulting compensatory adaptations have not been adequately studied relative to brain structure and activity, especially for lower extremity function in patients with bilateral involvement.

CSTs that originate in the motor cortex are responsible for skilled voluntary movement or selective motor control. The term "selective voluntary motor control" (SVMC) indicates the deliberate performance of isolated movements upon request (Fowler et al., 2010). Children with spastic CP and impaired SVMC may exhibit reduced speed of movement, mirror movements or abnormal reciprocal muscle activation patterns. Also, they are often unable to move their hip, knee and ankle joints in isolation, relying instead on closely coupled flexion and extension patterns to varying degrees (Fowler and Goldberg, 2009). In two studies, SVMC was more predictive of motor function than other aspects of CP (Østensjø et al., 2004; Voorman et al., 2007). Clinical measures of SVMC have been shown to correlate with mobility level (Fowler et al., 2009), gross motor function (Balzer et al., 2016; Noble et al., 2019) and gait (Fowler and Goldberg, 2009; Steele et al., 2015; Rha et al., 2016; Chruscikowski et al., 2017; Zhou et al., 2019).

Following a perinatal injury to the CSTs, alternative motor pathways develop that are forms of adaptive or maladaptive plasticity (Eyre, 2007; Friel et al., 2013; Gordon, 2016). This has been shown for animal models and the upper extremity of children with spastic hemiplegic CP. Ipsilateral CSTs from the uninvolved hemisphere can be preserved causing mirror movements and other impairments. In adults post stroke, it has been suggested that compensations by areas of the brain such as the rubrospinal tracts are utilized when damage to CSTs occur, producing synergistic flexor and extensor patterns in the involved extremities during voluntary movement (Yeo and Jang, 2010). While children with spastic CP sustain an early injury to the brain before the development of motor skills, similar compensatory pathways may be involved (Cahill-Rowley and Rose, 2014).

The structure of white matter tracts has been the focus of brain imaging studies in spastic CP (Scheck et al., 2012; Mailleux et al., 2020). Far less is known about neuromotor recruitment. Studies of brain activity during movement in CP have primarily focused on children with unilateral involvement during upper extremity fine motor or sensory tasks using functional magnetic resonance imaging (fMRI; Dinomais et al., 2013; Van de Winckel et al., 2013a,b). Only two fMRI studies investigating lower extremity movement in CP could be found (Phillips et al., 2007; Hilderley et al., 2018). All children were high functioning as they were able to walk and run independently (GMFCS level I) and could actively dorsiflex the ankle, which indicates a high level of selective movement. Despite these stringent inclusion criteria, excessive head movement during the motor task was problematic during fMRI data collection resulting in unusable data for some participants (Phillips et al., 2007) or limiting the number of available trials for analysis (Hilderley et al., 2018). Brain activation can also be studied using positron emission tomography (PET), a metabolic imaging technique that uses radioactive compounds to label functional brain metabolism (Phelps, 2000). A common biologically active molecule used is FDG, an analog of glucose. Regional glucose metabolism and accumulation represent the metabolic activity of the tissues (Alauddin, 2012). Radiotracer concentrations in specific regions of the brain are mapped on three-dimensional images of the brain that are reconstructed from MRI (Lee et al., 2007; Penny et al., 2011). Only one PET scan study could be found that investigated brain metabolism in CP (Lee et al., 2007) but it did not involve a motor task. An advantage of PET for evaluating neuromotor control is that motor task performance and tracer uptake occur before the imaging session. In contrast, the motor task occurs during imaging for fMRI requiring that head position be maintained during limb movement, excluding more children with CP from participation.

The purpose of this study was to examine the relationship between brain metabolism and SVMC in children with spastic bilateral CP during movement using PET. SVMC was evaluated using the Selective Control Assessment of the Lower Extremity (SCALE; Fowler et al., 2009). We hypothesized that a significant positive relationship between SCALE and the sensorimotor cortex would be found. Our secondary hypothesis was that significant correlations between SCALE and activation of other motor regions of the brain would be identified.

MATERIALS AND METHODS

Participants

Children with spastic bilateral CP were recruited from clinics and the community *via* mailings and flyers. This study was approved by the Human Subject Committee at the University of California, Los Angeles, CA, USA. Informed assents and consents were obtained from the participants and their guardians. Participants were recruited from the Center for CP at UCLA/OIC as well as the surrounding Los Angeles community. Data used for this analysis were collected as baseline information for a larger treatment intervention study. Inclusion criteria were: (1) age between 4 and 12 years; (2) diagnosis of spastic form of CP; and (3) ability to remain still for a minimum of 15 min. Exclusion criteria were: (1) attention deficit or hyperactivity disorder; (2) seizure within the last 6 months; (3) participation in a research study that involves the use of radiation in the past 12 months; (4) fear of enclosed spaces, breathing or swallowing problems, dizziness, or fainting spells; (5) pacemaker, intrathecal baclofen pump or metal implants in the head or neck, other than tooth fillings; and (6) mechanical, cystic or other structural abnormalities on MRI. Following informed consent, each participant received a structural MRI. Participants who were unable to lie still or who had MRI exclusion factors were discontinued from study participation. A physical therapist assessed mobility using the Gross Motor Function Classification

System (GMFCS; Palisano et al., 1997) and gross motor function using the Gross Motor Function Measure (GMFM; Bjornson et al., 1998).

Selective Voluntary Motor Control Assessment

Before PET scanning, SVMC was assessed by a physical therapist using SCALE, a validated and reliable clinical tool, which was developed for individuals with spastic CP (Fowler et al., 2009; Balzer et al., 2016). This assessment incorporates components of CST function including selectivity, reciprocation, and speed as well as the presence of involuntary movement at other joints including mirror movements of the contralateral extremity. Hip, knee, ankle, subtalar and toe joints are assessed using an isolated, reciprocal movement pattern and each joint is scored 0 (Unable), 1 (Impaired) or 2 (Normal). Scores are summed resulting in a possible score from 0 (absent SVMC) to 10 (normal SVMC) for each lower limb.

PET Scan Data Acquisition

PET scanning was used to acquire regional cerebral metabolic data. Participants were asked to fast for 3 h before the procedure to optimize glucose uptake. The process of injection and PET scan required approximately 2 h for completion. An intravenous line was placed and 185 MBq (FDG) was administered using standard aseptic technique. A single small blood sample was obtained to establish the starting level of blood glucose. PET scans were performed 40 min post-FDG injection.

During this uptake period, the participant performed an ankle movement task with the lower extremity that demonstrated the least impairment. The task was limited to one lower extremity to examine regions of the brain that controlled movement for the ipsilateral vs. contralateral limb. The child was instructed by a physical therapist to perform a series of isolated ankle dorsiflexion and plantar flexion movements that were initiated every 2 min followed by a brief rest period. If movement occurred at other joints, verbal feedback was provided for initial attempts but the feedback was discontinued if the motion was obligatory.

Whole Brain Analysis

Relative quantification of regional brain activity was performed using NeuroQ^{TM} (Syntermed Inc., Atlanta). This software corrects for tissue-based attenuation and then implements an algorithm for automatically measuring the number of radioactive events emitted by a positron source (gamma-ray lines of coincidence) per second detected by PET-scanner, emanating from pixel locations assigned by a computerized reconstruction algorithm. Statistical parametric mapping (SPM) methods were performed (Friston et al., 1995a,b) to co-register participant images and to reorient them into a standardized coordinate system using the SPM software package (Ashburner, 2009) from the Wellcome Department of Cognitive Neurology, Functional Imaging Laboratory (London, UK). Data were spatially smoothed and normalized to mean global activity as previously described (Silverman et al., 2011), except for a 12 mm (full-width half-maximum) smoothing filter that was applied to the images before statistical analysis. The set of pooled data were assessed with the t-statistic on a voxel-by-voxel basis, to identify the profile of voxels that significantly covaried with parameters characterizing each participant. To identify the anatomical label of the underlying voxel, we defined 240 standardized ROIs (sROIs) following the transformation of each PET scan to a template space (Tai et al., 1997) throughout the transaxial planes across the field of view. Normalized uptake values were determined for specific regions of the brain. Whole-brain voxel-wise Pearson correlations of metabolic activity vs. SCALE scores were performed. These results were correlated for multiple comparisons using cluster wise thresholding in SPM. All 240 sROIs and 47 volumes of interest (sVOIs) were used solely to obtain an anatomic parcellation of the brain and to identify the anatomical regions where there is cluster-wise statistical significance.

Secondary ROI Analysis

In the case of bilateral activation, it was necessary to further identify whether the FDG uptake was ipsilateral or contralateral to the moving limb. Therefore, a secondary ROI analysis was performed exclusively for those regions. Mean voxel activity for the bilateral ROIs was calculated following the transformation of each PET scan to a template space. This value was automatically normalized to the mean activity measured throughout that brain scan for each ROI and was used to correlate with SCALE. Importantly, for correlation analysis, only the anatomical ROI-based average instead of the statistical ROI-based average was used to avoid circular analysis.

RESULTS

Participant characteristics are shown for 10 children who were enrolled and underwent baseline testing in **Table 1**. The average age was 9 years, 4 months. Motor impairment ranged from mild (GMFCS Level II, GMFM 72.2, SCALE 7 bilaterally) to severe (GMFCS Level V, GMFM 36.0, SCALE scores ≤ 3). Two participants exhibited bilateral SCALE score = 0. Four children could walk and six used wheelchairs as their primary mode of mobility. One participant was dropped from the study after enrollment due to a significant structural abnormality that was identified on MRI. Of the remaining nine participants, eight had white matter damage including periventricular leukomalacia on MRI. Bilateral volume loss of the thalamus was additionally reported for one of these children.

During the ankle motor task, obligatory movement at other joints was observed in most participants. All six participants with low limb SCALE scores (0–2) were unable to isolate ankle motion and exhibited simultaneous hip and knee synergistic movement. The remaining three participants with limb scores of ≥ 5 exhibited impaired SVMC at their ankle, due to an inability to perform at least 15° of isolated ankle motion or the presence of movement at another joint. Mirror movement at the ankle was observed for one participant.

TABLE 1 | Participant characteristics.

Demographics		***n* = 10**
Age	Mean Age (SD) year, month	9, 4 (1, 4)
	Age range years	6–11
Gender	Male	6
	Female	4
Ethnicity	Hispanic	4
Race	African American	1
	Caucasian	9
GMFCS	II	2
	III	2
	IV	3
	V	3
CP Diagnosis-distribution	Diplegia	5
	Quadriplegia	4
	Total body involvement	1
GMFM	Mean (SD)	53.2 (11.9)
SCALE	Left Mean (SD)	2.7 (2.5)
	Right Mean (SD)	2.5 (2.6)

SD, standard deviation; GMFCS, gross motor function classification system; GMFM, gross motor function measure; SCALE, selective control assessment of the lower extremity.

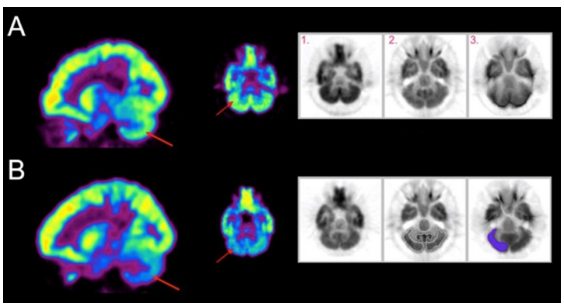

FIGURE 1 | Metabolic activity maps are shown for **(A)** an individual with a low Selective Control Assessment of the Lower Extremity (SCALE) score and **(B)** an individual with a high SCALE score. Red arrows indicate the right cerebellum. The gray scale images (inset) for each row show 1. Participant's original positron emission tomography (PET) scan, 2. Template PET scan on which standardized regions of interest are defined and 3. Activity resampled on the template. Relative hypoactivity was found in the cerebellum of the individual with a high SCALE score, indicated by the indigo color using a rainbow scale (violet being the lowest and red being the highest).

Qualitative Visualization of Whole Brain Metabolic Activity

Exemplar metabolic activity maps for individuals with contrasting SCALE scores can be seen in **Figure 1**. The metabolic maps in the first two columns are color-coded (rainbow scale) showing normalized activity for sagittal and axial slices. A contrast between cerebellar activation levels for two participants with low vs. high SCALE scores can be seen.

Whole-Brain Analysis

The results of SPM analyses examining correlations between metabolic activity and SCALE scores are shown in **Figure 2**. The sensorimotor (SM) and superior parietal (sPL) cortex contralateral to the moving limb were significantly positively correlated with SCALE scores (SM: $t = 8.06$, sPL: $t = 6.70$; $p < 0.0005$). In contrast, a significant negative correlation

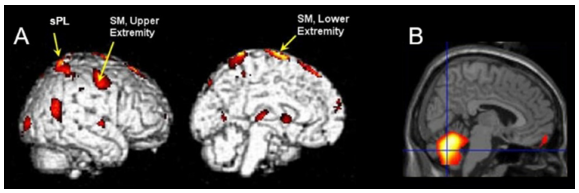

FIGURE 2 | **(A)** A three-dimensional volumetric rendering of significant positive correlations between SCALE and metabolic activity in the sensorimotor and the superior parietal cortex during movement of the contralateral limb shown on the lateral view and medial cross-section overlaid on an atlas ($p < 0.0005$, cluster corrected). **(B)** Voxels show significant negative correlations of metabolic activity with SCALE in the cerebellum ($p < 0.01$ cluster corrected) on the medial slice. Color indicates a significant relationship and yellow indicates a stronger relationship as compared to red. sPL, superior parietal lobe, SM, sensorimotor cortex.

of metabolic activity with SCALE was found in the entire cerebellum (peak $t = 7.23$, $p < 0.0005$). As both sides of the cerebellum were correlated with SCALE, the level of activation for the side ipsilateral vs. contralateral to the moving limb was not apparent from the whole-brain analysis. Therefore, a secondary analysis at the ROI level was performed.

ROI Analysis

We exclusively selected the cerebellum for further ROI analysis as it showed bilateral activation in the whole-brain analysis. Significant correlations between cerebellar ROI-averaged activity and SCALE score for the moving limb were found. As justified by tests of linearity, parametric Pearson correlation coefficients were used. A strong significant correlation was found between the SCALE scores for the moving limb and the ipsilateral cerebellum ($t = 5.27$, $p < 0.001$, **Figure 3A**). While the correlation between the activation level of the contralateral cerebellum and SCALE score was significant, the relationship was not as strong ($t = 2.43$, $p = 0.045$, **Figure 3B**).

DISCUSSION

This is the first study to document a relationship between impaired lower extremity SVMC and brain metabolic activity in children with CP. Previous researchers reported greater metabolism in bilateral motor and visual cortices and the cerebellum in children with spastic CP relative to typically developing children using PET; however, a motor task was not performed (Lee et al., 2007). As expected, children with higher levels of motor control in the present study exhibited greater activity in the cortical areas associated with motor function (sensorimotor and superior parietal cortices) contralateral to the moving limb. This finding is consistent with the primary motor cortex being the largest source of CSTs and the sensory cortex providing feedback during motor tasks. Further, the superior parietal cortex is known to be involved in adjusting posture and guiding movement of the limbs, particularly concerning visual-spatial perception and body awareness (Wolpert et al., 1998; Wolbers et al., 2003). A related finding from a fMRI study has shown activations in the primary motor and sensory areas

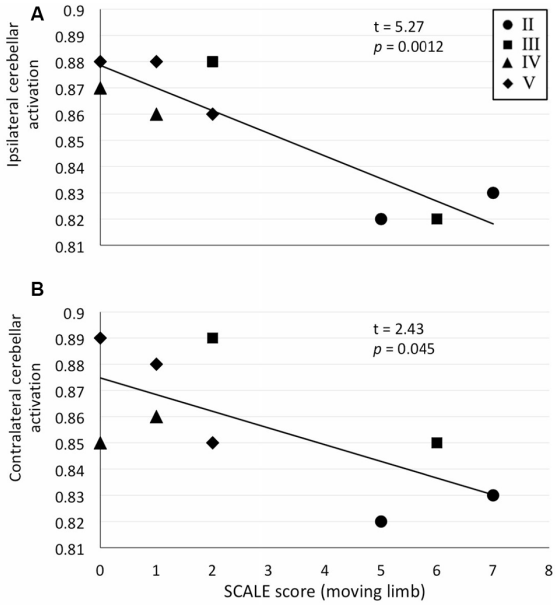

FIGURE 3 | Correlation plots for ROI-averaged cerebellar activation (normalized units) vs. SCALE score (from 0 = absent to 10 = normal) for the moving limb. **(A)** Ipsilateral cerebellum vs. SCALE score, R^2 = 0.80 and **(B)** Contralateral cerebellum vs. SCALE score, R^2 = 0.46. Gross Motor Function Classification System (GMFCS) level for each participant are indicated as II–IV.

in healthy adults performing a similar ankle dorsiflexion and plantarflexion task (Orr et al., 2008).

The sensorimotor region associated with the lower extremity exhibited a stronger correlation with SCALE than that associated with the upper extremity (**Figure 2B**). While activation of the sensorimotor cortex associated with the upper extremity would not be expected during ankle movement, the location of cortical activation has been found to vary for individuals with CP. Recently, motor evoked potentials with cortical stimulation were compared between adults with and without CP (Condliffe et al., 2019). Researchers reported that the "hotspots" for the soleus muscle of normal controls were in a tight cluster 2–3 cm lateral from the vertex (an anatomical landmark at the superior midpoint of the skull). For participants with CP, however, the hot spots were farther away from the vertex, more dispersed and, in some cases more lateral. Some hot spots appeared to be closer to the typical atlas site for the upper as compared to the lower extremity.

A unique aspect of this brain activation study was the inclusion of children with absent or very low levels of SVMC for whom greater cerebellar activation was found. Historically, the role of the cerebellum in normal movement production has been attributed to the control of balance and coordination. Although the exact role of the cerebellum is not fully known, studies have shown that it is involved with motor learning and motor control (Manto et al., 2012). Authors of a consensus article concluded that the cerebellar motor systems consist of an intrinsically connected network involved in the optimization of movement performance during the early phases of motor learning. It may also contain internal feedback models associated with unconscious skilled movement (Manto et al., 2012). This may explain increased activation in our participants with poor SVMC for whom this motor task was novel and more challenging.

An alternative explanation for greater cerebellar activation in children with reduced SVMC may be recruitment *via* alternative pathways that communicate with the cerebellum during movement. Although isolated ankle motion was requested, children with low SCALE scores produced simultaneous hip and knee motion (abnormal obligatory synergies). Rubrospinal tracts, which originate in the red nucleus and communicate with the cerebellum, have been associated with these more primitive synergies (Cahill-Rowley and Rose, 2014). Major afferents project from the cerebellar and cerebral cortices to the red nucleus and the rubrospinal tract projects to cerebellar nuclei before reaching the spinal cord (Darras and Volpe, 2018). Animal studies have shown that when the cerebellar nuclei are stimulated, stereotyped motor synergies are produced (Rispal-Padel et al., 1982). This may explain why children with larger deficits in SVMC may have a greater reliance on the cerebellum resulting in the production of less skillful patterned movements when higher centers of motor control are impaired.

While a stronger relationship with SCALE was found for the ipsilateral cerebellum, significance was also found for the contralateral side. Typically, there is an ipsilateral association between the cerebellum and limb movement; however, bilateral activation during unilateral movement has been reported in normal controls and adults post-stroke (Cui et al., 2000; Ehrsson et al., 2002; Nair et al., 2003; Kapreli et al., 2006; Dong et al., 2007). Normal adults performing a finger tapping task primarily activated their ipsilateral cerebellum when using their dominant hand but activated their cerebellum bilaterally when using their non-dominant hand (Dong et al., 2007). In the same study, patients post-stroke recruited their contralateral as well as their ipsilateral cerebellum while performing the task with their involved hand. While our patient population had bilateral rather than unilateral limb motor impairment, these data support our findings. Children with CP with greater impairment exhibited higher levels of bilateral cerebellar activation than those with less impairment.

Limitations

This study had a small sample size but comparative fMRI studies contained even fewer participants with CP (Phillips et al., 2007; Hilderley et al., 2018). A control group of typically developing children was not studied. While the goal was to examine varying levels of brain metabolism based on selective motor control within CP, knowledge of normal activation patterns under the same conditions is unknown. A common limitation in PET is the low anatomical resolution when mapping metabolic activity. Further, there may be smoothing of the metabolic maps when they are resampled to the SPM anatomical template, especially due to the lack of subject-specific MRI anatomical scan. However, this smoothing may also potentially lead to a gain in the signal to noise ratio locally over the image. Finally, due to statistical correction for a large number of voxel-wise multiple comparisons, there may be a loss of power although this loss

is mitigated by both cluster-wise thresholding methods and a separate *a priori* ROI-based analysis.

CONCLUSION

In this study, we examined neuromotor control during an ankle motor task that was challenging for children with spastic CP, particularly for those with low levels of motor control. As we hypothesized, there was a significant positive relationship between SVMC and metabolic activity in the sensorimotor cortex that was contralateral to the moving limb. Interestingly, we found that lower motor control was associated with greater cerebellar activation during the motor task. Decreased cortical and increased cerebellar activation in children with more impaired motor control may be related to task difficulty, activation of new motor learning paradigms in the cerebellum and potential engagement of alternative motor systems when CSTs are focally damaged. These results support SCALE as a clinical correlate of neurologic damage.

DATA AVAILABILITY STATEMENT

All datasets generated for this study are included in the article.

ETHICS STATEMENT

The studies involving human participants were reviewed and approved by Human Subjects Protection Committee, University of California, Los Angeles, USA. Written informed consent to participate in this study was provided by the participants' legal guardian.

AUTHOR CONTRIBUTIONS

EF, WO, MG, and DS designed and conducted the experiments. EF, DS, and SJ analyzed the data. EF wrote the article. LS, SJ, and WO contributed to the discussion and edited the article.

FUNDING

This study was funded by a grant from the United Cerebral Palsy Research and Education Foundation #R769-04.

ACKNOWLEDGMENTS

We thank the parents and children for their participation in this study.

REFERENCES

Alauddin, M. M. (2012). Positron emission tomography (PET) imaging with ^{18}F-based radiotracers. *Am. J. Nucl. Med. Mol. Imaging* 2, 55–76.

Ashburner, J. (2009). Computational anatomy with the SPM software. *Magn. Reson. Imaging* 27, 1163–1174. doi: 10.1016/j.mri.2009.01.006

Balzer, J., Marsico, P., Mitteregger, E., van der Linden, M. L., Mercer, T. H., and van Hedel, H. J. A. (2016). Construct validity and reliability of the selective control assessment of the lower extremity in children with cerebral palsy. *Dev. Med. Child Neurol.* 58, 167–172. doi: 10.1111/dmcn.12805

Bax, M., Tydeman, C., and Flodmark, O. (2006). Clinical and mri correlates of cerebral palsy: the european cerebral palsy study. *JAMA* 296, 1602–1608. doi: 10.1001/jama.296.13.1602

Bjornson, K. F., Graubert, C. S., Buford, V. L., and McLaughlin, J. (1998). Validity of the gross motor function measure. *Pediatr. Phys. Ther.* 10, 43–47. doi: 10.1097/00001577-199801020-00002

Cahill-Rowley, K., and Rose, J. (2014). Etiology of impaired selective motor control: emerging evidence and its implications for research and treatment in cerebral palsy. *Dev. Med. Child Neurol.* 56, 522–528. doi: 10.1111/dmcn.12355

Chruscikowski, E., Fry, N. R. D., Noble, J. J., Gough, M., and Shortland, A. P. (2017). Selective motor control correlates with gait abnormality in children with cerebral palsy. *Gait Posture* 52, 107–109. doi: 10.1016/j.gaitpost.2016.11.031

Condliffe, E. G., Jeffery, D. T., Emery, D. J., Treit, S., Beaulieu, C., and Gorassini, M. A. (2019). Full activation profiles and integrity of corticospinal pathways in adults with bilateral spastic cerebral palsy. *Neurorehabil. Neural Repair* 33, 59–69. doi: 10.1177/1545968318818898

Cui, S.-Z., Li, E.-Z., Zang, Y.-F., Weng, X.-C., Ivry, R., and Wang, J.-J. (2000). Both sides of human cerebellum involved in preparation and execution of sequential movements. *Neuroreport* 11, 3849–3853. doi: 10.1097/00001756-200011270-00049

Darras, B. T., and Volpe, J. J. (2018). "Evaluation, special studies," in *Volpe's Neurology of the Newborn, 6th Edition*, eds J. Volpe, T. E. Inder, B. T. Darras, L. S. de Vries, A. J. du Plessis, J. J. Neil and J. M. Perlman (Philadephia, PA, USA: Elsevier), 861–873.

Dinomais, M., Lignon, G., Chinier, E., Richard, I., Ter Minassian, A., and Tich, S. N. T. (2013). Effect of observation of simple hand movement on brain activations in patients with unilateral cerebral palsy: an fMRI study. *Res. Dev. Disabil.* 34, 1928–1937. doi: 10.1016/j.ridd.2013.03.020

Dong, Y., Winstein, C. J., Albistegui-DuBois, R., and Dobkin, B. H. (2007). Evolution of FMRI activation in the perilesional primary motor cortex and cerebellum with rehabilitation training-related motor gains after stroke: a pilot study. *Neurorehabil. Neural Repair* 21, 412–428. doi: 10.1177/1545968306298598

Ehrsson, H. H., Kuhtz-Buschbeck, J. P., and Forssberg, H. (2002). Brain regions controlling nonsynergistic versus synergistic movement of the digits: a functional magnetic resonance imaging study. *J. Neurosci.* 22, 5074–5080. doi: 10.1523/JNEUROSCI.22-12-05074.2002

Eyre, J. (2007). Corticospinal tract development and its plasticity after perinatal injury. *Neurosci. Biobehav. Rev.* 31, 1136–1149. doi: 10.1016/j.neubiorev.2007.05.011

Fetters, L., Chen, Y., Jonsdottir, J., and Tronick, E. Z. (2004). Kicking coordination captures differences between full-term and premature infants with white matter disorder. *Hum. Mov. Sci.* 22, 729–748. doi: 10.1016/j.humov.2004.02.001

Fowler, E. G., Staudt, L. A., and Greenberg, M. B. (2010). Lower-extremity selective voluntary motor control in patients with spastic cerebral palsy: increased distal motor impairment. *Dev. Med. Child Neurol.* 52, 264–269. doi: 10.1111/j.1469-8749.2009.03586.x

Fowler, E. G., Staudt, L. A., Greenberg, M. B., and Oppenheim, W. L. (2009). Selective control assessment of the lower extremity (SCALE): development, validation, and interrater reliability of a clinical tool for patients with cerebral palsy. *Dev. Med. Child Neurol.* 51, 607–614. doi: 10.1111/j.1469-8749.2008.03186.x

Fowler, E., and Goldberg, E. (2009). The effect of lower extremity selective voluntary motor control on interjoint coordination during gait in children with spastic diplegic cerebral palsy. *Gait Posture* 29, 102–107. doi: 10.1016/j.gaitpost.2008.07.007

Friel, K. M., Chakrabarty, S., and Martin, J. H. (2013). Pathophysiological mechanisms of impaired limb use and repair strategies for motor systems after unilateral injury of the developing brain. *Dev. Med. Child Neurol.* 55, 27–31. doi: 10.1111/dmcn.12303

Friston, K. J., Ashburner, J., Frith, C. D., Poline, J.-B., Heather, J. D., and Frackowiak, R. S. (1995a). Spatial registration and normalization of images. *Hum. Brain Mapp.* 3, 165–189. doi: 10.1002/hbm.460030303

Friston, K. J., Holmes, A. P., Poline, J. B., Grasby, P. J., Williams, S. C. R., Frackowiak, R. S., et al. (1995b). Analysis of fMRI time-series revisited. *NeuroImage* 2, 45–53. doi: 10.1006/nimg.1995.1007

Gordon, A. M. (2016). Impaired voluntary movement control and its rehabilitation in cerebral palsy. *Adv. Exp. Med. Biol.* 957, 291–311. doi: 10.1007/978-3-319-47313-0_16

Hilderley, A., Taylor, M., Fehlings, D., Chen, J., and Wright, F. (2018). Optimization of fMRI methods to determine laterality of cortical activation during ankle movements of children with unilateral cerebral palsy. *Int. J. Dev. Neurosci.* 66, 54–62. doi: 10.1016/j.ijdevneu.2018.01.004

Hoon, A. H. J., Stashinko, E. E., Nagae, L. M., Lin, D. D. M., Keller, J., Bastian, A., et al. (2009). Sensory and motor deficits in children with cerebral palsy born preterm correlate with diffusion tensor imaging abnormalities in thalamocortical pathways. *Dev. Med. Child Neurol.* 51, 697–704. doi: 10.1111/j.1469-8749.2009.03306.x

Kapreli, E., Athanasopoulos, S., Papathanasiou, M., Van Hecke, P., Strimpakos, N., Gouliamos, A., et al. (2006). Lateralization of brain activity during lower limb joints movement. An fMRI study. *NeuroImage* 32, 1709–1721. doi: 10.1016/j.neuroimage.2006.05.043

Lee, J. D., Park, H.-J., Park, E. S., Kim, D. G., Rha, D.-W., Kim, E. Y., et al. (2007). Assessment of regional $GABA_A$ receptor binding using 18F-fluoroflumazenil positron emission tomography in spastic type cerebral palsy. *NeuroImage* 34, 19–25. doi: 10.1016/j.neuroimage.2006.09.004

Lee, J. D., Park, H.-J., Park, E. S., Oh, M.-K., Park, B., Rha, D.-W., et al. (2011). Motor pathway injury in patients with periventricular leucomalacia and spastic diplegia. *Brain* 134, 1199–1210. doi: 10.1093/brain/awr021

Mailleux, L., Franki, I., Emsell, L., Peedima, M.-L., Fehrenbach, A., Feys, H., et al. (2020). The relationship between neuroimaging and motor outcome in children with cerebral palsy: a systematic review—Part B diffusion imaging and tractography. *Res. Dev. Disabil.* 97:103569. doi: 10.1016/j.ridd.2019.103569

Manto, M., Bower, J. M., Conforto, A. B., Delgado-García, J. M., da Guarda, S. N. F., Gerwig, M., et al. (2012). Consensus paper: roles of the cerebellum in motor control—the diversity of ideas on cerebellar involvement in movement. *Cerebellum* 11, 457–487. doi: 10.1007/s12311-011-0331-9

Nair, D. G., Purcott, K. L., Fuchs, A., Steinberg, F., and Kelso, J. S. (2003). Cortical and cerebellar activity of the human brain during imagined and executed unimanual and bimanual action sequences: a functional MRI study. *Cogn. Brain Res.* 15, 250–260. doi: 10.1016/s0926-6410(02)00197-0

Noble, J. J., Gough, M., and Shortland, A. P. (2019). Selective motor control and gross motor function in bilateral spastic cerebral palsy. *Dev. Med. Child Neurol.* 61, 57–61. doi: 10.1111/dmcn.14024

Orr, E. L., Lacourse, M. G., Cohen, M. J., and Cramer, S. C. (2008). Cortical activation during executed, imagined and observed foot movements. *Neuroreport* 19, 625–630. doi: 10.1097/wnr.0b013e3282fbf9e0

Østensjø, S., Carlberg, E. B., and Vøllestad, N. K. (2004). Motor impairments in young children with cerebral palsy: relationship to gross motor function and everyday activities. *Dev. Med. Child Neurol.* 46, 580–589. doi: 10.1017/s0012162204000994

Palisano, R., Rosenbaum, P., Walter, S., Russell, D., Wood, E., and Galuppi, B. (1997). Development and reliability of a system to classify gross motor function in children with cerebral palsy. *Dev. Med. Child Neurol.* 39, 214–223. doi: 10.1111/j.1469-8749.1997.tb07414.x

Penny, W. D., Friston, K. J., Ashburner, J. T., Kiebel, S. J., and Nichols, T. E. (eds.) (2011). Statistical parametric mapping: the analysis of functional brain images. London: Academic Press, Elsevier.

Phelps, M. E. (2000). PET: the merging of biology and imaging into molecular imaging. *J. Nucl. Med.* 41, 661–681.

Phillips, J. P., Sullivan, K. J., Burtner, P. A., Caprihan, A., Provost, B., and Bernitsky-Beddingfield, A. (2007). Ankle dorsiflexion fMRI in children with cerebral palsy undergoing intensive body-weight-supported treadmill training: a pilot study. *Dev. Med. Child Neurol.* 49, 39–44. doi: 10.1017/s0012162207000102.x

Rha, D., Cahill-Rowley, K., Young, J., Torburn, L., Stephenson, K., and Rose, J. (2016). Biomechanical and clinical correlates of stance-phase knee flexion in persons with spastic cerebral palsy. *PM&R.* 54, 11–18. doi: 10.1016/j.pmrj.2015.06.003

Rispal-Padel, L., Cicirata, F., and Pons, C. (1982). Cerebellar nuclear topography of simple and synergistic movements in the alert baboon (*Papio papio*). *Exp. Brain Res.* 47, 365–380. doi: 10.1007/bf00239355

Sargent, B., Reimann, H., Kubo, M., and Fetters, L. (2017). Infant intralimb coordination and torque production: influence of prematurity. *Infant. Behav. Dev.* 49, 129–140. doi: 10.1016/j.infbeh.2017.08.009

Scheck, S. M., Boyd, R. N., and Rose, S. E. (2012). New insights into the pathology of white matter tracts in cerebral palsy from diffusion magnetic resonance imaging: a systematic review. *Dev. Med. Child Neurol.* 54, 684–696. doi: 10.1111/j.1469-8749.2012.04332.x

Silverman, D. H., Geist, C. L., Kenna, H. A., Williams, K., Wroolie, T., Powers, B., et al. (2011). Differences in regional brain metabolism associated with specific formulations of hormone therapy in postmenopausal women at risk for AD. *Psychoneuroendocrinology* 36, 502–513. doi: 10.1016/j.psyneuen.2010.08.002

Steele, K. M., Rozumalski, A., and Schwartz, M. H. (2015). Muscle synergies and complexity of neuromuscular control during gait in cerebral palsy. *Dev. Med. Child. Neurol.* 57, 1176–1182. doi: 10.1111/dmcn.12826

Tai, Y.-C., Lin, K. P., Hoh, C. K., Huang, S. H., and Hoffman, E. J. (1997). Utilization of 3-D elastic transformation in the registration of chest X-ray CT and whole body PET. *IEEE Trans. Nuclear Sci.* 44, 1606–1612. doi: 10.1109/23.632740

Van de Winckel, A., Klingels, K., Bruyninckx, F., Wenderoth, N., Peeters, R., Sunaert, S., et al. (2013a). How does brain activation differ in children with unilateral cerebral palsy compared to typically developing children, during active and passive movements, and tactile stimulation? An fMRI study. *Res. Dev. Disabil.* 34, 183–197. doi: 10.1016/j.ridd.2012.07.030

Van de Winckel, A., Verheyden, G., Wenderoth, N., Peeters, R., Sunaert, S., Van Hecke, W., et al. (2013b). Does somatosensory discrimination activate different brain areas in children with unilateral cerebral palsy compared to typically developing children? An fMRI study. *Res. Dev. Disabil.* 34, 1710–1720. doi: 10.1016/j.ridd.2013.02.017

Volpe, J. J. (2009). Brain injury in premature infants: a complex amalgam of destructive and developmental disturbances. *Lancet Neurol.* 8, 110–124. doi: 10.1016/S1474-4422(08)70294-1

Voorman, J. M., Dallmeijer, A. J., Knol, D. L., Lankhorst, G. J., and Becher, J. G. (2007). Prospective longitudinal study of gross motor function in children with cerebral palsy. *Arch. Phys. Med. Rehabil.* 88, 871–876. doi: 10.1016/j.apmr.2007.04.002

Wolbers, T., Weiller, C., and Büchel, C. (2003). Contralateral coding of imagined body parts in the superior parietal lobe. *Cereb. Cortex* 13, 392–399. doi: 10.1093/cercor/13.4.392

Wolpert, D. M., Goodbody, S. J., and Husain, M. (1998). Maintaining internal representations: the role of the human superior parietal lobe. *Nat. Neurosci.* 1, 529–533. doi: 10.1038/2245

Yeo, S. S., and Jang, S. H. (2010). Changes in red nucleus after pyramidal tract injury in patients with cerebral infarct. *NeuroRehabilitation* 27, 373–377. doi: 10.3233/nre-2010-0622

Zhou, J. Y., Lowe, E., Cahill-Rowley, K., Mahtani, G. B., Young, J. L., and Rose, J. (2019). Influence of impaired selective motor control on gait in children with cerebral palsy. *J. Child. Orthop.* 13, 73–81. doi: 10.1302/1863-2548.13.180013

Conflict of Interest: The authors declare that the research was conducted in the absence of any commercial or financial relationships that could be construed as a potential conflict of interest.

frontiers in Neurology

ORIGINAL RESEARCH
published: 02 June 2020
doi: 10.3389/fneur.2020.00378

Treatment Response to Botulinum Neurotoxin-A in Children With Cerebral Palsy Categorized by the Type of Stretch Reflex Muscle Activation

Lynn Bar-On[1,2]*, *Erwin Aertbeliën*[3,4], *Anja Van Campenhout*[5,6], *Guy Molenaers*[5,6] and *Kaat Desloovere*[2,6]

[1] Department of Rehabilitation Medicine, Amsterdam UMC, Amsterdam Movement Sciences, Amsterdam, Netherlands, [2] Department of Rehabilitation Sciences, KU Leuven, Leuven, Belgium, [3] Department of Mechanical Engineering, KU Leuven, Leuven, Belgium, [4] ROB Core Lab, Flanders Make, Leuven, Belgium, [5] Department of Development and Regeneration, KU Leuven, Leuven, Belgium, [6] Clinical Motion Analysis Laboratory, University Hospital Leuven, Leuven, Belgium

While Botulinum NeuroToxin-A (BoNT-A) injections are frequently used to reduce the effects of hyperactive stretch reflexes in children with cerebral palsy (CP), the effects of this treatment vary strongly. Previous research, combining electromyography (EMG) with motion analysis, defined different patterns of stretch reflex muscle activation in muscles, those that reacted more to a change in velocity (velocity dependent –VD), and those that reacted more to a change in length (length dependent –LD). The aim of this study was to investigate the relation between the types of stretch reflex muscle activation in the semitendinosus with post-BoNT-A outcome as assessed passively and with 3D gait analysis in children with spastic CP. Eighteen children with spastic CP (10 bilaterally involved) between the ages of 12 and 18 years were assessed before and on average, 8 weeks post-treatment. EMG and motion analysis were used to assess the degree and type of muscle activation dependency in the semitendinosus during passive knee extensions performed at different joint angular velocities. Three-dimensional gait analysis was used to assess knee gait kinematics as a measure of functional outcome. Pre-treatment, 9 muscles were classified as VD and 9 as LD, but no differences between the groups were evident in the baseline knee gait kinematics. Post-treatment, stretch reflex muscle activation decreased significantly in both groups but the reduction was more pronounced in those muscles classified pre-treatment as VD (−72% vs. −50%, $p = 0.005$). In the VD group, these changes were accompanied by greater knee extension at initial contact and during the swing phase of gait. In the LD group, there was significantly increased post-treatment knee hyperextension in late stance. Although results vary between patients, the reduction of stretch reflex muscle activation in the semitendinosus generally translated to an improved functional outcome, as assessed with 3D gait analysis. However, results were less positive for those muscles with pre-treatment length-dependent type of stretch reflex muscle activation. The study demonstrates the relevance of categorizing the type of stretch reflex muscle activation as a possible predictor of treatment response.

Keywords: cerebral palsy, stretch reflex, spasticity, gait analysis, Botulinum toxin, treatment, tone reduction, muscle spindles

OPEN ACCESS

Edited by:
Maurizio Ferrarin, Fondazione Don Carlo Gnocchi Onlus (IRCCS), Italy

Reviewed by:
Isabella Campanini, Local Health Authority of Reggio Emilia (IRCCS), Italy
Tishya Wren, Children's Hospital of Los Angeles, United States

***Correspondence:**
Lynn Bar-On
l.bar-on@amsterdamumc.nl

Specialty section:
This article was submitted to Movement Disorders, a section of the journal Frontiers in Neurology

Received: *02 December 2019*
Accepted: *14 April 2020*
Published: *02 June 2020*

Citation:
Bar-On L, Aertbeliën E, Van Campenhout A, Molenaers G and Desloovere K (2020) Treatment Response to Botulinum Neurotoxin-A in Children With Cerebral Palsy Categorized by the Type of Stretch Reflex Muscle Activation. Front. Neurol. 11:378. doi: 10.3389/fneur.2020.00378

INTRODUCTION

Cerebral palsy (CP) is a common childhood physical disability caused by a non-progressive brain injury resulting in impaired development of the musculoskeletal system (1). The most common motor impairment among children with CP is spastic paresis (2), in which hindered development of the descending motor and sensory tracks results initially, in muscle paresis, followed very quickly by muscle alterations including increased sensitivity of the stretch reflexes (3, 4). When stretch reflexes, as measured at rest, are exaggerated in response to a changing stretch velocity, they are referred to as "spasticity" (5). In addition, studies carried out on different muscles of children with CP have reported exaggerated stretch reflexes in response to changes in muscle length, rather than velocity (6–9). In particular, length-dependent stretch reflex activation was most prevalent in the semitendinosus (6). Some hypothesize that this length-dependency reflects more severely affected muscles (2) or muscles with a more complex movement disorder (10). While several underlying pathophysiological mechanisms of the different types of stretch reflex muscle activation have been proposed (2), it is also relevant to verify whether treatment response differs between the two types of stretch reflex activation.

Reduction of hyperactive stretch reflexes is a key component of the therapy directed at children with spastic CP. For example, injections of Botulinum NeuroToxin-A (BoNT-A) to the semitendinosus are commonly included in a multi-level therapy approach (11). However, treatment success following BoNT-A injections varies strongly, especially in proximal leg muscles, such as the semitendinosus (12). This response variability necessitates more research to help delineate to whom such treatment should be directed. This is especially important given the concerns regarding the possible longitudinal impact of repeated BoNT-A injections on muscle growth (13, 14).

Instrumented assessments such as electromyography (EMG) and 3D motion analysis are becoming more accessible in clinical settings. Compared to ordinal clinical scales, these instruments allow more accurate diagnosis of impairments in children with CP, leading to more informed treatment decisions. In addition, given the low correlation between impairments assessed with the child at rest on an examination table and their assessment during gross motor function, such as gait, it is important that treatment effects are assessed in an instrumented way in both passive and active conditions (15). Therefore, using EMG and motion analysis during passive stretch and during gait, the aim of this study was to examine whether the type of stretch reflex muscle activation affects treatment outcome after BoNT-A injections in the semitendinosus of children with spastic CP. We hypothesized that those muscles with pure velocity-dependent reflexes pre-treatment will show greater improvement post BoNT-A compared to the muscles that show clear length-dependent reflex activations.

METHODS

Ethics Statement

Ethical approval was granted by the University Hospitals' Ethics Committee (B32220072814). Parents/guardians and subjects were informed of the procedure. Parents/guardians and children over the age of 12 provided written informed consent in accordance with the Declaration of Helsinki.

Participants

A convenience sample of 19 children with spastic CP aged 12–18 years were included (**Table 1**). Data from the instrumented spasticity assessment, but not their gait analysis, had also been analyzed for a previous study (16). One child from this sample did not undergo a gait analysis on the same day as the instrumented spasticity assessment and was therefore excluded from the current study, resulting in 18 subjects for final analysis. The exclusion criteria were as previously reported: a diagnosis (by a neurologist) of ataxia or dystonia; severe muscle weakness [<2+ on the Manual Muscle Test (17)]; poor selectivity (18); knee joint contractures that compromised passive knee joint motion to <20 degrees; cognitive problems that could impede the measurements; previous lower-limb orthopedic surgery; intrathecal baclofen pump; selective dorsal rhizotomy; BoNT-A injections 6 months prior to the first assessment.

Treatment

Subjects received BoNT-A injections in the semitendinosus as part of a multilevel treatment. BoNT-A dosage and muscle selection were based on patient weight, medical history, findings of a clinical examination, and 3D gait analysis. Injection was done under short general anesthesia, and ultrasound was used for visual identification of muscles and needle depth control (19). As part of the established and standardized integrated approach for BoNT-A treatment at the University Hospital, all patients received some casting during 1–2 weeks immediately following the injections. Some children only had ankle casting (i.e., below-the-knee), while for other children the ankle casts were combined with removable or non-removable full leg casts and an additional abduction-exorotation bar. As part of their regular care, physiotherapy was intensified during the first 4 weeks post-treatment such that three to five sessions of 30–60 min physiotherapy were provided per week. Details of the treatments are reported in **Table 2**.

Data Collection and Processing

3D Gait Analysis

Three-dimensional gait analysis data were collected using a 12 camera VICON system, operating at 100 Hz (VICON, Oxford Metrics, Oxford, UK). Fifteen reflective markers were placed at specific anatomical landmarks on the pelvis and lower limbs, according to the lower-limb Vicon Plug-in-Gait marker configuration (VICON, Oxford Metrics, Oxford, UK). All children walked barefoot at a self-selected walking speed along the walkway. A trial was considered successful when there

TABLE 1 | Included subject characteristics.

		Pre-treatment stretch reflex activation	
	All ($n = 18$)	**Velocity dependent ($n = 9$)**	**Length dependent ($n = 9$)**
Mean age (SD) (years)	9.78 (1.87)	9.65 (1.77)	9.89 (2.07)
Male/female (n)	12/6	6/3	6/3
Bilateral involvement (n)	11	4	7
Unilateral involvement (R/L) (n)	3/4	3/2	1/1
GMFCS (I/II/III) (n)	6/8/4	5/3/1	1/5/3
Median (range) number of previous BoNT-A injections in the medial hamstrings (semitendinosus, semimembranosus, gracilis)	2 (0–9)	2 (0–9)	0 (0–5)

GMFCS, gross motor functional classification scale; BoNT-A, botulinum neurotoxin-A.

TABLE 2 | Treatment details: number of injected muscles, average amount (SD) of Botulinum neurotoxin-A (botox®) injected per muscle, number of subjects prescribed with upper leg casts and number of lower and/or upper-leg casts, average number of casting days, physiotherapy sessions per week and duration.

			Pre-treatment stretch reflex activation pattern			
	All ($n = 18$)		**Velocity dependent ($n = 9$)**		**Length dependent ($n = 9$)**	
botox®	*n*	Units/kg	*n*	Units/kg	*n*	Units/kg
Psoas	13	1.85 (0.55)	6	1.50 (0.55)	7	2.14 (0.38)
Adductor	7	1.21 (0.57)	3	0.83 (0.29)	4	1.5 (0.58)
Rectus femoris	3	1.0 (0.50)	2	1.00 (0.71)	1	1.0 (0.0)
Medial hamstrings (semitendinosus, semimembranosus, gracilis)	18	4.44 (1.09)	9	4.32 (0.97)	9	4.56 (1.24)
Gastrocnemius	13	3.04 (1.33)	7	2.93 (1.64)	6	3.17 (0.98)
Soleus	8	1.91 (0.63)	4	1.69 (0.63)	4	2.13 (0.63)
Casting	*n*	Days in casts	*n*	Days in casts	*n*	Days in casts
Removable upper-leg casts	13	12.67 (1.97)	7	12.50 (2.07)	6	13.00 (2.00)
Non-removable upper-leg casts	4		2		2	
No upper-leg casts	1		0		1	
Non-removable lower-leg casts	16		9		7	
Physiotherapy	Sessions/week	Session duration (min)	Sessions/week	Session duration (min)	Sessions/week	Session duration (min)
	4.72 (2.37)	36.94 (12.14)	4.44 (1.01)	37.22 (11.74)	5.00 (3.28)	36.67 (13.23)

was good marker visibility. At least three successful trials were collected per participant.

Gait cycle events of initial contact and toe-off were visually determined in Nexus, Vicon (Oxford Metrics Group, UK) which was also used to apply the lower limb Plug-in-Gait for extracting 3D kinematic data. Further analysis was only carried out on the sagittal plane knee kinematics of the most affected knee organized in gait cycles. Firstly, statistical analyses of the entire kinematic waveforms were carried out in order to identify those phases of the gait cycle that significantly differed pre-post intervention. Secondly, the minimum knee extension angles during stance and during swing were calculated. These angles were previously found to be sensitive to treatment with BoNT-A in the semitendinosus (12), and to spasticity (20).

Instrumented Assessments During Passive Stretch

The degree and type of stretch reflex activation in the semitendinosus and its effect on passive knee extension was assessed by combining surface EMG, inertial measurement units and a hald-held dynamometer via a custom-built modular measurement system (compactRIO, National Instruments, Austin, Texas). The method has been extensively validated for use in children with CP, proving reliable and sensitive to the effects of BoNT-A (16, 21).

In children with unilateral CP, only the affected side was tested. In children with bilateral involvement, the most involved side was tested. The most involved side was defined as the side with the highest Modified Ashworth Scale score in the hamstrings (22) or, in case of symmetrical scores, an earlier knee catch angle as defined by the Modified Tardieu Scale (23). When sides were equally affected, the left side was selected. Patients lay supine and were instructed to relax. Circular Ag/AgCl electrodes (diameter of 2 cm) were placed on the muscle bellies of the semitendinosus and the rectus femoris, on specific landmarks with an inter-electrode distance of 2 cm according to the SENIAM guidelines. To minimize cable related movement artifacts on the EMG signal, EMG cables and receivers were taped to the skin. EMG data were collected using the Zerowire system (Cometa, Milan,

IT) at a sample rate of 2000 Hz. EMG recording were first collected at rest to define baseline activity. With the knee and hip stabilized by the examiner at 90 degrees, children were asked to carry out three repetitions of an isometric maximum voluntary contraction (MVC) with the knee flexors. The average recorded EMG data from the semitendinosus during the MVCs were used for normalization purposes of passive stretch EMG data collected pre-treatment. Since BoNT-A influences the EMG amplitude, the MVC pre- and post-treatment are not comparable. Therefore, much care was given to standardize the location of the EMG sensors, and EMG was not normalized post-treatment and when comparing pre to post-treatment.

Following the MVCs, the knee joint was passively moved by an examiner from knee flexion to full knee extension (from here on referred to as stretch trials). Firstly, the stretch was carried out at low velocity during ± 5s, then at an intermediate, medium velocity during ± 1s, and finally at high velocity, which was performed as fast possible. Three repetitions were carried out at each velocity. Repetitions were separated by 10 s intervals in order to avoid post-activation depression of the electrophysiological response to stretch (24).

A 6th order zero-phase Butterworth bandpass filter ranging from 20 to 500 Hz was applied to the raw surface EMG signal. The EMG envelope was extracted by taking the square root after applying a low-pass 30 Hz 6th order zero-phase Butterworth filter on the squared raw signal. Joint position and joint velocity were estimated from the data collected with the inertial measurement units using a Kalman smoother (25). From this, joint range of motion (ROM) and maximum angular velocity were obtained. All angular velocity-time profiles were bell-shaped. By visualizing the raw and processed data in a custom-made Matlab GUI, stretch repetitions were excluded when performed out of plane [see Supplement 1 in (21)], at inconsistent velocities between different repetitions within a velocity trial (difference of >5, 15, or 30°/s for low, medium, and fast stretch trials, respectively), in case of poor quality EMG (loss of signal, low signal-to-noise ratio or obvious artifacts), or in case of unexpected antagonist activation.

Stretch reflex sensitivity is related to the conditions from which the stretch is performed, including starting muscle length, stretch velocity and baseline muscle tone (26). To check whether these parameters were equal across groups and sessions, EMG recordings collected at rest, the average starting knee angular positions and maximum angular velocities from slow and fast stretch trials, and the average knee joint ROM from slow stretch trials, were extracted.

To quantify the amount of muscle activation during stretch, we studied the area under the EMG envelope relative to the position moved during stretch trials:

$$(1) integral\ EMG\ envelope = \int_{t_2}^{t_1} EMG_{envelope}\,(t\,)\,dt$$

$$(2) average\ EMG\ envelope = \frac{integral\ EMG\ evelope}{t_2 - t_1}$$

Where t_1 and t_2 are times corresponding to particular joint positions. Length-dependent muscle activation, termed EMG_{LD}, was expected to increase between the start and end of the slow stretch trials. Therefore, EMG_{LD} was calculated from slow stretch trials as the average EMG envelope during 60–90% ROM minus the average EMG envelope during 10–30% ROM. The extremes of the ROM (0–10 and 90–100%) were excluded as they were more likely influenced by the performance of the examiner and the comfort of the patient. EMG_{LD} was then expressed as a percentage of the pre-treatment average EMG envelope during the MVCs. Muscles with EMG_{LD} values ≥5%, were categorized as length-dependent (LD) and muscles with EMG_{LD} values <5%, as velocity-dependent (VD). Examples are provided in **Figure 1**.

In addition, the influence of increasing muscle stretch velocity on EMG amplitude was quantified using data from both the slow and the fast stretch trials. Specifically, the average EMG envelope during fast trials was computed over a time interval starting 200 ms prior to the time corresponding to maximum angular velocity and ending at the time corresponding to 90% of the ROM. Then, the average EMG envelope in the time interval corresponding to 10–90% ROM of the slow stretch trials was deducted from this value. This parameter is referred to as EMG_{VD}, and was calculated for all muscles, irrespective of categorization as LD or VD.

After accounting for the forces caused by gravity and inertia [based on estimates of the lower leg weight (27)], the net knee torque applied by the examiner was calculated from the external forces, moments, and measured moment arms [Figure 1B in (21)]. The (compensated) knee torque at 70 degrees knee flexion (an angle that corresponded to the overall mid-ROM of all subjects), further referred to as "Torque," was computed and the average value during slow stretch trials deducted from that during fast stretch trials. All data processing, visualization and analyses were carried out with custom-made MATLAB software (version 8.5.0 R2015a).

Statistical Analysis

Distribution normality of the data, divided by LD and VD groups, was assessed with Shapiro-Wilik tests and by inspection of *q–q* plots. Pre-treatment data were compared between LD and VD groups, while analysis of the effect of treatment was carried out separately for LD and VD groups as well as on the entire sample. Firstly, the knee kinematic waveforms in the sagittal plane during gait were compared with two-tailed unpaired (LD vs. VD) and paired (pre-post treatment) tests using a statistical parametric (SPM{t}) or non-parametric (SnPM{t}) map, over the gait cycle data (28). The minimum knee extension angles during stance and during swing were calculated per gait cycle and averaged per individual.

Discrete parameters (from passive stretch trials and gait) pre-treatment as well as the pre-post treatment change values were compared between LD and VD groups using unpaired *t*-tests or Mann Whitney U tests. Per group, as well as for the entire group, the effect of treatment on all discrete parameters (from passive stretch and gait) were carried out using paired *t*-tests or Wilcoxon Signed rank tests. Data of the groups were then combined to explore the relations between pre-post

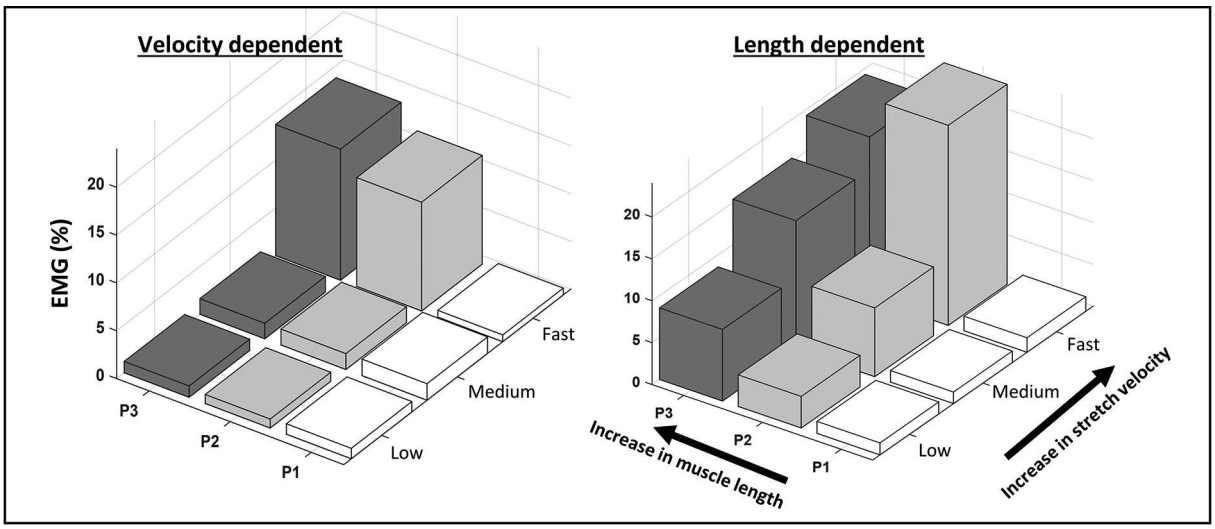

FIGURE 1 | Examples of velocity- and length-dependence of the stretch reflexes in the semitendinosus. The average normalized EMG envelope collected from the semitendinosus during passive knee extensions is shown across equally spaced zones of the range of motion (P1-3) at low, medium and fast stretch velocities. In the velocity-dependent activation pattern, EMG increases with increasing stretch velocity, but not across position zones. In the length-dependent activation pattern, EMG increases with stretch velocity and across position zones.

treatment changes in passive stretch parameters with changes in discrete gait parameters using either Pearson or Spearman correlation coefficients.

For all tests, the significance was corrected for multiple testing [$p < 0.025$ according to $p_{critical} = 1–(1–\alpha)^{1/N}$ (29)]. In addition to significance, pre-post treatment change values had to be larger than the minimal detectable change values extracted from previous reliability analyses on similar samples (21, 30). All statistical analyses were carried out using SPSS (IBM Statistics 24) and custom-made scripts in MATLAB (version 8.5.0 R2015a).

RESULTS

Subjects and Treatments

Included subject characteristics are reported in **Table 1**. Nine semitendinosus muscles were classified pre-treatment as having VD and nine as LD pattern. Children classified with VD patterns, tended to have a greater number of previous BoNT-A injections compared to those classified with LD patterns. Assessments were performed on average 59 ± 13 days after BoNT-A treatment. On average, 4.4 ± 1.0 units/kg BoNT-A were injected in the medial hamstring muscles (semitendinosus, semimembranosus and gracilis). Other muscles that received treatment are listed in **Table 2**. Post BoNT-A, the children wore lower and/or upper leg casts for an average of 12.67 ± 1.97 days (ranging from 10 to 14 days).

Gait Analysis

The children's knee kinematic waveforms before and after treatment together with age-related normative database of the gait laboratory (gray bands) are displayed in **Figure 2**. There were no significant differences in the pre-treatment knee kinematic gait curves between children with pre-treatment VD and LD muscles (**Figure 2A**). On the other hand, post-treatment, children categorized with an LD pattern showed significantly greater knee extension from mid- to terminal stance (**Figure 2B**). Those children with a pre-treatment VD pattern indicated greater post-treatment knee extension at initial contact, mid-stance and swing (**Figure 2D**). Comparison of the discrete gait parameters per group can be found in **Table 4**.

Instrumented Assessments During Passive Stretch

EMG_{LD} pre-treatment in those muscles categorized as LD was 45% higher than those muscles categorized as VD, indicating correct group allocation. In addition, pre-treatment EMG_{VD} was about 2-fold in muscles categorized as VD compared to LD. On the other hand, the pre-treatment baseline average EMG envelope, starting angular positions, ROM, and applied stretch velocities were not different between groups (**Table 3**).

Post-treatment results are reported in **Table 4**. Passive ROM significantly increased only in the VD group (+18%), while joint torque significantly decreased for the whole group (−30%) and for the LD group (−44%), but not for the VD group (−13%). EMG_{LD} significantly decreased in the whole group (−53%) and in the LD group (−68%), but tended to increase, though not significantly, post-treatment in the VD group. EMG_{VD} significantly decreased post-treatment by 60% for the whole group, and the reduction was significantly greater for the VD compared to LD group (−72% vs. −50%, $p = 0.005$). Significant positive correlations were found between the reduction in EMG_{VD} and increased knee extension at terminal swing ($r = 0.61$, $p = 0.021$).

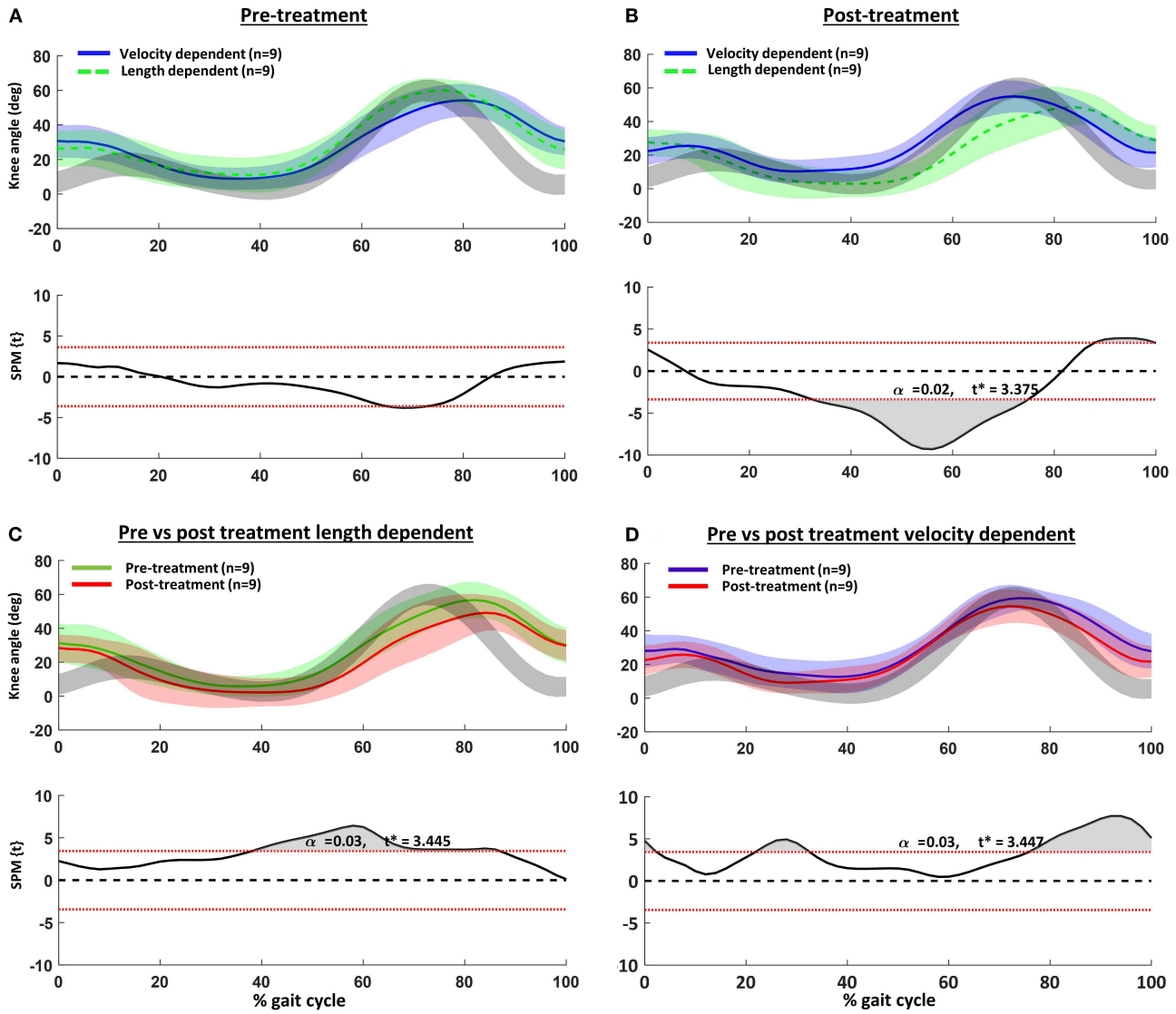

FIGURE 2 | Knee kinematics in the sagittal plane vs. normalized gait cycle and results of the statistical parametric mapping (SPM): **(A)** pre- and **(B)** post-treatment velocity vs. length-dependent muscles; **(C)** pre- vs. post-treatment for the length dependent muscles; and **(D)** pre- vs. post-treatment for the velocity dependent muscles. Gray curves are from a representative database of typically developing children.

DISCUSSION

In this study, we evaluated the outcome of BoNT-A treatment in the semitendinosus in children with CP on the impairment and activity level. We tested the hypothesis that the type of pre-treatment hyper-activation of tonic stretch reflexes during passive stretch (being velocity- or length-dependent) affects the outcome.

With the exception of highly trained athletes (31), a very high stretch velocity is needed to activate a tonic stretch reflex in a healthy relaxed muscle. In contrast, in subjects with an upper motor neuron lesion diagnosed with spasticity, this threshold is markedly reduced as stretch reflexes are hyperactive (32). Clinically, this results in an exaggerated velocity-dependent resistance to passively imposed movement about a joint (33). However, studies have reported that very low velocity joint rotations (<10–35 degrees/s) may already elicit a response in subjects diagnosed with spasticity (34). This would imply that in some cases, mechanisms other than velocity-dependency are at work when a muscle involuntarily contracts in response to an externally applied stretch. Furthermore, the dependency on velocity and/or length has been described as being muscle, subject and pathology-dependent (6, 7, 35). The current study is the first to report that, at least in the semitendinosus muscles of children with CP, the presence of length-dependent activation of tonic stretch reflexes helps characterize response to focal tone-reduction treatment. Those semitendinosus muscles with more length-dependency tended to react less favorably to treatment as assessed passively and during gait.

TABLE 3 | Average (and standard deviation) values of pre-treatment parameters in velocity-dependent and length-dependent muscles from the instrumented assessments during passive stretch.

	Pre-treatment stretch reflex activation pattern		
Passive stretch parameters	**Velocity dependent ($n = 9$)**	**Length dependent ($n = 9$)**	*p*-value
Starting position slow (deg)	114.9 (9.7)	118.2 (7.1)	0.419
End position slow (deg)	43.8 (10.5)	43.0 (8.0)	0.849
Starting position fast (deg)	115.9 (8.6)	118.9 (6.2)	0.400
End position fast (deg)	37.6 (6.8)	43.6 (9.9)	0.165
Max velocity slow (deg/s)	23.2 (3.5)	25.9 (7.3)	0.358
Max velocity fast (deg/s)	293.5 (29.8)	261.4 (33.2)	0.049
ROM slow (deg)	70.0 (6.8)	75.7 (12.6)	0.315
Torque (Nm)	8.6 (3.8)	9.1 (3.2)	0.752
Baseline EMG during slow stretch trials (%MVC)	2.6 (1.7)	7.7 (9.5)	0.065
Baseline EMG during fast stretch trials (%MVC)	2.8 (2.0)	8.4 (10.5)	0.067
EMG_{LD} (%MVC)	1.6 (1.6)	21.6 (23.8)	*0.012*
EMG_{LD} (μV)	2.2 (2.4)	15.8 (7.0)	*<0.001*
EMG_{VD} (μV)	25.7 (12.2)	11.6 (5.2)	*0.019*

Max, maximum; ROM, range of motion; EMG, electromyography; MVC, maximum voluntary contraction; EMG_{LD}, length dependent activation; EMG_{VD}, velocity dependent activation. $p < 0.025$.

TABLE 4 | Average and standard deviation values of parameters from the instrumented assessment during passive stretch and from the knee gait kinematics in the sagittal plane during gait pre- and post-treatment.

	All muscles ($n = 18$)			**Velocity dependent ($n = 9$)**				**Length dependent ($n = 9$)**				(VD vs. LD change)
	Pre	Post	*p*-value	Pre	Post	Change	*p*-value	Pre	Post	Change	*p*-value	*p*-value
Passive stretch parameters												
ROM slow (deg)	72.9 (10.5)	79.2 (8.0)	0.210	70.0 (6.8)	82.7 (6.0)	12.7 (10.4)	*0.011*	75.2 (12.6)	76.4 (8.6)	1.2 (9.0)	0.683	*0.023*
Torque (Nm)	8.9 (3.5)	6.0 (3.4)	*0.003*	8.6 (3.8)	7.0 (3.1)	1.6 (2.5)	0.107	9.1 (3.2)	5.2 (3.5)	4.0 (2.7)	*0.001*	0.077
EMG_{LD} (μV)	9.8 (8.7)	4.6 (4.2)	0.366	2.2 (2.4)	4.5 (4.4)	−2.2 (4.5)	0.205	15.8 (7.0)	4.7 (4.3)	11.2 (6.5)	*<0.00*	*< 0.001*
EMG_{VD} (μV)	17.9 (11.3)	6.1 (3.8)	*0.002*	25.7 (12.2)	7.3 (3.8)	18.4 (8.9)	*0.012**	11.6 (5.2)	5.3 (3.8)	6.6 (5.1)	*0.003*	*0.002**
Gait analysis parameters												
Min knee angle in stance (deg)	9.5 (8.1)	5.3 (8.3)	*0.008*	12.2 (8.9)	7.2 (7.7)	5.1 (6.5)	0.066	6.8 (6.8)	3.4 (9.0)	3.4 (5.1)	0.069	0.579
Min knee angle at terminal swing (deg)	27.7 (9.4)	24.1 (9.5)	*0.026*	27.6 (10.1)	21.1 (10.9)	6.5 (5.3)	*0.012**	27.8 (9.2)	27.1 (7.5)	0.7 (5.0)	0.707	0.041

*LD, length dependent; VD, velocity dependent. *Wilcoxon's signed rank test for non-normally distributed data. $p < 0.025$.*

In children with CP, spasticity in the semitendinosus is thought to restrict knee extension at terminal swing, resulting in reduced step length and excessive knee flexion at initial contact (36, 37). In accordance, pre-treatment, the knee kinematic gait pattern of the children included in the current study had excessive knee flexion in the second half of swing and during the first 10% of stance (**Figure 2A**). Flexion at these time points was slightly more exaggerated in those children categorized as having VD semitendinosus muscles, but the differences were not significant. Post-treatment, improvements of the knee angle at initial contact and terminal swing were only significant in those children with pre-treatment VD patterns. In contrast, post-treatment, children with LD patterns indicated knee angles approaching hyperextension in stance, as well as reduced and delayed knee flexion during swing. This pattern was also evident pre-treatment in the LD group, but was even more noticeable post-treatment.

In an extensive review of the effects of BoNT-A on gait in children with CP, Nieuwenhuys et al. (12) reported that increased knee extension in stance, similar to that observed in our LD group, was the only significant effect at the level of the knee. If our findings are confirmed, lack of reported response in other critical gait phases such as initial contact and swing in the studies included in the review, may have been due to the inclusion of children with LD, rather than VD muscles.

Furthermore, knee hyper-extension at terminal stance is not desirable and may be indicative of remaining gastrocnemius spasticity resulting in a pathological plantarflexion knee extension couple (38). While LD is less common in the gastrocnemius than in the semitendinosus (6), it may be possible that those subjects with LD semitendinosus muscles also have LD activation of their gastrocnemius and therefore reduced treatment effects. Another possibility for knee hyperextension at terminal stance is quadriceps weakness. This suggests that it may be worthwhile to explore possible differences in underlying muscle strength between LD and VD muscles. If LD muscles are indeed weaker, it may be hypothesized that the benefits of tone reduction do not outweigh the loss of

muscle strength. Alternatively, LD muscles may potentially benefit from additional strength training to outbalance the loss of muscle strength caused by treatment.

Although positive treatment response as assessed during passive stretch was evident in both groups, the reduction in EMG_{VD} was significantly greater in those muscles with a pre-treatment VD categorization. This reduction was associated with an improved knee angle at terminal swing, confirming that treatment of hyperactive tonic stretch reflexes improved the children's gait pattern, in particular in those subjects categorized as having muscles with VD patterns.

Unexpectedly, muscles categorized as LD, rather than VD, demonstrated a reduction in the torque measured during passive stretch. This parameter was calculated by subtracting the torque measured during low velocity stretch from that during fast stretch at a given joint angle (70 degrees knee flexion). Therefore, a change in joint angle, rather than torque also determines the outcome of this parameter. Since ROM improved in the VD group, the lack of significant reduction in torque at 70 degrees knee flexion in the VD group may be a result of a changing joint angle-moment relationship.

Pre-treatment values of EMG_{LD} helped categorize subjects into activation patterns. Therefore, EMG_{LD} was not included in the estimation of treatment response. Furthermore, given the definition of spasticity as velocity-dependent, changes in EMG_{LD} were not deemed directly meaningful to judge the effect of BoNT-A. Nevertheless, it was expected that BoNT-A results in general muscle paresis. This was indeed confirmed, since EMG_{LD} in muscles categorized as LD decreased significantly post-treatment. It is surprising however, that in VD muscles, the opposite effect was observed, i.e., EMG_{LD} tended to increase post-treatment. Yet, this increase was not significant and values were marginal to measurement errors reported from similar samples (21).

Limitations

The current study is not without significant limitations. Firstly, the study sample was small and heterogeneous, which did not allow us to explore more between-group differences. In particular, there were slightly more children classified as GMFCS level 1 in the VD group. Therefore, the distinction of the groups based on activation dependency alone, should be interpreted as preliminary. Additionally, previous studies included mixed forms of length and velocity dependency (6, 7). Such a mixed form is also evident in the LD example of **Figure 1**. Here, LD activation during slow and medium velocity stretch trials increases with increasing muscle length. Yet, this is not the case at fast velocity. This suggests an interaction between length and velocity dependent activation. While the current study is underpowered to do so, it may be interesting to further analyze the significance of these mixed patterns.

Secondly, while we refer to the semitendinosus only, its activity cannot actually be separated from that of the semimembranosus with surface EMG. Similarly, other muscles crossing the knee may have influenced the assessment of ROM and the calculation of net joint torque. Thirdly, some of the variation in post-treatment knee flexion during gait may be ascribed to the multilevel BoNT-A treatment and not by solely targeting the semitendinosus. Nevertheless, selected muscles and dosages were similar between groups (**Table 2**). Some subjects in the current study were also prescribed long-leg removable casts post- BoNT-A injection. While the number of children who received this were equally distributed among the groups, we are missing information regarding post-treatment cast adherence which may possibly have also influenced the results. Similarly, while all children received standardized post-treatment physiotherapy according to our hospital recommendations, we cannot exclude the possible effects of physiotherapy on treatment success.

Possible Etiology of Length and Velocity-Dependent Activations

The etiology behind why some muscles are more length, rather than velocity-dependent is unknown and beyond the investigations of the current paper. Nevertheless, there are some possibilities that may be considered.

Biomechanical Orientation

During passive muscle lengthening, motor neuron activation will be defined by excitation of different receptors: muscle-velocity sensing group Ia afferents, mono- and di-synaptic group II afferents that respond to a muscle's actual length, and poly-synaptic receptors from cutaneous mechanoreceptors, joint and tendon afferents. How and which sensors respond depends on the muscles starting lengths, morphological properties, stiffness, orientation of muscle fibers with regard to its tendon, as well as spinal and supraspinal control. Moreover, these characteristics are initially defined by posture and the muscles position within the limb. For example, studies have indicated biomechanical relationships between stretch reflex activation and starting muscle lengths (26, 39, 40). In the current study however, starting posture and joint orientation were similar between subjects and can therefore not explain the observed differences in activation thresholds between LD and VD muscles.

Muscle Properties

Compared to typically developing children, marked morphological alterations have been reported in the semi-tendinosus of children with CP, including smaller and shorter muscle bellies, and shorter fascicles that result in an altered moment-angle relationship (41). Short, stiff muscles may activate sooner as information is relayed more efficiently between fibers (3). Evidence for this has been reported in the elbow flexors of stroke survivors and in the medial gastrocnemius muscles of children with spastic CP, where muscle activation during slow passive joint rotation was related to reduced absolute fiber length (39) and reduced muscle lengthening (42). Therefore, it is likely that altered intrinsic muscle properties in CP are partly responsible for lowered activation thresholds during passive stretch.

In many studies examining muscles affected by spasticity in the passive state, EMG activation during low-velocity passive

joint rotation is regarded as indicating lack of muscle relaxation, and the data is discarded (4, 41, 43). We are fairly confident that the data presented in the current study did not reflect active participation by the subject. We were rigorous in monitoring both agonist and antagonist muscles during the passive stretch trials and carefully inspected the timing of any activation. Therefore, data were only selected from stretch trials where activation at low velocity gradually increased over the ROM. Our findings suggest that, rather than disregarding this data, capturing it may help identify children who require a different treatment approach.

Treatment History

There are concerns in the clinical community that repeated treatments with BoNT-A may irreversibly affect muscle volume and quality. If the hypothesis mentioned in the previous paragraph (i.e., that shorter, stiffer and more atrophied muscles elicit earlier stretch reflexes and thus LD patterns) is true, then it may be expected that those children with LD patterns would have undergone a larger number of previous treatments with BoNT-A. However, in our study, children with VD semitendinosus muscles tended to have a larger number of previous treatments with BoNT-A. Therefore, the suggestion that repeated BoNT-A detrimentally affects muscle integrity is not directly supported by our results. Rather, our finding that children with VD patterns more often underwent BoNT-A injections may reflect an appropriate subject selection and clinical decision-making. However, these are assumptions that need to be verified in future research. Given ongoing concern (14), careful monitoring of the long term effects of BoNT-A in children with CP is paramount.

Baseline Tone

Recently, it has been suggested that muscle spindle firing is modulated by fiber force, secondary to history-dependent features. In other words, muscles that are pre-activated (for example, when sustaining a standing posture) fire more strongly as reaction to stretch than when fully relaxed (44). In a simulation study, De Groote et al. (45) found an interaction effect between baseline tone (indicating higher intrinsic muscle force) and a reduced knee oscillation pattern when a leg with spasticity was simulated to undergo a pendulum test. Therefore, a possible explanation for a reduced activation threshold in some spastic muscles may be a higher resting muscle tone resulting in increased force detection by the spindles. Supporting this theory, in the current study, the baseline resting average EMG envelope tended to be higher in LD compared to VD muscles.

In conclusion, the clinical picture of CP is marked by heterogeneity. This emphasizes the importance of CP research focusing on disentangling and categorizing the clinical symptoms. A traditional clustering method is by the type of motor impairment, the most accepted distinguishing spastic, from dyskinetic and ataxic forms (1). Clinicians encountering mixed patterns of motor impairment, provide a diagnosis according to the most dominant and direct their treatment accordingly (1). We suggest that even within those muscles termed as spastic, deeper characterization of the reaction to passive stretch may be clinically meaningful and help direct treatment. Half of the muscles investigated in this small study sample demonstrated an activation pattern during passive stretch disparate to their original diagnosis of velocity-dependent spasticity. It is possible that these muscles possess factors that interact with their stretch reflex control. This possibly more complex disorder may explain their reduced post-treatment reaction at the muscle and joint level as well as reduced functional adaptability. If the current results are validated in larger studies, alternative treatments and closer follow-up may be more desirable than BoNT-A in children with LD muscles.

DATA AVAILABILITY STATEMENT (MS)

The raw data supporting the conclusions of this article will be made available by the authors, without undue reservation, to any qualified researcher.

ETHICS STATEMENT

The studies involving human participants were reviewed and approved by KU Leuven University Hospitals' Ethics Committee (B32220072814). Written informed consent to participate in this study was provided by the participants' legal guardian/next of kin.

AUTHOR CONTRIBUTIONS

LB-O, EA, and KD conceptualized the methods. LB-O processed the data. LB-O performed the formal analysis. LB-O, KD, GM, and AV acquired funding. LB-O, KD, GM, and AV conducted the investigation. LB-O, EA, and KD developed the methodology. LB-O, KD, GM, and AV administrated the project. LB-O, KD, GM, and AV provided resources. LB-O and EA developed the software. KD and GM supervised the project. LB-O, KD, GM, and AV validated the research outputs. LB-O and EA prepared the data visualization. LB-O drafted the manuscript. All authors edited the manuscript.

FUNDING

LB-O received a postdoctoral grant (12R4215N) from the Research Foundation Flanders (FWO) and a grant (016.186.144) from the Netherlands Organization for Scientific Research (NWO). The work was also supported by the IWT-TBM grant (IPSA-060799) and TBM grant (TAMTA-T005416N) both from the Research Foundation Flanders (FWO), Belgium; from the Doctoral Scholarships Committee for International Collaboration with non EER-countries (DBOF) of the KU Leuven, Belgium (DBOF/12/058) and from La Fondation Motrice, contract 2016/8.

REFERENCES

1. Rosenbaum P, Paneth N, Leviton A, Goldstein M, Bax M, Damiano D, et al. A report: the definition and classification of cerebral palsy April 2006. *Dev Med Child Neurol Suppl.* (2007) 109:8–14. doi: 10.1111/j.1469-8749.2007.tb12610.x
2. Baude M, Nielsen JB, Gracies JM. The neurophysiology of deforming spastic paresis: a revised taxonomy. *Ann Phys Rehabil Med.* (2019) 62:426–30. doi: 10.1016/j.rehab.2018.10.004
3. Gracies JMM. Pathophysiology of spastic paresis. I: paresis and soft tissue changes. *Muscle Nerve.* (2005) 31:535–51. doi: 10.1002/mus.20284
4. Willerslev-Olsen M, Lorentzen J, Sinkjaer T, Nielsen JB. Passive muscle properties are altered in children with cerebral palsy before the age of 3 years and are difficult to distinguish clinically from spasticity. *Dev Med Child Neurol.* (2013) 55:617–23. doi: 10.1111/dmcn.12124
5. Gracies JMM. Pathophysiology of spastic paresis. II: emergence of muscle overactivity. *Muscle Nerve.* (2005) 31:552–71. doi: 10.1002/mus.20285
6. Bar-On L, Aertbeliën E, Molenaers G, Desloovere K. Muscle activation patterns when passively stretching spastic lower limb muscles of children with cerebral palsy. *PLoS ONE.* (2014) 9:e91759. doi: 10.1371/journal.pone.0091759
7. Lebiedowska MK, Fisk JR. Knee resistance during passive stretch in patients with hypertonia. *J Neurosci Methods.* (2009) 179:323–30. doi: 10.1016/j.jneumeth.2009.02.005
8. van den Noort JC, Scholtes VA, Becher JG, Harlaar J. Evaluation of the catch in spasticity assessment in children with cerebral palsy. *Arch Phys Med Rehabil.* (2010) 91:615–23. doi: 10.1016/j.apmr.2009.12.022
9. van Doornik J, Kukke M, Sanger TD. Hypertonia in childhood secondary dystonia due to cerebral palsy is associated with reflex muscle activation. *Mov Disord.* (2009) 24:965–71. doi: 10.1002/mds.22282
10. Trompetto C, Currà A, Puce L, Mori L, Serrati C, Fattapposta F, et al. Spastic dystonia in stroke subjects: prevalence and features of the neglected phenomenon of the upper motor neuron syndrome. *Clin Neurophysiol.* (2019) 130:521–7. doi: 10.1016/j.clinph.2019.01.012
11. Graham HK, Aoki KR, Autti-Rämö I, Boyd RN, Delgado MR, Gaebler-Spira DJ, et al. Recommendations for the use of botulinum toxin type A in the management of cerebral palsy. *Gait Posture.* (2000) 11:67–79. doi: 10.1016/S0966-6362(99)00054-5
12. Nieuwenhuys A, Papageorgiou E, Pataky T, De Laet T, Molenaers G, Desloovere K. Literature review and comparison of two statistical methods to evaluate the effect of botulinum toxin treatment on gait in children with cerebral palsy. *PLoS ONE.* (2016) 11:e0152697. doi: 10.1371/journal.pone.0152697
13. Gough M, Fairhurst C, Shortland AP. Botulinum toxin and cerebral palsy: time for reflection? *Dev Med Child Neurol.* (2005) 47:709–12. doi: 10.1017/S0012162205001453
14. Multani I, Manji J, Ison TH, Khot A, Graham K. Botulinum toxin in the management of children with cerebral palsy. *Pediatr Drugs.* (2019) 21:261–81. doi: 10.1007/s40272-019-00344-8
15. Desloovere K, Molenaers G, Feys H, Huenaerts C, Callewaert B, Van de Walle P. Do dynamic and static clinical measurements correlate with gait analysis parameters in children with cerebral palsy? *Gait Posture.* (2006) 24:302–13. doi: 10.1016/j.gaitpost.2005.10.008
16. Bar-On L, Aertbeliën E, Molenaers G, Van Campenhout A, Vandendoorent B, Nieuwenhuys A, et al. Instrumented assessment of the effect of Botulinum Toxin-A in the medial hamstrings in children with cerebral palsy. *Gait posture.* (2014) 39:17–22. doi: 10.1016/j.gaitpost.2013.05.018
17. Hislop HJ, Montgomery J. *Daniels and Worthingham's Muscle Testing: Techniques of Manual Examination*. 6th ed. W. B. Philadelphia (Pa.) Saunders (1995).
18. Trost J. Physical assessment and observational gait analysis. In: Gage J, editor. *The Treatment of Gait Problems in Cerebral Palsy Clinics in Developmental Medicine No 164–165.* London: Mac Keith Press, (2002) 71–89.
19. Van Campenhout A, Molenaers G. Localization of the motor endplate zone in human skeletal muscles of the lower limb: anatomical guidelines for injection with botulinum toxin. *Dev Med Child Neurol.* (2011) 53:108–19. doi: 10.1111/j.1469-8749.2010.03816.x
20. Van Campenhout A, Bar-On L, Aertbeliën E, Huenaerts C, Molenaers G, Desloovere K. Can we unmask features of spasticity during gait in children with cerebral palsy by increasing their walking velocity? *Gait Posture.* (2014) 39:953–7. doi: 10.1016/j.gaitpost.2013.12.024
21. Bar-On, Aertbeliën E, Wambacq H, Severijns D, Lambrecht K, Dan B, et al. A clinical measurement to quantify spasticity in children with cerebral palsy by integration of multidimensional signals. *Gait Posture.* (2013) 38:141–7. doi: 10.1016/j.gaitpost.2012.11.003
22. Bohannon RW, Smith MB. Interrater reliability of a modified Ashworth scale of muscle spasticity. *Phys Ther.* (1987) 67:206–7. doi: 10.1093/ptj/67.2.206
23. Boyd RN, Graham HK. Objective measurement of clinical findings in the use of botulinum toxin type A for the management of children with cerebral palsy. *Eur J Neurol.* (1999) 6:23–35. doi: 10.1111/j.1468-1331.1999.tb00031.x
24. Grey MJ, Klinge K, Crone C, Lorentzen J, Biering-Sørensen F, Ravnborg M, et al. Post-activation depression of soleus stretch reflexes in healthy and spastic humans. *Exp brain Res.* (2008) 185:189–97. doi: 10.1007/s00221-007-1142-6
25. Rauch HE, Tung F, Striebel C. Maximum likelihood estimates of linear dynamic systems. *Am Inst Aeronaut Astronaut J.* (1965) 3:1445–50. doi: 10.2514/3.3166
26. Kamper DG, Schmit BD, Rymer WZ. Effect of muscle biomechanics on the quantification of spasticity. *Ann Biomed Eng.* (2001) 29:1122–34. doi: 10.1114/1.1424918
27. Jensen RK. Body segment mass, radius and radius of gyration proportions of children. *J Biomech.* (1986) 19:359–68. doi: 10.1016/0021-9290(86)90012-6
28. Pataky TC, Vanrenterghem J, Robinson MA. Zero- vs. one-dimensional, parametric vs. non-parametric, and confidence interval vs. hypothesis testing procedures in one-dimensional biomechanical trajectory analysis. *J Biomech.* (2015) 48:1277–85. doi: 10.1016/j.jbiomech.2015.02.051
29. Sidak Z. Rectangular confidence regions for the means of multivariate normal distributions. *J Am Stat Assoc.* (1967) 62:626–33. doi: 10.2307/2283989
30. Schwartz MH, Trost JP, Wervey RA. Measurement and management of errors in quantitative gait data. *Gait Posture.* (2004) 20:196–203. doi: 10.1016/j.gaitpost.2003.09.011
31. Ogawa T, Kim GH, Sekiguchi H, Akai M, Suzuki S, Nakazawa K. Enhanced stretch reflex excitability of the soleus muscle in experienced swimmers. *Eur J Appl Physiol.* (2009) 105:199–205. doi: 10.1007/s00421-008-0890-8
32. Lance J. Symposium synopsis. In: Feldman E, Young RG, Koella RR, editors. *Spasticity: Disordered Motor Control.* Chicago, IL: Yearbook medical, (1980) 485–94.
33. Sanger TD, Delgado MR, Gaebler-Spira D, Hallett M, Mink JW. Classification and definition of disorders causing hypertonia in childhood. *Pediatrics.* (2003) 111:e89–97. doi: 10.1542/peds.111.1.e89
34. Thilmann AF, Fellows SJ, Garms E, Thilman A, Fellows SJ, Garms E, et al. The mechanisms of spastic muscle hypertonus. Variation in reflex gain over the time course of spasticity. *Brain.* (1991) 114:233–44.
35. Lee HM, Huang YZ, Chen JJ, Hwang IS. Quantitative analysis of the velocity related pathophysiology of spasticity and rigidity in the elbow flexors. *J Neurol Neurosurg Psychiatry.* (2002) 72:621–9. doi: 10.1136/jnnp.72.5.621
36. Sutherland DH, Davids JR. Common gait abnormalities of the knee in cerebral palsy. *Clin Orthop Relat Res.* (1993) 288:139–47. doi: 10.1097/00003086-199303000-00018
37. Tuzson AE, Granata KP, Abel MF. Spastic velocity threshold constrains functional performance in cerebral palsy. *Arch Phys Med Rehabil.* (2003) 84:1363–8. doi: 10.1016/S0003-9993(03)00199-0
38. Gage JR. *The Identification and Treatment of Gait Problems in Cerebral Palsy*. 2nd ed. London: Mac Keith Press (2009).
39. Li S, Kamper DG, Rymer WZ. Effects of changing wrist positions on finger flexor hypertonia in stroke survivors. *Muscle Nerve.* (2006) 33:183–90. doi: 10.1002/mus.20453
40. Musampa NK, Mathieu PA, Levin MF. Relationship between stretch reflex thresholds and voluntary arm muscle activation in patients with spasticity. *Exp brain Res.* (2007) 181:579–93. doi: 10.1007/s00221-007-0956-6
41. Haberfehlner H, Maas H, Harlaar J, Brunner R, Becher J, Rutz E, et al. Knee moment-angle characteristics and semitendinosus muscle morphology in children with spastic paresis selected for medial hamstring lengthening. *PLoS ONE.* (2016) 11:e0166401. doi: 10.1371/journal.pone.0166401
42. Bar-On L, Kalkman BM, Cenni F, Schless S, Molenaers G, Maganaris C, et al. The relationship between medial gastrocnemius lengthening properties and stretch reflexes in cerebral palsy. *Front Pediatr.* (2018) 6:259. doi: 10.3389/fped.2018.00259

43. Lorentzen J, Grey MJ, Crone C, Mazevet D, Biering-Sørensen F, Nielsen JB. Distinguishing active from passive components of ankle plantar flexor stiffness in stroke, spinal cord injury and multiple sclerosis. *Clin Neurophysiol.* (2010) 121:1939–51. doi: 10.1016/j.clinph.2010.02.167
44. Blum KP, Lamotte D'Incamps B, Zytnicki D, Ting LH. Force encoding in muscle spindles during stretch of passive muscle. *PLoS Comput Biol.* (2017) 13:1–24. doi: 10.1371/journal.pcbi.1005767
45. De Groote F, Blum KP, Horslen BC, Ting LH. Interaction between muscle tone, short-range stiffness and increased sensory feedback gains explains key kinematic features of the pendulum test in spastic cerebral palsy: A simulation study. *PLoS One.* (2018) 13:e0205763. doi: 10.1371/journal.pone.0205763

Conflict of Interest: The authors declare that the research was conducted in the absence of any commercial or financial relationships that could be construed as a potential conflict of interest.

frontiers in Human Neuroscience

ORIGINAL RESEARCH
published: 09 July 2020
doi: 10.3389/fnhum.2020.00275

Structural Brain Lesions and Gait Pathology in Children With Spastic Cerebral Palsy

Eirini Papageorgiou[1,2†], Nathalie De Beukelaer[1,2†], Cristina Simon-Martinez[1,3], Lisa Mailleux[1], Anja Van Campenhout[4,5], Kaat Desloovere[1,2] and Els Ortibus[4]*

[1] Department of Rehabilitation Sciences, KU Leuven, Leuven, Belgium, [2] Clinical Motion Analysis Laboratory, University Hospitals Leuven, Leuven, Belgium, [3] Institute of Information Systems, University of Applied Sciences Western Switzerland (HES-SO), Sierre, Switzerland, [4] Department of Development and Regeneration, KU Leuven, Leuven, Belgium, [5] Department of Orthopedics, University Hospitals Leuven, Leuven, Belgium

The interaction between brain damage and motor function is not yet fully understood in children with spastic cerebral palsy (CP). Therefore, a semi-quantitative MRI (sqMRI) scale was used to explore whether identified brain lesions related to functional abilities and gait pathology in this population. A retrospective cohort of ambulatory children with spastic CP was selected [*N* = 104; 52 bilateral (bCP) and 52 unilateral (uCP)]. Extent and location-specific scores were defined according to the sqMRI scale guidelines. The gross motor function classification system (GMFCS), the gait profile score (GPS), GPSs per motion plane, gait variable scores (GVS) and multiple-joint (MJ) gait patterns were related to brain lesion scores. In all groups, the global total brain scores correlated to the GPS (total: $r_s = 0.404$, $p \leq 0.001$; bCP: $r_s = 0.335$, $p \leq 0.05$; uCP: $r_s = 0.493$, $p \leq 0.001$). The global total hemispheric scores correlated to the GMFCS (total: $r_s = 0.392$, $p \leq 0.001$; bCP: $r_s = 0.316$, $p \leq 0.05$; uCP: $r_s = 0.331$, $p \leq 0.05$). The laterality scores of the hemispheres in the total group correlated negatively to the GMFCS level ($r_s = -0.523$, $p \leq 0.001$) and the GVS-knee sagittal ($r_s = -0.311$, $p \leq 0.01$). Lesion location, for the total group demonstrated positive correlations between parietal lobe involvement and the GPS ($r_s = 0.321$, $p \leq 0.001$) and between periventricular layer damage and the GMFCS ($r_s = 0.348$, $p \leq 0.001$). Involvement of the anterior part of the corpus callosum (CC) was associated with the GVS-hip sagittal in all groups (total: $r_{pb} = 0.495$, $p \leq 0.001$; bCP: $r_{pb} = 0.357$, $p \leq 0.05$; uCP: $r_{pb} = 0.641$, $p \leq 0.001$). The global total hemispheric and laterality of the hemispheres scores differentiated between the minor and both the extension ($p \leq 0.001$ and $p \leq 0.001$) and flexion ($p = 0.016$ and $p = 0.013$, respectively) MJ patterns in the total group. Maximal periventricular involvement and CC intactness were associated with extension patterns ($p \leq 0.05$ and $p \leq 0.001$, respectively). Current findings demonstrated relationships between brain structure and motor function as well as pathological gait, in this cohort of children with CP. These results might facilitate the timely identification of gait pathology and, ultimately, guide individualized treatment planning of gait impairments in children with CP.

Keywords: cerebral palsy, brain lesions, structural brain MRI, motor function, gait pathology

OPEN ACCESS

Edited by:
Jessica Rose,
Stanford University, United States

Reviewed by:
Kornél Schadl,
Stanford University, United States
Rachel Vassar,
University of California,
San Francisco, United States

****Correspondence:***
Eirini Papageorgiou
eirini.papageorgiou@kuleuven.be

† These authors have contributed equally to this work and share first authorship

Specialty section:
This article was submitted to Motor Neuroscience, a section of the journal Frontiers in Human Neuroscience

Received: *28 November 2019*
Accepted: *18 June 2020*
Published: *09 July 2020*

Citation:
Papageorgiou E, De Beukelaer N, Simon-Martinez C, Mailleux L, Van Campenhout A, Desloovere K and Ortibus E (2020) Structural Brain Lesions and Gait Pathology in Children With Spastic Cerebral Palsy. Front. Hum. Neurosci. 14:275. doi: 10.3389/fnhum.2020.00275

INTRODUCTION

Children with cerebral palsy (CP) suffer from a non-progressive brain lesion that occurs in the developing fetal or infant brain (Rosenbaum et al., 2007). As a consequence, motor deficits (e.g., spasticity and muscle weakness) and functional disabilities (e.g., upper limb dysfunction and gait pathology) emerge during early childhood (Graham et al., 2016). The clinical severity of motor and functional impairments is frequently described by the topographic classification, i.e., bilateral (bCP) and unilateral (uCP) CP (Rosenbaum et al., 2007; Graham et al., 2016) and by the levels of the Gross Motor Function Classification System (GMFCS) (Palisano et al., 1997).

An increasing number of studies have explored the link between brain structure and functional impairments (Arnfield et al., 2013; Meyns et al., 2016; Mailleux et al., 2017a,b; Zhou et al., 2017; Cahill-rowley et al., 2019). Previous explorations in children with bCP, for example, have shown that increased damage to the total corpus callosum (CC) volume and increased lateral ventricle volume were associated with increased gait pathology (Meyns et al., 2016).

Neuro-imaging has played a substantial role in describing the pathogenesis and structure-function relationship in CP (Krägeloh-Mann and Horber, 2007; Himmelmann and Uvebrant, 2011). Because conventional magnetic resonance imaging (MRI) findings add considerable information to the early diagnosis of CP in children, harmonizing definitions is crucial (Novak et al., 2017). The Surveillance of Cerebral Palsy in Europe has suggested using the MRI Classification System (MRICS), where the predominant pathogenic lesion pattern is classified in broad categories, based on the presumed timing of the brain insult (Himmelmann et al., 2016). However, this classification system is restricted in providing a detailed neuro-anatomical characterization of the brain injury.

A reliable, semi-quantitative MRI (sqMRI) scale has recently been developed to assess both the extent and specific locations (e.g., layers, lobes, and subcortical structures) of the lesion. The scale is applicable in children from the age of 3 years onward, i.e., when myelination appears to be complete in both lobes and subcortical regions (Parazzini et al., 2002). In this scale, higher sqMRI scores indicate a higher brain involvement (Fiori et al., 2014). To date, this assessment, which has been developed specifically for CP, has shown correlations with communication in children with CP (Coleman et al., 2016; Laporta-Hoyos et al., 2018), upper limb sensorimotor outcomes and function in only uCP (Fiori et al., 2015; Pagnozzi et al., 2015; Mailleux et al., 2017a,b), as well as motor function and cognition in children with dyskinetic CP (Laporta-Hoyos et al., 2018). As a result, this semi-quantitative scale confirmed its potential to investigate structure–function relationships in children with CP after the age of 3 years (Fiori et al., 2014).

Nevertheless, the relationships between the sqMRI scale and general functional abilities of children with spastic CP and, more specifically, gait have not yet been investigated. This is crucial, since gait is one of the most frequent functional impairments in children with CP. Indeed, approximately 70% of children with CP are ambulatory (Ahlin et al., 2016). Gait in CP is commonly assessed with three-dimensional gait analysis (3DGA), which constitutes the "golden standard" (Wren et al., 2011; Meldrum et al., 2014). Gait indices, such as the Gait Profile score (GPS) (Baker et al., 2009), are commonly used outcome measures quantifying the overall degree of gait deviations, in comparison with gait data of typically developing (TD) peers. In addition, gait classification systems describe the walking patterns of children with CP and may be considered complementary to overall gait indices because they provide more insight regarding the direction of the observed deviation(s). The combination of gait indices and gait classification according to multiple joint (MJ) patterns (Papageorgiou et al., 2019a) may be key to comprehensively delineate gait pathology in children with CP and its relations to the brain lesion.

Children with bCP and uCP display differences in brain lesions (Krägeloh-Mann and Horber, 2007; Zhou et al., 2017), gross motor function (Himmelmann and Uvebrant, 2011; Holmes et al., 2018; Papageorgiou et al., 2019b), and gait (Meyns et al., 2016; Holmes et al., 2018). These population-based differences necessitate in-depth exploration of the possible interactions between the brain lesions of each group and their function or gait characteristics. Previous studies on the brain-gait relation in uCP and bCP included small samples (Meyns et al., 2016). Additionally, the combination of extent and location of the brain lesions has not been thoroughly investigated. Studies on the relationships between brain structure and functional disabilities of children with CP have used various methods, without comprehensive quantification of the respective pathologies. With respect to brain analysis, qualitative scales based on conventional MRI (Romei et al., 2007; Himmelmann and Uvebrant, 2011; MacFarlane et al., 2012; Taufika et al., 2012) and different neuroimaging modalities, such as diffusion tensor imaging (DTI) (Rose et al., 2007; Meyns et al., 2016; Cahill-rowley et al., 2019), have been applied. Regarding functional abilities and gait pathology, previous studies frequently used the gross motor function measure (Romei et al., 2007) and the GMFCS (Rose et al., 2007; Himmelmann and Uvebrant, 2011), gait patterns (MacFarlane et al., 2012; Taufika et al., 2012), spatiotemporal parameters (Cahill-rowley et al., 2019) or quantified outcome measures (Romei et al., 2007; Rose et al., 2007; Meyns et al., 2016; Cahill-rowley et al., 2019). The use of various brain and motor outcome measures might impede drawing overall conclusions concerning the structure–function relationship in children with CP. A deeper understanding of the underlying neural contributions could bridge the gap between the heterogeneous clinical presentations, as well as provide information and guidance for targeted, life-long treatments in children with CP (Rose et al., 2007; Graham et al., 2016; Zhou et al., 2017; Meyns et al., 2019).

Therefore, the aim of this retrospective study was to explore the relationships between the observed brain lesions in children with CP and their functional impairments with validated and easily obtainable tools, and with a special focus on gait pathology. This explorative study is the first to combine several previously explored, isolated parameters. The integration of several parameters is a new step towards a generalization of the findings. This methodological approach allows the comparison

of the new findings with previous studies and the delineation of novel associations that may have been lost in those previous studies. Hence, we explored whether the extent and location of the brain lesions scored according to the sqMRI scale were related to a comprehensive assessment of (a) the functional abilities, using the GMFCS, and (b) gait pathology, by means of the GPS and MJ patterns, in children with CP. These relationships were further separately explored in bCP and uCP children.

MATERIALS AND METHODS

Participants

A convenience sample was selected from the retrospective database of the Clinical Motion Analysis Laboratory of the University Hospitals Leuven, under the ethical approval provided by the Medical Ethical Committee of the University Hospitals Leuven (s56036). Permission to use and process retrospective patient data acquired during standard medical care was granted on condition that all patient information had been a priori anonymized and no patients would be included if they had requested so. Therefore, an informed written consent from all parents and/or patients was not acquired. This database comprised 3DGA sessions of more than 400 children, who were screened based on the following inclusion criteria: (a) a diagnosis of spastic bCP or uCP, (b) a 3DGA conducted between the ages of three and eight, (c) availability of a conventional brain MRI, acquired after the age of 3 years. Children were excluded if they showed marked clinical signs of dyskinesia or ataxia, if they had undergone any lower limb surgery in the past, more than three botulinum toxin type A (BoNT-A) treatments or if they had received a BoNT-A treatment less than 6 months before the 3DGA. These treatment criteria were applied in order to ensure homogeneity of the included sample, as well as to minimize the effect of treatment history on the analyses. In case multiple 3DGA sessions of the same patient fulfilled all criteria, the earliest one with sufficient data quality was chosen, to minimize the effect of treatment(s) or growth on gait. If multiple MRI scans were available, the first MRI after the age of 3 years and closest to the 3DGA was chosen. Additional data were collected and reported for all patients regarding commonly measured clinical impairments and comorbidities. Clinical impairments of the muscles acting in the sagittal plane were summed to form composite scores for spasticity, weakness, selectivity and passive range of motion (ROM) (Papageorgiou et al., 2019b). Comorbidities included visual, hearing and intellectual impairments, as well as a history of epilepsy. These were scored according to the guidelines of the Surveillance of CP in Europe (Cans et al., 2007).

Brain MRI

Each MRI scan was scored by a trained pediatric neurologist (EO) who was blinded to patient characteristics and 3DGA results, and who was also involved in the original reliability study of the sqMRI (Fiori et al., 2014). Firstly, the MRICS was used to qualitatively classify all children's brain lesions based on presumed lesion timing (Himmelmann et al., 2016). Only the predominant pattern based on the presumed timing of the lesion was reported for children who had multiple brain lesions, in accordance with the guidelines of the Surveillance of CP in Europe (Himmelmann et al., 2016). Children with a normal brain classification (i.e., category E) were not further scored with the sqMRI scale. The sqMRI scale is used to score the extent and location of the lesion and is preferably applied to the axial fluid-attenuated inversion recovery (FLAIR) sequences, which allow a clearer visualization of white matter lesions. If no FLAIR sequence was available for a patient, standard T1 sequences were used. The procedure was identical to that reported in the original publication, whereby the lesions were drawn on a paper template with six axial slices and scores were calculated based on the drawing (Fiori et al., 2014). Scoring brain lesions according to the sqMRI scale allows to score the extent and location of the lesion. In general, higher scores indicate larger damage, representing the extent of the brain lesion.

The *extent* of the brain lesion was expressed with the global total brain score (0–40), the global total hemispheric (0–24) and global total subcortical (0–10) scores, as well as the total CC and cerebellum scores (0–3, each). In addition to these, an adjusted global total brain score (0–37) was computed in case a sagittal MRI view was not available or was of poor quality, hindering the scoring of the CC. Finally, the laterality of the hemispheres was calculated based on the formula by Desmond et al. (1995), following the adaption by Coleman et al. (2016) (i.e., the difference between the two global hemispheric scores was divided by their sum, ranging between 0 and 1).

The *location* of the lesion was calculated based on detailed scores of the four brain lobes (i.e., frontal, parietal, temporal, and occipital; 0–3, each) in the most affected brain hemisphere. In cases of bilateral symmetrical lesions, the hemisphere that referred to the contralateral side of the most affected lower limb was used. Each lobe was further divided into three layers, namely periventricular, middle and cortico/subcortical (0–4, each). Lastly, all subcortical structures (the lenticular and caudate nuclei, the posterior limb of the internal capsule – PLIC, the thalamus and the brainstem) along with the individual parts of the CC (i.e., anterior, middle and posterior) were investigated in more detail (all scored as 0 or 1, indicating intactness or involvement, respectively).

Gait Analysis

For children with uCP, only the lower limb that displayed neurological symptoms and motor deficits was taken into account. For children with bCP, the most spastic and/or weakest side was chosen based on the clinical records of each patient. This was decided in order to account for the interdependence between the motions of both affected sides, as well as for enhanced comparability between the two patient groups.

Standardized 3DGAs at a self-selected walking speed and in a barefoot condition were selected from the retrospective gait database for all included children. Kinematic, kinetic and electromyographic data were recorded at the time of the gait analysis, which was planned as a routine clinical assessment. However, only kinematic data were considered for the current study. The measurement system consisted of 10–15 optoelectronic cameras (Oxford Metrics, Oxford, United Kingdom) set up around a 10 m walkway. Markers

were located on specific anatomical landmarks, according to the Vicon Plug-In-Gait model. Gait cycles were identified using the kinematic data as well as data from two force plates (Advanced Mechanical Technology Inc., United States) embedded in the walkway. After the identification of gait cycles, joint angles of the hip, knee and ankle, as well as segmental orientation of the pelvis and foot were calculated in Vicon Nexus software (Oxford Metrics, Oxford, United Kingdom). Next, all gait trials were imported into a custom-made Matlab® software (The MathWorks, Natick, MA, United States, 2015), to control for quality and any artifacts or potential outliers. To that end, the ROM and the knee varus-valgus angle values were taken into consideration as previously described (Schwartz et al., 2004). Outliers were defined by taking the average kinematic waveform of each lower limb as a reference and by inspecting the variability of the individual trials around the averaged waveform. A knee varus-valgus ROM $\geq 15°$, a knee valgus angle $\leq -10°$ during swing phase or increased variability in comparison to the average kinematic waveform led to trial exclusion. Subsequently, all available, good-quality gait trials were averaged in this custom-made software, thus creating a new trial for each child. These new, averaged gait trials were used for all further analyses.

Firstly, the GMFCS was reported because it is a widely accepted, frequently reported and validated measure of gross motor function for children with CP (Palisano et al., 1997, 2000). Gait is one of the components of the GMFCS, with the levels I to III expressing the ability to walk, and higher level referring to severe gait impairments (Molloy et al., 2010; Hassani et al., 2011; Massaad et al., 2014; Õunpuu et al., 2015). Secondly, the GPS was calculated. The GPS is an overall gait index that summarizes all relevant kinematic deviations from gait kinematics of TD children. The TD database consisted of 23 children with a median age of 7 years, 2 months (range 4 years, 2 months – 7 years, 11 months) and no neurological or musculoskeletal disorders. The GPS constitutes the root mean square difference between the gait vector of each patient and that of TD peers and is expressed in degrees of motion (Baker et al., 2009). Apart from the overall GPS, a GPS per separate motion plane was calculated (i.e., GPS – sagittal/coronal/transverse), as well as individual gait variable scores (GVS) for nine relevant joint motions in the three motion planes (Baker et al., 2009). For the bCP children, laterality scores were also calculated for the four GPSs, based on the formula of Desmond et al. (1995). Even though the GPSs and GVSs represent the severity of overall gait deviations, the direction of these deviations remains unclear. To overcome this limitation, an additional gait measure was used, i.e., classification of the average gait trials according to a recently reported classification system of MJ gait patterns. These MJ gait patterns represent a series of combined motions at different lower limb joints accepted by the clinical CP community (Papageorgiou et al., 2019a). All assigned patterns were merged into three broad categories, indicating the general direction of the gait deviations. These three categories included: (i) 'minor deviations,' including the children displaying minor gait deviations and children classified with a drop foot, (ii) 'extension patterns', including children presenting with the genu recurvatum, true equinus or jump gait MJ patterns, and (iii) 'flexion patterns,' including children presenting with apparent equinus or crouch MJ patterns. A brief explanation of the GPSs, GVSs and MJ patterns' classification can be found in **Supplementary Figure 1**.

Statistical Analysis

All patient characteristics, brain lesion scores and gait scores were summarized and descriptive statistics were extracted. Normality of the data was not confirmed in all cases based on the Shapiro–Wilk test, hence non-parametric statistics were applied. Between-group comparisons were carried out with the Mann–Whitney *U* (MWU) test, as well as the Pearson chi-squared test (χ^2) for the categorical outcomes, to identify whether the children with bCP and uCP showed baseline differences.

Due to the different types of study datasets, different statistical analyses were performed. A summary of all analyses can be found in **Supplementary Table S1**. The strength of all correlations was reported following the classification of Chan (2003). Correlation coefficients < 0.30 were classified as poor correlations and will not be discussed further. Coefficients between 0.30–0.50 and 0.50–0.80 were classified as fair and moderate correlations, respectively. Coefficients ≥ 0.80 were classified as very strong correlations (Chan, 2003).

Spearman's rank correlations (r_s) were performed to identify the relationships between the continuous or ordinal extent and location sqMRI scores and the GMFCS, the GPSs and the GVSs.

Point-biserial correlations (r_{pb}) were used to explore the relationships between the normally distributed dichotomous location scores and gait pathology. The MWU test was applied to identify differences in the ranks of continuous GPSs and GVSs between the non-normally distributed dichotomous sqMRI categories.

Kruskal–Wallis comparisons were carried out to explore the differences in the continuous sqMRI scores across the three MJ patterns. If differences were identified, post-hoc MWU tests were performed.

Finally, the Pearson chi-squared test (χ^2) was used to study the associations between the ordinal and dichotomous sqMRI scores and MJ patterns. The χ^2 test was also applied for the dichotomous scores and their associations with the GMFCS. In case of significant associations, their strength was defined based on Cramer's V, which depends on the degrees of freedom (DF) and was subsequently classified as weak, moderate or strong (Cohen, 1988). The interpretation rules of these values are described in **Supplementary Table S1**. The direction of these associations can be further examined with the adjusted standardized residuals (i.e., standardized residuals to control for the variations due to the sample size). The latter indicate which specific combinations of scores contribute more strongly to the identified associations. Adjusted standardized residuals follow a normal distribution [with '0' as mean and '1' representing one standard deviation (SD)]. Hence, values of adjusted standardized residuals larger than the mean +2 SDs indicate that two scores are observed more frequently together and are thus associated with each other. Similarly, values smaller than the mean −2 SDs indicate combinations that are statistically negatively associated with each other. All statistical analyses were performed in SPSS (IBM SPSS Statistics for Windows, version 24—IBM Corp.,

Armonk, NY, United States) with $\alpha = 0.05$. Due to the exploratory nature of the present study, correction for multiple testing was only applied for the *post hoc* MWU analyses that were run after the Kruskal–Wallis comparisons ($\alpha = 0.017$ – Šidák correction).

RESULTS

Sample, Brain Lesion and Gait Characteristics

A total of 104 children with spastic CP fulfilled the inclusion criteria and were selected for study enrollment. Patient characteristics are summarized in **Supplementary Table S2**. At the time of MRI, the median age was 8 years, 5 months (range 3 years, 0 months – 17 years, 7 months) and the median age at which the 3DGA was performed was 5 years, 10 months (range 3 years, 7 months – 7 years, 10 months) with an average time of 2 years, 7 months between the two evaluations. The sample consisted of an equal number of children with bCP and uCP ($n = 52$). At the time of the gait analysis, 51% of the entire sample was naive to BoNT-A treatment, while less than 7% of the children had undergone three BoNT-A treatment sessions. In total, the sample consisted of children who were mildly affected by spasticity, weakness, impaired selectivity or contractures, as indicated by the median composite scores (e.g., 4 out of maximally 16 for spasticity). Moreover, most of the children had no reported associated comorbidities. Finally, all children received physical therapy (ranging from 1 to 6 sessions, with a median duration of 45 min per session). The majority of children (i.e., 81%) used ankle foot orthoses during the day, while 40% of the children additionally used night orthoses.

Brain lesion scores are summarized in **Supplementary Table S3**. A standard T1 sequence was used for only three children with no FLAIR sequence availability. Brain lesions classified following the MRICS showed that the vast majority of children had predominantly white matter injuries. Global total sqMRI scores presented a median score of 12 (interquartile range = 1.7–16.5) out of 40. Nine children (i.e., 8%) had a global total brain score of 20 or above, with the maximum score being 28.5 in one child. Adjusted global total brain scores were used for a total of 21 children. Of the remaining 83 children, 27 (33%) showed no corpus callosum involvement. Cerebellar involvement was even more uncommon, with 91% of the children having an intact cerebellum. As far as the lesion location scores of the most affected brain hemisphere are concerned, the periventricular layer displayed the highest damage (median = 3.5, interquartile range = 2–4), with 36% of the children having the maximum score of 4. With respect to the subcortical structures, almost 40% of the children had an involved PLIC and thalamus.

Gait parameters are summarized in **Supplementary Table S4**. Most of the children in the total group were highly functional, i.e., GMFCS level I (62%). The highest median scores were reported for the GPS-sagittal (8.69, interquartile range = 7.33 – 11.53) and the GVS-knee sagittal (12.19, interquartile range = 9.15 – 15.11). Most of the children (i.e., 48%) displayed an extension MJ pattern whereas 21 and 31% presented a minor and flexion MJ pattern, respectively.

Relationships Between sqMRI Scores and Motor Function

All relationships between the brain lesion scores and the GMFCS, GPS and its derivatives and the MJ patterns are summarized in **Figures 1–3**. In these figures, each statistically significant relationship that was identified across the various statistical analyses is represented with shapes for each group: i.e., square for the total, circle for the bCP and triangle for the uCP. Only the statistically significant results are reported in the tables, separately for each group (**Tables 1–5**). No relationships were established between the cerebellum and any of the motor function scores.

Brain Lesion Extent Scores in Relation to the GMFCS and Gait Pathology

All statistically significant correlations are reported in **Table 1**. No correlations were found between the total CC and either the GMFCS or gait pathology.

Total group

The global total sqMRI score fairly correlated to the GPS ($r_s = 0.404$, $p \leq 0.001$) and the GPS-transverse ($r_s = 0.424$, $p \leq 0.001$), indicating that more extensive brain damage corresponds to higher gait pathology. The global total hemispheric score correlated to the GMFCS ($r_s = 0.392$, $p \leq 0.001$), GPS ($r_s = 0.387$, $p \leq 0.001$), GPS-sagittal ($r_s = 0.310$, $p \leq 0.001$), and GPS-transverse ($r_s = 0.372$, $p \leq 0.001$). None of these global scores were related to the GVSs. In addition, no correlations were identified for the total group regarding the global total subcortical score. Finally, the laterality hemispheres' score was negatively related to both the GMFCS level and the GVS-knee sagittal, indicating that children with more symmetric lesions, are classified in higher GMFCS levels and have more knee gait pathology, respectively.

Children with bCP

Fair correlations were identified between the global total sqMRI scores and the GMFCS, as well as the GPS ($r_s = 0.325$, $p \leq 0.05$). The global total hemispheric score correlated fairly to the GMFCS ($r_s = 0.316$, $p \leq 0.05$). In addition, all four global brain scores correlated to the GPS-transverse (i.e., global total – $r_s = 0.474$, $p \leq 0.01$; adjusted global total – $r_s = 0.566$, $p \leq 0.05$; global total hemispheric – $r_s = 0.346$, $p \leq 0.05$; and global total subcortical scores - $r_s = 0.370$, $p \leq 0.01$). Additional correlations were identified between the laterality of the hemispheres and the GVS-hip transverse ($r_s = -0.394$, $p \leq 0.01$), as well as between both the adjusted global total score and the global total subcortical score and the GVS-foot transverse ($r_s = 0.595$, $p \leq 0.05$; $r_s = 0.344$, $p \leq 0.05$, respectively).

Children with uCP

The global total sqMRI and the global total hemispheric scores were fairly correlated with the GMFCS ($r_s = 0.336$, $p \leq 0.05$; $r_s = 0.331$, $p \leq 0.05$, respectively), and the GPS ($r_s = 0.493$, $p \leq 0.001$; $r_s = 0.422$, $p \leq 0.01$, respectively). Additional fair correlations were identified between both of these global brain scores and the GPS-sagittal, the GPS-transverse and the GVS-hip sagittal. In this group, relationships were found between all four global scores and

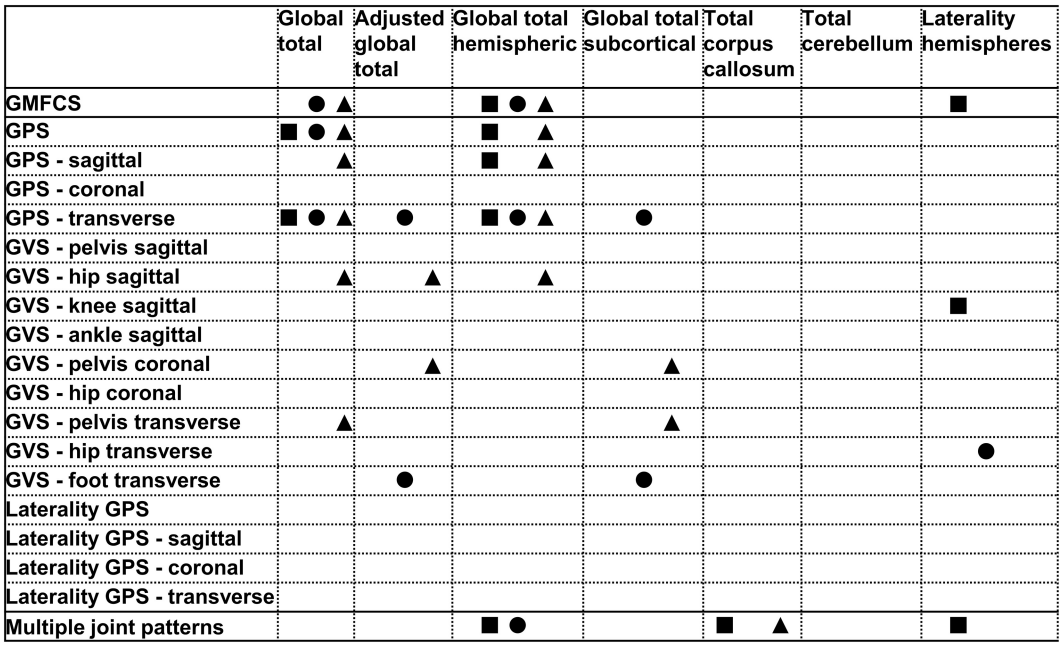

FIGURE 1 | Summary of all statistically significant relationships identified between the brain lesion extent scores and the functional and gait scores (i.e., GMFCS, GPSs, GVSs, and MJ patterns). The total group is depicted with a square, the bCP with a circle and the uCP with a triangle (from left to right: total, bCP, uCP). GMFCS, gross motor function classification system; GPS, gait profile score; GVS, gait variable score; MJ, multiple joint; bCP, bilateral cerebral palsy; uCP, unilateral cerebral palsy.

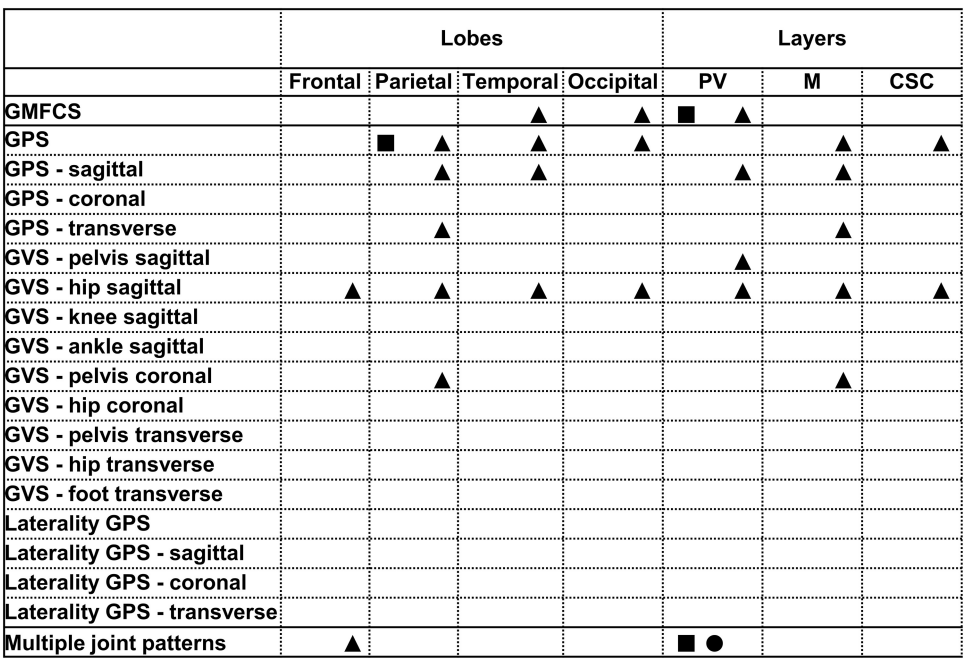

FIGURE 2 | Summary of all statistically significant relationships identified between the lobar and layers brain lesion location scores and the functional and gait scores (i.e., GMFCS, GPSs, GVSs, and MJ patterns). The total group is depicted with a square, the bCP with a circle and the uCP with a triangle (from left to right: total, bCP, uCP). GMFCS, gross motor function classification system; GPS, gait profile score; GVS, gait variable score; MJ, multiple joint; bCP, bilateral cerebral palsy; uCP, unilateral cerebral palsy.

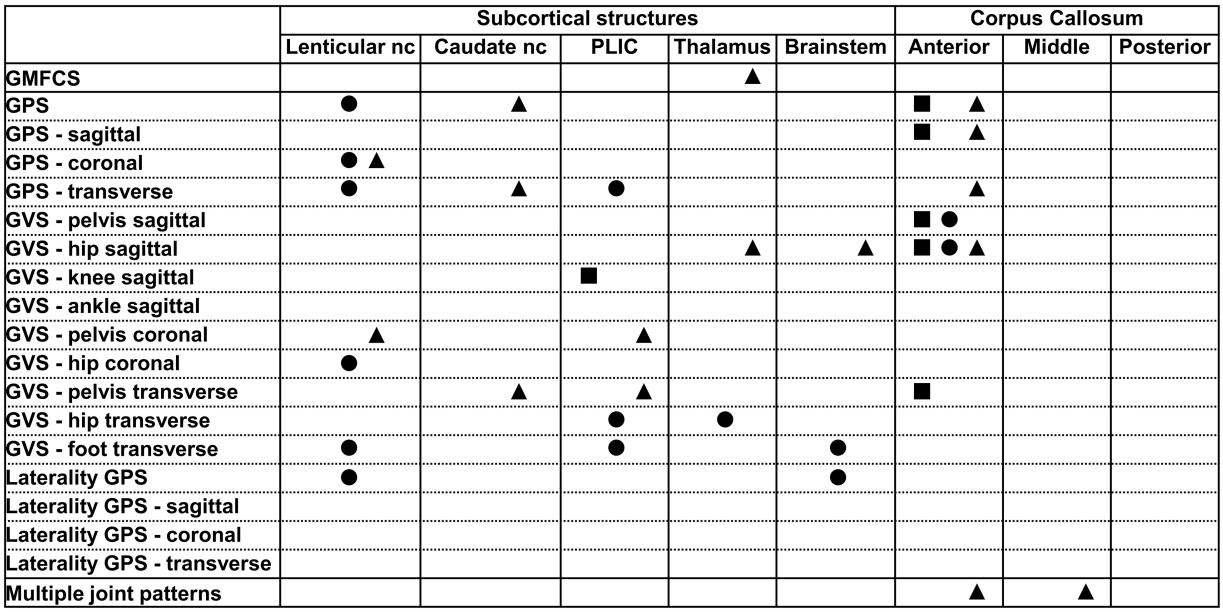

FIGURE 3 | Summary of all statistically significant relationships identified between the dichotomous brain lesion location scores (i.e., subcortical structures and parts of the corpus callosum) and the functional and gait scores (i.e., GMFCS, GPSs, GVSs, and MJ patterns). The total group is depicted with a square, the bCP with a circle and the uCP with a triangle (from left to right: total, bCP, uCP). GMFCS, gross motor function classification system; GPS, gait profile score; GVS, gait variable score; MJ, multiple joint; bCP, bilateral cerebral palsy; uCP, unilateral cerebral palsy.

TABLE 1 | Spearman's rank correlations between the sqMRI extent scores and the scores of functional ability and gait for the total (N = 104), bilateral (n = 52), and unilateral (n = 52) groups.

	Global total[a]	Adjusted global total[b]	Global total hemispheric	Global total subcortical	Laterality hemispheres
Total					
GMFCS			0.392***		−0.523***
GPS	0.404***		0.387***		
GPS – sagittal			0.310***		
GPS – transverse	0.424***		0.372***		
GVS – knee sagittal					−0.311***
bCP					
GMFCS	0.325*		0.316*		
GPS	0.335*				
GPS – transverse	0.474**	0.566*	0.346*	0.370**	
GVS – hip transverse					−0.394**
GVS – foot transverse		0.595*		0.344*	
uCP					
GMFCS	0.336*		0.331*		
GPS	0.493***		0.422**		
GPS – sagittal	0.396**		0.379**		
GPS – transverse	0.339*		0.335*		
GVS – hip sagittal	0.469***	0.821*	0.485***		
GVS – pelvis coronal		0.786*		0.304*	
GVS – pelvis transverse	0.320*			0.308*	

*$p \leq 0.05$; **$p \leq 0.01$; ***$p \leq 0.001$; sqMRI, semi-quantitative MRI scale [15]; GMFCS, gross motor function classification system; GPS, gait profile score; GVS, gait variable score; bCP, bilateral cerebral palsy; uCP, unilateral cerebral palsy; [a]n = 83, 37, 46, respectively; [b]global score when sagittal view MRI was missing, n = 21, 14, 7, respectively. Only the statistically significant results are shown.*

proximal gait impairment scores (i.e., GVS-pelvis in the coronal and transverse planes and GVS-hip sagittal). The strongest relationships were reported between the adjusted global total score and both the GVS-hip sagittal and GVS-pelvis coronal (for n = 7: r_s = 0.821, $p \leq 0.05$; r_s = 0.786, $p \leq 0.05$, respectively).

TABLE 2 | Spearman's rank correlations between the sqMRI location scores of the most affected brain side and the scores of functional ability and gait for the total (N = 104) and unilateral (n = 52) groups.

	Lobes				Layers		
	Frontal	**Parietal**	**Temporal**	**Occipital**	**PV**	***M***	**CSC**
Total							
GMFCS					0.348***		
GPS		0.321***					
uCP							
GMFCS			0.312*	0.409**	0.364**		
GPS		0.450***	0.371**	0.305*		0.444***	0.338*
GPS – sagittal		0.357**	0.369**		0.312*	0.395**	
GPS – transverse		0.331*				0.309*	
GVS – pelvis sagittal					0.372**		
GVS – hip sagittal	0.340*	0.408**	0.438***	0.440***	0.512***	0.486***	0.315*
GVS – pelvis coronal		0.306*				0.316*	

$^*p \leq 0.05$; $^{**}p \leq 0.01$; $^{***}p \leq 0.001$; sqMRI, semi-quantitative MRI scale [15]; PV, Periventricular; M, middle white matter; CSC, cortico/subcortical; uCP, unilateral cerebral palsy; GMFCS, gross motor function classification system; GPS, gait profile score; GVS, gait variable score. Only the statistically significant results are shown.

Brain Lesion Location Scores in Relation to the GMFCS and Gait Pathology

All statistically significant results are reported in **Tables 2–4**. No relationships were found between the middle or the posterior parts of the CC and either the GMFCS or gait pathology.

Total group

The periventricular layer of the most affected brain hemisphere correlated fairly to the GMFCS (r_s = 0.348, $p \leq 0.001$), as did the parietal lobe score with the GPS (r_s = 0.321, $p \leq 0.001$) (**Table 2**). Furthermore, regarding the dichotomous variables of the sqMRI scale, the involvement of the anterior part of the CC was fairly correlated to the GVS-hip sagittal (r_{pb} = 0.495, $p \leq 0.001$) (**Table 3**). Differences based on the MWU test demonstrated that the involvement of the anterior CC is related to increasing gait impairments (**Table 4**). In addition, an involved PLIC points to less severe pathology at the level of the knee in the sagittal plane (p = 0.03).

TABLE 3 | Point-biserial correlations between (i) dichotomous sqMRI scores and (ii) continuous gait scores for the total (N = 104), bilateral (n = 52), and unilateral (n = 52) groups.

	Subcortical structures		Corpus callosum[a]
	Lenticular nucleus	**Caudate nucleus**	**Anterior**
Total			
GVS – hip sagittal			0.495***
bCP			
GPS	0.430***		
GVS – hip sagittal			0.357*
uCP			
GPS	0.449***		
GPS – sagittal			0.439**
GPS – transverse		0.426**	
GVS – hip sagittal			0.641***

$^*p \leq 0.05$; $^{**}p \leq 0.01$; $^{***}p \leq 0.001$; sqMRI, semi-quantitative MRI scale [15]; PLIC, posterior limb of internal capsule; GVS, gait variable score; GPS, gait profile score; bCP, bilateral cerebral palsy; uCP, unilateral cerebral palsy; [a]n = 83, 37, 46, respectively. Only the statistically significant results are shown.

Children with bCP

No relationships were identified between the scores of the lobes or the layers and functional ability and gait in children with bCP (**Table 2**). As far as the dichotomous scores are concerned, two fair relationships were found, namely between (i) the lenticular nucleus and the GPS (r_{pb} = 0.430, $p \leq 0.001$), and (ii) the anterior part of the CC and the GVS-hip sagittal (r_{pb} = 0.357, $p \leq 0.05$) (**Table 3**). Differences based on the MWU test revealed that involvement of the lenticular nucleus, the PLIC, the thalamus, the brainstem and the anterior CC were associated with increasing gait pathology (**Table 4**).

Children with uCP

Positive, fair correlations were identified between the lobes and layers and the GMFCS, the GPSs and the GVSs (**Table 2**), indicating that increasing involvement of these lesion locations is observed with more pathological motor function. For example, the temporal and occipital lobes correlated to the GMFCS (r_s = 0.312, $p \leq 0.05$; r_s = 0.409, $p \leq 0.01$, respectively). Similarly, periventricular layer involvement was related to the GMFCS (r_s = 0.364, $p \leq 0.01$). Moreover, the involvement in three lobes (i.e., parietal, temporal and occipital) and two layers (i.e., middle and cortico/subcortical) correlated to the GPS. Moderate correlations were identified between the periventricular layer score and the GVS-hip sagittal (r_s = 0.512, $p \leq 0.001$).

With respect to the dichotomous lesion location scores, the GMFCS showed only one weak association with the thalamus in the uCP group (χ^2 = 4.13, $p \leq 0.05$, Cramer's V = 0.282, DF = 1). More specifically, GMFCS level I was associated with an intact thalamus, while the opposite was the case for children with GMFCS level II (**Supplementary Table S5**). Moreover, lesions of the subcortical structures and the anterior

TABLE 4 | Statistically significant differences based on Mann–Whitney *U* test between the continuous gait scores for the total (*N* = 104), bilateral (*n* = 52), and unilateral (*n* = 52) groups for the dichotomous sqMRI scores.

	Subcortical structures					Corpus callosum[a]
	Lenticular nucleus	Caudate nucleus	PLIC	Thalamus	Brainstem	Anterior
Total						
GPS						0.009
GPS – sagittal						0.009
GVS – pelvis sagittal						0.032
GVS – knee sagittal			0.030[†]			
GVS – pelvis transverse						0.039
bCP						
GPS – coronal	0.043					
GPS – transverse	0.006		0.012			
GVS – pelvis sagittal						0.045
GVS – hip coronal	0.020					
GVS – hip transverse			0.048	0.046		
GVS – foot transverse	0.004		0.011		0.010	
Laterality GPS	0.039				0.008	
uCP						
GPS						0.006
GPS – coronal	0.031					
GPS – transverse						0.041
GVS – hip sagittal				0.028	0.017	
GVS – pelvis coronal	0.006		0.012			
GVS – pelvis transverse		0.041	0.014			

sqMRI, semi-quantitative MRI scale [15]; PLIC, posterior limb of internal capsule; GPS, gait profile score; GVS, gait variable score; bCP, bilateral cerebral palsy; uCP, unilateral cerebral palsy; [a]n = 83, 37, 46, respectively; [†]an intact PLIC was related to a higher GVS – knee sagittal score. Only the statistically significant results are shown.

part of the CC were related to increasing gait pathology (**Tables 3**, **4**), with a moderate correlation between the anterior CC and GVS-hip sagittal (r_{pb} = 0.641, $p \leq 0.001$), shown in **Table 3**.

Brain Lesion Scores in Relation to the MJ Patterns

All statistically significant results are reported in **Table 5**, **Figure 4**, and **Supplementary Tables S6, S7**.

TABLE 5 | Statistically significant differences in sqMRI extent scores among the multiple joint patterns.

	Global total hemispheric	Laterality hemispheres
Total		
Kruskal-Wallis (p)	0.003	0.003
Minor vs. extension[a]	0.001	0.001
Minor vs. flexion[a]	0.016	0.013
Extension vs flexion[a]	NS	NS
bCP		
Kruskal–Wallis (p)	0.046	NS
Minor vs. extension[a]	NS	
Minor vs. flexion[a]	NS	
Extension vs flexion[a]	NS	

sqMRI, semi-quantitative MRI scale [15]; NS, not significant; bCP, bilateral cerebral palsy; uCP, unilateral cerebral palsy; [a]α = 0.017. Only the statistically significant results are shown.

Total group

In the total group, significant differences in two of the global extent scores among the three MJ patterns were found (**Table 5**). The post-hoc MWU comparisons showed that significantly smaller global total hemispheric scores were found in the children with minor MJ patterns in comparison with the extension ($p \leq 0.001$) and flexion ($p = 0.016$) MJ patterns. Additionally, higher laterality of the hemispheres scores were found in the minor deviations MJ patterns, compared to the extension ($p \leq 0.001$) and flexion ($p = 0.013$) patterns.

The total CC was moderately associated with the MJ patterns ($\chi^2 = 15.20$, $p \leq 0.05$, Cramer's $V = 0.303$, DF = 2) (**Figure 4** and **Supplementary Table S6**). An intact CC was associated with the extension MJ patterns, whereas an involvement of two parts (out of the three) of the CC was associated with the minor MJ patterns.

Furthermore, the periventricular layer was strongly associated with the MJ patterns of the total group ($\chi^2 = 32.56$, $p \leq 0.01$, Cramer's $V = 0.396$; DF = 2). This association further showed that a score of 2 was associated with the flexion patterns while the maximum involvement score of 4 was associated with the extension MJ patterns (**Supplementary Table S7**).

Children with bCP

Despite the observed differences in the global total hemispheric score among the MJ patterns ($p = 0.046$) none of the post-hoc comparisons was significant against the corrected α value (**Table 5**). Only the periventricular layer involvement

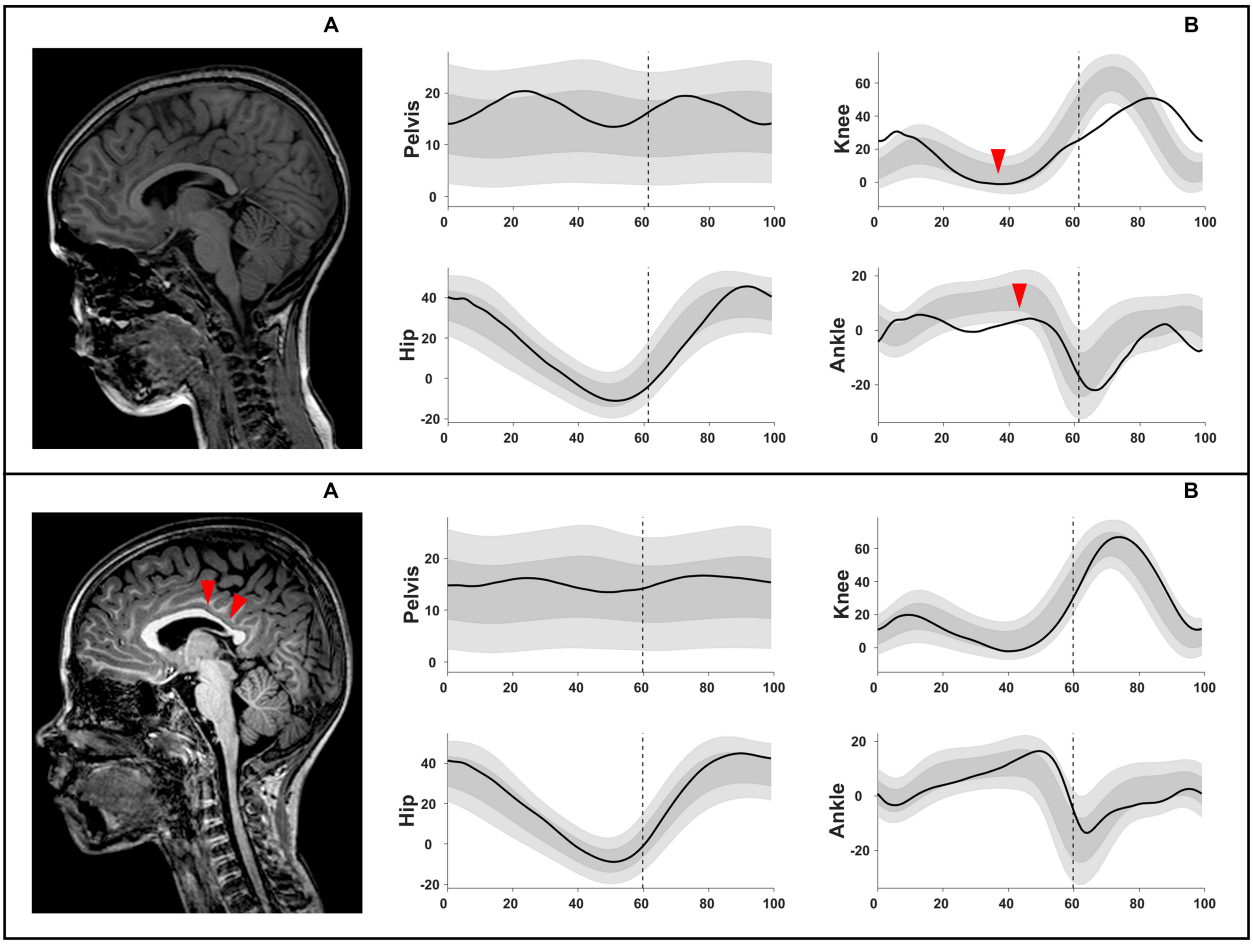

FIGURE 4 | Example illustration of chi-squared analyses, shown in **Supplementary Table S6**. Upper row: **(A)** intact corpus callosum (score 0 out of 3) associated with **(B)** an extension MJ pattern (increased knee extension during midstance and reduced dorsiflexion). Lower row: **(A)** corpus callosum with score 2 out of 3 (involved middle and posterior parts) associated with **(B)** a minor deviations MJ pattern. MJ, multiple joint.

was strongly associated with the MJ patterns (χ^2 = 23.74, $p \leq 0.05$, Cramer's V = 0.478, DF = 2). A score of 1.5 (out of 4) was associated with minor MJ patterns, a score of 2 (out of 4) with flexion MJ patterns and total periventricular layer damage was associated with the extension patterns (**Supplementary Table S7**).

Children with uCP

The global extent scores were not associated with the MJ patterns in this group, with the exception of the total CC score (χ^2 = 18.51, $p \leq 0.01$, Cramer's V = 0.454, DF = 2 – **Supplementary Table S6**). More specifically, an intact CC was associated with extension patterns, while a complete CC involvement was associated with flexion MJ patterns. Regarding the location scores, strong associations were found between the frontal lobe scores and the MJ patterns (χ^2 = 25.09, $p \leq 0.05$, Cramer's V = 0.491, DF = 2 – **Supplementary Table S7**). A minimal frontal lobe involvement (i.e., score of 0.5 out of 3) as well as a higher involvement (i.e., score of 2.5 out of 3) were associated with minor MJ patterns while a score of 1 was associated with flexion patterns. Finally, a moderate association was found between the anterior CC score and MJ patterns (χ^2 = 6.78, $p \leq 0.05$, Cramer's V = 0.388, DF = 1) and a strong association between the middle CC score and MJ patterns (χ^2 = 12.47, $p \leq 0.01$, Cramer's V = 0.526, DF = 1). An intact middle CC was associated with extension patterns. Anterior and middle part involvement were associated with flexion patterns (**Supplementary Table S7**).

DISCUSSION

The need to understand the relationship between the underlying brain structure and motor function in children with CP is largely reflected in the breadth of studies over the last decade (Arnfield et al., 2013; Meyns et al., 2016; Mailleux et al., 2017a,b; Laporta-Hoyos et al., 2018). However, these studies have focused on upper limb deficits, toddlers with CP or children with dyskinetic CP, and the relationship between the brain lesion and functional impairments, such as gait, remains unknown, especially after the brain has reached a full myelination and the gait pattern has

started to mature (Meyns et al., 2019). Therefore, the present study specifically aimed to investigate whether the extent and location of the brain lesion are related to measures of functional ability, as well as gait pathology, in children with spastic CP.

Differences in primary motor deficits (composite spasticity and passive ROM scores), as well as functional severity (i.e., GMFCS and gait) were found between the *two CP groups*, confirming that the children in the bCP group were more affected in comparison with the uCP group. When scored with the sqMRI scale, the structural damage of total hemispheres was larger in the bCP group, whereas the total subcortical and the laterality of the hemispheres scores were higher in the uCP group. For the latter, the lenticular, PLIC and brainstem were the most involved locations of the subcortical structures in the most affected brain side. The GMFCS levels were differently distributed among the two groups, with the children in the bCP group being less functional than those in the uCP group. All gait scores that were different between the two groups were significantly higher in children with bCP, representing a less impaired gait in children with uCP. Meyns et al. (2016) found the same trends of differences between bilateral and unilateral CP, even though they included fewer children in their study, with wider age ranges at the time of 3DGA and more uCP children with only unilateral brain lesions (4/25 versus 2/52 in the present study). In conclusion, our two groups reflected the expected differences in clinical presentation, extent, location and laterality of the lesion, as well as functional impairments (Fiori et al., 2015).

Brain Structure – Motor Function Relationship

The links between brain structure and motor function were firstly investigated between the *brain lesion extent scores* and measures of *gross motor function*. The overall white matter damage (i.e., global total hemispheric score) fairly correlated to the GMFCS in all groups. However, the global total brain score in the total group did not correlate to the GMFCS. This is contradictory with recent findings in dyskinetic CP, where the global brain score was found to be a significant predictor for the GMFCS (Laporta-Hoyos et al., 2018). This difference might stem from several factors. In the present study, children of up to level III of the GMFCS were analyzed, whereas in the study of Laporta-Hoyos et al. (2018), one third of the included children had GMFCS levels IV or V. Furthermore, one third of the patients in this study only had lesions in the basal ganglia or thalamus (Laporta-Hoyos et al., 2018), while all children enrolled in the present study had additional lesions. An additional explanation might be that lower global brain scores were reported by Laporta-Hoyos et al. (2018), with 49% of the participants presenting with a total global brain score of $\leq$5.5 (out of 40) (Laporta-Hoyos et al., 2018). In the present study, only approximately 10% of the patients presented with such low global brain scores. Lastly, the total group in this study showed an equal distribution between bCP and uCP children, whereas the study of Laporta-Hoyos et al. (2018) included mostly bCP dyskinetic children (Laporta-Hoyos et al., 2018).

Interestingly, the laterality of the two hemispheres in the total group showed a moderately negative correlation to the GMFCS, suggesting that more symmetrical brain lesions were observed in less functional children. This could also mean that these children showed a decreased potential for plasticity, through a diminished ability to retain or rewire locomotor circuitry (Fiori et al., 2015). Future studies focusing on the different associations between brain lesions and motor function, and, based on the amount of laterality of the brain lesion, may shed more light on this hypothesis.

The *extent* of the brain lesion (i.e., global total score) was fairly positively related to *gait pathology* (total GPS) in all groups. Furthermore, both the global total and the global total hemispheric scores were fairly related to the GPS-transverse in all groups, while in the total group, only the laterality scores correlated to any of the GVSs. It should be noted that none of these significant correlations were strong ones. Additionally, no correlations were observed for the adjusted global total and the global total subcortical scores with gait in this group. The observed relations between *lesion extent* and gait appeared to be different between the *two CP* groups. For example, in the transverse plane, two brain extent scores (i.e., the adjusted global total and the global total subcortical scores) were related to the GVS of the foot in children with bCP (moderate and fair correlations, respectively), whereas only the global total brain score was fairly related to the GVS of the pelvis in children with uCP. In addition, in this group, the brain *extent scores* were mostly related to *gait pathology* of the proximal joints, resulting in fair to strong correlations.

Stronger correlations were observed in the uCP group compared to the bCP and total groups. These findings could be the result of a more homogenous cohort of uCP children, with 86% being categorized as GMFCS level I and 62% being naive to BoNT-A treatment. Moreover, the global total brain scores and global total hemispheric scores were mostly related to overall gait outcomes, i.e., the GPS and GPS-transverse. Similar results were obtained in a study of Romei et al. (2007), which showed that children with more severe brain injuries had more gait deviations in comparison with children with milder brain lesions (Romei et al., 2007). The associations between brain *extent scores* and the GPS in children with uCP were not observed in the findings of Meyns et al. (2016). However, differences between the current and the previous study might explain the disagreement in findings, including the use of a different neuro-imaging modality (i.e., standard MRI versus DTI) and the variability in the included sample characteristics (e.g., number of patients and age).

The *lesion location scores* of the total group showed fair correlations between the parietal lobe scores and the GPS, as well as between the periventricular layer and both the GMFCS. Based on the MRICS classification, most of the children in this study had a predominant white matter injury (73%). This distribution and the present findings are in line with an earlier population-based study (Himmelmann and Uvebrant, 2011). Furthermore, the associations for these specific *location scores* are in agreement with previous studies that reported on the role of the white matter regions in gait pathology (Cahill-rowley et al., 2019; Toda et al., 2019), even though no associations, emerged between the

middle white matter or the cortico/subcortical layer and any of the functional measures in the total group.

Overall, the *lesion location* showed different correlations between the children with bCP and uCP. In the bCP group, only the subcortical structures, with the exception of the caudate nucleus, and the anterior part of the CC were associated with various gait scores (e.g., GVS-foot in the transverse plane). On the contrary, each of the lobar and layer scores, as well as all five subcortical structures' scores, fairly to moderately correlated to either the GMFCS or at least one gait measure in uCP. Because previous research also revealed fair to strong relationships between subcortical scores (i.e., PLIC and thalamus) and upper limb motor function in children with uCP (Mailleux et al., 2017a), the present findings further suggest a role of these *lesion locations* in the functionality of children with uCP.

MJ patterns were used in order to explore whether brain lesion scores differed according to the direction of the gait deviations. The global total hemispheric and laterality of the hemispheres scores indicated that the minor MJ patterns are different from both the extension and the flexion MJ patterns. Nonetheless, these *lesion extent scores* were not different between the more pathological MJ patterns. On the other hand, based on the total CC scores a differentiation between the extension and flexion MJ patterns in the total group was possible. Specifically, an intact total CC was moderately and positively associated with the extension MJ patterns and negatively associated with the flexion MJ patterns. Moreover, the *lesion location* scores additionally showed some differences between the two more pathological patterns. In the total and bCP groups, a score of 2 (out of 4) assigned in the periventricular layer was observed in children with flexion patterns while a fully involved periventricular layer was associated with extension patterns.

In the uCP group, strong positive associations were identified between an intact total CC and extension MJ patterns, but also between a fully involved total CC (score 3 out of 3) and flexion MJ patterns. Furthermore, an involved anterior or middle part of the CC was observed with flexion MJ patterns, whilst an intact middle part was related to extension patterns. Based on imaging studies, the anterior CC part seems important for actual and imagined walking, since premotor tracts are running through this location (Jahn et al., 2004; Bakker et al., 2008; la Fougère et al., 2010). The current results supported the emerging interest to investigate the CC and are in line with previous studies, where the anterior part of the CC was found to be significantly correlated to various gait metrics in toddlers (Rose et al., 2015; Cahill-rowley et al., 2019) or older children (Meyns et al., 2016). Those studies, however, have used more advanced imaging techniques (i.e., DTI). Hence, future investigations could explore the relationship of the CC –or its parts- to the GMFCS and gait patterns with more advanced measurements, such as measuring CC volume.

In summary, in the total group, the minor MJ patterns were associated with lower global total hemispheric and higher laterality scores, as well as an involvement of two CC parts and a score of 1.5 (out of 4) in the periventricular layer. The extension and flexion MJ patterns showed higher global total hemispheric and lower laterality scores in comparison with the minor MJ patterns. Additionally, for the extension MJ patterns, intactness of the total CC and maximal periventricular layer involvement were found. Lastly, the flexion MJ patterns were strongly positively associated with a score of 2 in the periventricular layer and were moderately negatively associated with an intact total CC.

Limitations and Future Directions

This study has some limitations related to brain and gait metrics. First, the vast heterogeneity in the clinical picture of CP poses numerous challenges. Unraveling the relationships between the structural lesions and functional impairments is not straightforward. Therefore, a sample as homogenous as possible was selected. MRI scans performed after the age of 3 years were included, as suggested in the protocol of Fiori et al. (2014). At that age, the brain lesion has reached quite a mature level, indicating that the lesion is more stable in comparison with the neonatal brain state (Parazzini et al., 2002; Hermoye et al., 2006; Welker and Patton, 2012). During the neonatal period, lesions might be incorrectly classified as normal, because periventricular lesions or lesions to the gray matter could remain undetected (Himmelmann et al., 2016). Previous research indicated that the myelination process is finished in both the lobes and subcortical regions by the age of 3 years (Parazzini et al., 2002), thus enabling assessment of white matter lesions. Even though brain maturation may still be ongoing in other regions, this study focused on presumably stable brain lesions. The children included in this study had undergone a 3DGA at a young age, namely after the age of three, but before the growth spurt or the development of severe secondary deformities. This age range restriction resulted in the inclusion of children who had not received neuro- or orthopedic surgery or were minimally treated with BoNT-A, further ensuring a homogeneous sample. Whether this minimal treatment history has an impact on the observed relationships remains to be explored.

Moreover, children are considered to have at least started to obtain a stable gait pattern around that age (Sutherland, 1997), with a mature gait pattern emerging around the age of 5 years (Simon et al., 1978). The current findings may be affected by the dynamic nature of gait in children with. Young children may be characterized by inconsistency between repeated gait trials, suggesting an immature gait pattern. However, at the time of the 3DGA, 86% of the children had already been ambulant for at least 24 months, ensuring sufficient maturation of their gait pattern. For the remaining 14%, who had only been ambulant for more than 12 months, the use of averaged gait data filters this inconsistency between the gait trials. It is important to highlight that the included study sample covers the current natural history of growing children with CP. Future studies with longitudinal data and large study samples may further explore to what extent changes in gait pathology throughout growth may influence the associations between brain lesions and motor outcomes. The choice of age ranges was necessary to ensure homogeneity of the included sample. Furthermore, even younger children have been included in previous studies investigating the relationships between brain lesions and gait metrics (Rose et al., 2015; Cahill-rowley et al., 2019). All studies have aspired to clarify these relationships, in light of timely and appropriate treatment

administration for children with CP. Due to the retrospective nature of this study and based on data availability, there was a substantial gap between the age at MRI and 3DGA. The median difference was 2 years, 7 months, with the MRIs having mostly been acquired at an older age. Assuming that the studied brain lesions are static, this difference in acquisition timings should not have influenced the current results.

Neuroimaging has established its role in the diagnostic process of CP, with brain MRI being increasingly accessible to clinicians (Novak et al., 2017). However, other imaging modalities, such as DTI, have advantages over the use and interpretation of structural brain MRI. These include higher sensitivity to identify white matter lesions (Hoon and Faria, 2010) or the involvement of certain locations, e.g., the volume of the CC. The use of conventional MRI could explain the diverse results in comparison with Meyns et al. (2016). MRI based on DTI, however, is not routinely available or used in clinical settings, rather (still) mostly applied for research purposes (Sutherland, 1997). Given that knowledge of the functional and gait characteristics is essential for clinical decision-making and treatment planning, the aim of our study was to provide insights in the neural correlates via a standardized and detailed scale using conventional neuro-imaging methods. The current findings delineated fair to strong associations between the brain lesions and motor function, based on conventional structural MRI, which is more clinically accessible and less time-consuming. The automation of the sqMRI brain scale could be a promising future direction to facilitate and optimize the transfer to clinical practice (Pagnozzi et al., 2015).

This exploratory study did not establish predictions of functional abilities and gait pathology based on the *extent and location* of the investigated brain lesions, nor did it apply statistical corrections for multiple testing. This study is a first step in providing a comprehensive quantification of the relationships of brain lesions with functional abilities and gait pathology in children with CP, using an extensive set of outcome parameters. Moreover, prediction analyses would require larger sample sizes, since the brain-gait interaction is considered obscure. Indeed, additional to neural injury, other factors are also suspected to be the causes of gait pathology in children with CP, such as the combination of the effect of spasticity, muscle weakness, and other motor deficits, as well as aberrant growth or compensation strategies (Baker et al., 2016). Future analyses can apply different statistics (e.g., logistic or linear regression models) on larger sample sizes, in order to accommodate for all different variable types within the sqMRI scale and the various motor function measures. The ultimate goal is to identify whether motor function and gait pathology can timely be explained and guided based on the underlying neurological correlates. Based on the current study results, preliminary treatment guidance can be suggested, in particular with respect to MJ patterns. Such clinical reasoning could, for example, be based on the moderate to strong associations of the intact total CC and full periventricular layer involvement with extension MJ patterns. Should these associations be validated by future studies, clinicians could promote adequate ankle dorsiflexion or limit knee hyperextension by adapting the physiotherapeutic exercise program accordingly, by providing properly tuned orthoses that prevent hyperextension, or by providing stimulating activities that facilitate the desired motions. Nevertheless, caution is needed before advising targeted and individualized interventions before the age of 3 years, based on the current findings.

CONCLUSION

In general, this is the first study that used the sqMRI scale to investigate the relationships between, on the one hand, the *brain lesion extent and location* and, on the other hand, *motor function*, with a focus on *pathological gait*. A comprehensive gait assessment was studied, including not only the GPSs and the GVSs, but also MJ patterns. The preliminary study findings seem promising, yet caution is warranted when interpreting these results due to the exploratory nature of this study. Nevertheless, the analyses based on the GMFCS as well as the GPSs and GVSs demonstrated that children with more extensive brain lesions have increased gait pathology, and differences in brain lesion scores were found among the MJ gait patterns. This study focused not only on a generic sample of children with spastic CP but also included two separate patient groups based on topographic classification. These additional analyses revealed more relations between the *lesion extent and location* and the *gait pathology* in children with uCP, suggesting that it may be especially interesting to further investigate the specific *locations* of the brain injury firstly in children with uCP. In addition, this study identified the neuro-anatomical characterization of the brain injury and gait pathology after the age of 3 years, suggesting some guidelines of treatment planning in children with mature brain lesions and stable gait patterns. Finally, this exploratory study confirmed the existence of a structure – function relationship, with a focus on pathological gait, in children with spastic CP which has not been extensively documented in the past.

DATA AVAILABILITY STATEMENT

The datasets generated for this study are available on request to the corresponding author.

ETHICS STATEMENT

The studies involving human participants were reviewed and approved by Medical Ethical Committee of the University hospitals Leuven (s56036). Written informed consent from the participants' legal guardian/next of kin was not required to participate in this study in accordance with the national legislation and the institutional requirements.

AUTHOR CONTRIBUTIONS

EP, ND, KD, and EO was designed the study. EP and ND were responsible for gait data acquisition. EO was responsible for brain MRI scoring. EP and ND conducted the all presented analyses. All

the authors had complete access to the study data throughout the study, contributed to the interpretation of the results, involved in the critical revision and editing of the manuscript, which was written equally by EP and ND and are co-first authors, approved the final version of the manuscript and agree to be accountable for the content of the work.

FUNDING

EP was supported by the SIMCP IWT-project (Agentschap voor Innovatie door Wetenschap en Technologie), a simulation platform to predict gait performance following orthopedic intervention in children with cerebral palsy (IWT 140184) and the Flemish Research Council (grant number T003116N). ND was supported by Internal Funds of KU Leuven (C24/18/103).

SUPPLEMENTARY MATERIAL

The Supplementary Material for this article can be found online at: https://www.frontiersin.org/articles/10.3389/fnhum.2020.00275/full#supplementary-material

REFERENCES

Ahlin, K., Himmelmann, K., Nilsson, S., Sengpiel, V., and Jacobsson, B. (2016). Antecedents of cerebral palsy according to severity of motor impairment. *Acta Obstet. Gynecol. Scand.* 95, 793–802. doi: 10.1111/aogs.12885

Arnfield, E., Guzzetta, A., and Boyd, R. (2013). Relationship between brain structure on magnetic resonance imaging and motor outcomes in children with cerebral palsy: A systematic review. *Res. Dev. Disabil.* 34, 2234–2250. doi: 10.1016/j.ridd.2013.03.031

Baker, R., Esquenazi, A., Benedetti, M. G., and Desloovere, K. (2016). Gait analysis: clinical facts. *Eur. J. Phys. Rehabil. Med.* 52, 560–574.

Baker, R., McGinley, J. L., Schwartz, M. H., Beynon, S., Rozumalski, A., Graham, H. K., et al. (2009). The Gait Profile Score and Movement Analysis Profile. *Gait Posture* 30, 265–269. doi: 10.1016/j.gaitpost.2009.05.020

Bakker, M., De Lange, F. P., Helmich, R. C., Scheeringa, R., Bloem, B. R., and Toni, I. (2008). Cerebral correlates of motor imagery of normal and precision gait. *Neuroimage* 41, 998–1010. doi: 10.1016/j.neuroimage.2008.03.020

Cahill-rowley, K., Schadl, K., Vassar, R., Yeom, K. W., Stevenson, D. K., and Rose, J. (2019). Prediction of gait impairment in toddlers born preterm from near-term brain microstructure assessed With DTI, using exhaustive feature selection and cross-validation. *Front. Hum. Neurosci.* 13:305. doi: 10.3389/fnhum.2019.00305

Cans, C., Dolk, H., Platt, M. J., Colver, A., Prasauskiene, A., Krageloh-Mann, I., et al. (2007). Recommendations from the SCPE collaborative group for defining and classifying cerebral palsy. *Dev. Med. Child Neurol.* 109, 35–38. doi: 10.1111/j.1469-8749.2007.tb12626.x

Chan, Y. H. (2003). Biostatistics 104: Correlational Analysis. *Singapore Med. J.* 44, 614–619.

Cohen, J. (1988). *Statistical Power and Analysis for the Behavioral Sciences*, 2nd Edn. Hillsdale: Erlbaum.

Coleman, A., Fiori, S., Weir, K. A., Ware, R. S., and Boyd, R. N. (2016). Relationship between brain lesion characteristics and communication in preschool children with cerebral palsy. *Res. Dev. Disabil.* 58, 55–64. doi: 10.1016/j.ridd.2016.08.015

Desmond, J. E., Sum, J. M., Wagner, A. D., Demb, J. B., Shear, P. K., Glover, G. H., et al. (1995). Functional MRI measurement of language lateralization in Wada-tested patients. *Brain* 118, 1411–1419. doi: 10.1093/brain/118.6.1411

Fiori, S., Cioni, G., Klingels, K., Ortibus, E., Van Gestel, L., Rose, S., et al. (2014). Reliability of a novel, semi-quantitative scale for classification of structural brain magnetic resonance imaging in children with cerebral palsy. *Dev. Med. Child Neurol.* 56, 839–845. doi: 10.1111/dmcn.12457

Fiori, S., Guzzetta, A., Pannek, K., Ware, R. S., Rossi, G., Klingels, K., et al. (2015). Validity of semi-quantitative scale for brain MRI in unilateral cerebral palsy due to periventricular white matter lesions: Relationship with hand sensorimotor function and structural connectivity. *Neuroimage Clin.* 8, 104–109. doi: 10.1016/j.nicl.2015.04.005

Graham, H. K., Rosenbaum, P., Paneth, N., Dan, B., Lin, J.-P., Damiano, D. L., et al. (2016). Cerebral palsy. *Nat. Rev. Dis. Prim.* 2:15082.

Hassani, S., Krzak, J., Flanagan, A., Bagley, A., Gorton, G., Romness, M., et al. (2011). Assessment of strength and function in ambulatory children with cerebral palsy by GMFCS level and age: a cross-sectional study. *Crit. Rev. Phys. Rehabil. Med.* 23, 1–14. doi: 10.1615/critrevphysrehabilmed.v23.i1-4.10

Hermoye, L., Saint-Martin, C., Cosnard, G., Lee, S. K., Kim, J., Nassogne, M. C., et al. (2006). Pediatric diffusion tensor imaging: Normal database and observation of the white matter maturation in early childhood. *Neuroimage* 29, 493–504. doi: 10.1016/j.neuroimage.2005.08.017

Himmelmann, K., Horber, V., De La Cruz, J., Horridge, K., Mejaski-Bosnjak, V., Hollody, K., et al. (2016). MRI classification system (MRICS) for children with cerebral palsy: development, reliability, and recommendations. *Dev. Med. Child. Neurol.* 59, 57–64. doi: 10.1111/dmcn.13166

Himmelmann, K., and Uvebrant, P. (2011). Function and neuroimaging in cerebral palsy: A population-based study. *Dev. Med. Child Neurol.* 53, 516–521. doi: 10.1111/j.1469-8749.2011.03932.x

Holmes, S. J., Mudge, A. J., Wojciechowski, E. A., Axt, M. W., and Burns, J. (2018). Impact of multilevel joint contractures of the hips, knees and ankles on the Gait Profile score in children with cerebral palsy. *Clin. Biomech.* 59, 8–14. doi: 10.1016/j.clinbiomech.2018.08.002

Hoon, A. H., and Faria, A. V. (2010). Pathogenesis, neuroimaging and management in children with cerebral palsy born preterm. *Dev. Disabil. Res. Rev.* 16, 302–312. doi: 10.1002/ddrr.127

Jahn, K., Deutschländer, A., Stephan, T., Strupp, M., Wiesmann, M., and Brandt, T. (2004). Brain activation patterns during imagined stance and locomotion in functional magnetic resonance imaging. *Neuroimage* 22, 1722–1731. doi: 10.1016/j.neuroimage.2004.05.017

Krägeloh-Mann, I., and Horber, V. (2007). The role of magnetic resonance imaging in elucidating the pathogenesis of cerebral palsy: A systematic review. *Dev. Med. Child Neurol.* 49, 144–151. doi: 10.1111/j.1469-8749.2007.00144.x

la Fougère, C., Zwergal, A., Rominger, A., Förster, S., Fesl, G., Dieterich, M., et al. (2010). Real versus imagined locomotion: A [18F]-FDG PET-fMRI comparison. *Neuroimage* 50, 1589–1598. doi: 10.1016/j.neuroimage.2009.12.060

Laporta-Hoyos, O., Fiori, S., Pannek, K., Ballester-Plané, J., Leiva, D., Reid, L. B., et al. (2018). Brain lesion scores obtained using a simple semi-quantitative scale from MR imaging are associated with motor function, communication and cognition in dyskinetic cerebral palsy. *Neuroimage Clin.* 19, 892–900. doi: 10.1016/j.nicl.2018.06.015

MacFarlane, S., Taufika, S., Guzetta, A., Edwards, P., and Boyd, R. (2012). The relationship between brain structure and gait patterns in children with congenital hemiplegia. *Neurorehabil. Neural Repair* 26:655. doi: 10.1177/1545968312448178

Mailleux, L., Klingels, K., Fiori, S., Simon-martinez, C., Demaerel, P., Locus, M., et al. (2017a). How does the interaction of presumed timing, location and extent of the underlying brain lesion relate to upper limb function in children with unilateral cerebral palsy? *Eur. J. Paediatr. Neurol.* 21, 763–772. doi: 10.1016/j.ejpn.2017.05.006

Mailleux, L., Simon-Martinez, C., Klingels, K., Jaspers, E., Desloovere, K., Demaerel, P., et al. (2017b). Structural brain damage and upper limb kinematics in children with unilateral cerebral palsy. *Front. Hum. Neurosci.* 11:607. doi: 10.3389/fnhum.2017.00607

Massaad, A., Assi, A., Skalli, W., and Ghanem, I. (2014). Repeatability and validation of gait deviation index in children: typically developing and cerebral palsy. *Gait Posture* 39, 354–358. doi: 10.1016/j.gaitpost.2013.08.001

Meldrum, D., Shouldice, C., Conroy, R., Jones, K., and Forward, M. (2014). Test-retest reliability of three dimensional gait analysis: Including a novel approach

to visualising agreement of gait cycle waveforms with Bland and Altman plots. *Gait Posture* 39, 265–271. doi: 10.1016/j.gaitpost.2013.07.130

Meyns, P., van den Bogaart, M., Theunissen, K., van der Krogt, M. M., Ortibus, E., and Desloovere, K. (2019). Editorial: motor control of gait and the underlying neural network in pediatric neurology. *Front. Hum. Neurosci.* 13:226. doi: 10.3389/fnhum.2019.00226

Meyns, P., Van Gestel, L., Leunissen, I., De Cock, P., Sunaert, S., Feys, H., et al. (2016). Macrostructural and microstructural brain lesions relate to gait pathology in children with cerebral palsy. *Neurorehabil. Neural Repair* 30, 817–833. doi: 10.1177/1545968315624782

Molloy, M., McDowell, B. C., Kerr, C., and Cosgrove, A. P. (2010). Further evidence of validity of the gait deviation index. *Gait Posture* 31, 479–482. doi: 10.1016/j.gaitpost.2010.01.025

Novak, I., Morgan, C., Adde, L., Blackman, J., Boyd, R. N., Brunstrom-Hernandez, J., et al. (2017). Early, accurate diagnosis and early intervention in cerebral palsy advances in diagnosis and treatment. *JAMA Pediatr.* 171, 897–907.

Õunpuu, S., Gorton, G., Bagley, A., Sison-Williamson, M., Hassani, S., Johnson, B., et al. (2015). Variation in kinematic and spatiotemporal gait parameters by Gross Motor Function Classification System level in children and adolescents with cerebral palsy. *Dev. Med. Child. Neurol.* 57, 955–962. doi: 10.1111/dmcn.12766

Pagnozzi, A. M., Fiori, S., Boyd, R. N., Guzetta, A., Doecke, J., Gal, Y., et al. (2015). Optimization of MRI-based scoring scales of brain injury severity in children with unilateral cerebral palsy. *Pediatr. Radiol.* 46, 1–10.

Palisano, R., Rosenbaum, P., Walter, S., Russell, D., Wood, E., and Galuppi, B. (1997). Development and reliability of a system to classify gross motor function in children with cerebral palsy. *Dev. Med. Child Neurol.* 39, 214–223. doi: 10.1111/j.1469-8749.1997.tb07414.x

Palisano, R. J., Hanna, S. E., Rosenbaum, P. L., Russell, D. J., Walter, S. D., Wood, P., et al. (2000). Validation of a model of gross motor function for children with cerebral palsy. *Phys. Ther. J. Am. Phys. Ther. Assoc.* 80, 974–985.

Papageorgiou, E., Nieuwenhuys, A., Vandekerckhove, I., Van Campenhout, A., Ortibus, E., and Desloovere, K. (2019a). Systematic review on gait classifications in children with cerebral palsy: an update. *Gait Posture* 69, 209–223. doi: 10.1016/j.gaitpost.2019.01.038

Papageorgiou, E., Simon-Martinez, C., Molenaers, G., Ortibus, E., Van Campenhout, A., and Desloovere, K. (2019b). Are spasticity, weakness, selectivity, and passive range of motion related to gait deviations in children with spastic cerebral palsy? A statistical parametric mapping study. *PLoS One* 14:e223363. doi: 10.1371/journal.pone.0223363

Parazzini, C., Baldoli, C., Scotti, G., and Triulzi, F. (2002). Terminal Zones of Myelination: MR Evaluation of Children Aged 20 – 40 Months. *AJNR Am. J. Neuroradiol.* 23, 1669–1673.

Romei, M., Galli, M., Fazzi, E., Maraucci, I., Schwartz, M., Uggetti, C., et al. (2007). Analysis of the correlation between three methods used in the assessment of children with cerebral palsy. *Funct. Neurol.* 22, 17–21.

Rose, J., Cahill-rowley, K., Vassar, R., Yeom, K. W., Stecher, X., Stevenson, D. K., et al. (2015). Neonatal brain microstructure correlates of neurodevelopment and gait in preterm children 18–22 mo of age: an Mri and dti study. *Pediatr. Res.* 78, 700–708.

Rose, J., Mirmiran, M., Butler, E. E., Lin, C. Y., Barnes, P. D., Kermoian, R., et al. (2007). Neonatal microstructural development of the internal capsule on diffusion tensor imaging correlates with severity of gait and motor deficits. *Dev. Med. Child Neurol.* 49, 745–750.

Rosenbaum, P., Paneth, N., Leviton, A., Goldstein, M., Bax, M., Damiano, D., et al. (2007). A report: The definition and classification of cerebral palsy April 2006. *Dev. Med. Child Neurol.* 49, 8–14.

Schwartz, M. H., Trost, J. P., and Wervey, R. A. (2004). Measurement and management of errors in quantitative gait data. *Gait Posture* 20, 196–203.

Simon, S. R., Deutsch, S. D., Nuzzo, R. M., Mansour, M. J., Jackson, J. L., Koskinen, M., et al. (1978). Genu recurvatum in spastic cerebral palsy. Report on findings by gait analysis. *J. Bone Joint Surg. Am.* 60, 882–894.

Sutherland, D. (1997). The development of mature gait. *Gait Posture* 6, 163–170.

Taufika, S., MacFarlane, S., Edwards, P., Guzetta, A., and Boyd, R. (2012). The relationship between brain structure and gait patterns in children with diplegia. *Neurorehabil. Neural Repair* 26, 655–656. doi: 10.1177/1545968312448178

Toda, K., Iijima, M., and Kitagawa, K. (2019). Periventricular White Matter Lesions Influence Gait Functions in Parkinson ' s Disease. *Eur. Neurol.* 81, 120–127.

Welker, K. M., and Patton, A. (2012). Assessment of normal myelination with magnetic resonance imaging. *Semin. Neurol.* 32, 15–28.

Wren, T. A. L., Otsuka, N. Y., Bowen, R. E., Scaduto, A. A., Chan, L. S., Sheng, M., et al. (2011). Influence of gait analysis on decision-making for lower extremity orthopaedic surgery: Baseline data from a randomized controlled trial. *Gait Posture* 34, 364–369.

Zhou, J., Butler, E. E., and Rose, J. (2017). Neurologic correlates of gait abnormalities in cerebral palsy: implications for treatment. *Front. Hum. Neurosci.* 11:103. doi: 10.3389/fnhum.2017.00103

Conflict of Interest: The authors declare that the research was conducted in the absence of any commercial or financial relationships that could be construed as a potential conflict of interest.

Advantages of publishing in Frontiers

OPEN ACCESS
Articles are free to read for greatest visibility and readership

FAST PUBLICATION
Around 90 days from submission to decision

HIGH QUALITY PEER-REVIEW
Rigorous, collaborative, and constructive peer-review

TRANSPARENT PEER-REVIEW
Editors and reviewers acknowledged by name on published articles

Frontiers
Avenue du Tribunal-Fédéral 34
1005 Lausanne | Switzerland

Visit us: www.frontiersin.org
Contact us: info@frontiersin.org | +41 21 510 17 00

REPRODUCIBILITY OF RESEARCH
Support open data and methods to enhance research reproducibility

DIGITAL PUBLISHING
Articles designed for optimal readership across devices

FOLLOW US
@frontiersin

IMPACT METRICS
Advanced article metrics track visibility across digital media

EXTENSIVE PROMOTION
Marketing and promotion of impactful research

LOOP RESEARCH NETWORK
Our network increases your article's readership